UNIVERSITY OF SOUTHAMPTON

THE ROLES OF HYDROGRAPHIC AND BIOGEOCHEMICAL PROCESSES IN THE DISTRIBUTION OF DISSOLVED INORGANIC NUTRIENTS IN A SCOTTISH SEA-LOCH SYSTEM

By

LOUISA JANE WATTS

A thesis submitted to the University of Southampton for the Degree of Doctor of Philosophy

Department of Oceanography
Southampton University
Highfield
Southampton
Hampshire

September 1994

TO MY MUM

AND ALL MY FRIENDS

UNIVERSITY OF SOUTHAMPTON

ABSTRACT

FACULTY OF SCIENCE

OCEANOGRAPHY

Doctor of Philosophy

THE ROLES OF HYDROGRAPHIC AND BIOGEOCHEMICAL PROCESSES IN THE DISTRIBUTION OF DISSOLVED INORGANIC NUTRIENTS IN A SCOTTISH SEA-LOCH SYSTEM

by Louisa Jane Watts

Fjords, like other estuaries form an important transition zone through which land-derived nutrients must pass before reaching the oceans. They possess topographic features which result in a unique type of circulation whereby water of marine origin may be retained and the flushing time of the system extended. These factors facilitate the study of nutrient distributions in the deeper waters of the basin because temporary or permanent isolation potentially enables these processes to be distinguished from hydrodynamic processes.

Work has been carried out over two field-seasons which spanned the spring months of March to May 1991 and February to April 1992, in the upper basin of Loch Linnhe, a sea-loch system based on the west coast of Scotland. Concentrations of nutrients (NO_3^-, PO_4^{3-}, dissolved Si) were measured, together with hydrographic and biological parameters, on samples from stations along the longitudinal axis of the upper basin.

Water in the upper basin of Loch Linnhe is vertically stratified. Water temperature plays a negligible role in determining the density structure of the water column. Water in the upper basin is essentially horizontally uniform in terms of its salinity and density properties although a slight gradient was present due to the freshwater input at the head of the loch. During both field-seasons a deep-water renewal event has been observed in which the system is flushed by incoming saline water. The timing of this event has been linked to a wind-driven upwelling event seaward of the sill, allowing high salinity water to enter the system. These flushing events occur on or close to large spring tides thus allowing relatively high volumes of saline water to enter the basin on a flood tide. In 1992 a temperature inversion was also observed throughout the water column prior to the renewal thus favouring its occurrence.

The main source of dissolved inorganic nitrate and phosphate to the system is the saline end-member, and that of dissolved silicon is the freshwater input of the rivers Lochy and Nevis. All three nutrients show a very weak relationship with salinity when the conventional steady-state, one-dimensional mixing diagram is employed. This is due to the presence of more than two mixing types in the system which is a result of (a) the inhibition of free-estuarine circulation due to the presence of the sill, and the resultant isolated bottom-waters which represent at least one other mixing type, and (b) the vertical stratification set up which, combined with the effects of observed temporally varying end-member concentrations within the flushing time of the system, gives rise to the presence of more mixing types. More than two mixing types results in deviations of nutrient behaviour away from a linear relationship with salinity, a phenomenon referred to as apparent non-conservative behaviour. Real non-conservative behaviour, which is caused by biogeochemical processes, has also been observed over the two field-seasons and includes (i) biological activity with the occurrence of a spring phytoplankton bloom, (ii) regeneration of nutrients from the sediments to the overlying bottom-waters and (iii) geochemical reactivity of phosphate suggested by its presence in the sediments and its association with fine-grained clay minerals.

To distinguish between real and apparent non-conservative behaviour of the nutrients, a simple, filling, one-dimensional box-model has been adapted. Driven only by observed meteorological and boundary condition data, it has successfully reproduced the hydrographic status of the upper basin for two years of data. Nutrients have been incorporated into the model as conservative tracers and the difference between observed and model predicted data show that non-conservative behaviour has occurred in the isolated bottom-waters of 1992. By initiating the model with a linear starting condition of the nutrient concentrations with salinity, it has been shown that the temporally varying end-member concentrations can explain up to 10 %, 3 % and 11 % of the variance of nitrate, phosphate and silicate concentrations respectively, in their relationships with salinity.

ACKNOWLEDGEMENTS

There are so many people that I need to thank for their support throughout the duration of my Ph.D. thesis that I don't know where to start. If I forget anybody please forgive me!

Thanks goes to the following people: Firstly to NERC for financing the Ph.D, including all of the conferences attended and courses abroad. To my supervisors; Dennis Burton, David Hydes and Ken Jones for their encouragement and support, particularly during the writing-up stage of the thesis. To Professor John Simpson and Dr. Tom Rippeth, UCNW, for their help in the collaborative work involved with the model. To Dr. Andrew Parker and Dr. Graham Paterson, Reading University, for the use of the XRD and XRF instrumentation.

To Dunstaffnage Marine Laboratory for accommodating me during the Ph.D. and for the provision of excellent on-hand facilities during the study period. This includes the use of the Research Vessels Calanus and Seol Mara, the crews of which I would especially like to thank for all their help and for being so cheery in all weathers during my field-trips. Without their help much of this data could not have been collected.

To Brian Grantham for his help and patience during the operation of the autoanalyser. To the Marine Physics gang; Jim Watson (thanks for the sweeties!), Anton Edwards, Jo Graham, Colin Griffiths, David Meldrum, Neil MacDougall, Katrine Smalley and Dave Ellett, for their extensive help and use of the tea-room and provision of Ginger Nuts (in the evenings!).

An enormous thankyou to Carol Phillips, without whose expertise on the photocopier this thesis would not have made it to the binders on time. Thanks also for all the gossiping sessions that kept me sane over the past three years.!

Thanks to Digby Harris for putting up with the chaotic mess in the office and with all the grumblings during the write-up. Thanks also to Tom Wilding, my flat-mate for putting up with domestic chaos! To Shona Sked (DML's very own glamour-puss!) for her cheery

smile every morning even when I'm in late. To Anton Edwards for his amazing support both technically and as a friend, for the long chin-wags and free business lunches. To Tom Rippeth for maintaining a gossip-line to UCNW via e-mail.

To all my friends for supporting me through all the ups and downs during the past few years.

To the Oban Inn for keeping me sane!

A huge "thankyou" to my Mum, Mrs. Jill Watts, for her never-ending moral support, patience, guidance and financial support throughout the whole of my education.

And last but not least, thanks to Karen Fretwell for her friendship and her smile.

LIST OF CONTENTS

LIST OF FIGURES AND TABLES

INTRODUCTION

Material from land-based sources that reaches the oceans has passed through a continuum formed by rivers, lakes, estuaries and coastal marine areas. In these environments biological and physicochemical processes occur leading to the transformation and immobilization of dissolved inorganic nutrients (Billen *et al.*, 1991). In this study the distribution of such dissolved inorganic nutrients in estuarine, sea-loch systems is considered. Such systems have been described as "geochemical reaction vessels" (Kaul and Froelich, 1984) due to the pronounced changes in physicochemical characteristics that occur during the mixing of river water and seawater and the close coupling between estuarine processes in the water column and in sediments which lead to a variety of reactions of geochemical significance (Burton, 1988). As stated by Kaul and Froelich (1984), biogeochemical processes regulate the input, recycling and removal of nutrients in estuaries and hence have a potentially major influence on their eventual transfer to the sea.

Since nutrient fluxes ultimately influence the level of productivity in the oceans, efforts to develop a quantitative basis for estimating the direction and extent of nutrient modification in estuaries will lead to a better understanding of the controls on global marine productivity and hence, variations in the atmosphere/ocean-CO_2 system and climate (Broecker, 1982; McElroy, 1983). Unfortunately the basic principles governing nutrient fluxes even through simple estuarine systems are not well-known (Kaul and Froelich, 1984) and it is on this basis that the present study has been undertaken.

This study is based on a system called Loch Linnhe, which belongs to a category of estuaries called fjords, or sea-lochs in Scotland. As with all estuaries, fjords are transitions between the land and open oceans and are therefore regions of strong physical and chemical gradients (Syvitski *et al.*, 1986). Most importantly fjords contain certain topographic features; submarine sills and deep, steep-walled basins, which enable them to encompass a number of distinctive oceanographic environments which make them particularly exciting sites for estuarine research.

The near-surface "estuarine-zone", (Syvitski *et al.*, 1986) basically common to all estuaries is underlain by marine water which in shallow-silled fjords such as Loch Linnhe, may be physically restrained in basin enclosures. Such coastal-zone, mini-ocean basins offer unique opportunities for studying terrestrial input into quasi-closed marine systems and this has great practical application since inputs and outputs can be more easily measured and modelled than in the larger and more remote open ocean systems (Syvitski *et al.*, 1986).

Like many of the sea-loch systems on the west coast of Scotland, Loch Linnhe possesses a shallow sill which impedes free estuarine-type circulation and hence the flushing time of the system is extended. This makes such environments particularly susceptible to pollution problems which, in this area of Scotland, are often connected with the fish-farming industry. There is growing concern over the effects of effluent from the local fish-farming industries on the nutrient composition of the seawater because of the influence of aquaculture on algal growth which has implications for public health, natural populations of fish and the viability of the aquaculture industries themselves (Munday *et al.*, 1992). Gowen and Bradbury (1987) report that the byproducts of culture species metabolism and feed leachates, provide nutrients that may enhance phytoplankton growth given the appropriate hydrographic conditions. Such variations in nutrient levels may lead to species changes in the composition of the phytoplankton (Officer and Ryther, 1980; Takahashi and Fukazawa, 1982) and the consequent formation of harmful algal blooms. Such biological activity may result in the production of toxins which can kill a wide range of aquatic organisms. In 1988 for example, a phytoplankton bloom occurred in Lochs Torridon and Diabeg causing mortalities in farmed salmon in these lochs (Gowen, 1988). Also the toxins produced by some algae may accumulate without danger in host organisms (often bivalve molluscs) but prove detrimental to man when ingested (Munday *et al.*, 1992). These toxins include those that cause diarrhetic and paralytic shellfish poisoning (PSP) in human beings (Munday *et al.*, 1992), which may result in the closure of shellfish farms. In the spring of 1990 for example, a number of sites along the north west coast of Scotland were banned from harvesting and marketing shellfish due to the presence

of the PSP toxin. This was attributed to the presence of a toxigenic dinoflagellate bloom entering the coastal waters (Berry, 1993).

It is obvious then that a knowledge of the circulation and hydrographic processes that occur in sea-lochs and the processes that govern them is desirable since these have a major role in the distribution of nutrients in such systems and hence on the biological activity. Carrying out such studies in a pristine environment such as Loch Linnhe, where there are no fish-farms, will prove useful because results can act as a baseline for predictions on more contaminated areas. Although pristine, it is of interest to note that the spring phytoplankton bloom that occurs in Loch Linnhe and its neighbouring sea-lochs (in which there are fish-farm sites), consists of diatoms and that these have the potential to cause damage to the gills and intestines of cultured fish in the area (Munday *et al.*, 1992). Hence study into the conditions that favour such blooms is important and the ability to predict the timing of the bloom could be of great significance to the fish-farmer who could then re-site cages if necessary.

The primary aim of this study has been to identify and isolate the particular processes that govern the distribution of dissolved inorganic nutrients in Loch Linnhe. It has involved an investigation into the circulation and hydrography of the upper basin of the loch with the emphasis being on their interaction with the biogeochemical processes that cause phase changes of the nutrients. It has also dealt with the individual biogeochemical processes themselves. This study has been achieved through the collection of hydrographic, biological and chemical data throughout the water column and along the salinity gradient of the upper basin over two time-periods in the years 1991 and 1992. Thus the collected data-sets have provided information on spatial and temporal variability and have enabled deductions to be made about the behaviour of the nutrients in the system. A small study on phosphorus in sediment deposited along the salinity gradient has also been carried out to investigate its association with different grainsizes of particulate matter and the elemental composition of the sediments of the basin.

The main approach taken in the study of the behaviour of the nutrients is that basically described by Burton (1976) and Liss (1976) which is to compare the observed nutrient distribution with that predicted for simple mixing of water bodies during which the nutrients are conserved. This is generally supplemented through the use of salinity as a mixing index and the creation of mixing diagrams which relate the nutrient concentrations with salinity. Under steady-state conditions, linear property/salinity distributions are expected when the time-scale of the changing end-member concentrations is greater than the hydrodynamic residence time of the estuary (Cifuentes *et al.*, 1990). However, this study has shown that the more complex circulation present in a sea-loch system leads to complications in interpretations using this simple two end-member mixing, steady-state model conventionally employed for such studies. For example, the extended flushing time of the water resident in the basin allows for significant variations in the end-member concentrations to occur within the flushing time of the system. This subsequently results in the presence of more than two mixing types in the system and gives rise to scatter of data away from a linear nutrient/salinity relationship thus producing apparently non-conservative behaviour. An important emphasis in this study has therefore been to find methods by which such apparent non-conservative behaviour can be distinguished from real non-conservative behaviour and, as far as is possible, to quantify their different contributions to property/salinity relationships.

Account can be taken of the factor of temporal variability in end-members by the application of a suitable model (Cifuentes *et al.*, 1990) and therefore substantial effort has been devoted in this study to such model development. This has involved the adaptation and further development of an extant one-dimensional simple filling box-model (Simpson and Rippeth, 1993) which has allowed the prediction of the hydrographic status of the system given varying meteorological conditions and nutrient distributions in the basin given conservative behaviour. From this a limited quantitative estimate of the real non-conservative behaviour in the basin has been made. Although results from the model are limited the model itself has acted as a good aid for investigations of hypotheses and, as stated

by Sharples and Tett (1992), has served "to educate our intuitions about the system".

CHAPTER 1 of this thesis describes the types of circulation and hydrographic processes that can be expected in a sea-loch system and **CHAPTER 2** considers the biogeochemical processes also operating. Both chapters are based on work reported in the literature and written with the emphasis on how to identify those processes which give rise to deviations away from linearity. In **CHAPTER 3** the literature available on circulation and nutrient status in the survey and surrounding areas is considered more specifically. **CHAPTER 4** provides descriptions of the methods and techniques used throughout the study and **CHAPTERS 5** and **6** deal with the hydrography and nutrient results from the two field-seasons undertaken in 1991 and 1992. **CHAPTER 7** describes the development and results from the numerical modelling approach and uses the field-observations from **CHAPTER 6** and from an archived 1990 data-set to test the applicability of the physical model and to compare results from the nutrient studies to allow for quantitative analyses. In **CHAPTER 8** a general discussion is presented of the conclusions that can be drawn from the study and some ideas for future work are given.

CHAPTER 1 FJORDS: CIRCULATION AND HYDROGRAPHY

A thorough understanding of the types of physical processes that may occur within a fjord is an essential basis for any chemical, biological or geological investigation of such a system. In the case of this study it is required because such processes will affect the transport and biogeochemical reactions, and thus the distributions, of inorganic nutrients within the sea-loch. The physical processes concerned are common to all fjords but the extent to which they operate significantly in any specific system depends upon the individual characteristics of the environment (e.g. detailed topography and its effects on circulation) and on local conditions, such as meteorological conditions and tidal motion. In this account the significance of the major processes is explained both in general terms and with specific reference to Loch Linnhe.

1.1 Definitions

Fjord: The usual scientific definition of a **fjord** is "a deep, high latitude estuary which has been (or is presently being) excavated or modified by land-based ice" (Syvitski *et al.*, 1986). Pearson (1988) defines fjords as "steep-sided, silled, overdeepened **estuarine** basins which, being high latitude features show strong seasonal variations in their biogeochemical properties". A typical **fjord** may be said "to combine a high length to breadth ratio with a glacially overdeepened basin behind a comparatively shallow sill" (Pearson, 1988).

Estuary: The definition of an **estuary** chosen for this thesis is taken from Pritchard (1952): "a semi-enclosed coastal body of water which has a free connection with the open sea and within which seawater is measurably diluted with freshwater derived from land drainage."

Sea-Loch: The common name for a fjord along the west coast of Scotland. There are approximately 50 sea-lochs in this area (Syvitski *et al.*, 1986).

Freshwater Plume: This may be formed when brackish river water floats out to sea over the salt water in a fjord (Officer, 1983).

The freshwater plume flowing within a fjord is commonly divided into two zones: a **near zone** (upper prodelta) and a **far zone** (lower prodelta). In the near-zone, the energy of the river flow controls the mixing and the distribution of the surface plume into its surroundings. In the far-zone, external factors such as tidal currents, wind, shoreline morphology, control transport and mixing (McClimans, 1978).

1.2 Fjord-Type Circulation

Because fjords are over-deepened basins which lie behind a comparatively shallow sill (Pearson, 1988), the type of circulation set up within a fjord is basically split into two components; the upper **surface system** and the less dynamic **basin system** that underlies it. The surface system will possess an estuarine-type circulation with saline water entering at the mouth and freshwater at the head. The underlying basin system exists because dense, saline waters resident in the basin itself, may become isolated and even stagnant for a period of days, weeks or sometimes years, if protected by a shallow enough sill (Edwards and Edelsten, 1977).

A main aim of this chapter is to show that although each of the systems is individual in terms of its circulation features and can therefore be considered separate from the other system, the two systems do interact. This occurs both continuously, by virtue of the fact that one system overlies the other and intermittently, when partial and deep-water renewal processes occur in the deeper basin waters. The following sections will describe in detail the circulation in each system with the main emphasis being on the competition set up between the buoyancy forces from the fresher surface layers and the processes which occur to break down the separation of the surface with the basin system, causing interaction.

1.2.1 The surface system: fjord-estuarine circulation:

1.2.1.1 Stratification and estuarine classification:

Since the surface layers in a fjord possess an estuarine-type circulation, their circulation will depend strongly on the level of stratification that the influx of freshwater can maintain. The level of stratification set up within the surface layers themselves and also between the surface system and the underlying basin system, is a balance between the buoyancy flux set up by the discharge of freshwater and those processes such as tide and wind-mixing which work to homogenize the water masses (Syvitski *et al.*, 1986).

Since climate governs the amount and type of precipitation, runoff and water temperature, stratification in a fjord can vary seasonally. Hence, the type of estuarine circulation within the fjord may change seasonally from (i) **two-layer estuarine** to (ii) **partially-mixed**, to (iii) **well-mixed** (Syvitski *et al*, 1986). These are defined by Dyer (1979) as:

i) **two-layer (salt-wedge) estuarine system**: the freshwater flows outwards over the surface of the seawater which penetrates as a salt-wedge along the bottom of the estuary. This creates a vertical salinity stratification with a sharp halocline (up to 30 PSU in half a metre depth of water). The main type of mixing in this process is by **entrainment**, where **entrainment** is defined as the process of one-way transport of fluid from a less turbulent to a more turbulent regime (Syvitski ***et al.***, 1986). This type of salt-wedge system may operate during the spring (snow-melt discharge), and autumn (rain-storm discharge);

(ii) **partially mixed system**: tidal movements may create turbulence within the water column. This mixes the water column more effectively than entrainment;

(iii) **well-mixed system**: the tidal range is very large and there is sufficient energy available in the turbulence to completely break down the vertical salinity

stratification so that the water column becomes vertically homogeneous.

1.2.1.2 Two-layer circulation: barotropic and baroclinic flow:

Barotropic flow: The discharge of freshwater at the head of a sea-loch will initially create a hydraulic head so that it will effectively flow downhill towards the sea. In this case a longitudinal hydrostatic pressure gradient is set up where the gradient is calculated from the geopotential surface and the free (actual) surface (see **FIGURE 1.1**). This is typically of the order of 1 cm/10 km (Farmer and Freeland, 1983). In such a situation where the horizontal pressure gradient is simply a function of the degree of the slope of the surface, the surfaces of equal pressure within the ocean i.e. the **isobaric surfaces**, are parallel to the sea-surface and to the surfaces of constant density i.e. the **isopycnic surfaces**. Such conditions are described as **barotropic** (Tritton, 1977). Tide, wind and varying meteorological conditions may all give rise to barotropic flow (Gade and Edwards, 1980). **FIGURE 1.2** illustrates that if the seawater density is constant at all depths then the horizontal pressure gradient force (i.e. the barotropic component) is equal at all depths and is equal to $\rho g \tan\theta$: the hydrostatic pressure acting at point A is given by

$$P_A = \rho g z$$

where z is the height of the overlying water column. At point B, where the sea-level is higher by an amount Δz,

$$P_B = \rho g(z+\Delta z).$$

The pressure at B is therefore greater than that at A by a small amount, Δp, so that:

$$\Delta p = P_B - P_A = \rho g(z+\Delta z) - \rho g z = \rho g \Delta z.$$

If A and B are a distance Δx apart, the horizontal pressure gradient between them is given by:

$$\Delta p/\Delta x = \rho g(\Delta z/\Delta x)$$

and since $\Delta z/\Delta x = \tan\theta$

$$\Delta p/\Delta x = \rho g \tan\theta.$$

Assuming Δp and Δx are extremely small ,

$\delta\rho/\delta x = \rho g \tan\theta$ and this is the horizontal pressure gradient force acting in the x direction.

Baroclinic flow: As the freshwater moves seaward under barotropic flow, it is mixed with more seawater due to: (a) entrainment of the saline water by random eddy motion from the shear set up between the surface outflowing layer and the underlying marine waters; (b) downward wind-mixing and (c) tidal motion. As the saline water is entrained into the outward-flowing surface layer, new seawater must enter the sea-loch at depth to provide the landward flux of salt required to maintain the salt-balance as determined by the conservation of mass (Officer, 1983). This return or "compensation" current is driven by a reverse internal pressure gradient arising from the generally sloping density field (Gade , 1976). Such internal pressure gradients which set up lateral variations in density will give rise to **baroclinic** (or **gravitational**) conditions and **baroclinic flow** from high to low pressure.

Steady-State Conditions: If the barotropic forcing is equal to the baroclinic forcing, then the system is said to be in **steady-state** (Gade, 1976). In nature this condition is very rarely met but it is possible that this type of system might be observed in a fjord basin where the only effective process in altering the density of the basin water is eddy-diffusion, i.e. in stagnant basin conditions. This results in a continuous lowering of density at all depths until the water column is completely uniform, determined by the upper boundary condition i.e. the fresh/brackish

FIGURE 1.1

Schematic with Extreme Vertical Exaggeration of Two-Layer Estuarine Circulation in a Fjord. Saltwater Entrained by the River Outflow is Replenished by a Net Inflow at Depth. (Taken from Thompson, 1981).

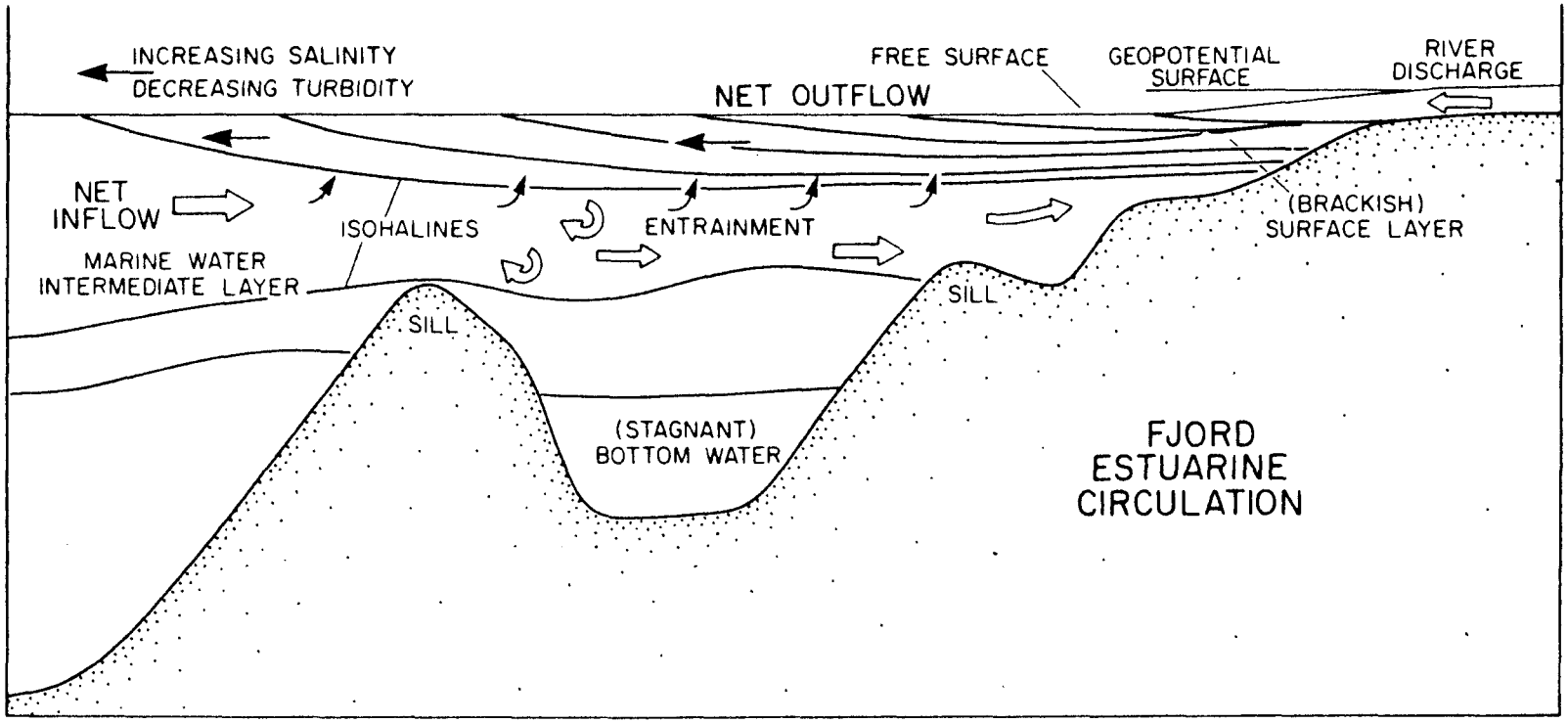

FIGURE 1.2

Schematic Diagram to Illustrate how a Sloping Sea-Surface Results in a Horizontal Pressure Gradient.

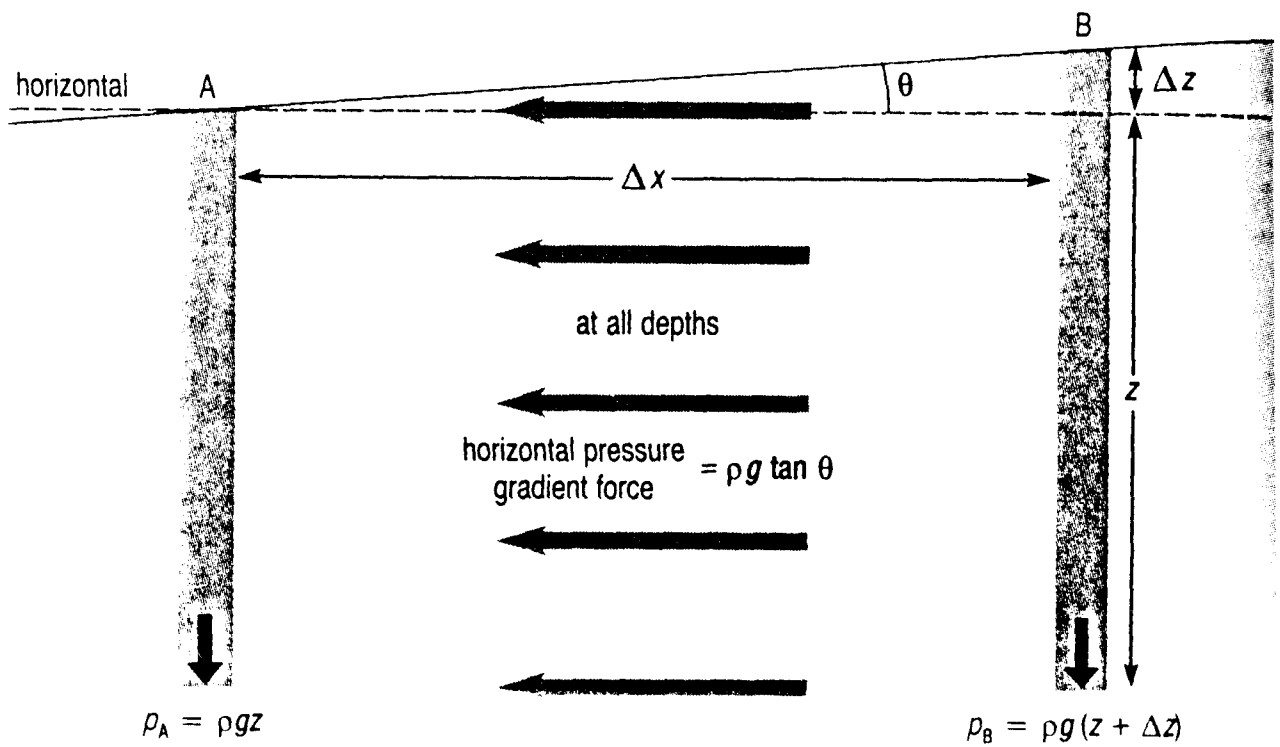

surface layer (Gade and Edwards, 1980). Provided the density stratification of the coastal water adjacent to such a fjord remains perfectly steady, seawater will be advected over the sill, developing into a density current as it sinks and sinking to the greatest depths in the basin at all times (provided that the water entering the basin is of a density greater or equal to the density of the resident water at the greatest depths). This will result in continuous renewal of the resident water in the fjord basin resulting in an aerated system (Gade and Edwards, 1980).

Barotropic vs baroclinic flow: Because the strength of the barotropic and baroclinic components in a system are governed by different factors, it is quite often the case that the two are not equal and that the steady-state situation described above does not exist. In highly stratified systems, for example, the baroclinic circulation may dominate or, at the opposite extreme, it may be resolvable only as a long-term mean flow, largely hidden by strong wind- or tidally-driven currents in unstratified or vertically mixed conditions. Nevertheless the baroclinic component is always present (Vaz *et al.*, 1989). The strength of the baroclinic component will depend not only on the magnitude of the horizontal density gradient, but also on the intensity of ambient turbulence; the more turbulent the conditions, the more momentum is imparted to vertical diffusion and less to horizontal baroclinic circulation (Vaz *et al.*, 1989). In highly turbulent conditions e.g. in areas with large tidal ranges, the baroclinic circulation may be slower than it would be in tranquil conditions, by one or two orders of magnitude (Vaz *et al.*, 1989). Laboratory experiments carried out by Linden and Simpson (1986; 1988), showed that in the undisturbed state the horizontal mass flux of salt was 10 times larger than in the turbulent, vertically-mixed state; "....the gravity current (baroclinic flow) is much more effective at transporting salt horizontally and the addition of turbulence decreases that flux" (Linden and Simpson, 1986). Therefore the more stratified a system is i.e. the higher the buoyancy input and the less turbulence (e.g. tide or wind generated) is present, the greater the strength of the horizontal, baroclinic flow.

"Tidal-throttling" in Loch Linnhe: In Loch Linnhe the size of the baroclinic flow

is hydraulically controlled due to the presence of the shallow sill at the Corran Narrows (~18m, see **CHAPTER 3**, section **3.3.2**). As is illustrated in **FIGURE 1.2** the barotropic component of the system will be the same at all depths ($\delta\rho/\delta x=\rho g\tan\theta$) if the seawater density is constant. The baroclinic component however increases with depth because of the difference set up by the lateral density difference of water at different depths. Since an increase in the baroclinic component is associated with an increase with depth, it is possible that the barotropic flow can reverse the baroclinic flow and particularly so if shallow sills are considered. Hence in Loch Linnhe a phenomenon known as "tidal throttling" is observed at the sill at Corran Narrows (Mr. A. Edwards, 1992, pers.comm., DML), where inflow is prevented on an ebb tide i.e. the barotropic reverses the baroclinic flow, and is augmented on a flood tide . This results in increased turbulence and mixing either side of the sill. The two-layer type estuarine circulation described in **section 1.2.1.2** is therefore not observed in the upper basin of Loch Linnhe, except possibly during slack water and exchange of water in the basin occurs instead by ebb pulses of low salinity water and flood pulses of high salinity water (Mr. A. Edwards, 1992, pers.comms., DML) .

1.2.2 The deeper basin system: vertical mixing processes

In order for water resident in a fjord basin to be displaced by the seawater entering across the sill, the inflowing water must have a density greater than the density of the water in the basin. This is the **density condition** which is referred to later in the text. There are several ways in which the density condition may be satisfied; in the short term by tide, wind or freshwater input and in the long term via seasonal changes, but there is only one way in which the density of the deeper basin water may alter during periods of isolation and that is through diffusive processes (Stigebrandt and Aure, 1989). These are thought to be continuous and caused by turbulence and result in a decrease of the basin water density (Stigebrandt and Aure, 1989).

The energy made available for mixing comes mainly from 2 sources, tides and

meteorological disturbances (Gade and Edwards, 1980):

1.2.2.1 Vertical diffusive mixing via tidal motion

The tides are the most effective energy source with the tidal energy being converted to turbulence via (a) boundary mixing, (b) tidal jets and (c) breaking of internal waves:

(a) Boundary Mixing: This occurs due to the tide which gives rise to a barotropic wave which creates tidal seiches in the fjord basin. At the fjord boundaries i.e. at the sides and the bottom, drag and friction processes are set up which result in vertical mixing and the formation of a water mass with a density higher than that of an adjacent water mass at the same depth, at the boundary. This results in baroclinic flow away from the wall with resultant lateral density currents and the vertical mixing of salt (Gade and Edwards, 1980). Much of this type of vertical mixing actually occurs in a bottom boundary layer (Stigebrandt and Aure, 1989). The thickness of the affected boundary layer is a strong function of the amplitude of the tidal current velocity and therefore will vary greatly within a fjord basin (Gade and Edwards, 1980).

Simpson and Bowers (1981) estimate that the efficiency of boundary mixing in working against the buoyancy forces in a sill basin is only ~ 0.4% of the total tidal energy available.

(b) Tidal plumes of excess density may contribute to the generation of turbulence and hence vertical mixing in the basin waters (Gade and Edwards, 1980). These arise when the tidal current through the fjord mouth is too fast for internal wave generation (Stigebrandt and Aure, 1989). This may occur in fjords with constrictions, such as narrow sounds or shallow sills, where the tidal currents become strong enough to separate from the walls and form jets and plumes penetrating the water masses of the fjord (Gade and Edwards, 1980).

Stigebrandt and Aure (1989) conclude that the mixing efficiency of tidal jets against the buoyancy forces is only ~1% of the total tidal energy lost to the basin.

(c) Tides generate internal waves in the vicinity of sills and other topographic features interacting with the tidal flow in stratified water (Gade and Edwards, 1980). In fjords internal waves of tidal period are often outstanding features, with the phenomenon being particularly well-developed where the sill reaches up to the pycnocline (Gade and Edwards, 1980). Stigebrandt (1976) proposed that the breaking of internal waves against the walls of a basin, created boundary turbulence which mixes with water of different density in the lower layer. He suggested that internal waves may be reflected off a fjord basin wall if the end wall is vertical or nearly vertical whilst complete absorption i.e. conversion to turbulence may occur when the end wall makes an appreciable angle with the vertical. From his study on Oslofjord, Gade (1970) considered the internal waves to be critical for the transfer of energy to turbulence and consequent vertical diffusive exchange. Similarly, a study made on the deep-water in the Arctic, Cambridge Bay (Gade *et al.*, 1974) pointed strongly towards internal waves as the main source of energy for generation of turbulence.

Stigebrandt and Aure (1989) considered a large number of sill basins off the Norwegian coast and used their measurements to establish a relationship between the observed mean rate of work against the buoyancy forces and the estimated energy input to the basin waters by internal waves and/or jets. They found that internal waves in basins could contribute up to 6% of the total available tidal energy to work against the buoyancy forces and thus cause vertical mixing.

1.2.2.2 Vertical mixing via convection

Another form of energy contributing to the fjord basin for mixing is that liberated by **convection** when water heavier than the resident water in the basin enters over the sill. Potential energy is released by the density current that forms and this is almost completely converted to turbulence within the basin (Gade and Edwards,

1980). The efficiency with which this liberated energy can be used for mixing is reported to be up to 10% i.e. 90% of the potential energy is converted to heat (Gade and Edwards, 1980). This may contribute to the turbulent diffusive processes occurring in the deeper basin-waters.

1.2.2.3 Measurement of vertical diffusion: the diffusion coefficient, k

Sill basins offer a unique opportunity to study vertical diffusion since only diffusive processes can change the density of the basin water during periods of stagnation (Stigebrandt and Aure, 1989). Stigebrandt and Aure (1989) describe how a horizontally integrated diffusion equation may be used to determine the turbulent vertical diffusivity i.e. the vertical diffusion coefficient, k. Such a horizontally integrated diffusion equation may be used only if "precision vertical profiles of density (salinity and temperature) have been obtained at two or more occasions during a stagnation period" (Stigebrandt and Aure, 1989).

Gade (1970), using data from Oslofjord found that vertical diffusivity in a fjord will depend on the vertical stability of the basin waters. He expressed the relationship of the diffusivity, k, with the buoyancy frequency (the Brunt-Väsiälä frequency) N in the following way:

$$k=\alpha(N^2)^{\beta} \qquad (1)$$

where α is a constant and β is a non-dimensional empirically determined constant and tends to lie in the range of $-0.8 < \beta < -0.4$ (Stigebrandt and Aure, 1989). The value of N^2 represents a measure of the density gradient;

$$N^2=g[(-1/\rho)(\delta\rho/\delta z)] \qquad \text{(Svensson, 1980)} \qquad (2)$$

where g is the gravitational constant, ρ is the density of the water and z is depth.

The diffusivity k is therefore not a constant but instead is a decreasing function of

the buoyancy frequency (Gargett, 1984) i.e. the larger the density gradient and therefore the larger the value of N^2, the lower the value of k. This would be because the more buoyancy input the more potential energy is required to mix down between the layers of stratification thus restricting the degree of vertical mixing within the system.

Measurement of k: The method used widely to determine diffusivity is known as the **budget method** (Gade, 1970; Gargett, 1984; Stigebrandt and Aure, 1989). It assumes that in periods of stagnation the density of the basin water may only change as a result of diffusive, vertical exchange. In order for this to be so, we treat the system as a stratified fluid in a closed system (Gargett, 1984). This is so as there is no flow and no exchange of heat and salt with the bottom sediments and no heat exchange from above into the basin water (Stigebrandt and Aure, 1989). The budget method deals in the horizontal plane with horizontal averages so as to avoid or minimize complications such as the volumetric effect of non-vertical basin walls (Stigebrandt and Aure, 1989). In periods of stagnation, the horizontally averaged conservation equation for the density, ρ of the basin water is a function of depth (z) and time (t):

$$\delta\rho/\delta t = 1/A(\delta/\delta z)[Ak(\delta\rho/\delta z)]$$

(Stigebrandt and Aure, 1989) **(3)**

where k=k(z)=horizontally averaged diffusivity and A=A(z)=the horizontal surface area of the basin.

By integrating this equation from maximum depth; z=b, to some level; z=u, one can obtain an expression for the vertical diffusivity at the upper integration level:

$$k_{z=u} = 1/(A\delta\rho/\delta z)_{z=u} \int_b^u (\delta\rho/\delta t)A \, dz$$

(Stigebrandt and Aure,1989) **(4)**

This equation may therefore be used for computation of k at different levels, u,

over time. $\delta\rho/\delta t$ and $\delta\rho/\delta z$ are estimated from repeated measurements of salinity and temperature at different depths of the basin (Stigebrandt and Aure, 1989). Gargett (1984) comments that in order to get representative estimates of k, the technique of Stigebrandt and Aure (1989) must be applied for periods in excess of a month.

Reported k values in the literature vary considerably for different geographical areas: Officer (1983) reports k values ranging from 0.1 $cm^2\ s^{-1}$ for the Vellar Estuary in India to 25 $cm^2\ s^{-1}$ in the Mersey Estuary, U.K. Hogg *et al.* (1982) report k values of 3-4 $cm^2\ s^{-1}$ for the Antarctic Bottom Water in the Brazil Basin, S. Atlantic, derived using the budget method. Edwards (1993, pers.comm.) reports a value of k of 0.5 $cm^2\ s^{-1}$ for Loch Linnhe during February to March 1990 increasing to 5 $cm^2\ s^{-1}$ in April 1990.

Later in this study, the budget method is used to obtain an average value for k in Loch Linnhe over the period of stagnation in 1990 (see **CHAPTER 7**, section **7.2.1.8 (i)**). Using this, a specific rate of work, w can be calculated:

Measurement of specific rate of work, w:

Once a value for k has been obtained and N^2 has been calculated from equation **(2)**, the mean rate of work performed by the turbulence against the buoyancy forces may be estimated.

Stigebrandt (1976, 1979) made the first successful attempt to relate the rate of vertical diffusion in fjords to a specific energy source for turbulence, which he took as internal waves. He defined the mean specific rate of work, w as:

$$w=1/V \int \rho k N^2 A\ \delta z \qquad \textbf{(5)}$$

where;

$$V = \int A\ \delta z \qquad \text{(Stigebrandt and Aure, 1989)} \qquad (6)$$

Equation **(5)** can therefore be used to give a total mixing rate to the level of inflow in a system and, thus a measure of turbulence.

Values of w reported in the literature vary, with Stigebrandt and Aure (1989) reporting values in the range of 0.054-1.67 mWm^{-2} for a suite of different Norwegian fjords and Simpson and Rippeth (1993) use a value of $0.162*10^{-3}$ Wm^{-2} for w in their model on the Clyde Sea area (Dr. T. Rippeth, pers.comms., 1993). Values of w may, however, be greater than these values depending on the value of k (see **CHAPTER 7**, section **7.2.1.8 (i)**).

1.2.3 Deep and partial renewal events

The surface and deeper basin systems in a fjord may mix via partial and deep-water renewal events:

Seawater entering a fjord basin via tidal advection (barotropic flow) and/or baroclinic flow will, if it is denser than the resident water in the basin, form a density current at the sill and sink to a level at which its density is equal to the surrounding water, displacing the resident water at that level upwards (Gade and Edwards, 1980). If this intrusion of saline water occupies the entire basin volume below the sill-depth, the renewal is said to be **complete** or **deep**. Otherwise it is described as a **partial** renewal event (Gade and Edwards, 1980).

Whether a renewal event is partial or complete will depend on (a) the density of the sill-water entering the basin relative to the resident water density and, (b) the volume of the water entering.

1.2.3.1 **Partial renewal events:** There are two main ways in which a renewal can be limited to being partial: (i) if the intruding shelf water is not sufficiently dense to replace the deepest water in the fjord, then it will sink to a level at which

its density is equal to the surrounding water and spread out from there, pushing the resident basin water out from that level upwards and, (ii) a thin plume of water from outside the basin may reach its appropriate level after having spent most of its potential energy entraining ambient water and overcoming bottom-friction; it therefore comes to rest without stirring up much of the resident basin water (Gade and Edwards, 1980).

There is also the case to consider where the water entering the basin has a density great enough that it can sink to the bottom of the basin, but there is an inadequate supply of the water to replace the volume of the resident water present i.e. the duration of the event is not sufficient to allow the whole basin to be filled. Deep-water renewal processes do not generally result in an exchange of the whole volume of the basin water; replacement of 20-80% is more common (Molvaer, 1980).

1.2.3.2 **Frequency of renewal events:** In section **1.2.1.2** it was discussed how continual deep-water renewal might occur in the steady-state case. However, such steady-state conditions are rarely met in nature due to fluctuations of the density field in the adjacent water which interfere with the inflow of sea-water (Gade and Edwards, 1980). Instead, deep-water renewal events tend to occur on an intermittent time-scale which ranges from daily tidal time-scales (**high frequency forcing**) to several weeks or even years (**low-frequency forcing**).

High-frequency forcing: This is a result of short-term processes such as (a) tidal motion, (b) the effect of winds, (c) variations in the freshwater runoff and (d) sill depth:

(a) Tidal Motion: For a renewal event to occur there has to be an inflow of relatively high density water into the fjord basin. Daily tides are important because they allow relatively high salinity water to enter the loch on a flood tide. As has been discussed in **section 1.2.1.2** the barotropic component in Loch Linnhe actually reverses the baroclinic component due to the presence of a shallow sill

hence the baroclinic inflow on the ebb tide is reversed but augmented on the flood tide. Therefore, for a renewal event to occur in Loch Linnhe, a flood tide (or possibly slack water) is required. Also the barotropic augmentation occurring due to the presence of the shallow sill, means that the Loch Linnhe system can carry more renewing water into the basin on a flood tide than a purely baroclinic driven system, and effectively increase the carrying capacity of the sill (Stigebrandt, 1977). As was discussed in section **1.2.1.2** inflow of water into the fjord basin will increase the ambient turbulence in the basin thus augmenting vertical diffusion within that basin water, with a resultant lowering of the water density.

When considering tidal motion the spring-neap cycle is also important in terms of renewals mainly because the volume of the water entering the basin will increase as the tidal cycle goes from neaps to springs. Spring tides enhance renewals by increasing the supply of the sill water to the basin and thus the energy for mixing, breaking down the stratification within the fjord and enhancing circulation (Stigebrandt, 1977). A study made by Edwards *et al.* (1980), on Loch Eil, a sea-loch adjoining Loch Linnhe at the northern end, showed that renewal events were controlled by the spring-neap cycle and so bottom-water stagnation was only present on a time-scale in the order of weeks. Stagnation occurred during the neap tides but deep-water renewals occurred regularly on the spring tides.

(b) Wind: A change in the wind strength and/or direction may cause high frequency intermittence. This is due to subsequent changes in the fjord water level which cause barotropic currents and a subsequent increase in baroclinic inflow of water over the sill (Gade and Edwards, 1980). This baroclinic inflow involves the uplift of high density, high salinity water seaward of the sill (referred to as **upwelling**) and is a result of the system settling back into an equilibrium state after a change in the meteorological conditions. This is illustrated for a sea-loch such as Loch Linnhe in **FIGURES 1.3 (a)** and **1.3 (b)**:

FIGURE 1.3 (a) shows the effect of a persistent south-westerly wind blowing up

FIGURE 1.3

The Theoretical Effect on Hydrography of (a) a Persistent South-Westerly Wind Blowing up a Sea-Loch System such as Loch Linnhe, Followed by (b) a Change in Wind Direction to North-Easterly.

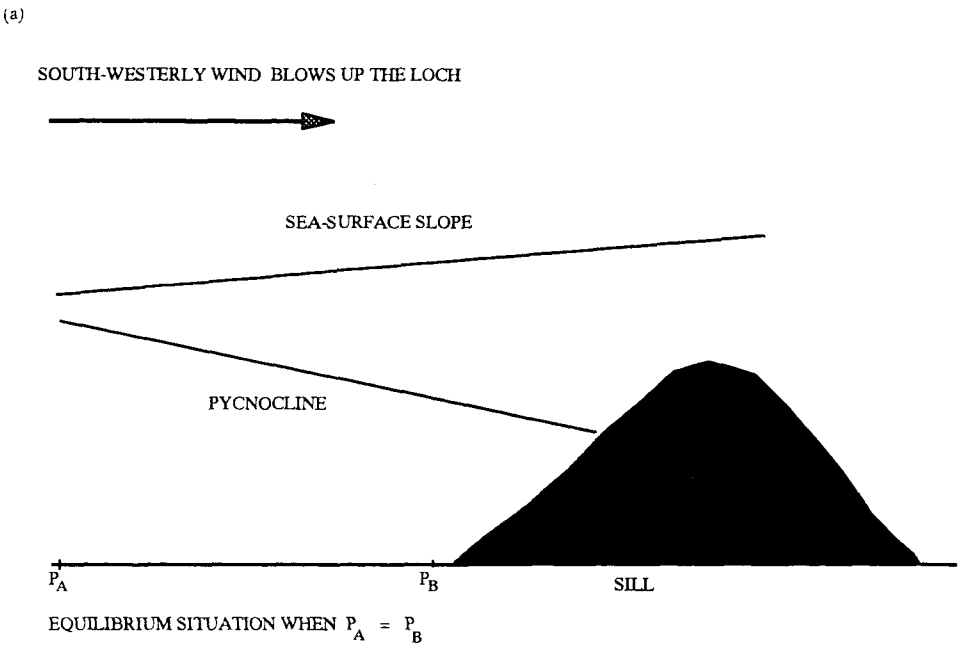

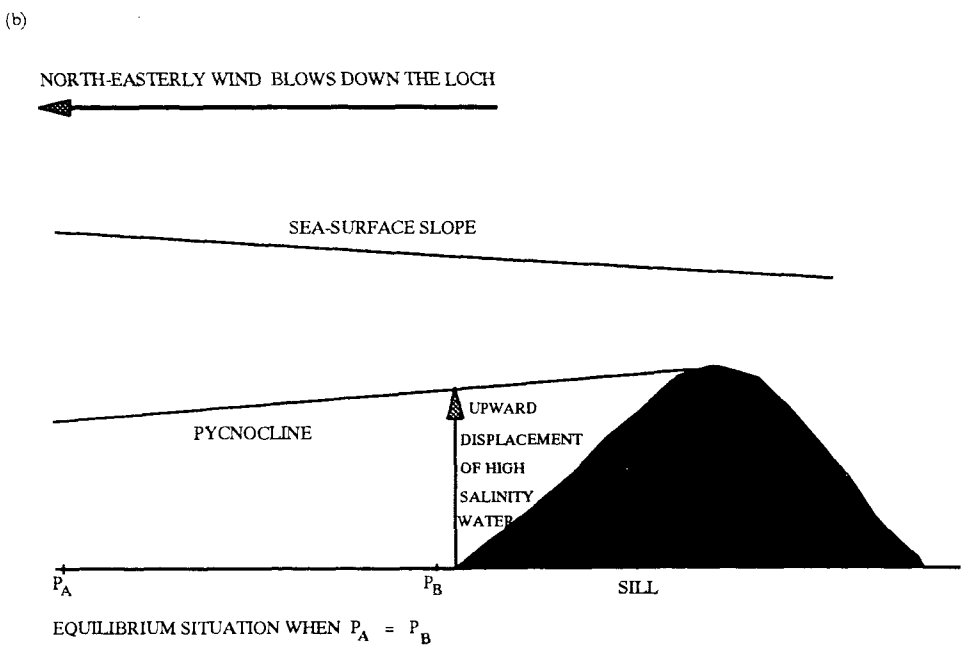

the loch along its longitudinal axis. It illustrates the situation seaward of the sill having achieved an equilibrium. The fresher surface layers, which are normally outward flowing in such a system are effectively retained to some extent by the wind, with the result that the sea-surface slope has increased up towards the head of the loch. In order to maintain an equilibrium situation so that the pressure at P_A is equal to that at P_B, the pycnocline (interface) adjusts itself so that the increase in the height of the water column experienced at P_B is balanced by an increase in the density of the water in the water column above P_A. **FIGURE 1.3 (b)** illustrates the equilibrium situation seaward of the sill after a change in the wind direction to north-easterly. As can be seen the gradient of the sea-surface slope is reversed and in order to maintain an equilibrium situation, the slope of the pycnocline has also reversed such that the increase in height encountered at P_A is compensated by an increase in the density of the water overlying P_B. From these two figures it can be seen that if a southwesterly wind stops blowing and/or a north-easterly wind starts up, in order to maintain an equilibrium state, the inclination of the pycnocline must alter such that denser water is available above P_B. This is achieved through **upwelling** i.e. the import and upward displacement of high salinity water to the region.

Upwelling events may be important to this study because they are a way of introducing high salinity water which may be nutrient-rich, to a fjord basin since they tend to occur seaward of a fjord entrance thus effecting the water just outside the sill (Gade and Edwards, 1980). This import of nutrient-rich water may be possible due to biogeochemical processes, such as the input of regenerated of nutrients from the sediments and the sediment porewaters (see section **CHAPTER 2**, section **2.3.2**), which might be occurring in deeper regions seaward of the sill area.

(c) Freshwater Runoff: Variations in freshwater runoff will effect the intermittency of renewals by (i) reducing the density of the water inside the basin via turbulent mixing and diffusive processes (see section **1.2.2**), thus increasing the likelihood of a renewal, or (ii) decreasing the density of the incoming sill water through mixing

as it passes over the sill. Even with an adequate supply of incoming water over the sill, a renewal event cannot take place if the density condition is not satisfied i.e. the condition that the inflowing water must have a density greater than the density of the resident water in the basin. This condition may fail if the incoming water although sufficiently dense is modified by mixing with lighter, fresher water during its passage over the sill (Gade and Edwards, 1980). If the freshwater runoff is so great that the surface layer approaches sill depth, no inflow will occur at all (Welander, 1974).

(d) Sill depth: This has a major part to play in deep-water renewal processes. Renewal of deep water is not only conditioned by the sill water being of a high density relative to the basin water, but also by the availability of an adequate supply of sill water to the basin. As already described in section **1.2.1.2**, the shallower the sill the greater its carrying capacity and the greater the likelihood of a renewal event on a spring flood tide for example. However the sill-depth has an important role to play in the degree of vertical mixing within the deeper basin waters because sills are regions of increased current, large shears and tidal jets and mixing is greater there than in the main fjord (Gade and Edwards, 1980) see section **1.2.2.1**.

Low-frequency forcing: This is caused by factors such as variations in the density structure of the adjacent coastal waters. Examples include Norwegian fjords where the major wind-field is monsoonal in nature, being predominantly northerly in the summer and southerly in the winter. This results in coastal divergence or convergence, giving rise to salinity maxima which can renew fjord water down to, at least 100 m (Gade and Edwards, 1980). Similarly, Cannon and Ebbesmeyer (1978) report that Puget Sound tends to respond to seasonal forcing of the oceanographic climate. In late summer the bottom-water is replaced due to coastal upwelling caused by northerly winds.

1.3 Summary and discussion

Circulation in a fjord can be considered as comprising two different systems which overlie each other; a surface system and a deeper basin system. This chapter has considered each system separately in terms of the processes that determine their hydrography and circulation and how these processes operate.

The surface system has been described in terms of two-layer estuarine circulation involving barotropic and baroclinic flow. It was described how the strength of each of these components is governed by different factors. For the barotropic flow tide, wind and varying meteorological conditions are important whereas for baroclinic flow the degree of stratification and therefore the buoyancy input is important; the higher the degree of stratification the greater the strength of the baroclinic component. In Loch Linnhe the barotropic component is greater than the baroclinic component due to the presence of the shallow sill. Thus the baroclinic flow is reversed during an ebb tide and augmented on a flood tide; a process referred to as tidal throttling. This results in turbulent mixing in the sill region.

For the deeper basin system, processes by which the density of isolated bottom-waters can change have been described. These processes involve the diffusion of salt via turbulent vertical mixing processes which are governed by (a) tidal motion giving rise to boundary mixing, the formation of tidal jets and the breaking of internal waves in the basin and (b) the convection of dense water entering the basin, sinking and releasing potential energy thus creating turbulence. Methods by which the extent of this vertical diffusion can be measured in bottom-waters have been discussed. They involve the calculation of a diffusion coefficient, k, which is a decreasing function of the buoyancy frequency. The measurement of k by the budget method has been described and reported values of k range from 0.1 to 25 $cm^2 s^{-1}$. It has then been shown that k is related mathematically to a total mixing rate and thus provides a measurement of the turbulence in the bottom-waters. Such vertical mixing results in decreasing the density of the bottom-waters

thus increasing the potential for deep-water renewal events. The tide, wind freshwater runoff and sill-depth all have important roles to play in determining the frequency of renewal events. The tide is important because it determines the frequency of deep and partial renewal events in terms of providing an inflow of saline water to the basin on a daily flood tide (or possibly slack tide) and an increased volume of saline inflow on a spring tide during the spring-neap tidal cycle. The wind is important because a change in its direction can cause upwelling events and the subsequent inflow of increased salinity water to the system. Freshwater runoff and sill-depth are important factors since increased freshwater runoff and increased vertical mixing will lower the density of the water inside the basin but also decrease the density of the inflowing water via mixing at the sill which will be increased with a shallower sill-depth.

An understanding of the circulatory features and the processes that govern them is crucial in terms of the interpretation of dissolved inorganic nutrient distributions in the system. When considering the roles of different processes in these distributions, it is important to be able to distinguish between changes in the nutrient concentrations caused by hydrographic processes e.g. the physical advection of water containing different concentrations of nutrients and those processes that actually affect the concentrations by causing a phase change i.e. biogeochemical reactivity. It is useful to be able to identify the presence of isolated bottom-waters from the hydrographic data for example, because then any changes observed in the nutrient concentrations in these waters over the isolation period (apart from those caused by diffusion), can be attributed to biogeochemical reactivity between the sediments and the overlying bottom-waters. To know which physical and meteorological processes affect the frequency of the renewal of such deep-waters is important in terms of the nutrient distributions because any accumulated nutrients in the isolated bottom-waters previous to the renewal will be displaced upwards as a result of the renewal. Also if these renewals occur only on a low frequency basis then there is a possibility that the bottom-waters may become depleted of oxygen due to the microbial oxidation processes occurring in the sediments. In extreme cases of deep-water isolation the basin water may

become anoxic, allowing the reduction of nitrate and sulphate and the creation of poisonous hydrogen sulphide (Richards, 1965). If this anoxic bottom water is vertically displaced to the surface due to a renewal event then there is the possibility of massive fish kills as have been observed in the Norwegian fjord of Hellefjord (Brogersma-Sanders, 1957).

Having considered the importance of physical processes in the determination of the nutrient distributions the following chapter will consider the biogeochemical processes that affect the nutrient concentrations and hence their distribution.

CHAPTER 2 FJORDS: THE BIOGEOCHEMICAL CYCLING OF NUTRIENTS

The distribution of nutrients in fjords is a function of the physical, biological and chemical processes which occur both in the water column and the sediments. The nutrients concerned in this study are the major dissolved inorganic micronutrients, namely phosphate, nitrate and silicate (dissolved silicon). This chapter considers the role played by biological and chemical activity in the recycling of these nutrients between the solid and dissolved phase in both the water column and the sediments. It initially considers the theory of estuarine mixing and then moves on to describe the primary inputs of nutrients to sea-loch systems, followed by a description of processes that lead to non-conservative and apparent non-conservative behaviour.

Notation and terms used in the text:

Phosphate: The notation, PO_4 used in the text represents the orthophosphate ion (PO_4^{3-}). The orthophosphate ion is largely protonated at the usual pH of seawater with about 10 % present as PO_4^{3-} ions and practically all remaining phosphate as HPO_4^{2-} ions (Grasshoff, 1983). Both these species react identically in the spectrophotometric determination of reactive phosphate and hence it is convenient to indicate the total concentration as PO_4.

Nitrate: The notation NO_3, is used to denote the charged inorganic species NO_3^-.

Silicate: The notation SiO_4, is used in the text to denote dissolved silicon. In river waters silicon is present in the particulate forms, mainly as detrital quartz and clay minerals, and as dissolved silicon. For waters of pH < 9, dissolved silicon (Si) will be present almost exclusively as silicic acid; $Si(OH)_4$ (Zwolsman, 1986) and this is the principal form of dissolved silicon in this study.

Biogeochemical: Geochemical processes are those that determine the distribution

of chemical species in natural systems, between the various components present - (solid phases, aqueous solutions) - the term biogeochemical is often used to indicate those processes in which biota have a particularly evident role (e.g cycling of major biogeochemical elements such as C, N, P, S). In aquatic and sedimentary systems however, almost all processes are biogeochemical in the sense that they are influenced by organisms, especially microorganisms.

2.1 Estuarine Mixing: Conservative and Non-Conservative Processes

In the absence of any biogeochemical processes that might lead to the addition (**source**) or removal (**sink**) of a nutrient, the physical mixing of the end-member waters i.e. the saline water and the freshwater, would result in a linear relationship between the concentrations of the nutrient and the proportions in which the two end-members which have undergone mixing. Usually salinity is used as an index of the extent of mixing (Liss, 1976; Burton, 1988; Chester, 1990). This physical mixing relationship thus offers a useful baseline for assessing the effect that biogeochemical reactivity has on the concentration and distribution of components such as dissolved inorganic nutrients in an estuarine system. Such a theoretical relationship is the basis of the utilization of **mixing diagrams**. **FIGURE 2.1** illustrates the theoretical relationships involved: If the concentration of a nutrient is controlled only by the degree of physical mixing in the system, then a plot of its concentration against a conservative mixing index, such as salinity, will result in a straight line, known as the **theoretical dilution line** (TDL), which joins the concentrations of the two end-members of the mixing series (Liss, 1976). If, by plotting the concentrations of a nutrient against the corresponding salinities such a straight line results, the nutrient is said to be **conservative** in its behaviour. Conversely, if the nutrient is involved in a biogeochemical reaction which results in a phase change either from (a) the dissolved to the solid state i.e. a **removal** from the system or **sink** or (b) to the dissolved state i.e. an **addition** to the system or **source**, then a plot of the concentrations against the salinities will result in deviations away from the TDL and the nutrient is said to be **non-conservative** in

FIGURE 2.1

Idealized Representation of the Relationship between Concentration of a Dissolved Component and a Conservative Index of Mixing, for an Estuary in which there are Single Sources of River and Seawater for a component (A) whose Concentration is Greater in Seawater than in River Water.

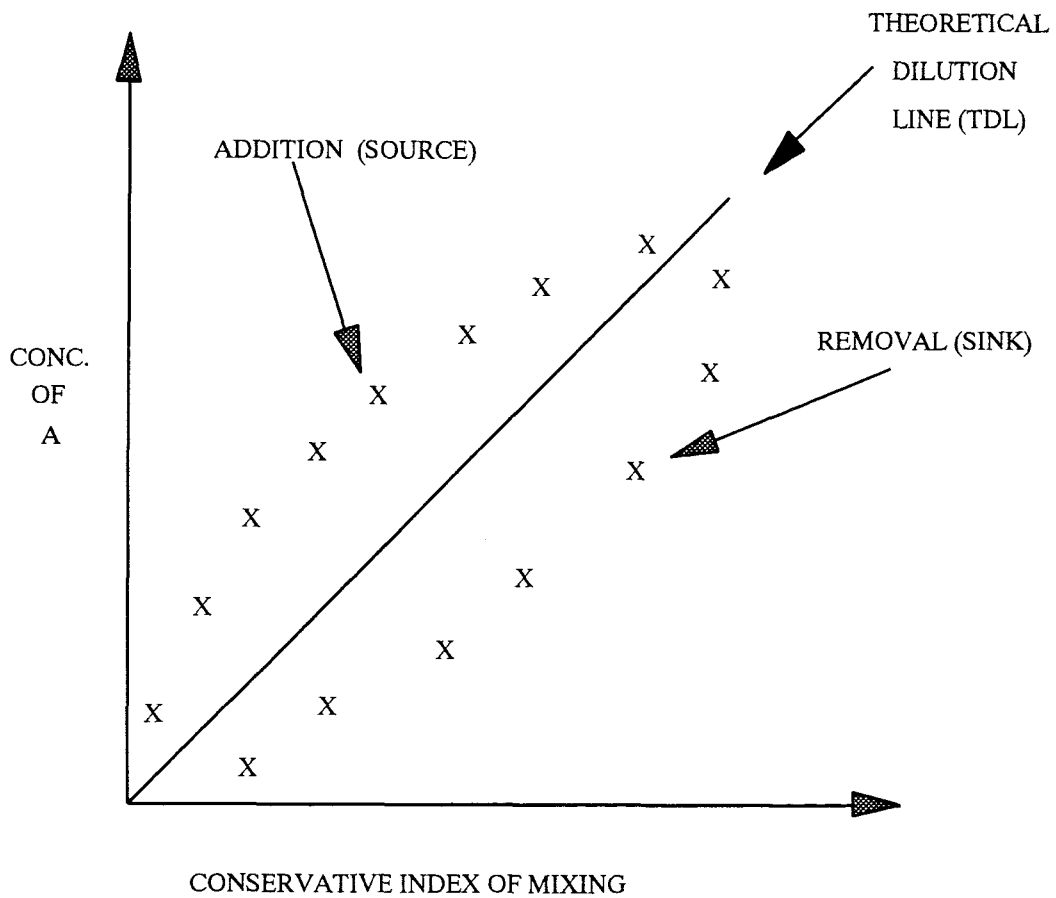

its behaviour (Liss, 1976; SCOR, 1988; Chester, 1990).

Examples of real non-conservative processes are (a) those resulting in a solution to solid state phase change: biological uptake of nutrients by phytoplankton; adsorption of nutrients onto SPM surfaces; association of the nutrient (principally PO_4) with colloidal material followed by flocculation/coagulation of the material to the solid phase; incorporation of the nutrient into the SPM structure itself via two-step solid phase sorption and (b) those resulting in a solid to solution phase change: release of regenerated nutrients from sediment porewaters; desorption from suspended particulate matter (SPM). Non-conservative behaviour of nutrients is discussed further in section **2.3**.

However, complications may arise in the interpretation of steady-state curvature since deviations from the TDL may also result when **apparent** non-conservative behaviour is occurring. This may be when (i) there are point inputs of nutrients within the estuarine zone either from pollution sources or complex river end-members (Butler and Tibbitts 1972), (ii) there are temporally varying end-member concentrations (Loder and Reichard, 1981; Officer and Lynch, 1981; Kaul and Froelich, 1984; Froelich, 1988; Cifuentes *et al.*, 1990) and (iii) nutrient-rich seawater is upwelled into the estuarine mixing zone (Stefansson and Richards, 1963) - see section **2.4**.

Hence the ability to differentiate between conservative, non-conservative and apparent non-conservative behaviour and, where possible quantify it, is crucial to the understanding of the control of nutrient distributions in a sea-loch system. It is important that any apparent non-conservative behaviour is identified and effectively eliminated if correct interpretations are to be made.

2.2 Nutrients in Sea-Lochs: Primary Inputs

The term **primary inputs** refers to the original sources of the nutrients to a system i.e. to riverine and, to a lesser extent, atmospheric input. This is because much of

the material mobilized during both natural crustal weathering and anthropogenic activities is dispersed by rivers, which transport the material towards the land/sea margins (Chester, 1990). River transported materials travel from their source across the estuarine (sea-loch) interface, through the coastal receiving zone and into the open ocean (Chester, 1990). The discharge of river water to the oceans is basically a function of net precipitation (precipitation minus evaporation) and basin area and is presently estimated at $35\text{-}40*10^3$ km^3 freshwater annually (Milliman, 1993).

Water which reaches the river environment originates from (i) the atmosphere (precipitation) which gives rise to surface runoff and groundwater circulation and/or (ii) the discharge of wastewater (i.e. anthropogenic input). The nutrients present in the river water are derived from the physical and chemical weathering of rocks, the decomposition of organic material, wet and dry atmospheric deposition and for some rivers, pollution (Chester, 1990).

Hence, river waters may exhibit wide variations in the concentration of and composition of dissolved nutrients due to temporal variations arising from differences in the proportions of groundwater flow and surface runoff (Livingstone, 1963; Meybeck, 1982; Meybeck, 1983; Walling and Webb, 1983; Kaul and Froelich, 1984; Meybeck, 1988).

2.2.1 Primary inputs of nitrate

Dissolved inorganic NO_3, which originates mainly from soil leaching, terrestrial run-off (including that from fertilized soils) and waste inputs, is the most abundant thermodynamically stable inorganic species of fixed nitrogen (N) in well oxygenated waters (Chester, 1990). Thermodynamically unstable forms of fixed N (NH_4^+, NO_2^-) however, can be a major constituent in surface waters under certain conditions e.g. high biological activity (Professor J.D. Burton, 1994, pers.comm.). The average concentration of total dissolved N in a wide range of unpolluted river systems has been estimated to be 375 $\mu g\ l^{-1}$ (27 μM), of which 115 $\mu g\ l^{-1}$ (8 μM) is

present as dissolved inorganic NO_3 and 260 $\mu g\ l^{-1}$ (19 μM) is in the form of the dissolved organic species (Meybeck, 1982).

Discharges of industrial and domestic waste may result in increased levels of organic matter and dissolved inorganic nutrients in natural waters and estuarine systems. For example, the River Ouse, which drains into the Humber Estuary is considered to be a polluted river with NO_3 concentrations of up to 380 μM (Morris, 1988) due to the intense agricultural activity in the catchment area. The River Scheldt in the south-west Netherlands drains densely populated and industrialised regions and as a result has NO_3 levels of up to 600 μM (Van Bennekon and Westeijn, 1990). The intense microbial activity which results from this input of nutrients and organic matter in domestic and industrial waste results in the almost complete consumption of dissolved oxygen in this region (Andreae and Andreae, 1989) with a permanently anoxic water column from May to October (Zwolsman, 1992). This affects PO_4 concentrations within the estuary (Zwolsman, 1992). The River Clyde, which drains into the Clyde Estuary on the West coast of Scotland, is highly enriched in NO_3 due to effluent from approximately half of Scotland's population and industry draining into it (Muller *et al.*, 1992). Winter levels of 171 μM NO_3 have been recorded (Haig, 1986). Such high NO_3 concentrations in the Clyde will increase those measured in the neighbouring lochs Striven and Fyne, for which the Clyde Estuary is a freshwater source (Tett *et al.*, 1985). It should be noted however, that a simple consideration of concentrations being input to an estuary is of limited value since what is of greater relevance to coastal waters is the flux of material through the estuary (Balls, 1992).

Due to the topography, soil type and bed-rock in the area surrounding Loch Linnhe (see section **3.2.2.1**), the land is not used for agricultural purposes and so the loch is not significantly affected by nutrient enrichment due to agricultural run-off. Neither is it affected significantly by direct discharges of waste water and sewage pollution by human activities (Mr. B. Bellwood, 1991, pers. comms., HRPB).

Also, the nutrient inputs from the surrounding mountainous areas would be expected to be small due to the thin coverings of generally nutrient-depleted soil present in such areas (Syvitski *et al.*, 1986). Therefore, the highest concentration of nitrate in Loch Linnhe is expected to be associated with the saline end member (see section **3.2.1**). Neighbouring Loch Etive also has its highest concentrations of nitrate in the higher salinity waters (Solorzano and Ehrlich, 1977).

It should be noted that for NO_3, atmospheric input in the Loch may be quite important since Grantham and Tett (1993) estimate an atmospheric input of ~10 μM dissolved inorganic nitrogen to the Clyde Sea area.

2.2.2 Primary inputs of phosphate

Rivers provide the major source of P to the sea (Froelich *et al.*, 1982). In unpolluted rivers the main form of dissolved P is orthophosphate which is derived from the natural weathering of minerals (Zwolsman, 1986). Orthophosphate occurs mainly as $H_2PO_4^-$ in the pH range of 3-7. In seawater where the pH is ~8, the principal dissolved species is HPO_4^{2-} (Stumm and Morgan, 1981). The global average river-water concentration of total dissolved phosphorus is 28 $\mu g\ l^{-1}$ (0.9 μM) and that of total particulate phosphorus is 530 $\mu g\ l^{-1}$ (17 μM), of which 320 $\mu g\ l^{-1}$ (10 μM) is in an inorganic form and 210 $\mu g\ l^{-1}$ (7 μM) is in an organic form (Meybeck, 1982). The sources of dissolved inorganic PO_4 in river waters include the weathering of crustal minerals e.g. aluminium orthophosphate and apatite during which it is liberated in large quantities as alkali phosphates and as dissolved or colloidal calcium phosphate (Grasshoff, 1983), and anthropogenic inputs e.g. from the oxidation of urban and agricultural sewage and the breakdown of polyphosphates used in detergents (Chester, 1990).

In recent years the PO_4 loading of many rivers has been increased due to soil disturbance (where the soil has been over-fertilized), and discharge of sewage and other human wastes (Smith and Longmore, 1980). However this riverine flux of PO_4 may be substantially modified by its deposition or dissolution in the estuarine

environment (Fox *et al.*, 1986). If excess PO_4 in urbanised rivers could be removed to the sediments of the receiving estuary, then this would reduce the influence of anthropogenic P inputs on adjacent coastal waters (Lebo and Sharp, 1992). However recent mesocosm experiments in well-mixed estuarine systems indicate that such systems may act as a conduit for P transport to coastal waters, exporting the majority of P they receive (Nowicki and Oviatt, 1990) which may give rise to increased growth of phytoplankton and macroalgae in coastal waters (Smith and Longmore, 1980).

Uncertainties regarding the reactions of phosphate adsorption on and desorption from suspended matter and sediment, are partially responsible for the problems encountered in estimating the fluvial fluxes of reactive P to the oceans (Froelich *et al.*, 1982). This is a complex aspect of the geochemical behaviour of phosphate and only a brief description is given here of how the primary PO_4 inputs may be altered by conversion to the colloidal or and/or solid phase before reaching the estuarine zone

2.2.2.1 Conversion to the colloidal phase

It has been shown by many workers that phosphorus (P) and iron (Fe) may be removed from the dissolved phase in river water through their conversion to the colloidal phase by their association with dissolved organic matter (DOM) present in the water (Eckert and Sholkovitz, 1976; Sholkovitz, 1976; Boyle *et al.*, 1977; Moore *et al.*, 1979 (does not deal with P removal); Smith and Longmore, 1980). The main consequence of this is that dissolved PO_4 derived from chemical and physical weathering for example, might enter the estuarine environment in the colloidal phase, undergo a phase change due to the aggregation the colloid as it encounters an increased salinity (see below) and then be released back into the dissolved phase before reaching the oceans, thus making it difficult to predict the impact of riverine inputs of PO_4 on the coastal waters.

The source of Fe in the river waters is through leaching of soils and peat bogs,

which is an important consideration in this study since Loch Linnhe lies in an area of peaty soils (see section **3.2.2.1**). The Fe is generally present in the colloidal phase and is in the form of oxyhydroxides (FeOOH) stabilised by DOM in the river water (Boyle *et al.*, 1977 and Moore *et al.*, 1979). River water DOM is composed to a large extent of "humic" substances which are complex macromolecular phenolic carboxyllic acids and exist in river water as true solutions of polyelectrolytes and/or as negatively charged hydrophylic colloids (Sholkovitz, 1976). Humic acid (HA) is a humic substance and is soluble above a pH of about 3.5 (Choppin and Clark, 1991). However, HA only accounts for 4-20% of the total DOM in Scottish rivers, indicating that fulvic acids and other non-humic substances predominate in river water organics (Sholkovitz, 1976).

Phosphate in natural waters can associate with both Fe colloids and HAs through binding by complexation, chelation and adsorption (Sholkovitz, 1976). As a consequence, the PO_4 is no longer in the truly dissolved phase, but is now associated with a colloidal phase. A property of colloids is that they tend to aggregate in electrolyte solutions such as seawater (Sieburth and Jensen, 1968), hence removing any Fe and/or PO_4 associated with them from the water column. This occurs by neutralisation of the negatively charged iron-bearing colloids (Boyle *et al.*, 1977) by calcium ions (Ca^{2+}) in the seawater (Sholkovitz and Copland, 1981) and also due to the reduction of the repulsive forces between the particles which stabilise the colloid (Professor J.D. Burton, 1994, pers. comms.). Eckert and Sholkovitz (1976), Sholkovitz (1976) and Boyle *et al.* (1977), have shown that DOM, dissolved Fe in river water and other trace elements, are all removed by this common process of aggregation which is dependent on salinity, (sometimes referred to as co-precipitation if both Fe and PO_4 are involved; Lucotte and d'Anglejan, 1988). Sholkovitz (1976), carried out laboratory experiments on filtered river water taken from 4 different Scottish rivers and showed that as it was mixed with filtered seawater, the extent of flocculation increased until it reached a maximum level at between 15-20 PSU. This flocculation resulted in removals of 200% P (showing that the seawater was acting as a source of P), 98% Fe and only 3-6% for Si, from the river-water.

2.2.2.2 Conversion to the solid phase

Other phase changes of PO_4 in natural waters include the adsorption of dissolved PO_4 onto the surface or into the structure of suspended particulate matter (SPM), including flocculants formed by the processes described above. Lucotte and d'Anglejan (1988) distinguish between adsorption (onto flocculants) and co-precipitation processes: Adsorption occurs when the Fe is precipitated before the PO_4 is added and co-precipitation when the Fe is precipitated after the PO_4 is added, although the removal efficiency of PO_4 is noted as being essentially identical for both processes.

It is widely recognised that dissolved PO_4 is highly particle-reactive, reacting rapidly with a wide variety of surfaces and being taken up by and released from particles through a complex series of "sorption" reactions (Froelich, 1988). Carritt and Goodgal (1954) first suggested that PO_4 could be removed from solution in turbid fresh waters by adsorption onto the particle surfaces, and thus transported into estuaries in this form. Since this early work the adsorption of PO_4 onto particulate surfaces has been studied extensively both in the laboratory and in the field by many workers. In summary, natural clay particles with a surficial coating of reactive Fe- and Al-oxyhydroxides, resulting from the chemical weathering of rocks and soils, have a high capacity for adsorbing PO_4 and thus for maintaining low PO_4 concentrations in natural waters (Froelich, 1988; Lebo, 1991).

With respect to the incorporation of PO_4 into the SPM structure, the kinetic control of dissolved PO_4 in natural waters and estuaries has been investigated by Froelich (1988), who described the mode of interaction of dissolved PO_4 with fluvial inorganic suspended particles as via a "reversible two-step sorption process". The first step in this involves the adsorption/desorption of PO_4 on surfaces and it has fast kinetics (in the order of minutes to hours), whilst the second step involves the slow reaction of solid-state diffusion of adsorbed PO_4 from the surface into the interior of particles and thus has slow kinetics, (in the order of days to months). Fox (1989) also reports on such a "two-step solid phase sorption" for inorganic PO_4

in river waters. He proposed that such a process controlled the concentration of PO_4, by effectively causing an equilibration of the dissolved PO_4 in the river water with a "solid-solution of amorphous ferric phosphate in amorphous ferric hydroxide." The first stage of this process is adsorption of PO_4 onto the metal hydroxide surfaces to form an amorphous metastable solid phase with a uniform distribution of P. Then, if the reaction time is long enough, or if temperatures or PO_4 levels are elevated, the second stage of the reaction may occur in which discrete iron phosphate phases are formed by initial sorption and subsequent diffusion of the PO_4 onto and into the metal hydroxide component of sediments and soils. At ambient temperatures this solid phase diffusion would be extremely slow, but at the amorphous, highly hydrated surface of metal oxides and in colloidal dispersions, diffusion might be rapid enough to influence the PO_4 concentrations within the residence times of waters in most rivers.

Hence PO_4 may enter an estuarine system in the solid phase as aggregated material or adsorbed onto particles, in natural waters. It should also be noted that whilst PO_4 can be removed from natural waters by the above processes, it may also be released back into the river water under certain pH, salinity and redox conditions: In section **2.2.1** it was described how the Scheldt River has a permanently anoxic water column from May to October. This results in the reduction of Fe (III) oxidation states to Fe (II) with the subsequent dissolution of Fe-bound PO_4, thus releasing it back into the river water column in the dissolved phase (Zwolsman, 1992). Such processes of PO_4 release into the water column are considered in more detail in section **2.3.2.3.**

2.2.3 Primary inputs of silicate

SiO_4 is present in river waters almost exclusively as silicic acid. It is mainly derived from the weathering of silicate and aluminosilicate minerals. Unlike NO_3 and PO_4, anthropogenic sources play a relatively minor role in the supply of SiO_4 to rivers (Chester, 1990). SiO_4 is a major constituent of river water, making up ~10% of the total dissolved solids, and its global average concentration has been

estimated to be 0.17 μM l^{-1} (Meybeck, 1979). Silicon is also present in river water in particulate forms, which include quartz and aluminosilicates and biological material e.g. from diatom skeletons (Chester, 1990).

Unlike PO_4, it would seem that SiO_4 is not significantly associated with colloidal phases in river water: Sholkovitz (1976), in his study on Scottish river water states that "...therefore, even in the river waters of Scotland, which contain considerable amounts of colloidal iron and humic substances, little removal of Si occurs." However, Morris *et al.*, (1981) did observe abiotic removal of SiO_4 from the water column, in their work on the Tamar Estuary and this occurred at low salinities of up to 15 PSU. However, the study was inconclusive with respect to the causes of this removal. It is possible that the removal was due to adsorption onto SPM.

2.3 Nutrients in Sea-Lochs: Non-Conservative Processes

2.3.1 Sinks/removal of nutrients from the estuarine system

This involves a phase change from the dissolved phase to the solid phase and includes biological activity and adsorption processes onto and/or into SPM:

2.3.1.1 Biological activity

Nutrients are utilized by phytoplankton for growth. NO_3 and PO_4 are essential elements in the cellular composition of the organisms whereas SiO_4 is only required for the growth of those organisms characterised by the presence of a frustule (diatoms) or by scales (chrysophycaes) made of biogenic opal (Burton, 1980; Burton, 1988; Billen *et al.*, 1991). Hence where phytoplankton are present, the removal of nutrients from the water column and hence the dissolved phase might be expected, causing deviations away from the TDL.

Nutrient Ratios and their importance: The proportions in which carbon (C), nitrogen (N), and phosphorus (P) are taken up by marine phytoplankton has been

generally found to be in the atomic ratio of 106:16:1 for C:N:P (Redfield *et al.*, 1963), known as the Redfield Ratio. Goldman *et al.* (1979) pointed out the remarkable constancy in the chemical composition of phytoplankton cells observing C:N:P ratios of 106:16:1, even under conditions of apparent nutrient depletion (i.e. in stable tropical waters). It seemed then that it was not the level of nutrients in the water that was important to growth so much as the atomic ratio in which they were present in the water (the Redfield ratio) and that this was particularly critical under low nutrient conditions. Redfield (1934) showed that seawater from different localities also contained nutrients in these constant proportions. Whether organisms evolved to use the 16:1 N:P ratio because it was there or whether marine organisms themselves established the ratio through time is still uncertain (Broecker and Peng, 1982). In shallower, more dynamic coastal areas (as compared with the deep, open ocean), there maybe rapid biological and geochemical reactivity occurring and point or diffuse (i.e. anthropogenic) inputs. This may lead to significant deviations of the nutrient ratios away from the Redfield values: N:P ratios of between 5:1 and 8:1 are common in inshore waters (Stefansson and Richards, 1963; Pratt, 1965) and in this study (1991) on Loch Linnhe N:P ratios in the saline end-member are found to be ~9:1 c.f. 13:1 for 1990 (Grantham, 1991). Also in enclosed or shallow waters, regeneration processes may not reach completion due to rapid recycling of nutrients within the water column, or short residence times (Grantham, 1986). Nitrogenous material tends to be more slowly regenerated than phosphorus hence N:P ratios may be low in the water column which may lead to nitrogen limitation. Billen *et al.* (1990), reports that phosphate is clearly remineralised much faster than nitrate. He reports that this is due to the fact that nitrogen compounds can be transported directly into the algal cells where they become incorporated in the biomass as amino acids, whereas phosphorus compounds cannot be transported as such across cell membranes.

In the case of areas where diatom growth predominates over other phytoplankton species, the uptake of silicon (Si) (as silicic acid) from the water column to build frustules needs also to be considered. Richards (1958) found that for water in the Western Atlantic silicon appears to enter the biochemical cycle in the same

proportions as nitrogen, so that the uptake ratio of C:N:Si:P for diatoms becomes 106:16:15:1. However, unlike N and P which can be present in ocean water in a fairly constant ratio of 16:1, concentrations of Si in the water column vary greatly in their proportion to P and N present (Redfield *et al.*, 1963). Such variation arises from the fact that in different parts of the oceans the proportions of diatoms to other phytoplankton, which do not require Si e.g. dinoflagellates, differ greatly and consequently the statistical composition of the plankton is variable with respect to Si. (Redfield *et al.*, 1963). Furthermore, the regeneration of Si back into the water column from the diatom tests may be expected to occur at different depths and different rates to the N and P. This is because animals which feed on phytoplankton have no use for Si and hence the diatom tests are rejected and tend to sink and dissolve at depth, whereas the N and P will be retained by the animal and be regenerated from its excretions and decomposition products in the upper layers of water (Redfield *et al.*, 1963). The rates of Si regeneration will be different to those for N and P because the regeneration processes of Si involve the slow non-biological process of opal dissolution (Billen *et al.*, 1991), whereas those for N and P are more directly related to the microbial oxidation of organic matter (Redfield *et al.*, 1963) and are therefore more rapid (Billen *et al.*, 1991). NO_3 is recycled more rapidly than SiO_4: Grantham and Tett (1983) report slow dissolution of particulate silicate relative to nitrate in the Clyde Sea; Officer and Ryther (1980) report 9-13 days for N recycling by decomposition which contrasts with the SiO_4 dissolution timescale of 45-190 days; Lerat *et al.* (1990) found in their study of the Bay of Morlaix, Brittany, that there was a 3 month delay between the release of NO_3 and that of SiO_4 following an input of organic matter to the sediment; Degobbis (1990) reports N:Si:P ratios of 15:47:1 for the Northern Adriatic Sea (<50m depth) which he attributes to denitrification in the sediment and the different regeneration rates of P and N (mainly regenerated in the water column) compared with biogenic SiO_4 (regenerated mainly in the sediments).

If the incoming water to a sea-loch contains nutrients in proportions which are lower than in the Redfield ratio, then phytoplankton growth might be expected to be nutrient limited. For example, if the N:P ratio is < 16:1 phytoplankton growth

might be expected to be nitrogen limited. This assumes that phytoplankton need to take up the nutrients in the 16:1 ratio, but it has been shown that phytoplankton can adapt to such conditions by changing their cellular atomic composition (Redfield *et al.*, 1963; Banse, 1974[1] and Banse, 1974[2]). Another response to nutrient limitation however, is a species change in the phytoplankton: Species changes have been observed where the dissolved silicon concentration is depleted: diatoms require silicate (SiO_4) for growth and the formation of their frustules or scales (chrysophyces) (Billen *et al.*, 1990). The N:Si ratio in marine species is generally in the order of 1.07:1 (Richards, 1958) and if the N:Si ratio is > 1.07:1 then there may be a species change to a less silicified diatom. This has recently been reported in the Mississippi River (Dortch *et al.*, 1992; Rabalais, 1992) where nitrate (NO_3) concentrations have doubled and SiO_4 concentrations halved since the 1950s, due to the use of PO_4 rich fertilisers (which tend to retain SiO_4). Such dramatic changes in the N:Si ratio of the river end-member have caused changes in the phytoplankton community with 3 different species of phytoplankton being observed under the changing conditions. When SiO_4 concentrations were high in the water moderately silicified diatoms predominated, when concentrations were low lightly silicified diatoms predominated, and when concentrations were depleted non-diatoms were present. Carbon fluxes in coastal zones and sea-loch systems might also be affected because lightly silicified diatoms or non-diatoms do not sink out of the water column directly and hence when these species predominate, carbon fluxes are lower thus reducing states of hypoxia in certain cases e.g the Mississippi (Dortch *et al.*,1992).

Changes in algal biomass and species composition could have implications for the fish farmer, if any additional growth or selection of species were in favour of a harmful species (Gowen, 1990). Officer and Ryther (1980) have argued in general terms that anthropogenic perturbation of the N:Si ratio may stimulate flagellates at the expense of diatoms. These flagellates could be toxic, such as occurred in 1988 in Lochs Torridon and Diabeg in Scotland with resultant mortalities to farmed salmon there (Gowen, 1988), and in 1990 a Queen Scallop fishery in Scotland had to be closed after a toxic dinoflagellate bloom occurred in the waters with the

result that paralytic shellfish poisoning developed in humans (UNESCO, 1991). With such examples in mind, the necessity to monitor the nutrient ratio status present in shallower, coastal environments is quite obvious.

2.3.1.2 Adsorption processes

As stated at the start of section **2.2.2.2** it is widely recognised that dissolved PO_4 is highly particle-reactive, reacting quickly with a wide variety of surfaces (Froelich, 1988). SiO_4 appears, from the literature, to be less particle-reactive and NO_3 not at all. This section therefore concentrates on the adsorption of PO_4 in a sea-loch environment and SiO_4 where appropriate:

Jitts (1959), in his study on adsorption of PO_4 by estuarine bottom deposits states that, "The studies on the effect of phosphate concentration on adsorption have shown that silts are capable of adsorbing very large quantities of phosphate, and that in the natural state they seldom even approach saturation with phosphate. It follows, that under average conditions the silt would act continuously as a trap of phosphate at the expense of the overlying water, particularly during the freshwater run-off cycle when highly oxygenated waters with low salinity are bringing down large quantities of terrestrial phosphate and silt."

Such associations of particle-bound P with natural solid phases, have been examined by workers using mainly chemical extraction procedures. In estuarine suspended and bottom sediments, particle-bound P has been found to be mainly associated with organic matter and phases of iron and aluminium (Upchurch *et al.*, 1974; Froelich, 1988; Lucotte and d'Anglejan, 1988; Lebo, 1991). Lebo (1991) showed that particulate P was associated with organic matter, aluminium (Al) oxides, iron (Fe) oxides and apatite, in all the areas of the Delaware Estuary. Krom and Berner (1980) showed that PO_4 is adsorbed onto ferric oxyhydroxide phases present in virtually all oxic sediments, but is less readily adsorbed onto Fe compounds such as siderite or ferrous sulphide.

Nutrient budgets of the Baltic Sea indicate that an increased loading of P to a great extent is counteracted by adsorption to the sediments, resulting in a comparatively small net increase of the P concentration in the water column (Carman and Wulff, 1989). This has important implications for pollution control in such an area since the P-loading in the Baltic Sea has increased eight-fold during this century and does not show any signs of decrease (Carman and Wulff, 1989).

Balls (1992), in his study on the Forth and the Tay estuaries, found that PO_4 was removed at the low salinity end of the estuaries especially during the summer. This could be explained by the removal of PO_4 from the river water by aggregation of PO_4 associated colloids to the solid phase, the removal of PO_4 by its adsorption of PO_4 onto such flocculants in the water column and/or by the adsorption of PO_4 onto other types of SPM, such as estuarine silts and riverine clay particles. Balls, however rules out the possibility of PO_4 removal by the aggregation of colloids by assuming that such processes would have to be linked to the presence of FeOOH colloids in the river water and that therefore such removal would be persistent all the year round. However, this assumes that the presence of FeOOH is not seasonal i.e. it does not vary with river flow, which may not be the case. Zwolsman (1992) for example, has found that in the Scheldt estuary, PO_4 removal has strong seasonal modifications dependent on the seasonal variation (with flow) of dissolved Fe in the river water. During spring and summer PO_4 and Fe are both removed in the low salinity zone by aggregation of colloids, but during the winter, when there was a low dissolved Fe concentration in the river water, such aggregation processes were not observed. Balls (1992) attributes the observed removal of PO_4 in the Forth and the Tay to adsorption onto SPM which is present at maximum concentrations in the summer due to the low river flows.

Balls (1992) also observed SiO_4 removal in the upper Forth Estuary in the summer which coincided with high SPM levels suggesting that SiO_4 was being adsorbed onto the SPM and thus removed from the dissolved phase. This backs up the findings of Liss and Spencer, (1970) who found in laboratory experiments that removal of SiO_4 increased with increasing SPM and salinity.

PO_4 may also be removed from the water column by adsorption onto flocculants produced by the aggregation of colloidal material during estuarine mixing.

2.3.2 Sources/addition of nutrients to the estuarine system

This involves a phase change from the solid phase to the dissolved phase and includes processes such as regeneration of nutrients from the sediments to the porewaters, and desorption of nutrients (principally PO_4) from SPM.

2.3.2.1 Nutrient regeneration processes

In temperate regions there is a distinct seasonal cycle of nutrient concentrations in the surface waters of fjords (Grantham, 1986). In the spring the water column tends to become stratified either by a radiation-induced thermocline or a freshwater-induced halocline, with the latter being the most important in Loch Linnhe. Such stratification allows phytoplankton to remain in the euphotic zone (Solorzano and Grantham, 1975), i.e. in the surface layers. Hence a spring bloom may occur, depending on the light conditions causing the nutrient levels in the surface layers of the fjord to become depleted (Raymont, 1963).

During a bloom a large percentage of the nutrients taken up by the phytoplankton may get rapidly recycled by grazing and subsequent excretion by zooplankton (Raymont, 1963). For example in highly productive estuarine systems, uptake of dissolved inorganic PO_4 by plankton may be sufficiently rapid to completely utilize the PO_4 many times during estuarine mixing (Sharp *et al.*, 1984; Fisher *et al.*, 1988; Lebo and Sharp, 1992).

Sinking of larger biogenic particles (faeces and corpses) and the vertical movements of zooplankton and other animals feeding on phytoplankton and detritus combine to cause a progressive downward movement of nutrients out of the euphotic zone (Parsons *et al.*, 1984). Hence the euphotic zone is continually being depleted of nutrients, and primary production would be inhibited unless there was vertical

mixing, or vertical advection of nutrient-rich water from greater depths (upwelling) (Parsons *et al.*, 1984). Such vertical mixing of the water column tends to occur during the winter and tends to be initiated by storms and gales. As a result, the seawater entering a fjord may have high nutrient concentrations corresponding to the winter maxima of the surrounding waters (Grantham, 1986).

In shallow coastal areas, a greater percentage of the nutrients tend to sink to the bottom in the form of organic matter, such as faecal pellets and debris from phytoplankton and zooplankton tissue. A high sedimentation rate may occur due to the shorter water column. The nutrients may then be regenerated in the sediments by bacterial activity (microbial decomposition of organic matter), and/or chemical processes which follow a change in the redox conditions in the sediment (Balzer, 1980). Such regenerated nutrients may be released back into the water column via the sediment-water interface by diffusion and/or bioturbation (Yen and Tang, 1977) or resuspension of the bottom sediments.

Edwards and Grantham (1986), made a detailed study of the regeneration of nutrients in the bottom waters of Loch Etive. The bottom water in the deepest basin of this loch may stagnate for months or years (Edwards and Edelsten, 1977). This bottom water is separated from the estuarine circulation in the upper 30 m by a secondary pycnocline which inhibits mixing and turbulent transfer (Edwards and Grantham, 1986). As the temperature and salinity change slowly in the bottom water, with the density subsequently falling slowly changes in the concentration of the inorganic solutes are dominated by the non-conservative, regenerative processes at work in the water column and in the sediment (Edwards and Grantham, 1986). Such processes involve the consumption and decomposition of organic matter. It was also found that at the start of stagnation, biogeochemical effects dominated because vertical differences were small, so that diffusion was negligible. But as the differences between the estuarine water and the stagnant water increased, so did the diffusive fluxes. Eventually a steady-state situation was attained whereby the diffusive and biogeochemical fluxes in the stagnant water became roughly equal and opposite, and little change was then observable in the

nutrient concentration whilst the water remained stagnant.

These processes require oxygen for the respiration of the decomposer organisms with the subsequent oxidation of the organic matter up to nitrate (NO_3) and carbon-dioxide (CO_2), (see equations I and II). In areas of high organic input, anoxic conditions may occur at the sediment surface due to the complete uptake of oxygen by the decomposer organisms. If this occurs then anaerobic bacteria can use nitrate (NO_3^-), nitrite (NO_2^-) and sulphate (SO_4^{2-}) the water column or sediment porewaters as terminal electron acceptors for the oxidation and consequent breakdown of organic material (Redfield *et al.*, 1963). The subsequent reduced products are ammonia (NH_3), nitrogen gas (N_2) and hydrogen sulphide (H_2S) which may accumulate in the sediment and the overlying water. Hence, in aerobic conditions the NO_3 concentrations will increase above the sediment as organic matter is broken down and in anaerobic conditions, the NO_3 and SO_4 concentrations are decreased in the water column with the subsequent production of N_2 and H_2S.

Phosphorus remains largely as phosphate during biological processes and hence, does not participate directly in this cycle of microbial reduction and oxidation to any significant extent (Billen *et al.*, 1990). Phosphate tends to be released back to the dissolved phase when conditions become sufficiently reducing that the Fe phases retaining the PO_4 in the sediment are reduced (see section **2.3.2.3**).

With respect to silicate regeneration, the dissolution of biogenic opal is a slow, non-biological process which simply requires the destruction of a protective organic coating after the death of the diatom (Billen *et al.*, 1990). Diatom skeletons tend to dissolve in estuarine sediments since estuarine waters are far from saturation with respect to silicic acid (Zwolsman, 1986). Silicate is therefore regenerated by purely physico-chemical processes, contrary to NO_3 and PO_4 which are regenerated mainly by microbial degradation (Zwolsman, 1986).

2.3.2.2 Stoichiometry of decay

The amount of oxygen taken up during the aerobic degradation of organic matter, depends on the chemical composition of the organic compound. As described in section **2.3.1.1**, Redfield (1934) and Goldman *et al.* (1979) found that the average molar ratio of carbon to nitrogen and phosphorus in phytoplankton and zooplankton was 106:16:1 (C:N:P) known as the Redfield ratio. The essentially reversible reactions that take place during the formation of organic matter by photosynthesis, and its subsequent destruction by respiration (oxidation), may be simplified in the following way:

For carbon;

$$CO_2 + H_2O \rightleftharpoons CH_2O + O_2 \qquad \textbf{(I)}$$

For nitrogen;

$$NO_3^- + H_2O + H^+ \rightleftharpoons NH_3 + 2O_2 \qquad \textbf{(II)}$$

These reactions move to the right during photosynthesis and to the left during respiration (Open University, 1989). From equation (**I**) it is clear that for every mole of carbon used during photosynthesis, one mole of oxygen is liberated; and for every mole of fixed nitrogen used, two moles of oxygen are liberated. Hence, oxygen may be included in the Redfield ratio: 106 moles of oxygen (O_2) are liberated, (or consumed) for every 106 moles of carbon fixed in, (or liberated from) organic tissue. From reaction (**II**), a further 32 moles of oxygen are liberated (or consumed) for the 16 moles of fixed nitrogen that accompany the carbon in the organic tissue. Increases in organic nutrient concentrations resulting from these oxidation processes, should retain the same proportionality as the elemental ratios in the decaying tissues (Grantham, 1986). However, this assumes that complete regeneration of the nutrients occurs within the flushing time of the particular system which may not be the case in shallower, coastal regions (see section **2.3.1.1.** for further details).

2.3.2.3 Other modes of PO_4 addition to the estuarine system

In section **2.2.2.1** it was described how PO_4 could enter the estuarine environment in the solid phase if incorporated into colloidal aggregated material. In section **2.2.2.2** it was seen that PO_4 could enter the system adsorbed onto the surface of riverine SPM or onto flocculant surfaces and in section **2.3.1.2** that it could be removed from the water column by adsorption onto SPM surfaces within the system. However, PO_4 can also be released back into the dissolved phase via desorption from the SPM. Such adsorption/desorption processes give rise to a phenomenon known as the PO_4 **buffer mechanism** which maintains dissolved PO_4 concentrations within a narrow range in some systems (Pomeroy *et al.*, 1965; Butler and Tibbitts, 1972; Fox *et al.*, 1985, 1986; Fox 1988, 1991; Froelich, 1988). It involves the equilibration of the dissolved PO_4 pool with a reservoir of particle-bound P, i.e. when the ambient PO_4 concentration differs from the equilibrium concentration, the PO_4 is either released or adsorbed until the equilibrium is achieved (Lebo, 1991). This PO_4 buffer phenomenon is very significant since it could be a significant process in maintaining the PO_4 concentration of rivers, streams and estuaries at nearly constant values and providing a large and potentially available reservoir of reactive PO_4 for phytoplankton growth in excess of that dissolved in the water (Froelich *et al.*,1988).

Effect of salinity and pH on desorption from the solid phase

Generally, in estuaries, an increase in salinity of the water has been reported to favour the release of PO_4 from SPM, including flocculants, back into the water column (Carritt and Goodgal, 1954; Lebo, 1991; Balls, 1992). This has been linked to the increase in pH which accompanies an increase in salinity (Carpenter and Smith, 1984; de Jonge and Villerius,1989; Balls,1992; Zwolsman,1992, pers. comms.). Zwolsman (1992, pers.comms.) considers that on increasing salinity and pH, the principal dissolved species of PO_4 in the water changes from $H_2PO_4^-$ to HPO_4^{2-} (Stumm and Morgan, 1981). Hence there is an increased repulsion between this species with an increased negative charge and any FeOOH colloids that the PO_4

might be associated with, and so the PO_4 is released back into the water column. Froelich (1988) however proposes that release of PO_4 at high salinities might happen for several other reasons: Firstly, surface seawater usually has a very low dissolved PO_4 concentration associated with it, and so when fluvial SPM (to which PO_4 is adsorbed), is swept into the sea, it encounters a medium where the PO_4 concentration is much lower than in typical rivers, and hence PO_4 is desorbed by a type of diffusion process, going from a high to a low concentration area; secondly, in seawater, anions which are capable of competing for the SPM surface sites to which the PO_4 is bound (e.g. OH^-, F^-, SO_4^{2-}, $B(OH)_4^-$) are present in concentrations orders of magnitude greater in seawater than in freshwater.

Lebo (1991) found that the release of particle-bound PO_4 by such desorption processes, would have been insufficient alone to maintain the constant PO_4 concentrations that he observed in the Delaware Estuary. From this he concluded that such release of PO_4 was being supplemented by the release of PO_4 from the bottom sediments, which was there due to remineralisation of organic matter formed during primary production and by the release of PO_4 from solid iron phases. During primary production the particulate organic P that is not remineralised in the water column eventually settles out into the sediment along with any inorganic PO_4 adsorbed onto SPM. Once in the sediments, remineralisation of organic P is continued until only a small refractory part remains which appears to be associated with nucleic acids (Kramer *et al.*, 1972; Zwolsman, 1986). Under aerobic conditions in the upper layer of the sediment, the orthophosphate produced during remineralisation may adsorb onto clay minerals and / or amorphous oxides of Fe and aluminium (Al) (Zwolsman, 1986). Dissolved PO_4 may be removed from porewaters by adsorption onto FeOOH coatings (Zwolsman, 1986; Sundby *et al.*, 1992). Resuspension of such bottom sediments may also result in release of PO_4 adsorbed onto the sediment surface back into the water column (Chase and Sayles, 1980; Fox *et al.*, 1986).

It has been shown that PO_4 may be released from bottom sediments without a change in the pH of the overlying water (Lucotte and d'Anglejan, 1988; Lebo, 1991)

however, it has also been shown that an increase in pH in the water overlying the sediments seems to favour the release of PO_4 from sediments (Seitzinger, 1991).

Effects of redox potential:

In the case of anaerobic conditions, brought about by microbial breakdown of organic matter or compaction of flocculant structures (Lucotte and d'Anglejan, 1988), the depletion of dissolved oxygen and perhaps NO_3^- and SO_4^{2-} leads to a lowering of the redox potential within the sediment, allowing the reduction of Fe (III) species to Fe (II) (Price, 1976). Dissolution of any Fe (III) species would thus occur under such conditions and any associated PO_4 would be released also (Krom and Berner, 1981; Balls, 1992). Thus large-scale release of Fe-associated PO_4 to the porewaters may take place when the sediments become completely anoxic. PO_4 may then be released back into the water column by bioturbation processes, resuspension of the sediments or diffusion across a diffusion gradient. However, it may readsorb onto Fe (III) surfaces as it migrates upwards out of the reducing zone and may actually be recycled several times across the redox boundary for Fe before escaping the sediment (Sundby *et al.*, 1992).

Since we are now entering an era in which nutrient and other pollutant inputs to many estuaries, rivers and lakes are decreasing as a result of water legislation (Seitzinger, 1991), a fuller knowledge of the effectiveness of pollution control methods is therefore required, and of particular concern is this long-term release of nutrients such as PO_4 from the sediment in response to changing water column conditions (Oviatt *et al.*, 1984).

2.4 Nutrients in Sea-Lochs: Processes Leading to Apparent Non-Conservative Behaviour

The main reason for apparent non-conservative behaviour is when end-member concentrations vary temporally within the time-scale of the flushing time of the system.

2.4.1 Upwelling of nutrient-rich seawater

Saline end-member concentrations may vary due to upwelling events. These quite often occur due to a change in aeolian conditions: The influence of the wind is two-fold: (i) it gives rise to barotropic currents by changing the fjord water level - this will diminish or augment inflow of water over the sill according to the direction of the wind and, (ii) it gives rise to baroclinic flow, which in the sill region can import renewing water (Gade and Edwards, 1980). This is described in **CHAPTER 1**, section **1.2.3.2**.

Upwelling events are important because they are a way of introducing high salinity, nutrient-rich waters to a fjord basin since they tend to occur seaward of a fjord entrance thus effecting the water just outside the sill (Gade and Edwards, 1980). This water may be nutrient-rich due to the regeneration of nutrients, as described in section **2.3.2.1** or just by virtue of changing inputs in surrounding coastal areas.

Other processes that give rise to temporally varying saline end-member concentrations are biogeochemical processes in the sill-region and / or the dilution effects of a temporally varying freshwater end-member being mixed down into the saline component.

2.4.2 Temporally varying freshwater nutrient concentrations

Source variations may introduce apparent removal and/or input signals into conservative profiles within an estuary. The direction and extent of these variations are dependent upon: (i) the direction in which the river source is changing (increasing or decreasing in concentration with time), (ii) the relative magnitude of the variation in the source concentration, (iii) the ratio of the period of source variation to the freshwater residence time in the estuary and, (iv) the rate at which the source variation is mixed and diluted down the salinity gradient (eddy diffusion) (Kaul and Froelich, 1984).

In a study made on a small Florida estuary, Kaul and Froelich (1984) report that up to 10% of the observed estuarine activity of nutrients could be attributed to variations in river concentrations:

Solorzano and Ehrlich (1977) made a study on the nutrients in Loch Etive, a neighbouring sea-loch to Loch Linnhe. They found that in Loch Etive the main contributors to the nutrient budget of the loch were (i) river run-off and (ii) seawater from outside the loch. The concentration of the nutrients in the rivers was found to vary throughout the year. With heavy precipitation, dilution and washout of nutrients is accentuated. During dry periods, the water is in contact with the soil for much longer periods and so the concentration of the nutrients increases. After long periods of dryness, the first rain produces a scouring of the river beds and the input of nutrients into the loch is high. In Loch Etive the highest concentrations of PO_4 and NO_3 is associated with the saline end member and so in periods of low rainfall and decreased river inflow, a rise in salinity and hence PO_4 and NO_3 concentrations is observed, with the lowest values of these nutrients being at the head of the loch (Solorzano and Grantham, 1975). Conversely SiO_4 concentrations are highest at the head of the loch and in dry periods the concentration decreases with rising salinities.

Webb and Walling (1985) in their study on the NO_3 loadings in the River Dart, Devon, also found that there was a marked seasonal variation, with dilution responses typical of the winter period and concentration effects more characteristic of summer months which they attributed to the influence of soil throughflow.

Smayda (1983) in his study on the Ythan River in northeastern Scotland found that there were seasonal fluctuations in the freshwater NO_3 and PO_4 concentrations, related to rainfall and to the seasonal application of fertilizers to agricultural land in the drainage area.

2.5 Summary and Discussion

This chapter has considered the role of biogeochemical cycling processes in the distribution of nutrients by considering the different processes that can lead to non-conservative and apparent non-conservative behaviour in an estuarine environment. This has been considered in the light of the estuarine mixing theory and the use of mixing diagrams and deviations of data from theoretical dilution lines for the interpretation of results.

It initially considered the possible primary inputs of the dissolved inorganic nutrients to a sea-loch system. In the case of nitrate it was shown that the main source originates from soil leaching, terrestrial runoff and waste inputs. For Loch Linnhe, which does not lie in an agricultural catchment area, the main source of nitrate is likely to be from the saline end-member. Any nitrate input from the freshwater end-member is likely to have its source from leaching from the soil.

The main source of phosphate in unpolluted river waters is from the weathering of crustal minerals such as aluminium phosphate and apatite. In polluted rivers, phosphate concentrations maybe increased due to over-fertilized land and discharge of sewage and other human wastes. The complex geochemical reactivity of dissolved inorganic phosphate in natural waters makes its concentration, and therefore potential impact on coastal waters, difficult to predict. In the rivers that enter Loch Linnhe at its head, this phosphate could be in the colloidal form since the rivers leach peaty soils and bogs and thus are likely to contain a significant amount of Fe and DOM in the form of humic acid. The implication of this is that the phosphate will be in an aggregated form as the rivers enter the estuarine system due to the coagulation of the colloidal material as it encounters an electrolytic medium. The high particle reactivity of dissolved inorganic phosphate was also considered in terms of adsorption processes onto and/or into SPM, namely natural clay particles with surficial coatings of Fe- and Al-hydroxides resulting from the chemical weathering of rocks and soils. Such adsorption processes will remove phosphate from the dissolved phase.

The main source of silicate is from the weathering of silicate and aluminosilicate minerals and not from anthropogenic sources. Unlike phosphate, silicate is not significantly associated with the colloidal phase in river water.

Removal of nutrients to the solid phase in estuarine systems was then discussed in terms of the resultant deviation away from conservative behaviour. Removal can occur via biological activity i.e. uptake of nutrients by phytoplankton for growth. Deviations from the oceanic Redfield ratio of C:N:P uptake in the ratio 106:16:1 and from the N:Si ratio of 1.07:1 predicted by Richards (1958), are expected in shallower coastal environments such as Loch Linnhe due to the rapid biological and geochemical reactivity occurring and the incomplete regeneration of nutrients in such a dynamic environment. Phosphate is likely to be regenerated faster than nitrate from the sediments and nitrate faster than silicate. Sinks of nutrients in the estuarine environment can also occur due to adsorption onto SPM. Such processes are most significant for phosphate and as such have only be dealt with for this nutrient. Dissolved inorganic phosphate can be scavenged from the water column by estuarine silts, riverine clay particles and aggregated colloidal material.

Sources of nutrients to the system have then been considered in terms of non-conservative behaviour and deviations away from a linear nutrient/salinity relationship. Such processes include the regeneration of nutrients from the sediments to the porewaters and ultimately to the overlying bottom-waters, and occur as a result of microbial oxidation and redox processes within the sediments. Additional mechanisms for the addition of phosphate back into the system have been considered which might arise through an increase in salinity and/or a decrease in redox potential, which would increase the potential for desorption of the phosphate from the solid phase.

Nutrient concentrations will also deviate from a linear relationship with salinity due to apparent non-conservative behaviour. This occurs due to temporally varying end-member concentrations of nutrients being input to the system within the flushing time of that system. In Loch Linnhe temporal variations in the

pristine riverine inputs are likely to be due to seasonal effects and in the saline inputs due to changes caused by upwelling seaward of the sill, advection of temporally changing water from adjacent coastal regions and possibly through dilution by a temporally varying freshwater end-member component.

This chapter has described many different processes that can affect the nutrient concentrations and hence their distribution in a sea-loch system. Identification and isolation of the individual processes involved is complicated for sea-loch systems due to the type of circulation set up, as described in the previous chapter. The use of mixing diagrams does not allow for a straightforward interpretation of the results in the identification of these processes and more careful consideration is required to distinguish between those processes leading to non-conservative behaviour and those leading to apparent non-conservative behaviour. However mixing diagrams and theoretical dilution lines are still potentially useful tools in such studies and thus will be used throughout this study.

CHAPTER 3 LOCH LINNHE AND SURROUNDING AREA: CIRCULATION AND PRIMARY INPUTS OF NUTRIENTS

In order to be able to look critically at the nutrient status of a system, quantitative and qualitative consideration must be given to the primary sources of nutrients entering that system. Only then can an accurate evaluation be made of the role of biogeochemical processes and their influence on the nutrient distribution within the system.

This chapter provides information on the origins and properties of the saline and freshwater inputs to the survey area, and it describes the relation of nutrient concentrations to the origins of waters around the west coast of Scotland. It also summarises some of the physical and hydrographic characteristics of Loch Linnhe.

3.1 Geographical Setting

The survey area is the upper basin of Loch Linnhe, a sea-loch system based on the west coast of Scotland (see **FIGURE 3.1**). Loch Linnhe is usually described as comprising two basins, the upper basin and the lower basin, although together with Loch Eil it does, in fact contain a total of 5 sills (Edwards and Sharples, 1986). The lower basin of Loch Linnhe is considered to start from Shuna Island (56° 35′ N, 5° 24′ W) and extends for 15.2 km NNE up as far as the Corran Narrows (West Coast of Scotland Pilot, 1974), (see **FIGURE 3.2**). The northern part of Loch Linnhe, i.e. the upper basin, is considered to start at the Corran Narrows (~ 56° 42′ N, 5° 17′ W) and extends for 16 km northwards to Fort William (56° 49′ N, 5° 06′W).

Loch Eil drains into the upper basin of Loch Linnhe through a channel of water called the Annat Narrows (see **FIGURE 3.2**). Together with Loch Linnhe they form the submerged western end of the Great Glen, the geological rift which divides the North from the Northwestern Highlands (Pearson, 1970). Feeding into the top of the upper basin are the rivers Lochy, Nevis and the Caledonian Canal.

FIGURE 3.1

Geographical Setting of the Survey Area, Loch Linnhe

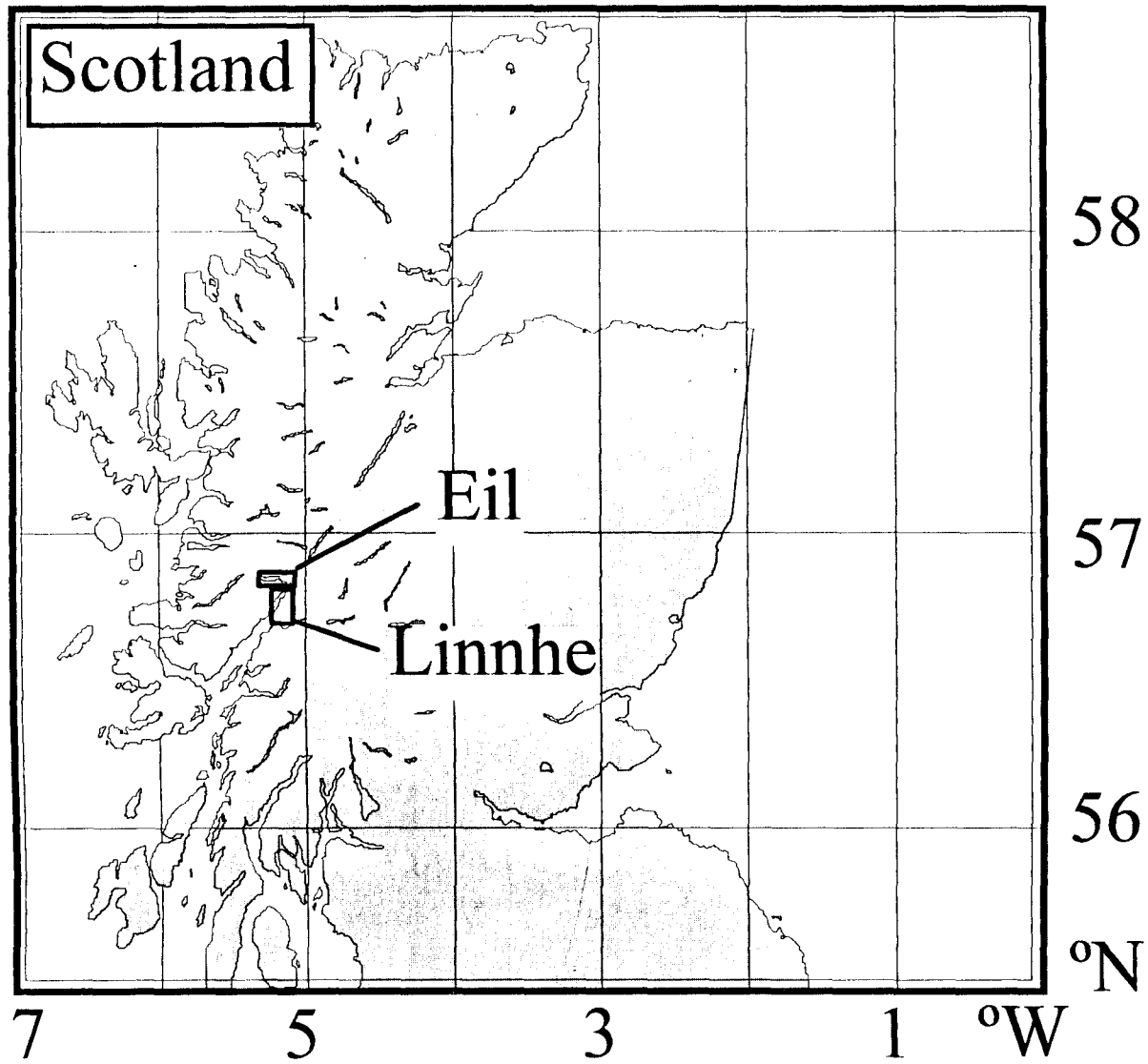

FIGURE 3.2

The Upper and Lower Basins of Loch Linnhe. Taken from West Coast of Scotland Pilot (1974)

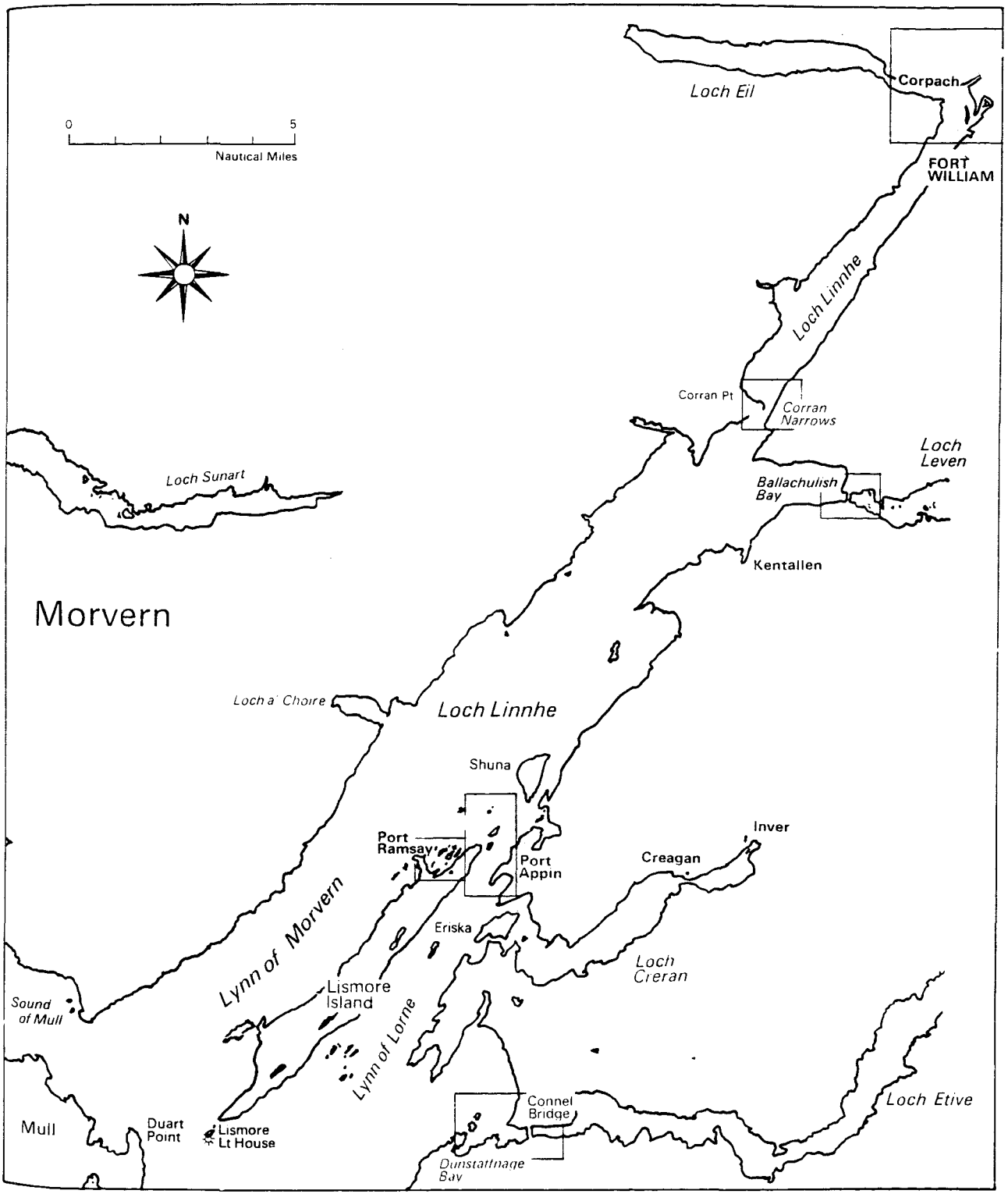

Beyond the lower basin of Loch Linnhe lies the Firth of Lorne, which opens out to the Atlantic.

3.2 Sources of Water to Loch Linnhe and Associated Nutrients

3.2.1 The saline end-member:

Different inputs of water to a system will contain different concentrations of nutrients. As stated in **Chapter 2**, section **2.3.1.1** the ratio of nutrients found in oceanic environments is expected to be 106:16:1 for C:N:P (Redfield *et al.*, 1963) and 16:15:1 for N:Si:P (Richards, 1958), providing there are no addition or removal processes modifying the nutrient concentrations within the water column. The saline water entering Loch Linnhe is not single-source oceanic water. It is a mixture of different water bodies, and as such is not likely to contain nutrients in the ratios predicted by Redfield *et al.* (1963) and Richards (1958).

FIGURE 3.1 shows the position of Loch Linnhe with respect to the Irish Sea, the North Channel and the Clyde Sea area and **FIGURE 3.3** indicates that the deeper, saline water entering the Loch originates from water moving up through the Irish Sea and the North Channel. Approximately 94 % of this water passes through the Firth of Lorne via the portion of the coastal current circulating west of Islay and only 6 % arrives at the Firth of Lorne via the Sound of Jura (Mackay and Baxter, 1985).

FIGURES 3.4 and **3.5** show that the composition of water entering the Firth of Lorne (and hence Loch Linnhe) consists of approximately 75 % Irish Sea/Clyde water and 25 % Atlantic water which enters the Firth of Lorne from the west. These figures were taken from Mackay *et al.*(1986) who investigated the patterns of circulation to the west of Scotland by tracing the passage of radiocaesium isotopes contained in the coastal current water.

FIGURE 3.3

Estimated Most Usual Net Water Movements Near the Bottom in the Waters around Scotland. (The Figures Indicate Very approximate Drift Speeds in Kilometres per Day). Taken from Craig (1959).

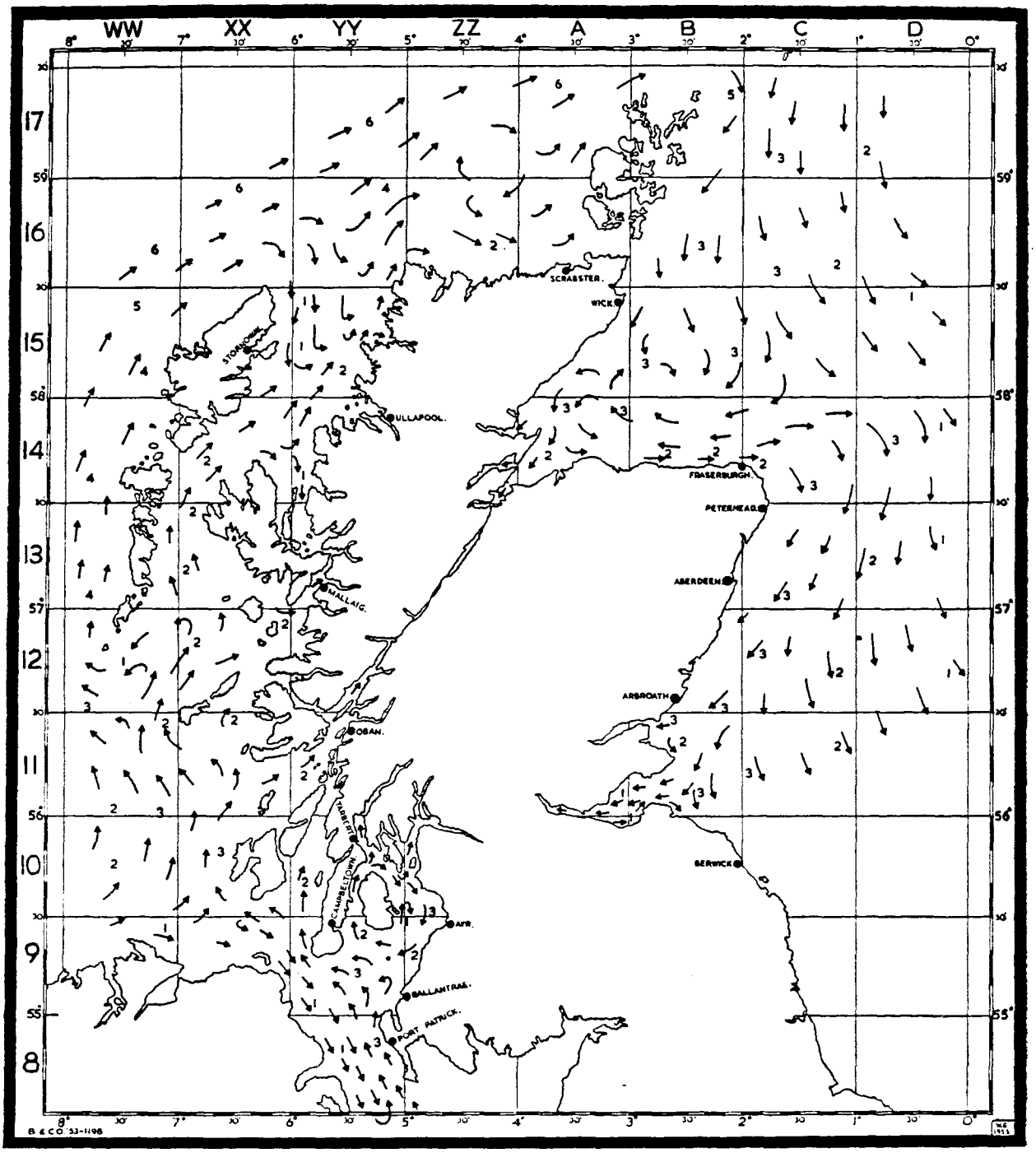

FIGURE 3.4

Relationship of Radiocaesium with Salinity for the Surface ^{138}Cs Observations taken in July 1981. Taken from Mackay *et al.*, 1986

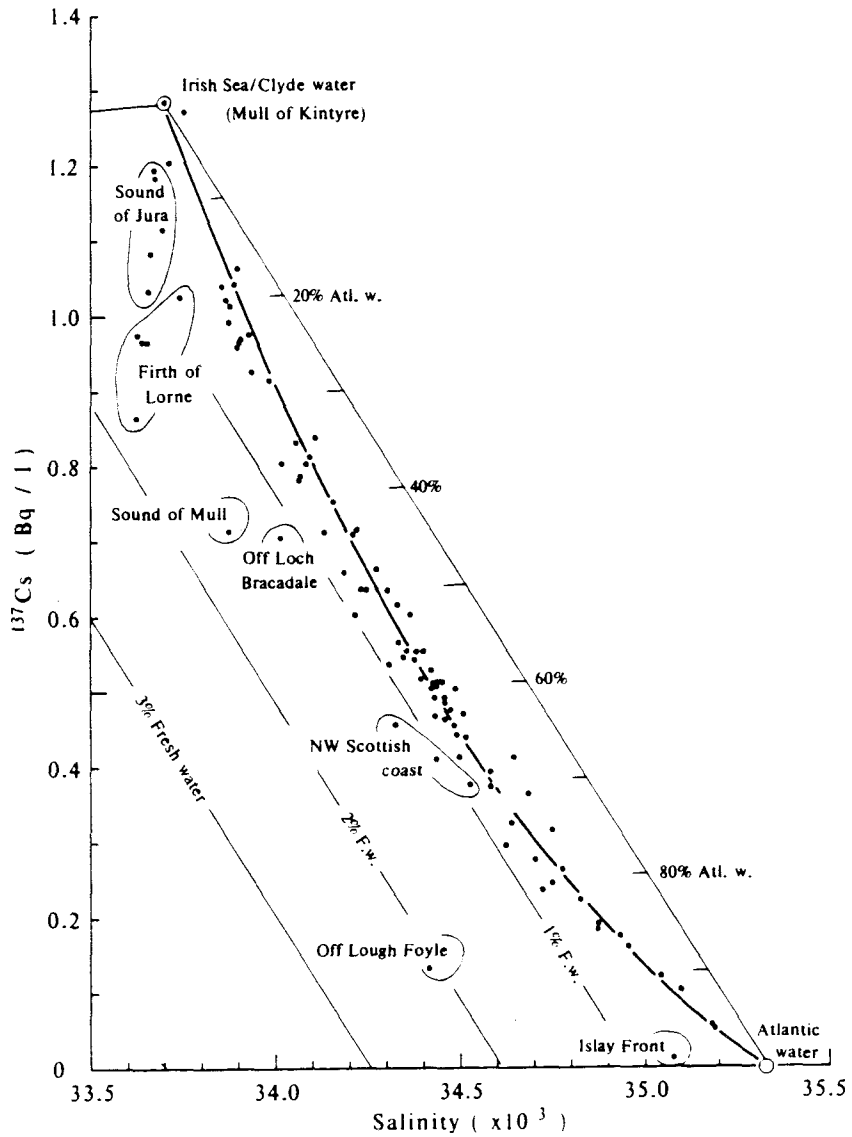

FIGURE 3.5

Radiocaesium/Salinity Mixing Diagram for the Three Main Water Types of the Scottish West Coast. Taken from Mackay *et al.*, 1986

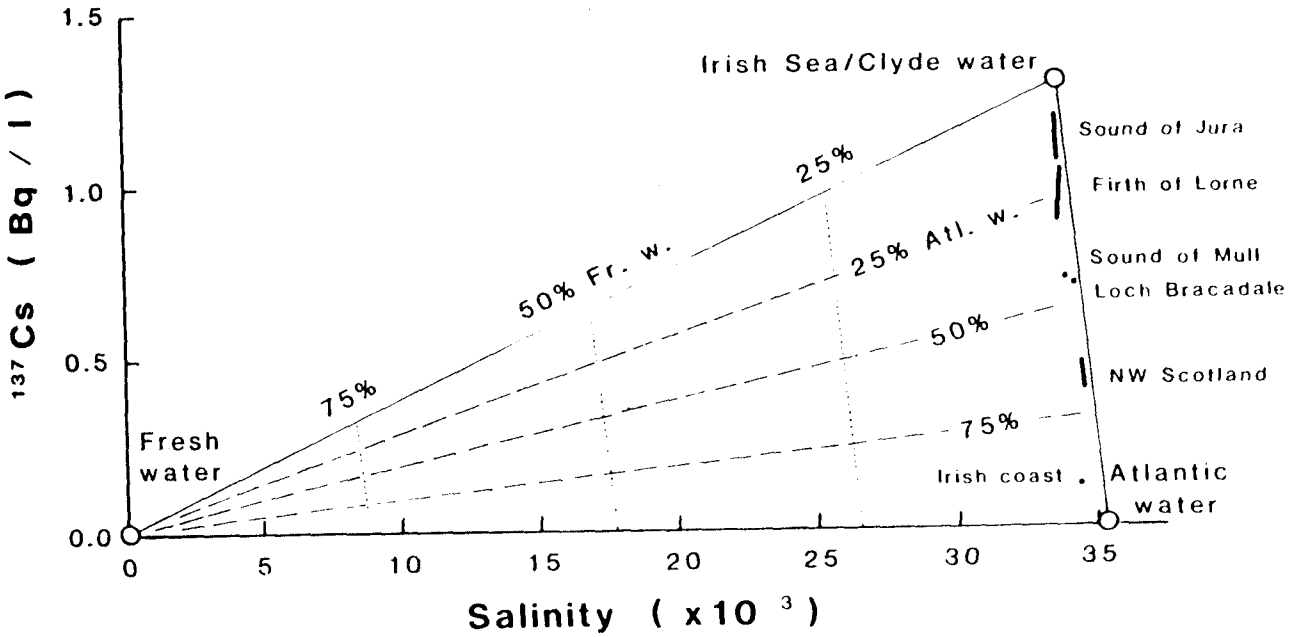

The range of nutrient concentrations entering a sea-loch will depend on the origin of the water. The nutrient composition of the saline water entering Loch Linnhe therefore depends on the composition of the Irish Sea/Clyde water predominantly, and of the Atlantic Ocean water to a lesser extent. It should be noted that the nutrient status of water passing up through the Firth of Lorne into Loch Linnhe may also be affected by the outflow of brackish water into it from neighbouring lochs e.g. Loch Etive, Loch Creran and Loch Leven.

3.2.1.1 Nutrient status of the Irish Sea:

Foster (1984) made a study on the winter regime of nutrients in the northern Irish Sea area. This study only extended from Anglesey, to the North Channel but the results showed that Atlantic water moving up through the Irish Sea was modified in its nutrient status due to mixing with the Irish Sea water. This was due to the different chemical characteristics of freshwater sources discharging into the northern Irish Sea which tended to generate a variety of different water types in the area. For example, marine waters along the Irish coast were found to be relatively enriched in silicon (Si), whilst waters adjacent to the eastern coastal boundary were relatively enriched by anthropogenic nitrogen sources. Results from this study showed that the distribution of nitrate (NO_3) through the Irish Sea was in the concentration range of 7.1 to 10.7 µM, (except for Liverpool Bay where the level was up to 29 µM). The SiO_4 was found to increase in concentration with decreasing salinity, indicating that the SiO_4 concentrations in the freshwaters were greater than that in the saline, receiving waters. Generally, the SiO_4 concentrations were in the range of 5.3 to 7.1 µM with values of >10.7 µM off the Irish coast waters and in the Liverpool Bay area. Phosphate (PO_4) concentrations were found to be less than those of NO_3 but greater than those of SiO_4, with concentrations in the range of 1.0-1.3 µM, but with elevated concentrations in the Liverpool Bay area of 2.3 µM. From this study, it can be seen how in its northwards passage through the Irish Sea, Atlantic water will be diluted with freshwaters from a variety of sources and its nutrient concentrations supplemented from the terrigenous sources. Nutrient ratios in this northern Irish Sea area, ranged between 7:1 to 10:1 (N:P) in

winter. Hence, if the uptake ratio during production is 16:1 (Redfield *et al.*, 1963), then these waters may become nitrogen deficient although phytoplankton can adapt to changes in nutrient ratios (see **CHAPTER 2**, section **2.3.1.1**). The N:Si ratio was generally found to be > 2:1. Assuming a value of approximately 1:1 to be typical for the N:Si utilization ratio (Richards 1958; Officer and Ryther, 1980), then the N:Si ratio in the northern Irish Sea can be described as "a delicate balance between availability and utilization, likely to exhibit variations from one winter to the next" (Foster, 1984).

3.2.1.2 Nutrient status of the Clyde Sea-water:

As seen from **FIGURE 3.1** water moving northward from the Irish Sea area through the North Channel, will have water from the Clyde Sea area mixing with it, thus altering its nutrient composition. Various studies have been made on the nutrient status of waters in the Clyde Estuary/Sea area and the results of these are summarised in the table below:

TABLE 3.1

Summary of Documented Nutrient Results Measured in the Clyde Sea Area in Winter Time.

AREA	NO_3 µM	PO_4 µM	SiO_4 µM	N:P	N:Si
River Clyde	171[1]	----	>100[2]	---	<1.71
Clyde Estuary	35[3]	3[3]	23[3]	12:1	1.52
Inner Firth	16.9[4]	----	15.6[4]	----	1.1
Inner Firth	29[2]	1.5[2]	18[2]	19.5:1	1.3
North Channel	6.8[4]	----	4.3[4]	----	1.6:1

(1): Haig (1986); **(2)**: Mackay and Leatherland (1976);

(3): Muller *et al.*, 1992; **(4)**: Grantham and Tett (1993).

From this table it can be seen that the concentrations of all three nutrients decrease as salinity increases i.e. from the freshwater in the Clyde River to the saline water in the North Channel. The River Clyde receives domestic and industrial waste from a population of nearly 2.5 million in and around Glasgow (Mackay and Leatherland, 1976; Haig, 1986). As a result it has high dissolved inorganic nitrogen levels. The high freshwater SiO_4 concentrations are due to the drainage of a lowland catchment area which overlies sedimentary rocks and due to the drainage of the sewage in the lowland areas (Grantham and Tett, 1993). These high concentrations are diluted as the Clyde Sea Water is mixed with the Irish Sea-water with the resulting North Channel water having lower nutrient concentrations. However, the NO_3 concentration quoted from Grantham and Tett (1993) of 6.8 µM respectively for North Channel water, seems exceptionally low for an area fed by such polluted waters. Balls (1992) reports that his measured NO_3 concentrations of up to 100 µmol l^{-1} for the Forth and the Tay rivers and estuaries are "not high" relative to those of contaminated rivers and estuaries such as the Rhine and the Scheldt where freshwater NO_3 levels have been measured at 450 and 600 µM respectively (Van Bennekon and Wetsteijn, 1990). Kaul and Froelich (1984) cite global average concentrations in "pristine" rivers of 7.4 µM-N (Meybeck, 1982) and 0.4 to 1.0 µM-P (Meybeck, 1982; Froelich *et al.*, 1982). Hence the concentrations of NO_3 in freshwaters in and adjacent to the survey area, which are in the range of 6 to 7 µM for Loch Etive (Solorzano and Grantham, 1975) and ~ 2 to 7 µM for Loch Linnhe (see **CHAPTER 5**, section **5.2.1.2**), and the low North Channel water concentration of 6.8 µM (Grantham and Tett, 1993), might be considered characteristic of an unpolluted/pristine environment (Meybeck, 1982; see **CHAPTER 2**, section **2.2.1**). It should be noted however, that this North Channel NO_3 concentration is just one measurement and that the very nature of anthropogenic dumping of pollutants gives rise to temporally varying riverine nutrient concentrations.

Using the concentrations quoted in Grantham and Tett (1993) a winter N:Si ratio of ~ 1.6:1 in the North Channel is predicted. PO_4 concentrations were not measured in this study but the report produced by Mackay and Halcrow (1976)

gave an average N:P ratio in the Inner Firth for January and February 1974 of ~ 19:1.

Thus the resulting North Channel water described above, will continue northwards mixing with a ~ 25% component of Atlantic Water which moves in from the west.

3.2.1.3 Nutrient status of the Atlantic Ocean water:

The 25% Atlantic water component, having come in from the west, probably originates from the Rockall/Malin Head region. Ellett and Martin (1973) made a study on the nutrients in this area, and found that the levels ranged from 2 μM SiO_4 at the surface in November 1965, to > 20 μM at 2000m in April 1965. Similarly PO_4 ranged from 0.5 μM PO_4 at the surface for November 1965 to > 1.0 μM at 2000m in April 1965. The NO_3 concentrations ranged from 10 μM at the surface for November 1965 to 20 μM at 2000m for April 1965. These results indicate an N:P ratio of ~20:1 for both the winter surface waters and for the spring-time deeper water, and similarly an N:Si ratio of ~5:1 for the surface waters and 1:1 at depth.

3.2.1.4 Prediction of nutrient ratios for the saline end-member:

As can be seen from this section, the three water masses influencing the nutrient composition in Loch Linnhe, namely the northern Irish Sea, the Clyde Sea water area and the Atlantic oceanic water, all have different nutrient ratios associated with them, as do the inputs of nutrients from the neighbouring sea-lochs, Etive, Creran and Leven. Also their nutrient levels will alter seasonally according to the levels of productivity occurring within them. The oceanic nutrient ratio of N:Si:P=16:15:1 is therefore not likely to be seen entering Loch Linnhe at the seaward end, since the saline water entering the Loch will be coastal dominated.

Assuming a 75 % Irish Sea water/Clyde Sea water (i.e. the North Channel) component and a 25 % Atlantic Oceanic water component (Mackay and Baxter,

1986), a predicted winter N:P and N:Si ratio for the saline end-member of Loch Linnhe can be estimated.

Since Grantham and Tett (1993) did not measure PO_4 levels in the North Channel a winter N:P ratio for this area has been estimated, assuming 50/50 mixing between the Irish Sea-water and the inner Firth water from the Clyde Sea area:

(19.5+9)/2 = N:P ratio of ~ 14:1.

The winter N:Si ratio for the North Channel from Grantham and Tett (1993) is ~ 1.6:1. The Oceanic ratios are N:P = 20:1 and N:Si = 5:1 (see above) and so a predicted N:P ratio for 75 % North Channel water and 25 % Oceanic water would be:

(75 % of 14:1)+(25 % of 20:1) = 15.5:1,

thus agreeing quite closely with that predicted by Redfield *et al.* (1963), and a predicted winter N:Si ratio would be:

(75 % of 1.6:1)+(25 % of 5:1) = 2.45:1.

This winter N:Si ratio seems rather high considering diatoms assimilate nitrogen and silicate in roughly equimolar quantities (Officer and Ryther, 1980) and it is well documented that the spring bloom in Loch Linnhe consists of diatoms (Solorzano and Grantham, 1975; Grantham, 1991; Grantham, 1992). However a likely explanation for this is that during the winter time the NO_3 will be remineralised more rapidly by from the sediment in the saline waters than the SiO_4 (organic N being remineralised at a faster rate than organic Si, (Grantham, 1986; Billen *et al.*, 1990)), hence increasing the N:Si ratio above 1:1. As the spring-time approaches the concentration of dissolved Si in the water will have increased and the N:Si ratio will be approaching 1:1 again.

From the literature then a predicted winter N:P ratio for the saline end-member to the survey area is ~ 15.5:1 and N:Si ratio is 2.45:1, probably approaching 1:1 by spring.

3.2.2. The Freshwater End-Member:

Upper Loch Linnhe receives water draining from the rivers Lochy, Nevis and the Caledonian Canal. It lies within an area of high natural rainfall, the annual average being 2200 mm (Edwards and Sharples, 1986). The catchment area of the River Lochy is 1252 km^2 and that of the River Nevis is 76.8 km^2 (data courtesy of the Highland River Purification Board; HRPB). For the years 1990, 1991 and 1992 the daily annual average flow of the River Lochy was 93.19, 55.44, 80.64 $m^3 s^{-1}$ respectively and for the River Nevis was 9.79, 5.65, 8.06 $m^3 s^{-1}$ (calculated from data provided courtesy of the HRPB). The high daily average rainfall for 1990 was due to a succession of 4 months with almost continuously high precipitation and, as a result the cumulative rainfall total for that year, up to June 1990, was 26% higher than the previous highest total recorded in 1989 (Grantham 1991).

Loch Eil receives a number of streams from the surrounding slopes but its catchment area is very small compared to that of the River Lochy and the River Nevis so that its freshwater input to Loch Linnhe is slight (Heath 1990).

For the Caledonian Canal there appears to be no available data on flow rates or catchment area due to the absence of monitoring by either the HRPB or the British Waterways Board. However there is no known discharge of high nutrients into Loch Linnhe from the Canal (Mr. B. Bellwood, pers. comms., HRPB, 1991).

3.2.2.1 Nutrient Status of the rivers Lochy and Nevis:

There is little existing literature on the nutrient status of rivers in the Argyll area of Scotland.

Nutrient levels entering the sea-loch via the rivers Lochy and Nevis, will depend not only on the contents of the precipitation (rainfall), but also on the type of vegetation, soils and bedrock with which the water is in contact (Låg, 1976). Both the River Lochy and the River Nevis flow through areas with peaty, brown soils containing humus-iron, derived from "gravels derived from acid rocks" (Mr. D. Merrilees, 1991, pers. comms., Scottish Agricultural College, Ayr), the presence of which will encourage the formation of colloidal PO_4 in the water column (see **CHAPTER 2**, section **2.2.2.1**). Since the soil types for the Loch Linnhe catchment area are generally acidic, with an average pH range of 3.5-5.0 the presence of PO_4 in the colloidal phase in natural waters may be favoured (see **CHAPTER 2**, section **2.2.2.1**). Indeed, Sholkovitz (1976), in his study of 4 Scottish rivers showed removal of inorganic PO_4 from the freshwater as it flocculated on meeting seawater indicating that the PO_4 in the river water was in the colloidal form. Balls (1992) in his study on the Forth and Tay estuaries in Scotland also reports removal of PO_4 from the freshwater but he attributes this to adsorption processes of the PO_4 onto SPM (see **CHAPTER 2**, section **2.3.1.2**). Solorzano and Ehrlich (1977), in their study on Loch Etive, a neighbouring sea-loch to Loch Linnhe, measured very low inorganic PO_4 concentrations of < 0.03 µmol l^{-1} in the surrounding rivers draining into the loch which would indicate that the inorganic PO_4 might be present in the organic colloidal form or adsorbed onto/into SPM present in the water. Solorzano and Grantham (1975) in their study on surface nutrients in three different Scottish sea-lochs, also report negligible PO_4 concentrations in the neighbouring Rivers Etive and Awe.

Average NO_3 concentrations of 6.2 µmol l^{-1} are reported for the Rivers Etive and Awe (Solorzano and Grantham, 1975).

For SiO_4, Solorzano and Grantham (1975) report that the highest concentrations are found in the areas of Loch Linnhe which receive the greatest freshwater runoff indicating a riverine source of SiO_4 in the area. This would be due to the natural weathering of the Si-containing bedrock in the area which is granite (see BGS map: Sheet 53, Ben Nevis, scale 1:50,000). Solorzano and Grantham (1975) also report

that Loch Linnhe showed higher SiO_4 levels than Loch Creran, which increased towards the head of the loch with concentrations of up to 16.2 µM SiO_4 being recorded in March 1974.

Thus knowing that the nutrient concentrations in the freshwater end-member will be a function of flow-rate and other parameters; temperature, pH, redox condition and suspended solids loadings of the water (see **CHAPTER 2**), all of which will vary temporally, it is difficult to predict N:P and N:Si ratios for the freshwater input to Loch Linnhe from the literature available. Part of the present study involves an investigation into the riverine nutrient concentrations entering the loch and how they vary with time and flow (see **CHAPTER 6**, section **6.2.1.1**).

What can be suggested from this section is that the contribution of inorganic PO_4 to Loch Linnhe from the rivers Lochy and Nevis will be negligible, but for NO_3 will be in the range of 6-7 µM and 15-20 µM for SiO_4, all of which will depend on flow-rates and other temporally varying parameters.

The outward moving brackish layer, which originates from the rivers at the head of Loch Linnhe results in net surface water movement out of the loch, mixing with the northward flowing water, moving up through the Sea of the Hebrides (see **FIGURES 3.6** and **3.1**).

3.3 Specific Physical Features of Loch Linnhe:

3.3.1 Dimensions and Tidal Ranges:

The lower basin of Loch Linnhe is 15.2 km long, extending from Shuna Island to the Corran Narrows (see section **3.1**). Its width varies from between 2.8 to 5.6 km, becoming contracted at the Narrows (West Coast of Scotland Pilot, 1974). The upper basin of the loch is about 16 km long, extending from the Corran Narrows to Corpach. Its width varies from about 1.5 to 3.0 km (see **FIGURE 3.2**).

FIGURE 3.6

Estimated Most Usual Net Water Movements at the Surface in the Waters around Scotland. (The Figures Indicate Approximate Drift Speeds in Kilometres per Day). Taken from Craig (1959)

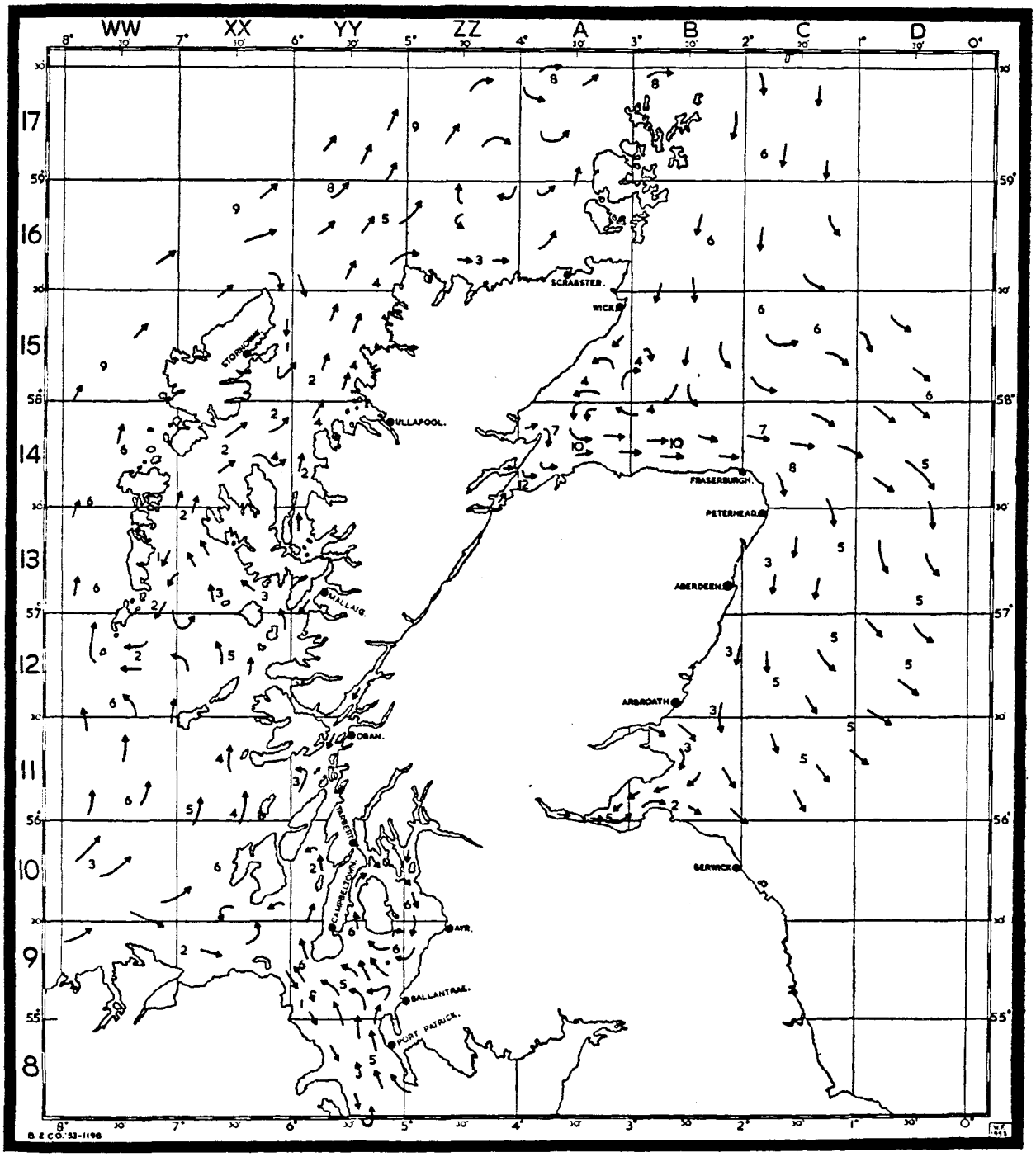

The maximum depth of the upper basin is 155 m at Lowest Astronomical Tide (LAT), (Admiralty Chart no. 2380) and its average depth is 50 m (Mr. A. Edwards, 1992, DML, pers.comms.).

The maximum tidal range for the upper basin is 3.7 m (where the maximum tidal range is taken as the range in the tidal height between mean high water springs and mean low water springs; Edwards and Sharples, (1986). The maximum tidal range for the lower basin is 3.6 m (Lawrence, 1990).

The minimum tidal range for the upper and lower basins is 1.6 m (Lawrence, 1990) (where the minimum tidal range is taken as the range in the tidal height between mean high water neaps and mean low water neaps).

From Admiralty Chart no. 2380, the surface area of the upper basin of Loch Linnhe which has been measured for this study is 20.08 km^2 at LAT. The surface area of the upper basin plus Loch Eil at high water is documented as 36.4 km^2 and at low water as 31.7 km^2 (Edwards and Sharples, 1986).

3.3.2 Sill Properties and Tidal Streams

The two sills described here are the sill at the Corran Narrows, which separates upper Loch Linnhe from lower Loch Linnhe, and the sill at the Annat Narrows, which separates upper Loch Linnhe from Loch Eil (see **FIGURE 3.2**):

(i) The sill at the Corran Narrows has a length of 1.17 km. It has a high water width of 290 m and a low water width of 270 m (Edwards and Sharples, 1986). It is difficult to specify one depth for the sill since the sill is not at a uniform depth across the loch, however Edwards and Sharples (1986) quote a mean sill depth of 18 m, based on a calculation of the sill area divided by the sill width at low water. Strong tidal streams run through the Corran Narrows, reaching 5 knots on a spring tide (Admiralty Chart 2380). These result in eddies forming on either side of the Narrows, mainly north of the narrows on the flood tide and south of them on the

ebb (Lawrence, 1990);

(ii) The sill at the Annat Narrows has a length of 1.97 km with a high water width of 290 m and a low water width of 270 m (Edwards and Sharples, 1986). The sill mean depth is quoted as being 6 m (Edwards and Sharples, 1986). Strong tidal streams also run through the Annat Narrows, reaching a maximum speed of 5 knots during springs and 3 knots during neaps (Admiralty Chart 2380).

Since the sill at both the Corran Narrows and the Annat Narrows is shallow, and the tidal ranges are high (especially during spring tides), a large volume of water will flood in and ebb out of the basin during every tidal cycle through a constricted cross-section. A consequence of this is that the tidal (barotropic) currents for Loch Linnhe will be sufficiently large to reverse baroclinic flow on an ebb tide, and also the outward flowing barotropic brackish water layer on a flood tide (see **CHAPTER 1**, section **1.2.1.2**). Such inhibition of baroclinic flow occurs during most of the semidiurnal tidal cycle associated with Loch Linnhe and is described as "tidal throttling" (Mr. A. Edwards, 1992, DML, pers. comms.). It will have important implications for the type of circulation that is set up in the loch due to the resultant turbulent mixing at the sill. In the case of Loch Eil which has a much shallower sill than in Loch Linnhe, such turbulence is only likely to affect the surface layers of the upper basin of Loch Linnhe and will not affect the water column at station LL19 used in this study (see **CHAPTER 5, FIGURE 5.1 (a)**)

Most exchange of water between the upper and lower basins of Loch Linnhe then, takes place by ebb pulses of low salinity water and flood pulses of higher salinity water drawn from around the sill depth at the Corran Narrows and discharged into the loch, settling at depths at which water is present of a similar density (Mr. A. Edwards, 1992, DML, pers. comms.). Hence the type of continuous two-layered estuarine flow discussed in **CHAPTER 1**, section **1.2.1** is not likely to be observed in Loch Linnhe.

3.3.3 Flushing Times in Loch Linnhe

Flushing time is defined as the time necessary to replace any given conservative quantity in a given volume of an estuary, river or coastal region at the rate at which that quantity is being injected into the volume (Officer, 1983). It is thus a measure of the residence time of a particle in an estuary or a portion of an estuary.

In this section a flushing time for the upper basin of Loch Linnhe is estimated from theoretical considerations using the "tidal-prism" method. This method is used by Edwards and Sharples (1986) in their catalogue on Scottish Sea-Lochs, and by the Scottish Office Agriculture and Fisheries Department (SOAFD) in their study on Loch Sween (Internal Report, Owen Paisley, 1993, pers. comms.) but is criticized by Falconer (1989) since it assumes complete mixing throughout the water column. For a more accurate value of the flushing time then this method is not appropriate for Scottish sea-lochs which quite often possess strong density gradients and are vertically stratified. It will however provide a useful estimation which can be used in comparison with a value calculated later in this study (see **CHAPTER 6**, section **6.1.2.2**) using the "freshwater fraction" method. This method uses freshwater as a conservative tracer to determine the residence time of water in a basin. It therefore requires an accurate knowledge of catchment area and rainfall (Kaul and Froelich, 1984; Officer and Kester, 1991).

Tidal prism method:

For a theoretical flushing time an average tidal range is considered;

$(1.6 + 3.7)/2 = 2.65$ m,

together with the average (between high and low water) total surface area of upper Loch Linnhe plus Loch Eil (since water entering upper Loch Linnhe will result in the same volume of water entering Loch Eil also);

$(36.4 + 31.7)/2 = 34.1\ km^2 = 34.1*10^6\ m^2$ = average total surface area of upper Loch Linnhe and Eil.

So the volume of water required to enter the system during a tidal cycle to achieve an average tidal range of 2.65m is

$2.65*34.1*10^6 = 9.04*10^7\ m^3$

Therefore if an average depth of 42.5m is taken for the upper basin of Loch Linnhe plus Loch Eil (Edwards and Sharples,1986), then the average flushing time for that system in one tidal cycle is:

(volume of the system/volume of water entering the system) tidal cycles;

$(34.1*10^6*42.5)/(9.04*10^7)$ = ~16 tidal cycles i.e. a flushing time of ~8 days for the whole system. If an average depth of 50 m is taken for the upper basin only (Mr. A. Edwards, 1992, DML, pers.comms.) then the flushing time for that basin is;

$(20.08*10^6*50)/(9.04*10^7)$ = 11.1 tidal cycles.

Therefore the upper basin of Loch Linnhe has a theoretical flushing time of ~6 days.

3.4 Summary

The survey area mainly comprises the upper basin of Loch Linnhe; a sea-loch system based on the west coast of Scotland. This basin is ~ 16 km in length and 1.5 to 3 km in width.

Saline water enters Loch Linnhe from the Firth of Lorne at the western end of the loch. This water consists of ~ 75 % mixed Irish Sea - Clyde Sea water and ~ 25 % Atlantic Ocean water. Based on values reported in the literature, winter N:P and

N:Si ratios for the saline end-member are estimated at 15.5:1 and 2.45:1 respectively.

The main freshwater input to Loch Linnhe is from the Rivers Lochy and Nevis at the head of the loch. The average annual daily flow-rate of the River Lochy is approximately ten times that of the River Nevis. These rivers flow through catchment areas consisting of peaty brown soils which contain humus iron and this favours the conversion of dissolved inorganic phosphate in the river water to the colloidal phase. This and the high particle reactivity of the phosphate contribute to the negligible phosphate concentrations reported in neighbouring Rivers Awe and Etive in the literature. It is suggested therefore that phosphate concentrations in the Rivers Lochy and Nevis will also be negligible although those for nitrate will lie in the range 6 to 7 μM and for silicate in the range 15 to 20 μM, with the silicate source being in the freshwater end-member.

The dimensions and tidal ranges for the upper basin have been specified in the chapter with the highest tidal range being 3.7 m and the lowest being 1.6 m. The sill depth is shallow at ~ 18 m and this results in tidal throttling and turbulent mixing at the sill. Using the tidal prism method the flushing time of the upper basin has been estimated at six days.

CHAPTER 4 METHODS AND TECHNIQUES

Two field-seasons were involved in this study; one in 1991 and the other in 1992. The 1991 field-season spanned the dates 20th March to 07th May which will be referred to in terms of Julian day numbers; days 79 to 127 respectively (starting from 01st January 1991). Sampling was carried out at two later dates also, on days 164 and 171. The 1992 field-season spanned the dates 19th February to 18th April, which are referred to as Julian day numbers 50 to 139 (starting from January 1st 1992). For both the field-seasons the sampling was carried out on a weekly basis on a flood tide, wherever logistically possible.

The sampling undertaken in 1991 served to provide preliminary basic observations which were then used to design the 1992 field-season to provide a more compact and complete picture of the hydrography and nutrient distributions in the upper basin of Loch Linnhe. This involved sampling at fewer stations over a greater range of depths during 1992.

4.1 Sampling Strategy

All sampling was carried out from the Dunstaffnage Marine Laboratory (DML) research vessel, R.V. Calanus; a 20m stern trawler equipped with a hydrographic winch and laboratory facilities.

4.1.1 Sampling stations

FIGURE 4.1 is a map of upper Loch Linnhe, showing the positions of the stations used in the 1991 field-season. Both hydrographic and chemical measurements were made at these stations for this field-season. Two extra stations; LL20 and LL21, further towards the freshwater end of the loch were incorporated into the sampling strategy on two sampling dates only as depicted in **FIGURE 4.1**. The positions and depths of all the stations are given in **TABLE 4.1**. Station LL0 is

FIGURE 4.1

The Upper Basin of Loch Linnhe: Sampling Stations Occupied in the 1991 and 1992 Field-Seasons

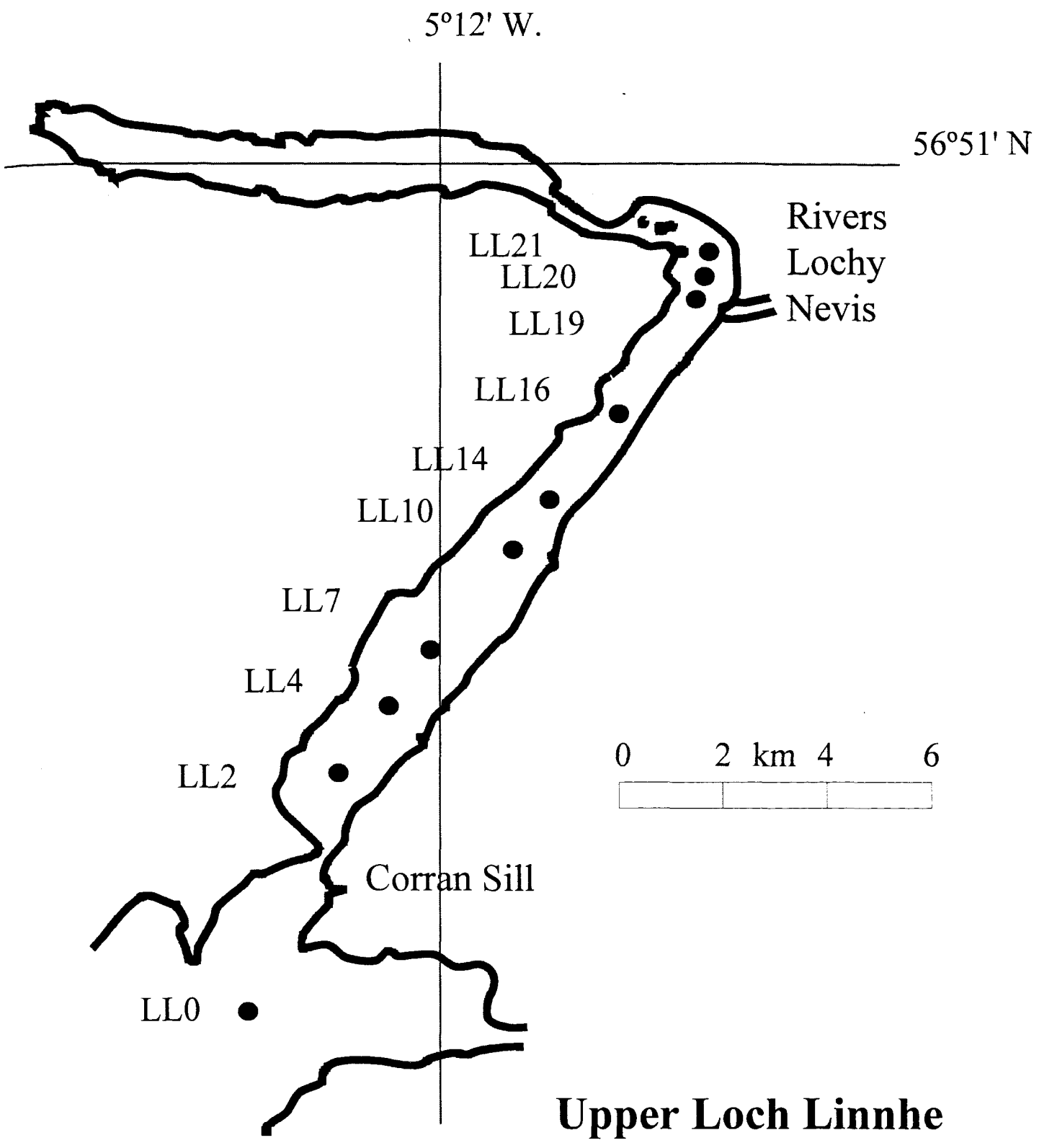

TABLE 4.1

Positions and Depths of Stations used During the 1991 and 1992 Field-Seasons

Station number	Position		Depth
	Latitude (°N)	Longitude (°W)	(m)
LL0[1,2]	56.41.20	5.17.60	42
LL2[1]	56.44.18	5.14.08	110
LL4[1,2]	56.44.61	5.13.53	110
LL7[1]	56.45.39	5.12.35	150
LL10[1]	56.46.29	5.11.20	153
LL14[1,2]	56.47.16	5.09.98	110
LL16[1]	56.48.01	5.08.81	122
LL19[1,2]	56.49.31	5.07.08	55
LL20[1,2]	56.49.60	5.07.10	25
LL21[1,2]	56.49.88	5.06.83	20

1 = stations occupied during the 1991 field-season

2 = stations occupied during the 1992 field-season

used to represent the saline end-member conditions and is situated seaward of the sill. Station LL14 is the most central station and is where currents generated from the riverine input and density currents formed at the sill region are most diminished. For the 1991 field-season, station LL19 is considered to represent the conditions at the freshwater end of the loch. The 1992 field-season incorporated far fewer stations for chemical analysis, namely LL0, LL14 and LL19 but for hydrographic measurements other stations were included: LL0, LL4, LL14, LL19, LL20 and LL21.

4.1.2 Hydrographic sampling techniques

For both field-seasons, temperature, salinity and depth measurements were made using an EG&G Ocean Products Neil Brown Instrument System, Conductivity, Temperature, Depth (CTD) profiling sensor. The recorded measurements were logged onto a chip-set 386 computer running Neil Brown Smart CTD software. From the temperature and salinity measurements the corresponding density data were calculated within the software. All data were then transferred onto floppy disc and converted to ASCII format back at the laboratory using locally developed Turbo Pascal programs (courtesy of Mr. A. Edwards, DML). Temperature data were obtained in units of °C, salinity in units of PSU and density (sigma-T) in units of kg m^{-3} (+1000) (UNESCO, 1991). Also attached to the CTD was a Sea Tech Inc fluorometer sensor (W.S Ocean Systems) from which measurements of fluorescence were made. These were smoothed using a three second time constant setting and the fluorescence data were converted to chlorophyll levels (µg l^{-1}) via a calibration developed at DML (sensitive to chlorophyll levels within the range of 0 - 10 µg l^{-1}), which was written into the Neil Brown software.

At each station the CTD was deployed on a hydrographic wire to a depth of approximately 10 m above the bottom of the loch. The CTD was deployed before the water sampling bottles on each occasion. Times of deployment, weather conditions and the amount of cable payed out (to compare to the pressure sensor reading) were recorded for each CTD deployment. At the end of each survey the

CTD was rinsed with freshwater and the individual sensors were carefully rinsed with deionised water to avoid corrosion.

4.1.3 Water sample collection

For both field-seasons water samples for nutrient analysis were collected using National Institute of Oceanography (NIO) polypropylene bottles (2.5 litre) lowered on a hydrographic wire. The depth of each bottle was determined from the amount of wire payed out, as indicated by a metre-wheel and from the spacing between the bottles (metres).

These water samples were collected at discrete depths throughout the whole water column at each station. At the shallower stations; LL0 and LL19, samples were collected at depths of 0, 5, 10, 20, 40 m. At stations LL20 and LL21, samples were collected at depths of 0, 5, 10, 15 and 20 m and 0, 5, 10, and 15 m respectively. At the deeper stations samples were collected throughout the water column during the 1992 field-season so that at station LL14, for example, samples were collected at depths of 0, 5, 10, 20, 40, 60, 80, 100, (100 - 110 m). In 1991 however, this was not the case and for the deeper stations from LL4 to LL16 the greatest depth at which samples were collected was 60 m so that sampling was at 0, 5, 10, 20, 40, 60 m only, for the majority of the field-season. Deeper sampling throughout the whole water column did take place as the field-season progressed but this was for three days only (days 113, 120 and 127) hence, information on the behaviour of the nutrients in the bottom-waters was limited for the 1991 study.

Polyethylene bottles (500 ml) were used for the temporary storage of the water collected from the NIO bottles. These had been rinsed three times previously with the sample before it was transferred to them. Filtration of the samples was carried out as soon as possible after collection and generally it was possible to filter the samples between the stations, with the maximum delay between collection and filtration being approximately 30 minutes. Filtering was carried out using polypropylene separating funnels, seven of which were connected in a line to an

electric vacuum pump so that seven water samples could be filtered simultaneously. Before filtering, each funnel was rinsed through with 250 ml of the sample and the filtrate was discarded. A further 250 ml of the sample was then filtered for use and the filtrate was subsampled into two separate polystyrene vials and placed into a freezer. Suction for the filtration was provided by an electric vacuum pump and was limited to between 100-150mm Hg as recommended for the filtration of chlorophyll samples (Tett and Grantham, 1978). The filter papers used were Millipore HA filter papers, 47 mm in diameter and with a poresize of 0.45 μm. The filters were handled by means of stainless steel forceps to minimise contamination introduced by handling errors.

4.1.4 Sediment sample collection

In 1993 a small study was made on the sediments in the upper basin with sediment samples being collected at stations LL0, LL4, LL14, LL19, LL20 and the River Lochy. This involved collecting one core per site using a Craib corer (Craib, 1965), although the riverine sample had to be collected manually.

4.2 Analytical Techniques for Water Samples

4.2.1 Filtration and storage of samples

After a seawater sample has been taken it continues to be influenced by biological activity, since bacteria and micro- and nano-plankton continue to digest and excrete material within the sample (Grasshoff, 1983). Hence the nutrient concentrations of the sample are likely to be altered. Also the walls of the sampling bottles and storage vials may act as surfaces for bacterial growth with the possibility of enhancing bacterial growth rates by several orders of magnitude (Grasshoff, 1983). In addition to this the material of which the sampling bottles are made may alter the dissolved nutrient concentration by processes such as adsorption of the nutrient. It is preferable then, that analysis of the nutrients be carried out as soon as possible after the sample has been collected and filtered. However, in the case

of this study, it was not logistically possible to analyse the samples immediately on the boat and hence, the samples had to be returned to the laboratory in the frozen state for analysis at a later date. In an attempt to minimise potential contamination of samples between collection and analysis, the filtration method, the type of storage vessel and the method of sample preservation had to be considered carefully:

4.2.1.1 Filtration of samples

As stated in section **4.1.3** the type of filter papers used for filtration of water samples throughout this study were Millipore HA filter papers of 0.45 µm poresize and 47 mm diameter. The reason that this type of filter paper was used as opposed to the cheaper Whatman GF/F and GF/C alternatives was that the latter filter papers contain silicate in their composition, being made of glass-fibre, and it was considered that this might cause contamination of the nutrient samples through leaching of the silicate into the sample. The Millipore HA filter papers are composed of cellulose esters and do not contain any significant amounts of nutrients that might contaminate the samples. The poresize of 0.45 µm was chosen so that only "dissolved" constituents were present in the filtrate, ("dissolved" being defined by Grasshoff (1983) as the components in a seawater sample that pass through a 0.45 µm filter paper), with the particulate fraction being retained on the filter paper. This assumption is, however not strictly correct, however, because a variety of very small particles and colloids may pass through a 0.45 µm filter (Grasshoff, 1983). Whatman GF/C and GF/F filter papers have larger poresizes of 1.2 µm and 0.7 µm respectively hence increasing the possibility for more particulate matter such as pico-planktonic cells to pass through the filter. Such large poresizes were considered unsuitable for this study.

Despite the small poresize in the filters used in this study any bacteria that might be present will be small enough to pass through the 0.45 µm poresize (K.Jones pers.comms, 1992) hence the requirement for preservation of the sample after its collection and filtration.

Filtration of the samples was by suction via a vacuum pump and this was kept to a pressure of between 100-150mm Hg (a pressure recommended for the filtration of chlorophyll samples; Tett and Grantham, 1978). Such a low pressure was used (double this pressure is recommended in Parsons *et al.*,1985), in order to minimise the possibility of contamination of the sample by destruction of planktonic cell membranes which would allow intercellular fluid into the filtrate (K. Jones, pers.comms., 1991).

4.2.1.2 Preservation and storage of samples

Method of preservation: As discussed in the previous section, even the use of a 0.45 μm poresize filter paper does not allow the eliminate all bacteria from the filtrate. Also it is assumed that filters have a uniform poresize which is rarely the case; the specified poresize is usually a mean value, hence there is a small potential for some particulate matter (i.e. > 0.45 μm in diameter) to pass through the filter paper (Grasshoff, 1983). While this is possible filter clogging will reduce the mean poresize once some water has been passed through. If any material that passes through the filter is planktonic then a combination of this and the bacterial activity may cause depletion of the original nutrient concentrations in the filtrate before it can be analysed. In order to try and minimise any such effect it was decided to preserve the samples through freezing until they were analysed. This should at least slow down any biological activity in the first instance and eliminate it once the sample is frozen solid. The addition of preservatives (such as chloroform or $HgCl_2$) was decided against since the addition of foreign substances to a sample increases the possibility of contamination and interference with the analysis of the nutrients themselves (MacDonald and McLaughlin, 1982). Also, as found by Fitzgerald and Faust (1967) addition of chloroform as a preservative, accelerates the release of labile phosphorus from plankton cells. Their samples were, however unfiltered. Despite this fact it was decided that addition of any phosphorus to the sample after filtration should not be risked, hence chloroform was not used in this study.

MacDonald and McLaughlin (1982) showed that freezing could be a reliable method of PO_4 storage provided turbid samples were first filtered. But they did find that the variance in the results increased if the samples were frozen for more than 2 months. For NO_3 they found that freezing was an acceptable method of storage although overall it caused a slight decrease in the measured NO_3 concentration. For SiO_4 they found that freezing was an effective method of storage for samples for which the salinity was > 27 PSU. Burton *et al.* (1970) had previously shown that samples for SiO_4 analysis which had salinities of < 27 PSU had to be left for several hours ("overnight") after thawing, before being analysed in order that polymeric Si might have a chance to depolymerise back to reactive silicon. Strickland and Parsons (1977) note that if analysis of nutrients has to be delayed for more than a few hours then the samples should be frozen in polyethylene bottles at a temperature not exceeding minus 20 °C, although they note that it is generally sufficient to put samples in a domestic-type freezer working at its lowest temperature setting. They state "we have found no evidence of changes in micronutrient concentrations at these low temperatures over a period of very many weeks". Grantham (1986) also used freezing (in polyethylene bottles) as a method of storage before analysis due to its simplicity as a storage method and its applicability to all the nutrients examined, which were NO_3, PO_4, SiO_4 and NH_4. He also used it in his Loch Linnhe study in 1990 (Grantham, 1991).

For the purposes of this study, an experiment was conducted to investigate the potential effects of freezing in the latter part of 1991, in connection with the analysis of some water samples collected for nutrient analysis in Spitsbergen, Norway. The aim of this was to check that no significant changes in the sample concentrations occurred during the transport of frozen samples from Norway to England in terms of their PO_4 concentrations. It involved the preparation of three standard PO_4 solutions by dissolving weighed quantities of NaH_2PO_4 (BDH) into Milli-Q deionised water in storage vials. These standards were then frozen along with all the other samples and their PO_4 concentrations analysed (after appropriate dilution) once back in England, after six weeks of storage. The maximum difference between the original concentration and the measured concentration was

5.3 % which was deemed satisfactory enough to run the rest of the samples. The reproducibility of the sampling was checked by collecting three samples from the survey area, filtering them through Millipore HA filter papers under vacuum, and then subsampling each sample into three separate vials with immediate freezing in a deep-freeze. The results for this were good with the maximum difference in results being 2 % of the average concentration for NO_3 and PO_4 and only 1% for SiO_4.

On the basis of this preliminary test and on the basis of the more extensive results from previous workers, the chosen method of storage for samples in this study was that of freezing. On the basis of the results from MacDonald and McLaughlin (1982) however, the samples were all analysed within two months of their collection in order to try and minimise any variations in the measured concentrations.

<u>Choice of storage vessel:</u> As stated previously the walls of the storage vessel may provide an excellent surface for the growth of bacteria and therefore the choice of storage vessel is an important factor in combatting bacterial growth. It is widely accepted however that there is no single universally applicable storage regime that will completely satisfy all requirements (Kirkwood, 1992). This introduces difficulties when one sample is retained for the analysis of a number of different nutrients. For example, storage in glass is unacceptable if silicate is to be analysed (Kirkwood, 1992) but Grasshoff (1983) recommends that glass bottles should be used for the storage of samples for analysis of PO_4 and NO_3. Zhiliang *et al.*, (1985) observed that polyethylene bottles were capable of halving the initial concentration of PO_4 in about 48 hours at room temperature whilst Kremling and Wenck (1986) have reported that polypropylene bottles are effective containers for the storage of PO_4 and other nutrients. Grantham (1986, 1991) used polyethylene bottles for storage of all nutrients.

The type of storage vessel used in this particular study was a disposable, polystyrene, 32 ml vial which, according to the manufacturer, Elkay Laboratory

Products, was "deionised and de-staticised to guarantee that each vial is particle free and chemically clean".

The polystyrene vials used in this study showed good precision for the samples collected as duplicates. For example, a random selection of the first ten samples collected on 03/04/91 showed that duplicate samples had an average precision of higher than 2 % for PO_4 analysis, whilst that for NO_3 was higher than 1 % and SiO_4 was 2.4 %. On the basis of this level of precision it was decided that the vials being used were adequate since it was probable that errors caused by adsorption onto vessel walls or uptake by bacteria would lead to erratic results and poor duplication between samples. It should be noted that this level of precision also includes the precision of the analysis itself i.e. the performance of the instrument (autoanalyser) plus any effects due to freezing of the sample between filtration and analysis.

4.2.2 Analytical methods for nutrient analyses

Automated analysis of the nutrients nitrate, phosphate and silicate were carried out using a hybrid Technicon/Chemlab autoanalyser (courtesy of B. Grantham, DML) using methods based on Grasshoff (1983). The autoanalyser was controlled by means of a BBC micro-computer and results were recorded both on this and on a 6 channel Chessell chart recorder.

The basic principles involved in the automatic analysis of nutrients are well-documented and not discussed here. For details of this aspect the reader is referred to Grasshoff (1983) and Hydes (1984).

4.2.2.1 Analysis of nitrate (NO_3)

The most sensitive and generally applied methods for the determination of NO_3 in seawater are based on the reduction of NO_3 to nitrite (NO_2), which is then determined via the formation of an azo dye. This basic method is based on the

work of Shinn (1941) and adapted for seawater by Bendschneider and Robinson (1952). Basically the NO_2 ion reacts with sulphanilamide to yield a diazo compound which then couples with N-1-naphthyl ethylene diamine dihydrochloride (NED) to form a soluble azo dye which can be measured photometrically.

The most common method of reducing NO_3 to NO_2 is via a heterogeneous reaction using cadmium granules coated in copper (which acts as a catalyst). It is described in Strickland and Parsons (1968) and is based on a method by Morris and Riley (1963) with some suggestions by Grasshoff (1964) and Wood *et al.*, (1967). Although this method is efficient and accurate, the preparation of the reduction column from cadmium is laborious, requiring the cutting and sieving of the filings. In addition, packing and regenerating the columns require special techniques to obtain efficient columns with satisfactory flow rates (Gardner *et al.*, 1976). To avoid such problems the type of column used in this study was that developed by Stainton (1974) in which a continuous cadmium (Cd) wire (1 mm diameter) is threaded inside teflon tubing of a similar diameter. Close matching of these diameters ensures good contact between the solution and the metal. The column is then activated by injecting 10ml quantities of 1M HCl distilled water, 2% copper sulphate solution and distilled water again.

As the NO_3 is passed through the column it is reduced to NO_2:

$$NO_3^- + Cd + 2H^+ \rightarrow NO_2^- + Cd^{2+} + H_2O$$

The yield of the reduction of NO_3 to NO_2 depends upon the metal used in the reductor, on the pH of the solution and on the activity of the metal surface (Grasshoff, 1983). In a neutral or weakly alkaline medium the Cd ions formed during the reduction of NO_3 react with hydroxyl ions and form a precipitate. This will obviously alter the pH and so a buffer is required; ammonium chloride (NH_4Cl) solution, adjusted to a pH of 8.5 to prevent further reduction of the nitrite leading to poor sensitivity and reproducibility (Collos *et al.*, 1992), is used for this

purpose. This is pumped through the column simultaneously with the sample. It also acts as a complexant:

$$2NH_4^+ \leftrightharpoons 2NH_3 + 2H^+$$

$$Cd^{2+} + 2NH_3 \leftrightharpoons [Cd\ (NH_3)_2]^{2+} \qquad \text{(Grasshoff, 1983)}$$

Use of this method means that any NO_2 already present in the sample before the reduction of the NO_3 will be measured along with the NO_2 from the reduction step. The method therefore gives a measure of the NO_3 plus the NO_2. NO_2 levels are, however, expected to be low in Loch Linnhe (Mr. B. Grantham, pers.comms., 1992); Solorzano and Ehrlich (1977) found the NO_2 levels in neighbouring Loch Etive to be low at ~0.2 µM, with highest values in the bottom water of up to 0.72 µM.

Interference in NO_3 Analysis: The most common problem to be encountered with this reduction method of NO_3 is that the reductor column may become less efficient with time. If the standard peak is reduced by < 10% then the reductor has to either be reactivated by passing approximately 200 ml of buffer solution through it containing ~ 100 µM NO_3 solution (Grasshoff, 1983), or else it should be replaced. The only other disadvantage with the method is that it does require the simultaneous determination of NO_2, as already noted.

4.2.2.2 Analysis of Phosphate (PO_4)

Dissolved inorganic phosphate (PO_4) exists in the sea in the form of orthophosphate ions. About 10% is present as PO_4^{3-} ions and practically all remaining PO_4 is present as HPO_4^{2-} ions (Grasshoff, 1983). Most methods allow for the measurement of orthophosphate and some easily hydrolysed organic phosphates and polyphosphates (although these will not be a major consideration as mentioned above), and it is now generally accepted that orthophosphate

approximates to the dissolved PO_4 immediately available to phytoplankton (Rigler, 1973).

All the methods for the determination of inorganic PO_4 in seawater are based on the reaction of the ions with an acidified molybdate reagent to yield a phosphomolybdate complex which is then reduced to a highly coloured blue compound. In early work, stannous chloride was used as the reductant. However, this reductant had several disadvantages including temperature dependence of the reduction rate and a salt error (Grasshoff, 1983). The automated analysis used in this study is the same as that described by Grasshoff (1983). This is based on a single reagent method first described by Murphy and Riley (1962). Essentially the method consists of the reaction of ammonium molybdate with PO_4 under acidic conditions to form a yellow colloidal phosphomolybdate complex. This is reduced to a highly coloured blue heteropoly compound by the ascorbic acid. Antimonyl ions present increase the rate of reaction and enter stoichiometrically into the product of this reaction resulting in a heteropoly complex containing antimony and phosphorus in the atomic ratio 1:1.

The single solution reagent is split into 2; the first reagent consists of sulphuric acid, ammonium molybdate and antimonyl ions, and the second consists of the ascorbic acid solution. By using 2 solutions the reagents are more stable (Grasshoff, 1983). To obtain a rapid colour development and to depress the interference of SiO_4, the final reaction pH must be < 1 and the ratio of the sulphuric acid to the molybdate, between 2 and 3 (Grasshoff, 1983).

Interference in PO_4 Analysis: The wash solution used in the analysis of PO_4 (and for all the nutrients) during this study was deionised water. This has the disadvantage that, when alternated with saline samples, it produces diffraction effects in the flowcell of the colorimeter at the changeover in liquids of differing densities (Grantham, 1986). This results in noisy signals at the beginning and end of each sample segment. The PO_4 method seems particularly prone to the problem. The remedy to this is to use a wash solution of the same salinity (and hence

refractive index) as that of the standard solutions and samples, but this requires large quantities of ANALAR grade NaCl, which is expensive. In the case of this study the PO_4 reading was based on the obvious peak between relatively noisy signals. Other possibilities of interference are that arsenate also reacts with molybdate under acid conditions and is reduced to a blue heteropoly acid. This reaction however, is much slower than the formation of the corresponding PO_4 compound and hence, the interference is insignificant at the low arsenate concentrations that may occur in seawater; 2.4×10^{-5} to 2.4×10^{-4} μM (Brewer, 1975). Silicate also forms a blue heteropoly acid with molybdate but only at a pH > 1 and the PO_4 reagent is acidified to a pH of 0.8-1.0.

4.2.2.3 Analysis of silicate (SiO_4)

The determination of SiO_4 in the orthosilicate form in seawater is based on the formation of a yellow silicomolybdate complex, when an acidified seawater sample is reacted with molybdate solution. It is feasible that absorption of this yellow silicomolybdic acid itself could be used to determine the SiO_4 concentration photometrically (Robinson and Thompson, 1948). However the sensitivity of this is such that only concentrations of >50 μM can be analysed. A blue heteropoly acid with a much higher extinction coefficient, may be obtained by the reduction of the silicomolybdic acid using metol (p-methylaminophenol sulphate) and sodium sulphite (Mullin and Riley, 1965), or ascorbic acid (Koroleff, 1976). Oxalic acid is also introduced into the sample stream to react with any excess molybdate and prevent the formation of a phospho-complex. The method used in this study is that described by Grasshoff (1976) which uses metol/sulphite as the reductor.

At the pH of seawater, silicic acid will readily polymerise. During the automated determination described above, only straight chain polymers of short length (up to 3 or 4 silicic units), will react with the molybdate in the time allowed for the reaction to occur. Hence the remainder is essentially unreactive (Grantham, 1986). This may be advantageous since the reactive portion of the dissolved SiO_4 probably represents that which is in a suitable form for uptake by phytoplankton, (Strickland

and Parsons, 1968).

For samples of salinities < 27 PSU, analysis should be carried out several hours after thawing (assuming they have been frozen for storage), in order that any polymeric silicon produced has a chance to depolymerise back to reactive silicon (Burton *et al.*,1970).

Interference in SiO_4 Analysis: There is no interference from other compounds present in natural waters other than PO_4 concentrations above 5 µM (Grasshoff, 1983), which do not occur in Loch Linnhe.

4.2.2.4 Blanks, Reagents and Manifold Configurations

Blanks and Standard Stock Solutions

The absorbance peak obtained by an automated system for a given nutrient in a seawater sample (when compared to a distilled water baseline) represents the sum of absorbance from at least four sources: (i) the light loss due to the differences in the index of refraction of the seawater and the distilled water (DW); (ii) reaction products (i.e. precipitates) of appropriate wetting agents and the seawater; (iii) the absorbance of coloured substances in the sample either particulate or dissolved and (iv) reaction products of the nutrient in the sample and the colour reagents (Glibert and Loder, 1977). These reaction products may be variable due to a salt error caused by the shift in the position of equilibrium as a function of a change in the ionic strength of the solution (Brewer and Riley, 1965).

For the automated analysis of all samples, a wash of deionised water (DW) between samples was used, which provided a baseline for the results. To avoid the problem of increased intensity of signal due to the difference in the refractive index between the DW and the samples the wash should have been of the same refractive index as the sample. However, as mentioned previously in connection with the PO_4 analysis, the use of artificial seawater (ASW) for this purpose would

be very expensive. In order to minimise this refractive index error, an ASW blank and a DW blank are run at the start and finish of every batch of samples. The average DW blank signal is then subtracted away from the ASW blank signal and the result is then subtracted from the signals of the standards to allow for any increased absorbance in the standard signal due to a difference in the index of refraction of DW and the standard solution and any increase in nutrients due to the composition of the ASW itself. The average ASW blank signal minus the average DW signal is also subtracted away from sample signals during a run to account for the refractive index error between samples and the DW wash, but doing this may cause errors:

Alvarez-Salgado *et al.*, (1992) investigated the use of a phosphate blank in the determination of nutrients by automated analysis. They considered the problem of increased intensity of nutrient signals due to the difference in the refractive index between the low nutrient seawater (LNSW) used for preparation of standard solutions and the zero nutrient blank used with the samples. They considered solving the problem by making up a blank with the same refractive index as the standards using an artificial seawater solution (ASW) prepared with sodium chloride (NaCl) but they point out the problem that no matter how pure the NaCl used it will contain PO_4 which might exceed the level of PO_4 in the LNSW and hence be unsuitable as a blank. To overcome this problem they used LNSW, from which the PO_4 had been removed through the addition of ferric chloride ($FeCl_3$), for making up both the standard solutions and the blank. Through the use of ASW for both the standard preparations and for the blanks in this study, subtraction of the average ASW blank signal minus the average DW signal, away from the standard signal would account for any additional PO_4 present in the ASW and there will be no difference in the refractive index between the standards and the blanks. In this study the average ASW blank signal minus the average DW blank signal is effectively subtracted from the sample signals as well to account for any increase in the absorbance due to a difference in refractive index between the DW wash and blank, and the sample so that if the ASW contains PO_4 then this will cause an underestimation in the PO_4 content of the samples. This error would

have been insignificant however, since the NaCl used to prepare the ASW (BDH analytical grade) contained only 0.0005 % by weight of PO_4, corresponding to 1.32 x 10^{-3} µmoles of PO_4 in 25 g NaCl, and the $MgSO_4$ also used in the preparation of the ASW does not contain any PO_4 as an impurity. It is now, however, standard practice to make up the standard solutions in PO_4 free ASW and to use the same medium as a PO_4 free blank in accordance with the methods described in Alvarez-Salgado *et al.*, (1992).

With regard to a salt error, caused by changes in salinity and thus the ionic strength of the sample solutions, these were minimised by preparing standard solutions for each nutrient from stock solutions prepared with ASW. The ASW was prepared according to Strickland and Parsons (1968): 25g NaCl + 8g $MgSO_4$ made up to 1 litre with DW. This results in ASW with a salinity of 28 PSU. It seems unlikely however, that a salt error will be significant for the nutrient analyses used in this study since Strickland and Parsons (1977) report that for NO_3 and NO_2 analysis the method is not effected by the salinity and Grasshoff (1983) report that a salt error of < 3 % is observed for SiO_4 for salinities ranging from 25 to 35 PSU (hence, for the majority of samples analysed in this study) and that it can be "neglected in most applications". Grasshoff (1983) does not mention a salt error in the PO_4 analysis and recommends that the stock standard solutions be prepared in DW (as c.f. ASW for SiO_4 standards). Strickland and Parsons (1977) also do not mention a salt error for PO_4. Atlas *et al.*, (1971) however, report that the salt error for the PO_4 analysis is < 2 % at a salinity of 33 PSU.

Reagents:

NO_3 Analysis: Reagents for this analysis were prepared exactly as described in Grasshoff (1983). They were (i) an NH_4Cl buffer: 75 g ammonium chloride is dissolved in 5 litres of distilled water and the solution is adjusted to a pH of 8.5 with about 12 ml of ammonia; (ii) sulphanilamide solution: 5 g sulphanilamide and 50 ml concentrated hydrochloric acid are transferred into 500 ml distilled water, dissolved and made up to 1 litre; (iii) a coupling reagent of NED: 0.5 g of

NED is dissolved in 1 litre of distilled water together with 1 ml of the surfactant, 10 % Brij 35 and (iv) a standard stock solution of 1.011 g potassium nitrate (KNO_3) prepared in 1 litre ASW (a modification to Grasshoff (1983) who recommends DW) to give a solution of 10 µ moles ml^{-1} NO_3 concentration.

PO_4 Analysis: Reagents were again prepared according to Grasshoff (1983); (i) Ascorbic acid solution: 6 g of ascorbic acid plus 1 ml of 0.5 % w/v sodium dodecyl sulphate detergent (a modification to Grasshoff (1983) who recommends Levor IV as a detergent) are made up to 1 litre with distilled water; (ii) the mixed reagent: 10 g of ammonium heptamolybdate tetrahydrate $(NH_4)_6Mo_7O_{24}.4H_2O$ plus 20 ml of an aqueous antimony potassium tartrate solution (2.3 %) and 67 ml of concentrated sulphuric acid (H_2SO_4), all diluted and made up to 1 litre and (iii) a standard stock solution of 1.361 g potassium dihydrogen phosphate made up to 1 litre in ASW (a modification to Grasshoff, (1983) which recommends DW), to give a solution of 10 µ moles ml^{-1} PO_4 concentration.

SiO_4 Analysis: Reagents were prepared according to Grasshoff (1983); (i) molybdate reagents: 7 g sodium molybdate ($Na_2MoO_4.2H_2O$) and 26 ml of 3.6 molar sulphuric acid are dissolved and made up to 1 litre with double distilled water; (ii) complexing reagent: 6 g oxalic acid ($C_2H_2O_4$) is dissolved and made up to 1 litre with double distilled water; (iii) reducing reagent: 10 g of metol (p-methylaminophenol sulphate) and 12 g of sodium sulphite are dissolved in 1 litre of double distilled water and (iv) a standard stock solution of 1.88 g sodium hexafluorosilicate (Na_2SiF_6) prepared in 1 litre of ASW to give a solution of 10 µ moles ml^{-1} SiO_4.

Manifold Configurations: All flowcells were 50 mm in length. Wavelengths in the colorimeter were set at 540 nm for NO_3; 880 nm for PO_4 and 810 nm for SiO_4.

Pumping rates, (determined by the diameters of the tubing used), for each analysis are given in **TABLE 4.2**

TABLE 4.2

Pumping Rates used for the Analyses of Nutrients on the Technicon / Chemlab Autoanalyser

Analysis	Parameter	Pumping Rate (ml/min)
Nitrate	Sample	1.00
	Buffer	0.60
	NED	0.10
	Sulphanilamide	0.10
	Air	0.42
	Pullthrough (flowcell)	1.00
Phosphate	Sample	1.40
	Ascorbic acid	0.16
	PO_4 mixed reagent	0.16
	Air	0.42
	Pullthrough (flowcell)	1.20
Silicate	Sample	0.60
	Molybdate	0.32
	Oxalic acid	0.32
	Metol/sulphite	0.32
	Air	0.32
	Pullthrough (flowcell)	1.00

4.2.2.5 Calibration and Precision of the Autoanalyser

The basic principle behind the automated analysis of dissolved nutrients is that a continuous stream of sample is taken from the sample vial, reagents added in a closed tubing system and the constituent in question converted to a compound that, in a flow-through colorimeter, produces an extinction related to its concentration. This relationship is often assumed to follow Beer-Lambert's law which states that the logarithm of the ratio of light intensities before and after passage through the sample solution is related linearly to the concentration of the detected component:

$$\log (I_o / I) = E.C.l$$

Where: I_o = Initial light intensity;
I = Intensity after passing through the sample solution;
E = Extinction coefficient;
C = Concentration of the absorbing compound;
l = optical path length;

(Grasshoff, 1983).

However, a non-linear relationship between extinction output and the concentration of the sample may occur due to a number of effects: ageing of the peristaltic pump tubing may modify the sample dilution; precipitates may form on the cuvette walls thus changing the colorimeter response; temperature effects may alter the position of the equilibrium of the reaction leading to the formation of the colorimetrically detected compound; the stability of some of the reagents is limited (Grasshoff, 1983). For this reason the linearity of the extinction output should be checked regularly through calibration experiments. During this study such experiments were carried out (a) at the start of any new batches of samples, (b) if the autoanalyser had been not been running for a length of time or had been physically moved for any reason and (c) if any parts of the autoanalyser had been replaced, for example the peristaltic tubing or the Cu / Cd reduction coil, which would affect the efficiency of the instrument.

Single concentration standards were then included with each run of samples to convert sample signals linearly to concentrations (micromolar).

The calibration experiments involve measuring the output of a standard dilution sequence so that the relationship between the output and a known concentration of nutrient can be established. These were carried out through the preparation and use of mixed standard stock solutions (reagents for which were listed in the previous section - section **4.2.2.4**). Seven mixed standard solutions were prepared and labelled A - G. The concentrations ranged from 1 - 10 µM for NO_3, 0.2 - 2.0 µM for PO_4 and from 2 - 20 µM for SiO_4 over the seven standards. The concentrations per standard can be found in **APPENDIX 4.1**. The standards were prepared in ASW as was the standard blank. The wash for the baseline determination was DW. Each standard was analysed four times and the carousel on the autoanalyser was set up so as the samples were run in the following order: DW, A - G, ASW, G - A, ASW*2, DW, A - G, ASW*2, G - A, ASW*2, DW, DW. From this both an estimate of the precision of each method could be obtained, and also the calibration curves for each nutrient could be plotted. A typical set of calibration results and plots from such a calibration experiment can be found in **APPENDIX 4.1**. For all of the calibrations carried out during this study the resultant plots were considered close enough to linearity (NO_3 concentrations within the limits of ± 0.21 µM away from a calibration line; PO_4 concentrations ± 0.08 µM and SiO_4 concentrations ± 0.23 µM) that the calculations of the nutrient concentrations from the autoanalyser traces could be carried out using a linear calibration. This was facilitated through the use of a program written into a Hewlett Packard 32S Scientific calculator, (courtesy of Mr. B. Grantham, DML).

The precision and limit of detection of each method were calculated from the standard deviation of the 28 standard samples, thus covering the whole of the analytical range during a calibration. The precision (95 % confidence limits) was taken as 2*standard deviation divided by the square root of Pi (from Youden, 1951) and the detection limit as 3*standard deviation of the DW blank. Results for precision and detection limits calculated from a typical calibration experiment are

given in **APPENDIX 4.1** and compared to results reported by Grasshoff (1983) in **TABLE 4.3.**

TABLE 4.3

Precision and Detection Limits for the Autoanalyser Based on Results from a Typical Calibration Experiment (precision and detection limits as reported by Grasshoff, (1983) given in brackets)

	NO_3 µM	PO_4 µM	SiO_4 µM
Precision	0.19 (0.1)	0.07 (0.06-0.10)*	0.13 (0.1)
Limit of Detection	0.04 (?)	0.01 (0.02)	0.10 (0.1)

* 0.06-0.10 µM is the precision for a range of samples from 1 - 3 µM PO_4 respectively.

4.3 Analytical Techniques for Sediment Samples

In 1993 a small study was made of the sediment composition of the upper basin of Loch Linnhe (see section **4.1.4**) with the aim of identifying any major mineralogical changes along the salinity gradient, from the saline end-member (LL0) to the freshwater end of the loch (the River Lochy), and how such changes might affect the phosphorus content of the sediment (see **CHAPTER 6**, section **6.2.1.2**). The two main analytical techniques used in this study were that of x-ray

diffraction (XRD) and x-ray fluorescence (XRF) and these were carried out at the Post-Graduate Research Institute of Sedimentology at Reading University with the help of Dr. G. Paterson and Dr. A. Parker. The sediment core samples were transferred to Reading University within four days of their collection and were transported in their original state in the core tubes with the overlying seawater present.

4.3.1 X-ray diffraction techniques

X-ray diffraction (XRD) is a technique that is used to qualitatively and semi-quantitatively analyse sample mineralogy. The following description of XRD is taken from Zussman (1977). The basis of XRD is that x-rays which are generated from the bombardment of a beam of electrons on a copper (Cu) target are allowed to strike the sediment sample, which is in the dried, ground state. The x-rays penetrate below the surface of any crystals present in the sediment and are then diffracted from successive atomic layers and these diffracted rays may or may not be in phase. The condition for a maximum diffracted intensity is that the contribution from the successive planes in the crystal lattice should be in phase. If interplanar spacing is denoted as d, then this condition is expressed by Braggs Law:

$$n.\lambda = 2.d.\sin\theta$$

where; λ = x-ray wavelength;

n = integer;

θ = Bragg angle.

So that for a given set of planes with spacing d, the diffraction can be regarded as occurring with a phase difference of $n.\lambda$.

Crystal planes with a given d value, which occur in a finely powdered specimen, occur in all possible orientations and give diffractions of x-rays along the surface of a cone, with semi-angle equal to $2.\theta$. These then hit the detector (a photographic film) to form two arcs, the distance between which is measured. From this

distance the corresponding Bragg angle can be determined and the d-values then obtained from Bragg's Law. Any set of d-values will be unique to a certain mineral and, as long as there is a reference relating the d-values to the mineral, the mineral content of the sediment can be determined. In this study the reference used was a table of key lines compiled by Pei-Yuan Chen (1977). Semi-quantitative analysis was carried out after Hooton and Giogetta (1977) (see also **CHAPTER 6**, section **6.2.1.2**). Semi-quantification of the minerals (in terms of percentage weight of the sample) is achieved through the measurement of peak heights from the XRD trace, each of which is then multiplied by an appropriate 'H' factor for that particular mineral. 'H' factors are unique for any one mineral for any one particular x-ray diffraction instrument and tables of these factors are therefore compiled for individual instruments. The theory behind the use of this factor is that it allows for the determination of the composition of a sample from the trace alone, without the use of standards and calibration curves in the analysis (Hooton and Giorgetta, 1977). H is determined for any one mineral through the 1:1 mixing of a pure mineral standard and the reference sample to be used on the machine and it is defined as:

$$H = [weight_{std} / weight_{ref}]*I_{ref} / I_{std}$$

where; I_{ref} = the intensity of the diffraction pattern of the reference sample,
I_{std} = the intensity of the diffraction pattern of the standard sample,
$weight_{ref}$ = the weight of the reference sample used,
$weight_{std}$ = the weight of the standard mineral used,

(G. Paterson, 1992, pers.comms.).

The factorised peak heights obtained are then added and the percentage of each factorised peak height of the total is then calculated. Further information on the physical methods involved in mineralogy can be found in Zussman (1977).

4.3.1.1 Sample preparation for XRD analysis

From each wet sediment core sample, approximately 8 cm^3 of sample was scooped

out of the surface, using a plastic spatula, and placed in a labelled crucible. This was then dried in an oven for approximately 6 hours at 60 °C which was then turned down to 40 °C and the samples left overnight. Samples were then ground to a fine powder using a ball mill (a Fritsch Pulverisette Analysette Laborette (made in Germany)). This consisted of pots each containing 5 sylon balls that pulverised the sample as the pots rotated in a planetary motion with the rest of the instrument. The fine powders were then transferred to greaseproof paper bags for storage.

For the XRD analysis the dried, ground specimens were packed into aluminium (Al) cavity mounts using the reverse-fill technique (see Zussman, 1977, for details) and were then ready for analysis.

4.3.1.2 XRD instrumentation

This consisted of :

(i) a Philips PW1050 goniometer;
(ii) a Philips PW1730 high voltage generator;
(iii) Sietronics SIE112 microprocessor control.

The instrument was set up for: 1 degree divergence, 0.2 degree scatter and 1 degree receiving slits with a nickel (Ni) filter.

Voltage was 35 kV; current, 55 mA and Cu K alpha radiation for the x-rays.

Scans were carried out to detect Bragg angles over the range of $2.\theta = 4 - 64°$ at 0.02 degree steps at a rate of 2 degrees per minute.

4.3.2 X-ray fluorescence (XRF) techniques

These allow for a chemical analysis namely the elemental identification of the sediment content, to be carried out on the dried sediment sample. The method

basically involves striking the sediment sample with a beam of x-rays generated from a Cu target (as for XRD). The energy emitted from the sample as fluorescence, as the electrons ejected from their orbitals as a result of the striking x-rays, fall down to fill lower energy levels, is characteristic for each element and thus elements can be identified through its measurement. Results from this analysis give the percentage weight fraction of the following compounds: P_2O_5; Fe_2O_3; Al_2O_3; Na_2O; MgO; SiO_2, K_2O; CaO; TiO_2 and MnO along with concentrations (ppm) of the trace elements: V, Cr, Co, Ni, Cu and Zn. See Zussman (1977) for more details on the methodology.

4.3.2.1 Sample preparation for XRF

Two grams of the dried powder sample, obtained as in section **4.3.1.1** for XRD analysis, is mixed with boric acid and pressurised to form pressed powder pellets which are then used in the XRF analysis. It should be noted that the accuracy of phosphorus measurements using XRF could be increased by using fusion beads instead of pressed powder pellets (G.Paterson, 1994, pers.comms.).

4.3.2.2 XRF instrumentation

The instrument used for XRF analysis was a Philips PW1480 sequential x-ray fluorescence spectrophotometer. The x-ray tube was a scandium / molybdenum dual anode with 3 kW at 100 kV maximum power. The analytical software used was Philips X40.

CHAPTER 5 RESULTS FROM THE 1991 FIELD-SEASON

In the **INTRODUCTION** it was explained that the main aim of this study is to identify and isolate the processes that control the distribution of dissolved inorganic nutrients in a fjord system such as a sea-loch. This involves (a) study into the main hydrographic processes that occur within the loch since these will determine the physical distribution of nutrients throughout the loch and, (b) a study into the biological and geochemical (i.e. biogeochemical) processes that will affect the distribution by affecting the phase changes of the nutrients. The 1991 and 1992 field-seasons were therefore designed to try and provide this information but, as was mentioned in **CHAPTER 4**, the 1991 field-season could only be considered a preliminary study since there were limitations in the nutrient sampling strategy, namely no sampling below 60 m on the majority of the sampling dates, which resulted in an incomplete picture of the nutrient distributions in the bottom-waters. However, basic deductions could be made from the 1991 field-season results and on the basis of these a fuller sampling strategy for the 1992 field-season was designed.

This chapter will initially present results from the 1991 hydrographic investigations, considering the spatial and temporal features observed. It will then progress to consider the nutrient results in a similar fashion.

5.1 Hydrographic Results

The hydrographic results to be described here are the salinity, density and temperature results collected as described in **CHAPTER 4**, section **4.1.2.** It should be noted at this point that the "density" referred to in the text is the quantity known as sigma-t, which is defined as the density difference of the water sample when the total pressure on it has been reduced to atmospheric (i.e. the water pressure is equal to zero), but the salinity and temperature are as *in situ* (Pickard and Emery, 1982). In terms of units, the density of seawater is expressed physically in units of kg m^{-3} and in the open ocean values range from about

1021.00 kg m^{-3} (at the surface) to 1070.00 kg m^{-3} (at 10,000 m depth). As a matter of convenience it is usual to quote only the last four of these digits so that sigma-t is equal to the density minus 1000. Because sigma-t of seawater is measured relative to pure water, strictly speaking it has no units, however in formulae and in this text it will be treated as having units of kg m^{-3} (following Pickard and Emery, 1982 and UNESCO, 1991[2]).

The hydrographic measurements were made at eight stations along the longitudinal axis of the loch (from station LL0, seaward of the sill to station LL19, at the freshwater end of the loch), for most of the field-season spanning Julian days 79 to 127 (with the Julian days starting from 01st January 1991). Two extra stations (LL20 and LL21) were included in the surveys on two dates towards the end of the field-season. All of the stations sampled, their positions and depths, are listed in **CHAPTER 4, TABLE 4.1.**

To illustrate the general spatial and temporal hydrographic features observed in 1991, only five of the eight stations have been selected for discussion, since it was found that all of the stations in the upper basin exhibited very similar trends in their salinity, density and temperature distributions (although CTD data from all eight stations were used to create the longitudinal sections in **FIGURES 5.1** to **5.3**). All of the CTD data is provided on floppy disc and labelled as **APPENDIX 5.1.** The five stations considered are (i) station LL0, a relatively shallow station (~ 40 m depth) situated seaward of the sill and chosen to represent the saline end-member condition, (ii) station LL4, a relatively deep station (~ 110 m depth) in the upper basin, at the seaward end, (iii) station LL10 which is also a deep station (~ 107 m depth) between stations LL4 and LL14; (iv) station LL14, a deep station (~ 110 m depth) situated in a relatively central position in the basin, such that the energy from the density currents set up at the sill at the saline end, and the currents set up by the barotropic flow of the rivers at the freshwater end, is generally dissipated at this station (Gade and Edwards, 1980), and (v) LL19 which is a relatively shallow station (~ 40 m depth) situated closest to the freshwater end of the loch.

5.1.1 Spatial features in the upper basin

This section considers spatial differences in the loch, by considering the upper basin in terms of a longitudinal section. Hydrographic parameters are presented for the longitudinal sections in the form of contour maps (**FIGURES 5.1** to **5.2**) for two separate sampling dates; day 79, the first day of the field-season and day 127, the last day of the field-season. These were produced using the UNIMAP software package, the settings for which are given in **APPENDIX 5.2**.

FIGURES 5.1 (a) and **(b)** show the longitudinal distributions of density and salinity respectively, as present in the upper basin on day 79. The water shows vertical stratification according to the density and salinity structures. This stratification appears to occur throughout most of the water column, which becomes relatively homogeneous only at depths of greater than 95 m throughout the basin, below which the total change in density is less than 0.1 kg m^{-3} and that of salinity less than 0.1 PSU, to the bottom. The salinity appears to determine the density structure of the water column with the salinity field exhibiting vertical stratification in exactly the same patterns as the density. The water temperature however, appears to play a negligible role, remaining relatively homogeneous throughout the water column as shown in **FIGURE 5.3 (a)** with an observed maximum change in temperature of 0.01 °C from 5 to 10 m depth to the bottom of the basin. In areas of temperate latitude sea temperatures (10 °C to 15 °C), a temperature change of 5 °C is required to bring about the same change in density as a 1 PSU change in salinity (UNESCO, 1981, 1983), which explains why the salinity field determines the density field in Loch Linnhe. At station LL14, for example the temperature difference between the surface (0 m) and the bottom-water (110 m) is 0.5 °C (see **FIGURE 5.3 (a)**) whereas the corresponding salinity change is much larger, at a value of 12.1 PSU. Such a large change in salinity would require a corresponding 60 °C change in temperature to bring about the same change in the density structure and hence the role of temperature in the loch is rendered negligible in determining the density.

FIGURE 5.1

Longitudinal Structure of (a) Density and (b) Salinity in the Upper Basin on Day 79, 1991.

(a)

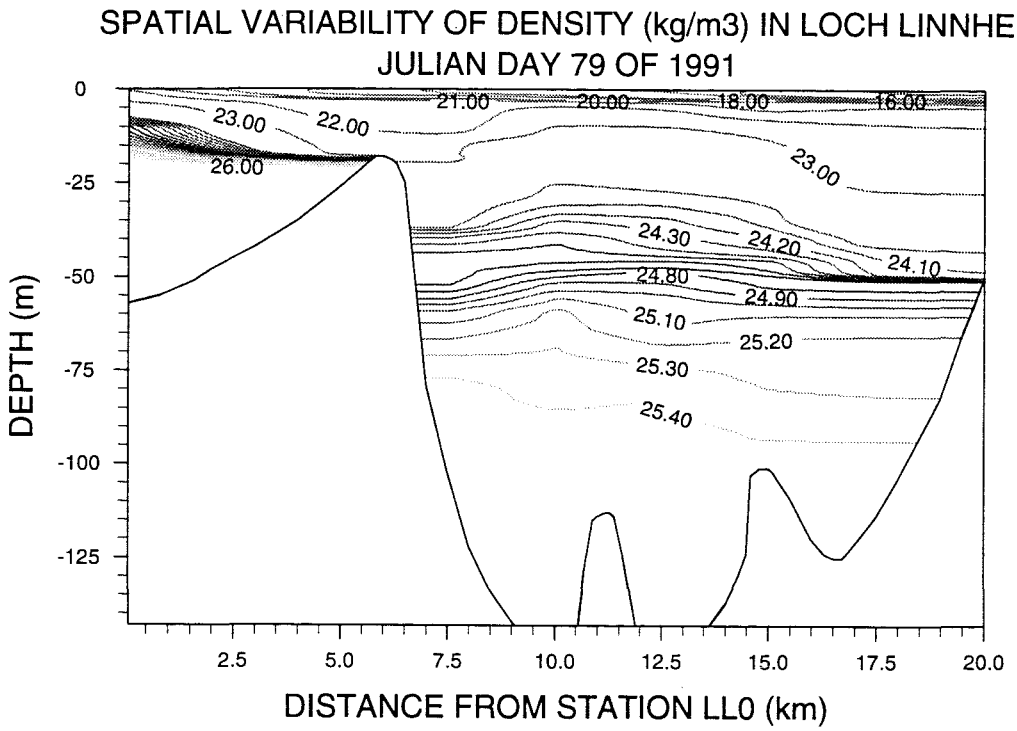

(b)

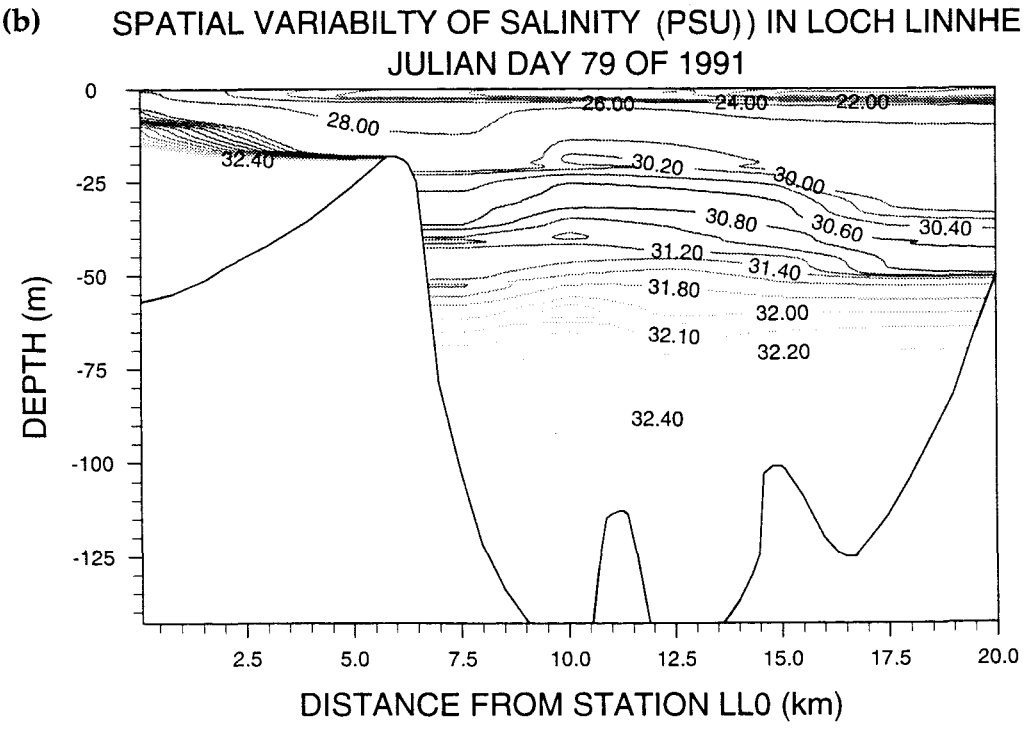

FIGURE 5.2

Longitudinal Structure of (a) Density and (b) Salinity in the Upper Basin on Day 127, 1991.

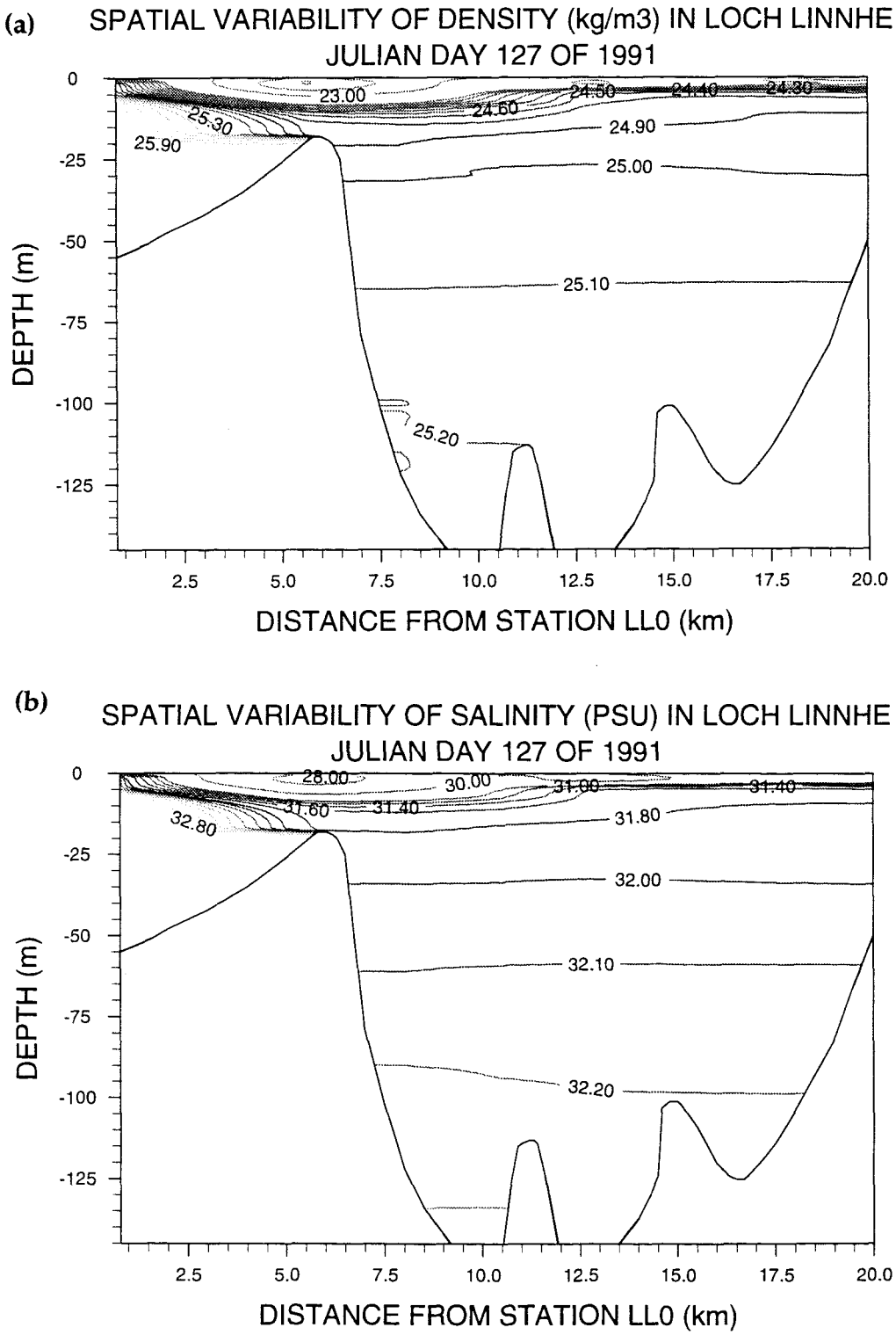

FIGURE 5.3

Comparison Between the Longitudinal Temperature Structure Present in the Upper Basin on (a) Day 79 with (b) Day 127, 1991.

(a)

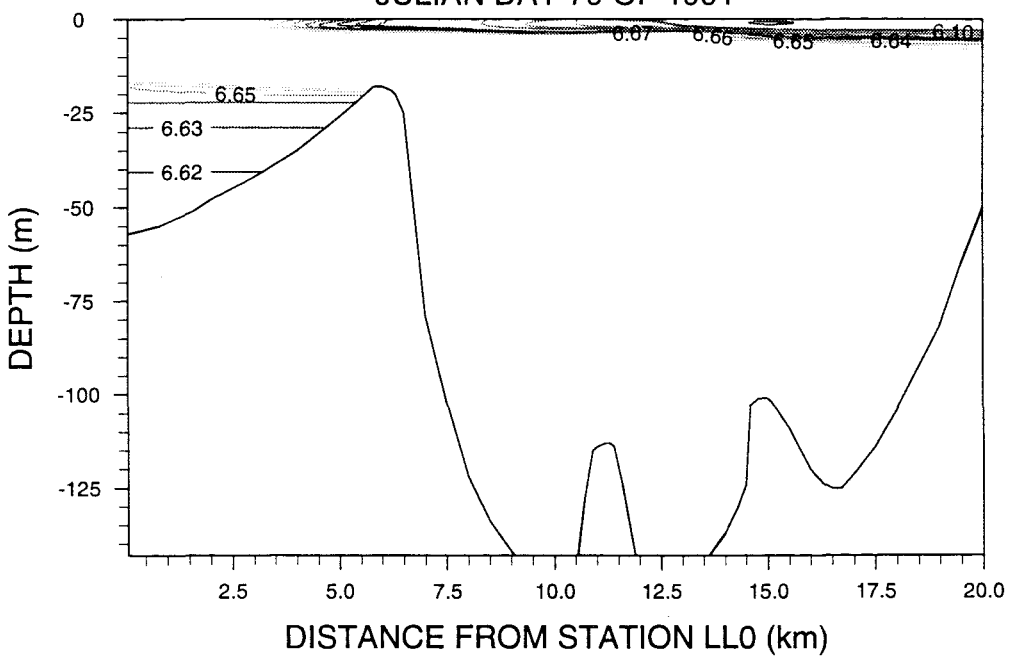

(b)

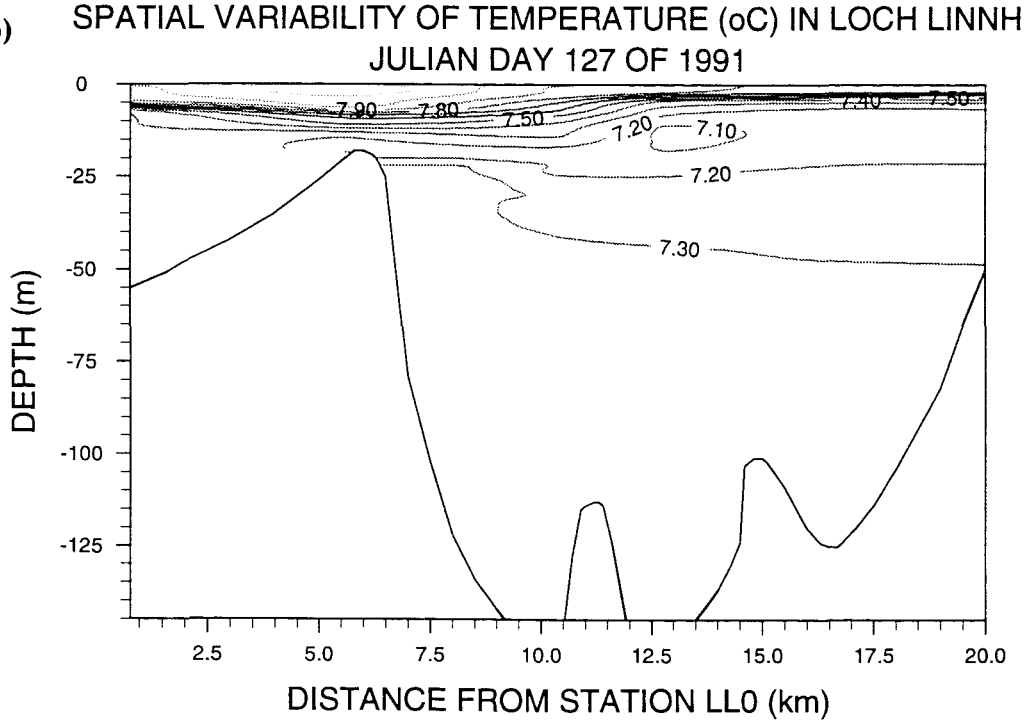

In terms of the horizontal structure of the basin, **FIGURES 5.1 (a)** and **(b)** show that the density and salinity are generally horizontally uniform. There are, however, slight horizontal gradients to be noted which are a reflection of the freshwater inputs from the Rivers Lochy and Nevis, at the head of the loch. For example, on day 79 surface (0 m) salinity values increase along the upper basin (although the trend is not of a continuous increase with distance in the centre of the loch), from station LL19 to station LL0 in the following way.

Station	**LL19**	**LL14**	**LL10**	**LL4**	**LL0**
Salinity (0 m, PSU)	14.45	20.34	20.29	19.97	28.64

The deeper more southerly stations show little variation in their surface salinities (maximum change is 0.37 PSU). Considering the spatial variations in the basin on the last day of the field-season (day 127) for comparison, it can be seen from **FIGURES 5.2 (a)** and **(b)** that the system is now relatively well-mixed with the maximum change in salinity between 15 m and the bottom of the basin being only 0.4 to 0.5 PSU as compared to a change of 2.4 to 2.5 PSU on day 79. Thus between days 79 and 127 some process has occurred throughout the basin to cause vertical mixing of the water column. Water becomes homogeneous on day 127, in terms of its density and salinity at depths greater than ~ 100 m throughout the basin, (where density changes are less than 0.1 kg m^{-3} and salinity changes less than 0.1 PSU), similarly to the situation on day 79. Again the temperature structure of the basin water on day 127 shows very little change throughout the whole water column with the maximum change in temperature recorded as 0.34 °C at station LL14 (**FIGURE 5.3 (b)**).

In terms of horizontal structure on day 127, again the density and salinity properties are generally horizontally uniform across the whole basin, with slight gradients (although not a continual trend) from the freshwater to the saline end:

Station	LL19	LL14	LL10	LL4	LL0
Salinity (0 m, PSU)	30.96	30.93	30.82	27.66	32.21

These salinity values are much higher than those observed on day 79 with a 16.51 PSU change in salinity observed between days 79 and 127 at 0 m at station LL19. This is a reflection of the drier weather around day 127 as confirmed by **FIGURE 5.4**, which shows the decreased total riverine flow into the system at and around this time. The total riverine inflow decreased from 180 m^3s^{-1} on day 79 to 9 m^3s^{-1} on day 127. The observed increase in salinity is also accompanied by an increase in the temperature of the surface layers with an increase of 1.90 °C between days 79 and 127.

5.1.2 Temporal variations in the hydrography

To investigate the temporal variations in the upper basin, time-series contour plots have been produced using data from the five aforementioned stations. The UNIMAP software package was again used to achieve this and the settings used are given in **APPENDIX 5.2**. The plots are given in **FIGURES 5.5, 5.6, 5.7, 5.8** and **5.9** for temporal changes in density and salinity at stations LL0, LL4, LL10, LL14 and LL19 respectively. Only one exemplary time-series plot to show temporal changes in the temperature structure is given and this is for station LL14 (**FIGURE 5.10**). This is because, as in the previous section, the role of water temperature will be negligible in terms of determining changes in the density structure of the water column.

FIGURE 5.4

Variation of the Mean Daily Flow Rate of the Total Riverine Flow (River Lochy plus River Nevis) with Time, Julian Day 0 to 366, 1991 (Data Courtesy of the HRPB).

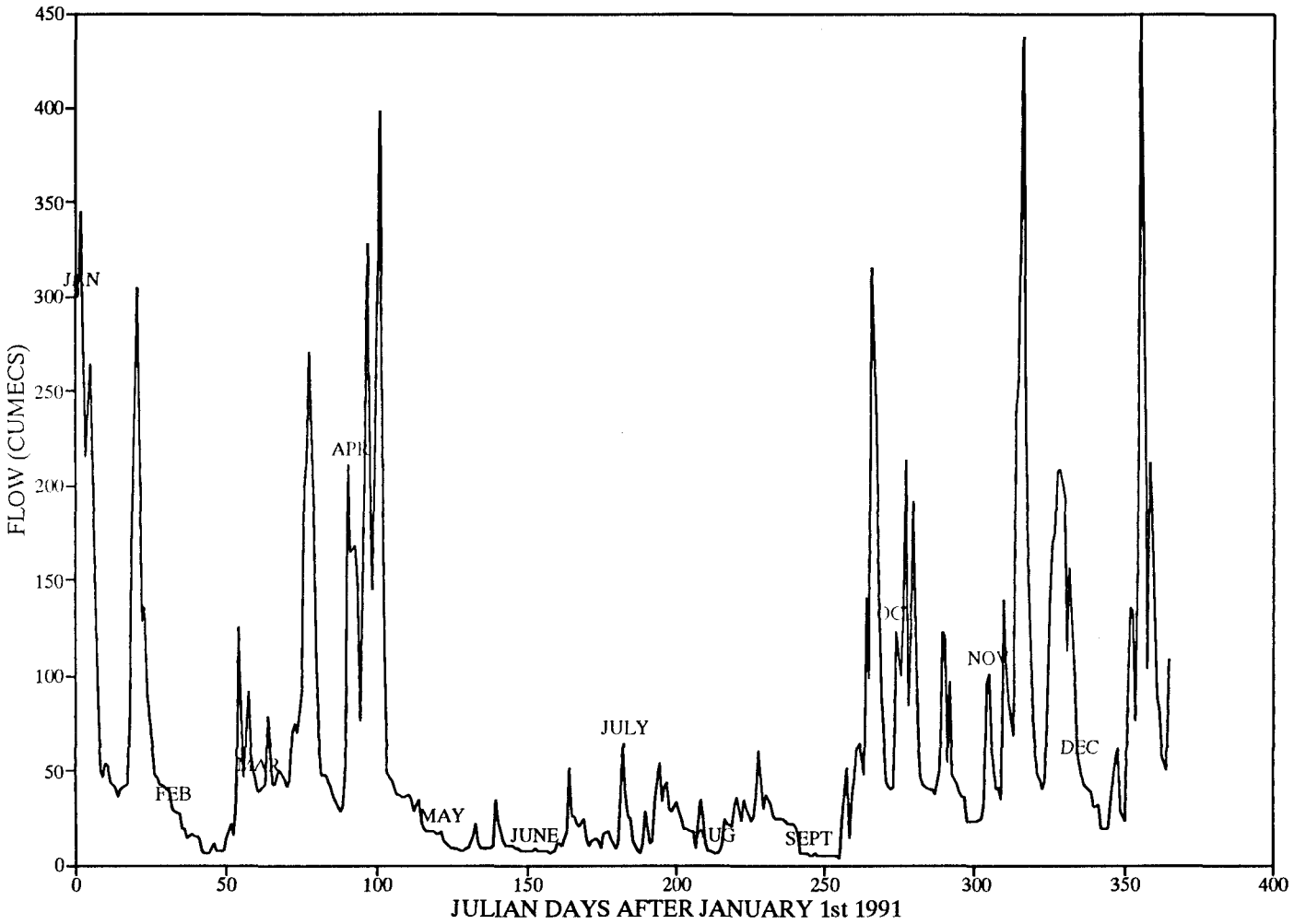

FIGURE 5.5

Temporal Variations in (a) the Density (kg m^{-3}) and (b) the Salinity (PSU) at Station LL0, Julian Day 79 to 127, 1991.

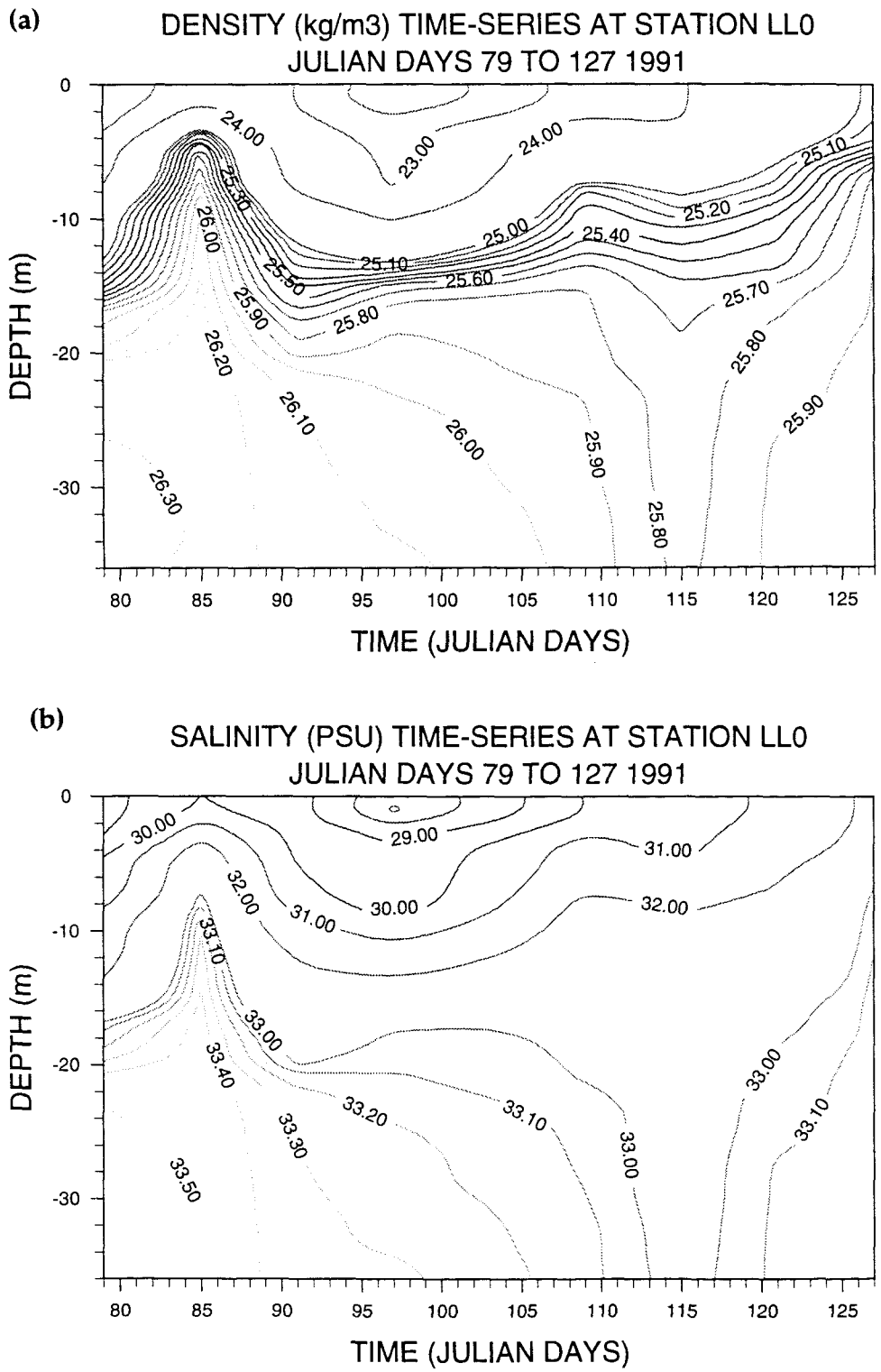

FIGURE 5.6

Temporal Variations in (a) the Density (kg m^{-3}) and (b) the Salinity (PSU) at Station LL4, Julian Day 79 to 127, 1991.

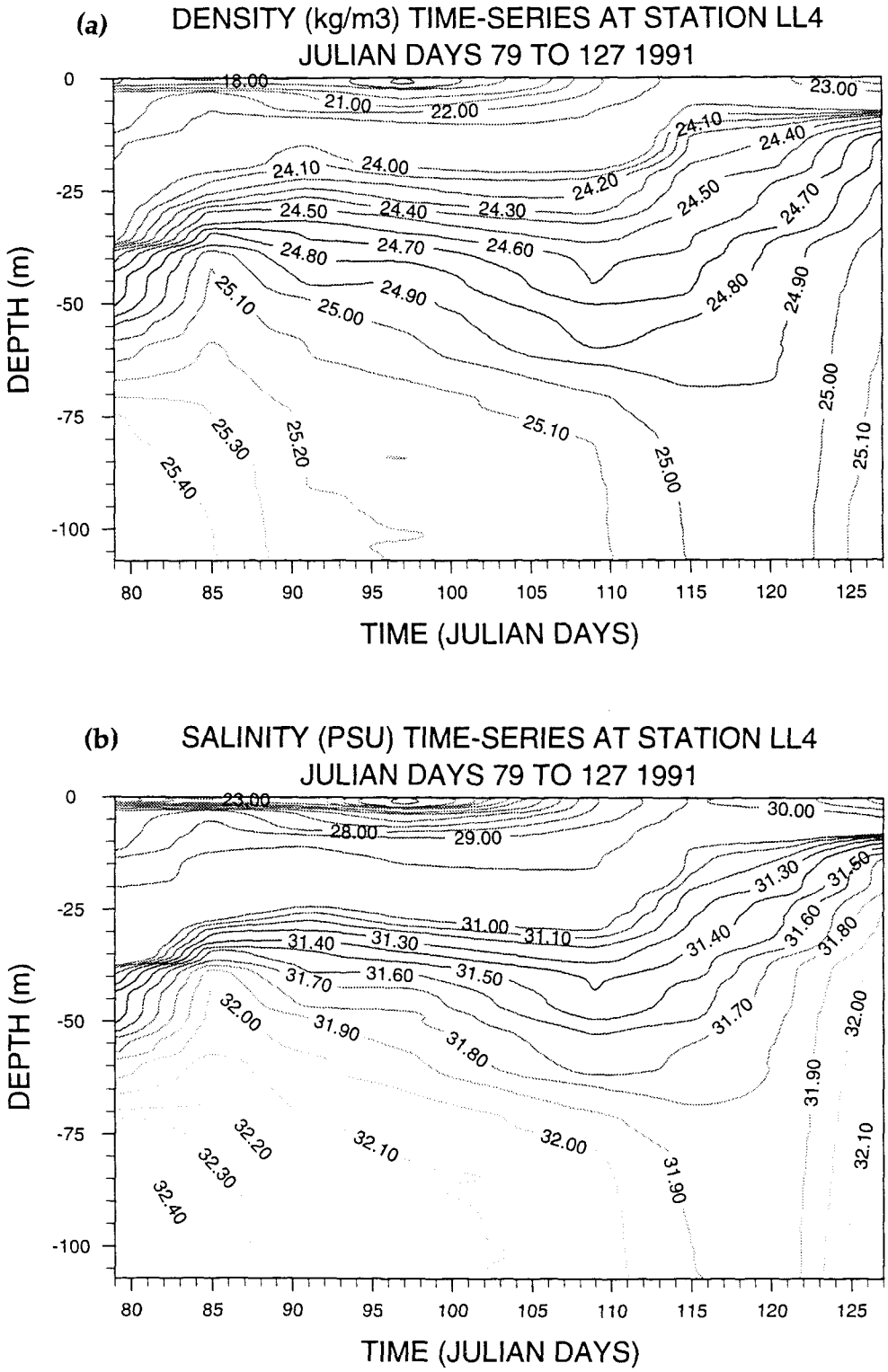

FIGURE 5.7

Temporal Variations in (a) the Density (kg m^{-3}) and (b) the Salinity (PSU) at Station LL10, Julian Day 79 to 127, 1991.

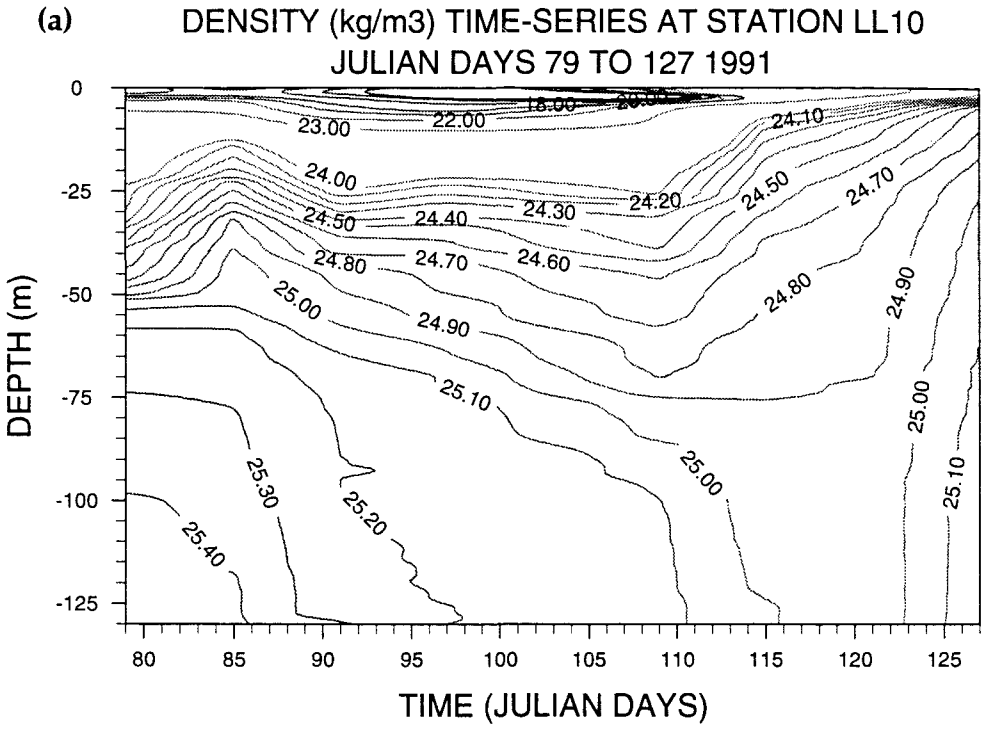

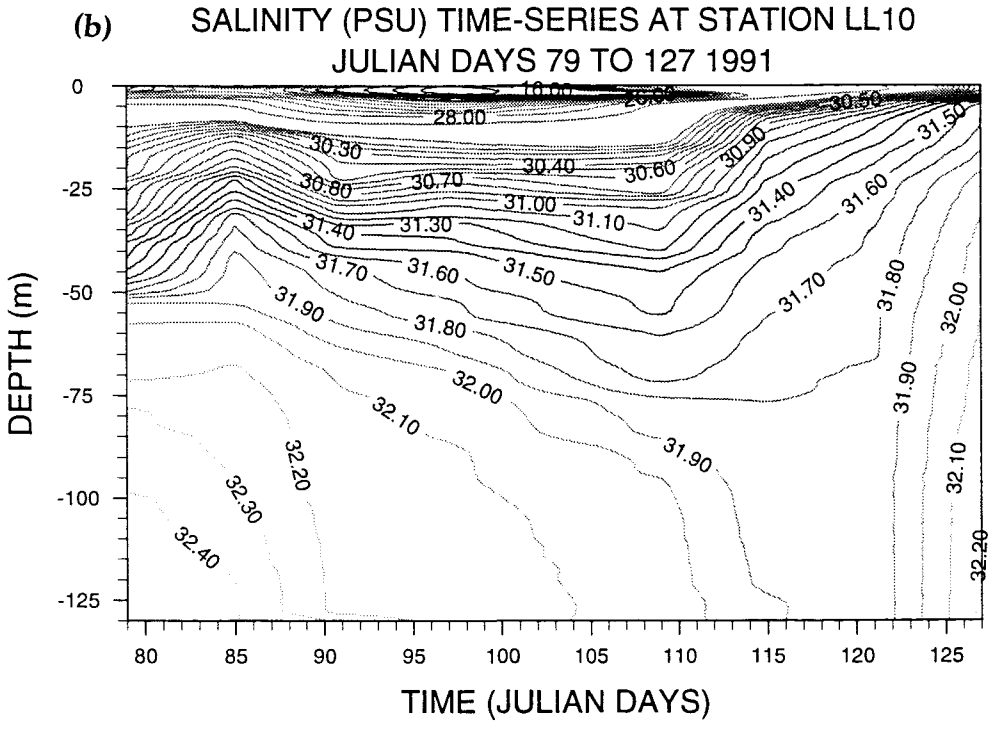

FIGURE 5.8

Temporal Variations in (a) the Density (kg m^{-3}) and (b) the Salinity (PSU) at Station LL14, Julian Day 79 to 127, 1991.

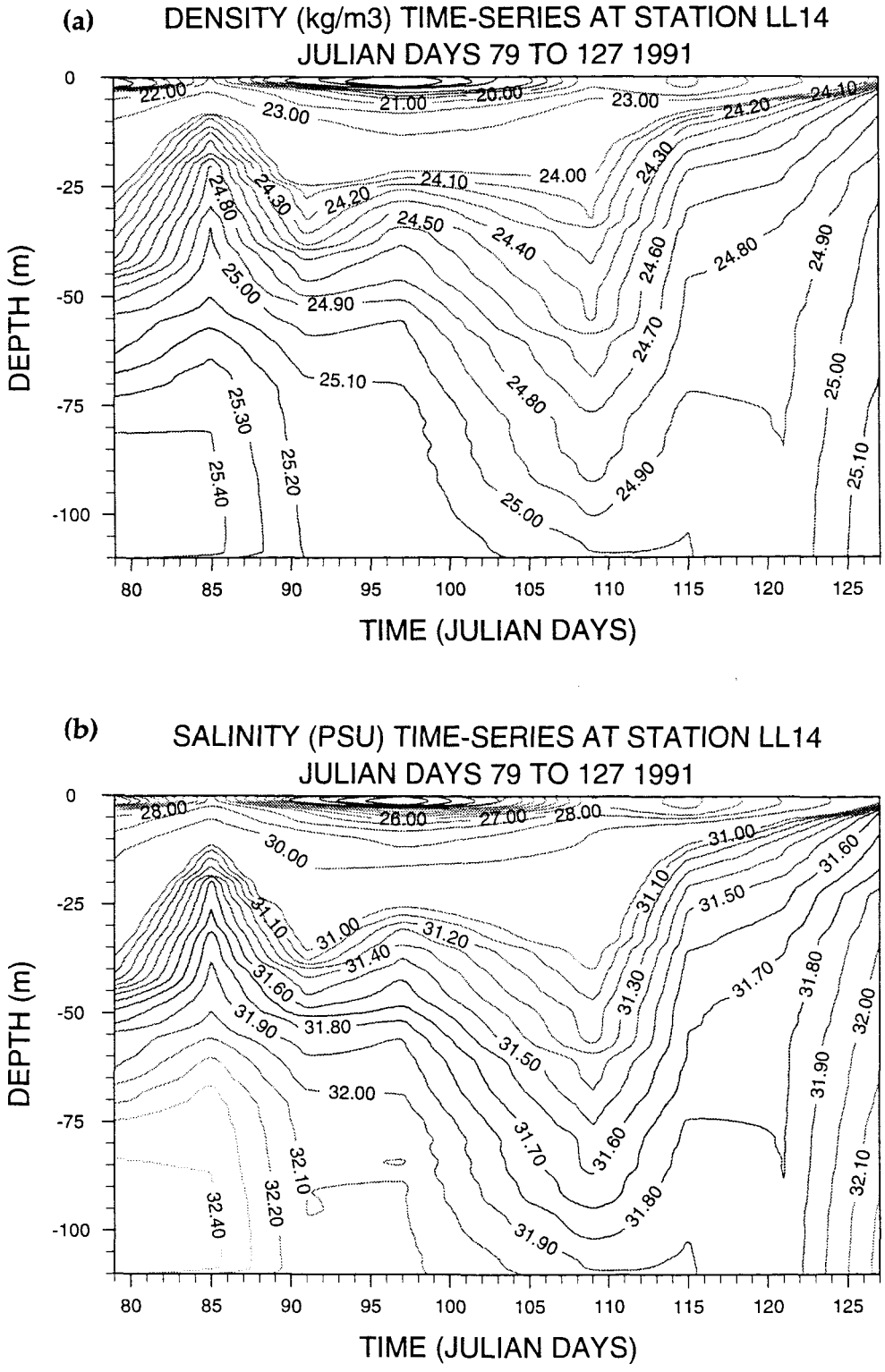

FIGURE 5.9

Temporal Variations in (a) the Density (kg m^{-3}) and (b) the Salinity (PSU) at Station LL19, Julian Day 79 to 127, 1991.

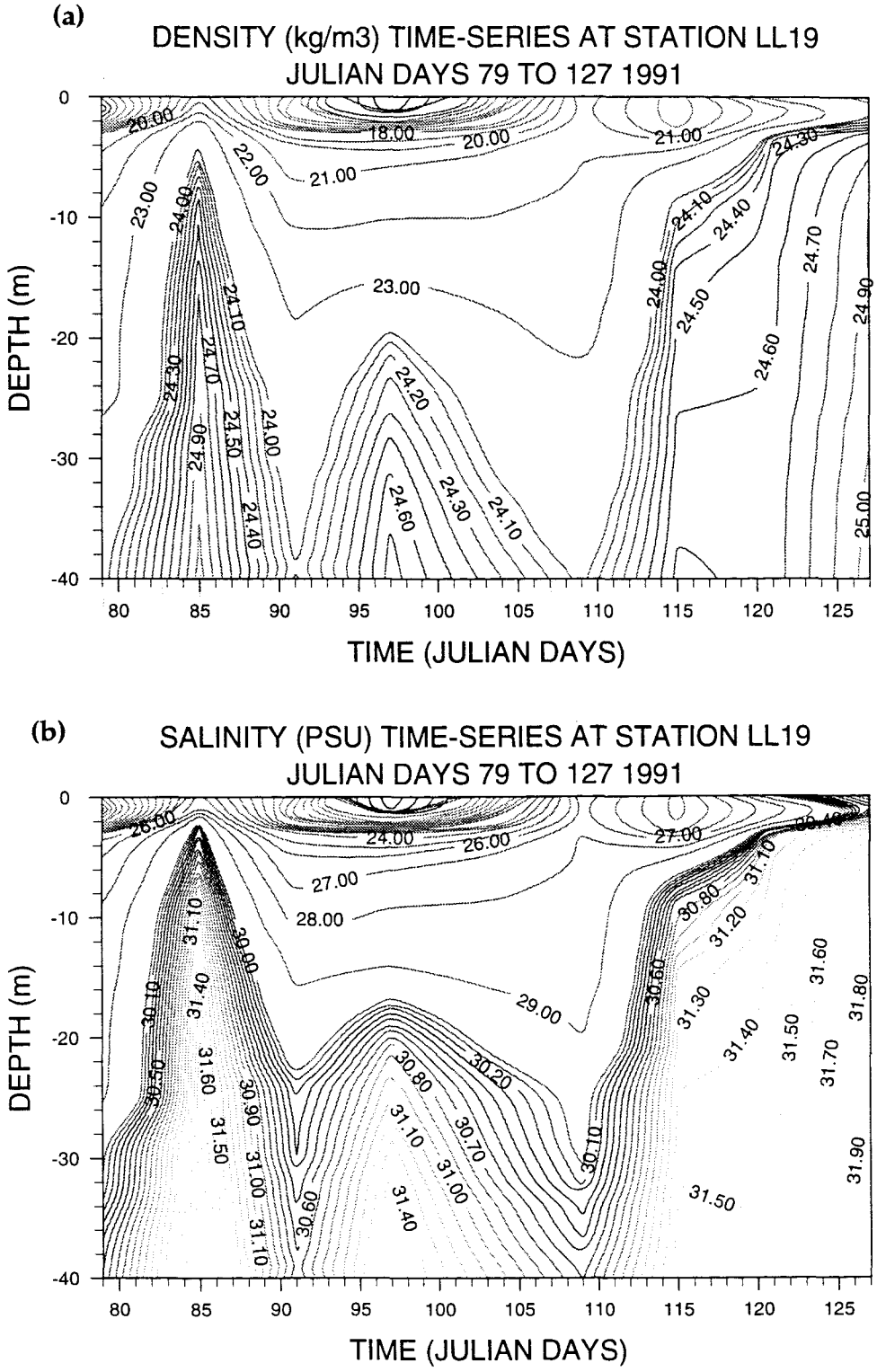

FIGURE 5.10

Temporal Variations in the Temperature at Station LL14, Julian Day 79 to 127, 1991.

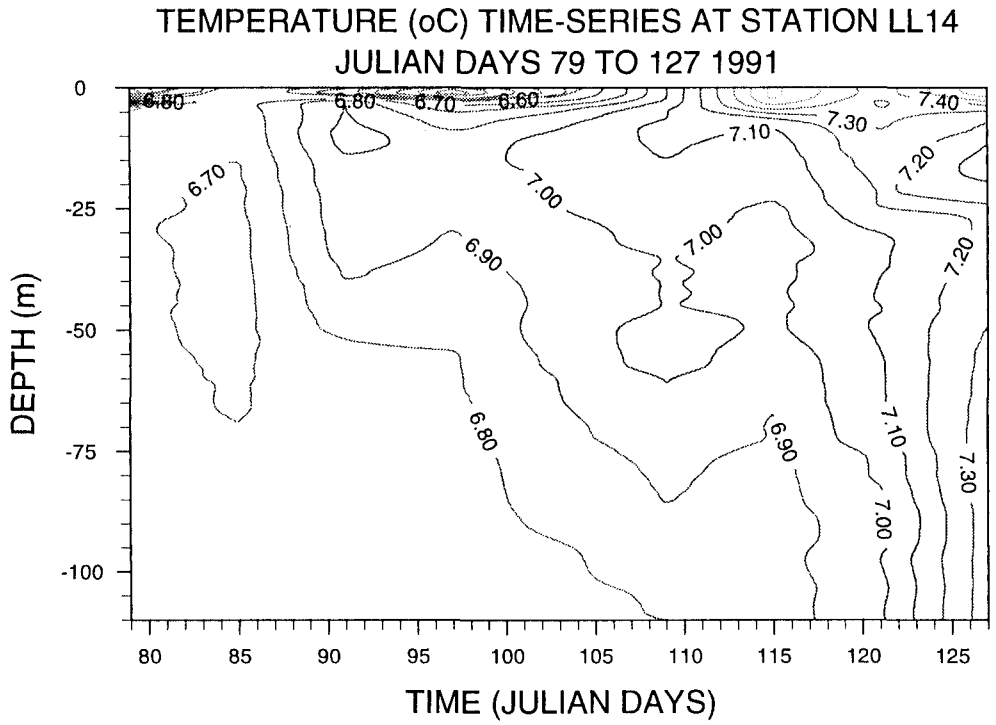

5.1.2.1 The surface layers of the loch

Looking at the time-series plot for changes at station LL19 (**FIGURE 5.9**), a marked depression in the isopycnals (**FIGURE 5.9 (a)**) and in the isohalines (**FIGURE 5.9 (b)**) is observed in the surface layers between days 93 and 107, when the density is observed to be less than 10.00 kg m^{-3} at 0 m depth and the salinity is observed to be < 18 PSU at 0 m depth. This is consistent with the increase in freshwater input around this time, as shown in **FIGURE 5.4** where the highest total flow rate of the river during the sampling period occurs on day 101 at 400 m^3 s^{-1}. The apparent depression of isohalines observed around days 113 to 120, does not indicate a temporal decrease in salinity because the salinity values have actually risen to ~ 24 PSU by this time, but rather an increased downward mixing of the relatively fresh layers into the underlying saline waters beneath them. This is confirmed in **FIGURE 5.4** where it is shown that the total freshwater flow-rate decreases markedly after day 103 (total riverine flow is 111 m^3s^{-1} on day 103 and 49 m^3s^{-1} on day 104), and onward to the end of the field-season, with the onset of the drier weather. The increased freshwater input observed between days 93 to 107 (in **FIGURE 5.9**) is reflected at all the stations through the depression of the isopycnals and isohalines in the surface layers (see **FIGURES 5.5** to **5.9**). The depression of the isopycnals is most marked at station LL19 which would be explained by its close proximity to the freshwater source. However, there is a marked depression in the isopycnals at the saline station, LL0 also. Possible explanations for this are (i) increased downward mixing of the relatively fresh surface layers with the more saline underlying waters due to the turbulent mixing encountered in the sill region caused by the process of "tidal throttling" (described in **CHAPTER 1**, section **1.2.1**), (ii) increased freshwater input in this region from neighbouring Loch Leven and/or (iii) the wedging of freshwater up against the sill by a south-westerly wind. At stations LL14, L10 and LL4, the extent of the mixing of the increased freshwater input around this time is not as marked which is likely to be due to their positions further from the freshwater source and the fact that the thickness of the freshwater will have decreased by the time it reaches these stations (see **CHAPTER 1**, section **1.2.1.2**). Also mixing of the water column at these

relatively southerly stations is regulated more by tidal motion, wind and shoreline morphology than by the kinetic energy of the riverine inflow which is likely to be more important for the surface layers at station LL19.

The variations in the temperature of the surface layers at station LL14, (**FIGURE 5.10**) show that the increase in freshwater observed around days 93 to 107 is accompanied by a drop in temperature, with values decreasing to 6.15 °C at 0 m around this time compared to temperatures of 6.79 °C as observed on day 85.

This section then, has shown that the density and salinity of the surface layers of the loch are essentially a function of the distribution of the freshwater input from the Rivers Lochy and Nevis (and, hence the rainfall patterns) and their distance away from the freshwater source.

5.1.2.2 Temporal variations in the bottom-waters: renewal events

An increase in the bottom-water density between two dates at any station indicates that water of an increased density has entered the basin between those dates and replaced the bottom-water that is resident at that station. Such deep and partial renewal events have been described in detail in **CHAPTER 1**, section **1.2.3**. In summary, water from the sill enters the basin on a flood tide (barotropic flow) or as baroclinic flow (possibly on slack tide), and sinks to a level where its density is equal to that of the surrounding water, displacing the water already resident at this depth and above it, upwards. If this inflowing water is of a great enough density and volume and has enough potential energy, then it can sink to the bottom of the basin and cause a complete renewal of all of the water present in the basin, referred to as a deep-water renewal. If, however the inflowing water is not of a great enough density or volume, or has lost some of its potential energy due to processes such as friction with the basin boundaries during its transport, then only a partial renewal of the basin-water will be observed. Because such renewal events result in the upward displacement of resident water, there will be an increase in the observed densities of the water at and above the level at which the inflowing

water intrudes, which will be at all depths if the renewal is a deep-water renewal.

On time-series plots such as those presented in **FIGURES 5.5** to **5.9**, such upward displacement of water will be evident from the uplift of isopycnals and isohalines with the subsequent vertical compression of the contour lines, due to the vertical compression of the horizontal layers as they expand laterally to fill the cross-section of the basin. Study of the contour plots would suggest that there are several renewal events throughout the whole field-season at station LL19 (**FIGURE 5.9**), the uplift of the isopycnals being particularly marked between days 79 and 85, 93 and 98 and 107 and 113, onwards to days 120 and 127. For the deeper stations; LL14, LL10 and LL4, renewal events seem less frequent, occurring only between days 79 and 85 and days 120 and 127 (see **FIGURES 5.8**, **5.7** and **5.6** respectively). **FIGURE 5.5** shows that there was a concomitant increase in the density of the inflowing water from LL0 on these dates. To determine the extent of these renewal events temporal changes in the densities of the bottom-waters at all of the stations (except for station LL0) have been considered. These are illustrated in **FIGURE 5.11** which shows that the trends in these densities over time seem to fall into two groups; those for the deeper stations; LL14, LL10 and LL4 and those for the shallower station; LL19. For the deeper stations the only time in which the bottom-water density is significantly increased is between days 120 and 127, whereas for the shallower station LL19, the bottom-water density is increased for the same time periods over which compression of the contour lines are observed at this station (**FIGURE 5.9**). This means that the inflowing water from LL0 (shown on **FIGURE 5.11** as data averaged over the top 15 m at station LL0) was of a great enough density to replace the bottom-water on these occasions at station LL19, but not necessarily at the deeper stations. In fact the inflowing water from LL0 was only of a great enough density to replace the bottom-waters at the deeper stations on one occasion, that between days 120 and 127 which would indicate that the uplift of isopycnals observed on the contour plots between days 79 and 85 must have been due to a partial renewal of water by the inflowing water, at a shallower depth. The reasons for the increased frequency of bottom-water renewals at station LL19 are likely to be (a) that it is closer to the freshwater

FIGURE 5.11

Temporal Changes in Bottom-Water Densities at Stations LL19, LL14, LL10, LL4 and Density of Water at Sill-Depth at Station LL0

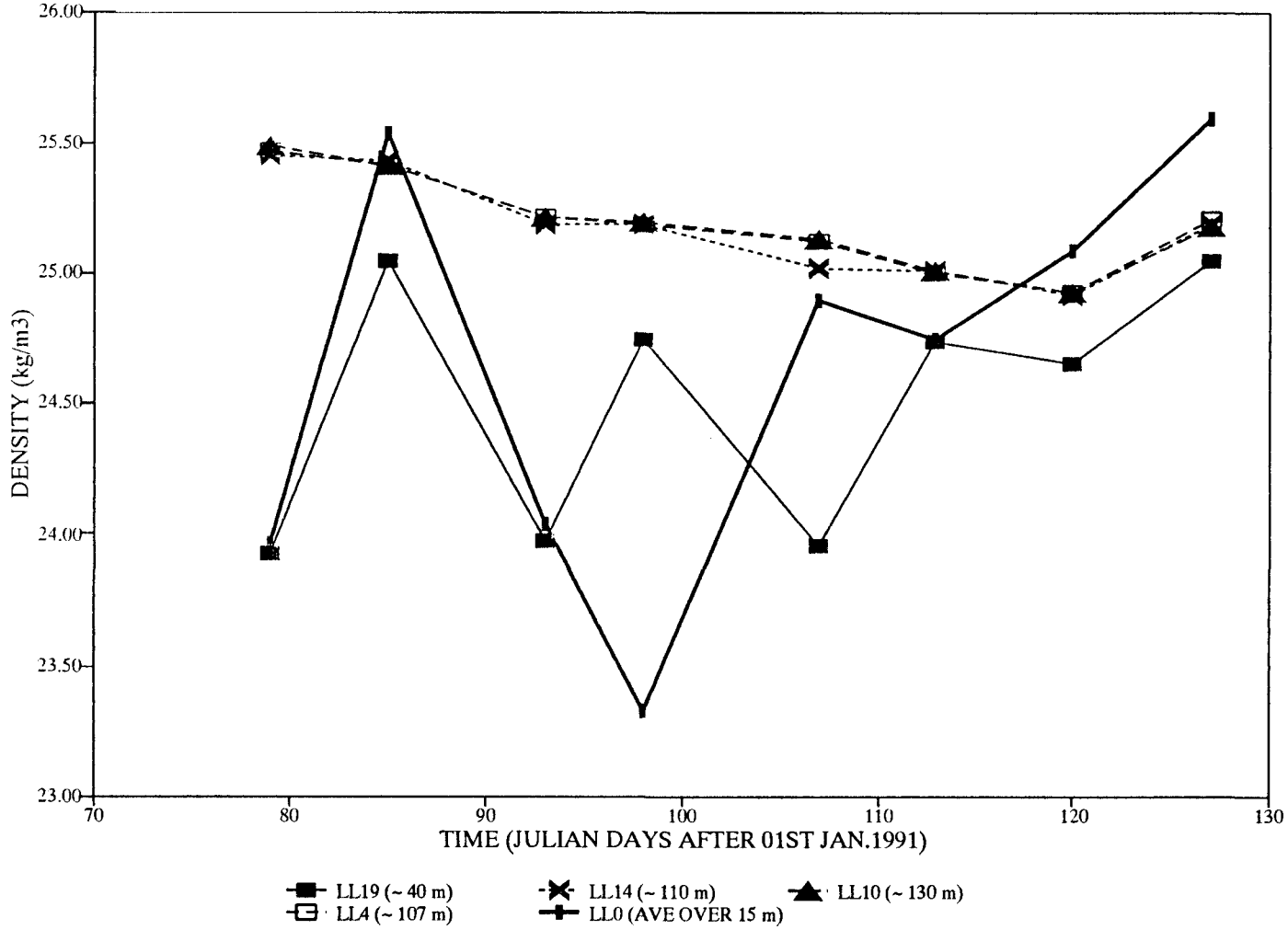

source than the other stations and thus has a higher proportion of freshwater in the water column, thus decreasing its density below that of the incoming water and, (b) that the station is relatively shallow and therefore undergoes more turbulent vertical mixing than the deeper stations due to a shorter water column for the energy inputs from the rivers, tide and wind to be dissipated through, thus increasing the efficiency of the downward mixing of the freshwater to the bottom-water depths (~ 40 m depth). From **FIGURE 5.11** it might be argued that a deep-water renewal should occur at all stations around day 79 if the relatively high density of the water present at station LL0 represents the water entering the basin over the sill. It is likely, however, that the water at station LL0 is of a higher density than the water that actually enters across the sill. Turbulent mixing of freshwater downwards will occur as the water from LL0 passes over the sill, such that the water that actually enters the basin is not of a high enough density to cause deep-water renewals at any but the shallower, fresher stations for the majority of the time.

Since all of the stations experience a marked increase in their bottom-water densities between days 120 and 127, it would seem likely that a deep-water renewal has occurred throughout the basin between these days. Reasons favouring the deep-water renewal event observed between days 120 and 127 were as follows.

(a) An increase in the density of the inflowing water around this time, illustrated in **FIGURE 5.11** from the LL0 density data. This could be due to the uplift of high salinity waters in the sill region due to an upwelling event, which would seem most likely since **FIGURE 5.5** shows a vertical compression of the contour lines at station LL0 around this time due to an uplift in the isopycnals. The phenomenon of upwelling has been described in detail in **CHAPTER 1**, (section **1.2.3.2**) and for a system such as Loch Linnhe is most likely to be caused by a change in the wind direction.

(b) The steady decrease in the densities of the bottom-waters in the basin during time leading up to the renewal event (see **FIGURE 5.12 (a)**).

FIGURE 5.12

(a) Temporal Variations in Bottom-Water (110 m) Density at Station LL14, Julian Day 79 to 127, 1991.

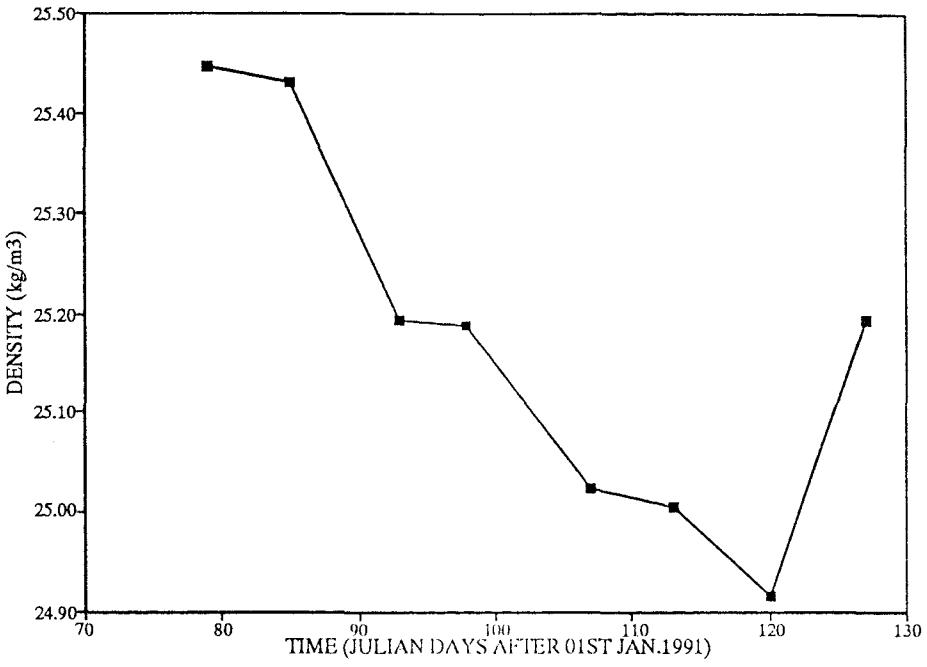

(b) Temporal Variations in Bottom-Water (110 m) Salinity and Temperature at Station LL14, Julian Day 79 to 127, 1991.

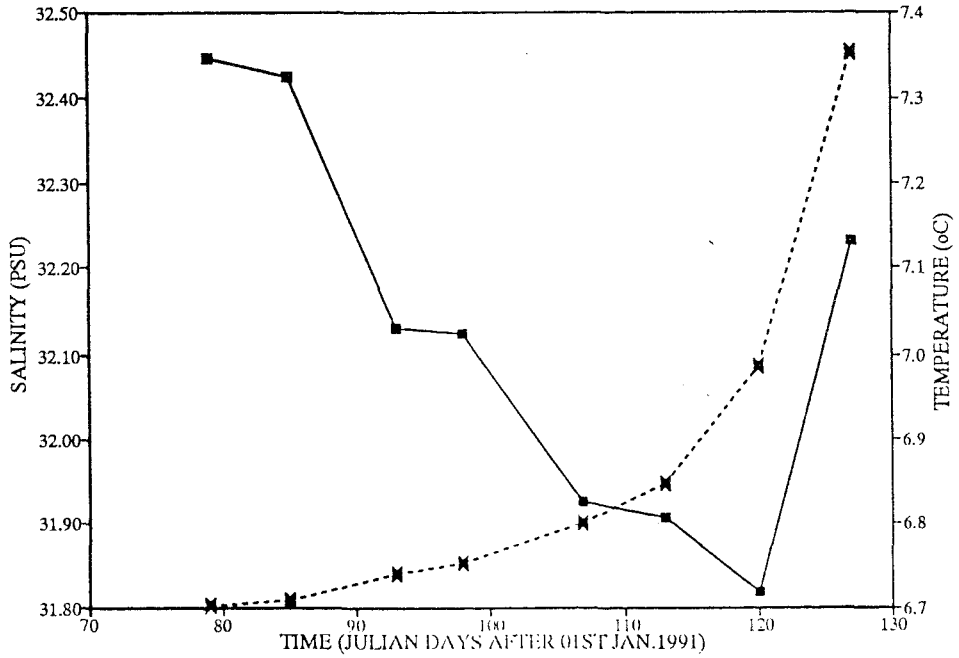

From **FIGURE 5.12 (b)** it can be seen that this is due to a diffusive (turbulent and molecular) salt flux out of the bottom-waters, up to the relatively less saline waters above them (see **CHAPTER 1**, section **1.2.2** for details), accompanied by a heat flux downwards from the relatively warm overlying waters to the bottom-waters below, both of which will contribute to the decreasing density.

(c) The increase in volume of the water entering the basin around this time due to the occurrence of spring tides on day 120, with a tidal range of 3.3 m. This would have resulted in relatively large volumes of water entering the basin leading up to the renewal, providing enough energy to break down the existing stratification in the water column, and enough volume to actually replace the resident water in the basin (see **CHAPTER 1**, section **1.2.3.2**). Also around the time of the renewal event the weather had become drier (see **FIGURE 5.4**) so that the buoyancy input supplied by the freshwater input to the surface layers was decreased thus reducing the degree of stratification present.

The importance of a hydrographic event such as a deep-water renewal, in terms of nutrient behaviour and distribution, is that if the bottom-waters at the deeper stations are not replaced by inflowing water at any point before days 120 and 127, then, effectively the bottom-waters can be described as being isolated. In **CHAPTER 2** (section **2.3.2.1**) it was described in detail how nutrients are regenerated from solid phase in the sediments, to dissolved inorganic forms in the porewaters, by various oxidative microbial processes and redox processes, and how they are ultimately released to the overlying bottom-waters via diffusive, bioturbative or resuspension processes. If the bottom-waters are isolated then this allows for an accumulation of the dissolved inorganic nutrients. Any subsequent upward displacement of this bottom-water via a deep-water renewal event, may result in a significant input of nutrients to the euphotic zone thus promoting biological activity and, perhaps triggering a phytoplankton bloom, given other favourable conditions such as enough light and stratification in the surface layers.

The nutrient results from the 1991 field-season are considered below.

5.2 Nutrients

This section considers the nutrient distributions in the light of hydrographic and biogeochemical cycling processes and highlights the problems in the identification and isolation (quantification) of such processes. All nutrient data are listed in **APPENDIX 5.3**.

As described in **CHAPTER 4** (section **4.1.1**) water samples were collected for nutrient analysis from the eight stations used for the hydrographic measurements reported in the previous sections. Two extra stations, LL20 and LL21 were incorporated at the end of the field-season which were situated closer to the freshwater source than LL19 (see **CHAPTER 4**, section **4.1.1**). Except for the last three sampling dates, days 113, 120 and 127, nutrient samples were not collected at depths greater than 60 m at the stations. The following sections will initially consider the nutrient data-set as a whole, and then the data collected from the four stations LL0, LL4, LL10 and LL19, using results from individual stations to highlight particular processes.

5.2.1 Nutrients and salinity: general behaviour

This section considers the behaviour of the nutrient concentrations relative to that of salinity in Loch Linnhe, in the light of the estuarine mixing theory which has been described in detail in **CHAPTER 2**, section **2.1**. In summary, when two end-members of an estuarine system physically mix then, providing there are no biogeochemical processes occurring in the system, the nutrient concentrations will be dependent only on the degree of physical mixing that has occurred within the system and, as such, will have a linear relationship with salinity. Such behaviour is termed conservative. Any deviation of behaviour from this linear relationship can be attributed to non-conservative processes (biogeochemical reactivity) and / or processes leading to apparent non-conservative behaviour (temporally varying end-member concentrations occurring within the flushing time of the system and also additional inputs of nutrients to the system such as point inputs). Details of

such processes can be found in **CHAPTER 2**, sections **2.3** and **2.4** respectively.

By plotting the nutrient concentrations against salinity for an individual day's data and then joining the end-member concentrations together, a mixing line is obtained referred to as the theoretical dilution line (TDL). If the nutrients are behaving conservatively and no processes leading to apparent non-conservative behaviour are occurring, then a regression analysis on the data concerned will give rise to a coefficient of determination (r^2) which has a value of one, since the plot will be linear. The definition of r^2 is as follows:

$$r^2 = [\Sigma (Y_{est} - Y)^2] \; / \; [\Sigma (Y - \bar{Y})^2]$$

where;

Y = the nutrient variable,

Y_{est} = the value of Y for a given salinity value estimated from a regression line of Y on salinity,

$\bar{Y}$ = the mean value of the nutrient data,

(Spiegel, 1972).

Values of r^2 lie between zero and one.

This type of analysis will be used throughout this study. It provides a measure of the dependency of the nutrient concentration on salinity and therefore how much of the variation in nutrient concentrations can be attributed to corresponding variations in the salinity. The main aim of this study is to identify and isolate the different processes that determine the distribution of the dissolved inorganic nutrients in the loch. The approach taken was to initially consider the data-set as a whole in terms of its relationship with salinity, and then to consider any deviations of r^2 from unity in the light of the different processes mentioned above. Data from all of the stations over the eight sampling dates are therefore considered together. These results are shown in **FIGURES 5.13 (a)** to **(c)**. It should be noted that because there are eight sampling dates then, effectively there are sixteen end-member concentrations on each plot. A TDL can only be drawn through the data if these end-member concentrations remain the same for each sampling date

Relationship of (a) Nitrate, (b) Phosphate and (c) Silicate Concentrations (Micromolar) with Salinity for Data from all Stations, 1991.

(a)

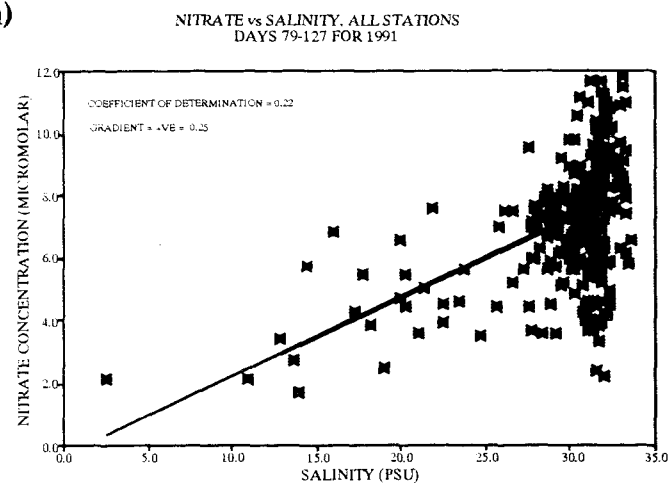

(b)

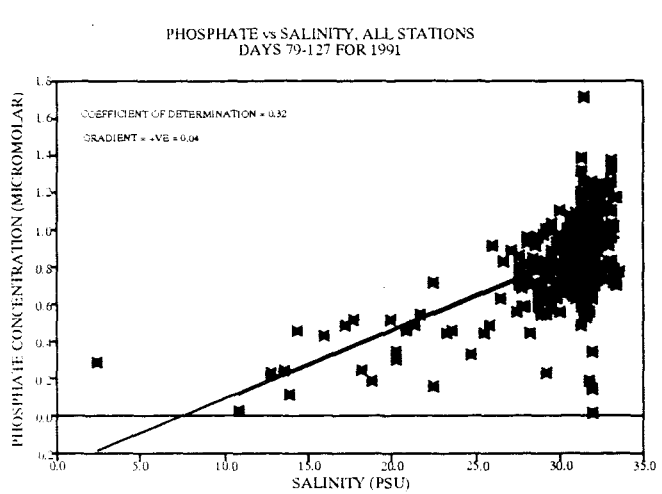

(c)

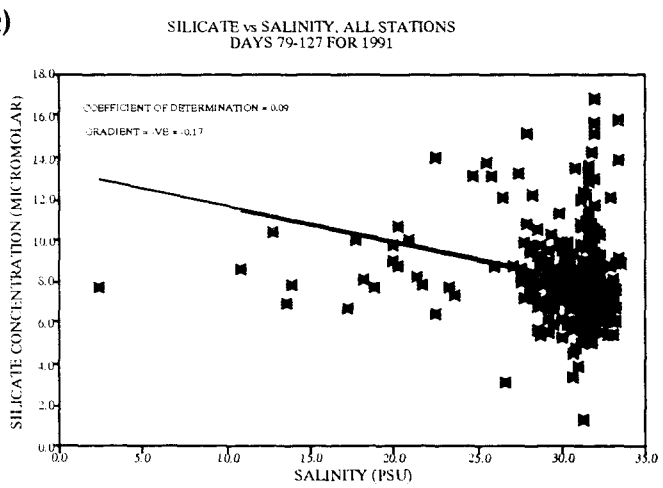

(although it is possible for the saline end-member concentrations to change as long as changes are linear with any linear nutrient / salinity relationships inside the basin), otherwise only a line of best fit can be drawn through the data. This defines the average composition of the end-members by the intercept and the slope and has been used in this study to define an average dilution line which assumes conservative behaviour. Deviations from this line therefore represent a measure of the total non-conservative and apparent non-conservative behaviour within the system over the whole field-season. No riverine freshwater data were available for the dates used in this field-season and the data for the lower salinities is from stations LL19, LL20 and LL21, which are closest to the riverine source.

From the gradients of the plots it is clear that the main source of NO_3 and PO_4 to the system is from the saline end, since the gradients are positive. The average concentration of NO_3 entering the loch for station LL0 (data averaged over the top 20 m for the entire field-season) is 7.76 µM and that of PO_4 is 0.92 µM. This gives rise to an average N:P ratio of 8.55:1. **FIGURE 5.13 (c)** shows a negative gradient for the plot of SiO_4 against salinity indicating that the main source is from the freshwater end. This is backed up by observations whereby the average concentration of SiO_4 over the whole field-season in the surface (0 m) at station LL19 is 13.78 µM for the whole field-season, whereas at the saline station LL0 the average concentration over the top 20 m is only 7.37 µM. The average N:Si ratio for water entering the loch is then 1.05:1. These findings for the sources of the nutrients are consistent with the literature available for this geographical area which has been described in **CHAPTER 3**, section **3.2**.

In terms of the correlation of the nutrients with salinity, it can be seen from the plots in **FIGURE 5.13** that there is a great deal of scatter about the lines of best fit for each nutrient. This is reflected in the low r^2 values of 0.22 for NO_3, 0.32 for PO_4 and 0.09 for SiO_4. This indicates that only 22 %, 32 % and 9 % of the variation in the NO_3, PO_4 and SiO_4 concentrations respectively can be attributed to changes in the salinity which leaves high percentages of the variances to be accounted for by fluctuating end-member concentrations within the flushing time of the system

(giving rise to apparent non-conservative behaviour) and biogeochemical (non-conservative) processes within the system. Evidence for these will now be considered.

5.2.1.1 Variations in the saline end-member concentrations

Each plot in **FIGURE 5.13** shows a large degree of scatter of data about the lines of best fit, particularly at the higher salinities. This indicates that the saline end-member concentrations are varying considerably within the time-span of the field-season and within the flushing time of the system (since scatter occurs over the time period for which there are isolated bottom-waters i.e. when no flushing of the system is occurring). **FIGURES 5.14 (a)** to **(c)** show such temporal variability in the saline end-member concentrations (taken as data from LL0 averaged over the top 20 m to account for the effect of mixing as the water passes over the sill), by considering the changes in the nutrient concentrations relative to salinity during the field-season. The fact that none of the plots show a linear relationship of the nutrients with salinity (r^2 = 0.32 for NO_3, r^2 = 0.42 for PO_4 and r^2 = 0.42 for SiO_4), indicates a temporal variation in the saline end-member concentrations which will cause scatter away from any linear relationship between nutrients and salinity inside the basin. This non-linear saline variation could be due to (i) the effect of dilution of the saline water by a temporally varying freshwater end-member concentration, (ii) the advection of water with different nutrient concentrations from the adjacent coastal regions, (iii) upwelling in the sill region of high salinity, nutrient rich seawater (see **CHAPTER 1**, section **1.2.3.2**), (iv) biogeochemical processes occurring in the sill-region such as adsorption / desorption of nutrients from SPM (as described in **CHAPTER 2**, sections **2.3.1.2** / **2.3.2.3**), or biological activity in the sill-region (see **CHAPTER 2**, section **2.3.1.1**).

In terms of dilution by a freshwater component **FIGURE 5.15** shows the changing salinities at 0, 10 and 20 m over time at station LL0. It shows that the salinities of the surface layers (0 and 10 m) vary much more than at 20 m which is fairly constant and probably represents the Irish Sea / Clyde-Sea and Atlantic water

FIGURE 5.14

Relationship of (a) Nitrate, (b) Phosphate and (c) Silicate Concentrations with Salinity at Station LL0 (Data Averaged Over the Top 20 m), 1991.

(a)

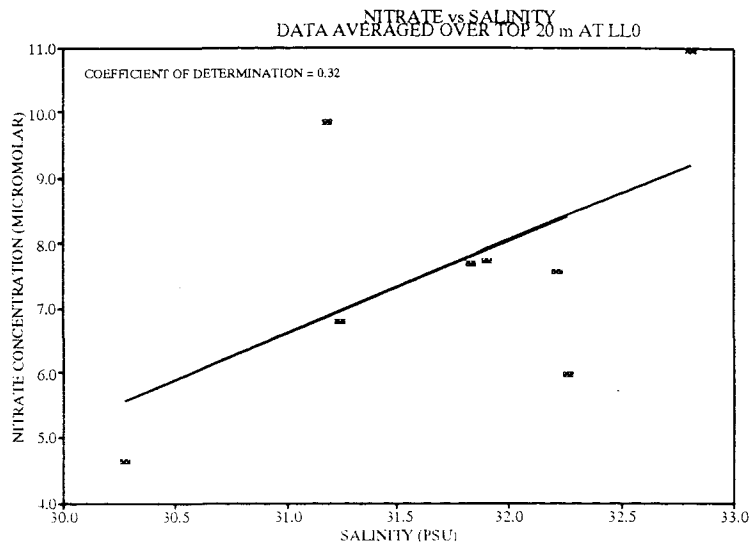

(b)

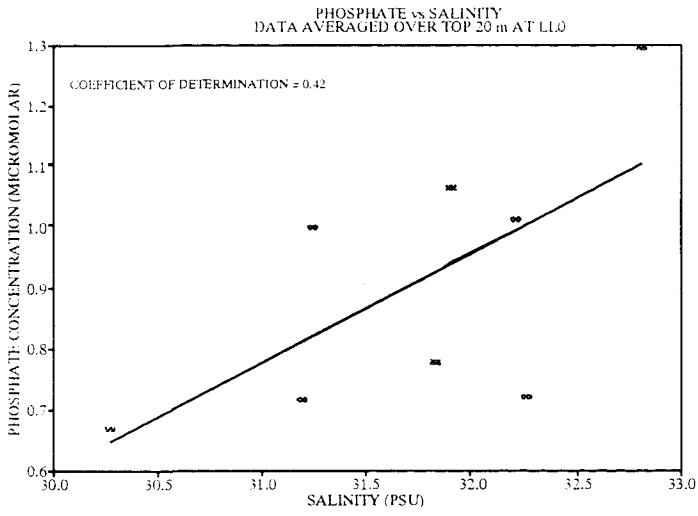

(c)

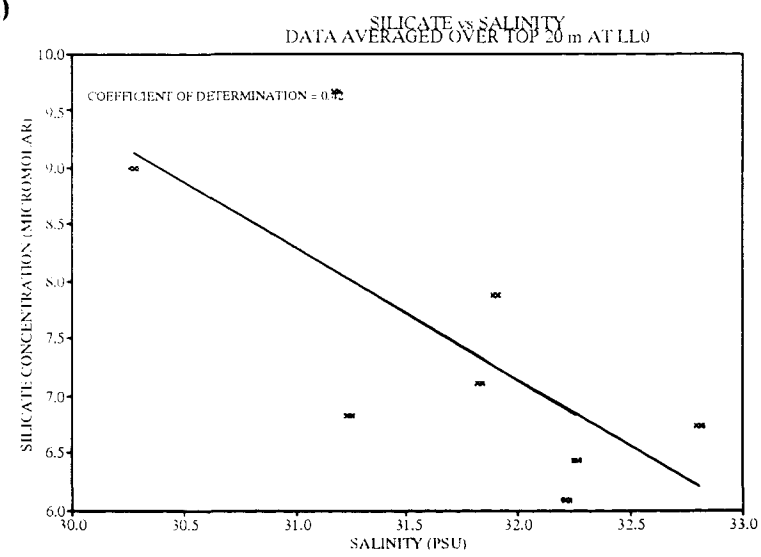

FIGURE 5.15

Variation of Salinity with Time at Different Depths at Station LL0, Julian Day 79 to 127, 1991.

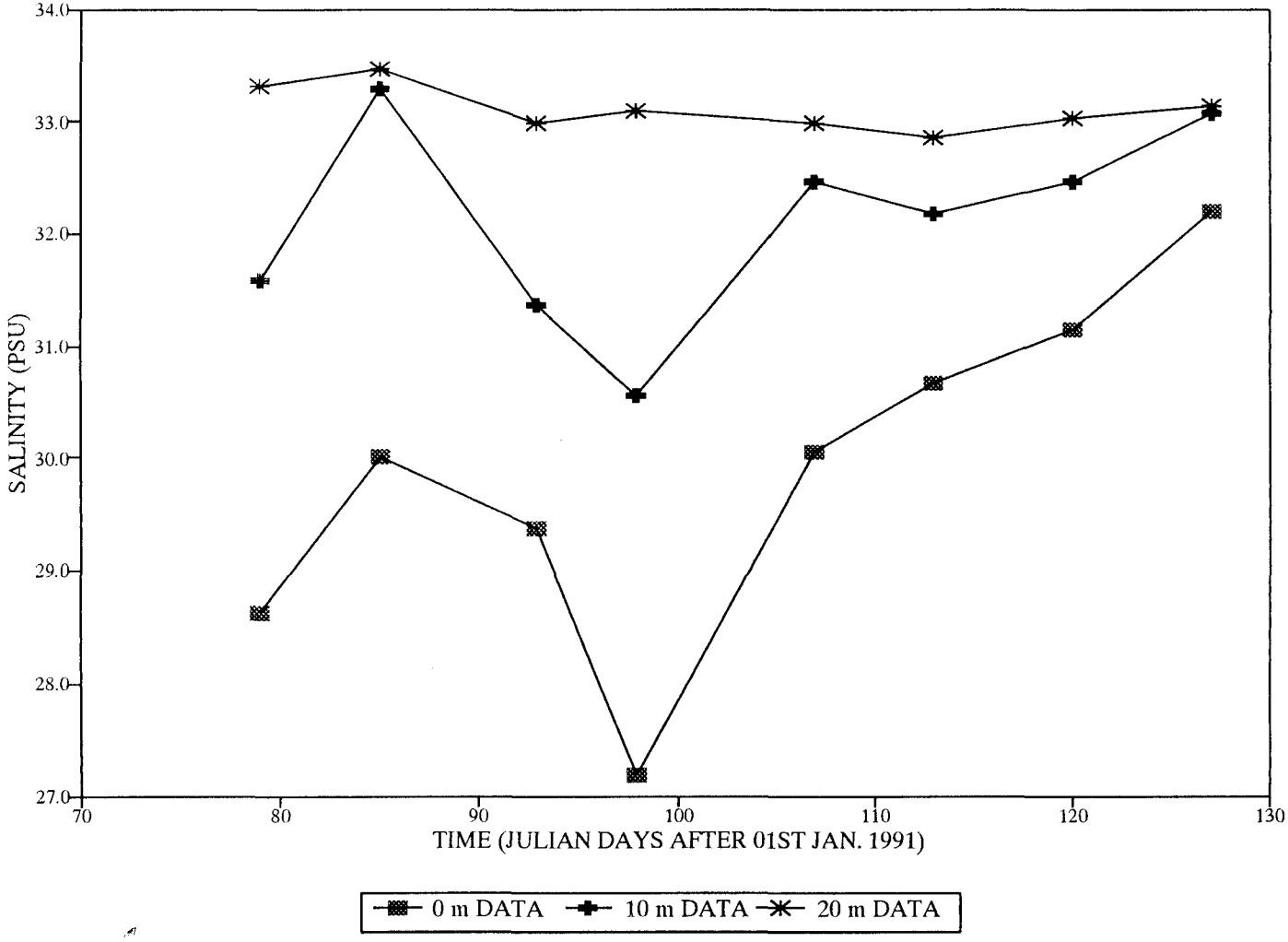

components in the saline end-member (see **CHAPTER 3**, section **3.2.1**). The patterns in the salinity changes at 0 m and 10 m depth are consistent with the freshwater inflow patterns as illustrated in **FIGURE 5.4**, showing decreased salinity between days 98 and 107 when the highest freshwater flow is being input to the loch. This freshwater component which is present down to depths of somewhere between 10 m and 20 m may cause a variation in the saline end-member concentrations if the nutrient concentrations in the freshwater vary with time (see section **5.2.1.2**) although, because the main source of nitrate and phosphate is from the saline end-member, then it is likely that this contribution to the scatter at the saline end will be minor.

In terms of variations in the saline component **FIGURE 5.16** shows the relationship of the 20 m data at station LL0 with salinity at this depth and shows that there are large deviations away from linearity for each nutrient ($r^2 = 0.01$ for NO_3, $r^2 = 0.20$ for PO_4 and $r^2 = 0.07$ for SiO_4). This then reflects the variations in the nutrients possibly caused by processes listed in (ii), (iii) and (iv) above.

5.2.1.2 Variations in the freshwater end-member concentrations

In **CHAPTER 2**, section **2.2** primary inputs of nutrients (riverine) to the estuarine system and reasons for their temporal variations were discussed in detail. A study into the variations in the freshwater end-member concentrations for 1991 was limited by the amount of data available, which were provided by the Highland River Purification Board (HRPB). A much more detailed study was carried out in connection with the 1992 field-season but which incorporated the 1991 data and this can be found in **CHAPTER 6**, section **6.2.1.1**. Briefly, the study showed that there are temporal variations in both the NO_3 and the PO_4 freshwater concentrations and that these variations have a higher correlation with the annual regime, which incorporates the effects of seasonality, than with short-term features such as river flow-rates (although this is only very slightly the case for PO_4). The NO_3 concentrations showed quite marked seasonal patterns in behaviour over time, generally increasing during the winter months due to (i) strong leaching of soluble

FIGURE 5.16

Relationship of (a) Nitrate, (b) Phosphate and (c) Silicate with Salinity at Station LL0, 20 m Depth, 1991.

(a)

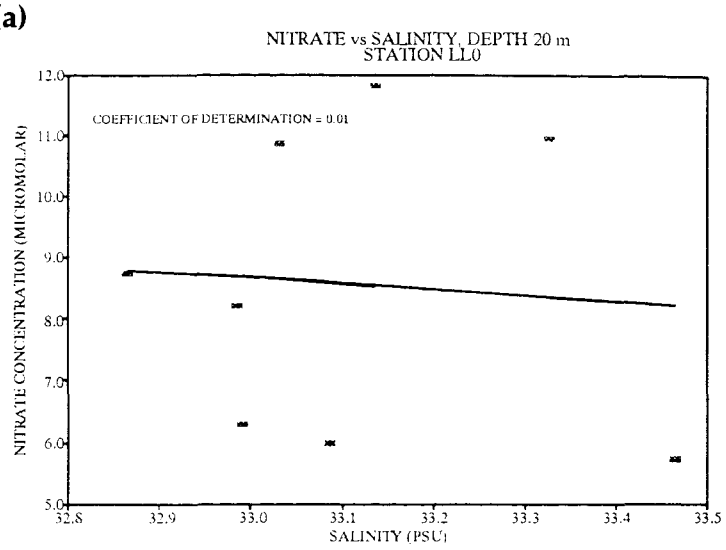

(b)

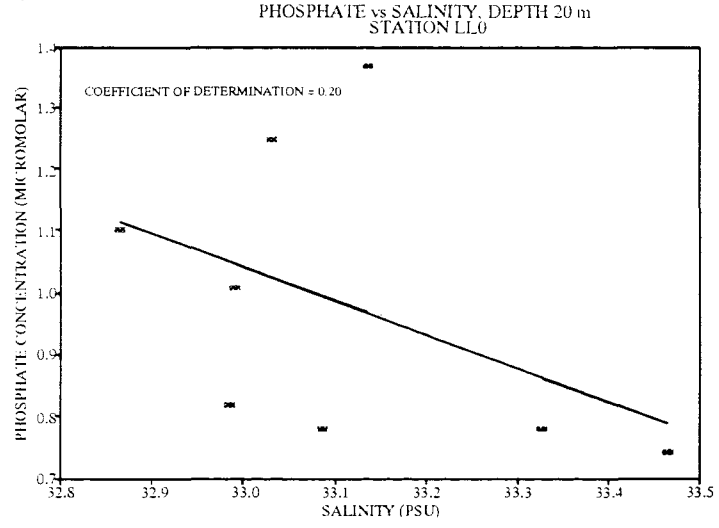

(c)

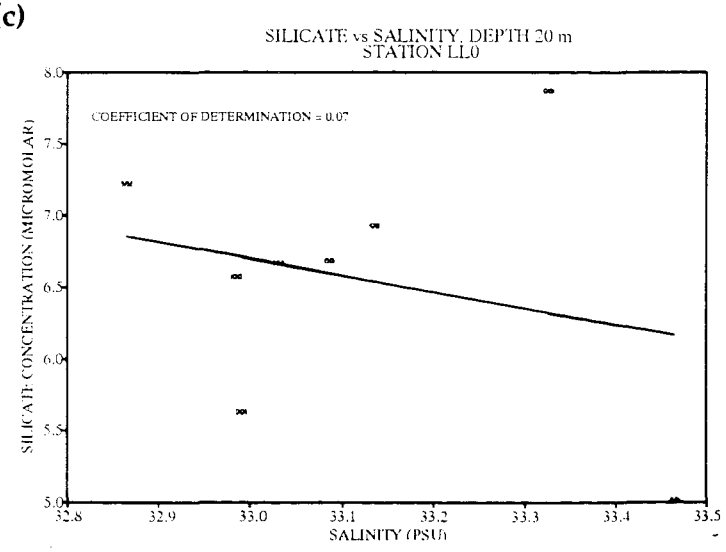

NO_3 ions by the water moving through the soil, (ii) the absence of nitrogen uptake by plants and (iii) the volume of saturated soil supplying runoff being at a maximum in the winter. In the summer the NO_3 concentrations generally decrease due to (i) diminished soil water movement, (ii) the dominance of bedrock as a source which is remote from the zones of relatively high nitrogen content located near the surface of the soil and (ii) losses of NO_3 due to uptake by growing crops or biological activity within the stream. Lack of correlation of NO_3 concentrations with the flow-rates was attributed to the temporal effect of water movement through the soil, resulting in the leaching of NO_3 from the soil into the runoff. The PO_4 concentrations in the freshwater however, were found to have weaker relationships with both river flow-rates and seasonality effects. This was attributed to its high and very complex geochemical reactivity in natural and estuarine waters (see **CHAPTER 2**, section **2.2.2**).

The freshwater data for the year 1991 show a range in the NO_3 concentrations of 2.5 to 9.0 µM with the higher concentrations being coincident with higher flow-rates (see **FIGURE 6.17** in **CHAPTER 6**). The freshwater PO_4 concentrations were much lower lying in the range of between 0.05 µM to 0.4 µM and showed no correlation with flow-rates. An average value for the SiO_4 concentration at the freshwater end was taken as the average of the 0 m data collected at station LL19 and was 13.78 µM.

It has been shown that the freshwater end-member concentrations of NO_3 and PO_4 do vary temporally and that this will give rise to scatter away from a linear nutrient / salinity relationship in the basin, particularly at the freshwater end but also, to a lesser extent at the saline end where there is a significant freshwater component in the inflowing water, although this contribution is likely to be minor for the variations in the saline-end member concentrations. Temporal variations in both the saline and the freshwater end-member concentrations will contribute to the scatter of the data and the deviations of r^2 values from one observed in the plots in **FIGURE 5.13**. Such variations are an example of processes that lead to apparent non-conservative behaviour.

5.2.1.3 Biogeochemical processes giving rise to non-conservative behaviour

The theory of biogeochemical processes has been considered in detail in **CHAPTER 2**, section **2.3**. The first to be considered is that of the removal of inorganic nutrients from the dissolved to the solid phase (causing a sink of nutrients from the system), via biological activity i.e. the uptake of nutrients by phytoplankton for growth.

(i) Evidence for biological activity in 1991: Such evidence was limited in the 1991 field-season because (a) chlorophyll a concentrations were not measured throughout the water column and (b) the phytoplankton bloom in Loch Linnhe occurred after the field-season had finished (chlorophyll a levels were not measured in the upper basin until day 135 by Dr. M. Heath, 1992, pers.comms.). Both of these deficiencies were rectified for the 1992 field-season when chlorophyll a data were collected through the use of a fluorometer attached to the CTD at each station (see **CHAPTER 4**, section **4.1.2** for details), and when the field-season covered the time of the bloom. Evidence for this activity is documented in **CHAPTER 6**. However, there is some evidence for biological activity in 1991. **FIGURES 5.17** to **5.21** are time-series plots which show the temporal variations of the nutrient concentrations at stations LL0, LL4, LL10, LL14 and LL19 (created with UNIMAP software - settings listed in **APPENDIX 5.4** including plots with superimposed data). These figures show that at all of the stations (apart from station LL19) there is a depletion of all three nutrients in the surface layers observed around day 120. This cannot be explained for NO_3 and PO_4 by dilution effects caused by increased freshwater inflow around this time because the weather was, in fact drier (see **FIGURE 5.4**); furthermore the silicate levels would have increased which was not the case. It would seem most likely that this depletion is due, instead, to biological activity, since the bloom had already been detected in the Firth of Lorne around day 119 (Dr. M. Heath, 1992, pers.comms.) and this would result in an inflow of algal cells and water with depleted nutrients to the basin.

FIGURE 5.17

Temporal Variations in (a) Nitrate Concentrations and (b) Phosphate Concentrations Station LL0, Julian Day 79 to 127, 1991.

(a)

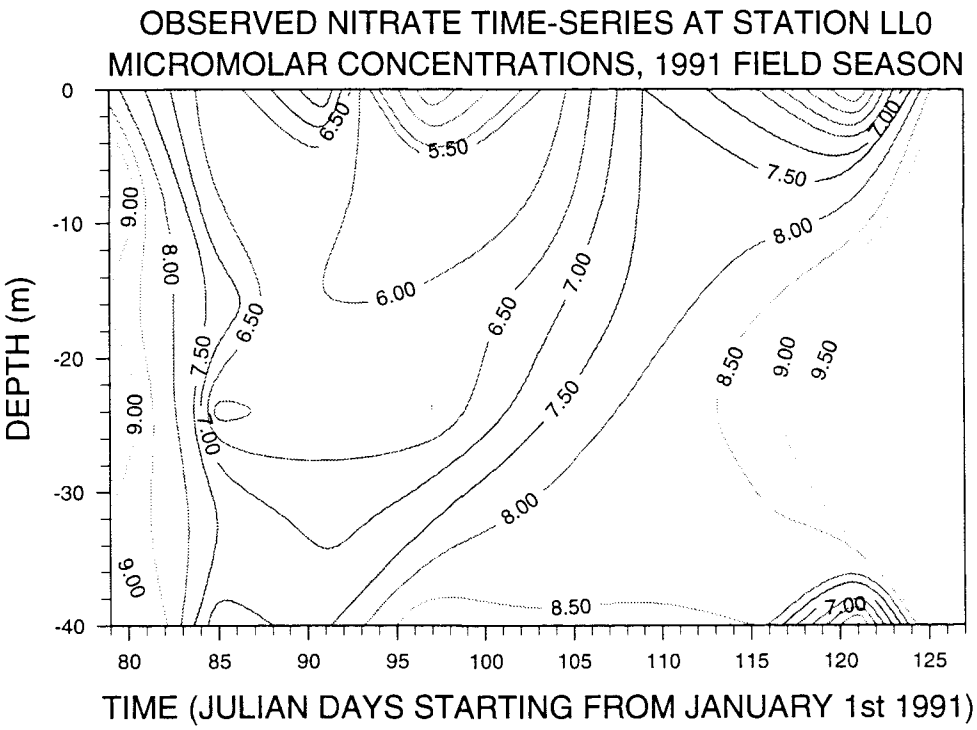

(b)

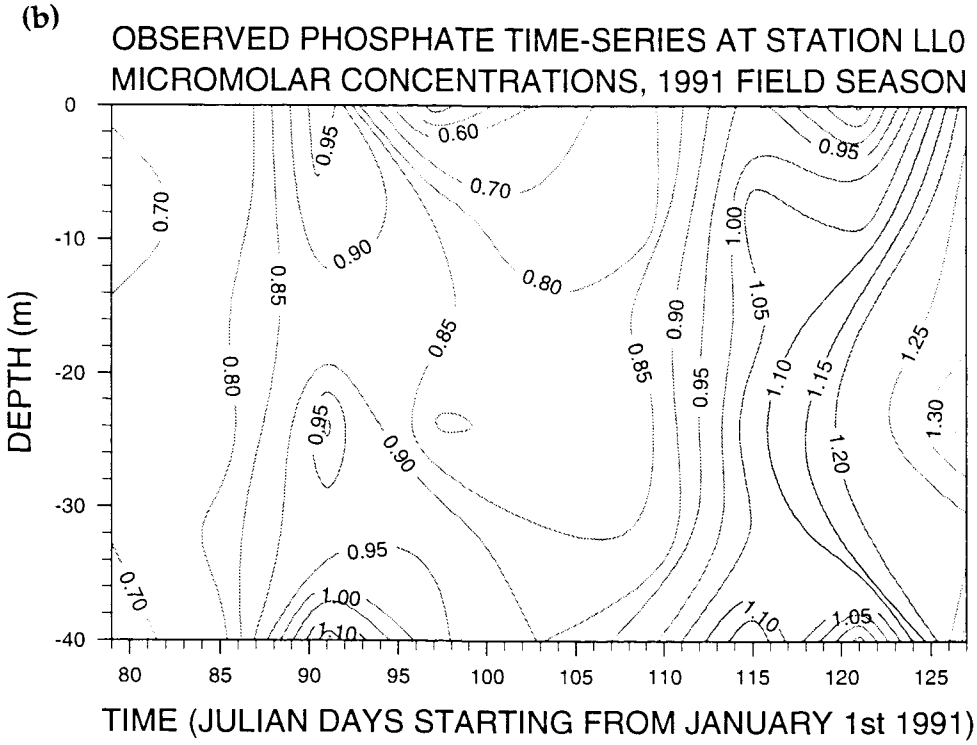

FIGURE 5.17

Temporal Variations in (c) Silicate Concentrations and (d) Salinity at Station LL0, Julian Day 79 to 127, 1991.

(c)

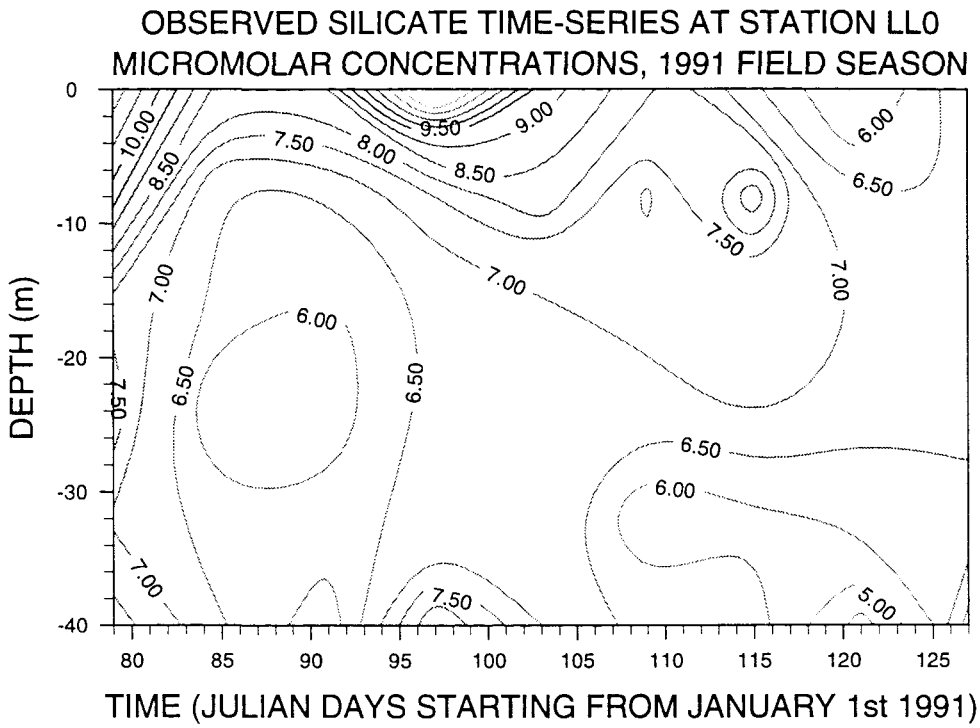

(d)

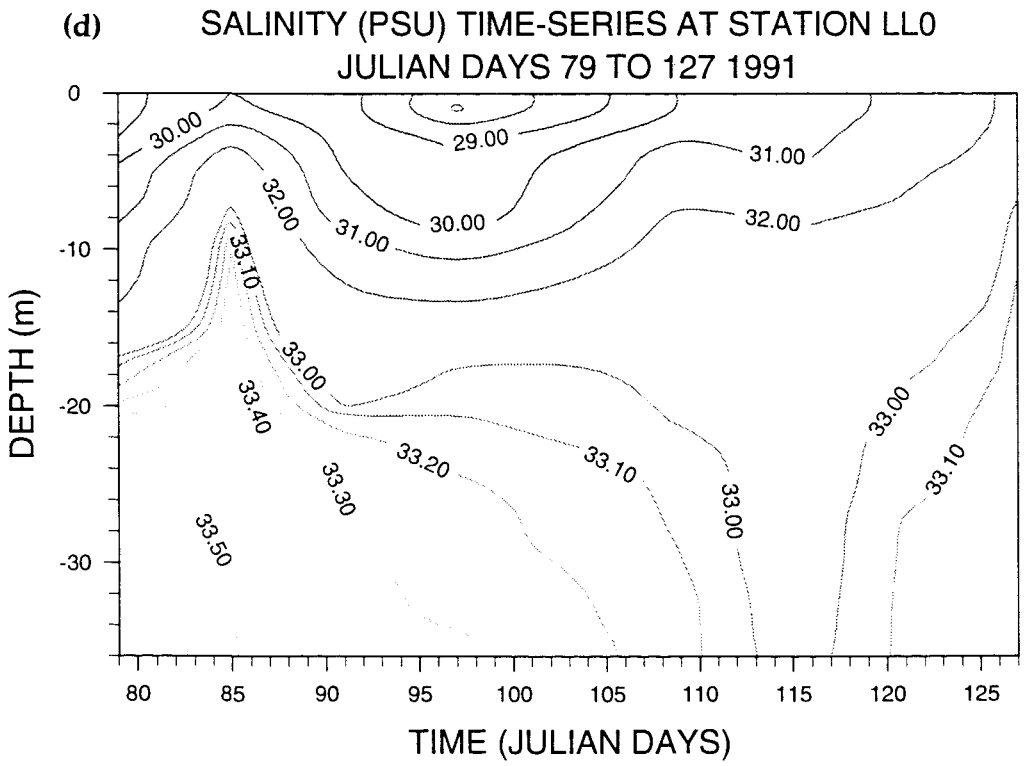

FIGURE 5.18

Temporal Variations in (a) Nitrate Concentrations and (b) Phosphate Concentrations Station LL4, Julian Day 79 to 127, 1991.

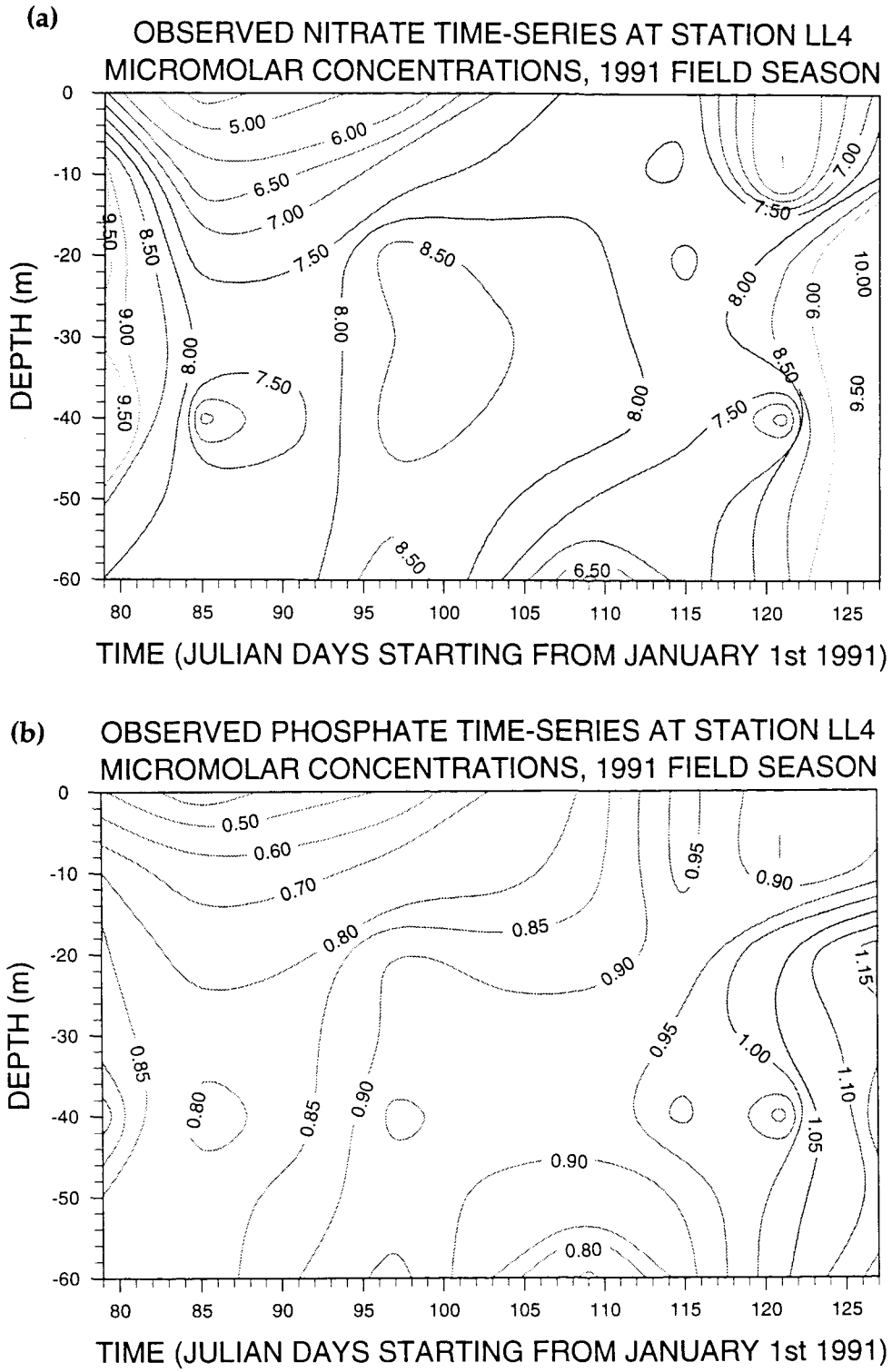

FIGURE 5.18

Temporal Variations in (c) Silicate Concentrations and (d) Salinity at Station LL4, Julian Day 79 to 127, 1991.

(c)

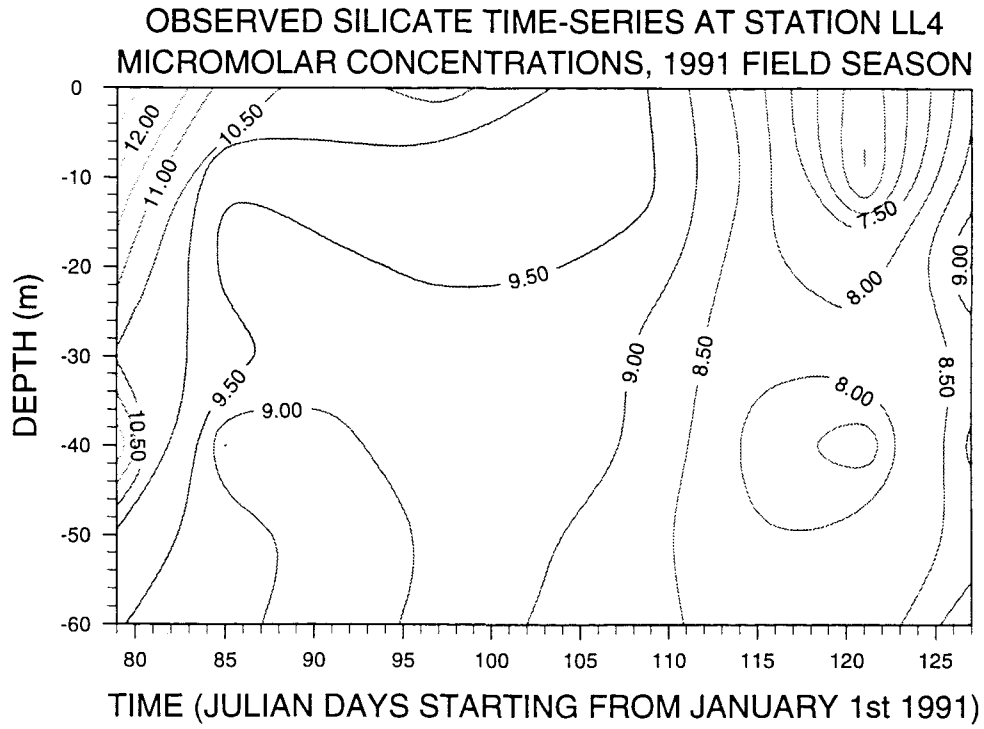

(d)

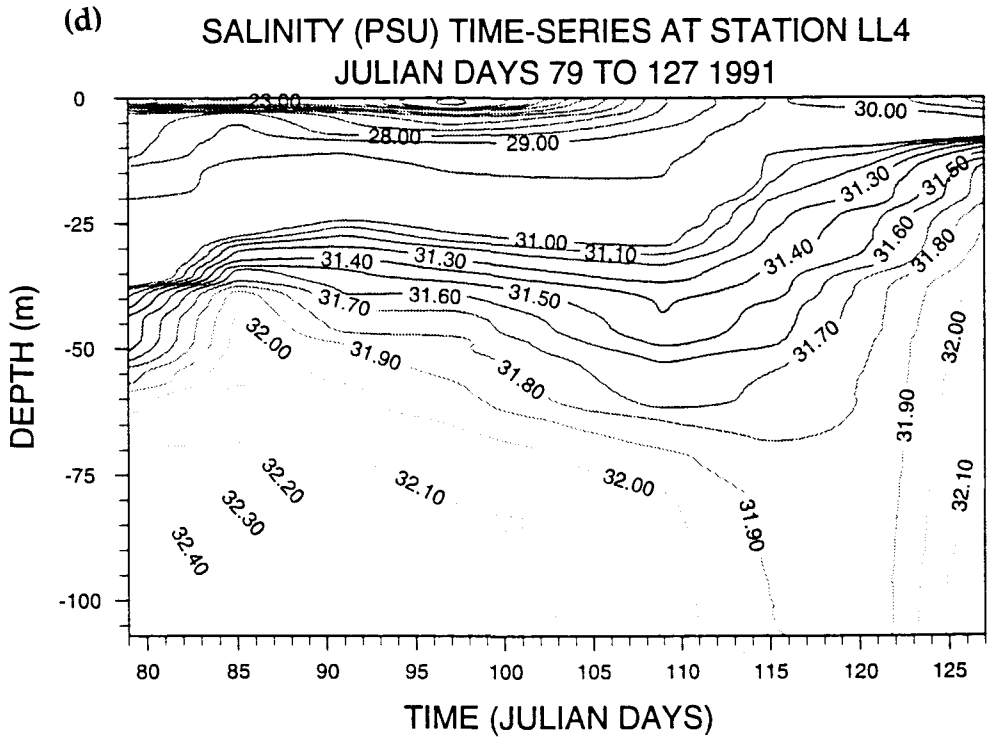

FIGURE 5.19

Temporal Variations in (a) Nitrate Concentrations and (b) Phosphate Concentrations Station LL10, Julian Day 79 to 127, 1991.

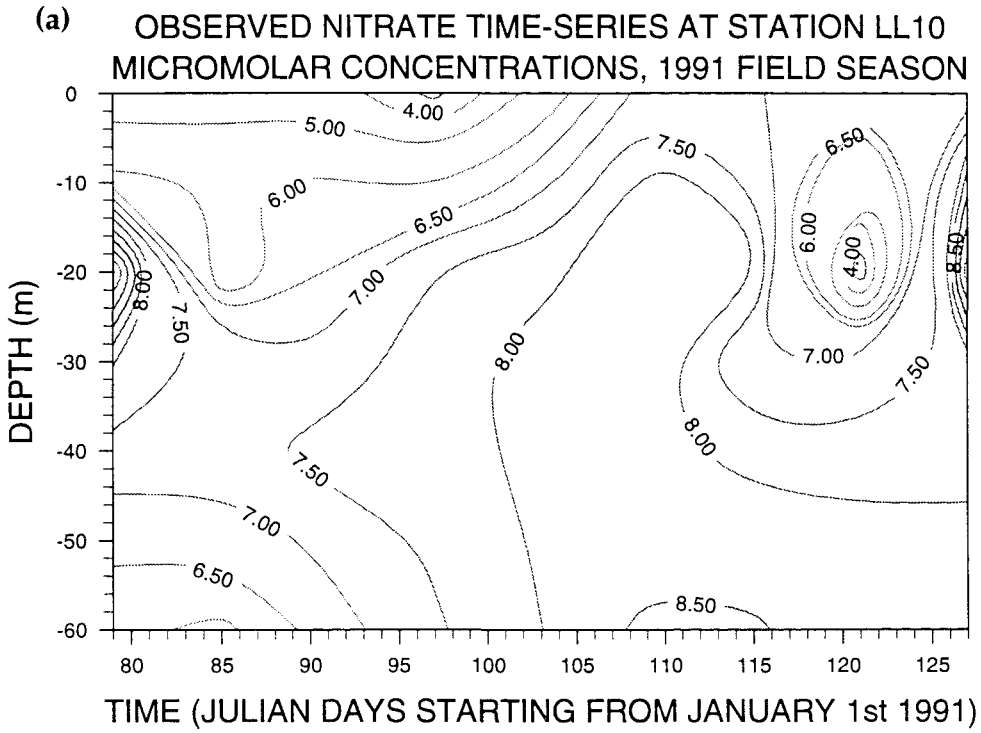

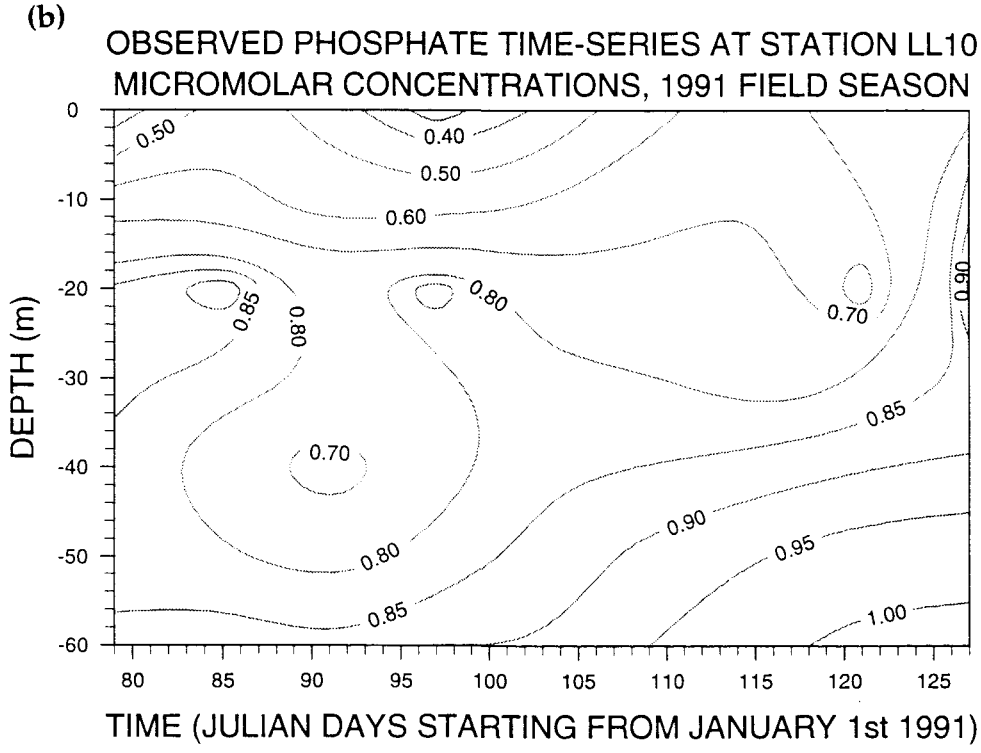

FIGURE 5.19

Temporal Variations in (c) Silicate Concentrations and (d) Salinity at Station LL10, Julian Day 79 to 127, 1991.

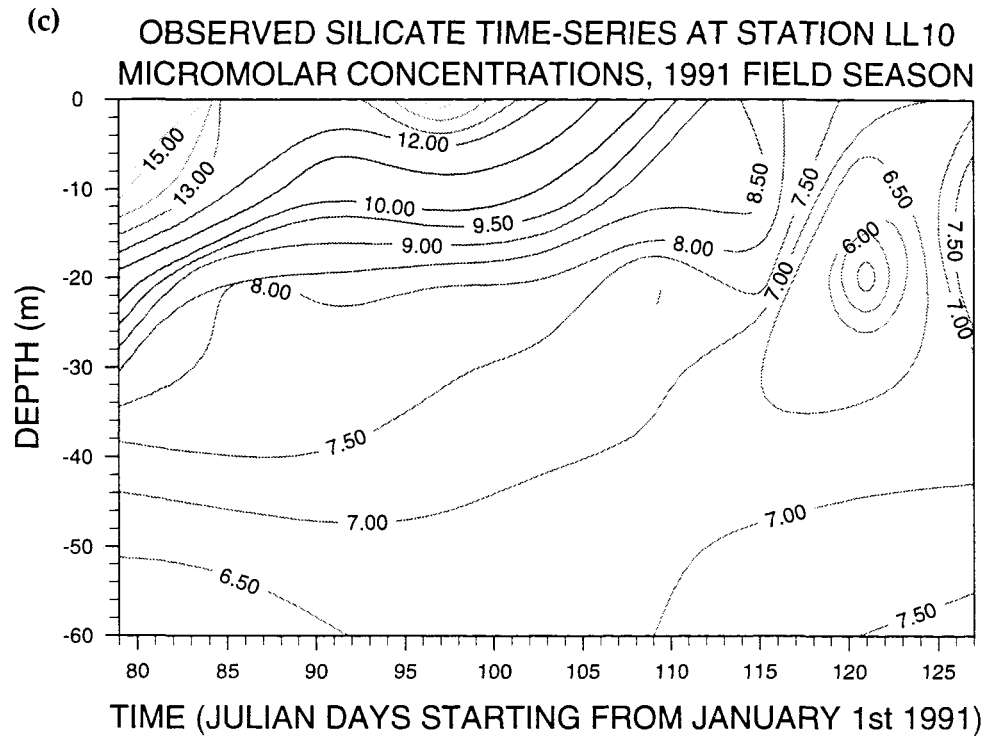

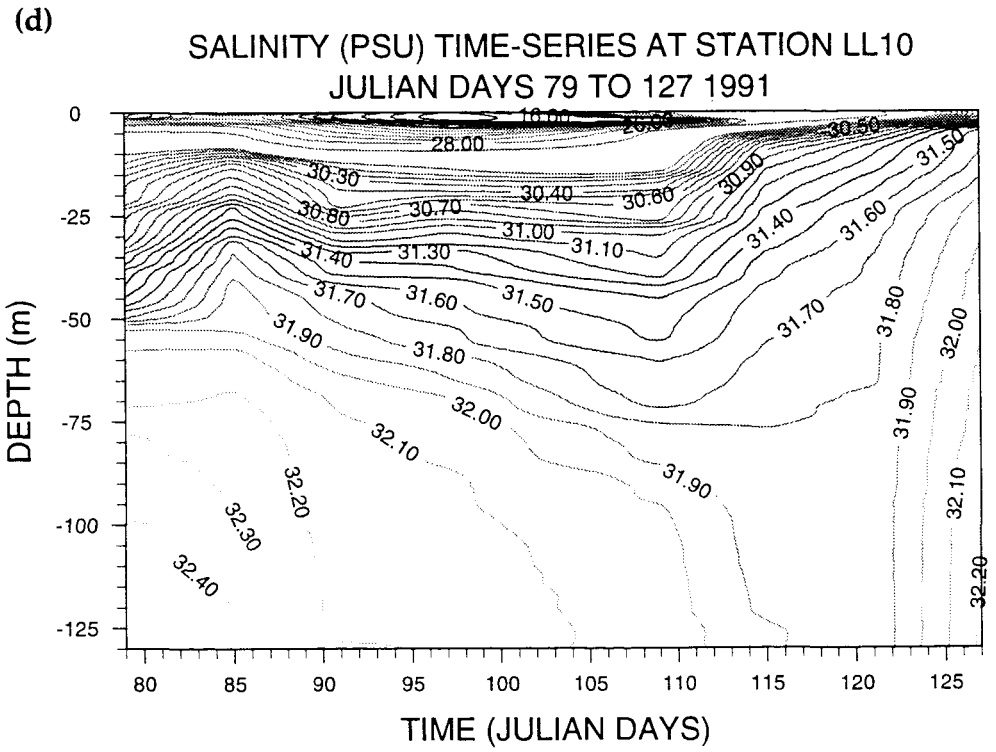

FIGURE 5.20

Temporal Variations in (a) Nitrate Concentrations and (b) Phosphate Concentrations Station LL14, Julian Day 79 to 127, 1991.

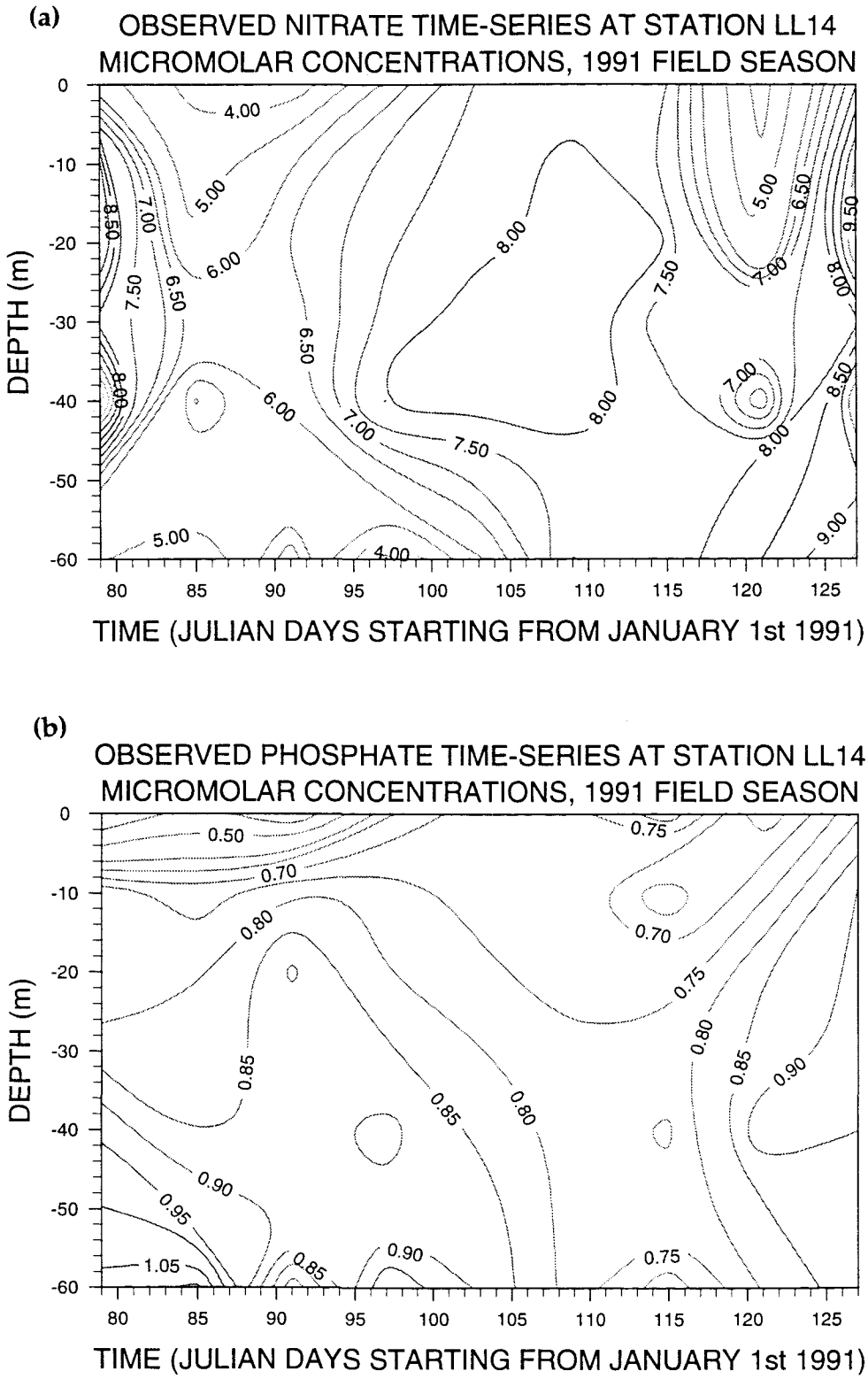

FIGURE 5.20

Temporal Variations in (c) Silicate Concentrations and (d) Salinity at Station LL14, Julian Day 79 to 127, 1991.

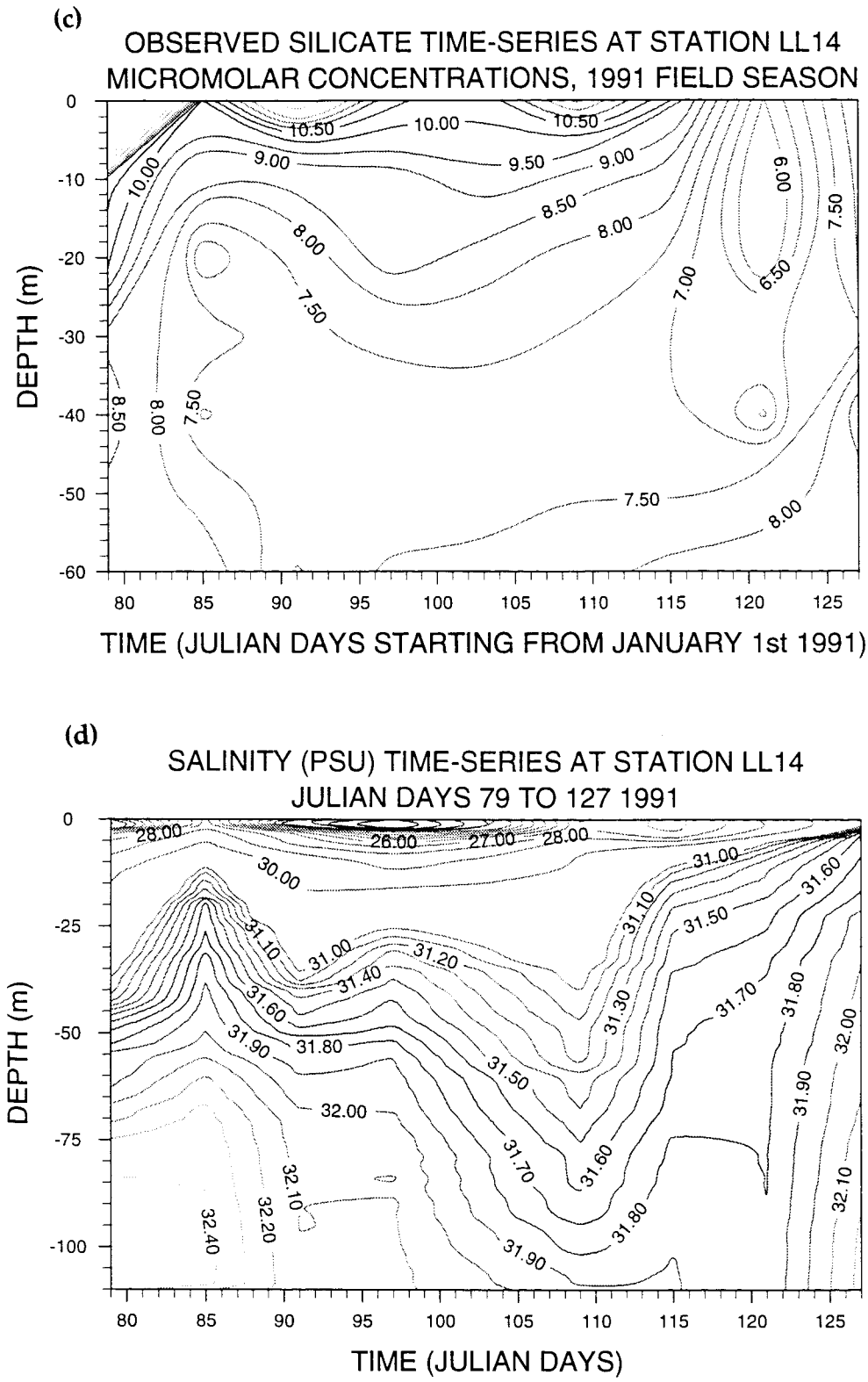

FIGURE 5.21

Temporal Variations in (a) Nitrate Concentrations and (b) Phosphate Concentrations Station LL19, Julian Day 79 to 127, 1991.

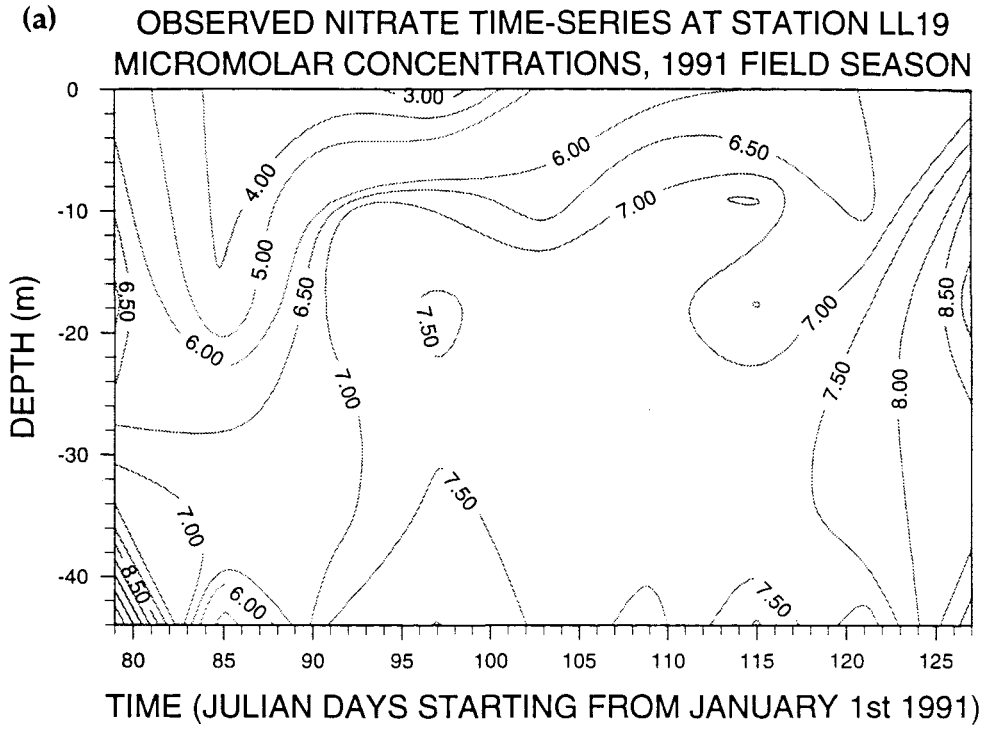

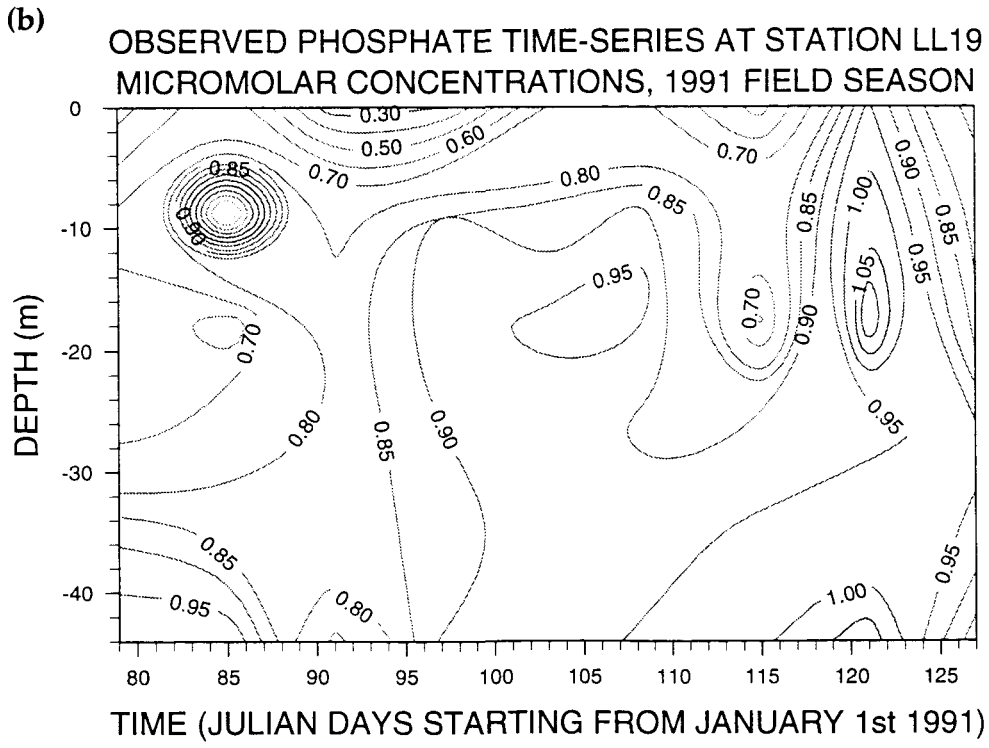

FIGURE 5.21

Temporal Variations in (c) Silicate Concentrations and (d) Salinity at Station LL19, Julian Day 79 to 127, 1991.

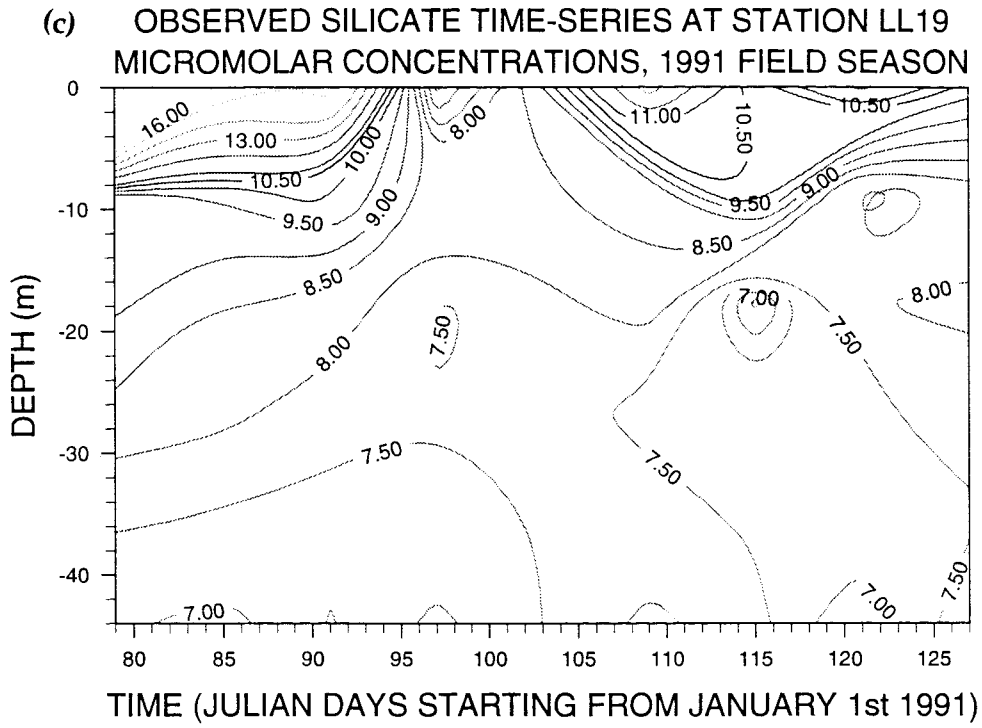

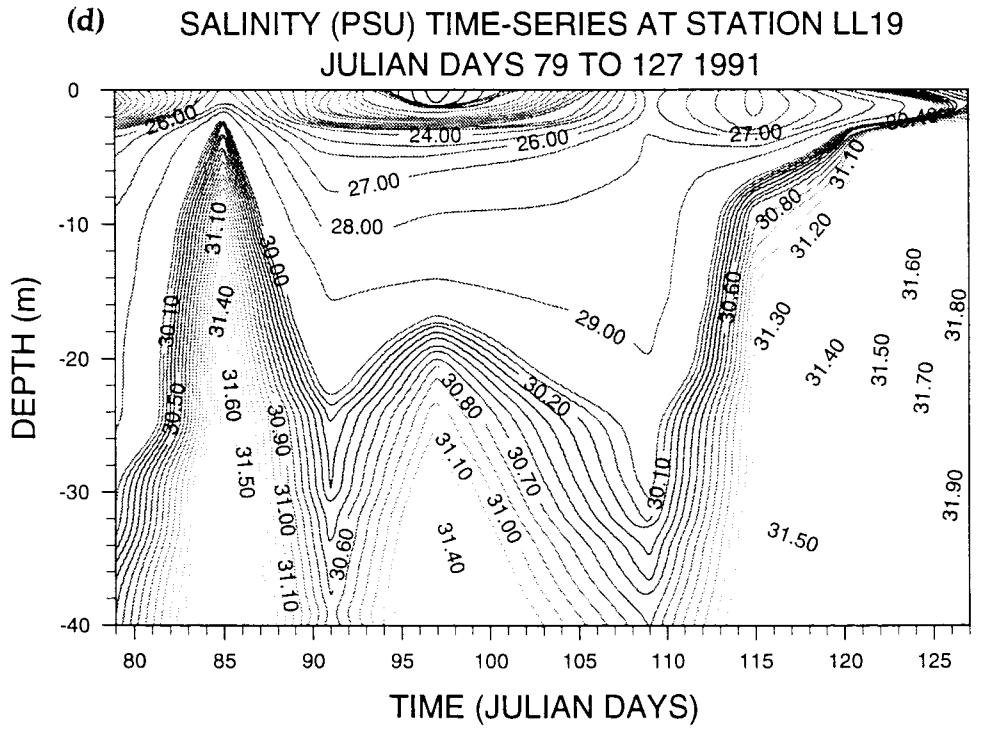

Further evidence is provided through hydrographic and nutrient data collected at two later dates, days 164 and 171, as part of this study. **TABLE 5.1** lists the data averaged over the top 10 m at stations LL4, LL10, LL14 and LL19 and over the top 20 m at LL0 for the dates, days 79 to 127 and **TABLE 5.2** lists similar data for the post-bloom dates, days 164 to 171.

TABLE 5.1

Station Number	**LL0**	**LL4**	**LL10**	**LL19**
Salinity (PSU)	31.86	28.05	27.75	27.01
NO_3 (µM)	7.76	6.76	5.84	6.34
PO_4 (µM)	0.92	0.79	0.64	0.76
SiO_4 (µM)	7.37	10.01	10.94	11.17
N:P RATIO	8.55:1	8.6:1	9.1:1	8.3:1
N:Si RATIO	1.05:1	0.68:1	0.53:1	0.56:1

This shows that the pre-bloom N:P ratios of the surface waters do not vary much across the loch (± 0.8) which indicates that the variations found in the NO_3 concentrations are accompanied by similar variations in the PO_4 concentrations. In **CHAPTER 2**, section **2.3.1.1** nutrient ratios were discussed in terms of their ecological importance as were deviations away from them and reasons for these (the Redfield Ratio predicting N:P values of 16:1 for the oceanic environment and the N:Si being predicted as 1.07:1 by Richards, 1958). The N:P ratios listed in **TABLE 5.1** lead to an average pre-bloom N:P ratio for the surface layers of the upper basin of 8.6:1 which is lower than the Redfield Ratio and would suggest that phytoplankton growth could be nitrogen limited in Loch Linnhe. The corresponding average N:Si ratio 0.68:1 is lower than the ratio predicted by Richards (1958) of 1.07:1 but it decreases with distance from the mouth of the loch from 1.05:1 for the top 10m at LL0 to 0.56:1 at station LL19. This is consistent with a simultaneous increase and decrease in SiO_4 and NO_3, respectively, with distance from the mouth. Average values for NO_3 µM from this table are 5.91 µM, and for PO_4 and SiO_4 are 0.46 and 11.26 µM respectively.

The phytoplankton bloom that occurred consisted of the diatom species ***Skeletonema costatum*** and was observed on day 135 in the upper basin. The data collected on days 164 and 171 therefore provide information on post-bloom conditions. **TABLE 5.2** shows the nutrient concentrations averaged over the top 10 m at stations LL4, LL10, LL14 and LL19, and over the top 20 m at station LL0.

TABLE 5.2

Station number.	**LL0**	**LL4**	**LL10**	**LL19**
Salinity (PSU)	31.08	31.79	31.41	31.56
NO_3 (µM)	1.79	1.73	1.39	2.60
PO_4 (µM)	0.39	0.53	0.42	0.75
SiO_4 (µM)	1.06	1.06	1.51	2.77
N:P RATIO	5.67:1	3.26:1	3.31:1	3.47:1
N:Si RATIO	1.69:1	1.63:1	0.92:1	0.94:1

This data shows that the average NO_3 concentrations measured over this time were 1.86 µM and so were 72% lower than the pre-bloom concentrations. The SiO_4 concentrations were even more depleted with average values at 1.58 µM, 84% lower than the pre-bloom concentrations. The PO_4 concentrations however, were only 32% lower than the pre-bloom averages, at 0.52 µM. Such observed depletions will be due to the phytoplankton bloom occurring between the two dates. Comparison of the average pre-bloom N:P value of 8.6:1 to the post-bloom average of 3.9:1 suggests that PO_4 is regenerated back into the water column more rapidly than either NO_3 or SiO_4, consistent with the literature (see **CHAPTER 2** section **2.3.1.1**). Comparison of the average pre-bloom N:Si ratio of 0.68:1 with the post-bloom value of 1.3:1 suggests also that NO_3 is being regenerated back into the water column faster than SiO_4.

Evidence for such biological activity supports the idea that removal of the dissolved inorganic nutrients to the solid phase via uptake for phytoplankton growth, (a non-conservative process) will be a process that will contribute to the

scatter of data observed in **FIGURE 5.13.**

Factors favouring the phytoplankton bloom: The growth of phytoplankton in sea-lochs is governed mainly by water column stability, nutrient supply and illumination (Grantham, 1981). The stability comes from the vertical stratification found within the sea-loch which is almost wholly due to the freshwater input. This stability (buoyancy input) however, affects phytoplankton growth in 2 opposing ways: (i) by reducing mixing of the surface layers it allows phytoplankton near the surface to maintain their position and receive illumination and (ii) by reducing mixing it also reduces the supply of nutrients from the deeper water when the surface nutrients have been depleted, thereby limiting the phytoplankton growth (Grantham, 1981). An adequate supply of nutrients is essential for phytoplankton growth and this can be provided to the surface layers via the runoff of freshwater and its distribution over the surface and also via vertical mixing, either through deep-water renewal events which displace deep-water upwards or wind-mixing which mixes the freshwater downwards. In terms of the role of nutrient supply by the freshwater runoff, section **5.2.1.2** showed that, generally the freshwater is deficient in PO_4 for phytoplankton growth with very low levels present at 0.05 to 0.4 µM although the input of NO_3 of 2.5 to 9.0 µM is relatively significant compared to the saline source. This leads to very variable N:P ratios ranging from 0.16:1 to 180:1 from the freshwater input to the loch, depending on seasonality effects for example. The SiO_4 concentrations are in excess due to the freshwater being their main source to the loch and they average 13.78 µM at 0 m at station LL19. Associated with high salinities and low freshwater runoff are high concentrations of NO_3 and PO_4 since their main source is from the saline end-member. Conversely, high SiO_4 concentrations are associated with relatively low salinities and high freshwater runoff. Around the time of the bloom, the weather had become drier (see **FIGURE 5.4**) and so the salinity of the surface layers would have been higher. The accompanying elevated concentrations of PO_4 and NO_3 and depressed concentrations of SiO_4 in the surface layers would favour the bloom.

Also favouring the bloom were the temporal changes in the nutrient concentrations

as observed at station LL0 (see **FIGURE 5.17**) for the two sampling dates leading up to the bloom, days 120 and 127. These show an increase in the concentrations of the NO_3 and PO_4 in the inflowing water and vertical mixing through the water column by day 127. The NO_3 concentrations are elevated to greater than 9.50 μM and the PO_4 concentrations to greater than 1.30 μM and the SiO_4 levels remain fairly constant at 6.50 to 7.00 μM. Such increases are likely to be due to the advection of increased nutrients from the coastal region due to the upwelling event described as occurring at station LL0 between days 113 and 120 in section **5.1.2.2**. The increased nutrient concentrations might be due to point inputs of nutrients in the Clyde-Sea area or an increased contribution from the Atlantic component which has typically higher NO_3 and PO_4 concentrations associated with it (Mr. B. Grantham, 1992, DML, pers.comms.). Hence this water containing increased levels of NO_3 and PO_4 will enter the basin and cause the deep-water renewal event described in section **5.1.2.2** which results in the upward displacement of the resident water in the basin, thus pushing up any nutrients from the saline waters into the euphotic zone. In **FIGURES 5.17** to **5.20** all stations show increased nutrient concentrations in well-mixed water columns by day 127 which would favour the bloom given more stratification in the surface layers, (which could well have occurred by day 135). Also favouring the bloom at this time is the fact that algal cells would have been being swept into the basin from the Firth of Lorne where elevated chlorophyll concentrations had been measured on day 119 (Dr. M. Heath, 1992, SOAFD, pers.comms.). Hence these could seed the bloom although another possibility for seeding the bloom is the uplift of diatom cells, once vegetative in the sediment, into the euphotic zone via resuspension of the sediment during the deep-water renewal event.

Having provided some limited evidence for biological activity which is a non-conservative process giving rise to real non-conservative behaviour and scatter of data from a TDL, the following section considers any evidence for further biogeochemical processes which will also lead to non-conservative behaviour thus contributing to the observed scatter.

(ii) Evidence for biogeochemical processes: This section considers evidence for further biogeochemical processes which may include (i) the conversion of nutrients from the solid to the dissolved inorganic phase via regeneration and (ii) adsorption of PO_4 from the dissolved to the solid phase via scavenging by SPM. Processes such as these which involve a phase change of the nutrients will lead to non-conservative behaviour and the scatter of data away from a linear nutrient / salinity relationship.

(a) The main problem with the consideration of regeneration of nutrients from the sediment using the 1991 data, is that changes in the nutrient concentrations of the bottom-waters could not be observed for this field-season because the sampling strategy was such that nutrient samples were not collected below a depth of 60 m for the majority of the field-season. There were only three days, (113, 120 and 127) when sampling took place fully, into the bottom-waters of the basin, at the deeper stations. This is unfortunate because the hydrographic results would suggest that for depths of approximately 90 m and greater, the water was isolated at least from at least day 79 to day 120, thus allowing time for the build-up of regenerated nutrients in the bottom-waters (as described in **CHAPTER 2**, section **2.3.2.1**). In 1990 for example, the period of deep-water isolation was considerably lengthened for the bottom-waters in the upper basin of Loch Linnhe, lasting from early February to mid-April, due to the exceptionally high rainfall during this period thus strengthening the vertical stratification throughout the water column. Accompanying this isolation were strong measurable signals of increased nutrient concentrations with the nutrient concentrations in the bottom-waters increasing to maxima of 13 µM for SiO_4, 1.2 µM for PO_4 and 9.8 µM for NO_3, (Grantham, 1992). For the 1991 field-season however, only data from the three days mentioned previously can be considered, using station LL4 as an example. Evidence for the benthic regeneration of nutrients into the bottom-waters from this is very weak. On the basis of this, the sampling strategy adopted for the 1992 field-season allowed for a more detailed study of the bottom-water processes, the results of which can be found in **CHAPTER 6** , section **6.2.1.2** (ii).

FIGURE 5.22 presents time-series plots of data from three days of observations for station LL4, created using the UNIMAP software package (settings listed in **APPENDIX 5.5**). It shows that all of the nutrients generally show vertical stratification throughout the water column on day 113, thus following the salinity distribution shown in **FIGURE 5.22 (d)**. The PO_4 concentrations tend to increase with salinity and depth ranging from less than 0.95 µM at the surface to greater than 1.00 µM at 110 m. The NO_3 concentrations also increase with salinity, ranging from less than 7.5 µM at the surface to greater than 8.5 µM at 110 m. This is consistent with the NO_3 and PO_4 having a saline source. SiO_4 concentrations decrease with depth ranging from greater than 8.0 µM at the surface to less than 6.5 µM at 60m depth, consistent with a freshwater source. At depths of greater than 75 m the SiO_4 concentrations begin to increase again reaching a maximum of greater than 7.5 µM at 110 m. This anomaly in the SiO_4 distributions is possibly due to inflowing water only penetrating to depths of 60 m to 75 m up to day 113 thus causing partial renewals of water to this depth with silicate concentrations above this depth reflecting those in the inflowing water. Concentrations of all three nutrients at depths greater than 75 m are relatively high compared to those in the water above them which could be due to (i) the original saline water that intruded to the bottom-waters of the loch containing high concentrations of all three nutrients, (ii) the incoming water which sank to 60 to 75 m containing lower levels of nutrients than the water at depths greater than 75 m and (iii) benthic regeneration processes releasing nutrients back into the water column from the sediment.

FIGURE 5.22 shows also that on day 120 there was an increase of NO_3 and PO_4 with depth although the bottom-water concentrations generally remain the same as on day 113. In general other observations from **FIGURE 5.22** are that in the top 75 m the concentrations of the nutrients have increased since day 113 and for SiO_4 the trend is now for a general increase in the concentration with depth throughout the whole water column. By study of **FIGURE 5.22** it can be seen how the contour lines have been lifted showing the higher concentrations of nutrients at shallower depths than day 113. This is likely to be due to a partial renewal of water to

FIGURE 5.22

Temporal Variations in (a) Nitrate Concentrations and (b) Phosphate Concentrations Station LL4, Julian Day 113 to 127, 1991.

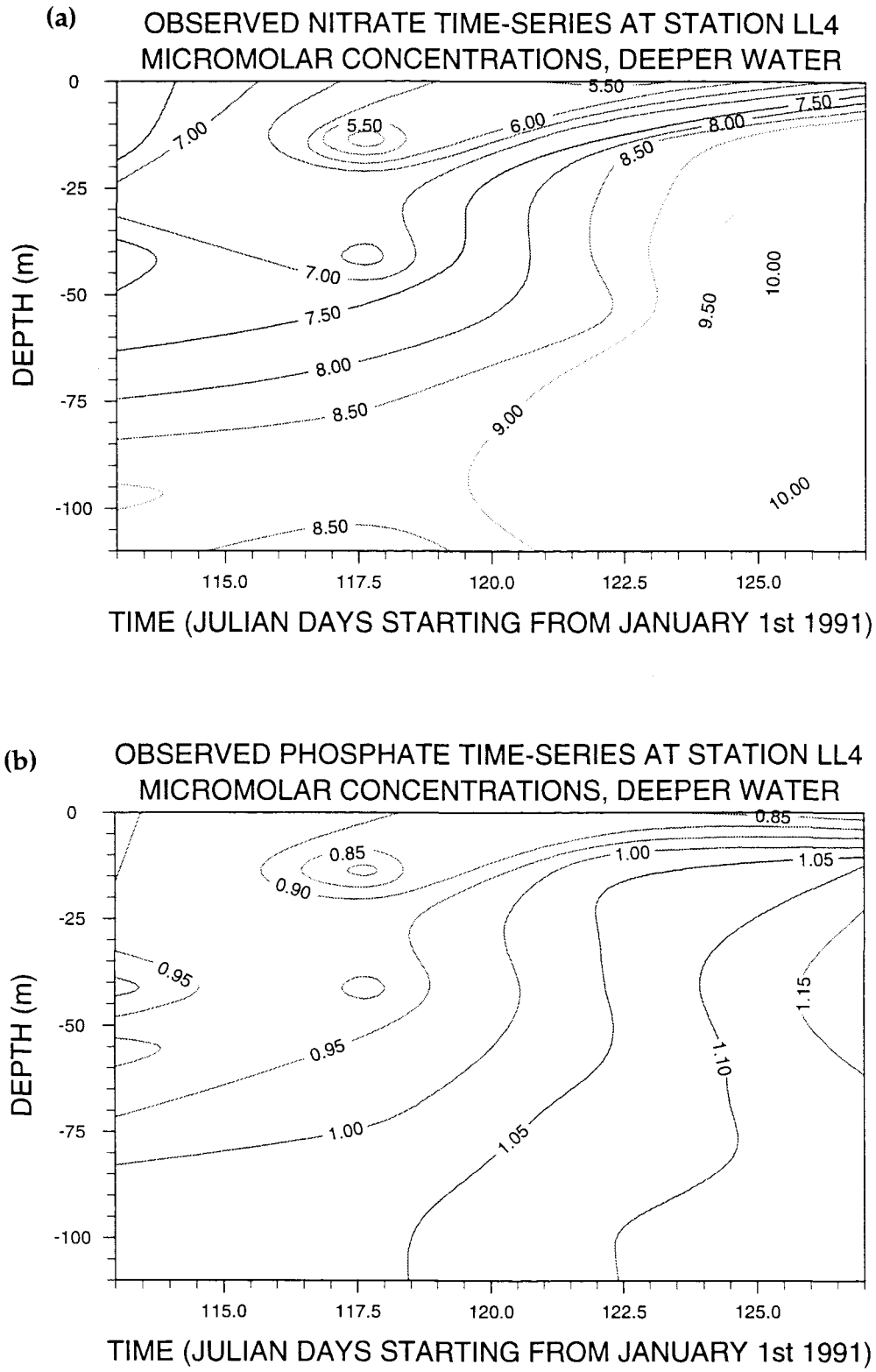

FIGURE 5.22

Temporal Variations in (c) Silicate Concentrations and (d) Salinity at Station LL4, Julian Day 113 to 127, 1991.

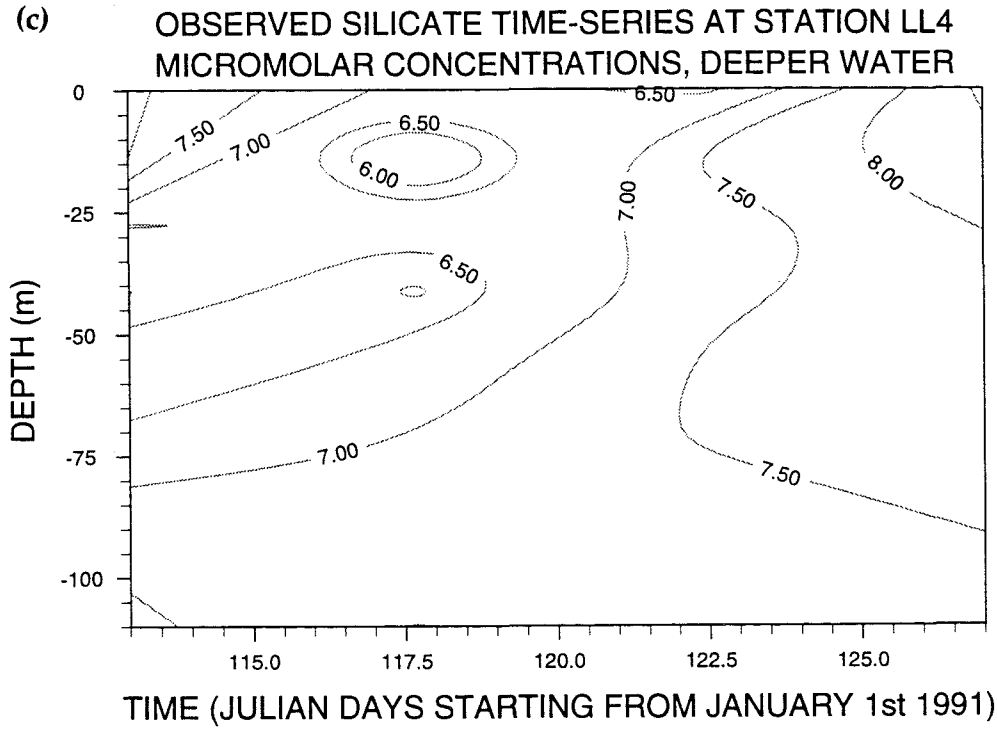

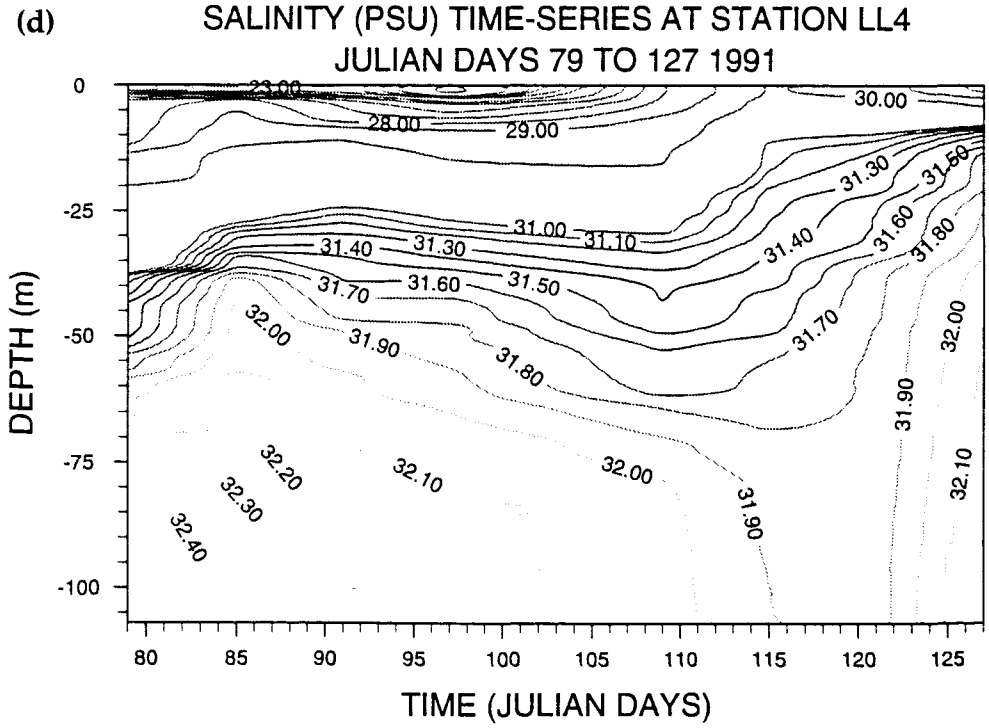

depths of between 60 to 75 m after day 113. Hence resident water at depths shallower than 75 m is displaced upwards by this event. As can be seen from **FIGURE 5.17** the concentration of the nutrients in the incoming sill-water was increasing over this time through to day 127 and this would explain the increase in the concentrations of the nutrients observed to 75 m at LL4. For SiO_4 the increase through the water column is only slight but this would be because the SiO_4 concentration of the incoming water is fairly constant over this time at 6.5 to 7.0 μM.

The high salinity water causing the deep-water renewal between days 120 and 127 has a high concentration of nutrients associated with it as noted before, especially NO_3 (~11 μM) and PO_4 (~1.3 μM) and the effect of this on the nutrient distribution at LL4 is evident from **FIGURE 5.22**; the renewal has resulted in breakdown of most of the vertical stratification within the water column (except for the top 10 m) causing the water below 10 m to be of a relatively high concentration (except for SiO_4) and relatively homogeneous in nature.

Hence, there is very little evidence from the 1991 data that significant regeneration of nutrients from sediments had occurred in the bottom-waters over the period of the observations.

(b) Dissolved inorganic PO_4 has a very complex geochemical reactivity associated with it in natural waters and this has been described in **CHAPTER 2**. Evidence for such behaviour from the 1991 data-set is again very sparse and so a limited study on the PO_4 content of the sediments in the upper basin was carried out as part of the 1992 field-season, the results of which can be found in **CHAPTER 6**, section **6.2.1.2** (ii). In 1991 there was however a slight suggestion of PO_4 removal from the water column from data collected at station LL21 on the last day of the field-season, day 127. Station LL21 is a more northerly station situated closer to the freshwater source to the basin, and is relatively shallow (~ 20 m depth) (see **CHAPTER 4**, section **4.1.1**). Thus increased vertical mixing might be expected at this station with resultant suspension of sediment and perhaps adsorption of the

particle reactive PO_4 onto the surfaces of the SPM. Results from day 127 then, are presented in **FIGURES 5.23, 5.24** and **5.25** for the PO_4, the NO_3 and the SiO_4 concentrations respectively as a function of salinity for stations LL21, LL20 and LL19. They show that the PO_4 concentrations are relatively independent of salinity at stations LL20 and LL19 and yet at station LL21 there appears to be a strong inverse relationship with the concentrations decreasing from ~ 0.8 µM at the surface to almost zero µM at a depth of 20 m. This decrease of PO_4 concentration with an increase in salinity is the opposite to what is expected based on the observations made in this chapter which show that the saline end-member provides the main source of PO_4 to the basin. **FIGURE 5.24** shows the corresponding changes in the NO_3 concentrations at these stations and shows them to behave as expected with positive gradients in their plots against salinity, indicating that the saline end-member provides the main source of NO_3. **FIGURE 5.25** shows that the SiO_4 concentrations also behave as expected with a negative gradient due to their freshwater source. Such a decrease of the PO_4 concentrations with depth and increasing salinities at station LL21 cannot then be explained by dilution effects by freshwater runoff since these would have caused a corresponding decrease in the observed NO_3 concentrations and increase in the SiO_4 concentrations. Hence there is the possibility that the decrease of PO_4 observed at station LL21 is caused by geochemical scavenging of the PO_4 onto particulate material; a non-conservative process that will lead to deviations of data away from a linear nutrient / salinity relationship.

FIGURE 5.23

Relationship of Phosphate Concentration with Salinity at (a) Station LL21, (b) Station LL20 and (c) LL19 on Day 127, 1991.

(a)

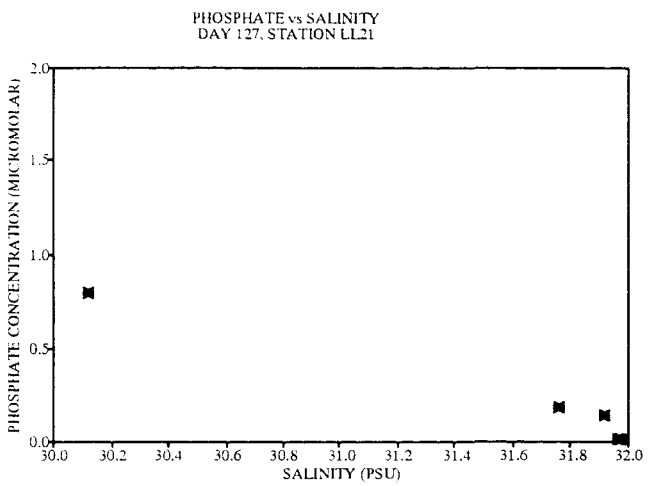

(b)

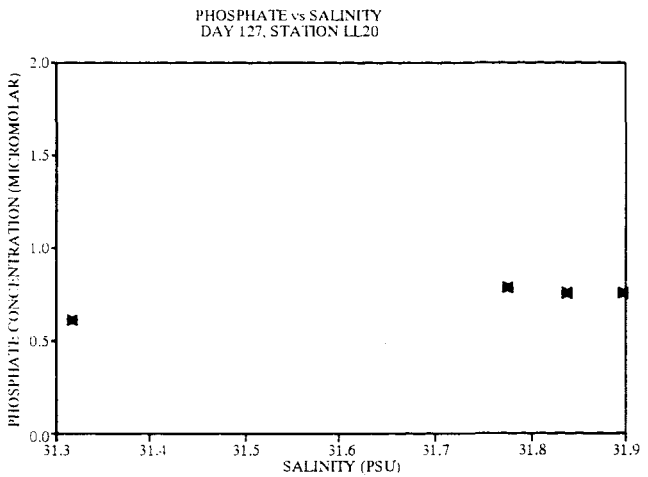

(c)

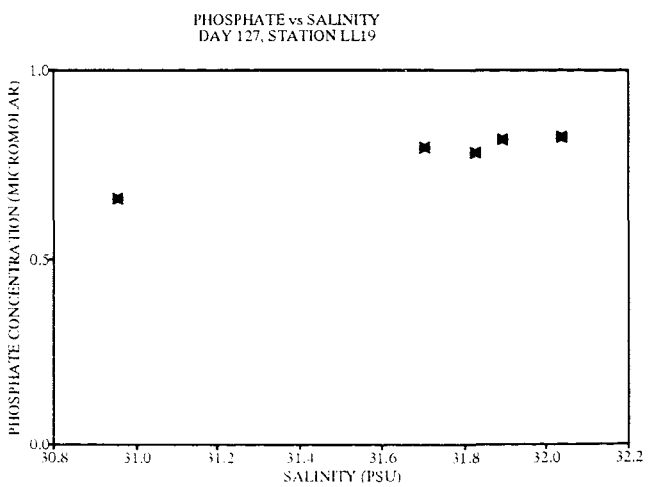

FIGURE 5.24

Relationship of Nitrate Concentration with Salinity at (a) Station LL21, (b) Station LL20 and (c) LL19 on Day 127, 1991.

(a)

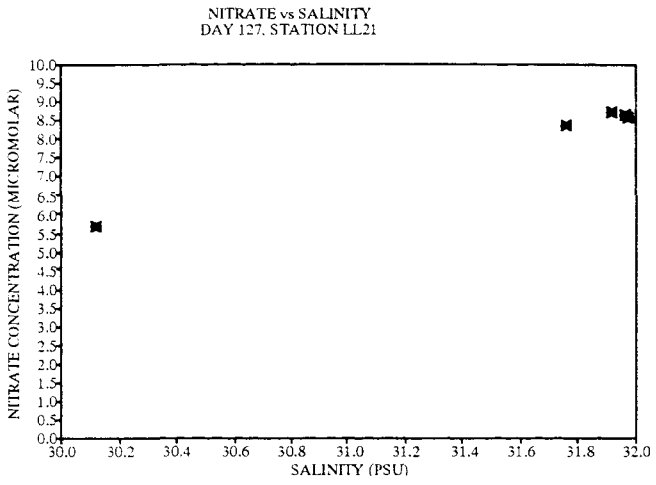

(b)

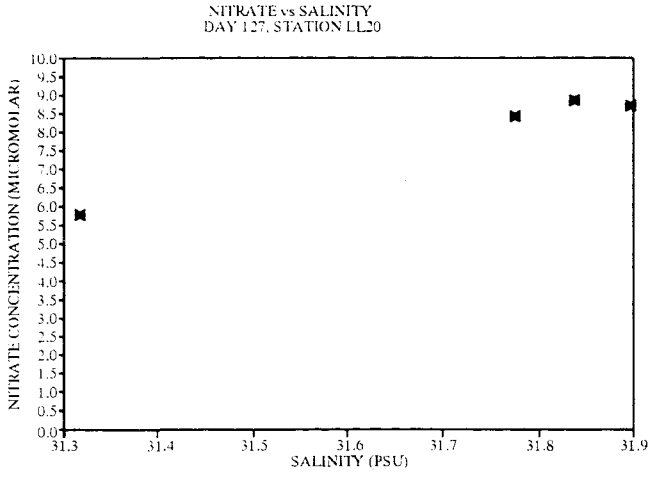

(c)

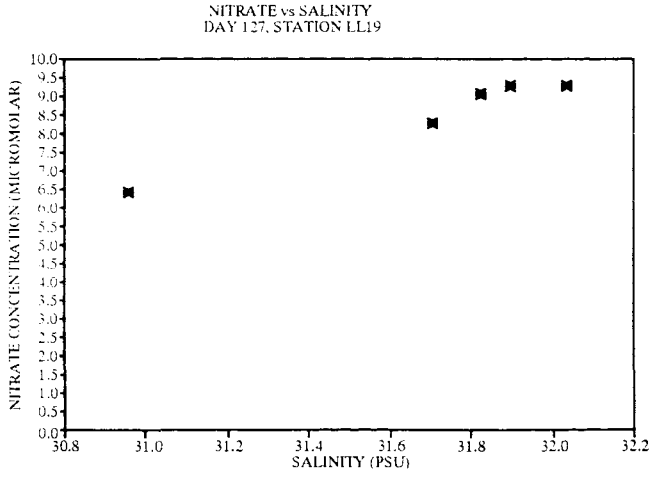

FIGURE 5.25

Relationship of Silicate Concentration with Salinity at (a) Station LL21, (b) Station LL20 and (c) LL19 on Day 127, 1991.

(a)

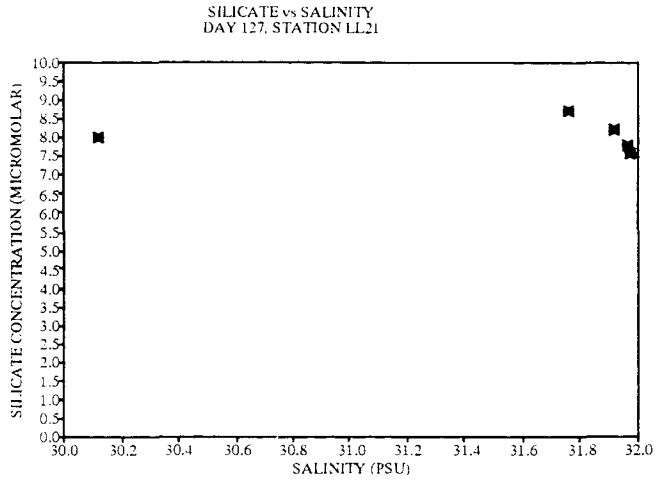

(b)

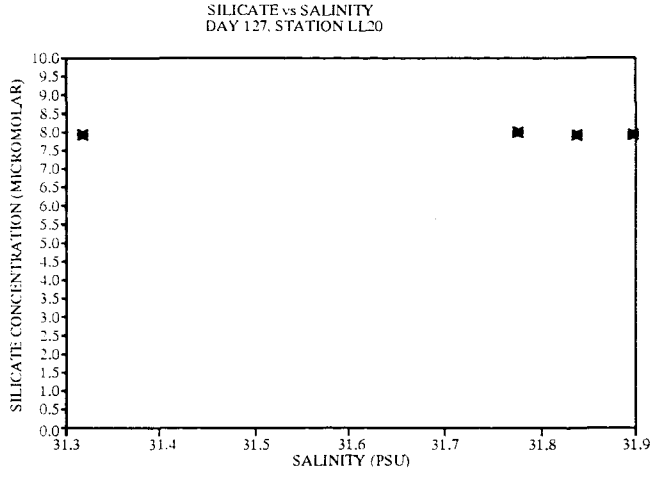

(c)

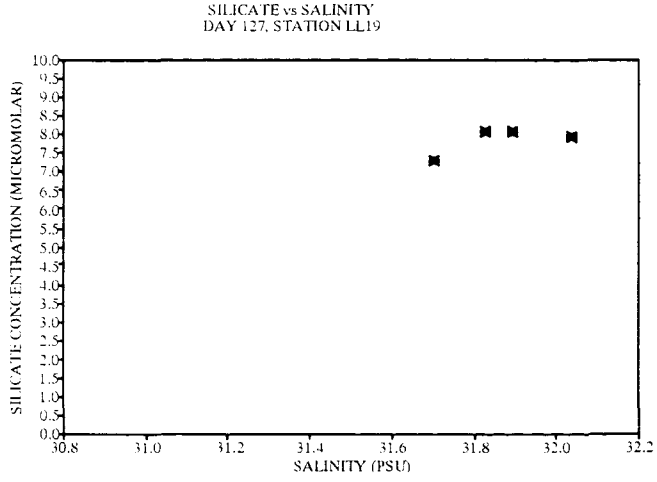

5.3 Summary and Conclusions from the 1991 Field-Season

5.3.1 Summary of the hydrographic observations

The 1991 hydrographic survey showed the following:

(i) The water in the upper basin of Loch Linnhe is vertically stratified according to its density and that the water temperature plays a negligible role in determining the density structure.

(ii) The basin is generally horizontally uniform in terms of density and salinity properties, although there are small gradients due to the freshwater source at the head of the loch.

(iii) The water below 95 m on day 79 showed near homogeneity with changes in the density and salinity from this depth to the bottom of the basin being only 0.1 kg m^{-3} and 0.1 PSU.

(iv) The water throughout the basin is relatively well-mixed by day 127 with the maximum change in salinity between 15 m and the bottom of the basin ranging from only 0.4 to 0.5 PSU compared to changes of 2.4 to 2.5 PSU on day 79.

(v) The hydrography of the surface layers is essentially dependent on the distance from the freshwater source and the riverine inflow.

(vi) Partial renewals of water were occurring throughout the basin intermittently throughout the field-season at the deeper stations, and these caused renewal of the bottom-waters at the shallower, fresher station LL19.

(vii) A deep-water renewal event occurred between days 120 to 127, favoured by (a) upwelling of high salinity water in the sill region, (b) salt and heat fluxes out of and into, respectively, the bottom-waters of the basin, thus decreasing their

density and (c) the occurrence of spring tides around day 120.

5.3.2 Summary of the nutrient results

Nutrient sampling in the 1991 field-season has shown the following:

(i) By plotting all of the nutrient data together as a function of salinity a strong linear nutrient / salinity relationship is not observed. Instead scatter of data occurs about a line of best fit which is due to the total non-conservative and apparently non-conservative behaviour of nutrients throughout the whole field-season.

(ii) General gradients show from the plots made above in (i) that the main source of NO_3 and PO_4 to the basin is from the saline end-member and for SiO_4 is from the freshwater end.

(iii) The saline end-member concentrations of all three nutrients are found to vary temporally and within the flushing time of the system (a deep-water renewal event is not observed until days 120 to 127). Such temporal variation has been attributed to (a) dilution by a temporally varying freshwater source and (b) a temporally varying saline component due to processes such as upwelling and the advection of temporally varying nutrient concentrations from adjacent coastal regions, and biogeochemical processes in the sill region.

(iv) The freshwater end-member concentrations have been found to vary temporally with the NO_3 concentrations showing a stronger correlation with the annual regime and therefore seasonality effects, than PO_4. Neither of these nutrients shows a strong correlation with riverine flow-rates which for NO_3 is explained by the temporal effect of water movement through the soil and for PO_4 by its complex geochemical behaviour.

(v) Limited evidence has been provided for the presence of biological activity in the upper basin, with a slight depletion of all three nutrients in the surface layers

of the basin being observed around day 120. Post-bloom data has shown significant decreases in the nutrient concentrations across the top 10 m of the basin with a 72 % decrease observed in the NO_3 concentrations compared to pre-bloom conditions, an 84 % decrease for the SiO_4 concentrations and a 32 % decrease for the PO_4 concentrations.

(vi) There is little available evidence for the regeneration of nutrients from the sediment into the bottom-waters. There is a suggestion of PO_4 removal from the dissolved phase at the shallow station LL21 possibly due to scavenging by SPM.

5.3.3 Concluding remarks

This chapter has highlighted the fact that in a sea-loch system there are processes other than biogeochemical processes that can give rise to scatter of data away from a TDL. These are namely temporally varying end-member nutrient concentrations occurring within the flushing time of the basin giving rise to apparently non-conservative behaviour and scatter away from a linear nutrient / salinity relationship when considering the field-season as a whole.

Although evidence has been presented for the different types of processes leading to apparent and real non-conservative behaviour, this has been rather limited, and on the basis of this a more detailed field-study was designed for the 1992 field-season, including sampling at greater depths throughout the basin and monitoring phytoplankton growth through the measurement of chlorophyll a levels. The hydrographic and nutrient surveys have shown the importance of understanding water movement in a sea-loch system, where the circulation is mainly horizontal and intermittent effects such as upwelling and renewal events can alter the distribution of the nutrients in the basin. Upwelling and deep-water renewal events occurred a week before the occurrence of the bloom, perhaps suggesting a link through the consequent upward displacement of high nutrient water into the euphotic zone thus triggering the bloom.

CHAPTER 6 will consider the results obtained in the 1992 field-season.

CHAPTER 6 RESULTS FROM THE 1992 FIELD-SEASON

This chapter presents, initially, results of investigations of spatial and temporal variability from the hydrographic survey made in 1992. It then describes the temporal changes in nutrient concentrations as observed at two stations in the basin system, selected for detailed examination.

6.1 Hydrographic Results

As was described in **CHAPTER 4**, hydrographic measurements were collected from six stations along the longitudinal axis of the loch (from station LL0 at the saline end to station LL21 at the freshwater, head of the loch) on a weekly basis from day 56 to day 139. In the following section data from selected stations only are used to illustrate particular hydrographic features, although the whole of the CTD data-set is present on floppy disc as part of the appendices (**APPENDIX 6.1**). Contour maps are, however, based upon all available relevant data; settings in the UNIMAP software used to produce these maps are given in **APPENDIX 6.2**.

6.1.1 Spatial features in the upper basin

This section considers the hydrographic features of the upper basin, as shown in a longitudinal section of the loch. Two days are chosen for the study: day 64, near the start of the field-season and day 139, the last day of the field-season. Contour maps, of hydrographic parameters are presented in **FIGURES 6.1** to **6.3** and which are produced using CTD data collected throughout the whole water column at the stations LL0, LL4, LL14, LL19, LL20 and LL21 (see **CHAPTER 4**, section **4.1.1.** for details).

FIGURES 6.1 (a) and **(b)** show the longitudinal density and salinity structures, respectively, as present in the upper basin on day 64. Vertical stratification and general horizontal uniformity of the density and salinity is a prominent feature of these plots. The salinity decreases slightly in the surface layers towards the head

FIGURE 6.1

Longitudinal Structure of (a) Density and (b) Salinity in the Upper Basin on Day 64, 1992.

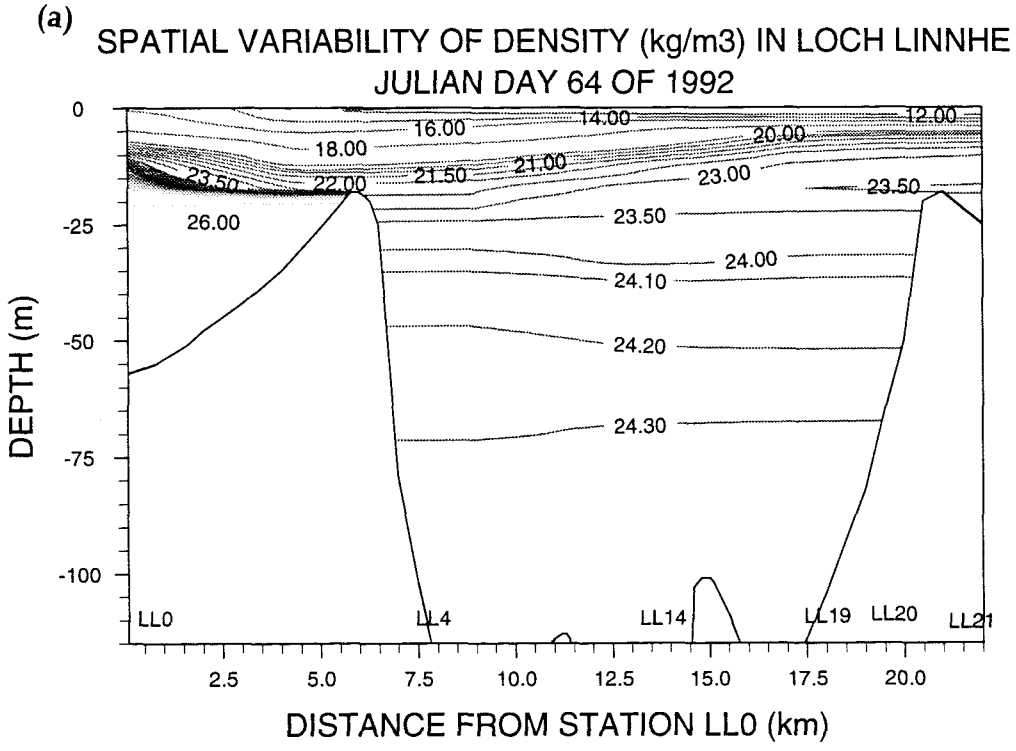

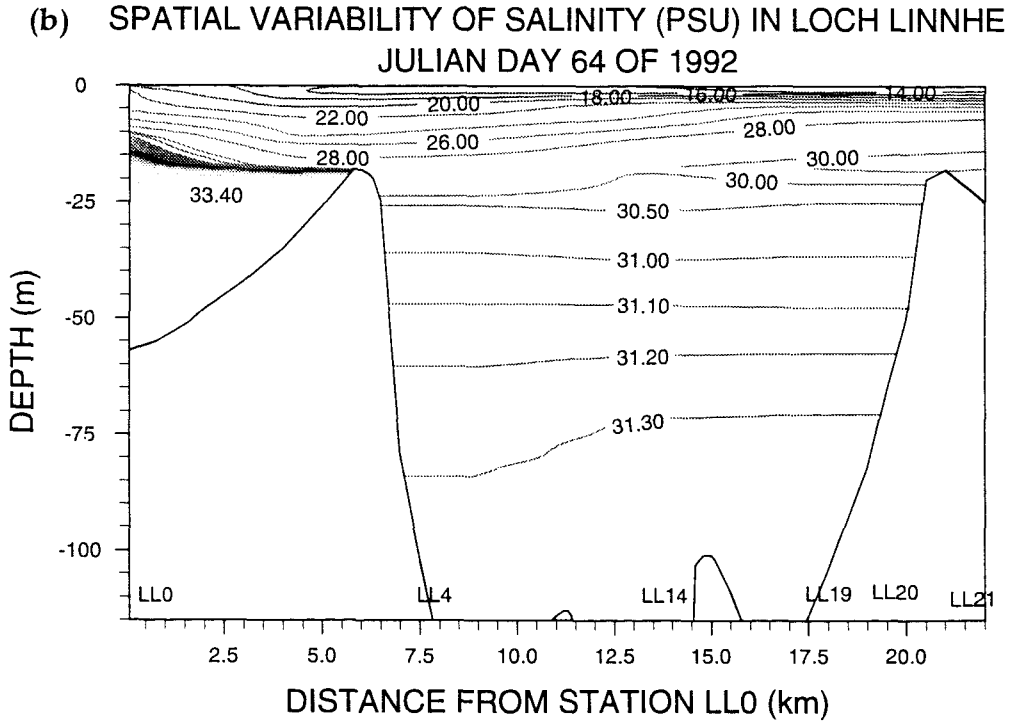

of the loch with its freshwater input; salinity values at 0 m depth for day 64 are 22.325 at LL0, decreasing to 13.609 at LL14 and 14.898 at LL21. The density and salinity of the water increases steadily with depth throughout the basin on day 64. At depths greater than 75 to 80 m the water appears to be homogeneous in the basin, with a density of between 24.3 -24.4 kg m^{-3} and a corresponding salinity of 31.3 - 31.4 PSU to the bottom-water depth of 115 m. (This bottom-water depth refers to the deepest data-point measured on that day i.e. 115 m at station LL14.)

FIGURES 6.2 (a) and **(b)** illustrate the longitudinal density and salinity structures in the upper basin for day 139, the last day of the field-season. The water is again vertically stratified in terms of both the density and the salinity structure of the basin and horizontal gradients are relatively small. Values of the salinity at 0 m depth decrease from 28.247 at station LL0 to 24.544 at LL14 and 21.566 at station LL21 reflecting the input of freshwater at the head of the loch. Again a steady increase in the density and salinity of the water with depth is observed with nearly constant density (24.8 - 24.9 kg m^{-3}) and salinity values (31.9 - 32.0 PSU) being found below ~ 80 to 90 m depth.

A comparison of hydrographic conditions on day 64 and day 139 shows that: (i) the surface salinity values have increased by day 139 which is most likely a reflection of the drier weather and thus decreased freshwater input to the loch around this time. This is illustrated in **FIGURE 6.4** which shows the temporal variation of the River Lochy flow; the mean daily flow was 147.88 m^3 s^{-1} on day 64 as compared to the much reduced flow of 33.45 m^{-3} s^{-1} as measured on day 139 (**APPENDIX 6.3** contains all river flow data); (ii) the density and salinity values in the bottom-waters of the basin have increased significantly by day 139; an increase of 0.5 kg m^{-3} for the density and 0.6 PSU for the salinity; (iii) the base of the layers in which there are measurable changes in density and salinity is deeper on day 139 than day 64, with the water becoming homogeneous at 80 to 90m as compared to 75 to 80 m on day 64. These changes in the bottom-water properties are indicative that the bottom-water has been replaced by water of a higher density and salinity throughout the basin at some point between days 64 and 139. Such

FIGURE 6.2

Longitudinal Structure of (a) Density and (b) Salinity in the Upper Basin on Day 139, 1992.

(a)

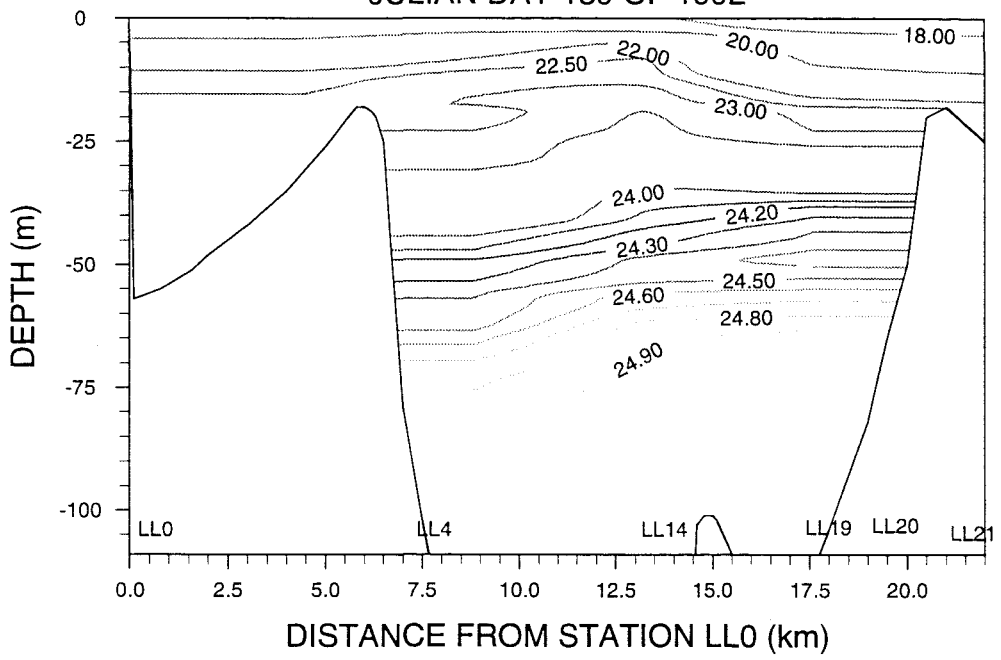

(b)

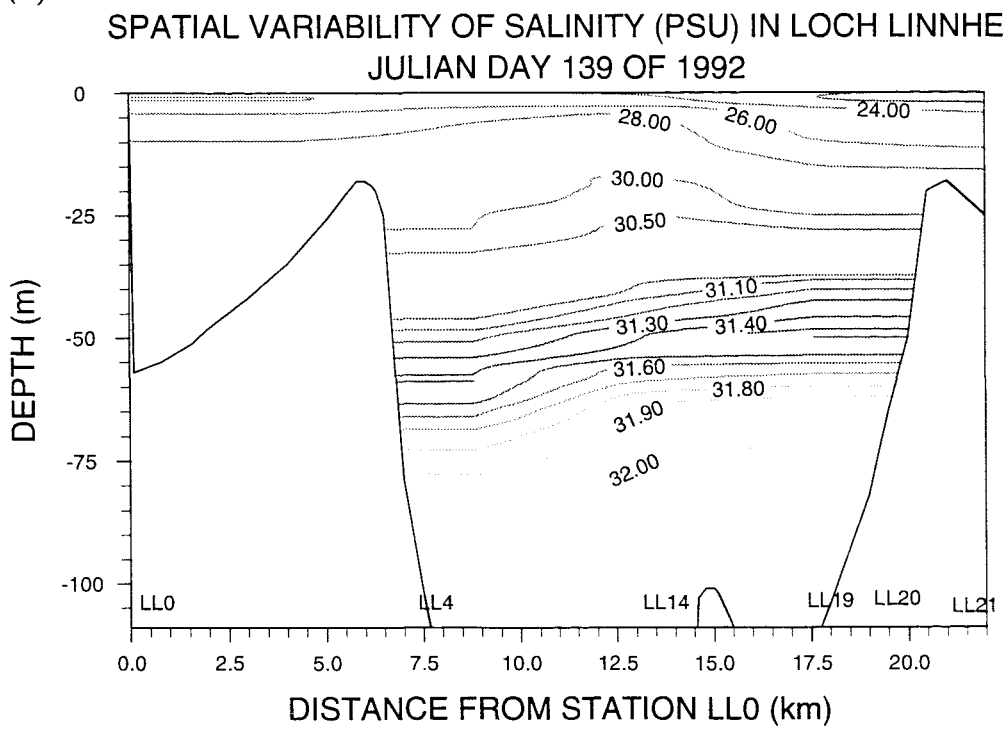

FIGURE 6.3

Comparison Between the Longitudinal Temperature Structure Present in the Upper Basin on (a) Day 64 with (b) Day 139, 1992.

(a) SPATIAL VARIABILITY OF TEMPERATURE (oC) IN LOCH LINNHE
DAY 64 1992 FIELD SEASON

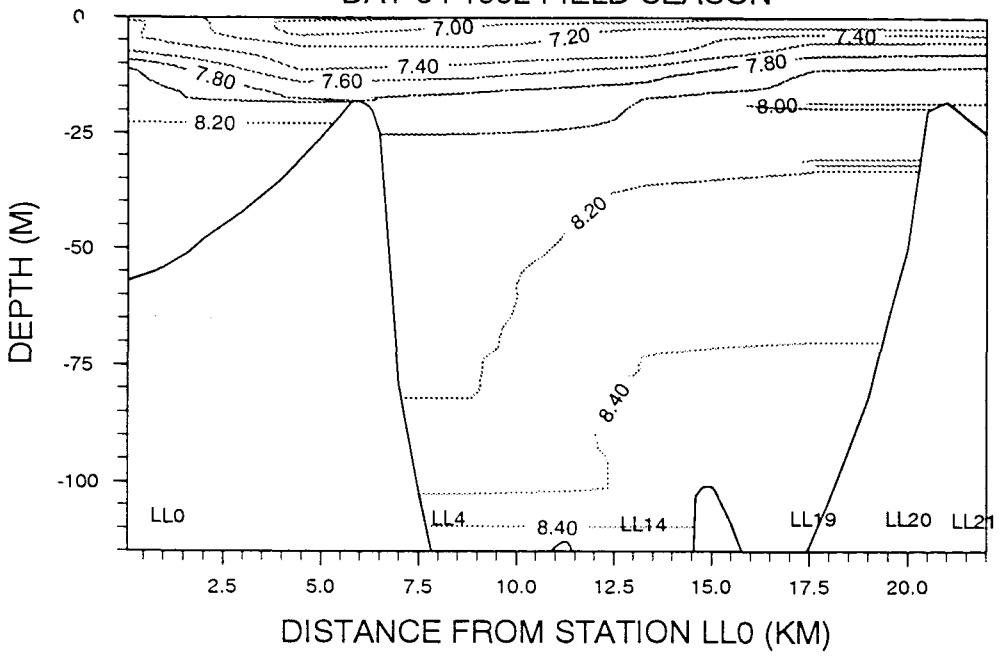

(b) SPATIAL VARIABILITY OF TEMPERATURE (oC) IN LOCH LINNHE
DAY 139 1992 FIELD SEASON

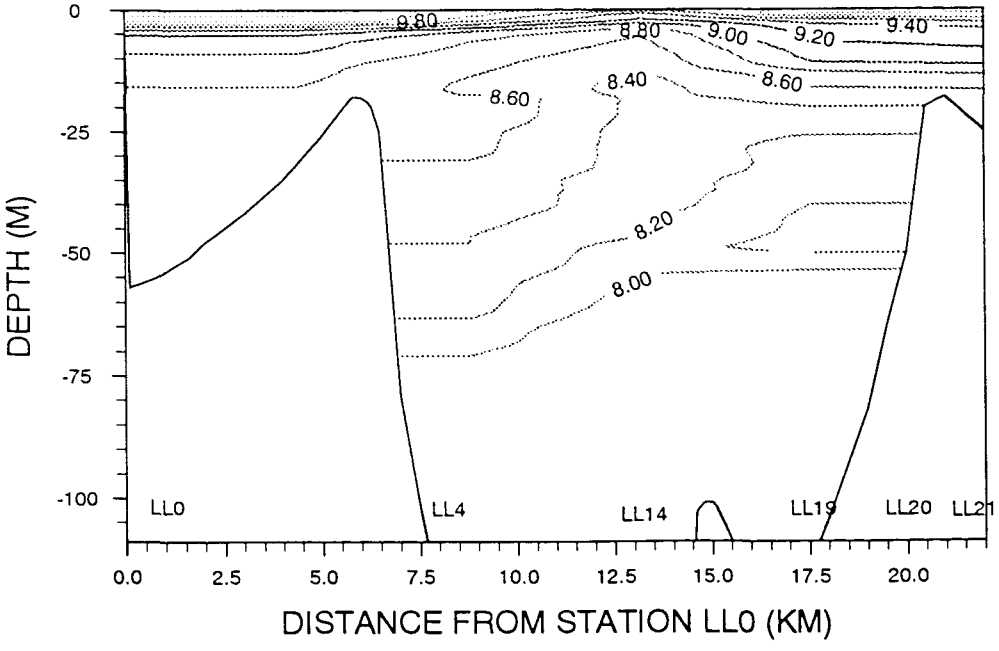

FIGURE 6.4

Variation of the Mean Daily Flow Rate of the River Lochy with Time, Julian Day 50 to 150, 1992 (Data Courtesy of the HRPB).

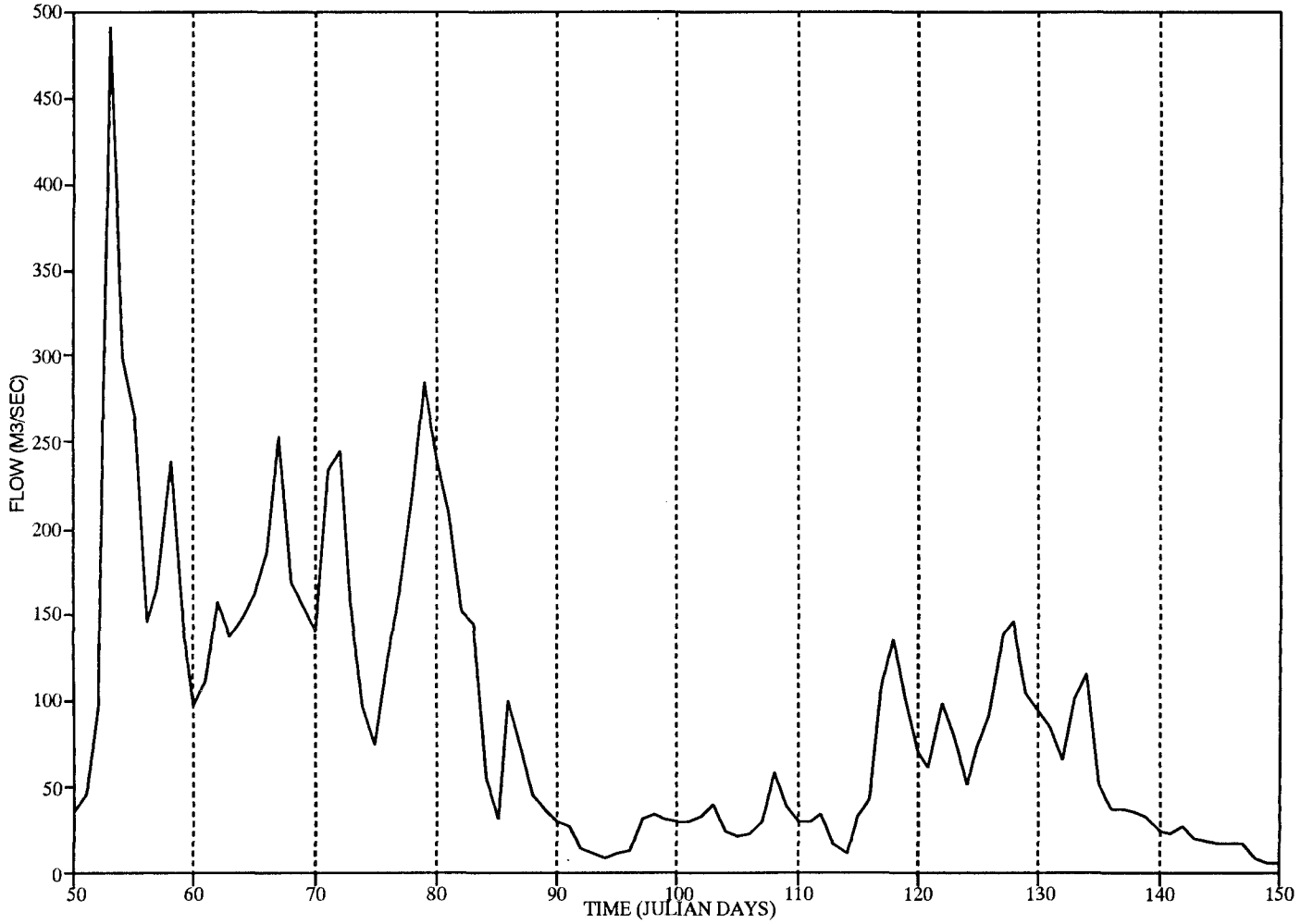

temporal variations in the structure of the water column are dealt with in more detail in section **6.1.2**.

FIGURES 6.3 (a) and **(b)** show how the temperature structure varies throughout the basin for days 64 and 139 respectively. As was described in **CHAPTER 5**, section **5.1.1** in temperate latitudes such as those for Loch Linnhe, a temperature change of 5 °C is required to bring about the same density change as is caused by a salinity change of 1 PSU (UNESCO 1981, 1983). From **FIGURES 6.1 (b)** and **6.2 (b)**, it can be seen that the maximum temperature difference at station LL14 for example, is only 1.43 °C on day 64 and 2.34 °C on day 139. If this is compared with the corresponding salinity changes at this station of 17.691 PSU on day 64 and 7.556 PSU for day 139 it is obvious that the salinity of the water will essentially determine the density structure of the basin whereas variations in the water temperature will have a negligible effect on the structure. On day 64 the surface temperature measured at station LL14 is lower than the bottom-water temperature (6.96 °C at the surface as compared to 8.39 °C at 115 m) and the temperature steadily increased with depth. This temperature inversion will favour a lowering of density in the lower layers to a small degree thus destabilising the water column in terms of the vertical density stratification, to a very small extent. By day 139 this situation is reversed and the surface temperature at station LL14 is greater than that at depth (9.30 °C at the surface as compared to 7.78 °C at 110 m) indicating that the bottom-waters of the basin have been replaced with cooler, denser incoming water. The increase in the surface temperatures of 2.30 °C at station LL14 between day 64 and day 139, reflects the input of warmer freshwater to the system, consistent with the warmer, drier weather around this time.

In the following sections, the temporal variations in the hydrography of the upper basin are considered.

6.1.2 Temporal features in the upper basin

In this section timeseries results from three stations are considered, namely LL0, the most seaward station; LL14 the deepest, most central station; and LL19, a shallower station situated near the head of the loch. Since variations in water temperature will have a negligible effect on the density structure of the water in the basin (see **CHAPTER 6**, section **6.1.1** and **CHAPTER 5**, section **5.1.1**), only the density and salinity features will be considered here.

6.1.2.1 Deep-water renewal events

FIGURES 6.5, 6.6 and **6.7** illustrate the temporal variations in the density and salinity at stations LL0, LL14 and LL19 respectively. As previously indicated the salinity determines the density in the basin.

The figures demonstrate vertical stratification in the water column for the majority of the time, except for the period between days 86 and 99 where there is evidence of vertical mixing throughout the whole water column. The figures show a compression of the contour lines around this time which would indicate that a deep-water renewal event, as observed in the 1991 field-season (see **CHAPTER 5**, section **5.1.2.2**), had occurred. This involves the advection of water over the sill which is denser and more saline than that present in the basin, thus causing upward displacement of the resident water from all depths and resulting in the vertical compression of the horizontal layers in the water column as they expand laterally to fill the cross-section of the basin. Such upward displacement of bottom-water of increased density, results in an increase of the water density at all depths in the basin, thus explaining the increase in salinity as noted on day 139 in section **6.1.1**.

FIGURE 6.8 illustrates the changes in the bottom-water densities of the stations over time. It shows how the density of the sill-depth water (taken as 15 m) at station LL0, decreases markedly between day 64 and day 79 and then increases

FIGURE 6.5

Temporal Variations in (a) the Density (kg m^{-3}) and (b) the Salinity (PSU) at Station LL0, Julian Day 56 to 139, 1992.

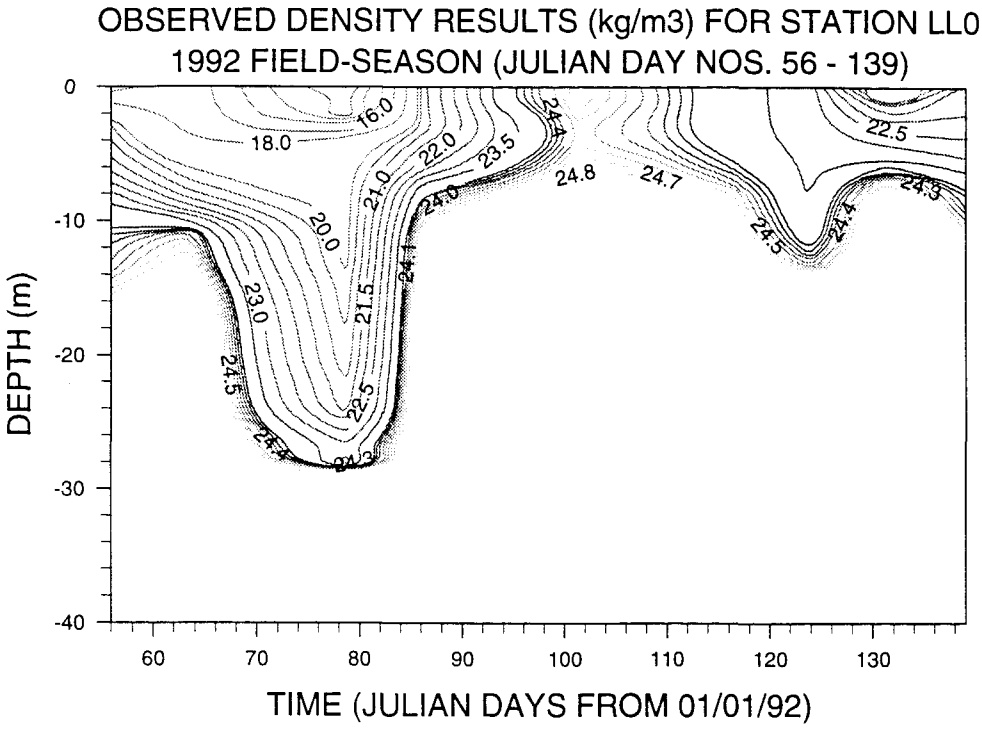

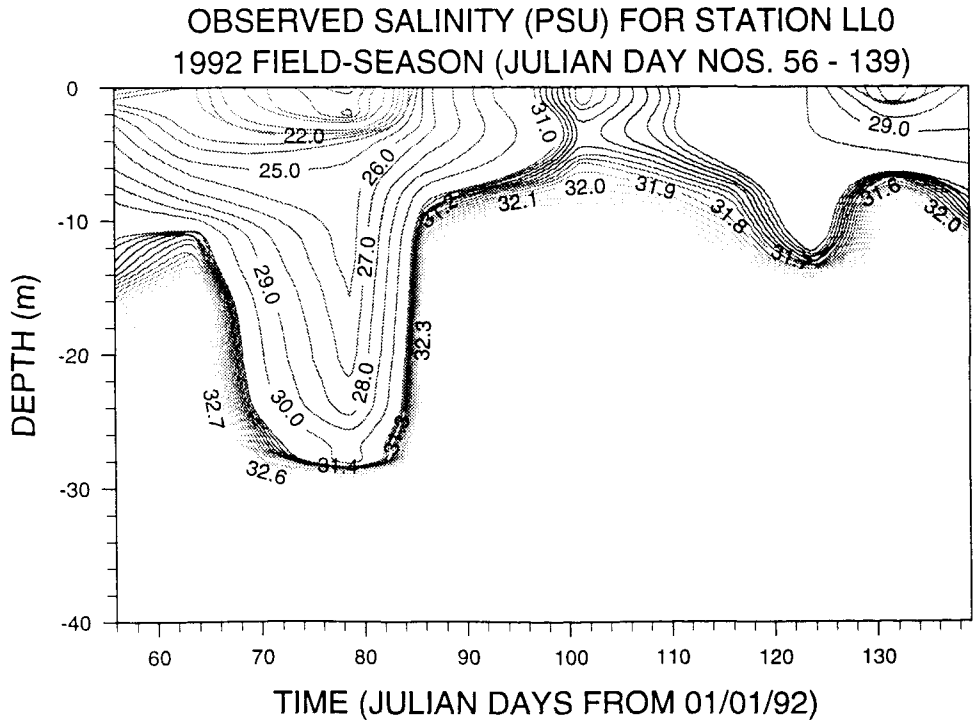

FIGURE 6.6

Temporal Variations in (a) the Density (kg m^{-3}) and (b) the Salinity (PSU) at Station LL14, Julian Day 56 to 139, 1992.

(a)

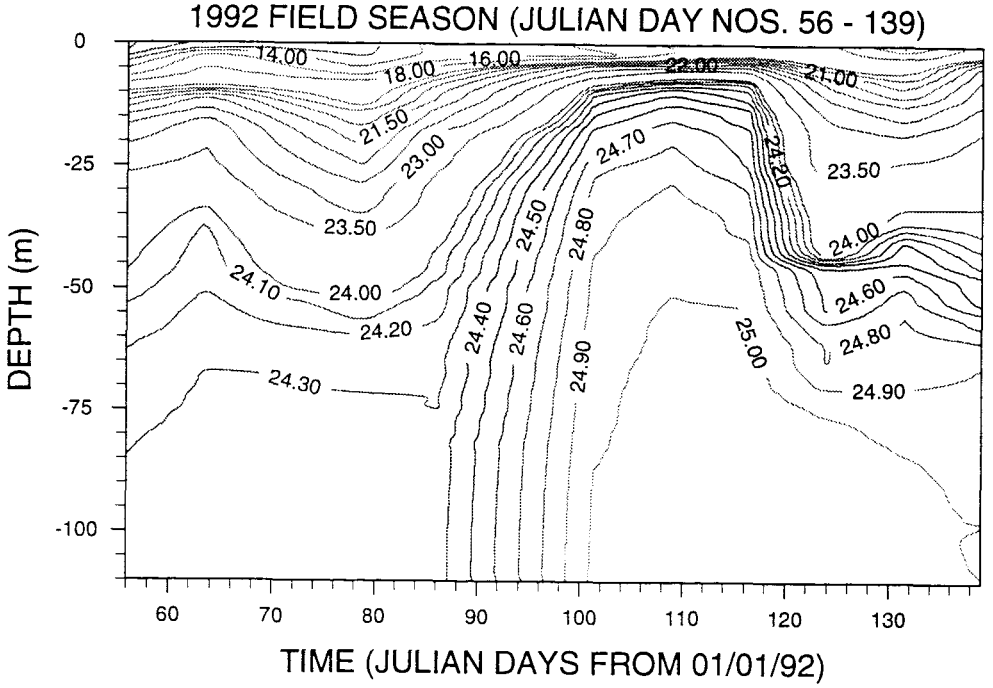

(b)

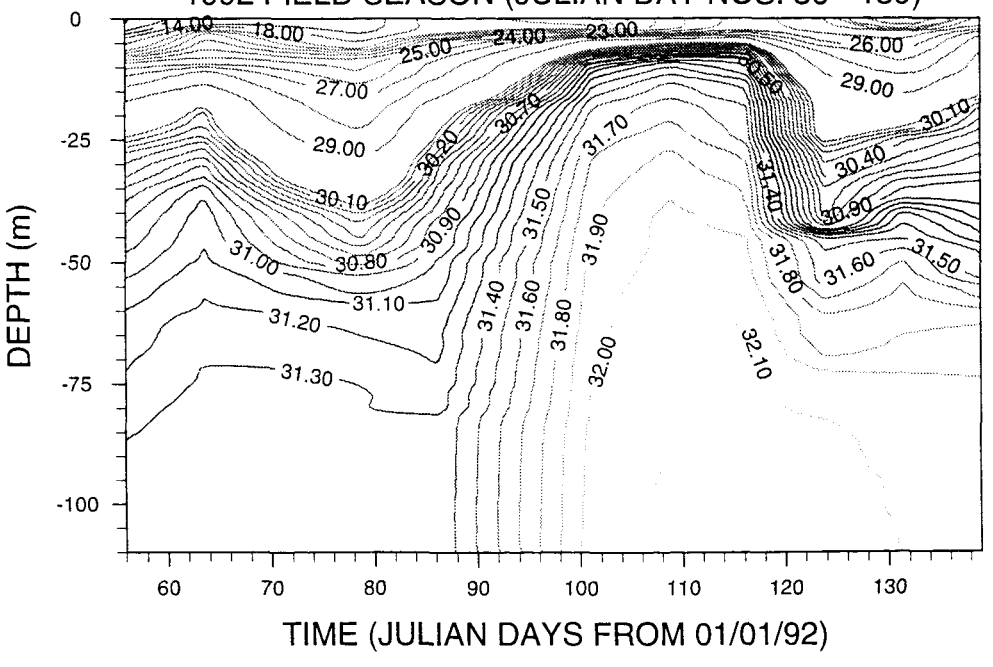

FIGURE 6.7

Temporal Variations in (a) the Density (kg m^{-3}) and (b) the Salinity (PSU) at Station LL19, Julian Day 50 to 139, 1992.

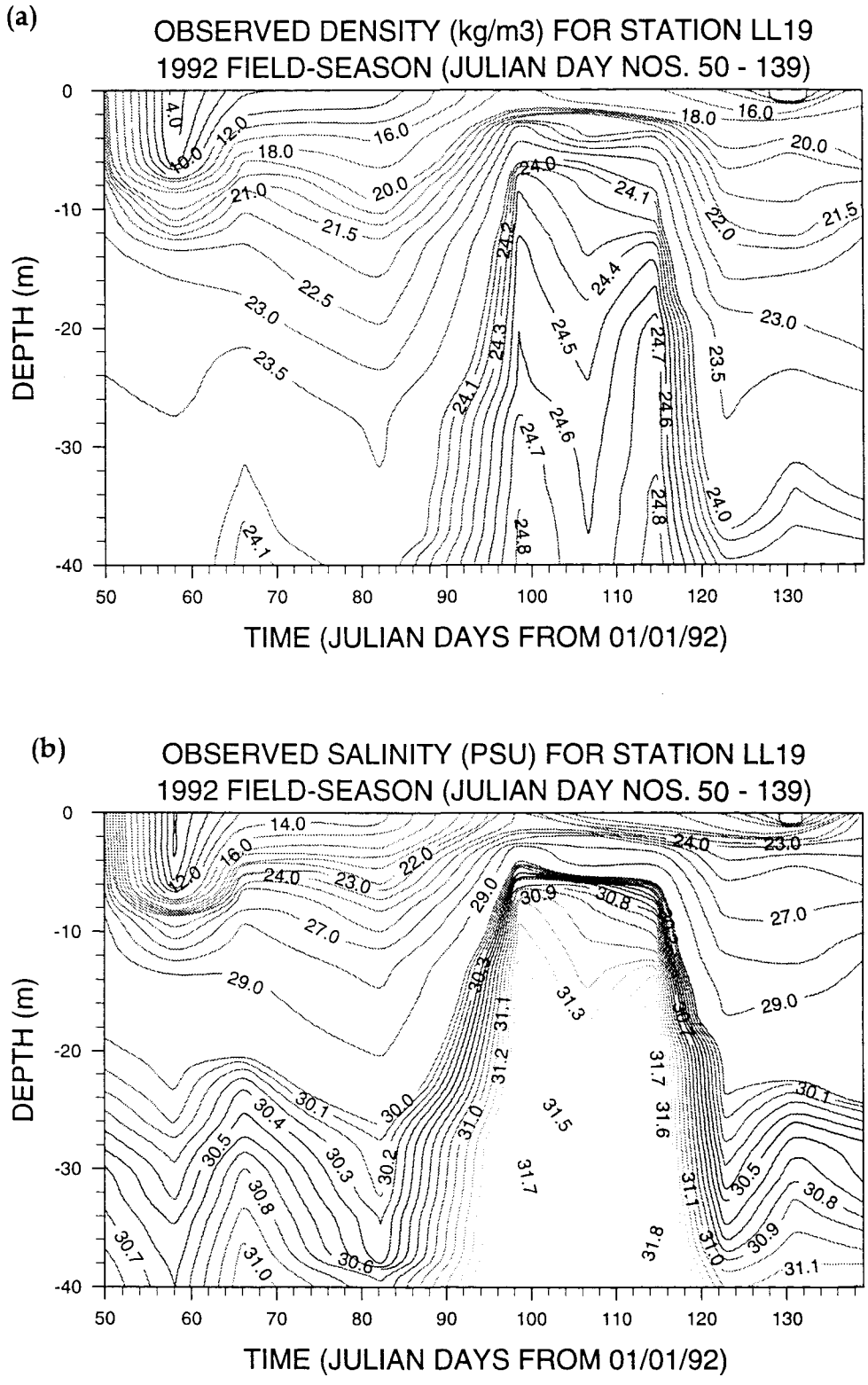

FIGURE 6.8

Temporal Changes in Bottom-Water Densities at Stations LL14 and LL19 and Density of Water at Sill-Depth at Station LL0

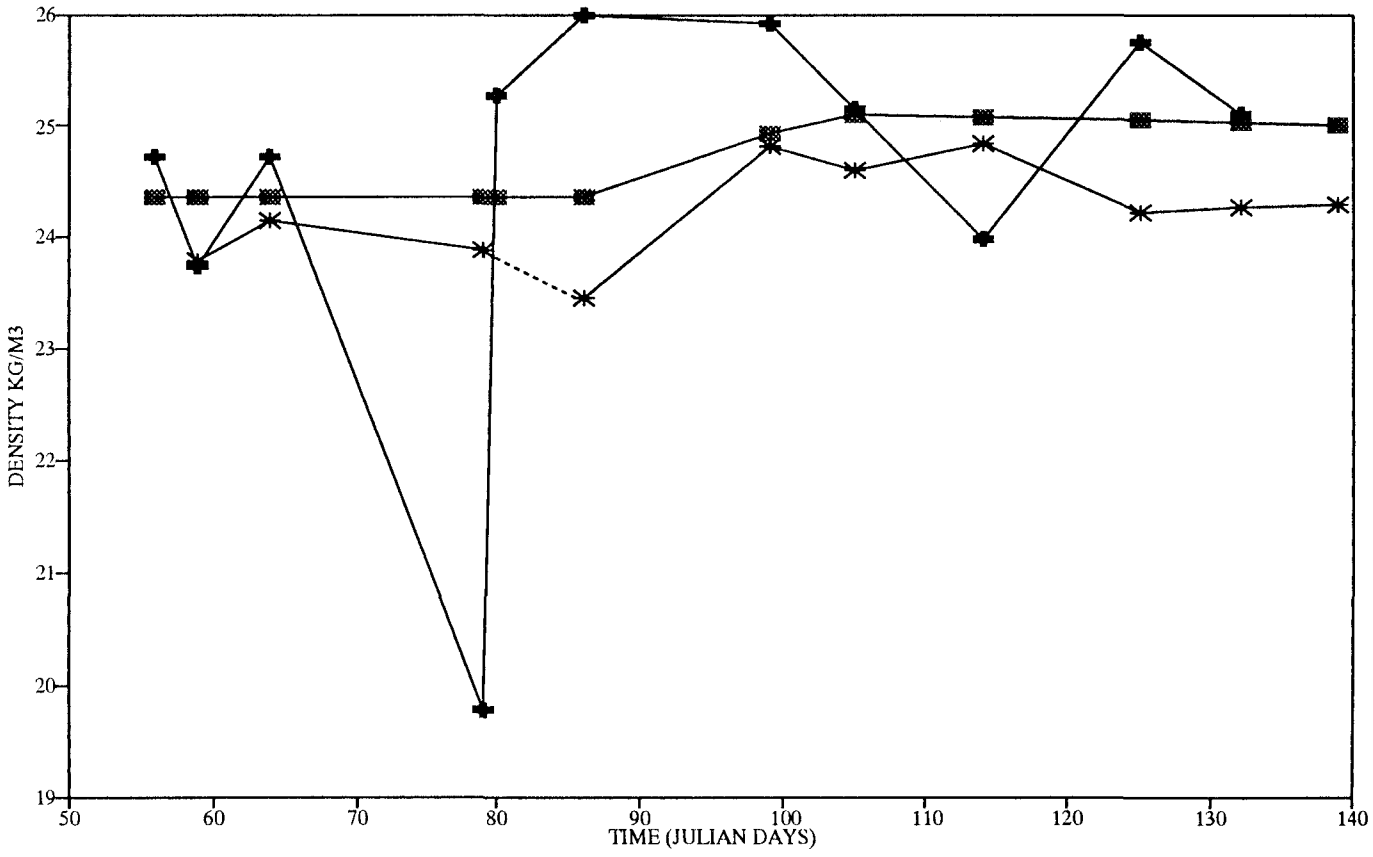

sharply by day 80 and on to day 86. By this time the water has become sufficiently dense to cause the displacement of the bottom-water at station LL14 (110 m) and station LL0 (40 m), thus causing the deep-water renewal event mentioned above. This is illustrated by the rise in the density of the bottom-waters at both stations LL14 and LL19 between days 86 and 99. Although the density of the water recorded at station LL0 on day 80 and day 86 is higher than that at the bottom-water depths of station LL14 and station LL19, a deep-water renewal does not occur in the basin. A possible reason for this is that the density of the incoming water from LL0 is likely to have decreased as it passes over the sill, due to the downward, turbulent mixing of the fresher surface layers with the inflowing water. Hence the density condition is not satisfied that the inflowing water must be of a higher density than the resident basin water to cause a renewal.

FIGURE 6.9 (a) illustrates the change in density over time at different depths at station LL14. The density of the water below 80 m remains almost constant until day 86 after which there is a sharp rise in the density at all depths due to the deep-water renewal event. This would suggest that prior to the deep-water renewal, water below 80 m depth is isolated which would mean that the only way in which the density of this water could change is through vertical diffusive processes (as described in **CHAPTER 1** section **1.2.2**). This may have important implications for the chemistry of this water in terms of biogeochemical processes (see **CHAPTER 2,** section **1.2.2**).

Figure 6.9 (b) illustrates how the same pattern of events occurs at station LL19, with a very slight increase of density at 40 m depth between days 59 and 64 followed by a steadily decreasing density at this depth up to day 86, followed by a sharp increase in the density due to the renewal event and then a stabilisation of the density as the basin stratification is re-established.

FIGURE 6.9

Variation of Density with Time at Different Depths at (a) Station LL14 and (b) Station LL19, Julian Day 50 to 139, 1992.

(a)

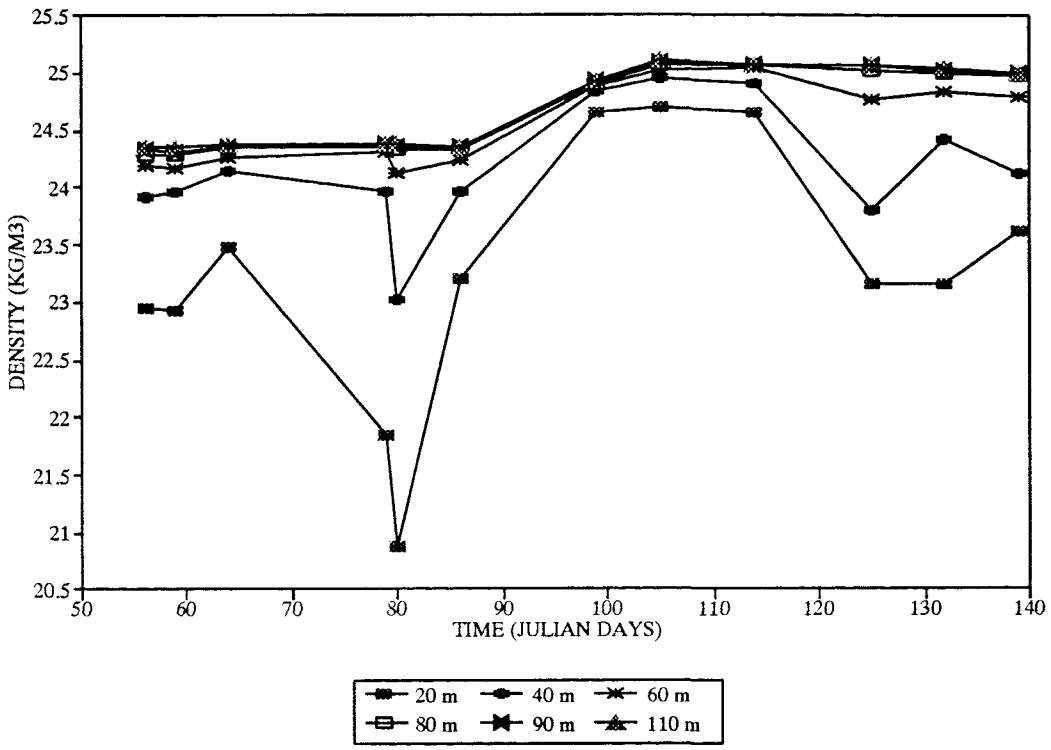

(b)

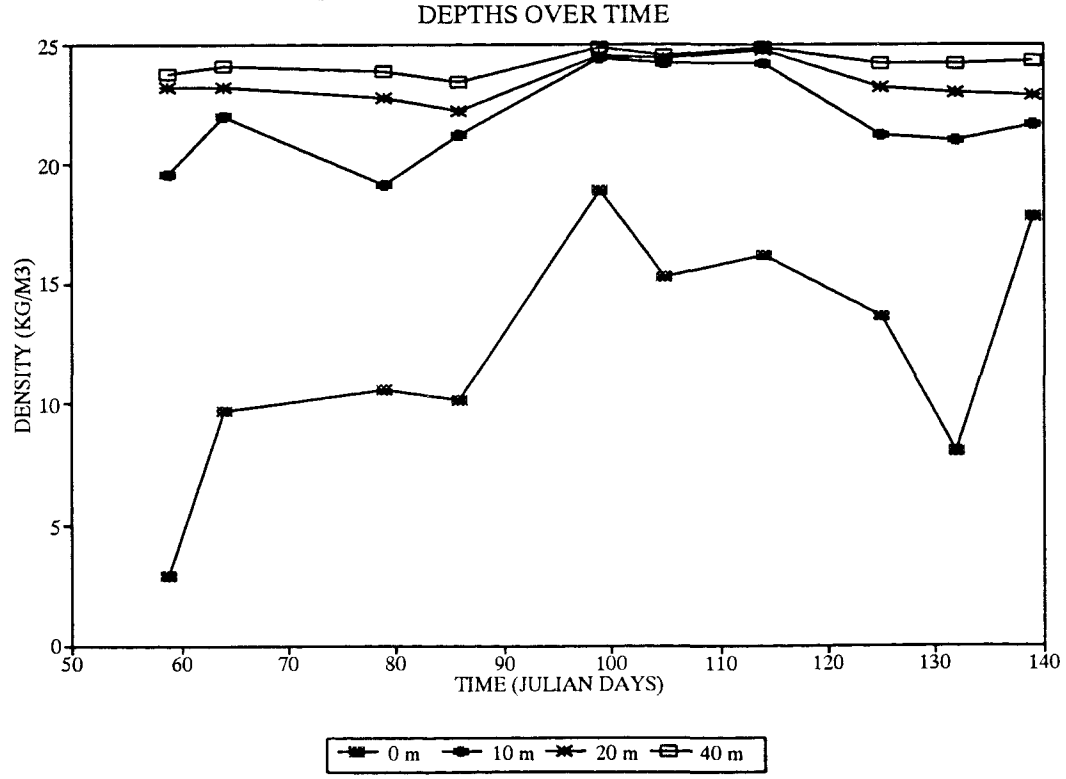

6.1.2.2 Factors contributing to the deep-water renewal event

As has been described in **CHAPTER 1** (section **1.2.3.2**), there are several factors that can affect the frequency of deep-water renewal events: **(1)** tidal motion, **(2)** the effects of the wind and **(3)** the temporal variation in the freshwater runoff to the system.

(1) Tidal motion: For the deep-water renewal event to occur there has to be an inflow of water to the system which has a higher density than the resident water in the basin and which is of an adequate volume to replace the water in the basin. The field results indicate that the deep-water renewal took place some time between day 86 and day 99 which coincides with the high spring tides occurring around day 95 (tidal range = 3.3 m) thus allowing for increasing volumes of water to enter the basin on the flood tides, and providing the energy required for mixing and breakdown of the vertical stratification in the loch. Therefore, if this factor dominated the renewal event, it is most likely to have occurred close to day 95.

(2)/(3) Wind and freshwater effects: The wind is important because a change in the wind direction and/or strength, may alter the gradient of the sea-surface slope and thus the barotropic forcing in the system. As the system strives to maintain a steady-state situation, baroclinic currents are set up which result in the upward displacement of water of increased density seaward of the sill, and the subsequent import of high salinity, nutrient-rich waters to the basin; a phenomenon referred to as **upwelling** (described in **CHAPTER 1**, section **1.2.3.2**). If this high salinity water is dense enough and of an adequate volume, then a deep-water renewal may occur inside the basin.

For the 1992 field season then, it is hypothesised that the wind will have the following effects on the system: **(a)** a persistent wind up the loch will cause retention of freshwater in the system; **(b)** a change in the wind direction will allow the freshwater to flow seawards thus altering the gradient of the sea-surface slope. This will result in upwelling of high salinity water seaward of the sill (at LL0)

which will lead to the deep-water renewals observed in the basin.

In order to investigate this **(a)** and **(b)** are considered separately:

(a) Retention of freshwater by the wind: Wind patterns over the field-season have been investigated and **FIGURE 6.10** shows the temporal changes in wind direction and velocity (as measured at DML) in terms of the component of the wind that acts along the longitudinal axis of the loch. Details of the theory behind this treatment of wind data may be found in section **7.3.1.1**. The figure shows that the wind was blowing up the loch i.e. in a south-westerly direction, prior to day 80, after which it relaxed. By day 90 the wind direction had changed to a north-easterly wind and the velocity of this wind peaked on day 94 when it reached 25 knots. It would seem likely from this wind pattern that for the time leading up to day 80, freshwater would be wedged and retained inside the basin by the persistent south-westerly wind. The effect of this would be reflected in a lowering of density in the surface layers at station LL14. However, the wedging of freshwater would also be expected in the shallower sill region which would be reflected in density changes at station LL0. Indeed, study of **FIGURE 6.11** shows how the density of the water at the seaward station LL0, varies temporally and at different depths. From the surface to sill-depth (15 m) and to 20 m also, it can be seen how the density of the water decreased markedly between days 64 and 80 which would indicate either a retention of the freshwater in the system by the wind, and/or a general increase in the input of freshwater to the system. **FIGURE 6.5 (a)** also illustrates the depression of isopycnals in the surface waters at LL0 prior to day 80, with water density 23 kg m^{-3} occurring at 10 m at the start of the field season on day 56, but at 25 m by day 80. This depression of the isopycnals in the surface layers is also observed inside the basin at station LL14 and is illustrated in **FIGURES 6.9 (a)** and **6.6 (a)**. **FIGURE 6.6 (a)** shows how water of density 23 kg m^{-3} which is present at a depth of ~20 m on day 56 at the start of the field season is found at 25 m depth by day 80. Hence the extent of isopycnal depression is greater at station LL0 than station LL14. This is likely to be due to increased wedging of freshwater up against the sill by the southwesterly wind.

FIGURE 6.10

Relationship of Wind Velocity Data (Resolved along the Longitudinal Axis of the Loch) with Time, Julian Day 30 to 140, 1992.

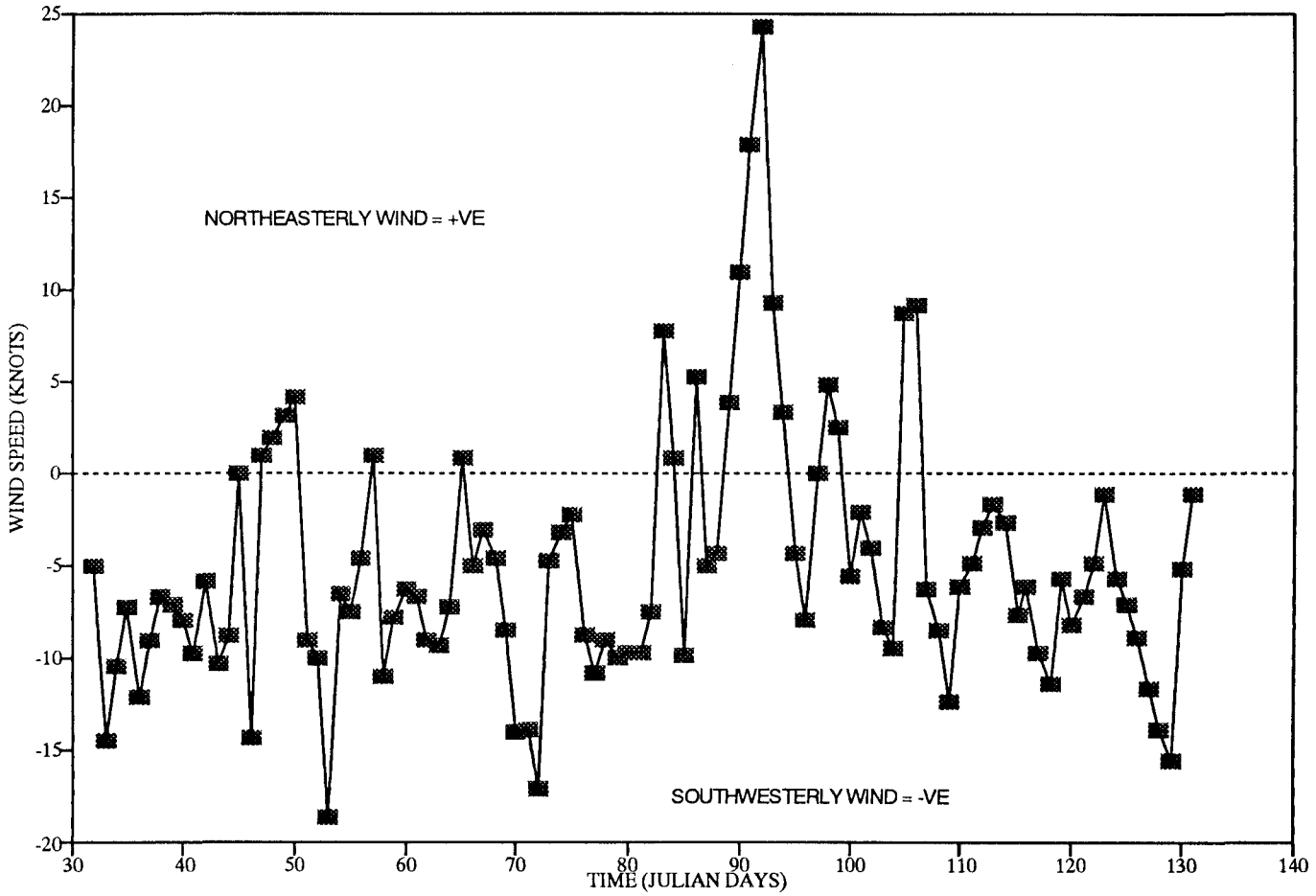

FIGURE 6.11

Variation of Density with Time at Different Depths at Station LL0, Julian Day 50 to 139, 1992.

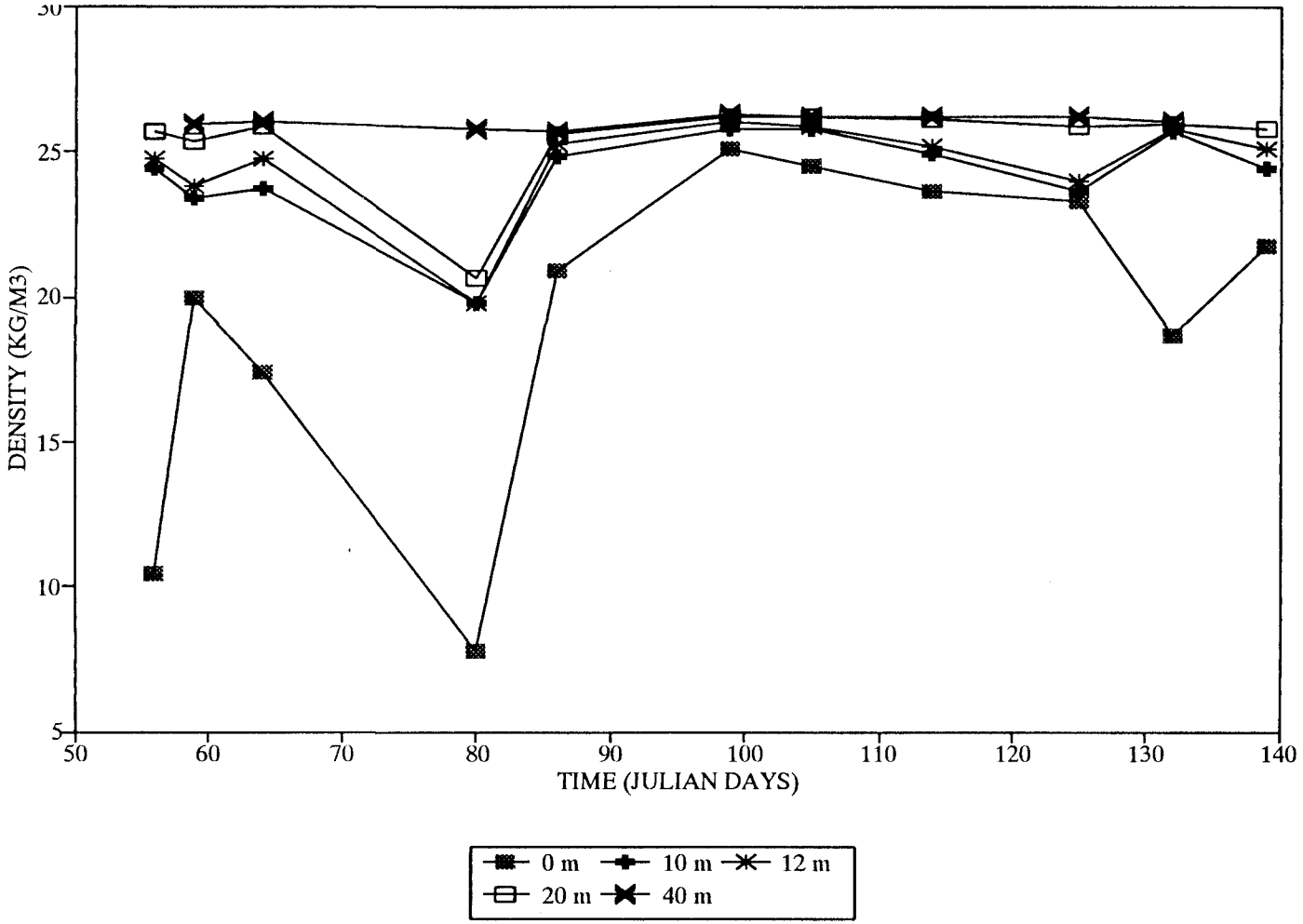

Regarding the freshwater input to the system during the period of sustained southwesterly winds, **FIGURE 6.4** illustrates the relatively high mean daily flow in the River Lochy prior to day 80 (flow data provided courtesy of the HRPB), with flow rates reaching levels of 492 $m^3 s^{-1}$ on day 53 and 286 $m^3 s^{-1}$ on day 79. This increased input of freshwater coupled with the south-westerly winds between days 56 to 80 will favour the retention of freshwater outside and inside the basin.

To investigate this retention of freshwater further, a study was made on the residence times of the freshwater inside the basin, at station LL14 over the field-season. The residence time (τ) is the average lifetime of a water particle in a given volume of the estuary (Officer and Kester, 1991). The method used in this study to determine values of τ for the freshwater present at station LL14 was based on that described in Officer and Kester (1991), in which the total volume of freshwater in the system is calculated and then divided by the rate of the freshwater input so that:

$$\tau = V_f / R_q \qquad \textbf{(6.1)}$$

Where; V_f = the total volume of freshwater in the basin (m^3),
R_q = the rate of freshwater input to the system ($m^3 s^{-1}$).

V_f can be calculated from:

$$V_f = [(S_0 - S) / S_0].V \qquad \textbf{(6.2)}$$

where; S_0 = the salinity of the incoming saline water;
S = the volume-averaged salinity of the portion of the estuary being considered;
V = the volume of the estuary (m^3),

(Officer and Kester, 1991)

A computer program was written in FORTRAN 77 so that V_f could be calculated for any one day for which there was salinity data for stations LL14 and LL0. V_f was calculated by integrating data for each 1 m layer through a depth, z:

$$V_f = \sum_{0}^{z} [(S_0 - S_{(i)}) / S_0].V_{(i)} \qquad \textbf{(6.3)}$$

Where; S_0 = the salinity of the incoming water from LL0;

$S_{(i)}$ = the salinity of layer (i);

$V_{(i)}$ = the volume of layer (i) (m^3);

z = the depth of water (m) (from the surface) for which the volume is calculated;

0 = the surface.

To minimise the problem of temporal fluctuations of S_0, S_0 was calculated by finding the average salinity through from 0 m to 15 m depth (sill-depth) at LL0 for each sampling date and then averaging these salinity values over two time-periods; days 56 - 79 and days 80 - 139 thus obtaining two values for S_0. These two values cover the pre-renewal period and the post renewal period, for which the values of S_0 were much higher at station LL0. Values of V_f were calculated for each day for which there was salinity data available at station LL14 and LL0 and the value of S_0 used for the calculation of V_f depended on whether the sampling day in question fell between days 56 - 79 or days 80 - 139. $S_{(i)}$ was obtained from the salinity profiles collected at station LL14 over time. $V_{(i)}$ was derived from the Admiralty Chart number 2380, through a method which is described in **CHAPTER 7**, section **7.3.1.1**. The depth z is taken as 10 m to represent the freshwater volume in the surface mixed layer at station LL0.

The V_f values obtained from the program could then be used to calculate the residence time, τ, according to the equation **6.1**. The value of R_q used was calculated from the sum of the daily mean flow-rates of the rivers Lochy and Nevis multiplied by 1.3 to take account of the difference between the catchment area of the loch and the watershed of the rivers. Details of this calculation may be found

in **CHAPTER 7**, section **7.3.1.1**. In Officer and Kester (1991) the value of R_q referred to is an average value but as can be seen from **FIGURE 6.4** the temporal variability of the river flow is too large for a meaningful average value to be taken. The approach taken for the calculation of τ from V_f and R_q therefore followed that described in the work done by Kaul and Froelich (1984) on the Ochlockonee Bay, Florida. In this procedure daily values of R_q were summed for a period prior to each sampling date at station LL14. The number of days over which values of R_q had to be summed so that the sum was equal (or closest,) to V_f was taken as the value of τ applicable to that sampling date. **FIGURE 6.12** illustrates the results from these calculations with a plot of the changing residence time of the freshwater in the system over the 1992 sampling period. It shows an increase in the residence time over the period from day 63 to 80 which would be consistent with the retention of freshwater at station LL14 due to the southwesterly wind blowing at this time. Over the period from day 80 to 86 there is a decrease in the residence time of this freshwater which coincides with the relaxation in the wind and the subsequent escape of the retained freshwater. Over the period from day 86 to 99 there is quite an increase in the residence time but this is most likely to be a reflection of the increased input of salt (due to the spring tides) that entered the basin from station LL0 as the density of the sill water was seen to increase at this time. Such an increase in the amount of salt entering the system means that S_0 and $S_{(i)}$ are disproportionate in equation **6.3** and hence the value of V_f (and thus τ) becomes less reliable around this time. The trends in the residence time of freshwater in the system are, however, consistent with the idea that the wind is likely to have a wedging effect as hypothesised. The values of τ calculated in this way are similar to that calculated in **CHAPTER 3**, section **3.3.3** by the tidal prism method (~6 days).

(b) As the wind changes direction and picks up speed after day 80, the freshwater as described above, would be allowed to escape from the system, thus relaxing the gradient of the sea-slope, resulting in upwelling and the import of high salinity water to the system. As described in section **1.2.3.2** the inclination of the interface (pycnocline) between the upper fresher waters and deeper denser waters seaward

FIGURE 6.12

Relationship of Freshwater Residence Time, Over the Top 10 m at Station LL14, with Time, Julian day 50 to 139, 1992.

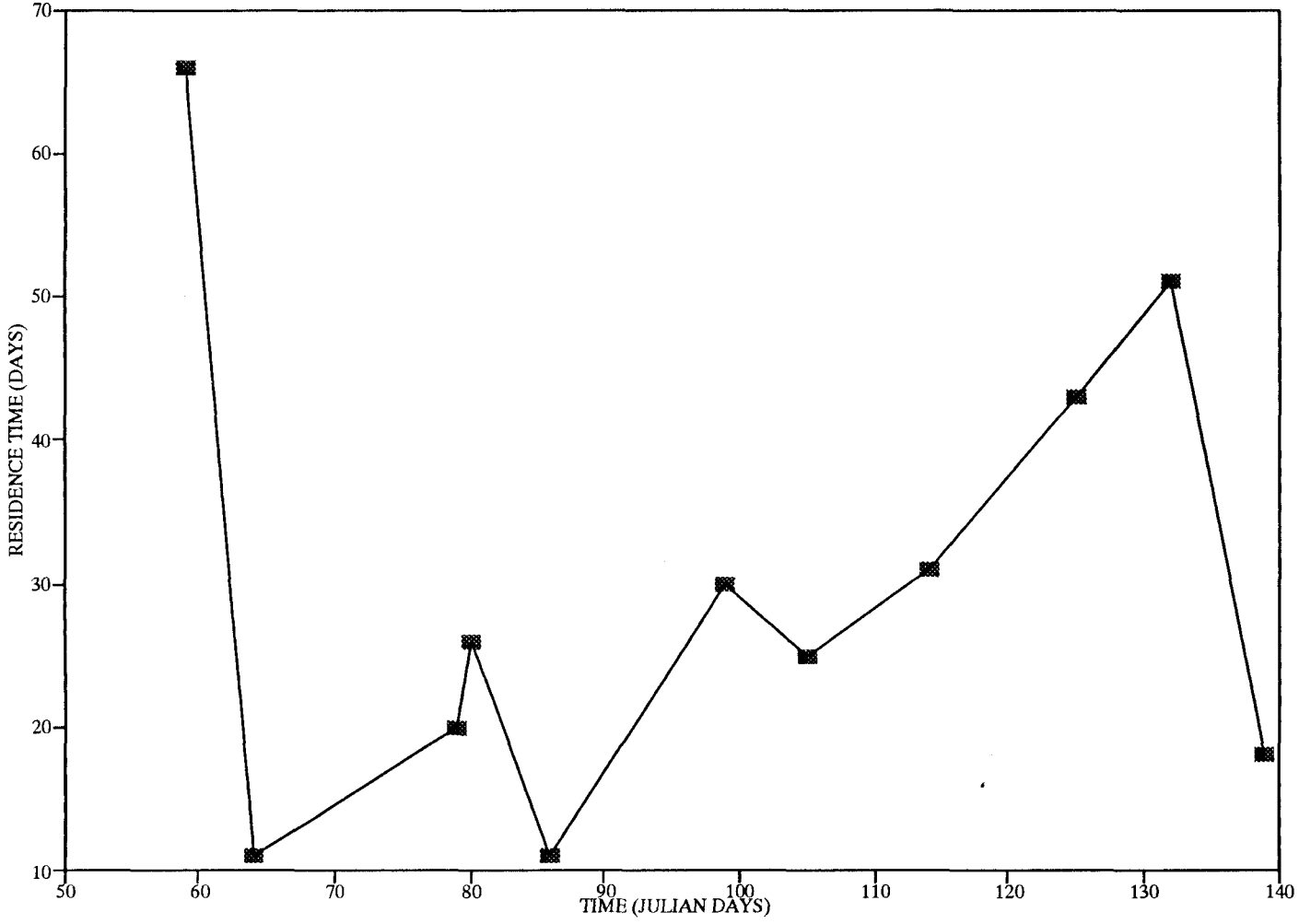

of the sill, alters with such a change in wind direction in order to maintain an equilibrium (steady state) situation and it is this that results in the upward displacement of saline water (upwelling). To investigate the feasibility of this upward displacement of the interface at station LL0 the distance through which this interface must move upwards is predicted mathematically for a given mean wind velocity.

When a wind has been blowing on a system persistently in the same direction then the system develops a steady-state/equilibrium situation whereby the force exerted by the wind is equal to the force exerted by the slope (barotropic force) which can be expressed mathematically as:

$$C_d.\rho_a.w^2 = g.s.\rho_w.h \qquad \textbf{(6.4)}$$

where C_d = the drag coefficient of the wind ($2*10^{-3}$);
ρ_a = the density of air (1.25 kg m^{-3});
w = mean wind velocity (m s^{-1});
g = acceleration due to gravity (9.81 m s^{-2});
s = slope of the sea-surface;
ρ_w = the density of the water (kg m^{-3});
h = height of the body of water concerned;

So that $s = (C_d.\rho_a.w^2) / (g.\rho_w.h)$ (Bowden, 1983)

If a prediction is to be made on the magnitude of displacement of water at LL0 then conditions throughout the whole of the lower basin as far as the Sound of Mull need to be considered (Mr. A. Edwards, 1994, DML, pers.comms.). The average wind velocity can be approximated as 5 m s^{-1} from **FIGURE 6.10**. The height h can be estimated to be equal to 10 m (from LL0 data) to represent the surface layer i.e. the depth of the mixed layer down to the first pycnocline. The slope of the interface is a function of the slope of the sea-surface and the density difference (Δ) between the surface layer and the layer beneath the pycnocline. This

density difference can be approximated at 1 kg m^{-3} for stations further down the lower basin of Loch Linnhe (Mr. A. Edwards, 1994, pers. comms.). Hence the slope of the interface can be expressed as:

$$\text{slope of the interface} = (\rho_w / \Delta).(C_d.\rho_a.w^2 / g.\rho_w.h)$$

$$\therefore \quad \text{slope of the interface} = (C_d.\rho_a.w^2 / g.\Delta.h)$$

$$= [2*10^{-3}.(1.25).25 / (9.81.1.10]$$

$$= 6.4*10^{-4}$$

If the slope of the interface is multiplied by the length of the lower basin as far as the Sound of Mull (31.8 km) then a value for the displacement through which the interface has moved may be approximated:

$$\text{Upward displacement of interface} = 20.35 \text{ m}$$

From this then it can be said that bottom-water at LL0 might be expected to undergo upward displacement of the order of ~20 m given the wind conditions observed for 1992.

This prediction is supported by observations at station LL0 and illustrated in **FIGURE 6.5** which shows how the uplift in isopycnals observed at all depths by day 86 and which is illustrated in **FIGURES 6.9 (a)** and **(b)**, is caused by the upward displacement of water through a height of at least 20 m which is thus consistent with a wind-driven upwelling event.

6.1.3 Conclusions from the hydrographic results

6.1.3.1 **Spatial variations:** Water in the upper basin of Loch Linnhe is vertically stratified according to its density throughout the upper basin, at the start and end of the 1992 field-season. The upper basin can be regarded as essentially uniform horizontally in terms of its density and salinity properties, although there is a slight salinity gradient in the surface waters due to the input of freshwater at the head of the loch. Between days 64 and 139 an increase in density is observed at all depths throughout the basin and the base of the layers in which there are measurable changes in density is deeper, at 80 to 90 m on day 139 as compared to 75 to 80 m for day 64. These observations would indicate the occurrence of a deep-water renewal event between these dates. The results from the temperature measurements also support this idea, with a temperature inversion present throughout the water column at station LL14 on day 64 which has reversed by day 139 with cooler, denser water resident at the bottom-water depths.

6.1.3.2 **Temporal variations:** A deep-water renewal event throughout the whole basin is observed to have occurred between days 86 and 99. It has been possible to show that there are various factors that favour such an event at this time and that a certain sequence of events probably causes it:

(1) Spring tides occurring on day 95 allow for larger volumes of higher salinity water to enter the basin. It is likely, therefore that the renewal event occurred around day 95;

(2) South-westerly winds blow persistently up the loch to day 80, retaining fresher water both outside the basin at station LL0 and to a lesser extent inside the basin at station LL14;

(3) The wind direction changes by day 90 to a north-easterly wind, resulting in the release of the retained freshwater and the ultimate upwelling of high salinity water outside the sill region. This occurs as a result of the upward displacement

of the pycnocline through a height of ~ 20 m at station LL0. This high density, high salinity water enters the basin causing a renewal of the deeper waters between days 86 - 99.

(4) To a much lesser degree the temperature inversion observed throughout the column on day 64 will act to destabilise the density structure of the water column thus facilitating the breakdown of the stratified layers by the incoming water, allowing the renewal event to occur.

6.2 Nutrients

The nutrient results to be considered in this section are those for station LL0, outside the sill region and taken as the saline source; those measured at station LL14, the deepest, most central station and the freshwater source of nutrients from the rivers[1]. Nutrient data have also been collected at station LL19 but are not used in this section because the aim of this section is to describe the nutrient results in a succinct way which can be easily related to the more quantitative approach to be presented in **CHAPTER 7**, section **7.6**. All nutrient data collected over the 1992 field-season (including the freshwater data provided courtesy of the HRPB) can be found in **APPENDIX 6.4**.

6.2.1 Nutrients and salinity: general behaviour

FIGURES 6.13 (a) to **(c)** illustrate the relationship of each nutrient (NO_3, PO_4 and SiO_4 respectively) with salinity for both the stations, LL0 and LL14 and the freshwater end-member concentrations, for the entire field-season (day 50 to day 139). For each nutrient the line of best fit is plotted through the data from which

[1] The HRPB provided nitrate and phosphate data for the rivers Nevis and Lochy, which had been collected on a monthly basis. Silicate data was not available.

FIGURE 6.13

Relationship of (a) Nitrate, (b) Phosphate and (c) Silicate Concentrations (Micromolar) with Salinity for Data from Stations LL14, LL0 and Riverine Inputs (Data Courtesy of the HRPB), 1992.

(a)

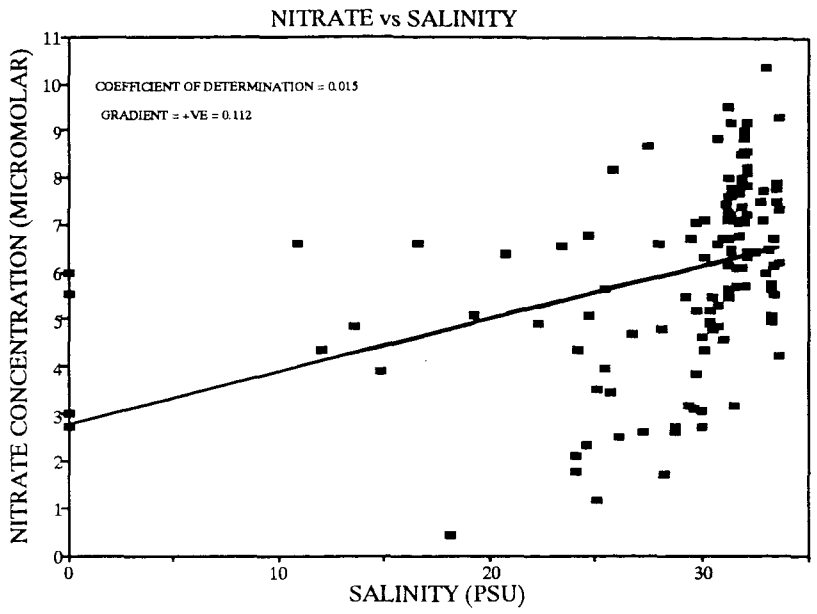

(b)

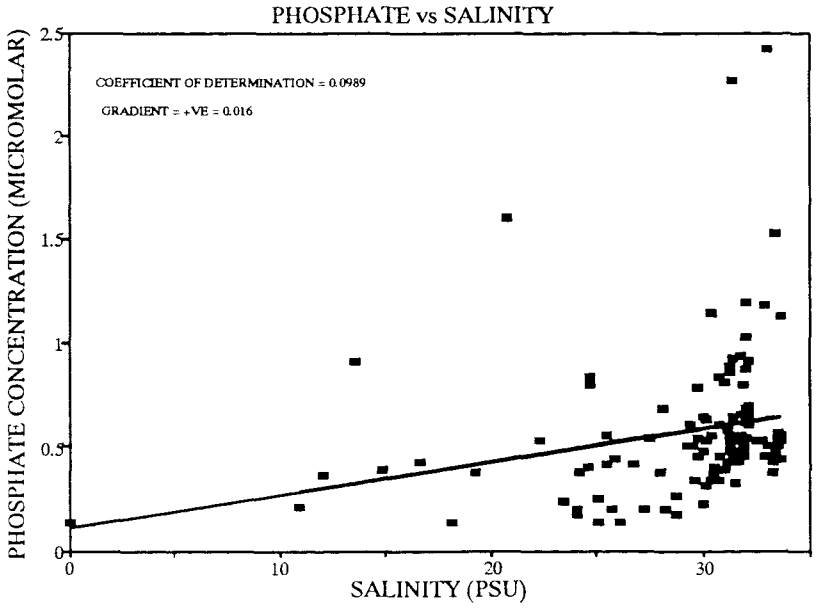

(c)

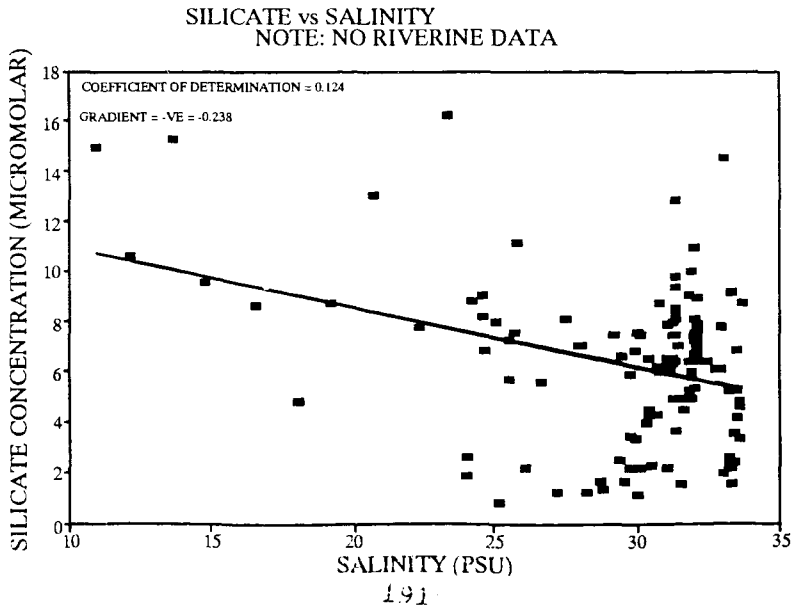

the gradient can be used as an indicator for the source of the nutrient, and the coefficient of determination (r^2) (see **CHAPTER 5**, section **5.2.1**) as an indicator of the degree to which dependency of the nutrient concentration is determined by salinity. A plot of nutrient concentration versus salinity for an individual sampling day's data will give rise to a theoretical dilution line (TDL) if the two end-member concentrations are joined together. Any scatter of data about this line can be attributed to deviations away from the steady-state distribution which is set up due from simple mixing of the two end-members. This can be due to real non-conservative behaviour (biogeochemical processes - see **CHAPTER 2**, section **2.3**) and/or apparent non-conservative behaviour (due to temporally varying end-member concentrations -see **CHAPTER 2**, section **2.4**). This theory of estuarine mixing is described in **CHAPTER 2**, section **2.1**. **FIGURES 6.13 (a)** to **(c)** contain all the data measured over the field-season and thus these plots display the scatter arising from the differences in end-member concentrations over the period and any real non-conservative behaviour within the basin. It is this scatter and the processes that cause it that are considered in the following sections.

Sources of the nutrients: From the gradients of the plots in **FIGURE 6.13** the following deductions can be made.

(a) The main source of nitrate to the upper basin is from the saline end-member with a plot of the nitrate versus salinity giving rise to a positive gradient of 0.112. The low gradient indicates however, low dependence of the nitrate concentration on salinity, and this is supported by a value of r^2 of only 0.015, i.e. only 1.5% of the variation in the nitrate concentration can be explained by the variation in salinity. Effectively 98.5 % of the scatter is due to other factors outlined above i.e. the temporal differences in end-member concentrations and any real non-conservative behaviour.

(b) The main source of phosphate to the upper basin is also from the saline end-member with **FIGURE 6.13 (b)** showing a positive gradient of 0.016. Again this is very low indicating a low dependence of the phosphate concentration on the

salinity. The r^2 value of 0.0989, indicates that only 10 % of the variation in the phosphate concentration can be explained by the corresponding variation in salinity. Thus, 90 % of the scatter around the line of best fit can be attributed to temporal variations in the end-member concentrations and any real non-conservative behaviour. Non-conservative processes are anticipated to be more complex for phosphate due to its high particle-reactivity and affinity for colloids (see **CHAPTER 2**, section **2.2.2**).

(c) The main source of silicate to the upper basin is from the riverine end with the best fit line in **FIGURE 6.13 (c)** showing a negative gradient of -0.238. This plot had to be created without any silicate riverine data but still the gradient is negative due to the freshwater components present at the stations LL0 and LL14. The value of r^2 is 0.124, indicating that 12 % of the variation in silicate is attributable to the variation in salinity leaving 88 % attributable to other factors as described above.

Evidence for processes leading to apparent and real non-conservative behaviour will now be considered for the 1992 field-season.

6.2.1.1 Processes giving rise to apparent non-conservative behaviour

Apparent non-conservative behaviour is observed in an estuarine system when the end-member nutrient concentrations vary with time such that the period of the oscillation in the end-member concentration is within the flushing time of the system. Obviously the amplitude of such oscillation is also important because such behaviour will contribute to the scatter in the nutrient / salinity relationships at station LL14. Such temporal variations are an important consideration in the interpretation of nutrient profiles since the scatter caused by them will lead to augmentation or damping of any curvature present due to real non-conservative and will therefore make such processes hard to identify and isolate.

Regarding the nutrient behaviour in the upper basin at station LL14, **FIGURES 6.14 (a)** to **(c)** show that a plot of the nutrient concentrations against salinity at

FIGURE 6.14

Relationship of (a) Nitrate, (b) Phosphate and (c) Silicate Concentrations (Micromolar) with Salinity for Station LL14, 1992.

(a)

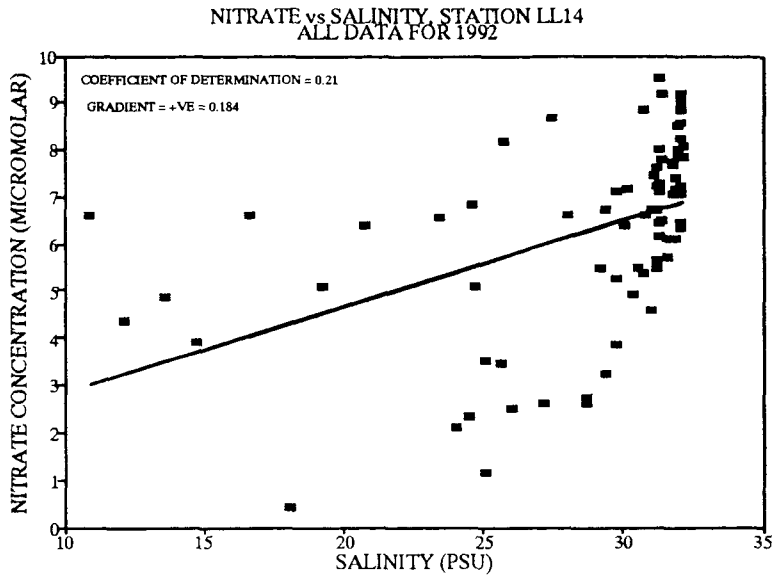

(b)

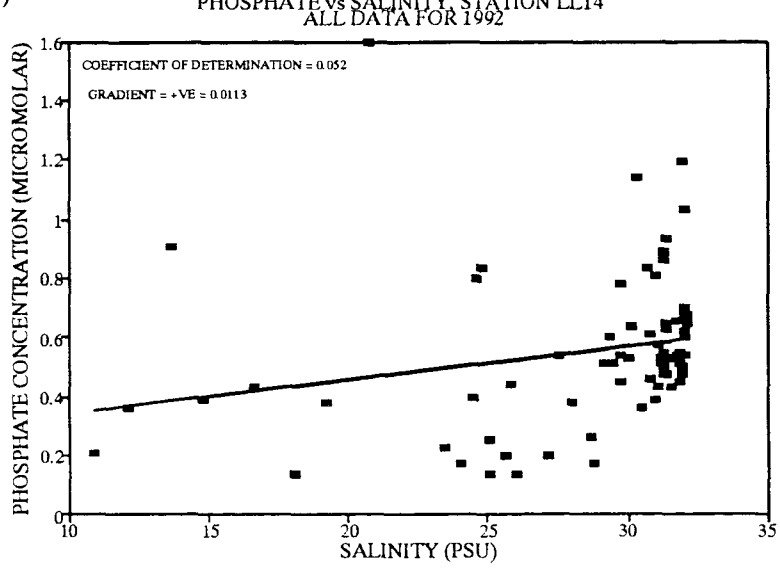

(c)

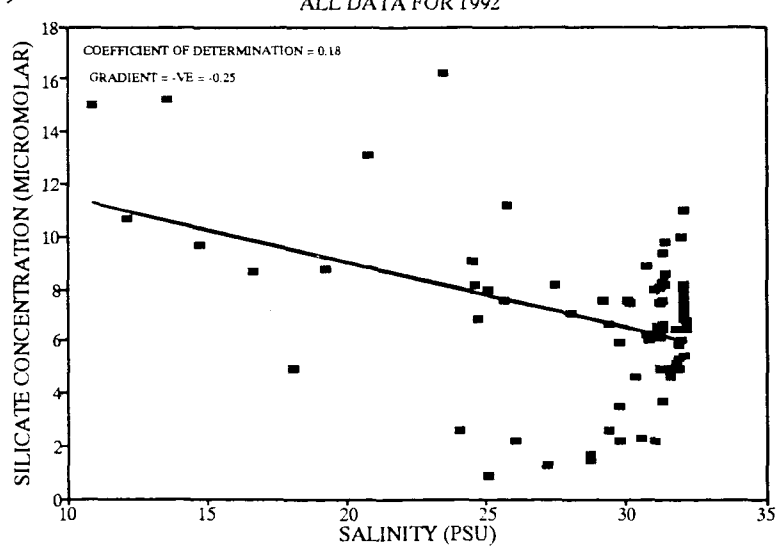

station LL14 for the whole field-season results in scatter of data about the average relationship. This scatter then is a reflection of the total apparent and real non-conservative processes occurring at this station over time. As mentioned above, the apparent non-conservative processes arise through temporal variability in end-member concentrations. In the case of a system like Loch Linnhe such oscillations in end-member nutrient concentrations, and their amplitudes, will give rise to enhancement in the scatter of data due to "memory effects" that will be observed in the nutrient measurements. This is due to the horizontal type of circulation set up within the system, made conspicuous by the observed vertical density stratification present within the upper basin (see sections **6.1.1** and **6.1.2.1**). This type of circulation is described in detail in **CHAPTER 1** but basically it involves the outward flow of fresher/brackish water across the fjord surface, compensated by inward-flowing saline water across the sill, forming a stratified system which is horizontally uniform in terms of the density and salinity (see section **6.1.1**). In Loch Linnhe this saline water originates from station LL0 and is mixed downwards as it passes over the sill due to the tidal throttling processes which result in turbulent mixing in the sill region (see section **1.2.1.2**). As it enters the basin it sinks to the depth at which there is neutral buoyancy i.e. its density is equal to the density of the surrounding water and then spreads out horizontally at this depth displacing resident water upwards. Hence this sill-water will only mix vertically with water which has a density less than or equal to its own, and the degree of horizontal mixing that it will undergo will depend on its volume and how much potential energy is still available for mixing after processes such as friction with the basin boundaries or heat loss through the sinking of the density current formed inside the sill. As has been shown from the hydrographic results in section **6.1.1** the density and salinity of water below 75 to 80m depth at station LL14 remained constant for the days leading up to day 86 indicating that the inflowing saline water had not been dense enough to sink to these depths, such that vertical mixing could have only occurred to depths down to 75 to 80 m maximum. Such a lack in vertical mixing within the basin will give rise to memory effects in the nutrient concentrations, reflected by scatter in the observed data.

The temporal variations in both the saline and freshwater end-member nutrient concentrations for Loch Linnhe will now be considered in turn.

Saline end-member variations: FIGURES 6.15 (a) to (c) are plots of nitrate, phosphate and silicate concentrations, respectively, versus salinity at station LL0 for all the data that was collected over the 1992 field-season. The data is averaged over the top 20 m of the water column so as to simulate the effect of mixing as the water passes over the sill, for each sampling date. For each plot a line of best fit is fitted through the data. If there is no temporal variation in these saline end-member concentrations then the coefficient of determination (r^2) for these lines will be equal to 1. However, as can be seen the values of r^2 are very low for all of the plots, with values of 0.00862 for nitrate, 0.0488 for phosphate and 0.0266 for silicate. Such temporal variations in the saline end-member concentrations will not only be a reflection of changes in the saline water brought about by: (i) upwelling (see section **1.2.3.2**); (ii) changing nutrient concentrations in adjacent source waters such as point inputs to the polluted Clyde and Irish Sea areas (see **CHAPTER 3**, section **3.2.1**); (iii) low nutrient concentrations in the source waters due to the advection of post spring-bloom water as the bloom is circulated up around the west coast ; (iv) real non-conservative behaviour via biogeochemical processes occurring in the sill region e.g. the depletion of nutrients via biological activity through advected phytoplankton cells to the sill region and adsorption/desorption processes of nutrients from SPM, due to the turbulent mixing that occurs in the sill region (see **CHAPTER 2**, section **2.3.1**). Although these phenomena will cause the majority of the concentration variability, they will also include any variations in the freshwater end-member concentrations since there will be a freshwater component in the water that is advected in over the sill, due to turbulent mixing in the sill area. This variation in nutrient concentration at station LL0, whether it be from temporal changes of water advected into station LL0, from biogeochemical processes in the sill region and/or a reflection of the changing freshwater concentrations, will give rise to temporally varying saline end-member concentration which will be reflected as scatter of data from measurements made at station LL14.

FIGURE 6.15

Relationship of (a) Nitrate, (b) Phosphate and (c) Silicate Concentrations with Salinity at Station LL0 (Data Averaged Over the Top 20 m), 1992.

(a)

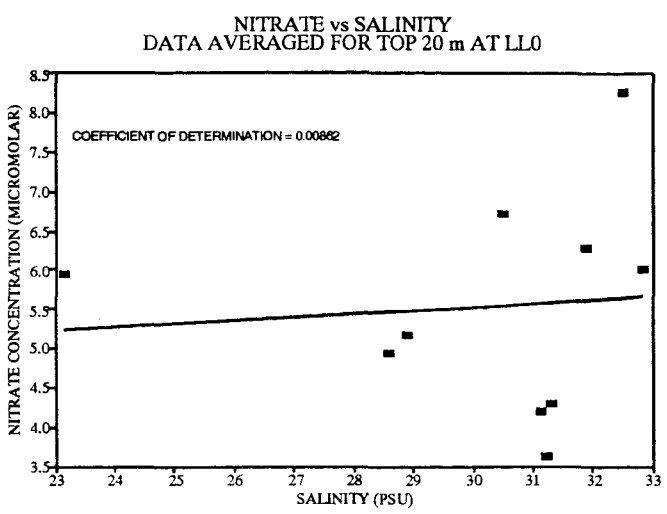

(b)

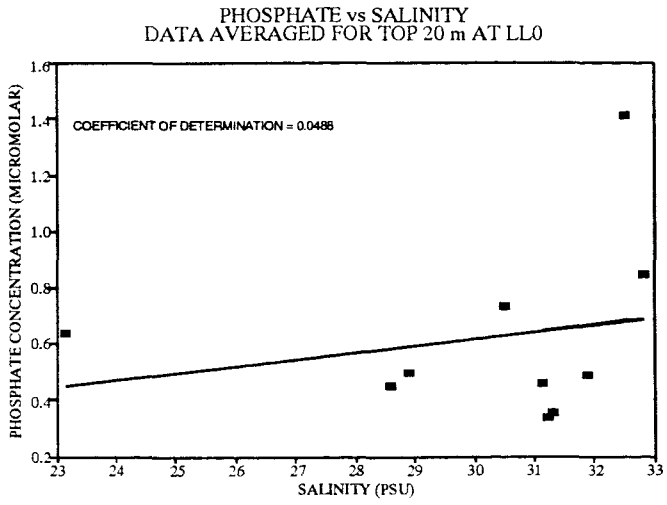

(c)

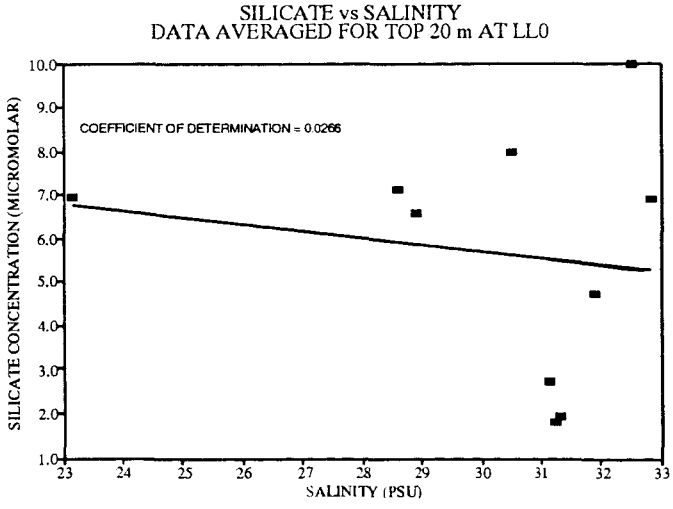

The 20 m averaged data shows NO_3 ranges within 4.94 - 8.28 µM, PO_4 from 0.64 - 1.42 µM and SiO_4 from 6.58 - 9.93 µM for the sill water entering the basin between the days 50 to 105. These concentrations were depleted to 3.6 µM, 0.34 µM and 1.8 µM for NO_3, PO_4 and SiO_4 respectively, by day 139.

Freshwater end-member variations: To consider temporal variations in the freshwater end-member concentrations, the monthly NO_3 and PO_4 riverine data and the daily riverine flow data (provided courtesy of the HRPB and listed in **APPENDIX 6.3**) have been studied:

FIGURE 6.16 (a) illustrates the daily temporal changes in river flow for the total river flow (Lochy plus Nevis flow) for the three years 1990, 1991 and 1992. These mean daily discharge values show that the flows vary erratically on a daily basis, with the flow varying by > 280 % from one day to the next at the start of 1992. If the relationships between monthly nutrient concentration, freshwater flow and time are to be investigated then the river flow data must be prefiltered to prevent aliasing in the results (where aliasing is the error brought about by a difference in the sampling frequencies between the observed monthly nutrient data and the measured daily river flow data). This filter allows for the data to be filtered around monthly average values and was achieved through a FORTRAN computer program (courtesy of Mr. C.R. Griffiths, DML). Results from this filtering are illustrated in **FIGURE 6.16 (b)**. This filtered data is appropriate for an examination of the relationships between riverine nutrient concentrations, time and flow rates.

Nitrate variations in the freshwater end-member:

Investigation into the annual regime. **Figure 6.17** illustrates the variation of monthly riverine NO_3 concentrations (averaged for the rivers Lochy and Nevis) with the filtered flow data over the three years, 1990, 1991 and 1992. The occurrence of generally increased NO_3 concentrations in the rivers Lochy and Nevis during the winter months may be related to the influence of several factors which include strong leaching of soluble NO_3 ions by water moving through the soil in

FIGURE 6.16

Relationship of (a) Total Riverine Flow (Lochy and Nevis) and (b) Filtered Total Riverine Flow Data with Time, Years 1990, 1991 and 1992. (Flow Data Courtesy of the HRPB).

(a)

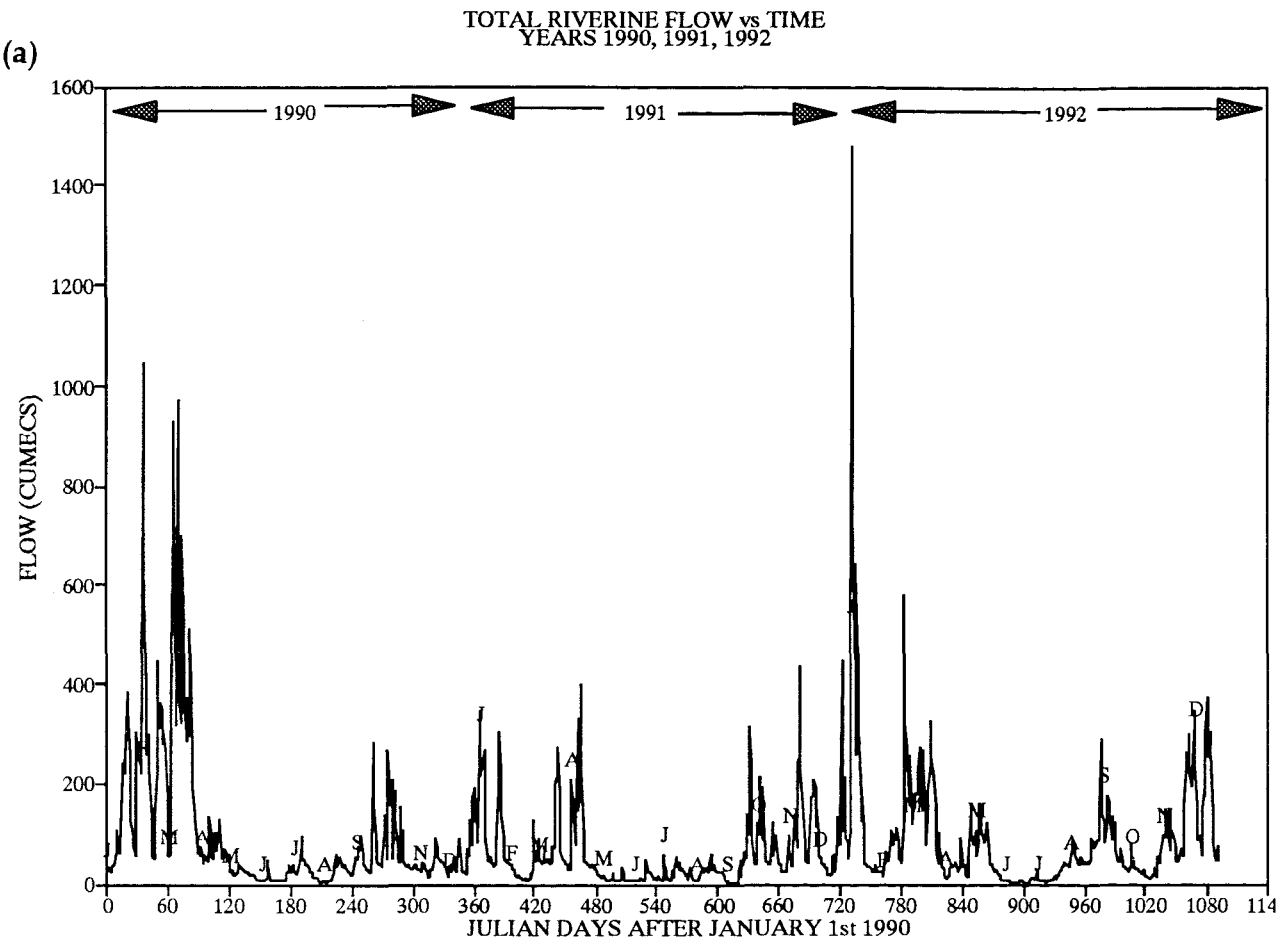

(b)

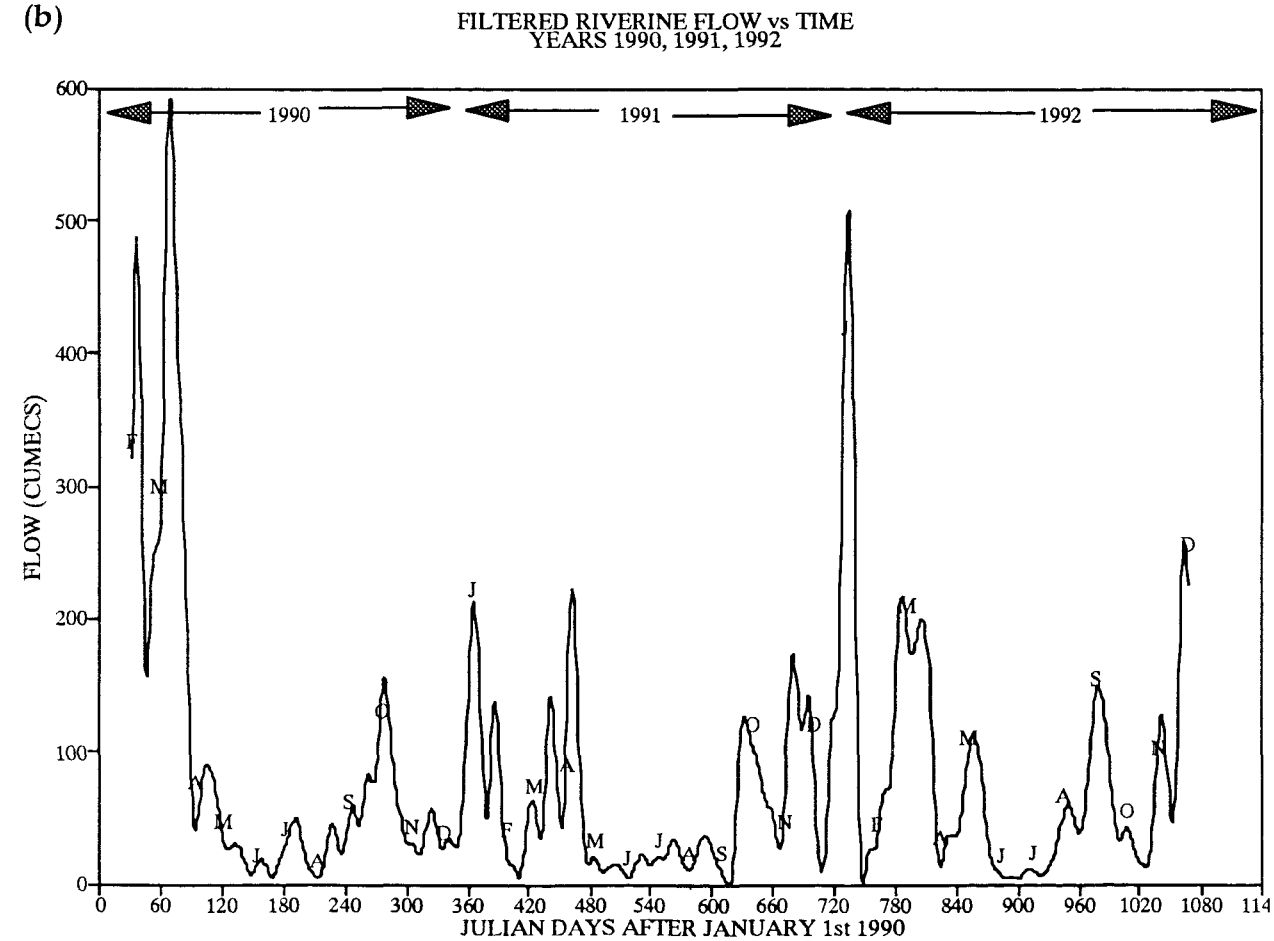

FIGURE 6.17

Relationship of Filtered Riverine Flow and Nitrate Concentrations with Time, Years 1990, 1991 and 1992.

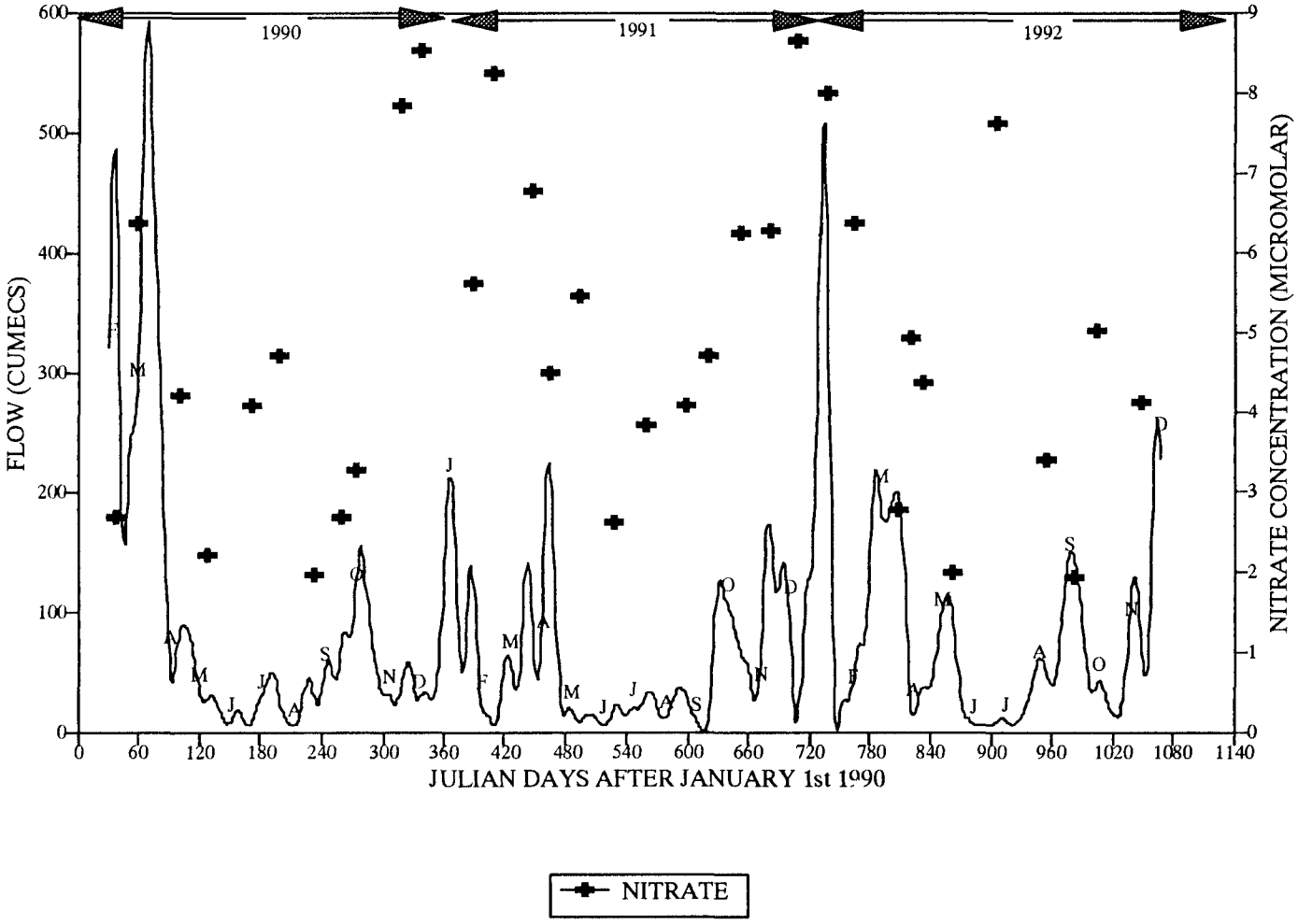

the winter period and the absence of nitrogen uptake by plants in the dormant season. Furthermore, the extent of the drainage network and the volume of saturated soil supplying runoff is at a maximum in the winter, allowing the tapping of NO_3 sources which may be unconnected to the main watercourse at other times of the year (Webb and Walling, 1985). There is also an argument that plant dieback is a gradual process supplying nitrogen to the soil well beyond the autumn months and that rates of mineral nitrogen production reach a maximum in the late rather than early winter (Roberts *et al.*, 1983).

Generally, around the summer to autumn months, when there is less rainfall, the concentrations decrease which is thought to reflect (i) the diminished soil water movement, (ii) the dominance of bedrock as a source which is remote from zones of relatively high nitrogen content located near the soil surface and (iii) losses of NO_3 due to uptake by growing crops and any biological activity within the streams (Webb and Walling, 1985). Any NO_3 that is accumulated in the soil during the drier months will be flushed out with the onset of the wetter weather thus contributing to the increased NO_3 concentrations as observed in the winter months.

To investigate further the extent of such long-term source variations in the NO_3 concentrations, a single harmonic function (a sine curve) with a period of one year which best fits the pattern of observed NO_3 concentrations over time in **FIGURE 6.17**, has been derived using the software package, MATHEMATICA (courtesy of Mr. A. Edwards, DML). This single harmonic function takes the form of the following equation:

$$Y_w = \alpha_0 + \alpha_1.[(\cos 2\pi.x)/365] + \beta_1 .[(\sin 2\pi.x)/365] \qquad \textbf{6.1}$$

Where; Y_w = the NO_3 concentration at a specified time within the yearly cycle;
x = time (Julian day number);
α_0 = the average NO_3 concentration over the three years = 4.93299 µM
α_1 and β_1 are coefficients and with units of concentration and take the values 1.74417 µM and 0.0147049 µM respectively.

FIGURE 6.18 shows the result of plotting this sine curve simultaneously with the observed NO_3 data over the three year time-period. As can be seen there does appear to be a correlation of the NO_3 concentrations with the annual regime. A regression analysis of the observed data on the predicted values derived from equation **6.1** results in an r^2 value of 0.32 which would indicate that 32 % of the variation in the freshwater NO_3 concentrations can be attributed to seasonal patterns within the annual regime. This agrees findings from a similar study carried out by Walling and Webb (1984) on NO_3 variations in the Exe Basin in Devon where values of r^2 ranged from < 1 % to > 40 %. Hence, the seasonal patterns (which are incorporated in the annual regime) in the NO_3 levels for the Linnhe area are relatively well-developed. Deviations of r^2 away from 1 may be mainly due to differences in the meteorological conditions over the three years in question. For example, it can be seen from **FIGURE 6.17** that the timing of the maximum rainfall varies from year to year and thus so will the timing of any flushing of increased NO_3 concentrations from the soil and the time available for leaching of NO_3 from the soil into the runoff.

Concentration-flow relationships: Regression analysis has been carried out of the monthly NO_3 concentration data on the corresponding filtered flow data and the results from this are illustrated in **FIGURE 6.19**. The value of r^2 is very low at 0.011. Such a low dependence of NO_3 concentrations on flow reflects the major importance of other parameters such as soil moisture and temperature (Walling and Webb, 1984). Also, despite the filtering of the flow data, there will still be uncertainties in the interpretation of r^2 values because of the strong intercorrelation between the discharge values for consecutive months due to the temporal effect of water movement through the soil which gives rise to a time-lag ("memory effect") of the nutrient signal.

Hence, the variations in riverine NO_3 concentrations appear to have a higher dependence on the timing of events and the seasonal cycles within an annual regime, than on shorter-term river-flow fluctuations.

FIGURE 6.18

Relationship of Riverine Nitrate Concentrations with the Annual Regime: Agreement of Nitrate Data with a Single Harmonic Function. (Riverine Data Courtesy of the HRPB).

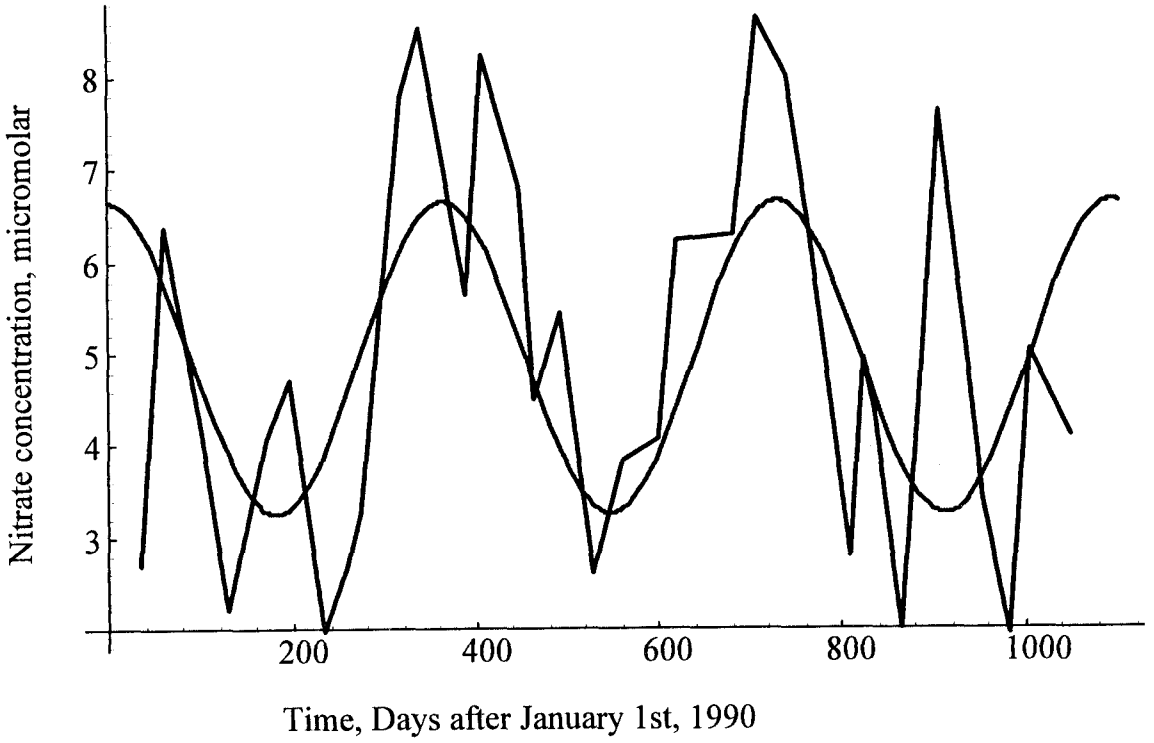

FIGURE 6.19

Relationship of Riverine Nitrate Concentrations (Averaged Lochy and Nevis Data) with Filtered Flow Data. (Data Courtesy of the HRPB).

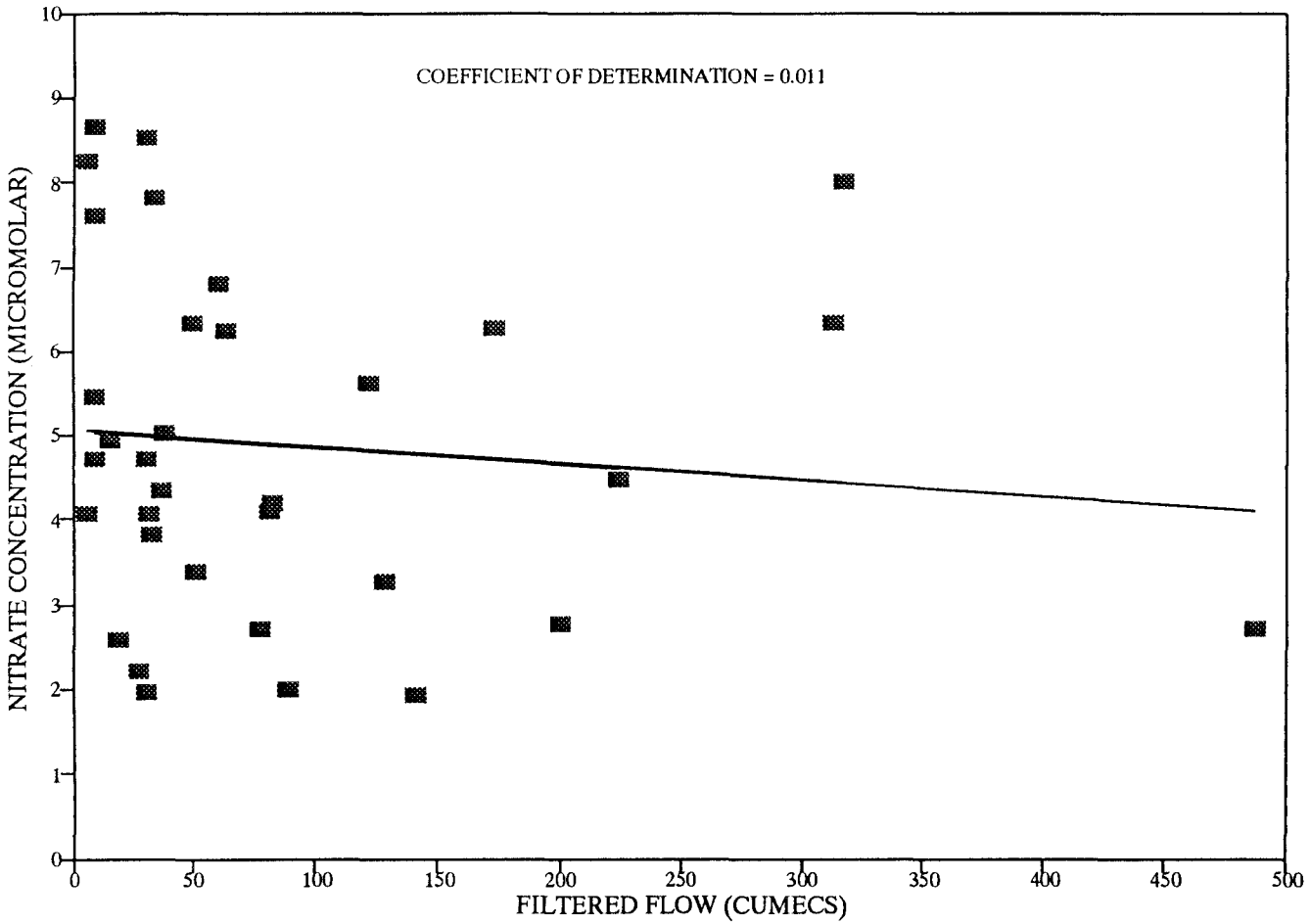

Phosphate variations in the end-member concentrations:

As is illustrated in **FIGURE 6.20** the pattern of riverine PO_4 concentrations with flow over time is far less pronounced than was for NO_3. The lack of a seasonal pattern in PO_4 concentrations is demonstrated quantitatively by carrying out the fitting of a sine curve with a period of one year in the same way as was undertaken for NO_3. **FIGURE 6.21** shows the results of fitting a sine curve of the form:

$$Y_w = 0.187012 - 0.099424.[(\cos 2\pi.x)/365] - 0.0543765.[(\sin 2\pi.x)/365]$$

where; Y_w = the PO_4 concentration at a specified time within the yearly cycle;
x = time (Julian day number).

This equation was obtained from the software package MATHEMATICA, (courtesy of Mr. A. Edwards, DML).

FIGURE 6.21 shows that there are no obvious seasonal patterns of PO_4 concentrations through the year and concentrations generally remain fairly constant throughout the whole of the three year period at values less than 0.3 µM. Exceptions were days 907 and 954, (in 1992) when increased concentrations of PO_4 of 0.48 µM and 1.68 µM respectively were the average values in the rivers. A regression analysis of the observed PO_4 concentrations on the predicted values obtained from the single harmonic function result in an r^2 value of 0.08. Analysis of the concentration-flow relationships of freshwater PO_4 concentrations indicates also very little dependence of concentration on flow. This is illustrated in **FIGURE 6.22**; regression analysis of the concentrations on the filtered flow data results in an r^2 value of 0.003.

A weak relationship between the PO_4 concentrations and flow and the lack of annual periodicity in concentrations are likely to be due to the high and very complex geochemical reactivity of PO_4 in natural and estuarine waters. This has

FIGURE 6.20

Relationship of Filtered Riverine Flow and Phosphate Concentrations with Time, Years 1990, 1991 and 1992.

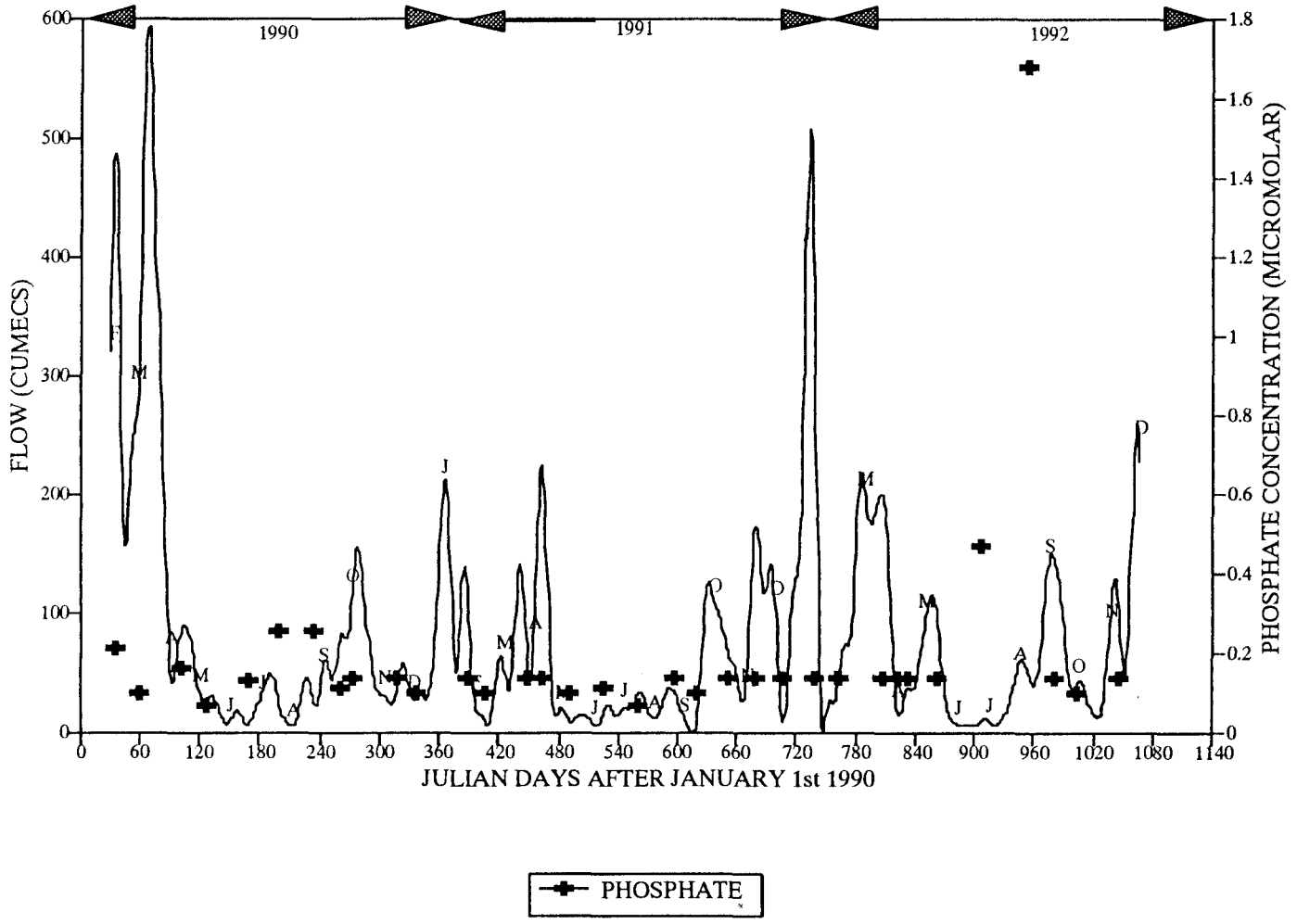

FIGURE 6.21

Relationship of Riverine Phosphate Concentrations with the Annual Regime: Agreement of Phosphate Data with a Single Harmonic Function. (Riverine Data Courtesy of the HRPB).

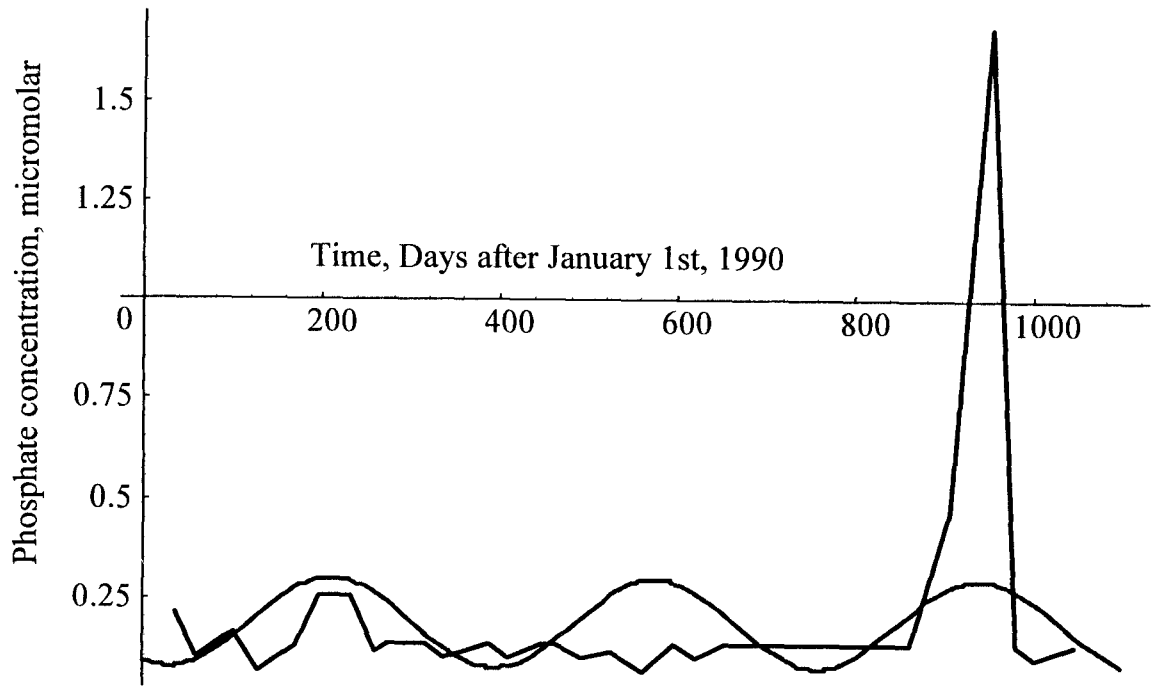

FIGURE 6.22

Relationship of Riverine Phosphate Concentrations (Averaged Lochy and Nevis Data) with Filtered Flow Data. (Data Courtesy of the HRPB).

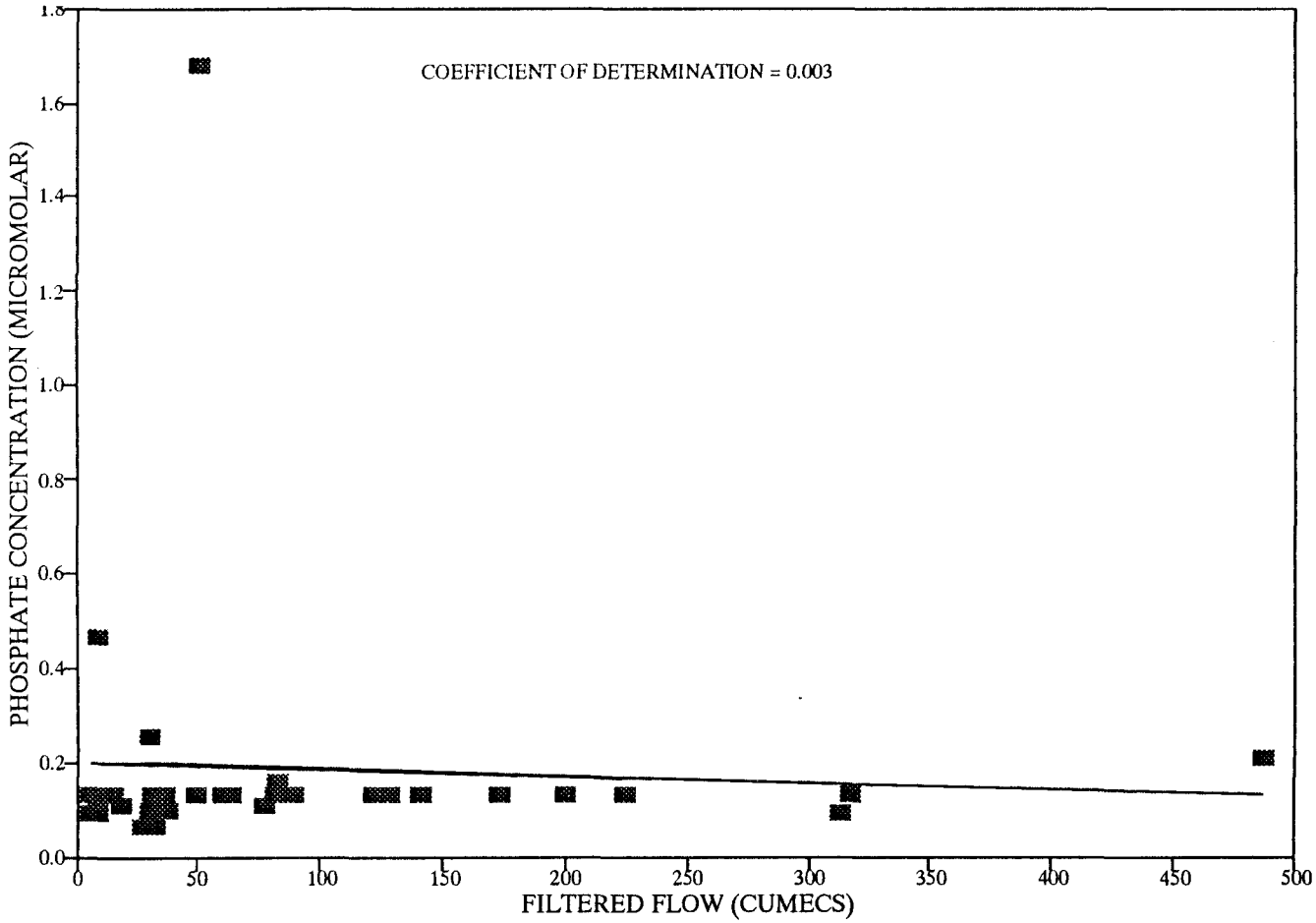

been summarised in **CHAPTER 2.** In these sections it was shown that the PO_4 concentration in true solution is very dependent on the amount of dissolved organic matter (DOM) and iron (Fe) present in the natural waters since it associates significantly with them to form a colloidal phase. In section **2.2.2.1** it was emphasized that this process of conversion to the colloidal phase may be of particular importance in the Loch Linnhe catchment area where there is acidic, peaty (Fe-rich) soil and the Fe in river water is likely to be present in the colloidal form, as oxyhydroxides stabilised by DOM. If the PO_4 is in the colloidal phase in the freshwater then it is likely to be removed to the solid phase when it enters the more saline, estuarine waters since a property of colloids is that they tend to aggregate in electrolyte solutions. This PO_4, once in the solid phase, may later be released back into the water column under certain conditions of pH, salinity and redox conditions. Section **2.2.2.2** describes the high particle-reactivity that is a property of the PO_4 ion and how it reacts with a wide variety of surfaces, being taken up by and released from particles through a complex series of sorption reactions. Hence PO_4 may be removed from the dissolved phase in natural waters through its adsorption onto and/or into the structure of suspended particulate matter (SPM), namely clays with surficial coatings of Fe and Al-oxyhydroxides, resulting from the weathering of rocks and soils and then released back into the estuarine water column under certain conditions of pH and salinity. The high geochemical and particle reactivity of PO_4 acts to complicate the prediction and modelling of its behaviour in natural and estuarine waters.

Conclusions from this section on freshwater end-member variations, are (i) that both nitrate and phosphate concentrations do vary temporally in the riverine input to the Linnhe system and these variations will contribute to the scatter of relationships of concentrations to salinity at station LL14 and, (ii) that these variations have a higher correlation with long-term phenomena such as the annual regime (although only very slightly for PO_4), which includes seasonal effects, than with short-term features such as variations in the river flow. For nitrate there are quite marked seasonal patterns in behaviour over time but with phosphate there are no such patterns which is most likely to be a consequence of its high

geochemical reactivity.

6.2.1.2 Processes giving rise to non-conservative behaviour

This section considers evidence for the occurrence of processes giving rise to real non-conservative behaviour in Loch Linnhe during the 1992 field-season, since these will contribute to the scatter of data in the nutrient / salinity relationships at station LL14. It considers evidence for the occurrence of (i) biological activity and (ii) biogeochemical processes in the basin system.

(i) Evidence for biological activity: **FIGURES 6.23, 6.24** and **6.25** show the temporal changes in the NO_3, PO_4 and SiO_4 concentrations respectively at stations LL0 and LL14 using timeseries plots which are in the form of contour maps. These contour maps have been created using the UNIMAP software package, the settings for which are listed in **APPENDIX 6.5**. The maps themselves can also be found in the **APPENDIX 6.5** with the data from which they were created superimposed onto them. The timeseries data span results collected on a weekly basis starting on day 59 and ending on day 139.

In **FIGURES 6.23 (a)** to **6.25 (a)** it can be seen that the concentrations of all three nutrients are markedly depleted in the top 10 m at station LL14 from day 105 onwards, with replenishment beginning again by the end of the field-season, day 139. This might be indicative of biological activity in the surface layers with all three nutrients being taken up from the dissolved phase by phytoplankton cells for growth, the NO_3 and PO_4 nutrients being essential elements in the cellular composition of the organisms (see **CHAPTER 2,** section **2.3.1.1**). The spring phytoplankton bloom that occurs in Loch Linnhe consists of diatoms and this is well-documented in the literature (see **CHAPTER 3**, section **3.2.1.4**). The SiO_4 is taken up in the dissolved phase by the diatoms and used in the development of the frustule in the diatom cell. The suggestion that the observed nutrient depletion is caused by the presence of the diatom bloom is supported by the chlorophyll a concentrations measured in the water column at this time (obtained from

FIGURE 6.23

Temporal Variations in Nitrate Concentrations at (a) Station LL14 and (b) Station LL0, Julian Day 50 to 139, 1992.

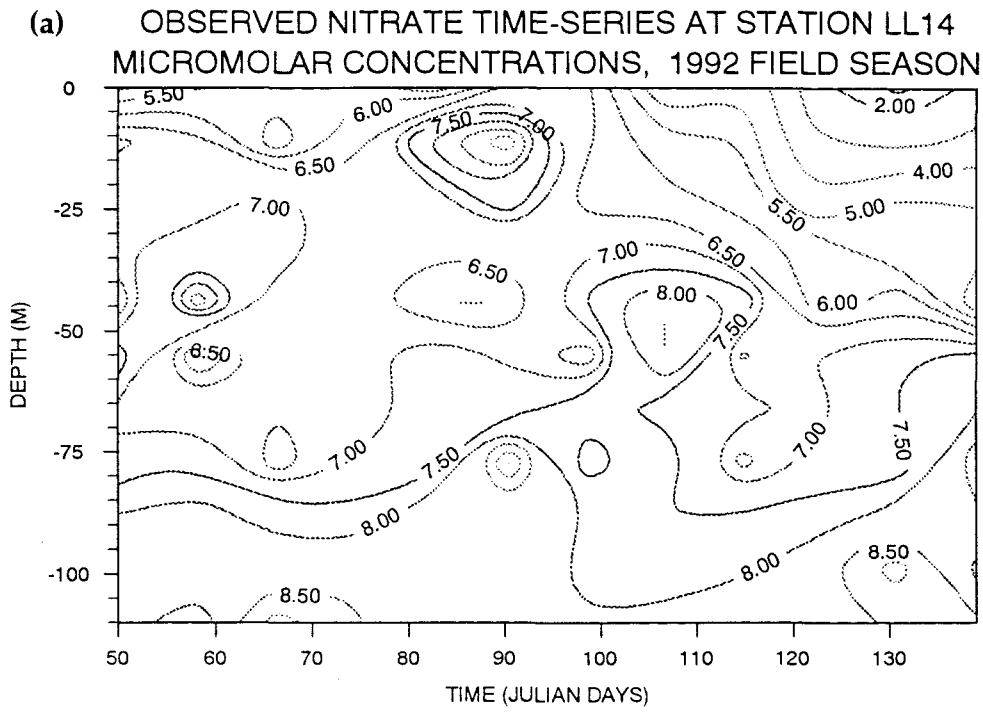

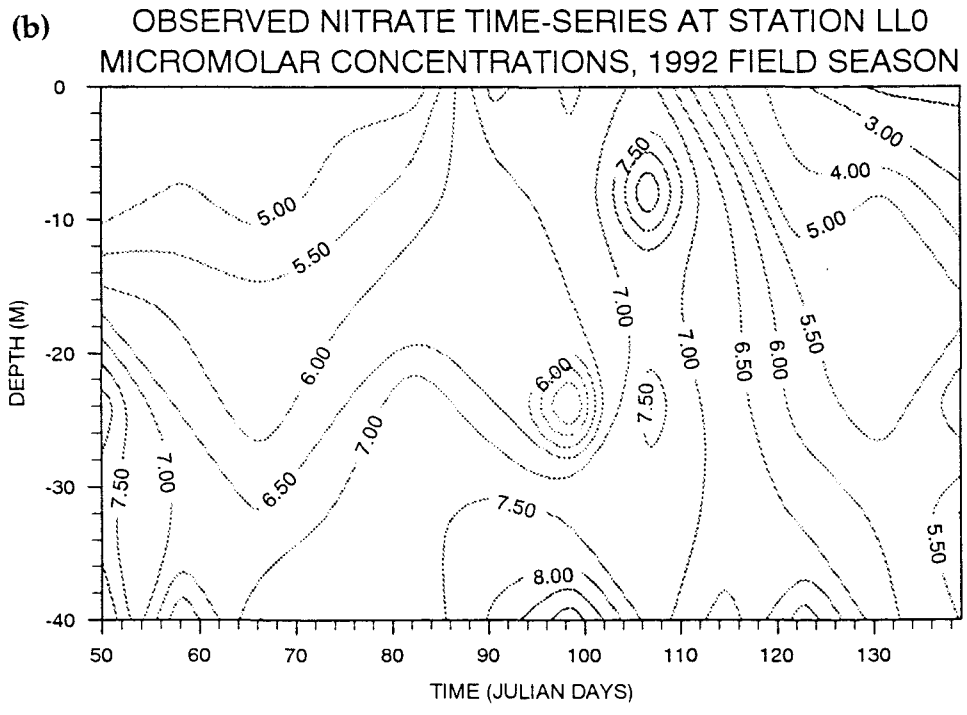

FIGURE 6.24

Temporal Variations in Phosphate Concentrations at (a) Station LL14 and (b) Station LL0, Julian Day 50 to 139, 1992.

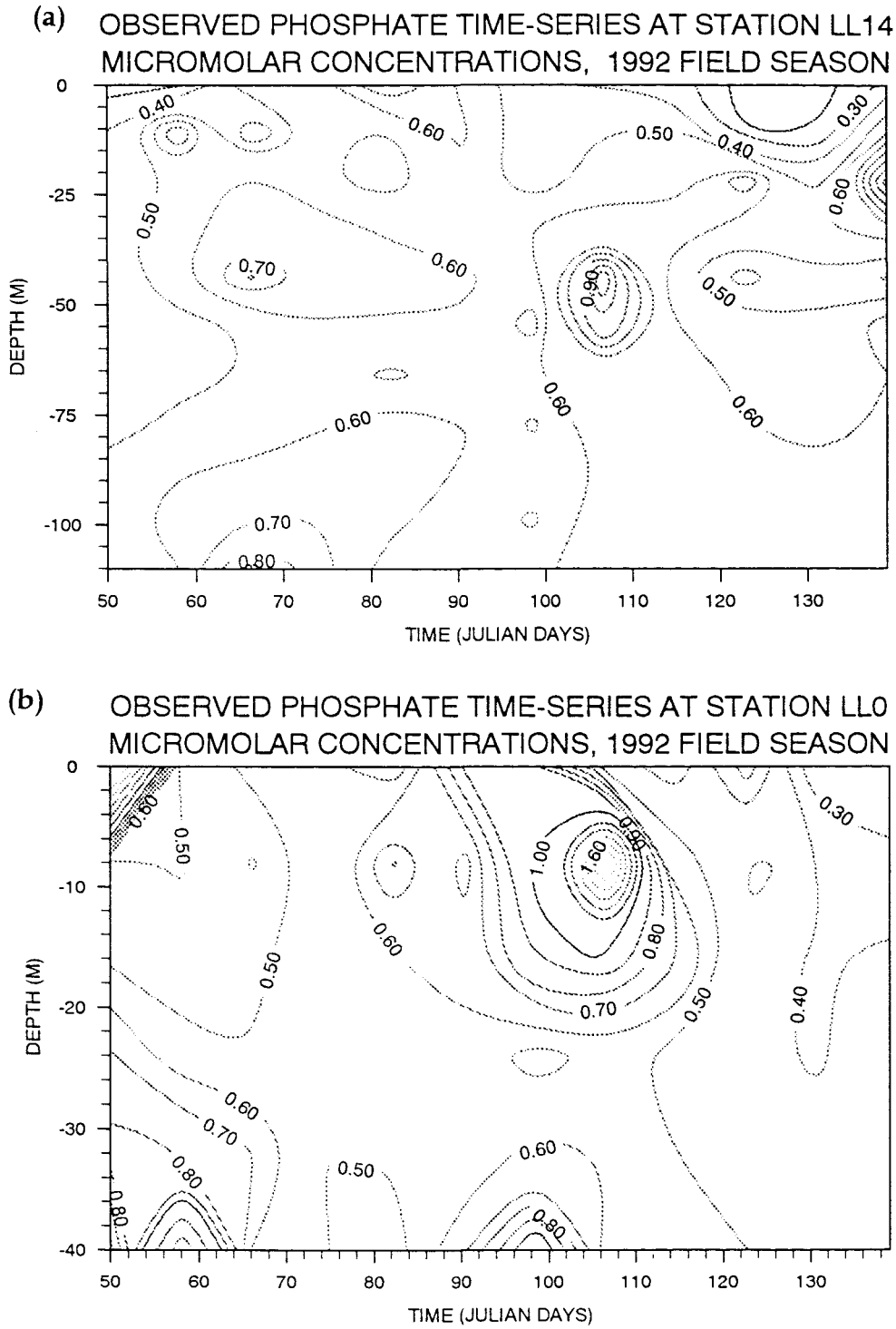

FIGURE 6.25

Temporal Variations in Silicate Concentrations at (a) Station LL14 and (b) Station LL0, Julian Day 50 to 139, 1992.

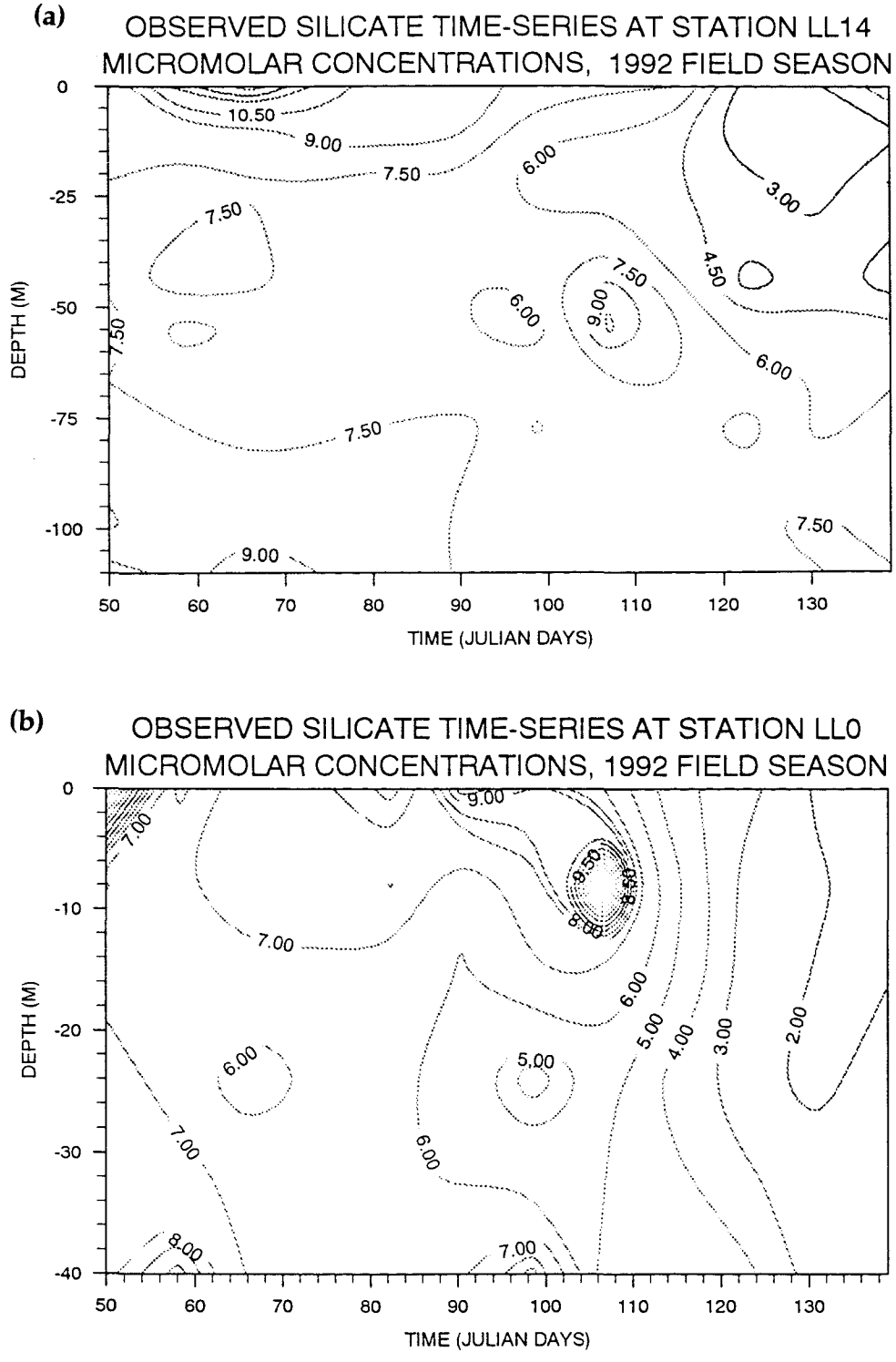

fluorescence measurements taken from the fluorometer attached to the CTD - data listed in **APPENDIX 6.1**). **FIGURE 6.26** shows the very marked increase in chlorophyll concentrations in the top 10 m at stations LL14 over this time, extending to a depth of 40 m by day 125 (probably due to downward vertical mixing of the surface layers or advection of inflowing cells to this depth via inflowing water from station LL0). **FIGURE 6.27** shows how a steady increase in the average chlorophyll concentrations over the top 10 m at station LL14, observed from day 99 onwards, values ranging from 0.13 $\mu g\ l^{-1}$ on day 99 to 8.27 $\mu g\ l^{-1}$ on day 125. This increase is concomitant with the steady decrease in the concentrations of all three nutrients in the surface layers between days 99 and 125, although there is a relatively sharp decrease in the nutrient concentrations between days 114 and 125 as the chlorophyll concentrations reach their maximum value. For the days 99 to 125 nutrient concentrations averaged over the top 10 m at station LL14 range from 6.66 to 2.45 μM for NO_3; 0.43 to 0.16 μM for PO_4 and 7.45 to 2.08 μM for SiO_4. After day 125 the nutrient concentrations begin to increase again, rising to concentrations of 2.71, 0.42 and 4.43 μM for NO_3, PO_4 and SiO_4 respectively by day 139, indicating die-off of the bloom.

Regarding the nutrient and chlorophyll status of the water originating from station LL0 around this time, **FIGURE 6.28** shows that for the average levels taken over the top 20m at the station there is a marked increase in the chlorophyll concentrations between days 99 and 125 with a range of between 0.10 $\mu g\ l^{-1}$ on day 99 to 8.47 $\mu g\ l^{-1}$ on day 125, decreasing sharply by day 132. This is also illustrated well in **FIGURE 6.29**. This increase in chlorophyll concentrations is again accompanied by a decrease in the concentrations of all three nutrients. Nutrient ratios of this inflowing water vary from N:P of 9.23:1 and N:Si of 0.85:1 on day 86, to N:P of 9.04:1 and N:Si of 1.55:1 by day 125, suggesting a maintenance of the pre-bloom NO_3 and PO_4 proportions either through regeneration of these nutrients or their uptake at the same rate, but indicating depletion of SiO_4 relative to NO_3. The presence of chlorophyll at station LL0 could be due to the advection of phytoplankton cells from the adjacent coastal regions (maximum chlorophyll concentrations being recorded in neighbouring Loch Creran on day 106; D.Harris,

FIGURE 6.26

Temporal Variations in Chlorophyll Concentrations (μg l^{-1}) at Station LL14, Julian Day 50 to 130, 1992.

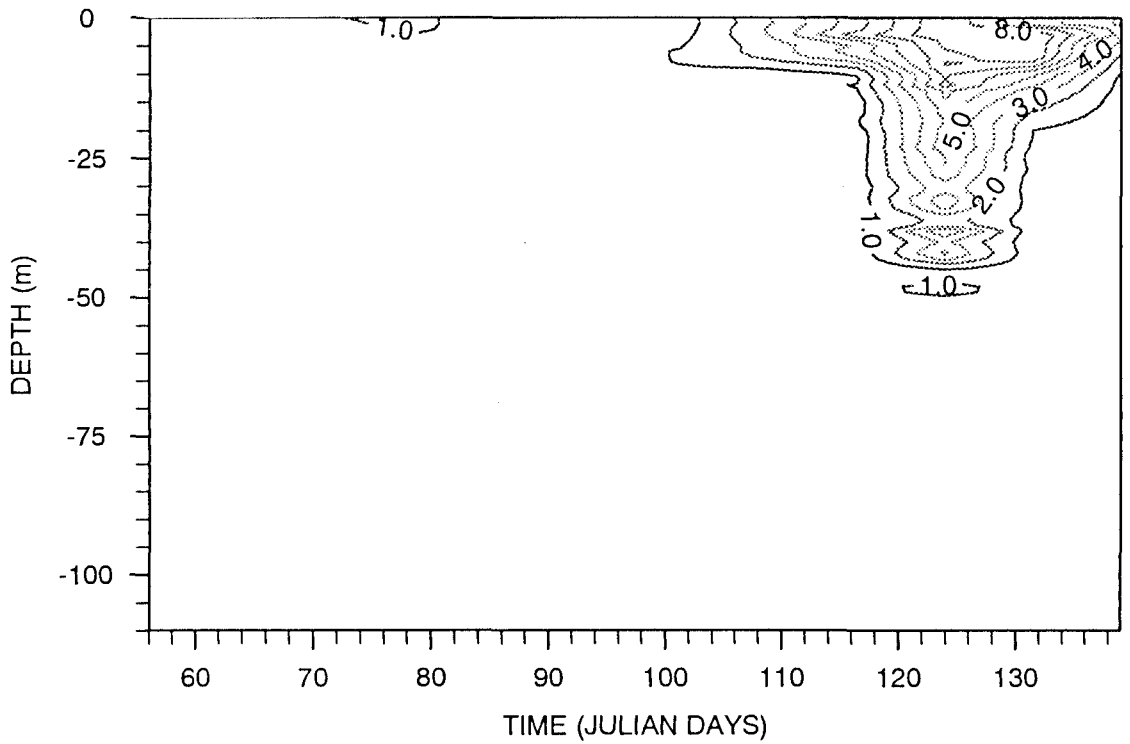

FIGURE 6.27

Relationship of Chlorophyll Concentrations (μg l^{-1}) with Nutrient Concentrations and Time at Station LL14, Julian Day 50 to 139, 1992. (Data Averaged over the top 10 m).

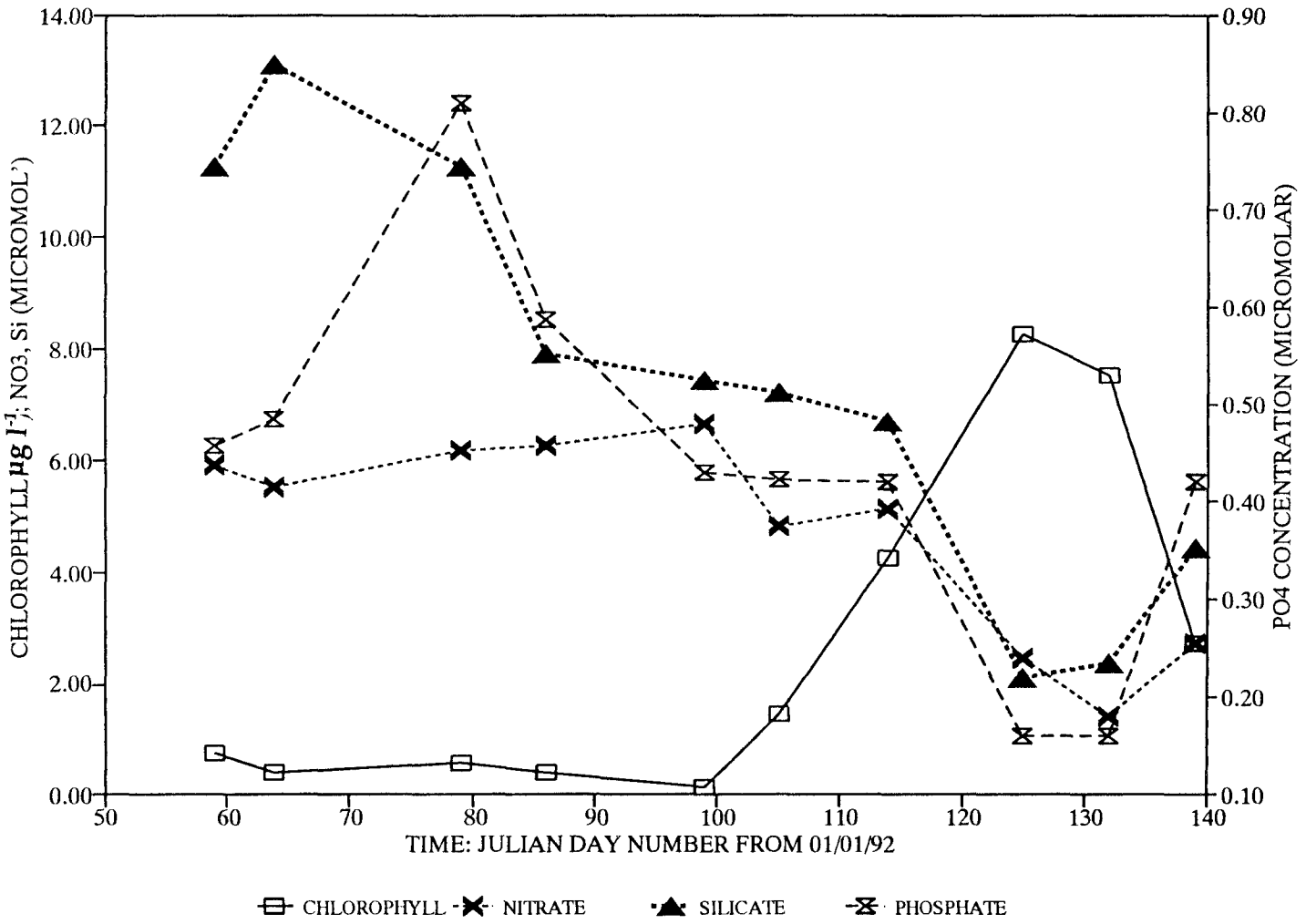

FIGURE 6.28

Relationship of Chlorophyll Concentrations (μg l^{-1}) with Nutrient Concentrations and Time at Station LL0, Julian Day 50 to 139, 1992. (Data Averaged over the top 20 m).

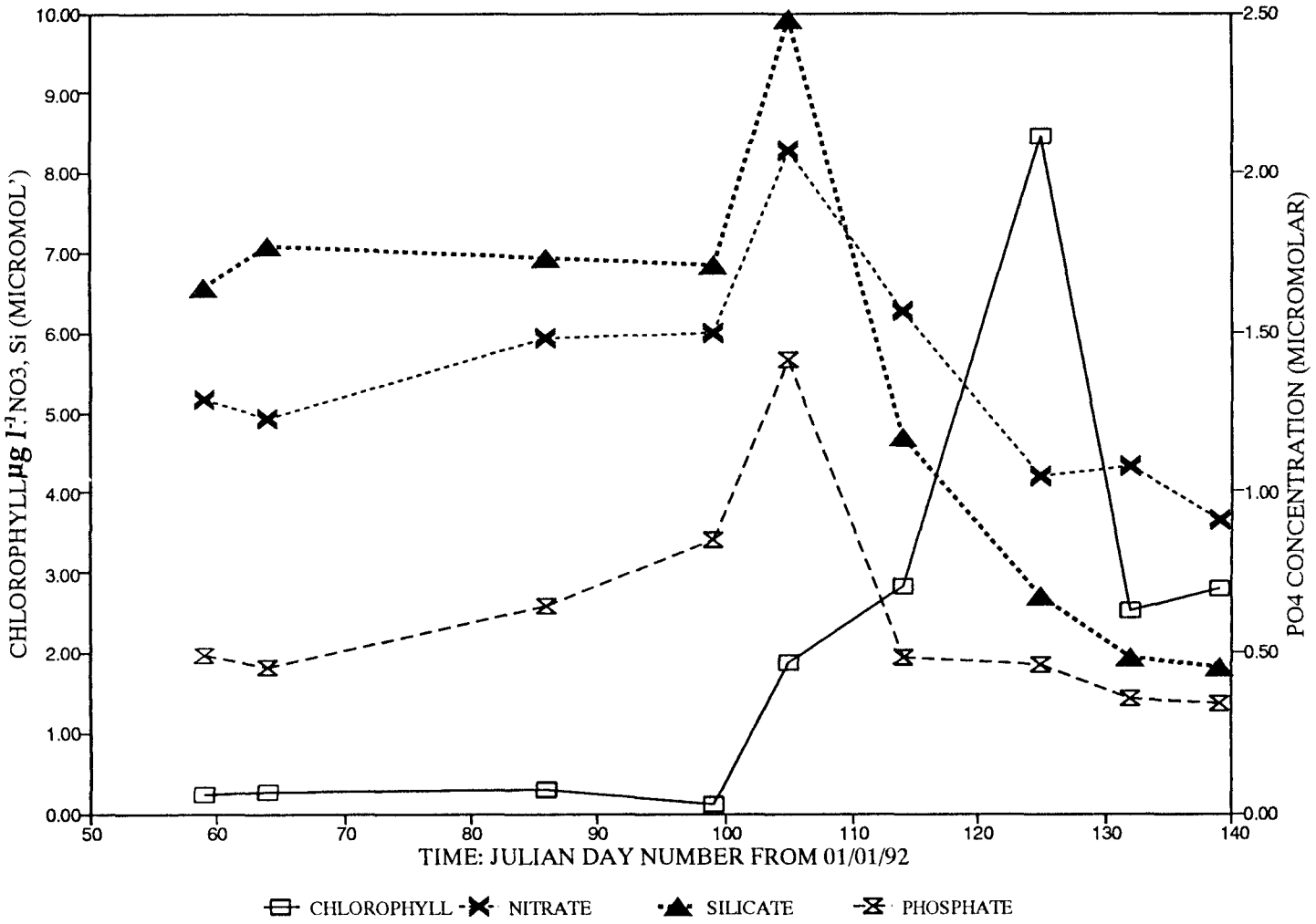

FIGURE 6.29

Temporal Variations in Chlorophyll Concentrations (µg l^{-1}) at Station LL0, Julian Day 50 to 130, 1992.

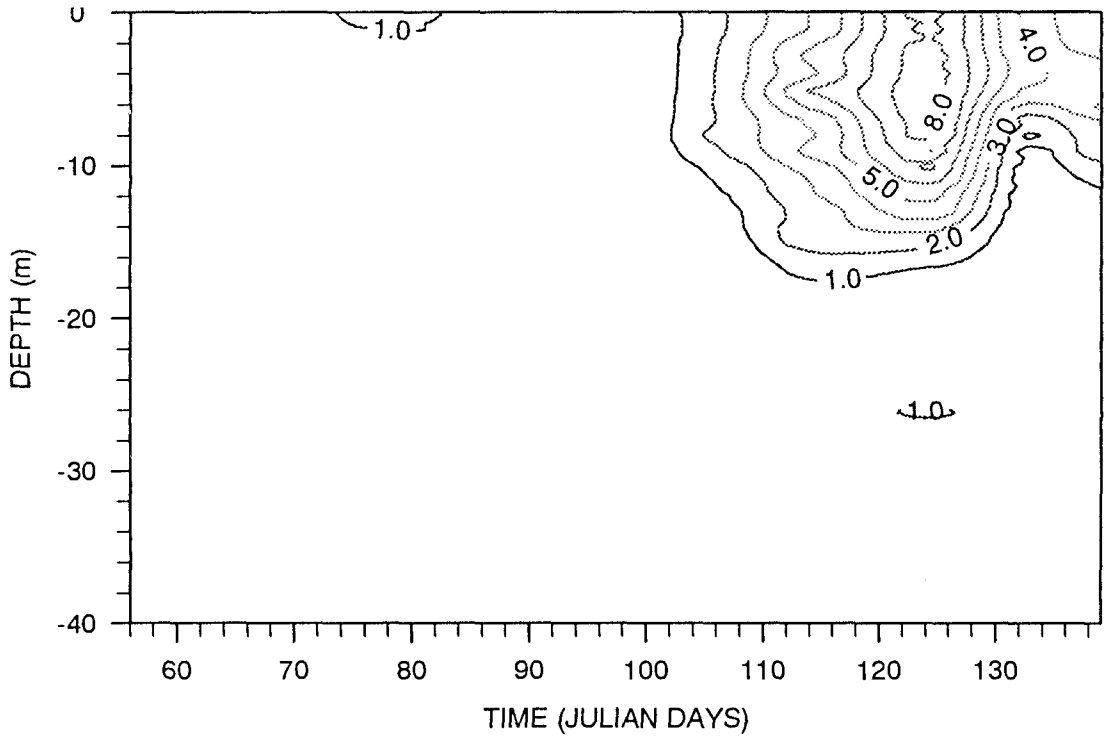

1994, pers.comm.), with the resultant seeding of the bloom inside the basin reflected by the elevated concentrations of chlorophyll present at station LL14, or it could be a reflection of the flushing out of phytoplankton cells and water with relatively low nutrient concentrations from the top 10 m at station LL14. This latter situation could arise if the bloom were seeded within the basin due to the uplift of diatom cells present in the sediment in a vegetative state over the winter but lifted back up into the euphotic zone by the spring, via a deep-water renewal event, as was observed between days 86 to 99 in Loch Linnhe (see section **6.1.2.1**).

Factors favouring the bloom: However the bloom is seeded in the upper basin, conditions must be favourable for algal growth for the bloom to occur once the phytoplankton cells are in the water column, and this requires the presence of nutrients in sufficient concentration and light in the water column (see **CHAPTER 2**, section **2.3.1.1**).

As has been shown in section **6.1** and summarised in section **6.1.3**, upwelling of high salinity water was observed by day 86 at station LL0, with the consequent upward displacement of the pycnocline through a height of approximately 20 m. This was concomitant with a change in the wind direction and a decrease in the residence time of the freshwater in the basin. Such upwelling events are important in fjord systems because the high salinity water that is upwelled seaward of the sill may be rich in nutrients due to the advection of higher salinity water from the adjacent coastal regions. In the case of Loch Linnhe, the intermittent, deeper topography of adjacent regions (pools effectively), allows nutrients that are diffusing out from the sediment porewaters to the water column, to accumulate in the isolated deeper waters. Such nutrient regeneration processes are described in detail in **CHAPTER 2**, section **2.3.2.1**. From **FIGURES 6.23 (b)**, **6.24 (b)** and **6.25 (b)**, it can be seen that increases in the concentrations of all three nutrients at 40 m depth at station LL0 are observed between days 86 and 99 with NO_3 increasing from 7.12 to 9.33 μM, PO_4 from 0.46 to 1.13 μM and SiO_4 from 6.17 to 8.76 μM between these dates. Such an increase of nutrient concentrations could be due to the import of high salinity, nutrient-rich water to the sill region due to the

upwelling events that are occurring around this time, from day 86 to day 105. In **FIGURE 6.28** the effect this has on the nutrient concentrations in the top 20 m at station LL0, is illustrated. All three nutrients show an increase in concentration around days to 86 to 105. The relatively high concentrations observed between days 99 and 105 are probably due to a combination of upwelled nutrients and possibly an input of water with high nutrient concentrations from the adjacent coastal waters (e.g. from the Clyde Sea area). In section **6.1** it was shown how this upwelled water at station LL0 had caused a deep-water renewal throughout the basin between days 86 and 99. This was evident from the increase in density and vertical mixing throughout the water column at stations LL14 and LL19. Hence, the saline water entering the basin at the time of the renewal event would contain increased levels of nutrients from LL0 plus any regenerated nutrients resident in the bottom-waters of the basin which would be displaced upwards into the euphotic zone by the dense, renewing water.

After day 105 the water column at station LL14 was observed to stabilise again, with an increased degree of vertical stratification. **FIGURE 6.4** showed that the freshwater input to the basin from the River Lochy, began to increase again after day 94 indicating that the rainfall had increased at this time. The total riverine freshwater input to the basin increased from 11 $m^3 s^{-1}$ on day 94 to 152 $m^3 s^{-1}$ on day 118 and 84 $m^3 s^{-1}$ on day 125, increasing the buoyancy input to the system and the stability of the surface layers. This allows for the retention of phytoplankton cells in the euphotic zone and hence enables the bloom to occur.

To summarise, it has been shown in this section that there is evidence for biological activity within the time-span of the 1992 field-season in the surface layers of the basin. This will give rise to scatter in the nutrient/salinity relationships at station LL14 due to the conversion of the nutrients from the dissolved to the solid phase during this process. This biological activity is due to the presence of a diatom bloom, the conditions for which are favoured by (a) increased nutrient concentrations in the incoming water from station LL0; (b) stabilisation of the water column in the basin through a buoyancy input of

freshwater to the water column; (c) the presence of algal cells in the basin water either via seeding from outside the loch or from seeding within the basin itself, caused by the potential uplift of diatom cells into the euphotic zone as a consequence of the deep-water renewal event observed previous to the bloom. Furthermore, as has already been mentioned, any increased nutrient concentrations in the bottom-waters of the basin will also be displaced upwards by the renewing water thus favouring phytoplankton growth in the euphotic zone. Such biogeochemical processes in the bottom-waters will now be considered.

(ii) Evidence for biogeochemical processes: This section will consider evidence for (1) the conversion of nutrients from the solid to dissolved phase via regeneration processes and (2) the conversion of PO_4 from the dissolved to the solid phase via adsorption and aggregation processes. Such biogeochemical processes produce real non-conservative behaviour and as such will cause scatter of data in the nutrient/salinity relationship at station LL14.

In **CHAPTER 2**, section **2.3.2.1**, the regeneration of nutrients from the solid phase in organic matter back to the dissolved inorganic phase in the water column, via microbial reduction processes, has been discussed in detail. Nutrients regenerated in this way in the sediment porewaters can be released back into the water column where they are available for use by phytoplankton, once in the euphotic zone. The dissolved inorganic nutrients are released across the sediment/water interface via (a) diffusive processes caused by the difference in nutrient concentrations between the porewater concentrations and the concentrations in the overlying waters, (b) bioturbation processes causing a disturbance of the sediment (c) the intrusion of short-term, high density pulses of water of a volume not great enough to cause a complete renewal of the bottom-waters of the basin, nor to cause a conspicuous rise in the densities measured there, but great enough to cause resuspension of the sediments. Once in the overlying waters, the increased nutrient concentrations may be transferred up to the euphotic zone via upward displacement by inflowing, renewing water.

The hydrographic results for 1992 (section **6.1.2.1**), showed that the density of the water present at depths greater than 75 to 80 m at station LL14 remained constant from the start of the field-season, day 50, to day 86 (inclusive) which was the last sampling date before the deep-water renewal event. It was therefore suggested that after this period water below about 80 m essentially was isolated from mixing with any incoming waters and that the only way that the nutrient concentrations can change over this time is through their simultaneous diffusion with salt. Any other changes in nutrient concentrations must therefore be due to non-conservative biogeochemical processes affecting the bottom-waters. **FIGURES 6.23 (a)** to **6.25 (a)** show marked increases in the concentrations of all three nutrients at depths below 80 m at station LL14 for the time leading up to day 86. **Figure 6.30 (a)** illustrates the temporal changes which appear to be occurring at 100 m depth at station LL14. Between sampling dates 59 and 64 the concentrations of all three nutrients have increased from 6.48 to 9.20 μM for NO_3, 0.65 to 0.93 μM for PO_4 and 8.57 to 9.76 μM for SiO_4. This would indicate that there has been an influx of nutrients to the bottom-waters, probably via a flux of regenerated nutrients from the sediment porewaters out across the sediment/water interface due to a disturbance of the sediment. **6.30 (b)** shows the effect of this input on the nutrient ratios in the bottom-waters at 100 m between these two dates. The N:P ratio is only slightly altered from 9.97 on day 59 to 9.89 on day 64 which shows that the proportion of NO_3 to PO_4 in the porewaters is the same as in the overlying waters although the actual concentrations of the nutrients may be different. It does indicate, however that if NO_3 and PO_4 are being regenerated within the sediment then they are doing so at the same rate. The N:Si ratio increases between these dates, tending towards 1 which would indicate that NO_3 is being regenerated faster in the sediments than SiO_4 which is consistent with the literature. (**CHAPTER 2**, section **2.3.1.1** provides a discussion of nutrient ratios and possible reasons for their deviation away from the Redfield N:P ratio of 16:1 and the predicted ratio of N:Si of 1:1.07 in marine species by Richards (1958)). Between days 64 and 79 all three of the nutrient concentrations are seen to decrease. The NO_3 concentrations, although decreased, are still relatively high to the starting concentration on day 59, being 8.01 μM. The PO_4 shows a much more pronounced decrease however,

FIGURE 6.30

Relationship Between (a) Nutrient Concentrations and (b) Nutrient Ratios with Time at 100 m Depth for the Time-Period Leading up to the Deep-Water Renewal. Station LL14, Julian Day 59 to 86.

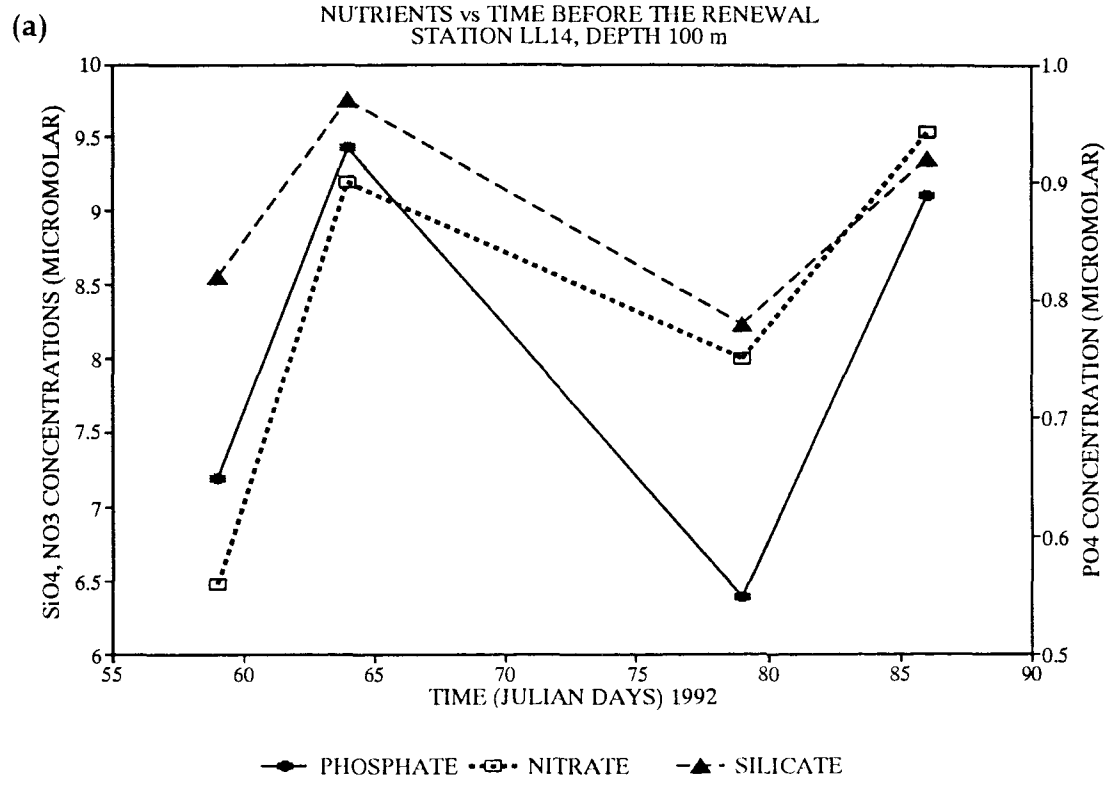

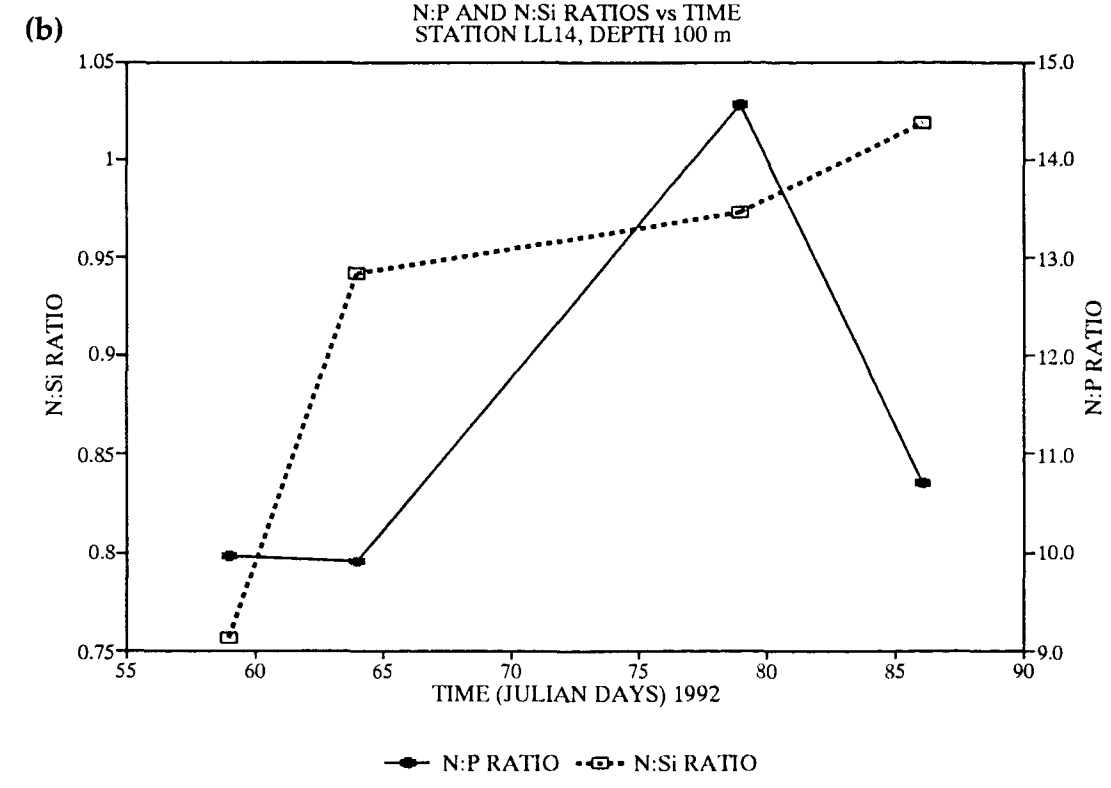

suggesting that there is some additional removal process, which is most likely to be due to its high geochemical reactivity and potential for being scavenged from the dissolved phase by SPM (namely clays - see **CHAPTER 2**). Silicate does not decrease so dramatically but because it did not rise so sharply initially, the concentration on day 79 is less than the starting concentration. The salinity change at 100 m depth between these two dates is < 0.2 PSU which would indicate that, assuming molecular diffusion of nutrient ions occurs at the same rate as salt, that the maximum change in the nutrient concentrations between these dates would be < 1 % of their concentration on the starting date and this will not explain the changes observed. As mentioned previously, enhanced removal of PO_4 may occur due to its geochemical reactivity and for SiO_4, also there is a slight possibility of being scavenged from the dissolved phase. But for NO_3 the observed decrease must be explained by some other mechanism. One possibility is that the molecular diffusion rate of the nutrients is higher than that of the salt in the bottom-waters. This is likely to be the case because the rate of molecular diffusion will depend on the gradients set up between the bottom-water concentrations and those in the water lying immediately above it, and between days 59 and 64 an influx of nutrients, but not salt, was observed at 100 m. Thus, the nutrient concentrations present at 100 m were higher than those in the water lying above it hence an increased molecular diffusion rate would be expected whereby the concentrations could decrease back to a steady-state situation given enough time. The fact that the PO_4 and SiO_4 concentrations fell below their starting concentrations would indicate enhanced removal by processes mentioned above. By day 86 the concentrations of all three nutrients have increased again at 100 m, from 8.01 - 9.54 μM for NO_3, 0.55 - 0.89 μM for PO_4 and 8.23 - 9.37 μM for SiO_4. In terms of the nutrient ratios, the N:P ratio is observed to decrease between these two dates from 14.56 on day 79 to 10.72 on day 86. This would suggest that the ratio is approaching that observed on day 64 and that the increased N:P ratio observed on day 79 could be due to the geochemical removal of PO_4 occurring in the water column and the lower N:P ratio observed on day 86 could be due to the influence of the nutrients in the porewaters as they are released into the overlying water. The N:Si ratio appears to be approaching the 1.07:1 ratio as predicted by Richards

(1958), indicating that the regeneration of nutrients has continued within the porewaters over time. **FIGURE 6.9 (a)** shows that there is no significant change in the salinity of the water at this depth between days 50 and 86 (delta salinity < 0.2 PSU), thus these temporal changes in the nutrient concentrations observed at this depth, provide evidence for the occurrence of non-conservative regenerative processes in the bottom-waters at station LL14. These result in a source of nutrients to the basin which, if transported upwards to the euphotic zone will encourage biological activity. Such inputs of nutrients to the system will cause scatter of data in a nutrient/salinity relationship at station LL14.

Further work was undertaken to investigate the potential role of solid-phase interactions of phosphate, with particular reference to sediments. In **CHAPTER 2** details have been given of processes that can lead to associations of dissolved inorganic PO_4 with solid phases, which can as a sink for the nutrient and cause scatter in a nutrient/salinity relationship. These include: the adsorption of PO_4 onto and /or into SPM structures in natural waters (section **2.2.2.2**); the conversion of PO_4 associated with the colloidal phase in natural waters to an aggregate in the estuarine environment (section **2.2.2.1**); the adsorption of PO_4 onto SPM surfaces in the estuarine environment (section **2.3.1.2**). In summary it was described how natural clay particles with a surficial coating of Fe and Al-oxyhydroxides have a high capacity for the adsorption of PO_4 and thus for maintaining low dissolved inorganic PO_4 levels in natural waters. The PO_4 may be incorporated into the clay structure itself via reversible two-step solid-phase sorption processes. When in the colloidal phase in natural waters the PO_4 can be converted to the solid phase by formation of aggregates when the colloid mixes with the electrolytic seawater solution in the estuarine environment. In the estuarine environment it has been found that silts have a high capacity for adsorbing PO_4 and particle-bound PO_4 has also commonly been found to be associated with organic matter and phases of Fe and Al.

Provided that there are no significant amounts of naturally occurring phosphate minerals, such as apatite, in the estuarine environment, evidence for the presence

of P in the solid phase would provide some evidence of removal of dissolved inorganic PO_4 from the water column to the solid phase, (although traces of P may be present in some non-phosphate minerals). This study did not aim to investigate localised processes of P geochemistry, but instead was designed to provide a more general picture of sediment composition along the salinity gradient of the upper basin of Loch Linnhe. To achieve this, sediment cores were collected from stations LL0 (the saline end-member), LL4, LL14, LL19, LL20 and the River Lochy (freshwater end-member), (details of the sampling strategy can be found in **CHAPTER 4**, section **4.1.4** and samples from the cores were analysed by x-ray diffraction (XRD) and x-ray fluorescence (XRF). This was carried out at the Post-Graduate Research Institute of Sedimentology, Reading University, with the help of Dr. Andrew Parker and Dr. Graham Paterson. Details of these techniques and the sample preparation involved can be found in **CHAPTER 4**, section **4.3**. Results are listed in **APPENDIX 6.6**.

Qualitatively the results from the XRD analyses showed the presence of the following minerals:

(i) Quartz (SiO_2): A coarse-grained mineral (> 2 μm diameter size fraction; Chester, 1990) obtained from the weathering of the bedrock, granite;

(ii) Feldspar (Ca^{2+}) or (K^{+}): This has the general formula $(M)Al(Al,Si)Si_2O_8(K^{+})$ where M is a cation (Fleischer, 1975) and is also a coarse-grained mineral in the same size fraction as quartz. It is derived from the weathering of the bedrock granite;

(iii) Chlorite: This has the general formula $M_{5\text{-}6}(Al,Si)_4O_{10}(OH)_8$ where M is one of many possible cations which include Fe^{2+}, Fe^{3+} or Al^{3+} (Fleischer, 1975). It is a clay mineral and as such is in the size fraction < 2 μm diameter; Chester, 1990). This is not derived from the weathering of granite and may have its source from the peat in the soil (G. Paterson, 1993, pers.comms.);

(iv) Mica: This has the general formula $(M)(M)_{2-3}(Al,Si)_4O_{10}(OH,F)_2$ where M is a cation and can include Fe^{3+} and Al^{3+} (Fleischer, 1975). It is also a clay mineral and as such is in the same size fraction as chlorite (Chester, 1990). It is derived from the weathering of granite;

(v) Amphibole: This has the general formula $M_2M_5(Si,Al)_8O_{22}(OH,F)_2$ where M can be one of a number of possible cations including Fe^{2+}, Fe^{3+} and Al^{3+} (Fleischer, 1975). It is a coarse-grained mineral and is thus in the same size-fraction as quartz; It is derived from the weathering of basalt (G. Paterson, 1993, pers.comms.)

(vi) Haematite: This has the general formula Fe_2O_3 and is likely to have its source in the biotite (Fe bearing mica) which is present in granite.

It should be noted that amphibole and haematite are only present in trace amounts (< 1%) in all samples, except for the sediment sample collected at station LL4 where the haematite is present as 3.5 % of the weight fraction. There are no phosphate minerals in detectable amounts.

FIGURE 6.31 (a) shows the composition of the sediments in terms of the coarser grained (quartz and feldspar) and finer-grained (clays: chlorite; mica) minerals and haematite as a function of distance from the saline end-member, LL0. The sediment at station LL14, the deepest and most central station in the upper basin, contains the highest proportion of fine-grained material i.e. clay minerals. This is most likely to be a reflection of the current regime in the upper basin with the fluvially derived clays being swept away from the head of the loch in a seawards direction, leaving the coarser grained material behind. Also any clays present in the vicinity of the sill will be swept towards the head of the loch by virtue of the density currents that are set up in the sill region. At station LL14 the currents are likely to have diminished from both directions (Gade and Edwards, 1980) allowing for the settling of the clays onto the sediment .

FIGURE 6.31

Relationship of (a) Sediment Size (Fine or Coarse Grained) and (b) Sediment content of Phosphorus, Iron and Aluminium Oxides with Distance in the Loch.

(a)

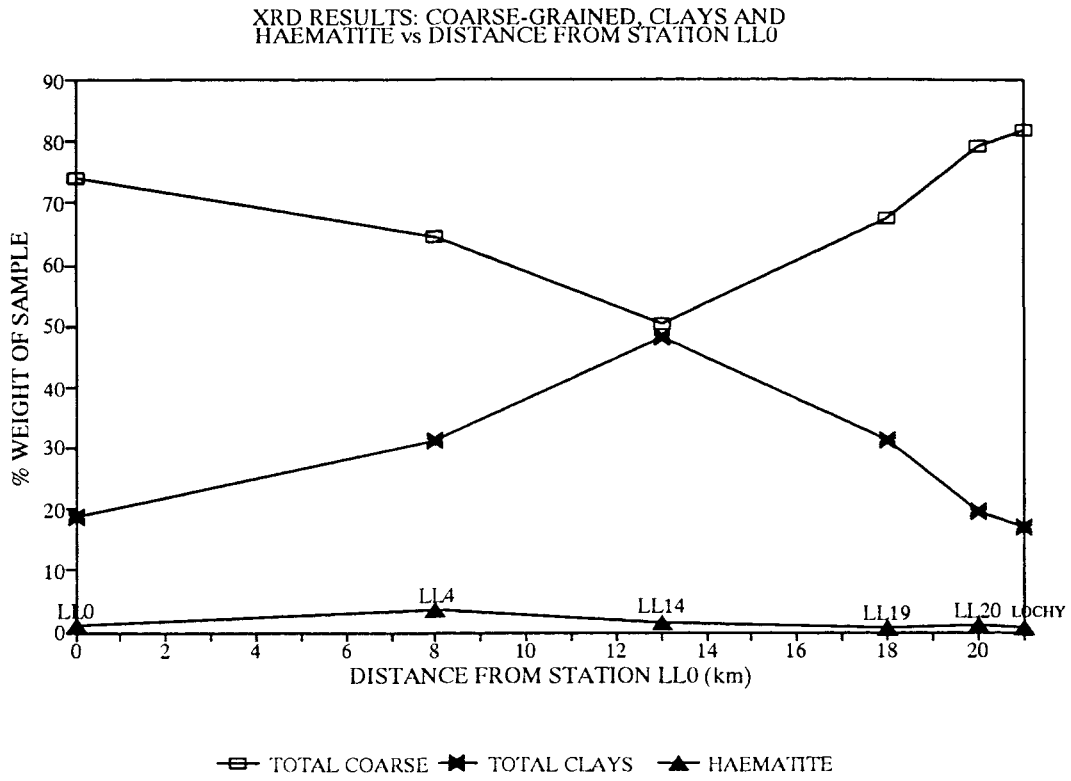

(b)

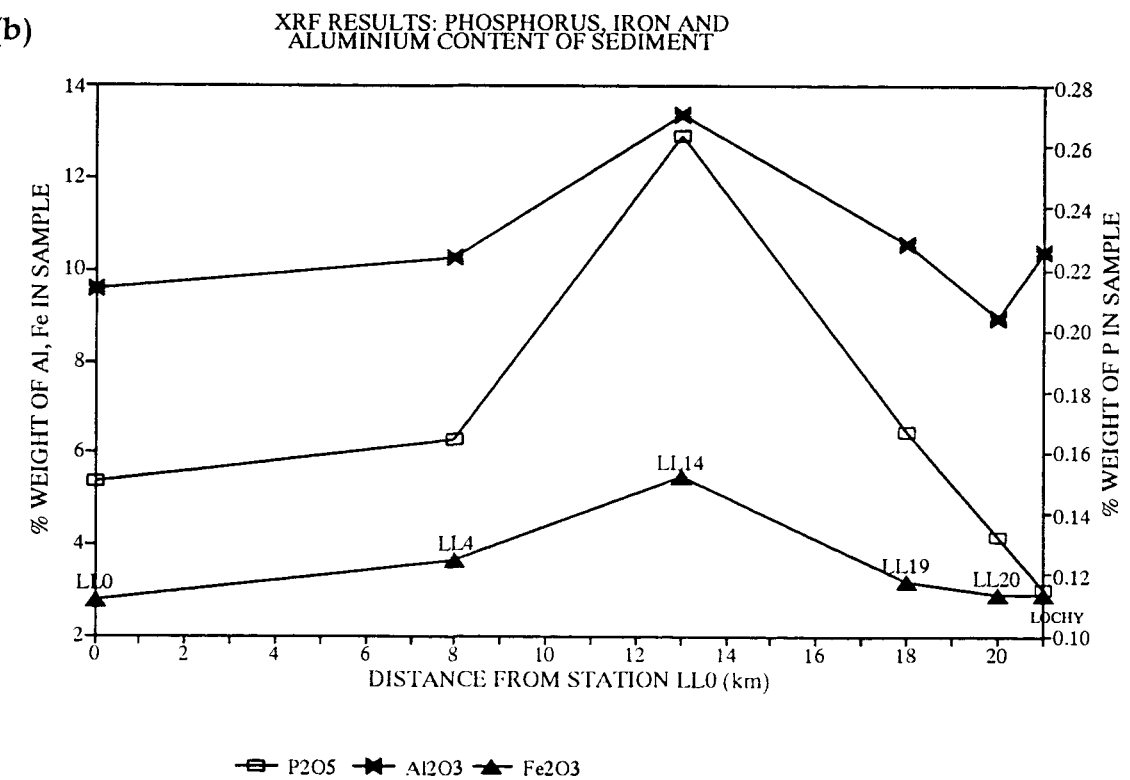

The main points to be made from the results of the XRD analysis are that (a) there are no detectable amounts of phosphate minerals present in the sediments at the stations studied and (b) that the finer grained clay minerals generated mainly from the weathering of the bedrock, granite, are in the highest proportion in the sediment collected from the central station LL14.

The next part of the study involved the analysis of the elemental composition of the sediment samples with the aim to see whether there was any P present in any of the sediments which would then be indicative of removal of this element, probably in the form of dissolved inorganic PO_4, from the dissolved phase. This was carried out using XRF techniques which have been described in **CHAPTER 4**, section **4.3**.

Only the results of the P_2O_5, Fe_2O_3 and Al_2O_3 content in the samples will be considered in this study, although all the results obtained are available on request from the author.

FIGURE 6.31 (b) shows the P, Al and Fe contents, expressed in terms of the oxides; P_2O_5, Fe_2O_3 and Al_2O_3, in the sediment samples along the salinity gradient. From this it can be seen that the sediment sample containing the highest proportion of all three elements; P, Fe and Al is that collected at station LL14 which, as was shown from the XRD results also contained the highest proportion of the finer-grained clay minerals (see **FIGURE 6.32 (b)**). The majority of the Al measured in the sediment samples will be crustally derived and therefore changes in the Fe:Al ratio along the salinity gradient will may be used as an indicator of the presence of Fe, in excess of that in the crustally derived minerals. The data in **FIGURE 6.32** show that the Fe content of the sediments is increased to that of Al at station LL14. The P:Al ratio also shows increased levels of P relative to Al at station LL14. The enrichment in Fe and P in the sediments at station LL14, would suggest that they have been removed from the dissolved phase onto SPM at some point during the transport and deposition of the sediment within the system. While a variety of mechanisms might contribute to this enrichment of Fe and P in these sediments,

FIGURE 6.32

Relationship of Iron:Aluminium and Phosphorus:Aluminium Ratios in the Sediment, with Distance in the Loch.

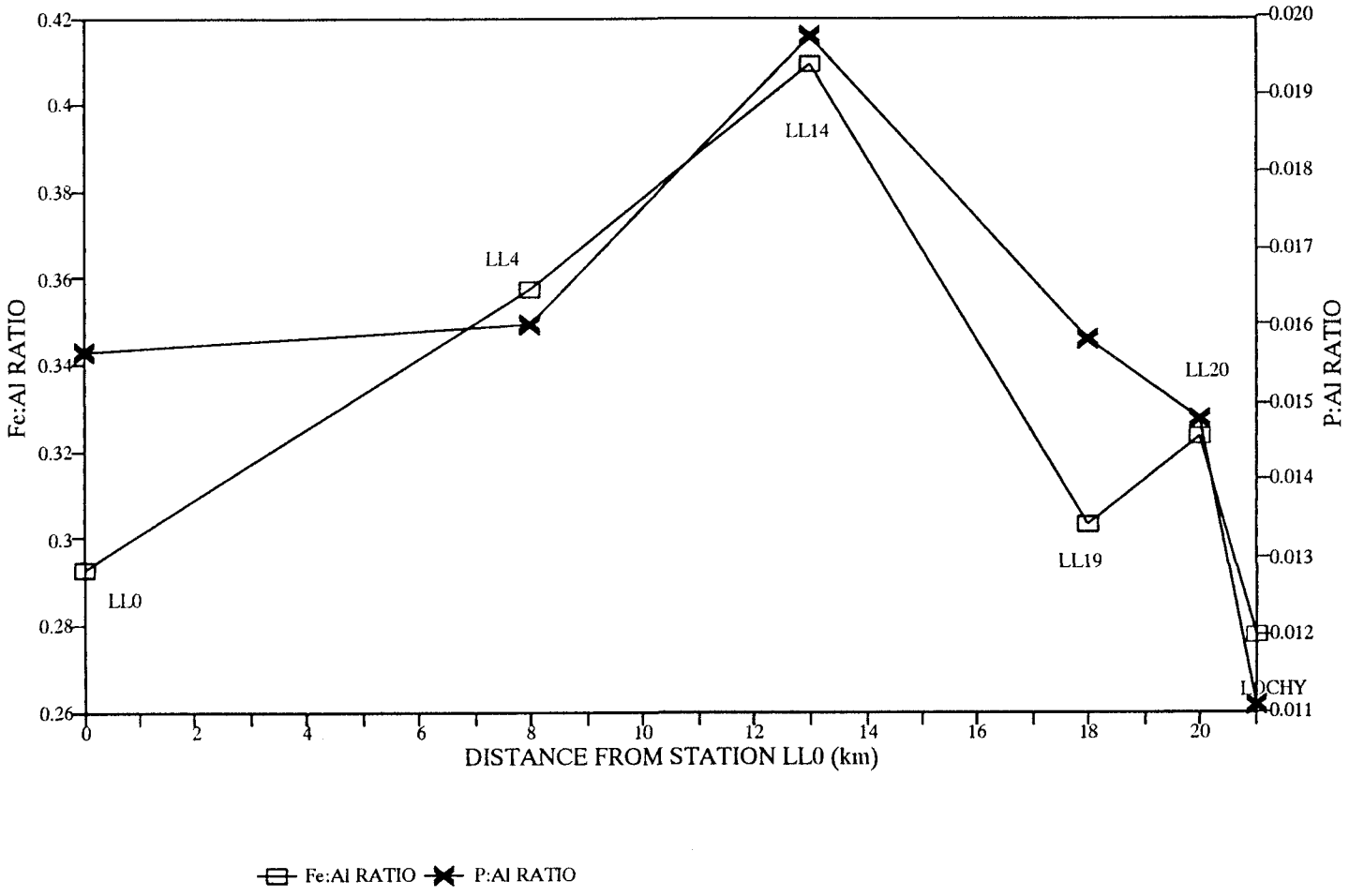

the known tendency of iron to form oxy-hydroxide coatings on mineral particles and that of phosphorus to become enriched in iron oxy-hydroxide phases, suggest that the simplest explanation is that these processes are responsible for the enrichment observed in the fine-grained sediments at station LL14, which present a larger surface area for the formation of coatings. This example of high particle-reactivity of PO_4 and thus association with the solid phase, provides evidence for the non-conservative behaviour of PO_4 in the estuarine environment and supports the suggestion that the enhanced decrease of PO_4 concentrations observed in the bottom-waters during the 1992 field-season (days 64 to 79) was due to the rapid scavenging of the PO_4 released from the porewaters. Such geochemical reactivity results will contribute to the scatter of data in a nutrient/salinity relationship such as is observed at station LL14.

It should be noted that although the levels of phosphorus measured in the sediment as P_2O_5 are very low, the increase in the levels from 0.11 % to 0.26 % between the River Lochy sample and the LL14 sample is a significant increase in terms of the precision of the measurement. It should also be noted, however, that because the phosphorus levels are so low there is the possibility that, if their source were from the mineral apatite, the XRD method would not be sensitive enough to measure these low levels of apatite. However, there is no obvious reason why apatite, if present in significant amounts in the sediments, should be more abundant in those at station LL14 than elsewhere in the loch and so it holds that the increase in observed P in the sediments at station LL14 can be explained by the mechanisms described above. The presence of phosphate associated with iron oxy-hydroxide phases represents an important potential source for sediment porewaters and the overlying water column if conditions become reducing either because the sediment becomes permanently anoxic or because rapid deposition of phytoplankton bloom material creates a reducing environment at the benthic surface. Thus the results from this study would suggest that the potential supply of PO_4 to the overlying water column is higher at station LL14 than at the other stations sampled.

In summary, the results from the XRD and XRF analyses of the sediment samples have shown (a) that the highest percentage of clay minerals to be found in the sediment is at the most central, deepest station, LL14, which is most likely to be a reflection of the current regimes at either ends of the basin and (b) that the levels of Fe, in excess of those due to crustally derived minerals, are also found to increase at station LL14 as do appear the levels of P found in the sediment. This is most likely to be due to the removal of iron and phosphorus from the dissolved phase onto the surface of the fine-grained particles during the transport of this SPM through the estuarine system, and the subsequent deposition of these sediments at station LL14 as the current slackens off. Such geochemical reactivity of PO_4 will give rise to a potential source of PO_4 for sediment porewaters and add to the scatter of data observed in a nutrient/salinity relationship in an estuarine system, for example at a station such as LL14.

6.2.2 Conclusions from the nutrient results

The main source of NO_3 and PO_4 are from the saline end-member in Loch Linnhe and that of SiO_4 from the freshwater end.

If all the available nutrient data is considered (i.e. that from station LL0, LL14 and the rivers), then the variations in the concentrations of the nutrients have a very weak dependency on salinity for the 1992 field-season taken as a whole with only 1.5 %, 10 % and 12 % of the variations in NO_3, PO_4 and SiO_4 concentrations respectively being attributable to changes in salinity. This low dependency is attributable to the occurrence of apparent and real non-conservative processes in the system, causing deviations from the steady-state distribution which would result from the simple mixing of the two end-members. The apparent non-conservative processes have been shown to include end-member concentrations that vary temporally such that the oscillations in their concentrations occur within the flushing time of the system. The variation in the saline end-member in Loch Linnhe can be attributed to (i) upwelling of increased nutrient concentrations seaward of the sill, (ii) changing concentrations in adjacent coastal waters, (iii)

depletion of nutrients through biological activity and (iv) adsorption/desorption processes of nutrients with SPM in the sill region plus any effects of the temporally varying freshwater nutrient concentrations. The NO_3 and PO_4 freshwater end-member concentrations have been shown to vary temporally and this variation has been shown to have a higher correlation with long-term phenomena such as the annual regime, which includes seasonal effects and patterns of the nutrient concentrations, than it does with riverine flow. Nitrate shows a stronger seasonal pattern than PO_4 due to the high geochemical reactivity of the latter.

Evidence has been presented for the occurrence of real non-conservative processes in the system during the 1992 field-season and this includes: (i) biological activity and the consequent depletion of nutrients, due to the formation of a phytoplankton bloom with maximum chlorophyll a concentrations being observed in the basin on day 125; (ii) regeneration of nutrients in the isolated bottom-waters, particularly between days 59 and 64 and days 79 and 86, (iii) the high particle-reactivity of dissolved inorganic PO_4 as it is removed from the dissolved phase to the solid phase through its association with clay minerals.

6.3 Overall Summary and Discussion

For the 1992 field-season the upper basin of Loch Linnhe has been shown to be vertically stratified according to its density structure and horizontally uniform also, in terms of its density and salinity properties, for the majority of the field-season. Within the time-span of the field-season a deep-water renewal was observed throughout the basin causing vertical mixing and an observed increase in the densities at all depths, between days 86 to 99. Factors favouring the renewal at this time were a change in wind direction around day 90 followed by high spring tides on day 95 and , to a lesser extent the presence of a temperature inversion through the water column thus destabilising the density structure of the water column slightly. The change in the wind direction allowed for any freshwater being retained in the system by the previous south-westerly wind, to escape, causing upwelling of high salinity, high density water seaward of the sill, as the

pycnocline was displaced up through a height of ~ 20 m at LL0. This high density water would have then entered the basin causing the observed deep-water renewal event.

The period between days 86 and 99 is relatively long compared to the weekly intervals for the majority of the sampling in 1992, and so from the observations it is hard to narrow down a more accurate date for the deep-water renewal. However, it is suggested that it occurs sometime between days 90 and 95 when the wind direction has changed and the volume of water flowing into the basin on the flood tides is at its maximum in the two week sampling period considered.

The nutrient results section has shown that the lack of correlation of nutrient concentrations with salinity in the basin is due to the presence of (a) apparently non-conservative processes: oscillations in the concentrations of the end-members occurring within the flushing-time of the system and (b) the occurrence of real non-conservative processes: biological activity in the form of a phytoplankton bloom; regeneration of nutrients from the sediment to the isolated bottom-waters; the geochemical reactivity of dissolved inorganic PO_4 with clay minerals. Evidence for the occurrence of all of these processes during the 1992 field-season has been provided.

Considering the hydrographic and nutrient results together, it is suggested that there is a sequence of events that occurs during the 1992 field-season and that these events occur in the following order:

1. A southwesterly wind blows persistently up the loch until day 90, thus retaining freshwater in the system, which is conspicuous by the increase in the residence time of the freshwater in the basin around this time.

2. The wind direction changes and the freshwater that was retained by the southwesterly wind is allowed to escape.

3. To retain a steady-state situation, an upwelling event occurs outside the basin at station LL0, evident from the observed upward displacement of the pycnocline through a height of ~ 20 m.

4. The upwelled, high salinity, high density water enters the basin and causes renewal of the bottom-waters throughout the basin some time between days 86 - 99. The change in wind direction around day 90 and the increased volumes of inflowing water around day 95 would suggest that the renewal occurred at some point between these two dates.

5. The upwelling of saline water at station LL0 results in the presence of increased nutrient concentrations seaward of the sill which is most likely to be due to the advection of high salinity, high nutrient (probably regenerated) water from adjacent coastal regions.

6. These high nutrient levels thus enter the basin around the time of the renewal so that the levels of nutrients present in the euphotic zone are potentially increased and also the renewal event itself will displace any increased nutrient concentrations resident in the bottom-waters, up towards the euphotic zone.

7. This, in combination with increased daylight hours given springtime, and an increased buoyancy input to the surface layers after the renewal event, will favour the formation of a phytoplankton bloom as observed in the loch a week after the renewal event took place (days 105 to 125).

If this sequence of events were to occur every year then, provided that the timing of renewal events could be predicted accurately, an estimation of the timing of the bloom could be made. Such information might be useful to the fish-farmer for example, where variable dissolved nutrient concentrations might give rise to the formation of toxic algal blooms, detrimental to the health fish and/or human-beings. Also if the aforementioned sequence of events is correct, then to be able to isolate and quantify the processes which affect the nutrient concentrations and

distributions in the loch (apparent and biogeochemical processes), that are evident as occurring in the 1992 field-season, would be most beneficial particularly for the correct interpretation of mixing diagrams.

The possibility of obtaining such hydrographic and chemical aims through numerical methods is investigated in the next chapter.

CHAPTER 7 LOCH LINNHE: A MODEL OF THE STRATIFICATION, MIXING AND NUTRIENT DISTRIBUTIONS

In an attempt to achieve the aims set out at the end of Chapter 6, a numerical model has been incorporated into this study.

This chapter briefly sets the application of the present model in the context of other work in this area and describes its main aims. It then presents a detailed description of the model and the treatment of the field data used to drive the model and, finally the results obtained from its application. The physical model is considered first, followed by the model as adapted for nutrients:

7.1 Past Work and Aims of the Model

Tett and Edwards (1984) wrote a review aimed at encouraging collaboration between oceanographic disciplines, with respect to numerical modelling. Since this time models have been developed with this aim in mind: Tett *et al.*, 1986; Tett, 1987; Sharples and Tett, 1992. Sharples and Tett (1992) coupled two existing physical and biological numerical models with the aim to investigate the interaction between the physical processes of stratification and vertical mixing, and the closely dependent microbiological processes of phytoplankton growth and respiration. The framework for the biological part of the numerical model followed Tett *et al.* (1986) and Tett (1987) and the physical component incorporated a turbulent closure scheme. Biological observations were "satisfactorily" reproduced by the model but the model did not attempt to deal with any biogeochemical processes in the water column.

Several successful numerical and mathematical models exist for estuarine and shelf-sea areas (Simpson and Bowers, 1981; Simpson and Sharples, 1991; Sharples *et al.*, 1994) and specifically for Scottish sea-loch systems (Falconer, 1989; Gillibrand, 1993; Simpson and Rippeth, 1993) but these are designed to simulate only the physical processes within the systems. Other numerical models which

have attempted to integrate other processes, to the point of modelling whole marine ecosystems, appear to be extremely complex and to contain so many parameters that the models would probably be difficult to test given a particular data-set, for example, Aksnes and Lie (1990), Ross *et al.*[1] (1993) and Ross *et al.*[2] (in press). Also the latter 2 papers do not consider the physical regime of the system other than by simple diffusive processes, which is not realistic for such dynamic coastal systems.

The model developed during this study was a simple 1-dimensional (1-D) box model. The aim was to develop a model that could reproduce the salinity field (and hence the density field - see results in **CHAPTER 5**, section **5.1.1** and **CHAPTER 6**, section **6.1.1**) in Loch Linnhe (i.e. the upper basin), given varying saline and freshwater boundary conditions with simultaneously varying meteorological conditions, over given periods of time. The time-periods in this case were the 1992 field season (see **CHAPTER 4**) and a 1990 field season (a 4 month field season carried out in Loch Linnhe by DML) which was used for test data. Once the salinity field could be accurately reproduced, including the simulation of deep-water renewal events, the model could then be used to predict the nutrient distributions in the loch, assuming conservative behaviour. Using this information deductions could then be made about the degrees of real and apparent non-conservative behaviour within the observed data.

Similar approaches have been used by workers in the past. Edwards and Grantham (1986) studied the inorganic nutrient regeneration in the bottom-water of Loch Etive and used salinity as conservative tracer. They used it to calculate salt diffusion rates between the stagnant bottom water and the overlying estuarine circulation from which the diffusive changes in the non-conservative properties could be estimated, thus allowing for the measurement of nutrient regeneration rates from the sediment. Loder and Reichard (1981), Officer and Lynch (1981), Kaul and Froelich (1984) and Cifuentes *et al.* (1990) also used the idea of effectively subtracting conservative behaviour away from observed behaviour to give an estimate of the effect of a temporally varying freshwater end-member concentration

in an estuarine system. However, none of these used numerical modelling in their analyses; they used analytic models. More recently, models which aim to predict nutrient concentrations in estuarine environments have been documented (Lebo and Sharp, 1992; Pejrup *et al.*; 1993), but again they are analytic models using equations such as that of salt-conservation (Pejrup *et al.*, 1993) and advection-dispersion equations for salt/nutrient transport (Lebo and Sharp, 1992). They are not numerical, iterative models such as the one developed in this study. This is probably because they deal with shallower systems (<10m) for which solutions at discrete depths are not required.

7.2 Description of the Model

The model used here is an adaptation and continuation of the model derived by Simpson and Rippeth (1993) for the Clyde Sea area. Work on the model was done in collaboration with Dr. T.P. Rippeth and Professor J.H. Simpson of the University College North Wales (UCNW), Bangor. The code was written in FORTRAN 77 and the model was compiled and run on the Decstation at DML using a UNIX operating system.

The model is described as a filling box model which uses a 1-D depth-resolving grid. It considers the interaction between basic stratifying and stirring processes and as such is driven by buoyancy inputs of freshwater and heat (although the heating component to buoyancy can be considered negligible for Loch Linnhe - see results **CHAPTER 5**, section **5.1.1** and **section 7.2.1.6**) and by mechanical stirring processes involving wind-stress, tidal forcing and convective motion.

The model is based on a simplifying assumption that the structure in the interior of Loch Linnhe can be treated as being horizontally uniform which is justified by many of the observations (see **FIGURES 5.1** and **5.2**; **FIGURES 6.1** and **6.2**). It produces results in the form of 1 m interval profiles of the water column, so that salinity, density and nutrient profiles can be obtained over time at a fixed position which can be taken to apply to any point in the loch (based on the assumption of

horizontal invariance made above). These results are tested against the observations collected at station LL14. This station was chosen because being the most central station in the loch, it was considered to provide the best average representation of water column properties.

The following sections describe the basic model (Simpson and Rippeth, 1993) and how it was adapted to reproduce the physical conditions within Loch Linnhe. Further adaptations were required to study the nutrient regime and these are described in section **7.6**.

7.2.1 The basic model: The physics

The data files required to run the model are:

1. **Check92.run**: Contains the boundary conditions for the model and the meteorological data;
2. **Check92.str**: Contains the initial temperature (T), salinity (S) and density profile at station LL14;
3. **Linnhe.run**: Contains constants such as sill depth, maximum depth of the loch, time-step, depth interval and surface area;
4. **Linnhe.area**: Contains depth-specific, cross-sectional area data.

A description of these data files, and how they were compiled, including the treatment of the data, is detailed in section **7.3.1**. The data themselves are listed in **APPENDIX 7.1**.

Basically, the model starts with an initial profile of the T, S and density of the water column (depth interval of 1 m), from station LL14, measured on the first day of the field season (file **Check92.str**). Boundary conditions; the daily saline input entering over the sill plus the daily freshwater volumes entering the loch mainly via the Rivers Lochy and Nevis are then read in (from **Check92.run**) along with treated wind, dew point temperature, solar irradiance and freshwater temperature

data (see section **7.3.1**). Using a specified time-step, depth step and sill depth (from **Linnhe.run**), plus cross-sectional area variation data (from **Linnhe.area**) the model then enters the main loop of the program, where the commands listed below are carried out on the initial profile to result in a new profile per time-step. These commands are shown schematically in **FIGURE 7.1**.

In each time-step:

1. Calculation of the volume inflow and outflow to the loch;
2. Determination of the depth of neutral buoyancy for the inflowing water and the subsequent mixing at that level;
3. Upward displacement of existing water above the level of neutral buoyancy to sill depth;
4. Simulation of tidal throttling above sill level;
5. Addition of freshwater to the surface layer;
6. Addition of heat;
7. Addition of wind-mixing;
8. Addition of tidal mixing.

FIGURE 7.1

ORDER OF PROCESSES OPERATING IN THE FILLING BOX MODEL

Adapted from Simpson and Rippeth, 1993

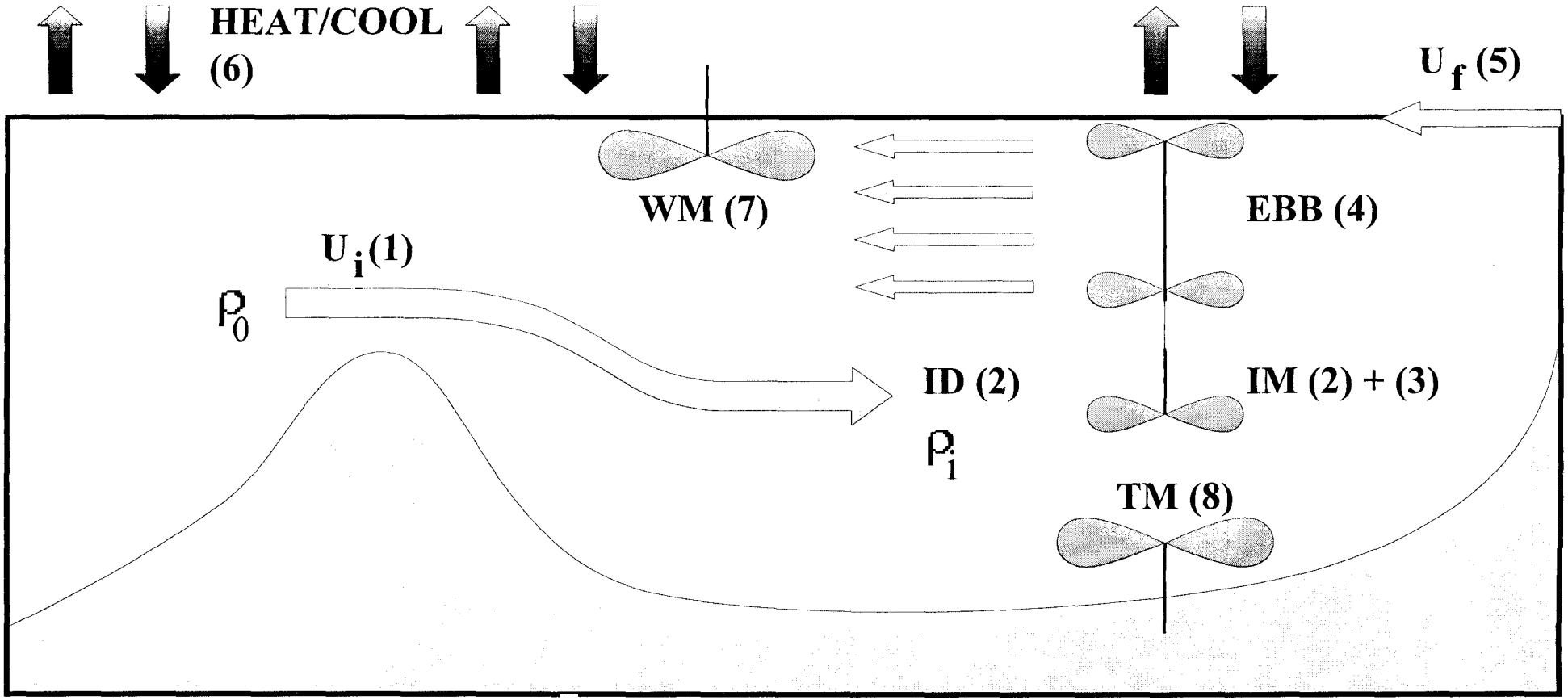

U_i = VOLUME OF SALINE WATER ENTERING; ρ_0 = DENSITY OF SALINE INFLOW; ρ_1 = DENSITY OF WATER AT INFLOW DEPTH; ID = INFLOW DEPTH; IM = INFLOW MIXING (TO SILL-DEPTH) +UPWARD DISPLACEMENT AND MIXING OF RESIDENT WATER; EBB = MIXING OF WATER DISPLACED UPWARDS FROM SILL-DEPTH TO SURFACE + EBBING OUT OF WATER; U_f = VOLUME OF FRESHWATER ENTERING THE LOCH; WM = WIND MIXING; TM = TIDAL MIXING

Each of these commands may now be considered in turn:

7.2.1.1 Calculation of the volume inflow and outflow

This is based on the following equation for conservation of volume and thus assumes no longterm rise or fall in sea-level. Also changes within a tidal cycle are not simulated:

$$U_o = U_i + U_f \qquad (1)$$

where: U_o = outflow volume i.e. volume of water leaving the loch (m^3);

U_i = inflow volume i.e. volume of water entering the loch over the sill (m^3);

U_f = volume of freshwater inflow from the Rivers Lochy and Nevis plus remaining catchment area (m^3).

U_o and U_i are unknown whilst U_f is an observed daily value.

The calculation of U_i for Loch Linnhe required a different approach to that taken for the Clyde Sea area. In the version of the model for the Clyde Sea area, U_i was calculated from U_f and U_o, which was calculated as the product of a Hansen-Rattray coefficient and the density difference between the incoming saline water and the surface water of the basin, $(\rho_o - \rho_s)$. U_o could be calculated this way because for the Clyde Sea area the exchange of water in and out of the basin could be assumed to be driven mainly by baroclinic flow allowed by a relatively deep sill compared to Loch Linnhe (45 m c.f. 15 m). The definition of the Hansen-Rattray coefficient (HR) is the ratio of the longitudinal diffusive or non-advective tidal exchange flux to the total longitudinal flux of an index quantity usually taken as salt (Officer and Kester, 1991). Therefore if HR $\rightarrow$ 1 then non-advective tidal processes (i.e. barotropic flow giving rise to vertical diffusion via turbulence - see **CHAPTER 1**, section **1.2.2.1**) are dominant and if HR $\rightarrow$ 0, gravitational circulation

processes (i.e. baroclinic flow - see **CHAPTER 1**, section **1.2.1.2**) are dominant. For the Clyde Sea area HR was taken as 0.2 to simulate the greater baroclinic component. In Loch Linnhe however, the size of the baroclinic flow is hydraulically controlled due to the presence of the shallow sill at the Corran Narrows and as a result the barotropic reverses the baroclinic flow; a phenomenon known as "tidal throttling", so that inflow is prevented on an ebb tide but augmented on the flood (see section **1.2.1.2**). Hence the model had to be adapted at this point to allow for this. Instead of using $HR.(\rho_o - \rho_s)$ to define U_o and allow for the determination of U_i, U_i is determined independently in the Linnhe model using a tidal equation of the form;

$$U_i = [Z_o + H.\cos(\omega.t + p)].dt \qquad \textbf{(2)}$$

where:

Z_o = a constant = the average daily flow of water entering the loch over a spring-neap tidal cycle ($m^3\ s^{-1}$);

H = the amplitude of the tidal flow curve ($m^3\ s^{-1}$);

ω = the angular velocity = $2\pi/T$, where T = the period of the spring-neap cycle and = 14.7653 days;

p = the phase of the tidal cycle;

dt = the time-step of the model = 108 secs (needed to convert flow to volume, m^3);

t = day number (Julian days).

Values for these parameters are:

Z_o = 2018 $m^3\ s^{-1}$;

H = 799.6 $m^3\ s^{-1}$;

ω = 0.4255 $days^{-1}$

p = 3.0069

dt = 108 secs

Calculations for the above parameters can be found in section **7.3.2.1.**

Z_o and H take into account the semi-diurnal component (M2) of the tide and ω and g take into account the spring-neap tidal cycle.

Having calculated U_i, U_o is then calculated from equation **(2)** with the known U_f value.

Having determined U_i and U_o, the next step is to inject U_i into the Linnhe basin at a depth of neutral buoyancy.

7.2.1.2 Determination of the depth of neutral buoyancy for the inflowing water and mixing at the inflow level

This part of the model uses a loop to compare the boundary condition density (ρ_0); the average daily density of the water coming in over the sill (see section **7.3.1.1**), with the density of the water already present at discrete depths in the water column, ($\rho_{(i)}$), (where (i) is the depth (metres) as an integer). It works through the loop until it finds a level where the two are equal within a particular range. This level is taken as the level of neutral buoyancy i.e. the inflow depth and the range is determined by averaging $\rho_{(i)}$ with the densities above and below it. By taking averages in this way, the accuracy of the level of the inflow depth is increased by a factor of 2.

Having determined the inflow depth, the water entering the loch; U_i must then mix with the resident water already at that level from the previous time-step. Mixing is simulated in the model by changing the T, S and density properties proportionally. The proportion of water at the inflow depth which is replaced by U_i, takes on the T, S and density properties of the replacing water in that proportion with the remainder of the water at that level retaining the properties from the previous time-step.

Having mixed the inflowing water at the inflow depth, the next step is to simulate the resultant upward displacement of resident water from that depth.

7.2.1.3 Upward displacement of existing water above the level of neutral buoyancy to sill depth

Seawater enters the basin over the sill, sinks to a depth appropriate to its density and displaces resident water upwards from that depth. This sequence of events renews water inside the basin either partially or completely (see **CHAPTER 1**, section **1.2.3**). The model simulates upward displacement via a loop: The water flowing in over the sill of volume U_i, sinks to the inflow depth and this same volume is then displaced into the layer above . From this layer the same volume is displaced up into the next layer and so on up to sill depth. The upward displacement of water is actually simulated via the mixing processes described in section **7.2.1.2** i.e. using the T, S and density properties in proportions corresponding to the volume of water being displaced upwards relative to the volume of the layer being displaced into.

So water has now been displaced up to sill level and the next part of the model then deals with the upward displacement of water from the sill level to the surface. As mentioned in section **7.2.1.1** and described in **CHAPTER 1**, section **1.2.1.2**, the tidal exchange across the sill in Loch Linnhe is dominated by the barotropic component because of the shallow sill. It is this type of cross-sill exchange that the next part of the model simulates.

7.2.1.4 Simulation of tidal throttling above sill level

The main difference between the Clyde model and the Linnhe model with respect to exchange of water across the sill is that, in the Clyde, because the sill is relatively deep compared to that in Linnhe (45 m c.f. 15 m), the system is effectively split into an upper estuarine surface system and a deeper basin system which underlies it. The consequence of this is that there is an outward moving surface layer (barotropic flow) which is compensated by a saline, inward-flowing baroclinic current beneath it. Such a circulation is described in section **1.2** and is simulated in the Clyde model through the calculation of U_i and use of a Hansen-

Rattray coefficient (see section **7.2.1.1**). This volume of water is displaced upwards from the inflow depth in the same way as that described in section **7.2.1.3**. and the loop is extended so that the same volume of water gets displaced upwards from the inflow depth right to the surface. The Clyde model then has a certain volume of water entering the loch and the same volume leaving the loch after mixing. Therefore the circulation is assumed to be steady-state (see **CHAPTER 1**, section **1.2.1.2**). In the Linnhe model however, the circulation has to include tidal throttling, so that instead of a continual exchange of water across the sill, exchange occurs via ebb pulses of low salinity water and flood pulses of higher salinity water. In this model the inflow is tidally driven (barotropic), simulated through the calculation of U_i (see section **7.2.1.1**). Once all this water has mixed with the resident water present in the basin, as far as the sill, it must then be allowed to escape through ebb conditions. Again a loop is used but the volume of water displaced upwards from the sill depth to the surface is no longer equal to the volume of water coming in on the flood tide but, instead is equal to a fraction of U_i, the denominator being the sill depth. This fraction is mixed with the resident water present in the layer into which it is being pushed and the remaining fraction is assumed to move outwards across the sill, under ebb conditions. As the fraction of U_i gets pushed progressively upwards through the layers to the surface, the fraction decreases uniformly so that the same fraction of U_i is being lost through ebb conditions for each layer. Such outward ebbing from the sill depth to the surface, together with the barotropically driven inflow, effectively simulates tidal throttling.

The next step of the model is the addition of freshwater to the surface layer:

7.2.1.5 Addition of freshwater to the surface layer

The freshwater inflow is mixed with layer 1 in the model. This occurs in the same way as described in section **7.2.1.2** via proportions of freshwater properties relative to the volume of the surface layer. Effectively the salinity and temperature of the top layer are diluted through mixing with the freshwater with the freshwater

salinity taken as 0 and the freshwater temperature being that based on observed values. This freshwater is then mixed vertically downwards via the subroutine **windmix** which simulates the effects of wind-mixing.

7.2.1.6 Addition of heat

This is carried out via the subroutine **heating**, which considers the heat flux through the sea-surface (i.e. the top 1 m layer of the model). The flux of heat through the sea-bottom is small and can therefore be neglected (Bowden, 1948), as can the heat flux through the sides of the water column (Simpson and Bowers, 1984). The heat flux, Q, through the sea-surface is approximated according to Edinger *et al.* (1968) and Brady *et al.* (1969);

$$Q = Q_s + k.(T_d - T_s) \qquad \textbf{(3)}$$

where, Q_s = the solar flux at sea-level (short-wave radiation) obtained from the observed irradiance data (mW hours cm^{-2});

k = a thermal exchange coefficient (Wm^{-2} $°C^{-1}$);

T_d = dew-point temperature of the atmosphere, calculated from the wet and dry-bulb temperatures (° C);

T_s = sea-surface temperature (°C).

Since T_s is normally greater than T_d, the second term on the right hand side of equation **(3)** represents a heat loss rate which increases with rising surface temperature. The value of k is not constant and depends on wind speed (w in ms^{-1}), T_s and T_d. The value of k is determined using the following equations from Edinger *et al.*, (1974):

$$k = 4.5 + 0.05.T_s + (\beta + 0.47).f(w) \qquad \textbf{(4)}$$

where: $\beta = 0.35 + 0.0015.T_m + 0.0012.T_m^2$;

$T_m = 0.5.(T_s + T_d)$

and $f(w) = 9.2 + 0.46.w^2$ (Brady *et al.*, 1969)

The first step in the subroutine is to work out the value of $k.(T_d - T_s)$ from equation **(3)** using observed values of w, T_d and T_s. It then divides this by the heat capacity of the layer of water and adds the resultant value on to the temperature of the water in layer 1 (the surface layer). It goes on to allow for the effect of irradiation on the heat flux by distributing the observed irradiance (Q_s) so that 55% is retained in the first layer and the remaining 45% is distributed exponentially with depth. This distribution is typical of the absorption of solar radiation in coastal waters (Ivanoff, 1977).

However, it has been found that the **heating** subroutine is not suitable for the Loch Linnhe system because the only way that heat can be lost from the system back to the atmosphere is via layer 1, through the term, $k.(T_d - T_s)$. This is not a problem in the Clyde version of the model (Simpson and Rippeth, 1993), because in this case the top layers of the model are mixed down with the underlying layers via wind-mixing. In Loch Linnhe however, the freshwater volume input is so large and the density stratification so strong in the surface layers that the top layers do not get mixed downwards very effectively with the wind-power available (see section **7.2.1.7**). Hence, the heat in the surface layers (which is greater than that below due to the exponential distribution of heat), effectively gets trapped at depths > 1 m. so, although the top 1 m temperatures predicted by the model look reasonable (~ 6 - 9 °C) the results at depths below it do not (~ 20 °C). Hence the results from the model are inaccurate in terms of temperature results. However, in terms of predicting the hydrographic status of the system, this is not a problem since for the same change in density affected by a 1 PSU salinity change, a 5 °C

temperature change is required in temperate waters (UNESCO, 1983). The observed salinity changes over the field seasons concerned (1992 and 1990) are far higher than the temperature changes (16 PSU c.f. 2 °C). Hence the temperature of the water in Loch Linnhe will have a negligible effect on the density structure of the water column as compared to the effect of salinity, (as shown in the **CHAPTERS 5** and **6**) and can therefore, for the purposes of this model, be ignored. The **heating** subroutine is therefore omitted from the final version of the Linnhe model.

7.2.1.7 Addition of wind mixing

The wind has 3 main effects on the circulation in the loch:

1. It creates a well-mixed layer near the surface, the thickness of which varies in an annual cycle as well as in its daily response to fluctuations in wind-speed and buoyancy flux through the sea-surface (Stigebrandt, 1987);

2. It generates wind-driven currents which are of central importance in the generation of turbulence. However, such currents generally diminish with depth and reduce strongly below the pycnocline (where diffusion rates are reduced) (Gade and Edwards, 1980);

3. Wind-driven currents result in a change of the fjord water level e.g. wedging of freshwater against a land boundary, which can cause barotropic currents leading to baroclinic flow of saline water over the sill (Gade and Edwards, 1980).

However, in terms of the model, such freshwater wedging cannot be simulated because the model is 1-D and assumes horizontal uniformity, hence it only uses wind velocity data and does not take account of the wind direction. The surface layer is only mixed vertically downwards in the model so that there is no horizontal motion of water.

From the observations reported in **CHAPTER 6**, it was hypothesised that the south-westerly wind was causing the wedging of freshwater up the loch and that the change in wind direction, from south-west to north-east during the 1992 field season, resulted in an upwelling event i.e. the inflow of saline water from outside the loch, followed by a deep-water renewal event in the loch. Because the effect of wind direction cannot be simulated by the model such wedging of freshwater cannot be reproduced. This will be shown from the model results, however, not to be a problem in predicting the deep-water renewal because it is an increase of salinity in the inflow caused by a change in wind direction which causes the renewal. Therefore, provided that the saline boundary condition reflects this then the wind direction is not required. This conclusion is supported by Gade and Edwards (1980) who suggest that although renewal events are influenced by tides, wind and other meteorological disturbances in that these all cause barotropic flow which influences the inflow, it is the tides, not the wind, which usually predominate in their influence.

The model simulates vertical wind-mixing with the subroutine **windmix**. Within **windmix** is a loop which incorporates the following 2 main commands: (i) the calculation of the amount of power available from the wind, followed by, (ii) the calculation of the mixed layer depth i.e. the depth to which the wind is effective in mixing, from the surface downwards and mixing to this depth:

(i) Calculation of the energy available from the wind:

The energy available from the windstress is calculated from the power available (P_w), from the following equation, which is described in Simpson and Bowers (1984):

$$P_w = \delta.k_s.\rho_a.w^3 \qquad (5)$$

where; w = wind-speed (ms^{-1});

ρ_a = density of air (1.2 kg m^{-3});

δ = the efficiency of wind-mixing = 0.023 (Simpson and Bowers,1984)

k_s = the product of the drag coefficient (0.003) and the slippage factor = $6.4*10^{-5}$ (Simpson and Bowers, 1984).

The wind speed used is a daily value. By multiplying the calculated power by the time-step, the energy available is calculated.

(ii) Determination of the mixed-layer depth and mixing to this depth:

Having calculated the energy available from the wind, the loop then compares this with how much energy is required in each time-step to mix the water column from the surface downwards. This is achieved through consideration of the potential energy (P.E.) of the water column and the approach used is related to the **potential energy anomaly (φ)**, (Simpson and Bowers, 1981). It considers the amount of energy per unit volume required to change a stratified water column to its corresponding homogeneous state (Vaz *et al.*, 1989) so that:

$$\varphi = (P.E._{mixed} - P.E._{strat}) \qquad (6)$$

where; $P.E._{mixed}$ = the P.E. of the whole mixed water column;
$P.E._{strat}$ = the P.E. of the water column in the stratified case.

where the P.E. of a thin layer of water is defined as;

$$P.E. = \rho.A.g.z.dz \qquad (7)$$

where; ρ = the density of the water (kg m^{-3});
A = the surface area of the water column (m^2);
g = acceleration due to gravity (ms^{-2});
z = vertical coordinate (positive upwards) (m);

z = 0 at the surface,

z = -H at the bottom;

dz = the thickness of the layer (m).

If the water column is completely mixed then $\rho = \bar{\rho}$. The density of the water column is the same at all depths and is the average of all the densities of the different layers, $\rho(z)$. $\bar{\rho}$ may be determined from:

$$\bar{\rho} = 1/V.\int_{-H}^{0} \rho(z).A(z).dz \qquad \textbf{(8)}$$

where; V = the volume of the basin (m^3);

A(z) = the cross-sectional area of the layer at depth z (m^2);

dz = thickness of the layer at z;

z = -H = maximum depth of the water column (m);

z = 0 at the surface.

Through incorporation of the term A(z), the algorithm allows for the variation in the cross-sectional area with depth in the loch and the effect this has on the average density, ρ. To allow for the effect of this variation on the P.E. of the water column, the P.E. per unit area is calculated as the integral of **(7)**:

$$P.E._{mixed} = 1/A_0.\int_{-H}^{0} \bar{\rho}.A(z).z.g.dz \qquad \textbf{(9)}$$

where, A_0 = surface area of the basin (m^2);

If the water column is stratified according to its density then the value of ρ will be unique for each stratified layer so that the P.E. of the water column in the stratified case ($P.E._{strat}$) can be described as;

$$P.E._{strat} = 1/A_0.\int_{-H}^{0} \rho(z).A(z).z.g.dz \qquad \textbf{(10)}$$

$\therefore$ from equation **(6)** φ may be described by;

$$\varphi = [1/A_0.\int_{-H}^{0} \bar{\rho}.A(z).z.g.dz] - [1/A_0.\int_{-H}^{0} \rho(z).A(z).z.g.dz] \qquad \textbf{(11)}$$

By substituting equation **(8)** into equation **(11)**:

$$\varphi = g/A_0.\{[(1/V.\int_{-H}^{0} \rho(z).A(z).dz).\int_{-H}^{0} A(z).z.dz] - [\int_{-H}^{0} \rho(z).A(z).z.dz]\}$$

Discretising this expression for the model code with a depth interval D, results in the following expression:

$$\varphi = (g.D)/A_0.\{[(\Sigma\rho(i).A(i).\Sigma A(i).h(i))/\Sigma A(i)] - [\Sigma\rho(i).A(i).h(i)] \qquad \textbf{(12)}$$

where, h(i) = distance from the surface to the centre of mass of layer i.

The model works through the loop carrying out this type of summation. It starts at the surface, where i=1 and it calculates how much P.E. is associated with layer 1. It then does the same thing for layer 2, adding this P.E. onto that for layer 1. The amount of P.E. required to convert layers 1 and 2 from the stratified to the mixed state can then be calculated from equation **(12)**. This is compared with the amount of energy available, calculated from equation **(5)**. If the energy available exceeds that required for mixing, the loop begins again, calculating the amount of energy required to mix layers 1, 2 and 3 and this sequence continues until the amount of energy available for mixing is less than that required to mix to the depth (m+1). At this point the model exits the loop and the water column is mixed down to the depth (m). Mixing is simulated by straightforward averaging of the salinity and density properties of all the layers down to the layer (m), taking into account the variation in the cross-sectional area of the loch with depth. Any residual energy is carried over into the next time-step unless the water column is completely mixed, in which case no energy is carried over, simulating the conversion of P.E. to some other form of energy e.g. heat.

Having simulated the effect of the wind in terms of its ability to form a surface mixed layer via downward, vertical mixing, the next step in the model is the

simulation of mixing via tidal effects.

7.2.1.8 Addition of tidal mixing

The effects of tidal mixing in the deeper basin waters are simulated via the subroutine **tidemix**.

When considering the effect of the tide, the 3 main types of mixing are (i) that caused by barotropic flow (flood and ebb of the tide), (ii) that caused by baroclinic flow density-driven current) and (iii) that caused by turbulent vertical diffusion of the deeper basin system.

A detailed account of barotropic and baroclinic flow may be found in **CHAPTER 1**, section **1.2.1.2** which includes a description of tidal throttling, as observed in cross-sill exchange in Loch Linnhe. This effect of barotropic flow reversing baroclinic flow, thus preventing baroclinic flow on an ebb but augmenting it on the flood, has already been accounted for through the barotropic inflow and mixing calculations followed by the ebbing of all water above sill-depth (sections **7.2.1.1** - **7.2.1.3** and **7.2.1.4** respectively). Thus processes (i) and (ii) have been dealt with in the model and tidal mixing simulated to the level of neutral buoyancy. However, the effect of the tide on mixing in the deeper basin waters has not and it is this that the subroutine **tidemix** aims to simulate.

Tidemix works in exactly the same way as **windmix** in that it (i) calculates the energy available for mixing from the tide and (ii) it calculates the depth to which this mixing is effective and mixes to this depth:

(i) Calculation of the energy available for bottom-mixing from the tide:

In the Clyde-Sea version of the model (Simpson and Rippeth, 1993), the energy available for mixing is calculated from the sum of the power made available from (a) the barotropic forcing in the system, (b) the turbulent diffusion caused by the

breaking of internal waves and (c) mixing via convection of the inflowing water over the sill. As mentioned above, the effects of (a) have already been considered in the Linnhe model and are therefore not considered again in **tidemix**. Instead, **tidemix** considers the energy available for turbulent diffusion in the basin waters and that from convective motion.

The processes that can cause turbulent vertical diffusion in the deeper basin waters of Loch Linnhe are discussed in detail in **CHAPTER 1**, section **1.2.2.1** and include (a) boundary-mixing, (b) tidal jets and (c) the breaking of internal waves off the walls of the basin. As described in section **1.2.2.1** the process of internal wave breaking in the basin is the most efficient in terms of such mixing and presumably this is why this process was chosen to represent the mixing in the bottom-waters in the Clyde-Sea version of the model. In the Linnhe version of the model a different approach was taken to represent such effects. As mentioned at the start of section **1.2.2**, the only way in which the density of the deeper basin water may alter during periods of isolation is through diffusive processes such as (a), (b) and (c) above (Stigebrandt and Aure, 1989). Hence, if an amount of diffusion can be measured over a period of time within the isolation period, then this can be related to the amount of work required to bring about this level of diffusion, which can then be substituted as the power available for bottom-water mixing thus replacing the term for mixing caused by internal waves in the Clyde-Sea model. Such an approach could be adopted for the Linnhe model because an extensive data-set from the year 1990 was made available which included 30 CTD measurements made at the same station LL14. Using these data, the amount of vertical diffusion which had taken place in the bottom-waters during the 4 month isolation period for 1990 could be determined through the determination of a diffusion coefficient, k. From this a rate of work, w, could be determined and substituted into **tidemix** as the variable, **wmix**. Details of the theory and literature underlying this approach can be found in **CHAPTER 1**, section **1.2.2.3**. For the purposes of the Linnhe model, a computer program was written by Dr T. P. Rippeth (UCNW, Bangor) from which k, the Brunt-Väsiälä frequency (N^2) (see section **1.2.2.3**) and w could be determined given precision vertical profiles of density during the isolation

period. Actual results from this program can be found in section **7.3.2** but a description of the program itself will be given here:

Program for the calculation of the diffusion coefficient (k), the Brunt-Väsiälä frequency (N^2) and the amount of work required, (w):

The program was based on an approach known as the **Budget Method** (Gargett, 1984) already described in **CHAPTER 1**, section **1.2.2.3**. It requires that a density profile taken at the start of the specified time-period from a particular station (in this case LL14) be input along with one of an identical length and depth interval taken at the end of the time-period at the same station. The program then determines k for each layer using equation **(4)** in section **1.2.2.3**:

$$k_{z=u} = 1/(A_0.\delta\rho/\delta z)_{z=u}.\int_b^u (\delta\rho/\delta t).A(z).dz \quad \textbf{(13)}$$

(Stigebrandt and Aure, 1989).

for a layer at a discrete depth (z), working upwards from the bottom of the basin (b) to some upper level (u). So it effectively calculates the total diffusion per unit area for a specified period of time within the isolation period, for a layer of water at depth z=u.

Gargett (1984) suggests that the time-periods used should be in excess of a month in order to get representative values of k. However, during treatment of the data available it was found that during the 1990 isolation period (total number of 80 days), the density decreased smoothly in the bottom-waters over 4 separate time-periods, only one of which was longer than a month. The reason for this intermittent density decrease during the isolation period is that, although the inflowing water during this time was not of a high enough density and/or large enough volume to cause a complete deep-water renewal in the basin it is possible that it may have been sufficiently dense to cause smaller partial renewals with, perhaps smaller volumes of high density water penetrating the resident water in the basin down to depths of 100m. Such partial renewals are conspicuous by the

slight increase in density observed between time-periods. Details of the treatment of the 1990 data-set may be found in section **7.3.2.**

Having calculated a k value for each level over the 4 specified time-periods, the actual value of k used in the model was determined by averaging the values of k for each of the 4 time-periods up to the level of inflow and then averaging these 4 average values to give a resultant k value. The level of inflow is the level to which the saline inflow has penetrated after the specified time-period. It can be determined by consideration of equation **(12)** where k is determined for each layer through the calculation of the density change over time in that layer. In order for the program to calculate k it requires an initial CTD profile and a final CTD profile, as already mentioned and so not only is the k value for each layer output by the program but also the initial salinity (S1) and final salinity value (S2) (from the profiles). By studying S1 and S2, the level to which the inflow has occurred at the end of the time-period can be determined since at that level S2 > S1. The resultant value of k obtained from the program was 3.62 $cm^2\ s^{-1}$ for the isolation period (see section **7.3.2** for the calculations) which is within the range of other k values reported in the literature and given in **CHAPTER 1**, section **1.2.2.3.**

Having calculated k, the program then calculates N^2, which is the Brunt-Väsiälä frequency and is representative of the degree of buoyancy in the system. It has already been described by equation **(2)** in section **1.2.2.3**, so that for a layer of water at a discrete depth (z),

$$N^2 = g[-1/\rho(z).(\delta\rho/\delta z)] \qquad \text{(Svensson, 1980)} \qquad \textbf{(14)}$$

The program uses this equation to calculate a value of N^2 for each layer.

The next step of the program is to calculate the work (w) required to cause the degree of diffusion measured by k i.e. the work required to cause the diffusion that is observed from the bottom of the basin to the inflow level. To do this the model uses the following equation:

$$w = 1/V.\int \rho(z).k(z).N^2.A(z).dz \qquad \textbf{(15)}$$

(Stigebrandt and Aure, 1989)

N^2 is substituted from equation **(14)**, so that **(15)** simplifies, leaving w simply as a function of k and density change with depth, also allowing for the effects of the variation in cross-sectional area with depth in the basin. Values of w for each of the 4 time-periods are thus calculated by the model and an average value is used in the model (see section **7.3.2** for calculations). This resultant w has a value of $3*10^{-2}$ Wm^{-2} which is 2 orders of magnitude larger than that used by Simpson and Rippeth (1993) in the Clyde version of the model, where $w = 0.162*10^{-3}$ Wm^{-2} (Rippeth, pers. comms., 1993). This is indicative of a higher level of stratification in Loch Linnhe where the freshwater input is high, as compared to the Clyde i.e. the buoyancy forces in Linnhe are evidently greater than that in the Clyde, leading to higher values of N^2 and thus higher values of w, in accordance with equation **(12)**. The value of w is entered into **tidemix** as a variable called **wmix**.

Also considered as a source of energy for mixing at the top of the deeper basin-water, is the energy released by the convective motion of the inflowing water. This has been described in **CHAPTER 1**, section **1.2.2.2** and is calculated in the model via the subroutine **ifm**. **Ifm** simply calculates the potential energy available from the density current that forms from the inflowing water, as it falls from the sill-depth to the level of neutral buoyancy. The basic equation used is:

$$P.E. = \rho.vol.g.h \qquad \textbf{(16)}$$

where ρ = the density of the inflowing water relative to the density of the resident water present between the sill-depth and level of neutral buoyancy (kg m^{-3}); vol = volume of inflowing water in 1 time-step (see section **7.2.1.1**); g = acceleration due to gravity (m s^{-2}) and h = the height through which the inflowing water falls (m). Since less than 10 % of this P.E. is used for mixing (Gade and Edwards, 1980), a variable **ei** is introduced into the equation which represents the efficiency of such mixing and is set at 0.07 (7 %). The calculated P.E. is thus multiplied by **ei**. The

result is then added to **wmix** along with any residual energy from the previous time-step (as in **windmix**) and the sum is then taken as the energy available for bottom-mixing from the tide.

(ii) Determination of the bottom mixed-layer depth and mixing to this depth

This works in exactly the same way as in **windmix** using the P.E. anomaly (φ) approach (see section **7.2.1.7 (ii)**), so that the power available from the tide is compared with the power required to convert a stratified system to a mixed one. The main difference between **tidemix** and **windmix** is that in **tidemix** the summation described in equation **(12)** is carried out from the bed to layer i = m′, where (m′-1) is the first layer at which φ is greater than the power available and (m′.dz) is the bottom mixed-layer depth. Again any residual energy is carried over onto the next time-step. Mixing is simulated by averaging properties of the layers from the bottom of the basin to m′.

Having carried out the addition of tidal-mixing of the water column, the model then outputs the resultant salinity and density profiles at station LL14, since **tidemix** is the last command to be carried out within a time-step in the model. The model then begins another time-step.

7.3 Input Files, Treatment of Data and Determination of Model Variables

This section begins with consideration of the input data files required for the model: the data they hold, their origin and how they are treated before it is used in the model. This will be followed by details of the calculations used to determine the variables in the model including those used in the calculation of the inflow volume, U_i (see section **7.2.1.1**), and the variables k and w used in the subroutine **tidemix** (see section **7.2.1.8**). The data files themselves are listed in **APPENDIX 7.1**.

7.3.1 Input files and treatment of data

As stated in section **7.2.1**, the data files required to run the model are (1) **check92.run**, (2) **check92.str**, (3) **linnhe.run** and (4) **linnhe.area**. In this section each will be considered individually:

7.3.1.1 Check92.run:

This file contains the daily data for the boundary conditions (the saline and freshwater inputs to the loch), plus the meteorological data required for the model.

The saline boundary condition: Daily values of salinity and temperature averaged over the top 15 m (sill-depth) from the most seaward station, LL0, were used for the 1992 field-season. These were obtained from the results from the study of the 12 CTD profiles taken at weekly intervals during the 1992 period. Because these profiles were measured during a flood tide when possible, the averaged results could be used to simulate the saline inflow. Linear interpolation between these observed averages was carried out for both the salinity and temperature data in order to obtain daily values for the data-file.

The same method was used for the 1990 data-set using the 30 CTD profiles obtained from biweekly sampling over the 4 month period at station LL0.

The freshwater boundary condition: This includes daily values of the total riverine input (River Lochy plus River Nevis) to the loch. These volumes (in $m^3 s^{-1}$) were obtained courtesy of the Highland River Purification Board (HRPB). Having considered the riverine freshwater inputs, the freshwater input from rainfall had also to be considered. The total catchment area for the Rivers Lochy and Nevis had been accounted for in the river-flow data, but the total watershed of Loch Linnhe and Loch Eil is larger than this total catchment area and needed to be accounted for to allow for the extra freshwater input due to rainfall:

Total catchment area of Rivers Lochy and Nevis = 1252 + 76.8 = 1328.8 km^2 (see **CHAPTER 3**, section **3.2.2**) and the watershed of Linnhe and Eil = 1820 km^2 (Edwards and Sharples, 1986). Therefore, the volume of freshwater being input is increased proportionally:

$$1820/1328.8 = 1.37$$

and the freshwater riverine input is multiplied by 1.37 in the model to allow for the extra catchment area. Daily rainfall data is actually available from DML but it was decided that it would be more accurate to make the rainfall deficit in the model a function of the river flow in the Linnhe area, since the DML area and the Linnhe area differ in terms of topography and hence rainfall and meteorological patterns would be expected to differ between the 2 areas.

Temperatures of the river water were only available from the HRPB on a monthly time-scale. However, the temperatures of the rivers Lochy and Nevis had been measured on a weekly basis as part of the 1992 field season and so these data were added to the monthly data-set. Since the temperatures of the 2 rivers were always very similar (within 2 °C of each other), an average of the 2 was used and linear interpolation was carried out between the days for which there was data, to give daily values for the data file.

Check92.run also contains the meteorological data required for the model: (i) the solar irradiation data; (ii) the dew-point temperature of the atmosphere and (iii) the wind-speed:

(i) Daily values for the total solar irradiation (mW hours cm^{-2}) falling onto a horizontal surface were provided courtesy of DML. This data is logged at an hourly rate using an irradiation card affixed to the roof-top at DML at position 56° 28′ N, 05° 26′ W;

(ii) Daily dew-point temperatures were determined from daily measurements of

dry-bulb and the depression of the wet-bulb temperatures, using Hygrometric Tables (1970) available from the Meteorological Office. The dry and wet-bulb data is recorded on a daily basis at 0900 hours GMT at DML;

(iii) The wind-data used were average, daily wind velocities (m s^{-1}) provided by DML. The data were in the form of hourly anemograph data recorded on the roof-top at DML. As described in section **7.2.1.7**, the model does not take into account the direction of the wind, being a 1-D model and so only the wind velocity is required. This is not an ideal situation since it was shown in **CHAPTER 6** that the wind direction influences the amount of freshwater in the surface layers through the wedging and retention of freshwater in the loch. Hence there is a problem in simulating the salinity field of the surface layers of the loch (see section **7.4.1.2**) but, as described in section **7.2.1.7**, lack of wind direction is not a problem in terms of prediction of the deep-water renewal events, provided that the saline boundary condition is accurate. However, it was decided to treat the DML wind data before use in the model to try to account for the mountainous topography surrounding Loch Linnhe which is different to that surrounding DML. The theory behind this data treatment was that since the longitudinal axis of the loch lies in the NE/SW direction (see **FIGURE 3.2** in **CHAPTER 3**), i.e. at bearings of 045°/225° from true North, then any wind direction deviating from these angles will not be as effective in its speed and mixing as if it was blowing straight up or down the longitudinal axis of the loch. The way in which this could be represented was through modification of the corresponding wind velocities by resolving them to cos 45° so that:

$$\text{resolved wind velocity} = \text{measured wind velocity}.\cos(\theta - 45°)$$

where θ = the measured wind direction.

Thus if the wind direction is 45° or 225° then the measured wind velocity is multiplied by 1. The main problem with doing this is that the maximum velocity that the wind can ever have is equal to 1 x that recorded at DML hence no allowance is made for the possibility of enhancement of the wind velocity through

funnelling of the wind up the loch along the glen. So, to investigate the hypotheses that (i) the velocity of the wind recorded at DML should be resolved along the longitudinal axis and (ii) that the wind does not need to be increased above that recorded at DML, a data-set was studied which had been collected from a meteorological (met) buoy placed in the loch at station LL14 during the month of March 1992. This provided the wind speeds and directions actually observed at station LL14 (recorded on a 20 minute interval), and could be compared with the measurements made over the same time-period from DML. The 20 minute met buoy data was averaged to give comparable hourly data. **FIGURE 7.2 (a)** shows a plot of the wind speeds measured at both DML and at the met buoy versus time (the first 4 days of March 1992). From this plot it can be seen how the velocities recorded at DML are rarely less than those recorded by the met. buoy and hence there is no requirement that the DML data be multiplied by >1. In fact it can be seen how the wind velocities measured at DML are at times much greater than the met buoy data. If these peaks are isolated then the corresponding data are:

Time	**Wind Direction (° from**		**Wind velocity (knots)**	
(number of hours)	**true North)**			
	DML	Met Buoy	DML	Met Buoy
14	290	270	16	9
18	270	148	9	3
37	240	255	17	8.5
52	270	191	18	8

From these results it can be seen that the largest discrepancies between the DML and met buoy data are when the wind direction at DML is westerly (~270°). These winds are reduced in speed and their direction made more easterly as they blow up the loch. **FIGURE 7.2 (b)** shows that by resolving the wind velocity along the longitudinal axis of the loch, these peaks are removed with the resultant wind velocities slightly lower. However, resolving the data along the longitudinal axis of the loch does not improve the correlation between the DML and the met. buoy

FIGURE 7.2

Relationship between Wind Velocity and Time for Data Measured at the Met. Buoy and at DML during March 1992

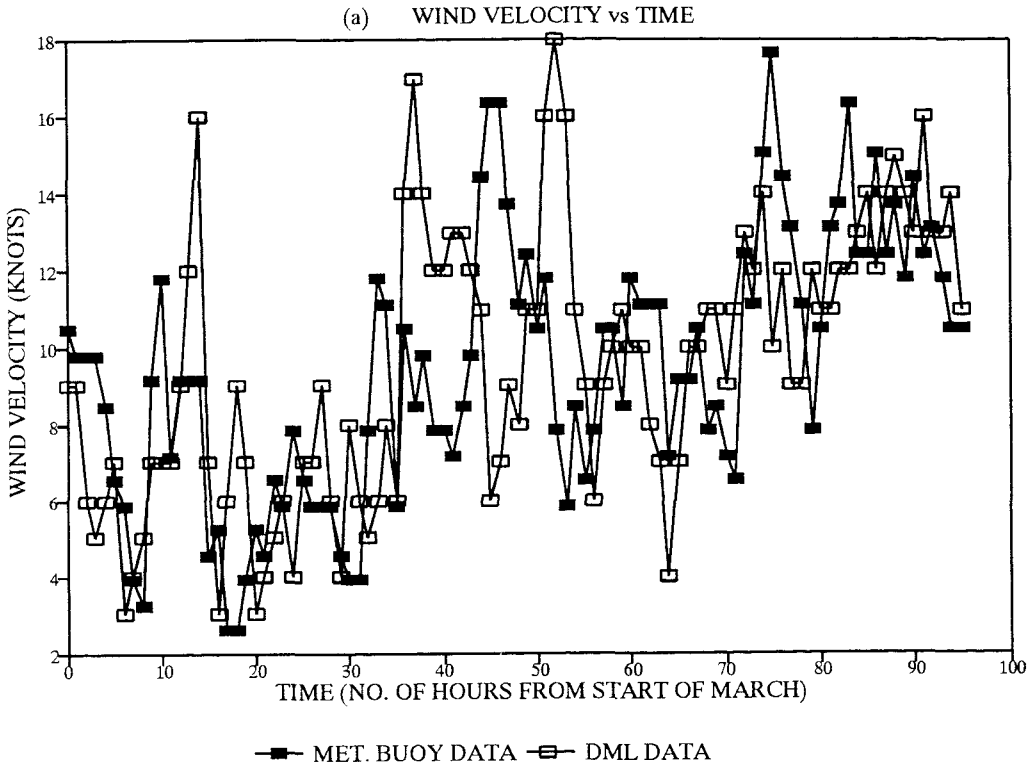

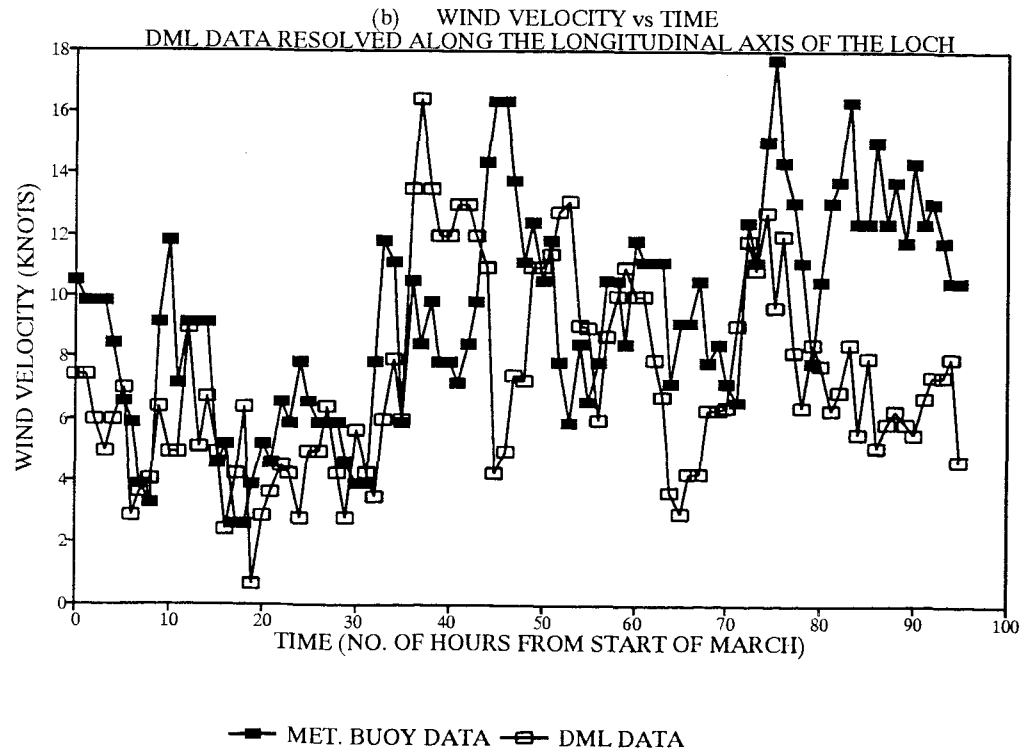

data: The correlation coefficient for a comparison of the resolved DML data with the met. buoy data is calculated as 0.32 as compared to 0.45 for a comparison of the unresolved DML data with the met. buoy data. This shows that the unresolved wind velocities are in closer agreement with the met. buoy data in terms of temporal trends. The data-sets also appear to be more similar numerically: The average wind velocity for the unresolved data-set is 9.59 knots (standard deviation = 3.54 knots) comparing with an average wind velocity of 9.44 knots (standard deviation = 3.37 knots) for the met. buoy data and 7.25 knots (standard deviation = 3.13 knots) for the resolved data. In order to decide which data-set to use in the model, the model was tested with both resolved and unresolved met buoy data. The results from both model runs were identical. This is likely to be due to the fact that vertical wind-mixing in the surface layers of the loch will not be very effective due to the very strong stratification due to the freshwater buoyancy input resulting in a high value of φ (see section **7.4.1.2**). It was decided to leave the unresolved data-set in **check92.run**.

Wind direction data is not used in the model but out of interest **FIGURE 7.3** shows that generally the wind direction lies between 180° and 270° for both the met buoy and the DML data and that the largest discrepancies occur when wind in a northwesterly or a northeasterly direction is recorded on the met. buoy. This is very likely to be due to topographic effects from the surrounding mountains.

7.3.1.2 Check92.str

This file holds the CTD data for the initial profile recorded at station LL14 at the start of the field-season and provides a profile for the model to work on. It contains depth (at 1 m intervals), temperature, salinity and density data (although the density data are not used in the model since it calculates density from salinity and temperature itself, using the subroutine **sigmat**). Because the maximum depth in the model is set at 155 m (the maximum depth of the basin) and not 110m which is the maximum depth at station LL14, the data from **check92.str** had to be interpolated to the sea-bed i.e. to 155 m. This is done within the model after the

FIGURE 7.3

Relationship between Wind Direction and Time for Data Measured at the Met. Buoy and DML during March 1992.

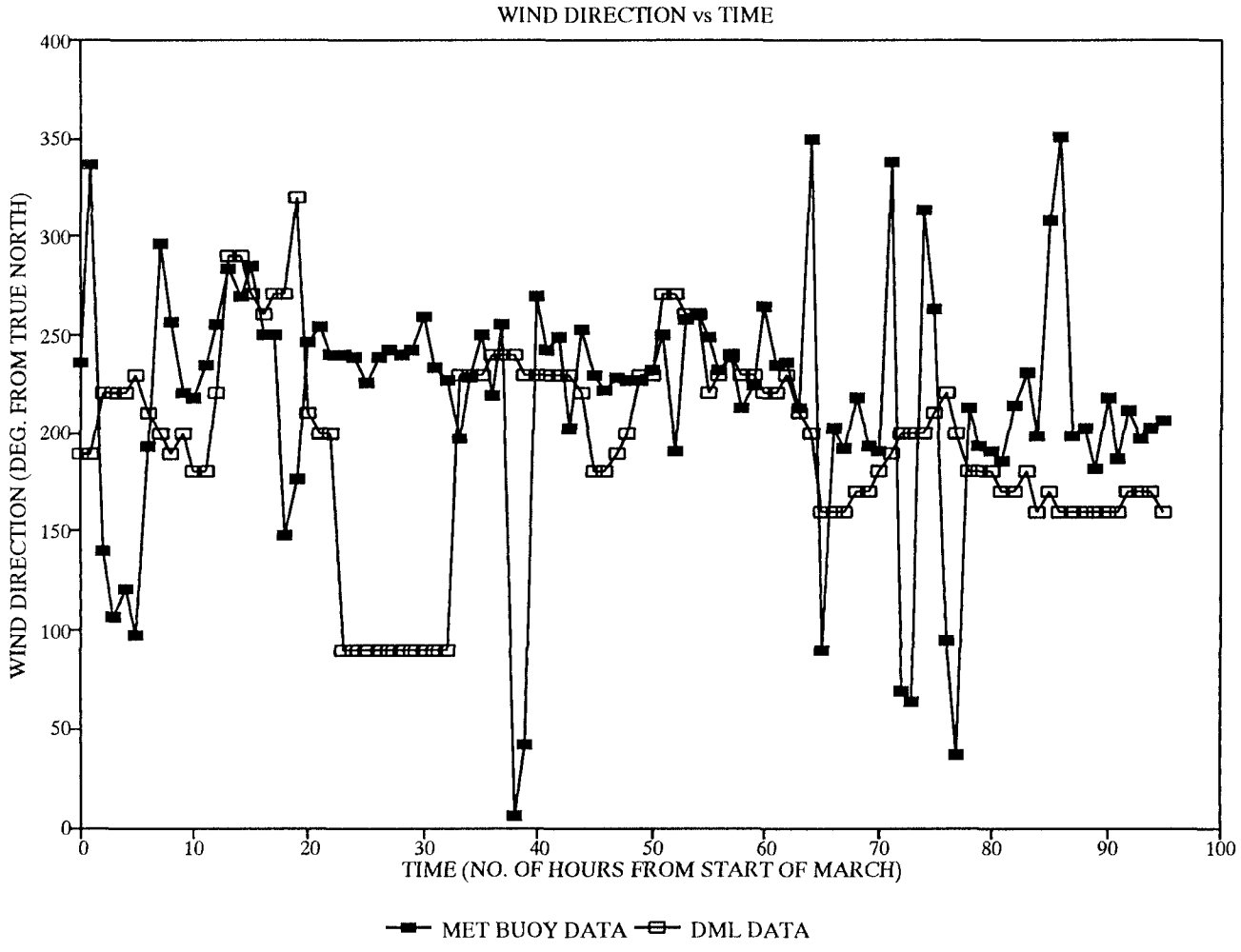

CTD data has been read in, by making all the data between the maximum depth in **check92.str** and 155m equal to those recorded at the maximum depth. Hence, when comparing model predictions with observations at station LL14, only data down to a depth of 110m is considered.

7.3.1.3 Linnhe.run

This contains variables for the model. It actually contains more information than is required for the Linnhe model due to the fact that the file is an adaption of that used in the Clyde version, where different approaches were used throughout. The variables used in the Linnhe model and stored in **Linnhe.run** are (i) **ei**; the inflow mixing efficiency coefficient described in section **7.2.1.8** and set at 0.07 (Gade and Edwards, 1980), (ii) **dt**; the time-step of the model, set at 0.00125 days (108 seconds), (iii) **ntime**; the total number of time-steps in the model, depending on the length of the data-set being used, (iv) **dz**; the depth interval set at 1m, (v) **mdepth**; the maximum depth of the basin, set at 152 m, (vi) **sdepth**; the sill depth, set at 15 m (an arbitrary number decided upon from a combination of data from Edwards and Sharples (1986) and study of Admiralty Chart no. 2380), (vii) **sarea**; the surface area of the upper basin of Loch Linnhe, set at $20*10^6$ m^2, calculated from Admiralty Chart no. 2380.

7.3.1.4 Linnhe.area

This contains loch cross-sectional area data for depth intervals of 2 m plus the area of each of these layers as a fraction of the surface area. This information was derived from Admiralty Chart no. 2380: cross-sectional areas for Loch linnhe at different depths were determined by measuring the areas within the contours on the chart corresponding to depths of 0, 10, 20, 30, 50 and 100 m, taking the value at 155 m as 0 m^2, plotting these areas against depth (see **FIGURE 7.4**) and then extrapolating values for 2 m intervals from the surface to 154 m. Once these data have been read into the model, areas for the layers at 1m intervals are made equal to the areas of the layer above them, read in from **linnhe.area.**

FIGURE 7.4

Cross-Sectional Area Data for Loch Linnhe Obtained from Admiralty Chart Number 2380.

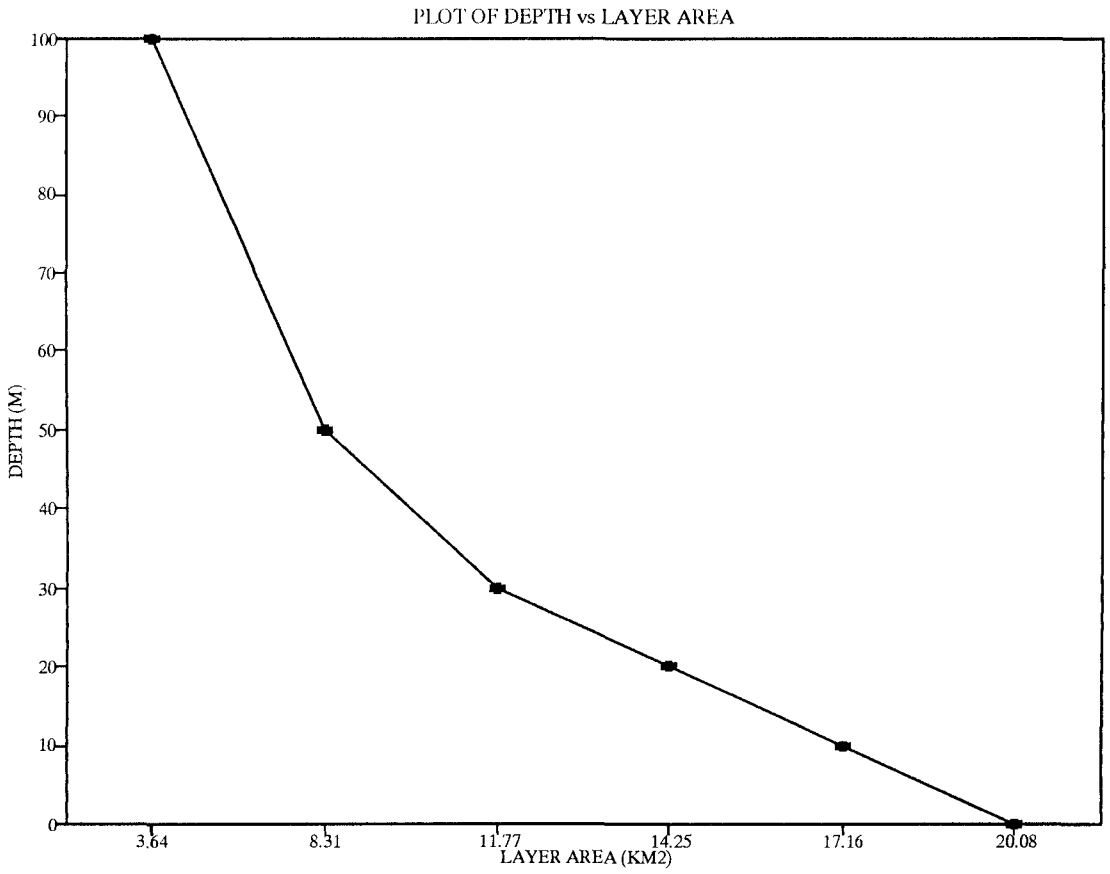

7.3.2 Calculation of variables used in the model

This section contains details of (i) the calculation of the inflow, U_i, (see section **7.2.1.1**) and (ii) the calculations for the degree of diffusion (k) and amount of work (w) required to cause this through tidal mixing (see section **7.2.1.8**).

7.3.2.1 Calculations required for U_i

In section **7.2.1.1** it was described how U_i was calculated using the basic tidal equation:

$$U_i = [Z_o + H.\cos(\omega.t + g).dt]$$

The calculation of values for each of the parameters in this equation is now considered.

(i) Z_o = a constant = the average daily rate of water entering the loch over a spring-neap cycle (m^3s^{-1}).

This calculation considers the average surface area of Lochs Linnhe and Eil:

Mean high water surface area = 36.4 km^2 (from mean high water springs data) and mean low water surface area = 31.7 km^2 (from mean low water springs data), (Edwards and Sharples, 1986).

$\therefore$ the average surface area of Lochs Linnhe and Eil = 34.05 km^2.

Maximum tidal range (springs) = 3.7 m (Edwards and Sharples, 1986) and minimum tidal range (neaps) = 1.6 m (Lawrence, 1990).

$\therefore$ the average tidal range = 2.65 m.

Average volume of water entering Loch Linnhe daily = $2.65*34.05*10^6$ m^3

$\therefore$ the rate of water entering the loch per tidal cycle =

$(2.65*34.05*10^6)/(3600*12.42060122) = 2018$ m^3 s^{-1}.

(ii) H = the amplitude rate of the tidal curve (m^3 s^{-1}).

The calculation for this considers the amplitude of the spring-neap tidal curve i.e. (maximum tidal range - average tidal range for Loch Linnhe) = 3.7 - 2.65 = 1.05 m.

$\therefore$ the average amplitude rate per tidal cycle = $(1.05*34.05*10^6)/(3600*12.42)$

$\therefore$ H = 799.62 m^3 s^{-1}.

(iii) ω = angular velocity = $2\pi/T$

where, T = the period of the spring-neap cycle.

$\therefore$ $\omega = 2\pi/14.7653 = 0.4255$ $days^{-1}$.

(iv) p = the phase of the tidal cycle i.e. the distance along the spring-neap tidal curve from the start of the year.

For the 1992 data-set the model starts on julian day 56 .
$\therefore$ t = 56 days and $\omega.t = 0.4255*56 = 23.8280$.

Day 56 is 4 days after a spring tide, therefore the model starts 4/14.7653 = 0.2709 into a tidal curve. Since 4 spring tides have already passed the position on the tidal curve from the start of the year = $4.2709*2\pi = 26.8349$.

$\therefore$ p = 26.8349 - 23.8280 = 3.0069.

7.3.2.2 Calculations required for tidal mixing

Determination of the diffusion coefficient (k): As reported in section **7.2.1.8**, 4 separate time-periods were used over the 1990 field-season for the determination of an average k value. A plot of density versus time for various depths at station LL14 is shown in **FIGURE 7.5** and through consideration of the data at 100 m in this plot, time-periods were chosen where the density gradient was negative. These time-periods and the resultant k and w values computed from the program described in section **7.2.1.8** are given below:

TABLE 7.1

Table of Average k and w Values up to Inflow Levels for 4 Different Time-Periods

Time (Julian days)	k ($cm^2\ s^{-1}$) (average to inflow level)	($W\ m^{-2}$)
38-47	6.39	$2.91*10^{-2}$
54-68	1.91	$4.05*10^{-2}$
68-79	2.96	$4.47*10^{-2}$
79-108	3.22	$5.03*10^{-3}$

From these results, the average value for w = $2.98*10^{-2}$ W m^{-2} and the average value for k = 3.62 $cm^2\ s^{-1}$. These are the values used in the subroutine **tidemix**.

7.4 Hydrographic Results from the Model

Having described in the previous sections how the model works and the data required to run it, this section considers the hydrographic results obtained from the model. Output files were created within the model so as to be compatible with the UNIRAS software packages; UNIMAP and UNIGRAPH. Macros were written within these packages so that timeseries contour maps and 2-D graphs could be easily obtained after model runs. Details of the settings used within UNIMAP are given in **APPENDIX 7.2.**

FIGURE 7.5

Relationship between Density and Time at Various Depths for Station LL14, Julian Day 38 to 151, 1990.

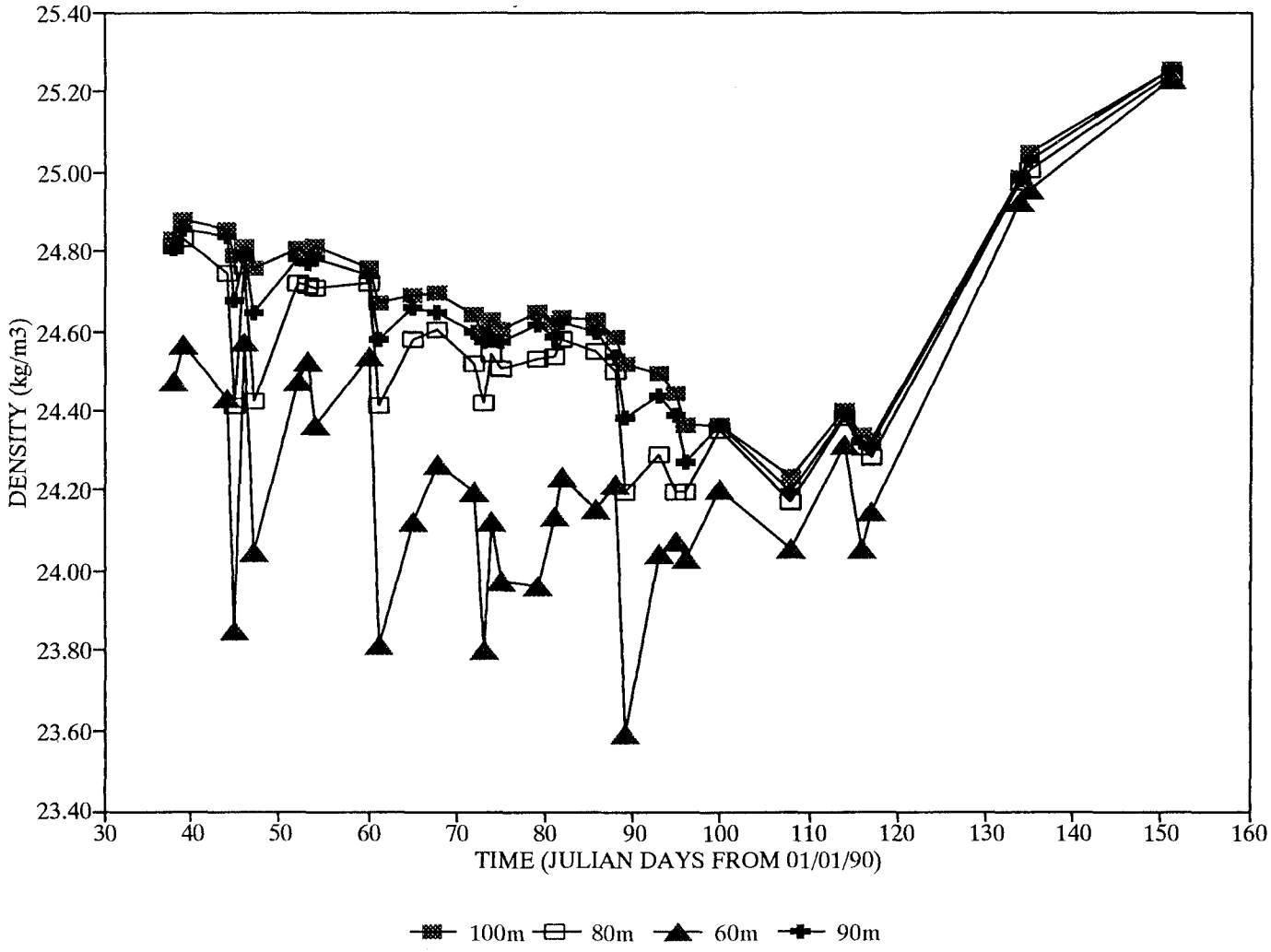

7.4.1 Results for the 1992 field-season

The actual hydrographic properties and results from the 1992 field-season data have been described in section **CHAPTER 6**, section **6.1**. This section will concentrate on how closely the model predictions agree with the observed data and try to account for any discrepancies.

Running the model with the data input files created from the 1992 field-season data, the following results were obtained: **FIGURE 7.6 (a)** shows a time-series plot of the model predictions for the density field at station LL14 for a depth of 0 - 110 m over the time-period of Julian days 56 - 139 1992. This can be compared with **FIGURE 7.6 (b)** which is the density field as obtained from CTD measurements collected during the 1992 field-season. As can be seen the model appears to provide an adequate prediction of certain features over time. The main features to compare between model predictions and real observations are (1) the timing of the deep-water renewal event at station LL14 and (2) the density structure of the water column for any particular day:

7.4.1.1 Timing of the deep-water renewal event

By studying the output file used to create **FIGURE 7.6 (a)**, the timing of the deep-water renewal (at 110 m), as predicted by the model was determined as being between Julian days 93 - 94. This agrees with the observations as shown in **FIGURES 7.6 (b)** and **7.7**, the latter illustrating the timing of the sharp salinity increase which accompanies deep-water renewal events for both the model and the observation data. In **CHAPTER 6**, section **6.1.2** it was stated that the deep-water renewal event occurred between days 86 - 99 which coincided with the high spring tides on day 95 (tidal range = 3.3 m). This was derived from observations. However the model narrows this timing down to between days 93 - 94, which corresponds well with the increasing tidal range around this time as springs are approached on day 95. It was also shown in **CHAPTER 6**, section **6.1.2.2** how the wind had been blowing continually in a south-westerly direction up the loch up

FIGURE 7.6

Comparison between (a) Model Predicted and (b) Observed Density Data for Station LL14, 1992.

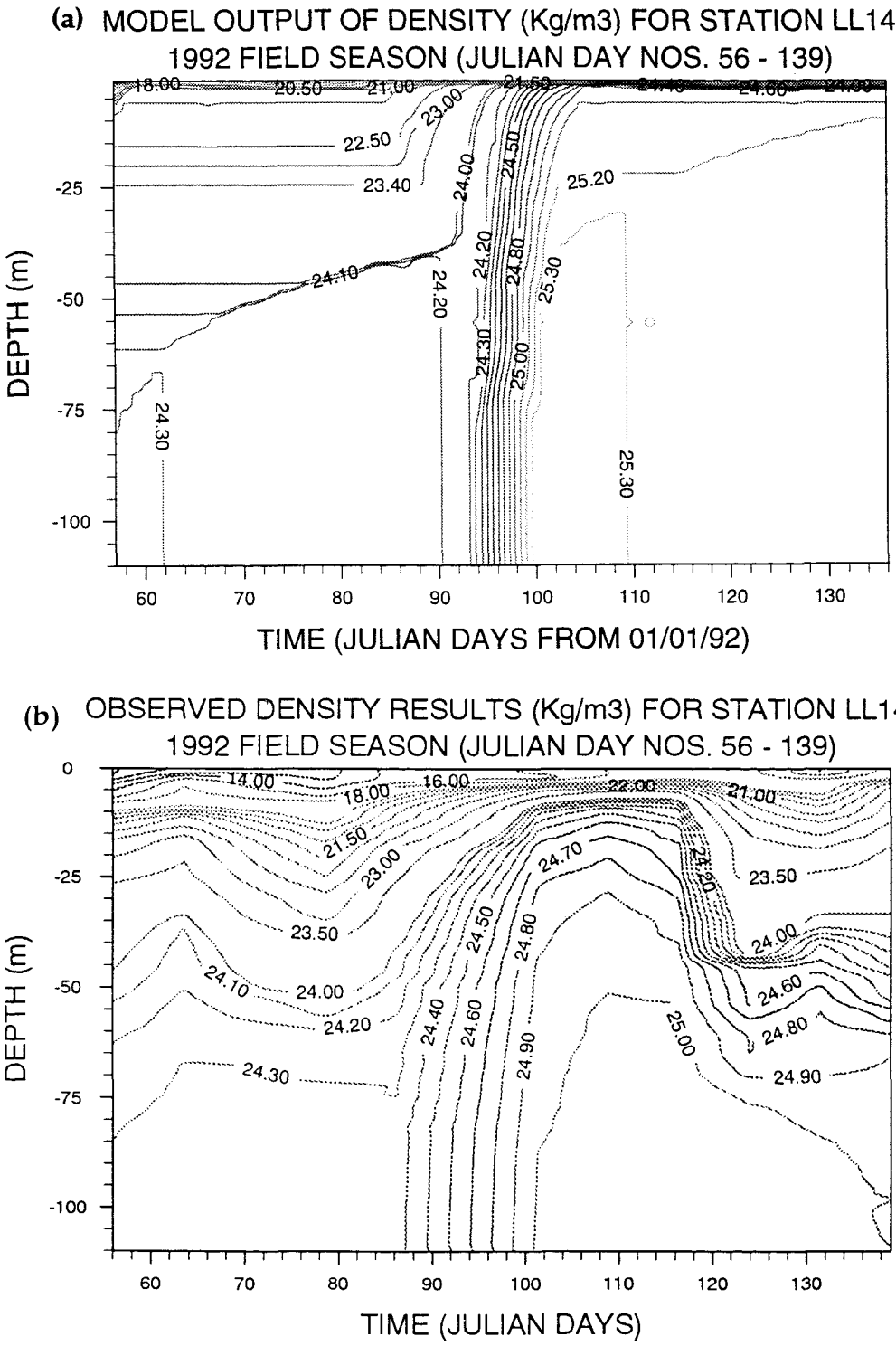

FIGURE 7.7

Comparison between Model Predicted and Observed Salinity Data for Bottom-Waters (110 m) at Station LL14, Julian Day 56 to 139, 1992.

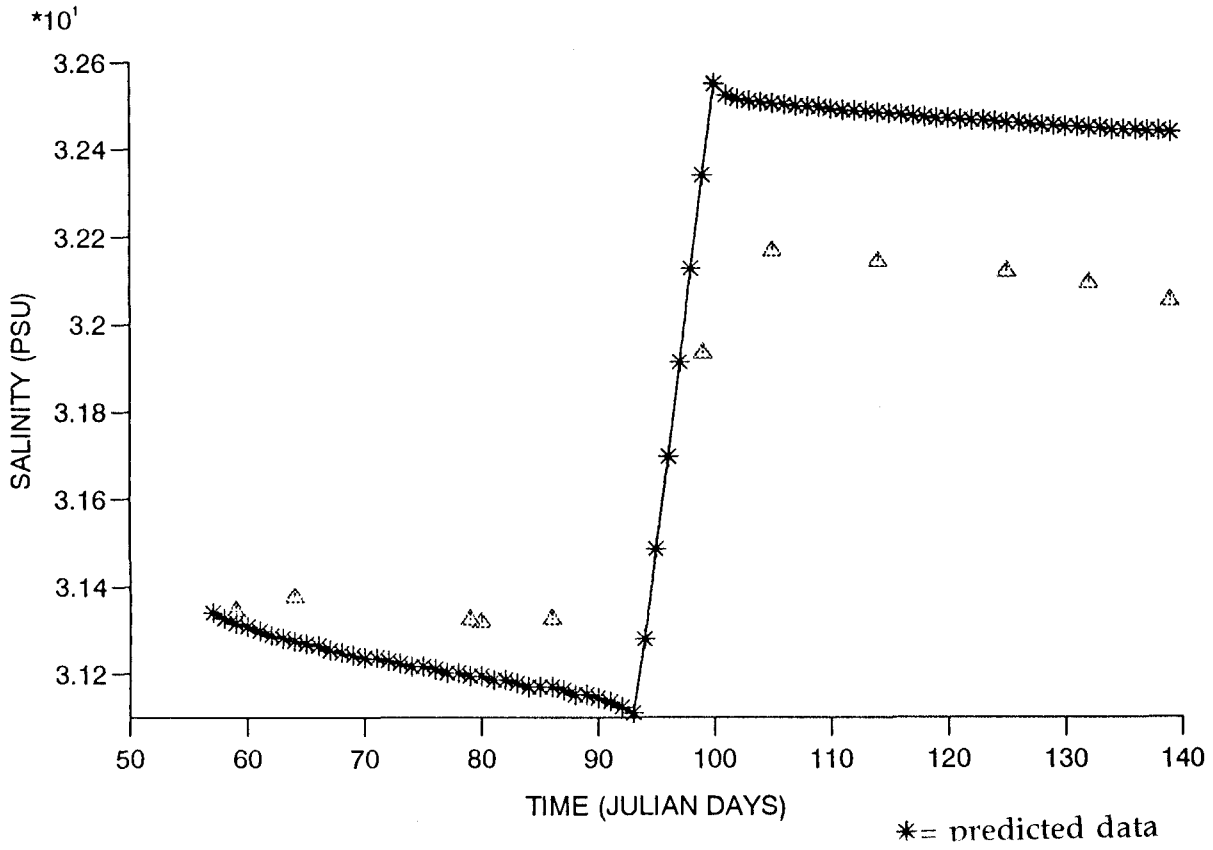

until day 88 when it changed direction to a north easterly wind with wind velocities increasing up to day 91 (see **FIGURE 6.10**). It was suggested that the change in wind direction was responsible for the upwelling of saline water outside the loch causing the renewal. Hence the model results back this hypothesis up by predicting the renewal event just a week after the wind direction changed.

7.4.1.2 Model vs observations for the density field at station LL14

Although the density fields shown by **FIGURES 7.6 (a)** and **7.6 (b)** appear to be very similar in shape, both showing vertical stratification as indicated by the salinity field (see **FIGURE 7.8**) and the same timings of the deep-water renewal event, closer inspection of the surface layers shows discrepancies. In order to investigate this and the accuracy of the model with respect to the observations, it was decided to look at salinity data rather than density data since it is the salinity which dominates the density of the water column and hence any discrepancies in density will be due to a difference in the salinity. Also, in the sections that follow the behaviour of nutrients in terms of conservative and non-conservative properties will be considered and hence their behaviour with salinity (not density) will be dealt with.

To illustrate that the discrepancies fall mainly in the surface layers, a set of figures (**FIGURES 7.9 (a) - (k)**) is given in which values for the difference between the observed results and the model predictions are plotted against depth for each day for which there is observed data available. To get an idea of the accuracy of the model predictions with depth, each plot has been considered individually and the values for the observed results minus the model predictions, studied to establish the depth below which the model is accurate within certain salinity limits:

FIGURE 7.8

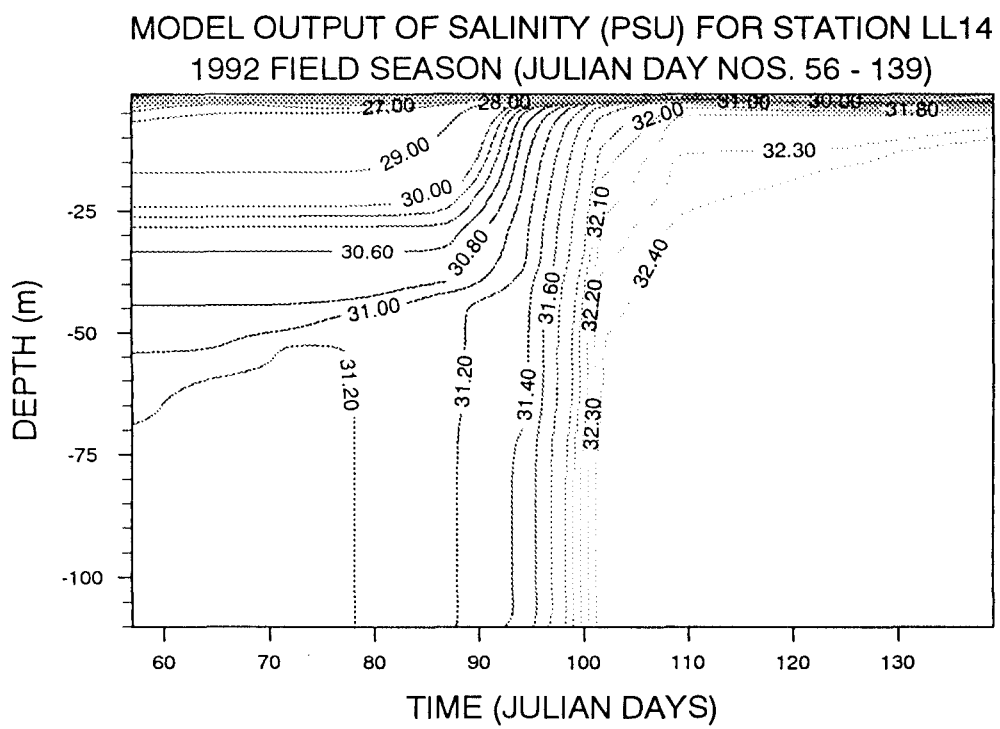
MODEL OUTPUT OF SALINITY (PSU) FOR STATION LL14
1992 FIELD SEASON (JULIAN DAY NOS. 56 - 139)
27.00
28.00
29.00
30.00
30.60
30.80
31.00
31.20
31.40
31.60
31.80
32.00
32.10
32.20
32.30
32.40
32.30
DEPTH (m)
-25
-50
-75
-100
60
70
80
90
100
110
120
130
TIME (JULIAN DAYS)

FIGURE 7.9

Comparison between Depth Variations in Model Predicted and Observed Salinity Data, Julian Day 59 to 139, 1992.

(a - c)

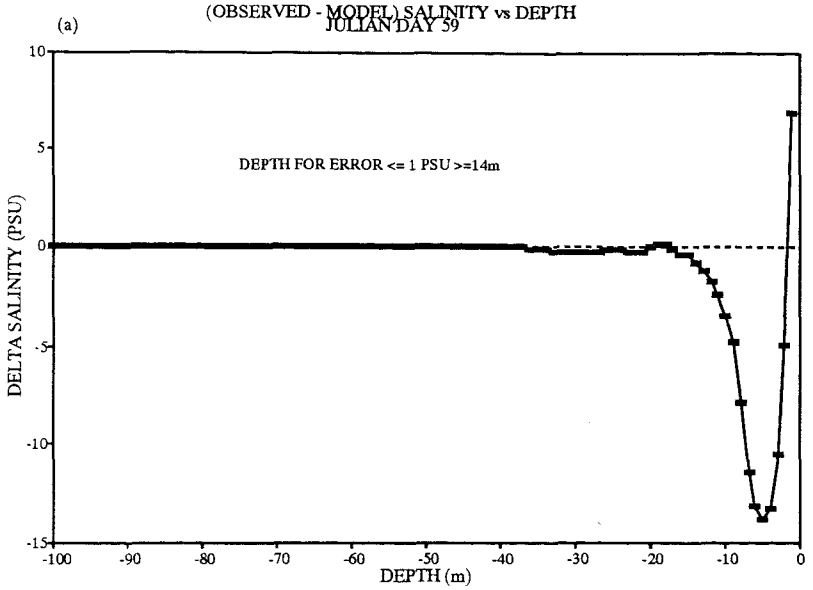

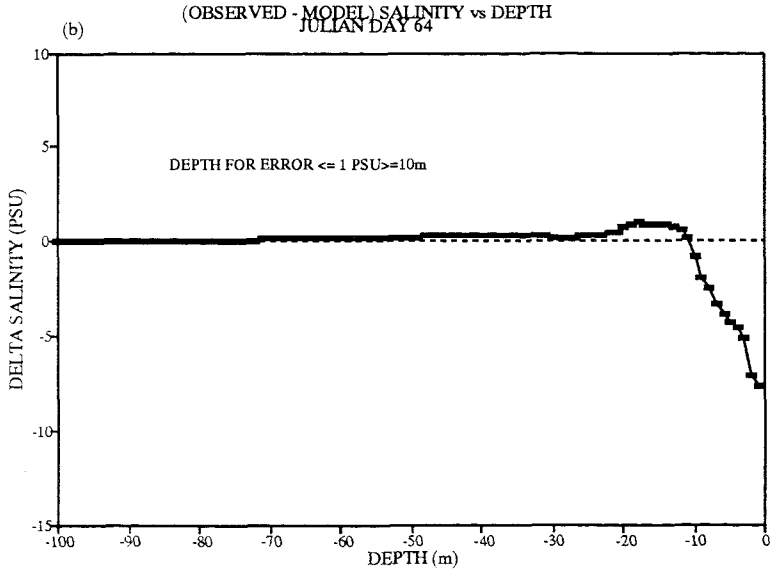

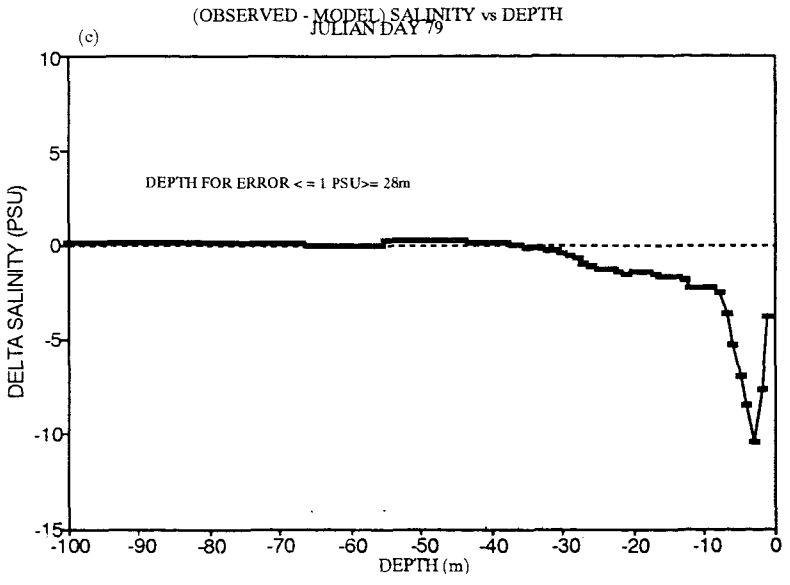

FIGURE 7.9

(d - f)

(d)

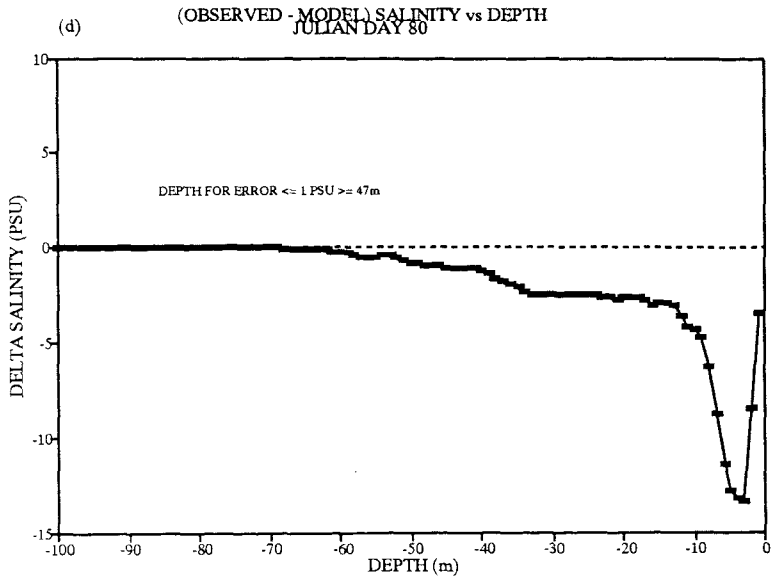

(e)

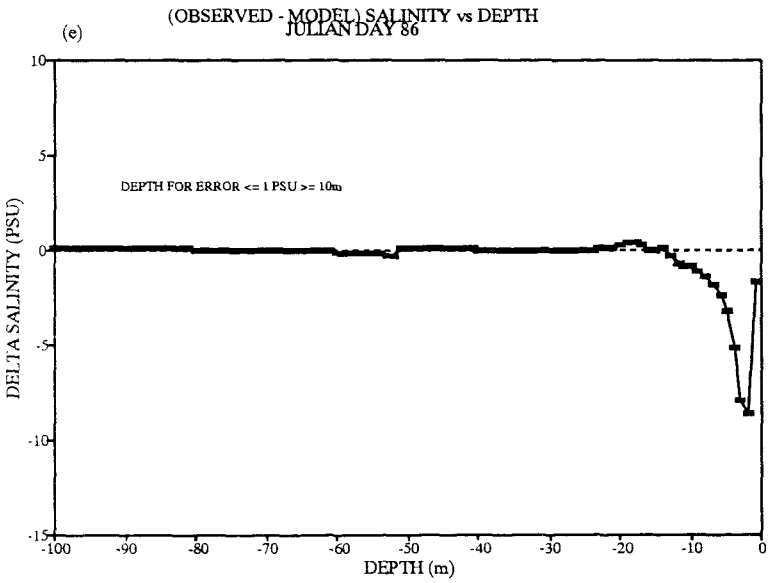

(f)

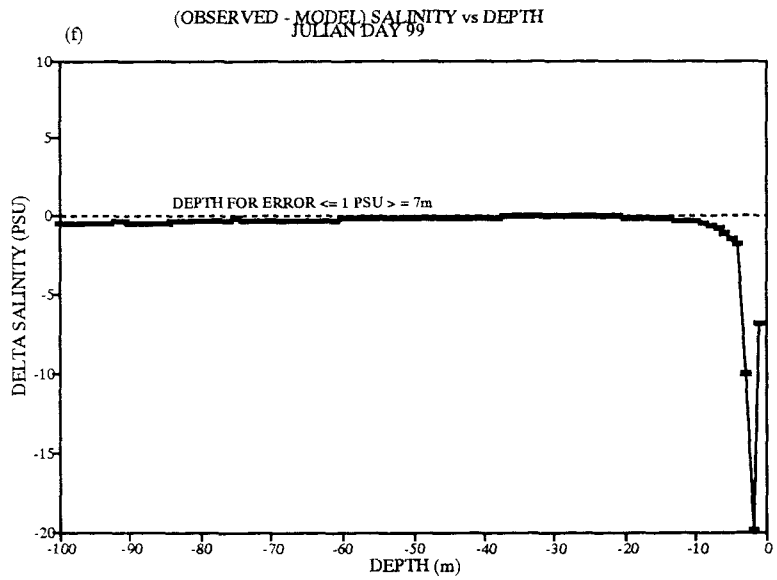

FIGURE 7.9

(g - i)

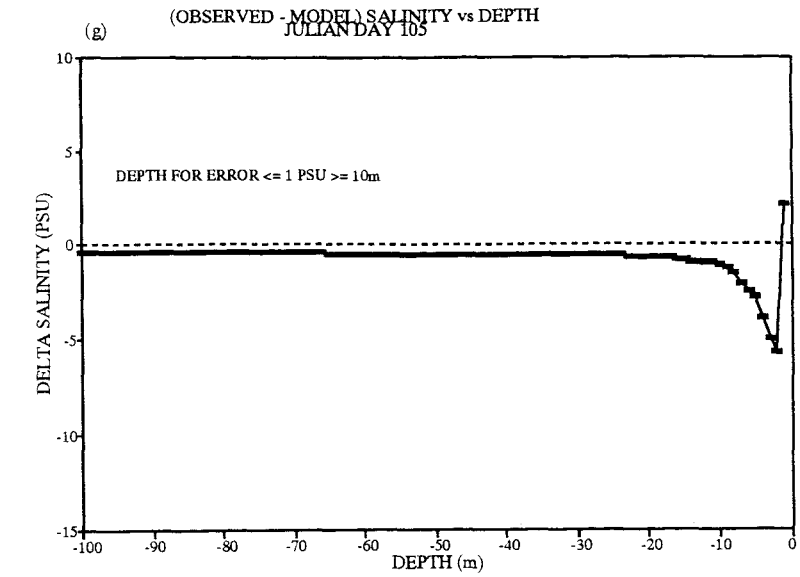
(g)
(OBSERVED - MODEL) SALINITY vs DEPTH
JULIAN DAY 105
DEPTH FOR ERROR <= 1 PSU >= 10m
DELTA SALINITY (PSU)
DEPTH (m)

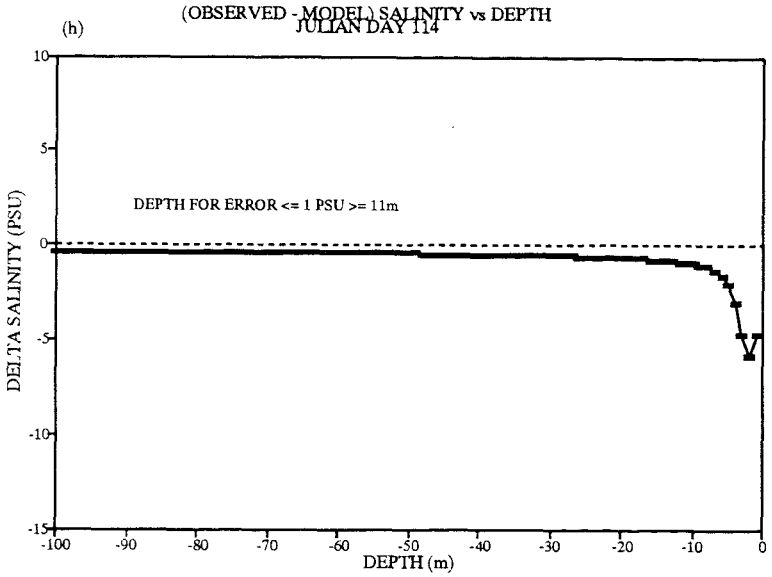
(h)
(OBSERVED - MODEL) SALINITY vs DEPTH
JULIAN DAY 114
DEPTH FOR ERROR <= 1 PSU >= 11m
DELTA SALINITY (PSU)
DEPTH (m)

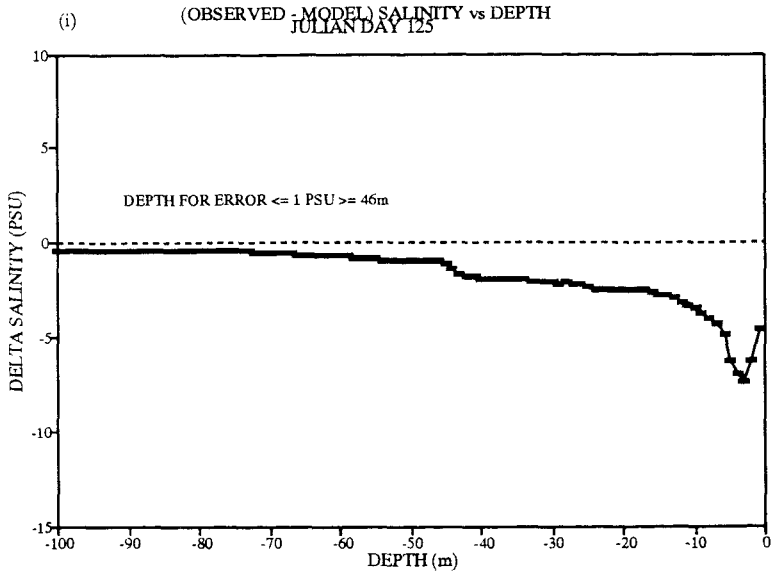
(i)
(OBSERVED - MODEL) SALINITY vs DEPTH
JULIAN DAY 125
DEPTH FOR ERROR <= 1 PSU >= 46m
DELTA SALINITY (PSU)
DEPTH (m)

FIGURE 7.9

(j - k)

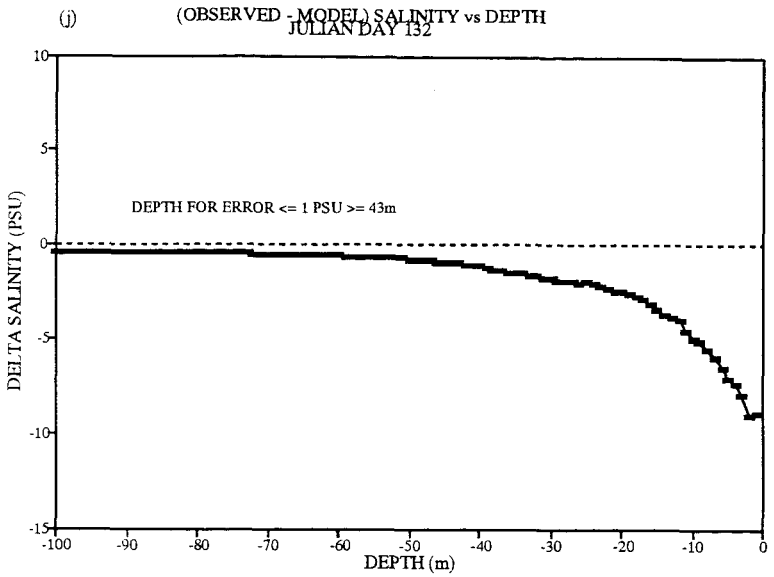
(j)
(OBSERVED - MODEL) SALINITY vs DEPTH
JULIAN DAY 132
DEPTH FOR ERROR <= 1 PSU >= 43m
DELTA SALINITY (PSU)
DEPTH (m)
10
5
0
-5
-10
-15
-100
-90
-80
-70
-60
-50
-40
-30
-20
-10
0

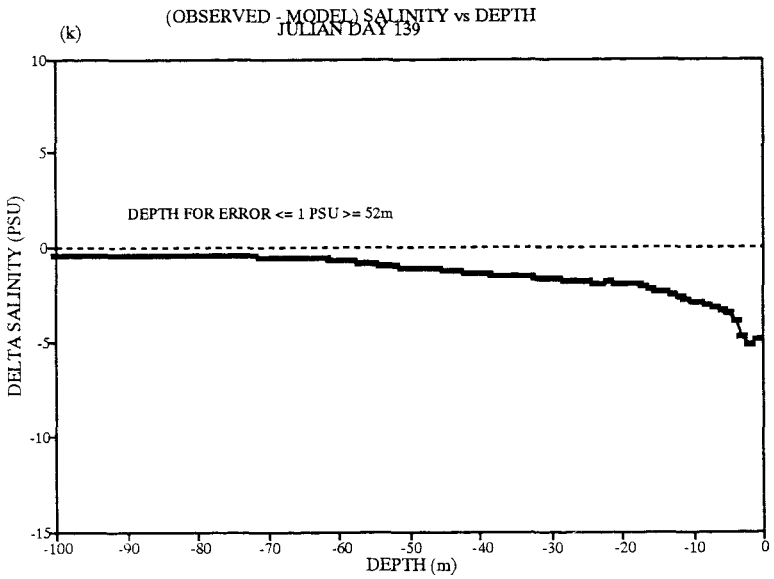
(k)
(OBSERVED - MODEL) SALINITY vs DEPTH
JULIAN DAY 139
DEPTH FOR ERROR <= 1 PSU >= 52m
DELTA SALINITY (PSU)
DEPTH (m)
10
5
0
-5
-10
-15
-100
-90
-80
-70
-60
-50
-40
-30
-20
-10
0

TABLE 7.2

Accuracy of the Model Salinities Relative to Observations

Julian day no. (for observed data)	Depth below which (observed - model) salinity = ± 1 PSU	Depth below which (observed - model) salinity = ± 1.5 PSU	Depth below (observed - model) (salinity = ± 2 PSU)
59	14 m	13 m	12 m
64	10 m	9 m	9 m
79	28 m	18 m	13 m
80	47 m	39 m	36 m
86	10 m	8 m	7 m
99	7 m	5 m	4 m
105	10 m	8 m	7 m
114	11 m	7 m	6 m
125	46 m	44 m	34 m
132	43 m	36 m	27 m
139	52 m	34 m	19 m

From these results it is possible to say that:

For	(Observed - model) salinity = ± 1 PSU:	(Observed - model) salinity = 1.5 PSU:	(Observed - model) salinity = 2 PSU:
Below this Depth (m)	% Within Limits	% Within Limits	% Within Limits
10	36	45	45
20	45	64	73
30	64	64	82
40	64	91	100 (from 36m)
50	91	100	100
52	100	100	100

This shows that within the limits of ± 1 PSU the model predictions agree entirely with the observations for depth below 52 m. Within the limits of ± 1.5 PSU and ± 2 PSU, respectively, agreement is obtained for depths below 40 m and 36 m.

By study of the output from the model the depth below which the bottom-waters can be considered isolated (before the deep-water renewal event), is determined as 81 m. This is the depth below which no change in salinity is observed other than that caused by diffusive processes. From the 1992 field-data, the depth below which the water is considered to be isolated over days 56 - 99, is 75 - 80 m (see **CHAPTER 6**, section **6.1.1**). Below this depth it can be assumed that any changes in nutrient concentrations, other than those due to diffusive processes, are due to real non-conservative biogeochemical processes as described in **CHAPTER 6**, section **6.2.1.2**. Since the hydrographic model predictions are accurate within the salinity limits of ± 1 PSU for depths below 52 m, the model can be used to investigate nutrient concentration changes in the bottom-waters during the isolation period (see section **7.6**).

However, the top 20 m of the salinity field at LL14 are not well produced by the model. From **FIGURE 7.10** it can be seen that the predicted model surface (1 m) salinities are higher than the observed values. **FIGURES 7.6 (a)** and **(b)** also show that the densities of the model surface layers are higher than that of the observed densities, particularly in the top 10 m where the model results are never less than 18 kg m^{-3}, whereas the observed values are less than 14 kg m^{-3} on occasion. From an examination of the output files themselves, it can be seen that the problem lies in the lack of mixing between the top 2 layers of the model: For example, the output file shows that for day 58 the model predicts the following data for the surface layers:

Depth (m)	Salinity (PSU)	Density (kg m^{-3})
1	8.5	6.62
2	23.56	18.38
3	26.71	20.81

FIGURE 7.10

Comparison between Model Predicted and Observed Salinity Data for Surface Waters (1 m) at Station LL14, Julian day 56 to 139, 1992.

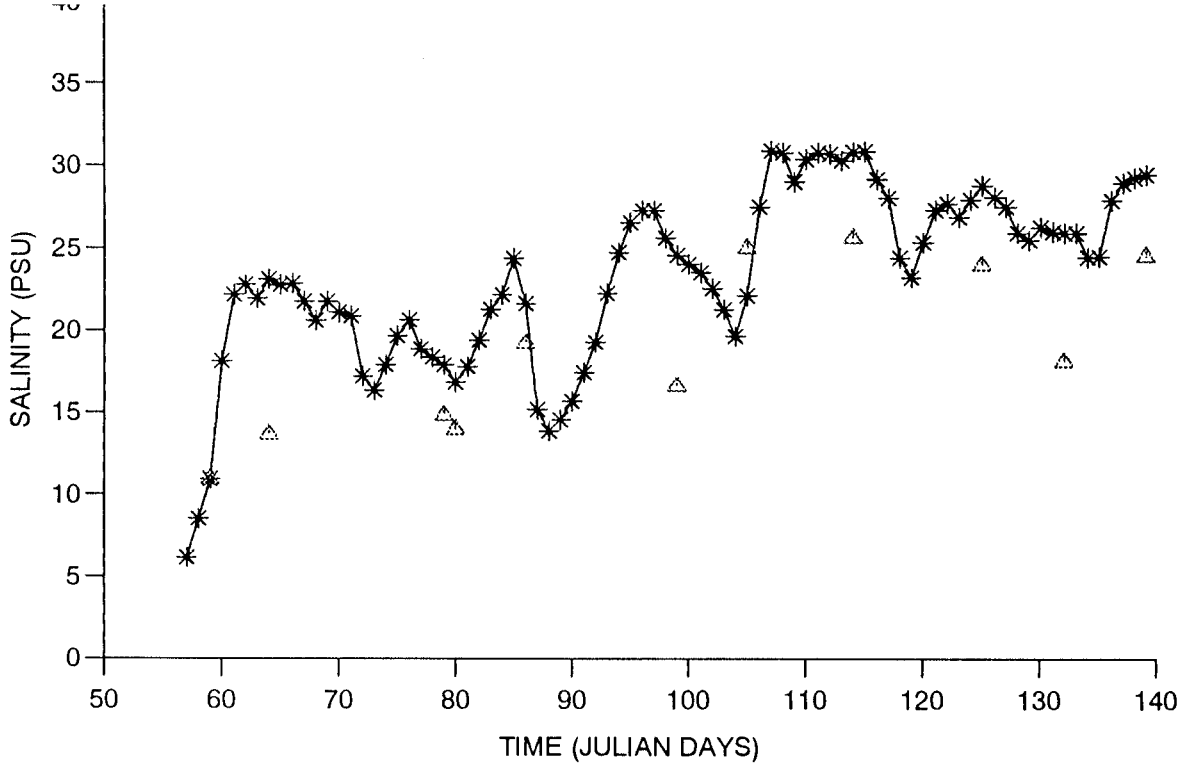

* = predicted data △ = observed field data

which would suggest that the top layer in the model is quite isolated from the rest of the water column. Possible reasons for such high predicted salinities and densities in the surface layers are as follows.

(a) There is not enough freshwater entering the system i.e. the freshwater boundary condition, **Rq**, is inaccurate. **Rq** was determined as accurately as possible, taking into account the extra input of freshwater to the system due to the watershed of the loch exceeding the catchment areas of the inflowing rivers (see section **7.3.1.1**). However, it is possible that the saline boundary condition is too saline since linear interpolation between the observed data values had to be carried out in order to obtain daily input values for the model (see section **7.3.1.1**). Hence it is possible that increases occurring in the freshwater input in the saline boundary condition have been omitted due to lack of observational data. However, the timing of the renewal is predicted well by the model and for this to be the case accurate trends in the saline boundary condition are required. Thus, an alternative suggestion is required.

(b) The retention of freshwater observed in the system due to the wedging effect of the wind blowing up the loch cannot be replicated by the model. In **CHAPTER 6**, section **6.1.2.2** it was shown how the residence time of the freshwater in the water column at station LL14 increased over time prior to the renewal, and this was attributed to an increase in the freshwater input to the system prior to day 80, coupled with a persistent south-westerly wind blowing up the loch (see **FIGURE 6.10**), thus retaining the freshwater both at the sill and inside the basin. Since the model is a 1-D model it only considers wind velocity and cannot utilize wind direction data, hence this effect cannot be simulated by the model. The only way in which the model can use the wind data is to mix the surface layers vertically downwards via the subroutine **windmix** (see section **7.2.1.7**). For mixing to occur, the energy available from the wind must exceed the potential energy anomaly (φ) of the first 2 layers of the model at least, but looking at the magnitude of the wind velocities input to the model (see file **check92.run** in **APPENDIX 7.1** it can be seen that these are not high with an average wind velocity of 10.16 knots

(force 3 to 4 on the Beaufort wind scale). Hence, it is probable that the energy available from the wind will not exceed the resultant φ between the surface layers of the model, rendering **windmix** quite ineffective in terms of downward mixing of freshwater.

The possibility was also considered that there was downward mixing of freshwater through convection of water caused by heat loss from the surface layers (at night for example). This had to be considered separately due to the lack of any allowance for heating in the model. To do this, the day with the maximum observed surface temperature was considered (day 139) and the density calculated for this layer using the UNESCO (1981) algorithms. Then assuming that the very lowest temperature (T) that the freshwater will fall to is 4 °C, (although in reality the temperature of the water will probably only fall by 0.5 ° C, (Dr. D. Ellett, 1994, DML, pers. comms.)), the density of the same water is calculated for this temperature :

Density of water at T = 9.3 ° C and salinity = 24.5 PSU is 18.87 kg m^{-3};
Density of water at T = 4 ° C and salinity = 24.5 PSU is 19.42 kg m^{-3}.

Therefore, this large drop in temperature gives rise to a density difference of 0.55 kg m^{-3}. Looking at the model output for the top 4 m for day 139:

Depth (m)	Salinity (PSU)	Density (kg m^{-3})
1	29.47	22.92
2	30.63	23.83
3	32.19	25.06
4	32.19	25.06

it can be seen that, in order for the top 2 layers of the model to mix, a drop in T is required that will give rise to a density difference of ~ 0.9 kg m^{-3}. Since this is not the case it was concluded that, in terms of mixing down layer 1 into layer 2,

effects of convection of water through heat loss are negligible.

7.4.2 Results from the 1990 field-season

Having looked at the performance of the model in predicting observations for one year, 1992, it was decided to check it against a data set taken from a different year, 1990, for which the meteorological conditions were different. The data set used was that collected during a 4 month period at station LL14 consisting of 30 CTD profiles. These data were made available courtesy of Mr. A. Edwards (DML) and were used to make up input files for the model (see section **7.3.1**), along with relevant meteorological data also provided by DML. The year 1990 had a particularly high rainfall, with the cumulative rainfall total up to June of that year being 26 % higher than the previous highest recorded, in 1989 (Grantham, 1991). For example the cumulative river flow from the start of 1990 to April 1990 for the River Lochy was 24,547 $m^3 s^{-1}$ as compared to 14,235 $m^3 s^{-1}$ for the same period in 1992. It was deemed that such a difference in the 2 years would be useful in testing the reliability of the model's performance. Running the model for 1990, under exactly the same conditions as for 1992, but with different input data, the predicted density field at LL14 shown in **FIGURE 7.11 (a)** was produced. As can be seen the model produces an adequate prediction of the observed density field shown in **FIGURE 7.11 (b)**. **FIGURE 7.12** shows the accurate model prediction of the timing of the deep-water renewal in 1990. This was predicted to occur between Julian days 121 - 122, which agrees with the observed data set which shows the renewal occurring somewhere between days 117 - 134. Again the model has narrowed down the time-scale in which the renewal occurs, with days 121 -122 being 4 -5 days after a spring tide of tidal range 2.1 m. However, in spite of this accurate prediction of the bottom-water behaviour, **FIGURES 7.11 (a)** and **7.13** again highlight the problem of high predicted salinity values in the top layer of the model. This can again be explained by wind effects.

FIGURE 7.11

Comparison between (a) Model Predicted and (b) Observed Density Data for Station LL14, Julian Day 38 to 151, 1990.

(a) MODEL OUTPUT OF DENSITY (Kg/m3) FOR STATION LL14.
1990 FIELD SEASON (JULIAN DAY NOS. 38 - 151)

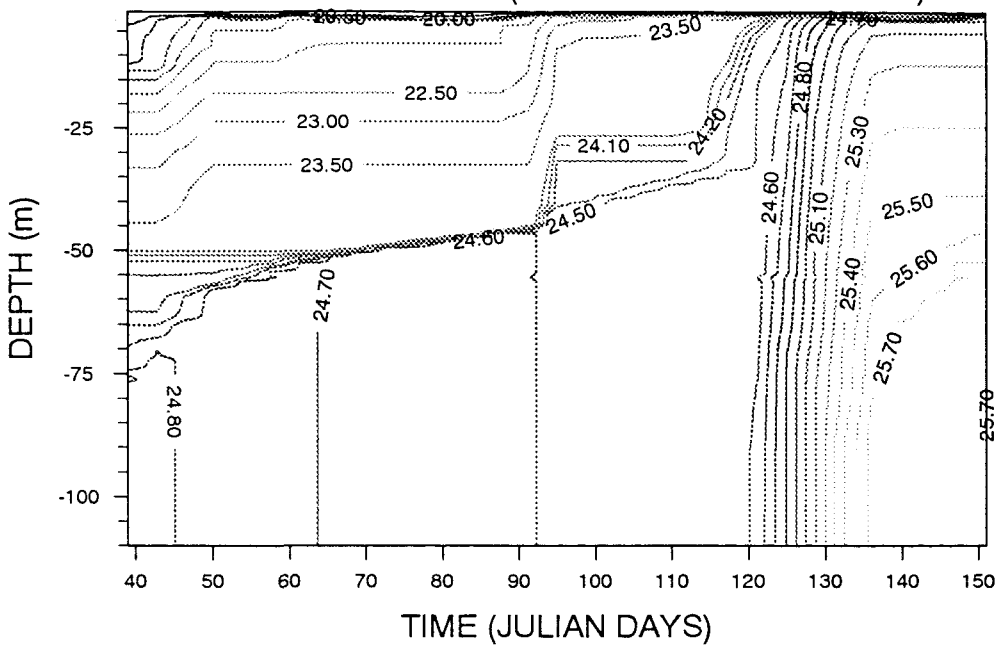

(b) OBSERVED DENSITY (KG/M3) TIME-SERIES AT STATION LL14
1990 FIELD SEASON

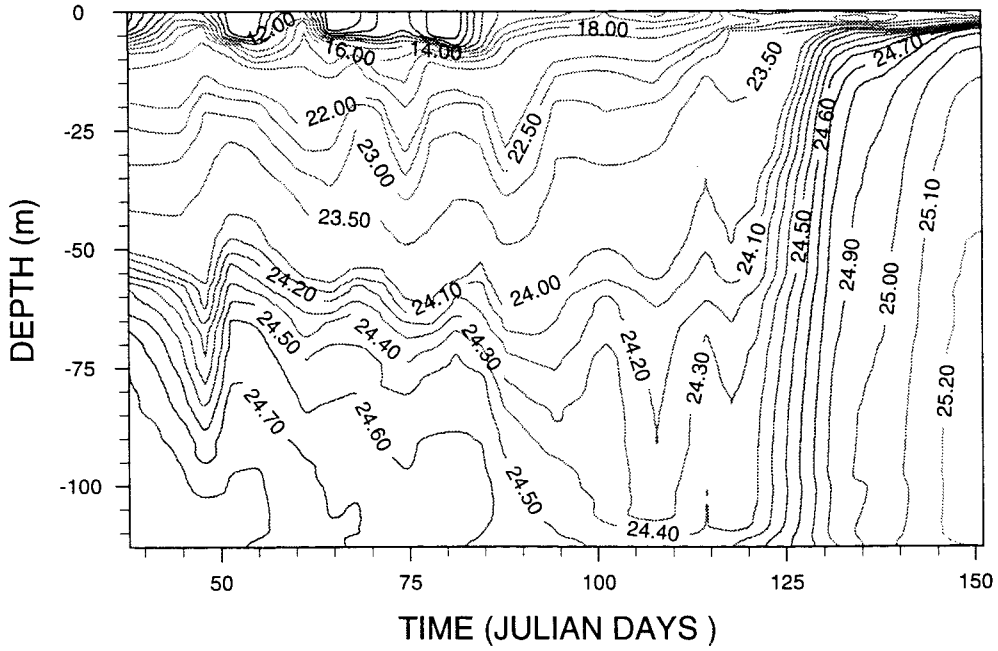

FIGURE 7.12

Comparison between Model Predicted and Observed Salinity Data for Bottom-Waters (110 m) at Station LL14, Julian Day 38 to 151, 1990.

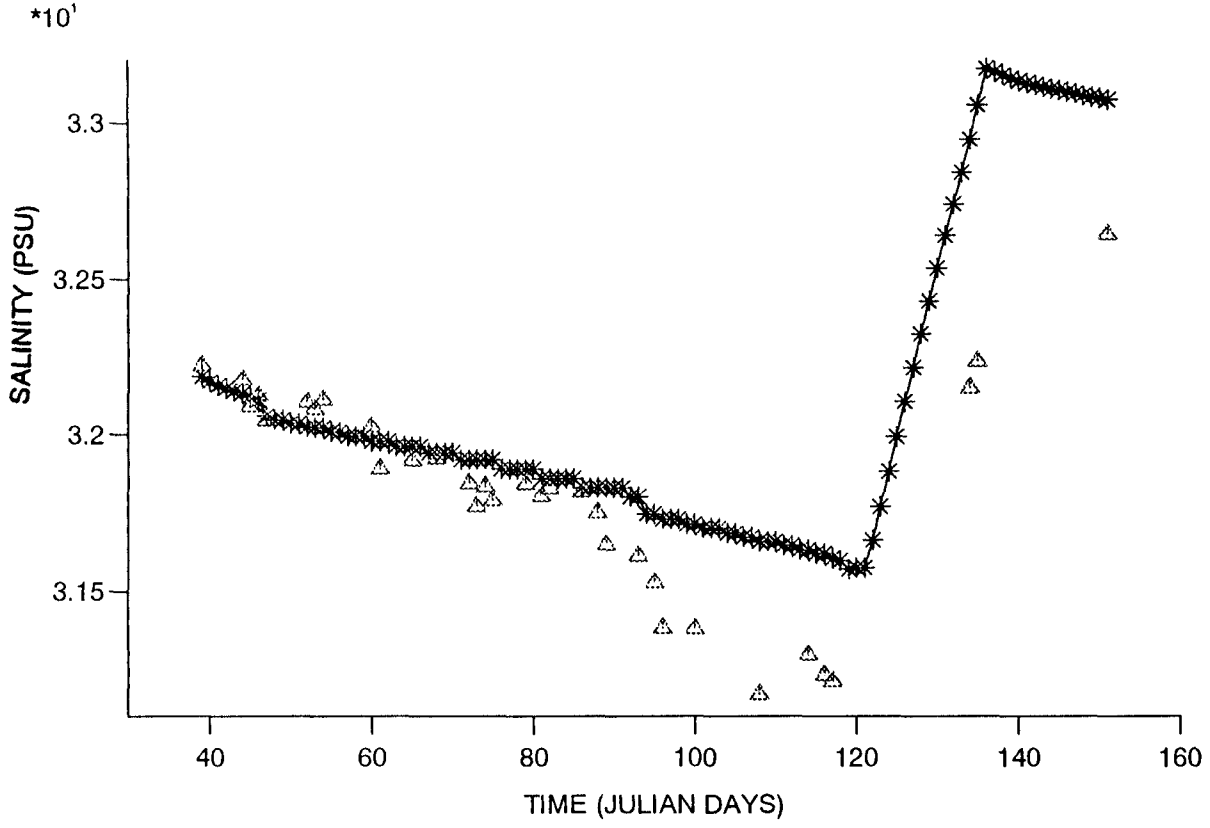

* = predicted data △ = observed field data

FIGURE 7.13

Comparison between Model Predicted and Observed Salinity Data for Surface Waters (1 m) at Station LL14, Julian Day 38 to 151, 1990.

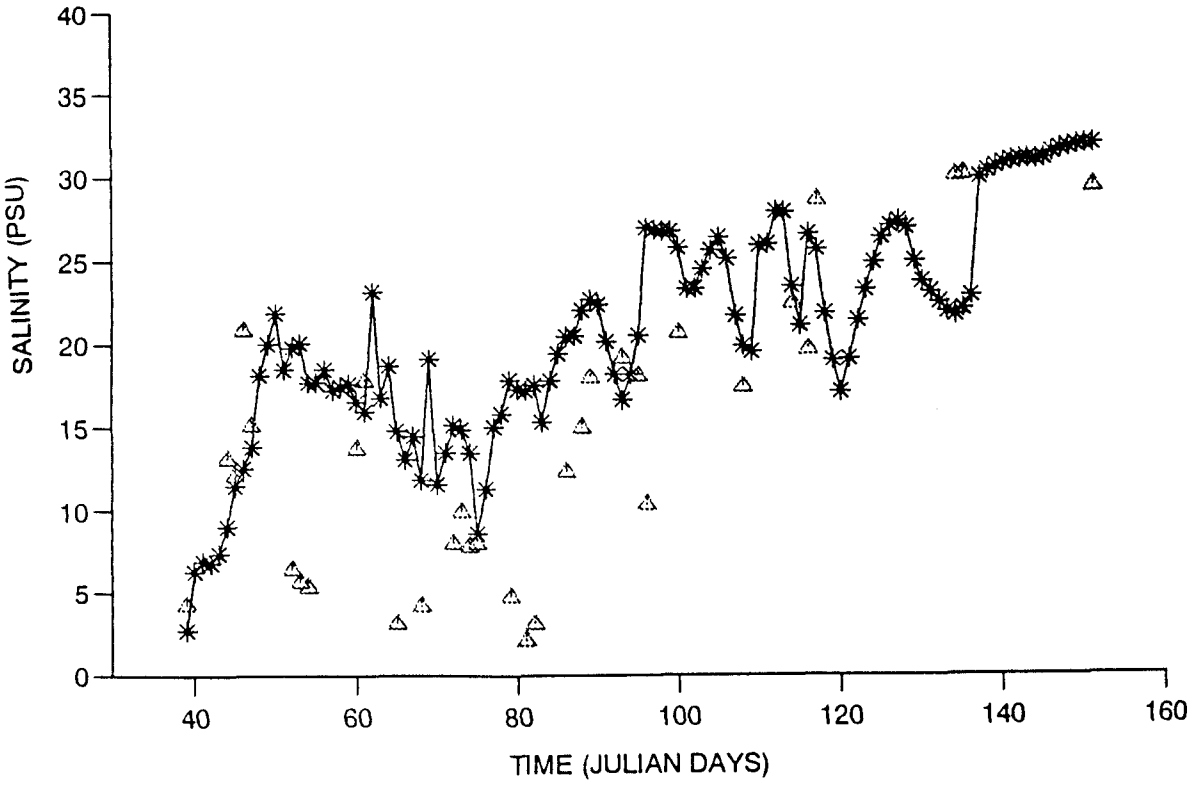

✳ = predicted data △ = observed field data

7.5 Conclusions from hydrographic model results

(1) The hydrographic model predictions are accurate within the salinity limits of ± 1 PSU for water below 52 m in the loch. Hence, the model is deemed adequate for use in investigating the behaviour of the nutrients in the isolated bottom-waters (below 81 m) for the 1992 field season.

(2) The top 20 m of the observed salinity field at LL14 are not accurately reproduced by the model. This is due to a deficit of freshwater in the model, making the predicted surface salinities too high. The most likely explanation for this is the inability of the model to account for wind direction and hence the lack of simulation of freshwater retention in the system. Also downward mixing of the surface layers is not very effective in the model due to the low wind velocities compared to the high values of φ between the top 2 layers.

(3) Convective mixing of water in the surface layers due to heat loss can be assumed to be negligible in the model.

(4) The model is reliable in reproducing field observations below a depth of 52 m for different data sets.

7.6 Development of the Physical Model for the Study of Nutrient Behaviour in Loch Linnhe

The aim behind this part of the study was to develop the physical model for prediction of nutrient distributions over time in the upper basin of Loch Linnhe, and also to quantify the extent of any apparent and real non-conservative behaviour of the nutrients basin.

The rationale behind this part of the study involved a number of steps, as follows:

(1) To develop the physical model so that nutrients could be input to the system in such a way that they behaved conservatively within the system but retained their temporal variability in the saline and freshwater end-members (the boundary conditions of the model);

(2) To use the results from **1** to estimate the contribution of the temporally varying end-member concentrations to the deviation of observed nutrient concentrations away from the corresponding theoretical dilution line (TDL);

(3) To verify the models performance with nutrients by checking that the predicted changes in nutrient concentrations in the isolated bottom-waters are correlated entirely with diffusive changes in the salinity;

(4) On the assumption that step **3** confirms the validity of the model for the prediction of the nutrient distribution in the bottom-waters in the absence of non-conservative behaviour, to compare this prediction with the observed distribution (before the deep-water renewal event) and thus to evaluate the influence of non-conservative processes in the bottom waters. Such processes will cause deviations of data from the TDL.

The results from these steps will be given in the subsequent sections.

7.6.1 Development of the Physical model and the Input of Nutrient Data

Theory: As described in **CHAPTER 2**, section **2.1** and **CHAPTER 5**, section **5.2.1**, if the concentration of a nutrient in a system is controlled only by the degree of physical mixing of two end-members in the system, then a plot of its concentration against salinity will result in a straight line, known as a theoretical dilution line (TDL). Regression analysis of nutrient concentrations on salinity as the independent variable will give rise to a coefficient of determination (r^2) equal to 1 (see **CHAPTER 5**, section **5.2.1** for details of r^2). Values of $r^2 < 1$, will occur if there are:

(a) factors leading to apparent non-conservative behaviour such as temporally varying end-member concentrations with variations of significant period relative to the flushing time of the system;

(b) real non-conservative processes such as biogeochemical reactions occurring within the water column and the sediment and;

(c) point inputs of nutrients to the system.

Points (b) and (c) give rise to more source than the two end-member sources.

For the Loch Linnhe system only (a) and (b) need be considered as potential contributors to deviations of the nutrient concentrations away from a linear relationship with salinity. In fact in both **CHAPTERS 5** and **6** it was shown that the effect of the temporally varying end-member concentrations was such that a single TDL could not be drawn through the data due to the range of the end-member concentrations within the field-seasons. Hence a line of best fit was drawn instead, which defined an average dilution line and which assumed conservative behaviour. Scatter of data around this was taken as an indicator of the apparent and real non-conservative behaviour occurring within the basin over the whole of each field-season. If the model is developed such that the incoming nutrient concentrations are forced to behave conservatively once inside the basin, then the value of r^2 for the behaviour of the nutrients relative to salinity would always be equal to 1, provided that the end-member concentrations remain constant. Values of r^2 are therefore expected to be less than 1 due to the observations discussed above, and the value of $(1 - r^2)$ may be used to estimate the degree of apparent non-conservative behaviour in the system.

The first part of this study then, involved developing the physical model to incorporate the nutrient data in such a way that they behaved conservatively once inside the basin, and then to determine r^2 values from the model results.

Procedure: The main adaptations that had to be made to the basic physical model involved writing additional FORTRAN code to allow for (i) the input of the nutrient files to the model, (ii) the simulation of conservative behaviour of the nutrients in the same manner as salinity in the basin system and (iii) the output of the predicted nutrient profiles with the corresponding salinity predictions.

(i) Code was written to allow the input of a nutrient data file (**nutsal.92**) which contained daily boundary condition data. This file was read into the model simultaneously with the physical boundary conditions (**check92.run**). Initial nutrient profiles (**nutpro.prn/nutlin.prn**) were read into the model simultaneously with the hydrographic profile (**check92.str**) and on the basis of these the model carried out the commands listed in section **7.2.1**. Details of how these files were compiled may be found in section **7.6.1.1** and the data files themselves are listed in **APPENDIX 7.3**.

(ii) The simulation of conservative behaviour of the nutrients was achieved through the mixing of nutrients through the water column simultaneously and by processes identical to those used to determine the salinity in the physical model (see section **7.2.1.2**).

(iii) Output files for the nutrients and salinity were created within the model so as to be compatible with the UNIRAS software package, UNIMAP, and the QUATTRO PRO for Windows software package from which regression analyses could be carried out.

7.6.1.1 Input files and the treatment of data

Because the nutrient model is a further development of the physical model, all of the physical data files described in section **7.3.1** are also required for the nutrient model. The additional files required for nutrient predictions have been mentioned in the previous section and are called (i) **nutsal.92** and (ii) **nutpro.prn/nutlin.prn**. It should be noted that these files start on Julian day 59 and not Julian day 56 (as

for the physical data) due to a lack of nutrient data for day 56.

Nutsal.92: This contains the daily nutrient data for the boundary conditions i.e. the concentrations of nutrients in the saline and freshwater inputs to the loch.

The saline boundary condition: Daily values of phosphate, nitrate and silicate concentrations averaged over the top 20 m from the most seaward station, LL0, were used for the 1992 field-season. A depth of 20 m had to be used and not 15 m (as for the physical data) because there was no available nutrient data at 15 m depth, the nutrient samples being collected at discrete depths of 0, 5, 10, 20, 40, 60, 80, 100, 110 m (see **CHAPTER 4**, section **4.1.3**). By using a 20 m average to obtain daily nutrient values and not a 10 m average, higher concentrations of nitrate and phosphate are assigned (since these nutrients increase in concentration with an increase in salinity) which allows for greater sensitivity in the detection of the occurrence of geochemical inputs of nutrients to the bottom-waters, of the system. Linear interpolation between these observed (weekly) 20 m average values was carried out for all the nutrients in order to obtain daily values for the data-file. This approach was adopted to match that used to determine the daily salinity values (see section **7.3.1.1**).

The freshwater boundary condition:

As described in **CHAPTER 6**, section **6.2.1.1**, the relationship of freshwater nitrate and phosphate concentrations with time (annual variations) is stronger than with flow. Hence, the daily freshwater nutrient concentrations were determined as a function of time using the single harmonic equation:

$$Y_w = \alpha_0 + [\alpha_1.\cos(2\pi.x)]/365 + [\beta_1.\sin(2\pi.x)]/365$$

where;

Y_w = nutrient concentration;

α_0 = mean nutrient concentration determined from monthly HRPB nutrient data;

α_1 and β_1 are coefficients with units of concentration;

x = time in days.

This equation and the results from such treatment of data have already been described in section **6.2.1.1**.

Only nitrate and phosphate concentrations in freshwater could be obtained using this method since no silicate data was available from the HRPB. Therefore the freshwater silicate concentration had to be estimated and a constant average value of 13.78 μM was used based on measurements made at 0 m depth at the most northerly station, LL19, during the 1991 field season (see **CHAPTER 5**, section **5.2.1.2**). This is obviously a more inaccurate estimate than that for the nitrate and phosphate concentrations in the end-members but it was deemed adequate for investigation into the biogeochemical processes in the bottom-waters, since the original source of nutrients to the bottom-waters would be in the denser saline input as opposed to the freshwater input (although some mixing down of freshwater might be expected at the sill).

Nutpro.prn/nutlin.prn: **Nutpro.prn** and **nutlin.prn** are two different files which contain the nutrient profiles which are used to initiate the model. The reason that there are two different files is that they contain nutrient profiles which are compiled in different ways: **Nutpro.prn** contains the profiles of NO_3, PO_4 and SiO_4 concentrations based on nutrient measurements made at discrete depths throughout the water column (0, 5, 10, 20, 40, 60, 80, 100, 106 m) on the first day of the field-season (day 59 in the case of the nutrients). These profiles were compiled through the linear interpolation between the data points to give profiles with a depth interval of 1 m. **Nutpro.lin** contains the nutrient profiles with data at depth intervals of 1 m but which are simulated conservative profiles. This means that the nutrient data has been forced to be linear with the recorded salinities throughout the water column so that the only observed nutrient concentration data to be used is that found at 0 m on day 59.

All other settings in the model are the same as those used in the physical model although the number of time-steps had to be changed in the Linnhe.run file to account for the fact that Julian days 56 - 59 were missing for the nutrient concentration data and the phase of the tidal cycle was correspondingly altered to 4.284.

7.6.1.2 Results from the Nutrient Model run with Nutpro.prn for the Initial Profiles

The model was initially run with the data files in **nutpro.prn** entered as the original profiles. Knowing that the model predicted salinity accurately within 1 PSU below 52 m depth, the model was set so as to output data from (a) 0m and (b) 60 m downwards to 110 m (to coincide with the nutrient data collected at 60 m and downwards). From these output files (a) contour maps of the predicted nutrient distribution timeseries could be obtained using the UNIMAP software (details of the UNIMAP settings are given in **APPENDIX 7.4**) and (b) regression analyses could be carried out within the QUATTRO PRO software package to investigate the variance of the predicted nutrient concentrations relative to the variance of the predicted salinity below 60 m (within the limits of the 1 PSU salinity prediction), respectively.

To carry out these regression analyses, data points were used from the predicted profiles from 60 m downwards for the total time-period (4080 data points) and the coefficient of determination (r^2) was obtained. The value of r^2 therefore provides a measure of how much of the variance of nutrient concentrations can be explained by a linear regression of their concentrations on salinity and will be equal to 1 if the nutrients behave entirely conservatively and there are no processes that can lead to apparent non-conservative behaviour occurring in the model.

FIGURES 7.14 (a), (b) and **(c)** show how results from the model can be used to predict nutrient distributions and their changes with time at station LL14 in the loch. By comparison with the corresponding observed nutrient time-series plots

FIGURE 7.14 (a)

Comparison between Model Predicted and Observed Nitrate Data (Micromolar) for Station LL14, Julian Day 60 to 139, 1992.

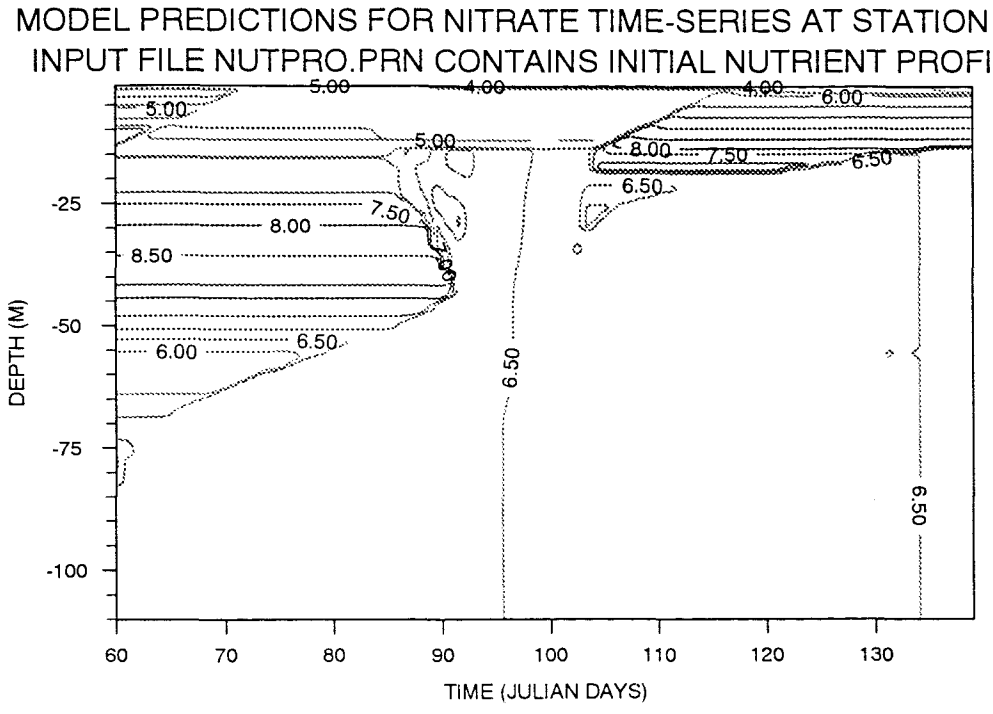

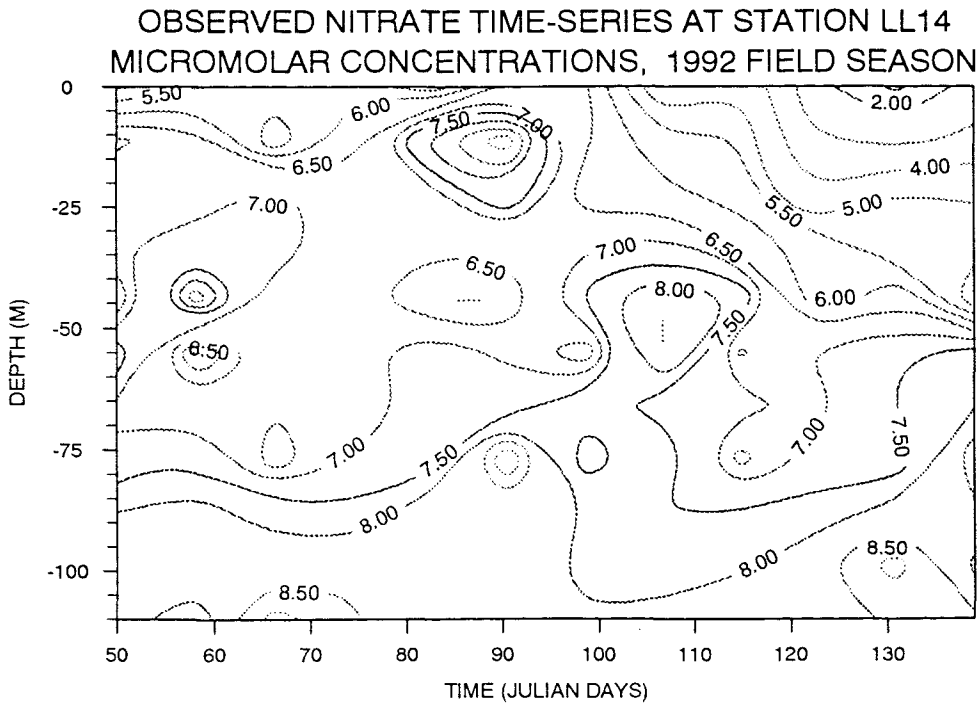

FIGURE 7.14 (b)

Comparison between Model Predicted and Observed Phosphate Data (Micromolar) for Station LL14, Julian Day 60 to 139, 1992.

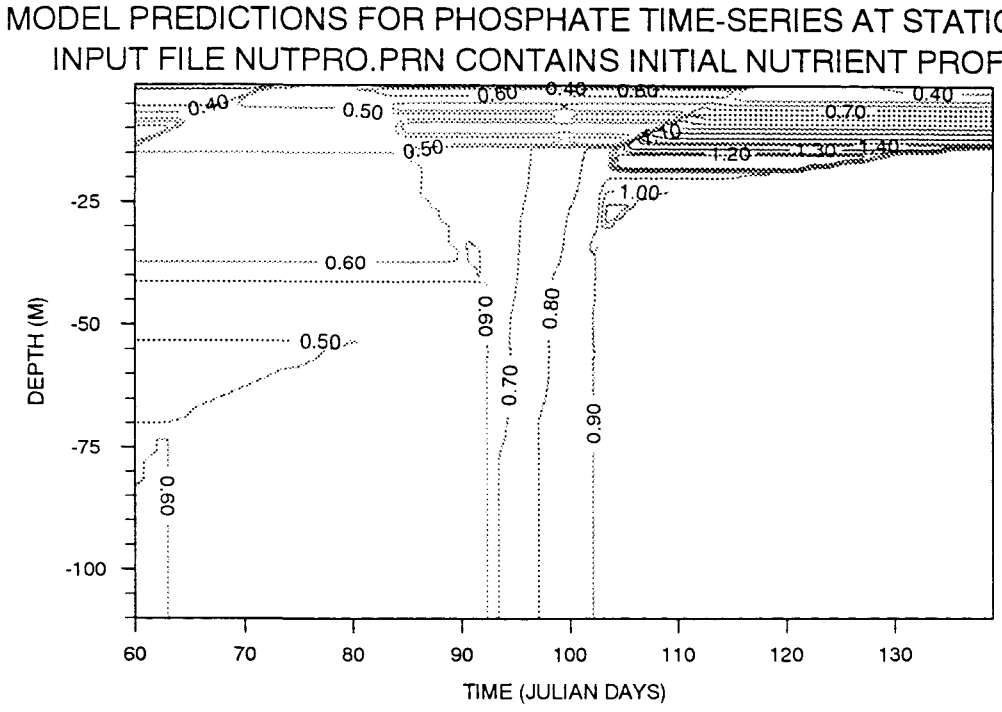

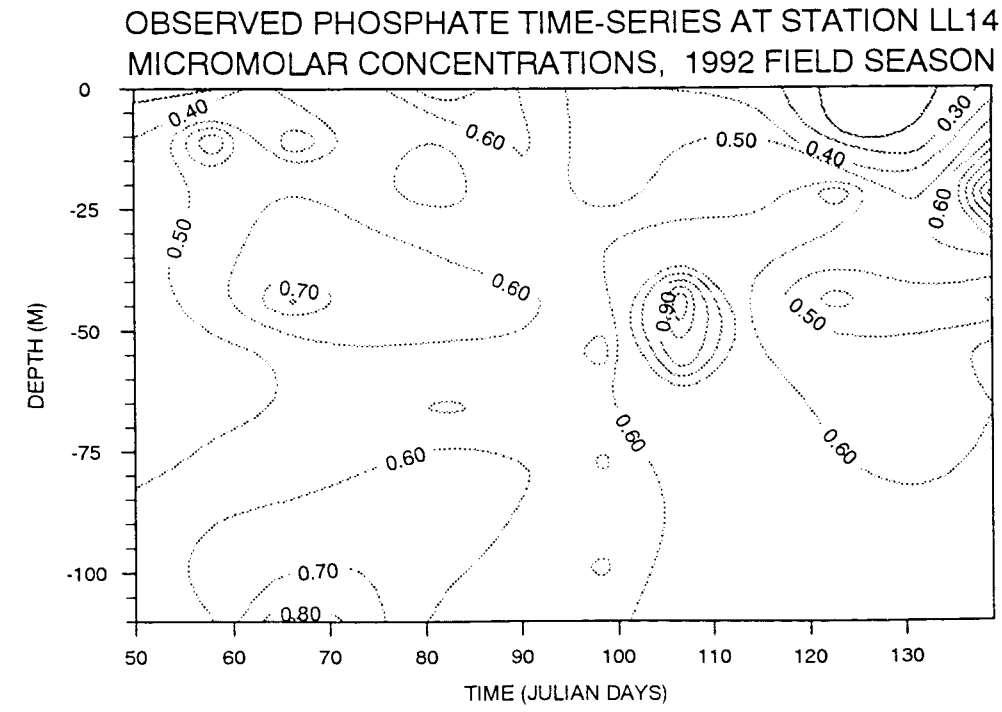

FIGURE 7.14 (c)

Comparison between Model Predicted and Observed Silicate Data (Micromolar) for Station LL14, Julian Day 60 to 139, 1992.

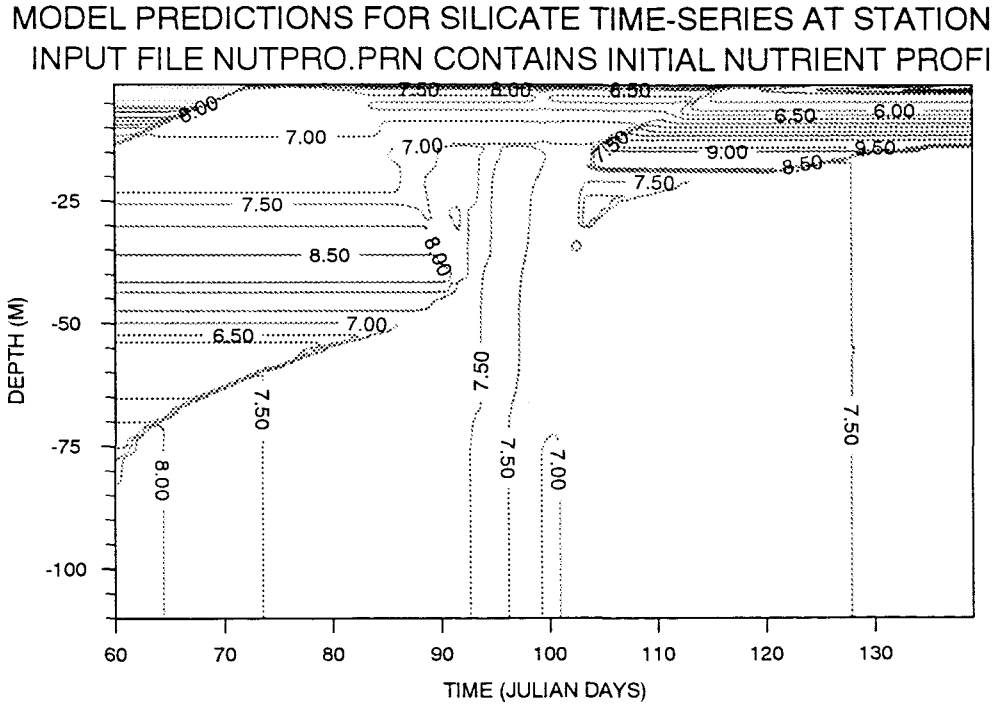

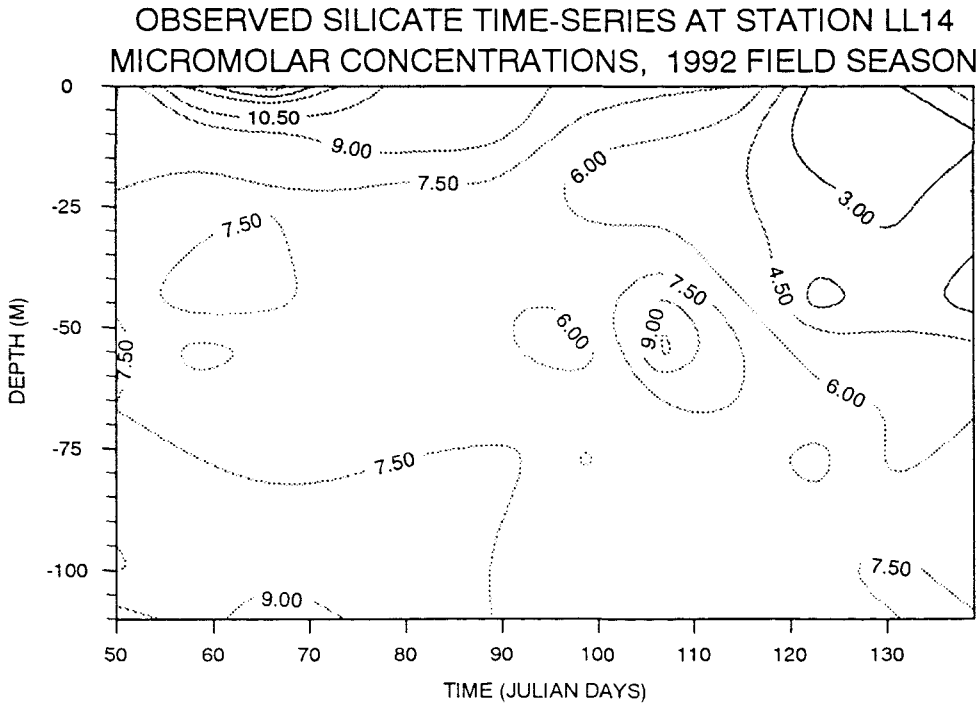

also shown in these figures, (all UNIMAP settings are kept constant for the model and observed results), it is clear that notable differences exist between the model predicted and observed nutrient concentrations in the isolated bottom-waters. For example, between day 60 and day 70 an increase in the observed concentrations of all three nutrients is observed at depths greater than 100 m, with the NO_3 concentrations increasing to > 9.0 μM, PO_4 concentrations increasing to > 0.9 μM and SiO_4 levels increasing to > 9.0 μM (see **CHAPTER 6**, section **6.2.1.2 (ii)**). The observed and predicted SiO_4 concentrations are generally of similar magnitude in concentration in the bottom-waters, 7.5 - 8.0 μM, indicating that the saline input of SiO_4 is more important in the bottom-waters than the freshwater inputs, since the freshwater inputs are inaccurate being set as constant in the model, at 13.78 μM. Such increases are not present in the model results, where the only changes in the bottom-water concentrations are due to diffusive processes (shown in section **7.6.3**). Hence the increases are likely to be due to biogeochemical processes as was suggested in **CHAPTER 6**. Also the complexity of the contour maps produced from the observed data as compared to those for the model results, emphasizes the roles of temporally varying end-member concentrations and their incomplete mixing relative to the flushing time of the system, plus biogeochemical processes in the definition of the nutrient distributions in such a system. Such comparisons between the time-series data can only be qualitative however, since problems are found to arise when quantitative analyses are performed on these model results.

From regression analyses of predicted nutrient concentrations on predicted salinity data (within the limits of the 1 PSU salinity prediction), the following results are obtained:

	NO_3	**PO_4**	**SiO_4**
r^2	0.29 %	0.96 %	0.00 %
% explained variance	29 %	96 %	0 %
% unexplained variance	71 %	4 %	100 %

These results would suggest that 71 %, 4 % and 100 % of the variance of the concentrations of NO_3, PO_4 and SiO_4 respectively cannot be explained by variations

in the salinity. These results seem erroneously high for SiO_4 and NO_3. A likely reason for this is that the initial nutrient profiles in **nutpro.prn** do not themselves correspond to a linear relationship with salinity and this is illustrated in **FIGURE 7.15**. Thus 62 %, 39 % and 20 % of the variances in the NO_3, PO_4 and SiO_4 concentrations, respectively, are unexplained by the variance in salinity. Hence the model, on reading these files in, effectively assigns nutrient concentrations corresponding to particular salinity values on a basis which incorporates a considerable degree of apparent and real non-conservative behaviour. So, although the nutrients behave conservatively once read into the model because they follow exactly the same mixing patterns as the salinity in the water column, this conservative behaviour is not reflected in the results because of the departure from linear behaviour assigned at the point of reading in the nutrient profiles. The procedure is therefore internally inconsistent in that degrees of apparent and real non-conservative behaviour are incorporated into the model before it starts carrying out its commands on the data. This means that a comparison of the predicted and observed nutrient contours over time will only be informative if the starting condition for the comparison can be identified under which the nutrient distributions are close to linear. This is most likely to be the case after a deep-water renewal event when the water column is well mixed.

7.6.2 Running the Model with Nutlin.prn for the Initial Profiles: Estimation of the Degree of Apparent Non-Conservative Behaviour

In order to solve the quantitative problem discussed in section **7.6.1.2**, it was decided to make up input profiles for each nutrient which were linear with salinity and to run the model again. As mentioned in section **7.6.1.3** this involved using the nutrient and salinity data measured at 0 m at station LL14 on day 59 and calculating nutrient concentrations at 1 m depth intervals in such a way that their concentrations varied in a 1:1 relationship with the salinity. Thus the r^2 value for these profiles was 1 as was the gradient of the plots of nutrient concentration against salinity (except SiO_4 where the gradient was -1). These profiles were read into the model from the file **nutlin.prn**.

FIGURE 7.15

Relationships of Nutrient Concentrations with Salinity in Input File nutpro.prn

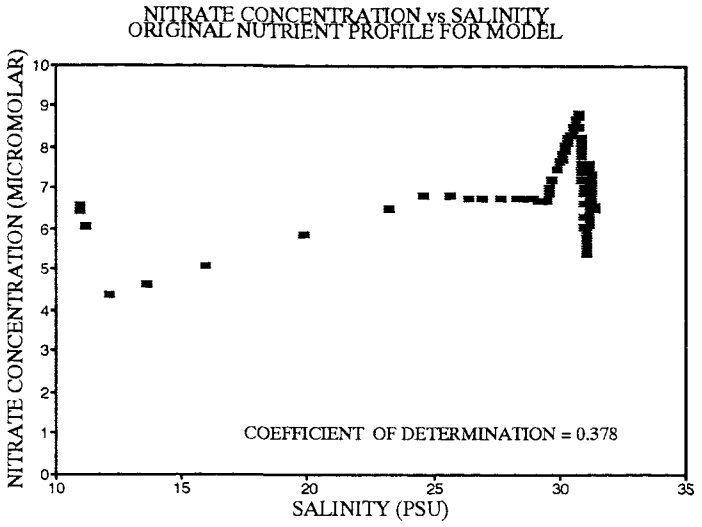

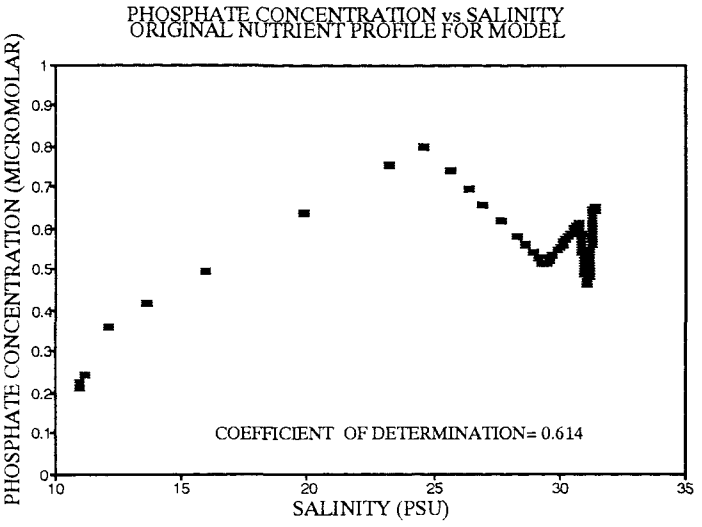

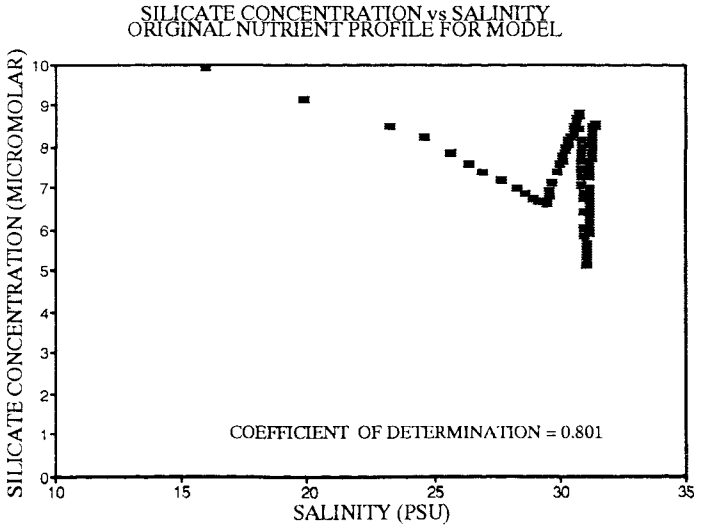

By running these conservative profiles through the model the nutrients will behave conservatively throughout the basin as before and r^2 will be equal to 1 if the boundary conditions are constant. Any deviation of r^2 from 1 will be due to temporally varying end-member concentrations which produce a non-steady-state condition and consequent deviations away from the initial TDL.

Results from this run are:

	NO_3	PO_4	SiO_4
r^2	0.90	0.97	0.89
% explained variance	90 %	97 %	89 %
% unexplained variance	10 %	3 %	11 %

These results show that by initiating the model with a linear conservative profile (nutrient concentration:salinity = 1:1) the temporal variations in the end-member concentrations give rise to 10 %, 3 % and 11 % of the variance of NO_3, PO_4 and SiO_4 concentrations respectively (below 60 m).

Since the same number of data points are used in the regression analyses for the two aforementioned runs of the model, the r^2 values obtained for the results can be compared. From such a comparison it can be said that for the initial run of the model 61 %, 1 % and 89 % of the unexplained variance for NO_3, PO_4 and SiO_4 respectively was attributable to the scatter caused by the non-linearity in the nutrient-salinity relationship in the original profiles in **nutpro.prn**.

Having obtained an estimate of the contribution of apparent non-conservative behaviour to the deviations from the model TDL, this estimate can now be applied to the observed nutrient behaviour at depths below 60 m for the 1992 field season.

FIGURE 7.16 shows the relationships of observed NO_3, PO_4 and SiO_4 data with salinity at station LL14. Regression analyses of these relationships give the following results:

FIGURE 7.16

Relationships of Observed Nutrient Concentrations with Salinity at Station LL14, 1992.

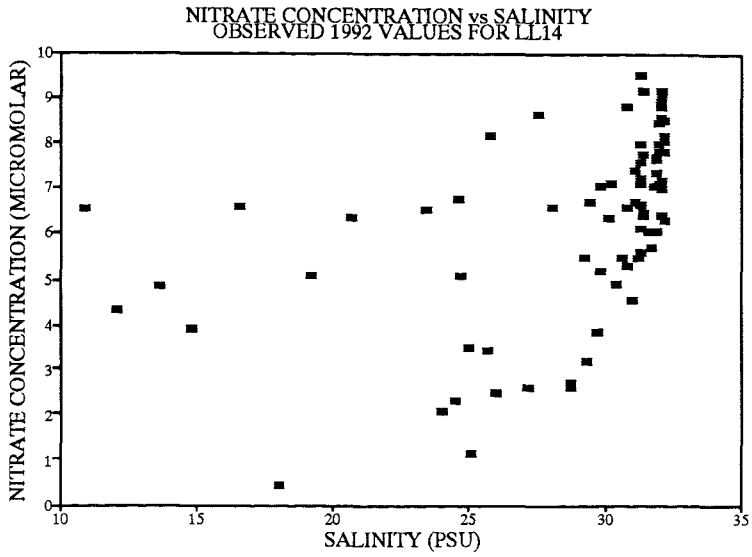

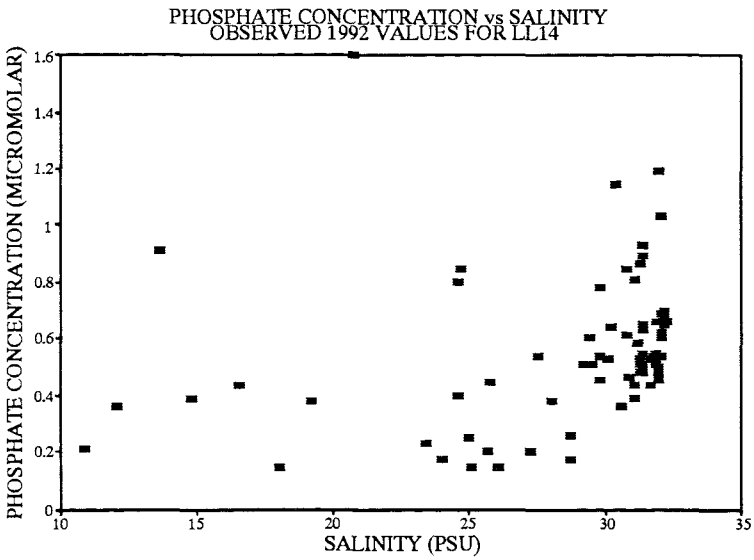

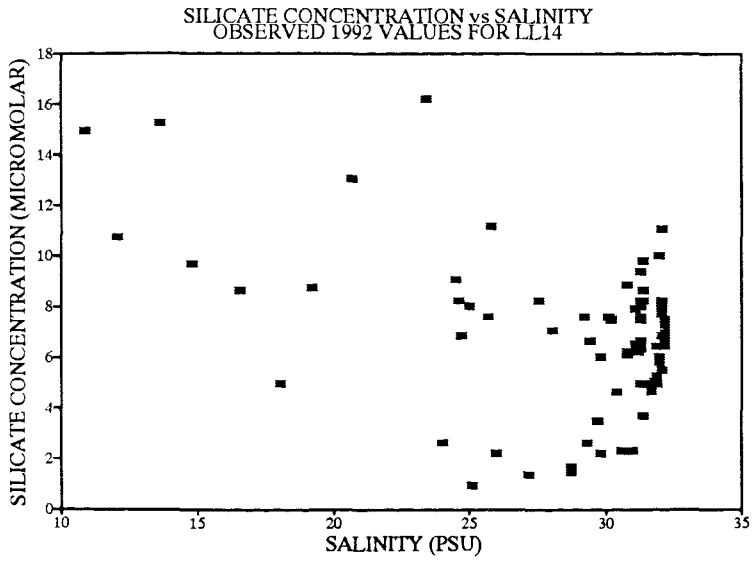

	NO_3	PO_4	SiO_4
r^2	0.025	0.005	0.030
% explained variance	2.5 %	0.5 %	3 %
% unexplained variance	97.5 %	99.5 %	97 %

Thus below 60 m, 97.5 %, 99.5 % and 97 % of the variance of the observed NO_3, PO_4 and SiO_4 concentrations is due to some process other than the variation in salinity. If it is assumed, for illustrative purposes, that the fractions of the variances attributable to the temporal variations in the end-member concentrations are equal to those estimated in the previous section (namely 10 %, 3 % and 11 % for NO_3, PO_4 and SiO_4 respectively) then the results would suggest that fractions of 88 %, 96.5 % and 86 % of the respective variances arise from real, as distinct from apparent non-conservative processes.

7.6.3 Using the Model to Investigate the Isolated Bottom-Waters

The biogeochemical processes mentioned above are likely to modify the properties of the isolated bottom-waters of the system, which will exist below depths of 81 m (see section **7.4.1.2**) during the time leading up to the deep-water renewal. As a pre-requisite to attempting to quantify these biogeochemical processes a check was run on the proper operation of the model as regards nutrients, to make sure that only diffusive processes could cause changes in the nutrient concentrations in the bottom-waters. This was achieved by running the model with the conservative initial profiles in **nutlin.prn** and then running regression analyses on the results obtained below 81 m up to and including day 93, the day before the deep-water renewal event. Results were as follows:

	NO_3	PO_4	SiO_4
r^2	0.999984	0.999968	0.999984
% explained variance	100 %	100 %	100 %
% unexplained variance	0 %	0 %	0 %

Therefore the nutrients are behaving entirely conservatively with the salinity

changes through diffusive processes in the bottom-waters, before the deep-water renewal, indicating that the temporally varying end-member concentrations have no effect on the bottom-waters. (Data from day 94, after the renewal event give reduced r^2 values for NO_3, PO_4 and SiO_4 of 0.3281, 0.1160 and 0.2948 respectively).

7.6.4 Estimation of the Degree of Non-conservative Behaviour in the Isolated Bottom-Waters

Knowing that r^2 will be equal to 1 if the nutrients behave entirely conservatively in the isolated bottom-waters and that the only process to affect their concentrations is that of diffusion, it is possible to make a limited analysis of the degree of biogeochemical behaviour occurring in the bottom-waters. The reason that the analysis is limited is that the problem again arises that r^2 will only be equal to 1 if the diffusion is occurring within a profile which originally has an r^2 value of 1, i.e. the initial situation must be defined by a linear relationship between the nutrients and salinity. With this in mind, changes in the observed nutrient concentrations relative to the changes in salinity over time have been examined at a constant depth (105 m) in the bottom-waters, using regression analysis. Assuming that the rate of diffusion of nutrients is equal to that of salt, then any deviation of r^2 from 1 will be due to biogeochemical processes and $(1-r^2)$ will give an approximation of the extent of these processes. Results from these regression analyses are as follows:

	NO_3	PO_4	SiO_4
r^2	0.03	0.1	0.17
% explained variance	3 %	10 %	17 %
% unexplained variance	97 %	90 %	83 %

These results show that at 105 m, 97 %, 90 % and 83 % of the variance in NO_3, PO_4, SiO_4 concentrations cannot be explained by diffusion or by temporally varying end-member concentrations. This unexplained variance is therefore likely to be due to biogeochemical processes occurring in the water column. These reflect sources of nutrients to the system (the above analyses show positive gradients). It

should be noted however that these results are based on only 4 data points representing 4 days before the renewal event for which nutrients were measured at 105 m.

7.7 Summary and Conclusions from the Nutrient Model Results

(1) The physical model has been successfully adapted to accommodate nutrient distributions to the Linnhe basin system. The model assumes the nutrients to behave conservatively with salinity once inside the basin, but the end-member nutrient concentrations are allowed to vary temporally. It thus allows prediction of any apparent non-conservative behaviour, attributable to temporal variability in end-member composition

(2) Using observed data as the starting point for the model, only qualitative deductions concerning the extent of genuine non-conservative behaviour can be made from the comparison of observed and model contour plots. This is because degrees of apparent and real non-conservative behaviour are incorporated into the model at the start through its initiation with the observed nutrient profiles.

(3) Using a simulated linear profile to initiate the model (where nutrient concentrations : salinity = 1:1), quantitative estimates of the contribution of temporally varying end-member concentrations (apparently non-conservative behaviour) to the observed scatter away from a TDL may be made. For depths greater than 60 m for the 1992 field-season such contribution is estimated at 10 %, 3 % and 11 % to the total observed scatter for NO_3, PO_4 and SiO_4 TDLs, respectively.

(4) The model has been used to show how only diffusive processes can affect the isolated bottom-water nutrient concentrations during the period leading up to the deep-water renewal event; temporally varying end-member concentrations do not affect these waters. Hence quantitative estimates of the contribution of biogeochemical processes to observed scatter has been made possible with the

result that up to 97 %, 90 % and 83 %, of the NO_3, PO_4 and SiO_4 behaviour in the isolated waters at 105 m, can be attributed to biogeochemical processes, resulting in inputs of nutrients to the system. This analysis required consideration of nutrient changes over time at a constant depth and could be greatly improved in terms of its accuracy if more data was available, through increasing the sampling frequency in the loch.

7.8 Overall Summary and Discussion

The results in this chapter have shown how a simple 1-D box model, originally written to reproduce hydrographic features of the Clyde Sea area, has been successfully adapted and developed to reproduce hydrographic features in the upper basin of Loch Linnhe, providing a tool for the study of nutrient distributions in the system. In terms of the physical features of the loch, the model reproduces the salinity field observed during the 1992 field-season to within ± 1 PSU for depths greater than 52 m. The model is particularly useful in that it accurately predicts the timing of the deep-water renewal event, given only an initial hydrographic profile and varying end-member properties and meteorological conditions. This predictive capability is important if the renewal event is a significant contributor to the timing of the phytoplankton bloom in the loch, as was suggested in **CHAPTER 6**. The fact that the model cannot accurately reproduce observations in the top 20 m of the water column is indicative of the inability of the model to simulate retention of freshwater in the system. This is because the model is only 1-dimensional and so cannot simulate the directional effect of the wind. This supports the hypothesis put forward in **CHAPTER 6**, section **6.1.2.2** that the direction of the wind is fundamental in the wedging of freshwater up the loch, thus explaining the increase in the residence time of the freshwater in the system for the period leading up to the deep-water renewal event.

The model has also shown that temperature variations within Loch Linnhe are negligible in terms of their role in defining the hydrographic regime of the system.

The model has successfully reproduced hydrographic observations, for depths > 52m, in Loch Linnhe for 2 different years for which the meteorological conditions were distinctly different. This indicates that the model is robust in reproducing the correct salinity field for the Linnhe system, given certain limits of accuracy for varying depths: an accuracy to between ± 1 PSU for depths below 52 m; ± 1.5 PSU for depths below 50 m and ± 2 PSU for depths below 36 m.

From this basis the model has been successfully developed further to incorporate nutrients into the system. The model can be used to predict changes in the nutrient concentrations over time, on the assumption that behaviour within the basin is conservative. It successfully takes account of apparent deviations from conservative behaviour arising from temporal variability in the end-member concentrations. In terms of the isolated bottom-waters in the system, the model has shown that only diffusive processes can alter the nutrient concentrations in these waters and that this process is a conservative one. Any deviations way from this conservative behaviour have therefore been attributed to biogeochemical processes in the bottom-waters, since the model results showed that the temporally varying end-members do not penetrate the bottom-waters. Such biogeochemical processes leading to the increase of nutrients in the bottom-waters of Loch Linnhe will ultimately increase the nutrient levels in the euphotic zone, after the deep-water renewal event for example which may have important implications for the timing of the bloom as discussed in **CHAPTER 6.**

While the work has demonstrated the potential of the model as a tool for better understanding of processes affecting nutrient distributions, some limitations are evident. The most important is that the starting condition of the model must involve a conservative (linear) nutrient profile in order that any quantitative estimates can be made on the degrees of deviation of nutrient distributions away from conservative behaviour, caused by various processes. Such a profile can be simulated for the model for this purpose but in a real world situation such linearity of nutrient concentrations with salinity is only likely to be observed when the system has been well-mixed, after a deep-water renewal event for example.

Hence the model cannot be used to realistically predict the nutrient distributions in the Loch Linnhe system for the majority of the time, since renewal events in Loch Linnhe are not a continual feature in the hydrography.

Further work should include:

(1) Incorporation of the directional effect of the wind either by making the model 2-dimensional or, more simply, by developing an algorithm which will allow for the prediction of the degree of freshwater retention in the system given varying meteorological conditions;

(2) Improvement of the accuracy of the predictions of the temporal changes in nutrient concentrations by using a higher resolution nutrient profile to initiate the model e.g to use a profile in which there are values at 5 m depth intervals. Also an observed data-set with as high a sampling frequency as possible is recommended to improve the basis for comparisons between the model predicted and the observed results.

In conclusion, this part of the study has demonstrated the potential through the use and development of existing hydrographic models, to gain information on the processes that determine the nutrient distributions in estuarine systems. While the resulting model from this study has limitations, as already discussed, it has allowed some degree of quantitative analysis of processes which, previously, could only be suggested as affecting the variance of the nutrient behaviour in the water column. The logical sequence of steps embodied in the model provides a sound basis for future model development.

CHAPTER 8 CONCLUDING DISCUSSION

The aim of this research has been to investigate the roles of hydrographic and biogeochemical processes in the distribution of nutrients in a sea-loch.

It has been shown that in a sea-loch system, although non-conservative behaviour will cause changes in the nutrient distributions through changing the nutrient concentrations, it is ultimately the hydrographic processes themselves that determine where, and to what extent, these biogeochemical processes can occur and thus have a more determinant effect on the distribution of the nutrients in a sea-loch system.

It has been shown that for such a system complications arise in interpretation of mixing diagrams and the simple, two end-member, steady-state model conventionally employed for such estuarine nutrient studies. This is because such one-dimensional, steady-state conditions do not exist in a sea-loch system due to the complex circulation and hydrography which are set-up. These lead to extended flushing times such that the end-member concentrations being input to the loch vary within this flushing time and the bottom-waters can become isolated, giving rise to the presence of more than two-mixing types on a mixing diagram. This results in scatter about the theoretical dilution line on the mixing diagram, i.e. non-linearity of nutrient concentrations with salinity. Such deviations from non-linearity are normally attributed to non-conservative behaviour when using mixing diagrams since in a simple steady-state, two end-member model the assumption is that a linear relationship between nutrient concentrations and salinity exists in the absence of non-conservative behaviour. However, in Loch Linnhe this is not the case and such deviations from linearity do not necessarily indicate non-conservative behaviour since they are a consequence of the circulation and hydrography set up as mentioned previously. Such behaviour is referred to as apparent non-conservative behaviour and it is essential that apparent (caused effectively by the hydrography of the system) and real non-conservative behaviour (caused by biogeochemical processes) be distinguished from each other if the correct interpretation of mixing diagrams is to be carried out.

The study has therefore focused mainly on identifying the processes, and the factors that govern them, that produce non-linear relationships between nutrients and salinity, with the ultimate aim of quantifying and distinguishing between those that lead to real non-conservative behaviour and those that lead to apparent non-conservative behaviour. Such a study is important for the prediction of nutrient distributions in systems which ultimately affect the concentrations and ratios of nutrients and hence, potentially the phytoplankton populations and their productivity, in the adjacent coastal waters and in the systems themselves. The study has shown that deviations from linearity are caused by:

(i) Apparent non-conservative behaviour, brought about by temporal changes in the concentrations of nutrients being input introduced by both the saline and the freshwater end-member sources; changes that occur within the flushing time of the system. Variations in the freshwater end-member concentrations of nitrate and phosphate have been shown to have a stronger correlation with the annual regime (i.e. seasonal effects) than with riverine flow, with the freshwater nitrate concentrations showing quite marked seasonal patterns. The freshwater phosphate concentrations do not, however, have a strong correlation with either the annual regime or with riverine flow which is attributed to its high geochemical reactivity in natural waters. Temporal variations observed in the saline end-member concentrations of all three of the nutrients studied (nitrate, phosphate and silicate) can be attributed to: (a) advection of temporally varying concentrations from the adjacent coastal regions; (b) advection of high salinity, nutrient rich waters during the process of upwelling seaward of the sill; (c) biogeochemical processes occurring in the shallow, dynamic sill region and possibly (d) the temporally varying freshwater component present, diluting the saline end-member

(ii) Real non-conservative behaviour, brought about by biogeochemical processes affecting the waters within the mixing series and which involve a phase change from dissolved to solid (resulting in a sink of nutrients) or from solid to dissolved (resulting in a source). In Loch Linnhe this has been shown to occur via (a) biological activity with the formation of a spring phytoplankton bloom consisting

of diatoms, thus resulting in removal of nutrients from the surface layers and constituting a sink for the nutrients; (b) the regeneration of nutrients from the sediments to isolated overlying bottom-waters, via microbial oxidation and redox processes in the sediments; (c) geochemical reactivity of phosphate and its removal from the dissolved to the solid phase by adsorption onto fine-grained clay minerals containing surficial iron oxide coatings.

The main hydrographic and circulatory features shown to occur in Loch Linnhe and which can affect these biogeochemical processes and the nutrient distributions are:

(i) Vertical stratification of water in the upper basin according to its density (and hence salinity) set up due to a horizontal type of circulation caused by the presence of the sill at one end and the barotropic freshwater flow from the other end. Because the main source of nitrate and phosphate is from the saline end-member (high salinity water) and that of silicate is from the freshwater end-member (low salinity), such vertical stratification will affect the nutrient distributions with the nitrate and phosphate concentrations generally increasing with depth and those for silicate decreasing. Also the distribution of nutrients in the surface layers has been found to be a function of distance from the freshwater source due to its mixing with saline water.

(ii) Deep-water renewal events inside the basin. Partial and deep-water renewal events have been observed, with the shallower and fresher areas of the loch undergoing replacement of their bottom-waters by inflowing, saline water more frequently than the deeper more saline areas. Deep-water renewal events have been shown to be an important way of upward displacement of high salinity water with associated nutrient concentrations to the surface layers of the loch and, have been suggested to be linked to the triggering of biological activity i.e. phytoplankton growth, in the euphotic zone. Also because the deep-water renewals have been shown to be intermittent, occurring close to spring tides, dry weather and upwelling events seaward of the sill caused by a change in wind

direction, they allow for a period of isolation of the bottom-waters from the incoming waters, during which biogeochemical processes and exchanges between the sediments and the overlying waters can occur with the subsequent accumulation of nutrients in the bottom-waters.

(iii) Density currents generated in the sill region and those set up at the head of the loch by the inflowing freshwater, result in the transport of finer-grained sediments to the centre of the loch. These clay minerals have phosphorus associated with them which is most likely to be due to scavenging of dissolved inorganic phosphate from the water column during transport processes of the sediments. An increase in the phosphorus concentration of the sediments is thus observed in the centre of the loch where the currents are diminished and the percentage of finer-grained particles in the sediment is increased.

Having identified the main hydrographic and biogeochemical processes that could lead to a non-linear nutrient/salinity relationship in a sea-loch, it was then attempted to investigate these processes with a more quantitative approach. This was achieved through the use of a one-dimensional box model originally written for the Clyde Sea area. This model was adapted for Loch Linnhe so that it could adequately reproduce the density and salinity structures of the upper basin for two field-seasons; that carried out in 1992 and a more intensive and meteorologically contrasting one carried out in 1990. It was found that given only an initial hydrographic profile and the variations in meteorological conditions, the model could reproduce the salinity fields to within ± 1 PSU of the observations for depths of greater than 52 m which includes the isolated bottom-water depths from the 1992 field season (greater than 75 to 80 m) and, very significantly, the model could also accurately predict the timing of the deep-water renewal events for both the years. This predictive capability is particularly useful if there is a link between the deep-water renewal events and the timing of the bloom, as suggested by the present observations. It was also shown that the hydrography of the top 20 m of the water column in the basin could not accurately be reproduced accurately by the model and this was attributed to a deficit of freshwater in the model

predictions caused by the inability of the model to simulate the directional effect of the wind i.e. the retention of freshwater in the system by a wedging effect, since the model is only one-dimensional. From the field observations it was suggested that the reason for the upwelling at the sill prior to the deep-water renewal event was that prior to the event a south-westerly wind was blowing up the loch thus causing a retention of freshwater in the loch and in the sill region, reflected by an increase in the residence time of the freshwater in the centre of the loch. This was then followed by a change in wind direction which allowed the freshwater to escape with the subsequent upward displacement of the pycnocline through a height of 20 m outside the sill. Thus the model supports this sequence of events to some extent, through its inability to simulate the directional variability of the wind reflected by a freshwater deficit in the surface layers.

Having successfully adapted the model for the hydrographic data, it was then adapted to incorporate nutrient data, given conservative behaviour in the basin. The data set tested in the model was that collected during the 1992 field-season. From this part of the study it was found that for depths of greater than 60 m the temporally varying end-member concentrations, leading to apparent non-conservative behaviour, could account for up to 10 %, 3 % and 11 % of the variability in the relationship with salinity for nitrate, phosphate and silicate respectively. For depths of 105 m, over the period of bottom-water isolation, it was estimated that 97 %, 90 % and 83 % of the variability in the relationship with salinity of nitrate, phosphate and silicate respectively, could be attributable to biogeochemical processes, i.e. to real non-conservative behaviour. It was thus shown that, although rather limited, the model could be used to give some degree of quantification of the different categories of process that would give rise to non-linearity of nutrients with salinity in a sea-loch system.

An aspect of the present work that would particularly merit further investigation is the hypothesis that the timing of the spring phytoplankton bloom is related to a deep-water renewal event which, as discussed above, may be triggered by a change in wind direction: A south-westerly wind blows persistently up the loch

prior to the renewal event retaining freshwater in the system and, this is followed by a change in wind direction with the subsequent upward displacement of the pycnocline seaward of the sill resulting in the uplift of high salinity, nutrient rich water over the sill and into the basin causing a deep-water renewal event and triggering a phytoplankton bloom in the surface layers of the basin. This sequence of events could be easily investigated via high frequency sampling of hydrographic, biological and meteorological parameters over the spring months on a yearly basis. This could be achieved through deployment of InterOcean Systems electromagnetic S4 current meters, attached to a mooring, at discrete depths above the sea-bed at a deep station in the sea-loch e.g. station LL14. These current meters will detect any water movement at increased depths caused by renewal events and since this type of current meter can incorporate temperature and conductivity probes also, density changes at different depths caused by renewal events can also be detected. A fluorometer should be attached to the mooring in the surface layers to allow for the measurement of chlorophyll in the water and a meteorological buoy deployed alongside the mooring for the simultaneous measurement of wind velocity and direction. A land-based annenometer would also be of use for comparison between the meteorological buoy measurements and those collected on land (which would be less expensive). If the hypothesised sequence of events is found to occur every year prior to the spring bloom, then the timing of this bloom in Loch Linnhe could be estimated through the timing of the deep-water renewal predicted by the one-dimensional model developed in this study. Simple adaptations of the model for different sea-lochs would make this model very useful in the context of fish-farming since the timing of the bloom could be predicted from observed hydrographic and meteorological changes thus allowing the fish-farmer to re-site cages if necessary, as mentioned in the **INTRODUCTION**. It should be noted, however, that in order for the bloom to occur there also has to be enough light and stability in the euphotic zone to sustain algal growth. It would of interest to see how important these factors are relative to the presence of increased nutrient concentrations, introduced by the renewal event.

With further improvements of the model such as were suggested at the end of

CHAPTER 7, the hydrography of the surface layers of the loch may also be simulated. The model could then be adapted to incorporate chlorophyll data which is possible if it is introduced with the saline boundary conditions thus simulating seeding by algal cells being swept in from the Firth of Lorne. A comparison between the predicted chlorophyll distributions (which must assume conservative behaviour with salinity) and observed data might then yield some information on productivity rates versus export of cells via grazing sedimentation and advection of water. This is because any difference between the model predicted and observed chlorophyll concentrations must be due to factors other than the physical distribution of algal cells i.e. primary production and export processes. If the observed data are higher than those predicted by the model then the primary productivity rates must exceed the rate of export and if they are lower then vice versa. Such a quantitative investigation into processes in the euphotic zone are likely to be more straightforward than that undertaken for nutrients throughout the whole water column in this study, because the starting condition for the model in terms of chlorophyll distributions will be less complicated. At the start of the field season the initial profile will contain zero concentrations throughout the whole water column indicating independence of salinity (and an r^2 value of zero for a regression analysis of chlorophyll concentrations on salinity). As the chlorophyll data are input to the model via the saline boundary condition, they will begin to act completely linearly (and conservatively) with salinity so that as the model progresses r^2 tends towards one (although it will never be equal to one because of the independent nature of the chlorophyll regression below the euphotic zone). If only the top 10 m is considered, however, then the probability of r^2 being equal to one at some point during the execution of the model (probably when chlorophyll concentrations are at their maximum values) is increased so that information can then be gained by comparison with observed data.

Leading on from here, the model could then be adapted to link this net primary productivity information to predicted nutrients and nutrient ratios in the surface layers so as they are altered proportionally to simulate the effects of non-conservative behaviour as observed in the surface layers. Once this has been

achieved there is scope for investigating possible changes in phytoplankton species given information on the tolerance of different species to different nutrient ratios.

Another aspect of this work has shown that future observational programmes designed to investigate the behaviour of dissolved inorganic phosphate in a sea-loch environment could yield some useful information for the interpretation of phosphate data and to aid the prediction of its behaviour in such systems. It is suggested that three programmes could be carried out:

(i) At the freshwater end of the loch to determine the relative concentrations of phosphorus entering the system in the colloidal, adsorbed and dissolved inorganic phases. This information can then be linked to the variables of Fe and DOM concentrations, suspended solid loadings, mineralogical content of the SPM, and pH all of which should be investigated in terms of their correlation with the annual regime;

(ii) On variations in dissolved inorganic phosphate concentrations in isolated bottom-waters over a significant period of time i.e. months to years (in Loch Etive, for example) to allow for a steady-state to be set up between the sediments and the overlying bottom-waters. These should then be related to the dissolved oxygen concentrations in the water and also to the conditions in the sediments themselves i.e. changes of redox conditions and mineralogical composition of the sediments with depth in the sediments and also phosphate concentrations in the sediment porewaters. This might yield further information on the idea that phosphate concentrations exist in an equilibrium situation between the solid and the dissolved phase, referred to as the phosphate buffer mechanism (see **CHAPTER 2**) and recently suggested as existing between porewater and sediment surface adsorption sites in coastal marine sediments (Sundby *et al,,* 1992). The effects of resuspension events on the concentrations of dissolved inorganic phosphate in the bottom-waters can also be investigated at the end of the isolation period when a deep-water renewal event occurs and relationships with suspended solids loadings can be investigated through the use of a transmissometer;

(iii) A fuller investigation (i.e. more replicate core samples) into phosphorus concentrations and their associations with different elements and grain sizes in sediment as a function of salinity and distance from the source of currents.

Such information obtained from observational programmes is essential if the concentrations of dissolved inorganic phosphate in sea-loch systems are to be predicted by numerical models, since the different parameters that can affect the concentrations need to be assessed in terms of their impact and relationships need to be established numerically so that phosphate concentrations can be estimated from the predictions of other parameters or combinations of parameters.

APPENDICES AND REFERENCES

APPENDIX 4.1

TYPICAL CALIBRATION RESULTS TAKEN FROM A CALIBRATION EXPERIMENT MADE ON 23/07/92

PHOSPHATE RESULTS: CALIBRATION

SAMPLE	A	B	C	D	E	F	G	ASW	DW
CONCENTRATION (MICROMOLAR)	2	1.8	1.6	1.4	1	0.4	0.2		
SIGNAL (mm)	120	115	101.5	102.5	70	49	30.5	23.0	9.0
	122	115	103	91	71.5	44.5	34	22.8	8.8
	116.5	108.5	100	90	69	37.5	36	23.0	8.9
	121	115	102.25	96.75	70.75	46.75	32.25	22.5	8.5
AVERAGE SIGNAL	119.9	113.4	101.7	95.1	70.3	44.4	33.2	22.8	8.8
SIGNAL MINUS (AVE ASW - AVE DW)	106.0	101.0	87.5	88.5	56.0	35.0	16.5		
	108.0	101.0	89.0	77.0	57.5	30.5	20.0		
	102.5	94.5	86.0	76.0	55.0	23.5	22.0		
	107.0	101.0	88.2	82.7	56.7	32.7	18.2		
AVERAGE SIGNAL	105.9	99.4	87.7	81.0	56.3	30.4	19.2		
LINEAR CALIBRATION	105.9	96.3	86.6	77.0	57.7	28.8	19.2		
DIFFERENCE BETWEEN SIGNAL AND LINEAR CAL. (mm)	-0.1	3.1	1.0	4.0	-1.4	1.6	-0.0		
DIFFERENCE BETWEEN SIGNAL AND LINEAR CAL. (MICROMOLAR)	-0.00	0.06	0.02	0.08	-0.03	0.03	-0.00		
STD DEVIATION OF DW BLANK SAMPLES		0.19							
CONVERTING STD DEVIATION TO CONCENTRATION (MICROMOLAR)		0.004							
DETECTION LIMIT (MICROMOLAR) = 3*STD DEVIATION OF DW		0.01							

PHOSPHATE: CONCENTRATION vs PEAK HEIGHT
CALIBRATION OF AUTOANALYSER, JULY 1992

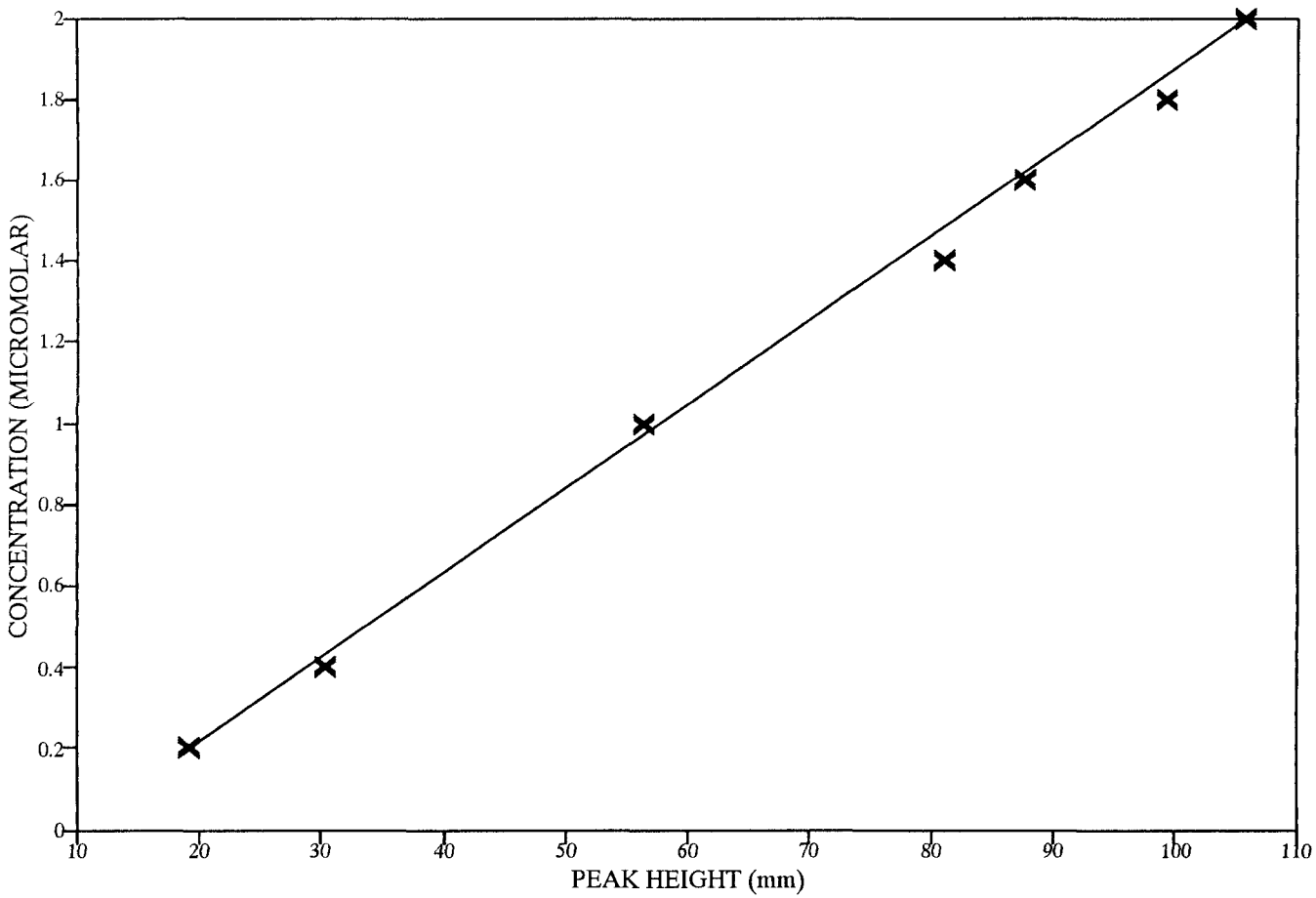

PHOSPHATE RESULTS: PRECISION

SAMPLE	A	B	C	D	E	F	G	
CONCENTRATION (MICROMOLAR)	2	1.8	1.6	1.4	1	0.4	0.2	
SIGNAL (mm)	106.0	101.0	87.5	88.5	56.0	35.0	16.5	
	108.0	101.0	89.0	77.0	57.5	30.5	20.0	
	102.5	94.5	86.0	76.0	55.0	23.5	22.0	
	107.0	101.0	88.2	82.7	56.7	32.7	18.2	
TOTAL SIGNAL (mm)	423.4	397.4	350.65	324.15	225.15	121.65	76.65	
NUMBER OF ANALYSES, n	4	4	4	4	4	4	4	
SQUARES OF DATA	11230.7	10196.0	7651.9	7827.8	3133.2	1223.3	271.4	
	11658.6	10196.0	7916.6	5925.2	3303.4	928.7	399.0	
	10501.1	8925.5	7391.7	5772.2	3022.3	551.1	482.9	
	11443.7	10196.0	7783.7	6843.4	3217.7	1070.9	332.2	
SUM OF SQUARES OF DATA	44834.08	39513.38	30743.78	26368.6	12676.55	3773.978	1485.478	
(TOTAL SQUARED)/n	44816.9	39481.7	30738.9	26268.3	12673.1	3699.7	1468.8	
DIFFERENCE	17.1875	31.6875	4.921875	100.2969	3.421875	74.29688	16.67188	
SUM OF SQUARES	248.4844							
DEGREES OF FREEDOM	3	3	3	3	3	3	3	= 21
QUOTIENT GIVES VARIANCE		11.83						
STD DEVIATION		3.44						
CONVERTING STD DEVIATION TO CONCENTRATION (MICROMOLAR)		0.06						
PRECISION (MICROMOLAR) = (2/SRTQ OF Pi)*STD DEV.		0.07						

TYPICAL CALIBRATION RESULTS TAKEN FROM A CALIBRATION EXPERIMENT MADE ON 23/07/92

NITRATE RESULTS: CALIBRATION

SAMPLE	A	B	C	D	E	F	G	ASW	DW
CONCENTRATION (MICROMOLAR)	10	9	8	7	5	2	1		
SIGNAL (mm)	159.0	144.5	129.5	115.0	79.2	25.0	11.0	7.5	3.5
	160.5	147.5	130.0	116.5	79.0	26.2	12.0	6.0	4.0
	160.5	148.9	132.5	116.9	81.5	27.5	13.0	7.5	3.7
	171.5	146.2	126.0	116.2	81.5	28.3	12.5	6.5	3.9
AVERAGE SIGNAL	162.9	146.8	129.5	116.2	80.3	26.8	12.1	6.9	3.8
SIGNAL MINUS (AVE ASW - AVE DW)	155.9	141.4	126.4	111.9	76.1	21.9	7.9		
	157.4	144.4	126.9	113.4	75.9	23.1	8.9		
	157.4	145.8	129.4	113.8	78.4	24.4	9.9		
	168.4	143.1	122.9	113.1	78.4	25.2	9.4		
AVERAGE SIGNAL	159.8	143.7	126.4	113.1	77.2	23.7	9.0		
LINEAR CALIBRATION	159.8	143.0	126.3	109.5	76.0	25.8	9.0		
DIFFERENCE BETWEEN SIGNAL AND LINEAR CAL. (mm)	0.0	0.7	0.1	3.5	1.2	-2.1	-0.0		
DIFFERENCE BETWEEN SIGNAL AND LINEAR CAL. (MICROMOLAR)	0.00	0.04	0.01	0.21	0.07	-0.13	-0.00		
STD DEVIATION OF DW BLANK SAMPLES		0.19							
CONVERTING STD DEVIATION TO CONCENTRATION (MICROMOLAR)		0.01							
DETECTION LIMIT (MICROMOLAR) = 3*STD DEVIATION OF DW		0.04							

NITRATE: CONCENTRATION vs PEAK HEIGHT
CALIBRATION OF AUTOANALYSER, JULY 1992

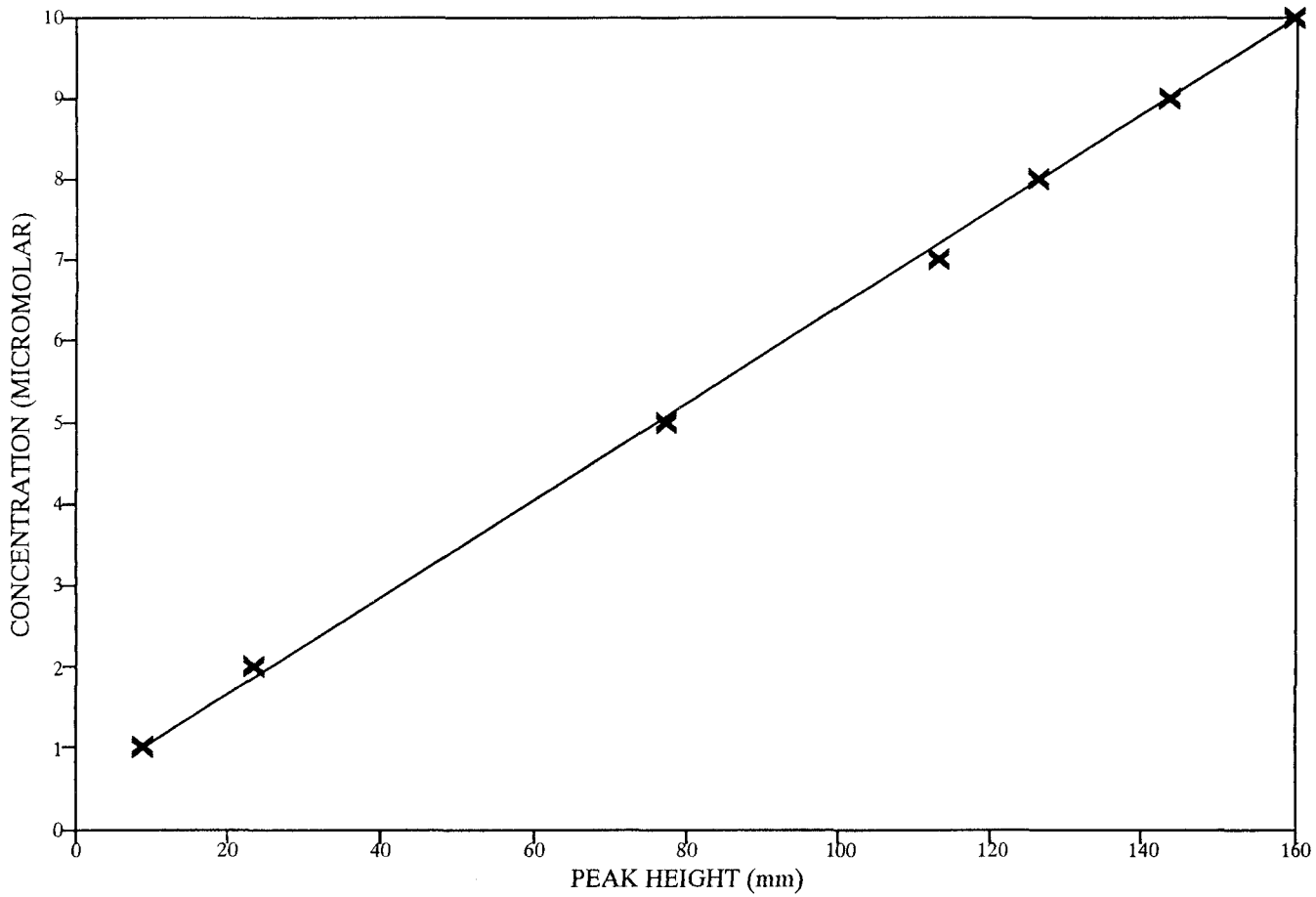

NITRATE RESULTS: PRECISION

SAMPLE	A	B	C	D	E	F	G	
CONCENTRATION (MICROMOLAR)	10	9	8	7	5	2	1	
SIGNAL (mm)	155.9	141.4	126.4	111.9	76.1	21.9	7.9	
	157.4	144.4	126.9	113.4	75.9	23.1	8.9	
	157.4	145.8	129.4	113.8	78.4	24.4	9.9	
	168.4	143.1	122.9	113.1	78.4	25.2	9.4	
TOTAL SIGNAL (mm)	639.1	574.7	505.6	452.2	308.8	94.6	36.1	
NUMBER OF ANALYSES, n	4	4	4	4	4	4	4	
SQUARES OF DATA	24304.8	19994.0	15977.0	12521.6	5791.2	479.6	62.4	
	24774.8	20851.4	16103.6	12859.6	5760.8	533.6	79.2	
	24774.8	21257.6	16744.4	12950.4	6146.6	595.4	98.0	
	28358.6	20477.6	15104.4	12791.6	6146.6	635.0	88.4	
SUM OF SQUARES OF DATA	102212.9	82580.6	63929.3	51123.2	23845.1	2243.6	328.0	
(TOTAL SQUARED)/n	102112.2	82570.0	63907.8	51121.2	23839.4	2237.3	325.8	
DIFFERENCE	100.7	10.5	21.5	2.0	5.8	6.3	2.2	
SUM OF SQUARES	149.0							
DEGREES OF FREEDOM	3	3	3	3	3	3	3	= 21
QUOTIENT GIVES VARIANCE		7.10						
STD DEVIATION		2.66						
CONVERTING STD DEVIATION TO CONCENTRATION (MICROMOLAR)		0.17						
PRECISION (MICROMOLAR) = (2/SQRT OF Pi)*STD DEV.		0.19						

TYPICAL CALIBRATION RESULTS TAKEN FROM A CALIBRATION EXPERIMENT
MADE ON 23/07/92

SILICATE RESULTS: CALIBRATION

SAMPLE	A	B	C	D	E	F	G	ASW	DW
CONCENTRATION (MICROMOLAR)	20	18	16	14	10	4	2		
	208.5	191	171.8	156	109.5	54	29.5	7.5	3.5
(mm)	206.5	190.5	171.5	155.5	110.8	55	31	7.0	4.0
	207	186	174.5	156	112	57	32.5	7.5	4.5
	207.5	190.75	171.65	155.75	110.5	54.5	30.25	7.8	3.9
AVERAGE SIGNAL	207.4	189.6	172.4	155.8	110.7	55.1	30.8	7.5	4.0
SIGNAL MINUS	205.0	187.5	168.3	152.5	106.0	50.5	26.0		
(AVE ASW - AVE DW)	203.0	187.0	168.0	152.0	107.3	51.5	27.5		
	203.5	182.5	171.0	152.5	108.5	53.5	29.0		
	204.0	187.3	168.2	152.3	107.0	51.0	26.8		
AVERAGE SIGNAL	203.9	186.1	168.9	152.3	107.2	51.7	27.3		
LINEAR CALIBRATION	207.4	187.8	168.2	148.5	109.3	50.4	30.8		
DIFFERENCE BETWEEN SIGNAL AND LINEAR CAL. (mm)	-3.5	-1.7	0.7	3.8	-2.1	1.2	-3.5		
DIFFERENCE BETWEEN SIGNAL AND LINEAR CAL. (MICROMOLAR)	-0.21	-0.10	0.04	0.23	-0.12	0.07	-0.21		
STD DEVIATION OF DW BLANK SAMPLES		0.36							
CONVERTING STD DEVIATION TO CONCENTRATION (MICROMOLAR)		0.03							
DETECTION LIMIT (MICROMOLAR) = 3*STD DEVIATION OF DW		0.10							

SILICATE: CONCENTRATION vs PEAK HEIGHT
CALIBRATION OF AUTOANALYSER, JULY 1992

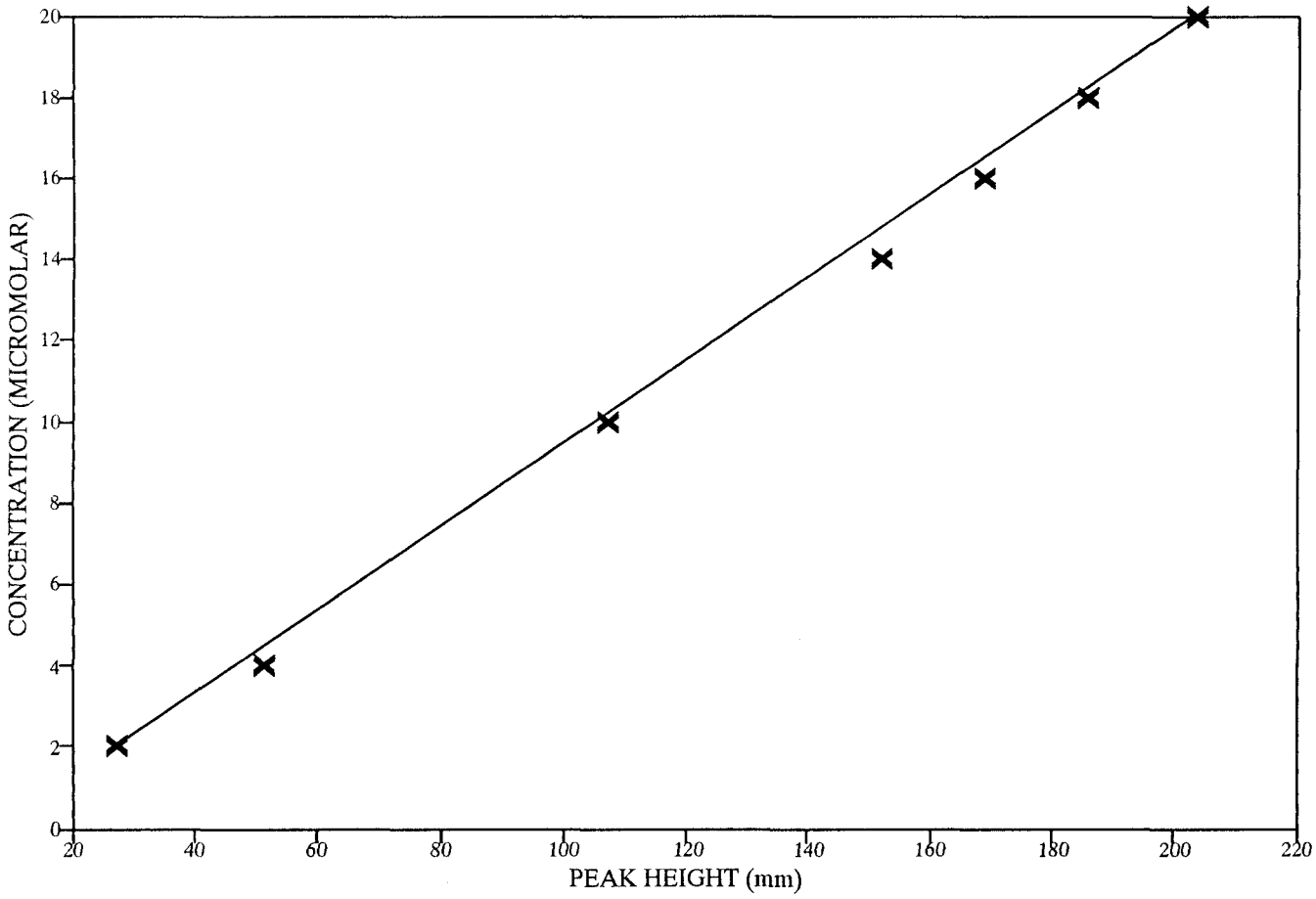

SILICATE RESULTS: PRECISION

SAMPLE	A	B	C	D	E	F	G	
CONCENTRATION (MICROMOLAR)	20	18	16	14	10	4	2	
SIGNAL (mm)	205.0	187.5	168.3	152.5	106.0	50.5	26.0	
	203.0	187.0	168.0	152.0	107.3	51.5	27.5	
	203.5	182.5	171.0	152.5	108.5	53.5	29.0	
	204.0	187.3	168.2	152.3	107.0	51.0	26.8	
TOTAL SIGNAL (mm)	815.6	744.35	675.55	609.35	428.9	206.6	109.35	
NUMBER OF ANALYSES, n	4	4	4	4	4	4	4	
SQUARES OF DATA	42035.3	35165.6	28333.3	23263.9	11241.3	2552.8	677.3	
	41219.2	34978.4	28232.4	23111.6	11518.7	2654.8	757.6	
	41422.4	33315.4	29249.6	23263.9	11777.7	2864.9	842.5	
	41626.2	35071.9	28282.8	23187.7	11454.4	2603.6	716.9	
SUM OF SQUARES OF DATA	166303.0	138531.3	114098.1	92827.0	45992.0	10676.1	2994.3	
(TOTAL SQUARED)/n	166300.8	138514.2	114092.0	92826.9	45988.8	10670.9	2989.4	
DIFFERENCE	2.2	17.0	6.1	0.2	3.2	5.2	4.9	
SUM OF SQUARES	38.8							
DEGREES OF FREEDOM	3	3	3	3	3	3	3	= 21
QUOTIENT GIVES VARIANCE		1.85						
STD DEVIATION		1.36						
CONVERTING STD DEVIATION TO CONCENTRATION (MICROMOLAR)		0.13						
PRECISION (MICROMOLAR) = (2/SRTQ OF Pi)*STD DEV.		0.15						

APPENDIX 5.2

UNIMAP SETTINGS FOR FIGURES 5.1 TO 5.3: SPATIAL VARIABILITY OF HYDROGRAPHIC PROPERTIES.

The file from which the plots are made up contains data from eight stations arranged in columns and each column has a 1 m depth resolution. It is of the format:

Distance from LL0 (Km) Depth (m) Temperature (°C) Salinity (PSU) Density (Kg m^{-3})

Therefore temperature, salinity and density data are read into UNIMAP as three z variables. A file containing distance data of the stations from station LL0 is also read into UNIMAP as a fault file. The basic set-up within the UNIMAP software is as follows:

DATA:	IRREGULAR	
	FORMAT:	NUMBER OF Z VARIABLES = 3
		COLUMNS
		FORTRAN FORMAT = *
	RATIO:	X = 1.6
		Y = 1
		Z = 1
	READ	
INTERPOLATE:	METHOD:	BILINEAR
	OPTIONS:	DISTANCE WEIGHTED
	GRIDCELLS:	X DIRECTION = 7 (for the 8 stations used)
		Y DIRECTION = 140
MAP:	GALLERY:	2D LINE
SMOOTH:	SMOOTHING LEVEL: MED	
STYLE:	ANNOTATE	
	METHOD:	OVERLAY
CLASS:	LIMITS:	AS ON PLOTS]

APPENDIX 5.2

UNIMAP SETTINGS FOR FIGURES 5.5 TO 5.9: TEMPORAL VARIABILITY OF HYDROGRAPHIC PROPERTIES, CONTOUR PLOTS.

The files from which the timeseries plots are made up contain data arranged in columns and each column has a 1 m depth resolution. They are of the format:

Time (Julian Day) Depth (m) Temperature (°C) Salinity (PSU) Density (Kg m^{-3})

Therefore temperature, salinity and density data are read into UNIMAP as three z variables. The basic set-up within the UNIMAP software is as follows:

DATA:	IRREGULAR	
	FORMAT:	NUMBER OF Z VARIABLES = 3
		COLUMNS
		FORTRAN FORMAT = *
	RATIO:	X = 1.6
		Y = 1
		Z = 1
	READ	
INTERPOLATE:	METHOD:	BILINEAR
	OPTIONS:	DISTANCE WEIGHTED
	GRIDCELLS:	X DIRECTION = 8 (weeks)
		Y DIRECTION = 36 (LL0), 107 (LL4), 128 (LL10) 110 (LL14), 40 (LL19).
MAP:	GALLERY:	2D LINE
SMOOTH:	SMOOTHING LEVEL: MED	
STYLE:	ANNOTATE	
	METHOD:	OVERLAY
CLASS:	LIMITS:	AS ON PLOTS]

APPENDIX 5.3

ALL NUTRIENT DATA FROM 1991 INCLUDING
THAT COLLECTED FROM STATION LL16, LL7 AND LL2.
NOTE THAT WHERE THERE IS A "99" IN THE TEXT
THIS MEANS THERE IS NO DATA FOR THAT DEPTH ("99" USED
IN UNIMAP)

STATION	J.DAY	DEPTH (m)	NO3	PO4	Si04
			MICROMOLAR CONCENTRATIONS		
LL19	79	0.00	5.71	0.46	25.98
	79	-10.00	6.35	0.72	9.42
	79	-20.00	7.19	0.68	9.10
	79	-40.00	11.11	1.00	99.00
LL16	79	0.00	3.41	0.23	25.98
	79	-10.00	7.10	0.62	10.35
	79	-20.00	7.82	0.79	9.75
	79	-40.00	8.35	0.75	9.71
LL14	79	0.00	5.47	0.30	25.98
	79	-10.00	9.21	0.79	10.65
	79	-20.00	9.79	0.76	10.28
	79	-40.00	10.94	0.94	9.01
LL10	79	0.00	4.40	0.34	25.98
	79	-10.00	8.90	0.80	8.75
	79	-20.00	10.55	0.86	99.00
	79	-40.00	8.59	0.75	99.00
LL7	79	0.00	6.76	0.44	99.00
	79	-10.00	7.36	0.80	9.47
	79	-20.00	7.87	0.81	7.36
	79	-40.00	9.31	0.96	1.38
LL4	79	0.00	6.57	0.51	25.98
	79	-10.00	9.57	0.80	99.00
	79	-20.00	9.81	0.88	8.58
	79	-40.00	11.65	0.98	99.00
LL2	79	0.00	7.54	0.54	25.98
	79	-10.00	5.99	0.59	10.78
	79	-20.00	6.70	0.66	9.05
	79	-40.00	8.19	0.81	8.60
LL0	79	0.00	8.21	0.71	11.35
	79	-10.00	10.39	0.66	9.76
	79	-20.00	10.94	0.78	7.86
LL19	85	0.00	3.60	0.70	15.17
	85	-10.00	3.64	1.38	9.51
	85	-20.00	3.86	0.53	8.35
	85	-40.00	4.56	1.00	6.82
LL16	85	0.00	3.68	0.59	13.05
	85	-10.00	3.69	0.88	8.92
	85	-20.00	4.01	0.82	7.44
	85	-40.00	4.17	0.95	7.98
	85	-60.00	4.69	0.93	7.00
	85	-80.00	4.95	0.96	7.50
LL14	85	0.00	3.60	0.45	9.96
	85	-10.00	4.48	0.72	8.00
	85	-20.00	4.43	0.78	6.54
	85	-40.00	3.91	0.82	6.92
	85	-60.00	4.16	1.11	8.36
	85	-80.00	4.48	1.00	7.64
LL10	85	0.00	4.43	0.55	12.20
	85	-10.00	4.84	0.77	8.59
	85	-20.00	5.34	0.94	7.54
	85	-40.00	5.78	0.92	6.89
	85	-60.00	5.86	0.89	6.00

	85	-80.00	5.88	0.91	6.02
LL7	85	0.00	4.43	0.45	13.28
	85	-10.00	5.59	0.77	7.74
	85	-20.00	6.26	0.76	7.17
	85	-40.00	6.00	0.74	6.66
	85	-60.00	6.51	0.75	7.95
	85	-80.00	5.74	0.72	7.07
LL4	85	0.00	3.52	0.33	13.78
	85	-10.00	5.94	0.63	8.74
	85	-20.00	7.06	0.76	7.29
	85	-40.00	6.34	0.75	8.37
	85	-60.00	7.57	0.82	7.75
	85	-80.00	8.27	0.88	7.49
LL2	85	0.00	5.00	0.50	13.05
	85	-10.00	6.76	0.77	8.13
	85	-20.00	6.93	0.81	6.85
	85	-40.00	6.56	0.76	7.74
	85	-60.00	6.37	0.77	6.22
	85	-80.00	7.53	0.80	7.93
LL0	85	0.00	6.06	0.71	8.25
	85	-10.00	6.14	0.71	6.04
	85	-20.00	5.74	0.74	5.02
	85	-40.00	6.58	0.77	6.54
LL19	93	0.00	3.82	0.24	16.77
	93	-10.00	7.01	0.77	10.33
	93	-20.00	7.20	0.82	8.47
	93	-40.00	7.59	0.68	7.53
	93	0.00	4.53	0.17	15.79
LL16	93	-10.00	6.70	0.57	8.95
	93	-20.00	6.70	0.55	8.04
	93	-40.00	6.91	0.65	8.02
	93	-60.00	7.30	0.60	7.30
	93	-80.00	7.42	0.87	7.03
LL14	93	0.00	4.70	0.51	14.00
	93	-10.00	6.12	0.83	8.41
	93	-20.00	6.61	0.91	7.59
	93	-40.00	6.24	0.88	7.46
	93	-60.00	6.88	0.72	6.86
LL10	93	0.00	3.61	0.46	15.14
	93	-10.00	6.13	0.54	9.75
	93	-20.00	7.29	0.70	7.84
	93	-40.00	7.74	0.63	7.53
	93	-60.00	8.29	0.66	7.17
LL4	93	0.00	4.60	0.45	11.65
	93	-10.00	6.55	0.67	10.02
	93	-20.00	7.44	0.79	7.01
	93	-40.00	7.34	0.82	7.43
	93	-60.00	7.77	0.90	7.11
LL2	93	0.00	3.89	0.71	8.66
	93	-10.00	5.61	0.91	7.74
	93	-20.00	7.02	1.07	7.13
	93	-40.00	7.72	1.71	6.88
	93	-60.00	7.26	1.10	6.28
LL0	93	0.00	7.93	1.00	8.50
	93	-10.00	6.17	0.98	6.38
	93	-20.00	6.31	1.01	5.62
	93	-40.00	7.42	1.18	5.67
LL19	98	0.00	2.12	0.29	6.40
	98	-10.00	6.98	0.93	8.51
	98	-20.00	7.62	0.94	7.30
	98	-40.00	8.02	0.91	6.88
LL16	98	0.00	2.15	0.04	12.02
	98	-10.00	5.85	0.65	9.14
	98	-20.00	7.73	0.72	7.68

	98	-40.00	7.96	0.66	7.51
	98	-60.00	7.77	0.63	6.74
LL14	98	0.00	1.70	0.11	13.64
	98	-10.00	7.31	0.79	8.61
	98	-20.00	7.42	0.79	8.85
	98	-40.00	8.51	0.92	7.00
	98	-60.00	8.54	0.99	7.60
LL10	98	0.00	2.72	0.25	15.63
	98	-10.00	7.00	0.23	7.86
	98	-20.00	7.81	0.88	7.97
	98	-40.00	6.47	0.80	5.93
	98	-60.00	7.43	0.90	6.61
LL7	98	0.00	2.51	0.19	12.90
	98	-10.00	6.20	0.67	6.94
	98	-20.00	8.05	0.79	6.77
	98	-40.00	9.16	0.88	6.71
	98	-60.00	8.51	0.87	6.39
LL4	98	0.00	5.44	0.51	14.27
	98	-10.00	7.29	0.75	7.72
	98	-20.00	8.93	0.93	7.08
	98	-40.00	8.96	0.97	6.65
	98	-60.00	8.96	0.97	6.90
LL2	98	0.00	4.29	0.50	9.33
	98	-10.00	6.62	0.79	10.09
	98	-20.00	7.70	1.00	6.19
	98	-40.00	8.42	0.99	5.66
	98	0.00	2.25	0.35	12.88
LL0	98	-10.00	5.61	0.88	7.39
	98	-20.00	5.99	0.78	6.68
	98	-40.00	9.08	0.96	8.44
	98	-60.00	7.96	0.70	13.41
LL19	107	0.00	5.98	0.70	13.41
	107	-5.00	7.41	0.95	8.81
	107	-10.00	7.22	0.94	8.73
	107	-20.00	7.03	0.97	8.32
	107	-40.00	6.78	0.96	8.13
LL16	107	0.00	5.19	0.63	13.83
	107	-5.00	6.28	0.95	8.33
	107	-10.00	6.25	0.89	8.35
	107	-20.00	6.42	0.93	7.74
	107	-40.00	6.61	0.95	8.18
	107	-60.00	6.71	0.87	7.81
LL14	107	0.00	7.68	99	12.12
	107	-5.00	8.13	99	9.83
	107	-10.00	8.36	99	7.66
	107	-20.00	8.08	99	7.77
	107	-40.00	8.48	99	7.13
	107	-60.00	8.01	99	99
	107	-120.00	9.03	99	8.40
LL10	107	0.00	7.68	99	11.01
	107	-5.00	8.28	99	8.57
	107	-10.00	8.30	99	8.19
	107	-20.00	8.47	99	6.88
	107	-40.00	8.52	99	6.85
	107	-60.00	8.63	0.95	99.00
	107	-120.00	9.02	0.74	9.95
LL7	107	0.00	7.61	0.74	8.22
	107	-5.00	7.70	0.70	9.82
	107	-10.00	7.97	0.72	9.25
	107	-20.00	8.08	0.74	8.12
	107	-40.00	8.20	0.79	9.29
	107	-60.00	8.10	0.70	8.57
	107	-140.00	8.83	0.82	8.97
LL4	107	0.00	7.71	0.81	10.69

	107	-5.00	7.94	0.83	9.90
	107	-10.00	7.82	0.81	10.84
	107	-20.00	8.17	0.87	10.58
	107	-40.00	8.36	0.93	9.01
	107	-60.00	5.87	0.68	7.59
LL2	107	0.00	6.89	0.76	11.92
	107	-5.00	7.77	0.82	10.90
	107	-10.00	7.68	0.82	10.12
	107	-20.00	7.25	0.66	9.93
	107	-40.00	8.30	0.72	9.61
	107	-60.00	8.54	0.72	8.81
	107	-90.00	8.54	0.76	8.76
LL0	107	0.00	7.51	0.78	8.12
	107	-5.00	7.49	0.72	7.57
	107	-10.00	7.60	0.79	6.16
	107	-20.00	8.23	0.82	6.57
	107	-35.00	8.36	0.82	5.47
LM10	107	0.00	8.15	0.76	8.10
	107	-5.00	8.16	0.74	7.27
	107	-10.00	7.64	0.70	7.30
	107	-20.00	8.36	0.74	7.86
	107	-40.00	8.67	0.77	8.24
	107	-60	8.58	0.77	7.42
LL19	113	0	5.67	0.46	10.12
	113	-5	7.37	0.54	13.17
	113	-9	7.90	0.99	8.47
	113	-19	6.47	0.59	5.89
	113	-44	8.06	0.99	7.66
LL16	113	0	6.96	0.50	11.47
	113	-5	7.36	0.58	10.84
	113	-10	8.00	0.72	8.07
	113	-20	3.95	0.48	3.09
	113	-40	7.51	0.67	7.08
	113	-60	7.60	0.72	7.43
	113	-110	8.33	0.95	8.26
LL14	113	0	7.52	0.83	10.10
	113	-5	7.39	0.59	8.42
	113	-10	7.27	0.63	8.12
	113	-20	8.16	0.71	7.66
	113	-40	7.74	0.74	7.18
	113	-60	7.74	0.67	8.21
	113	-100	7.42	0.67	6.64
	113	-115	8.84	0.98	8.25
LL10	113	0	7.23	0.85	9.63
	113	-5	7.67	0.70	8.87
	113	-20	8.30	0.77	7.97
	113	-40	9.42	0.98	8.20
	113	-60	8.55	0.99	7.39
	113	-100	5.22	0.57	4.83
	113	-145	5.84	0.79	5.62
LL7	113	0	7.99	0.81	8.10
	113	-5	8.04	0.81	8.32
	113	-10	8.10	0.86	7.93
	113	-20	6.98	1.32	29.46
	113	-40	9.00	0.96	7.13
	113	-60	8.13	0.96	6.94
	113	-100	8.68	0.94	7.76
	113	-145	8.74	0.94	8.38
LL4	113	0	7.91	0.97	8.00
	113	-5	7.80	0.94	8.21
	113	-10	8.59	1.01	7.60
	113	-20	7.31	0.91	8.40
	113	-40	7.89	1.02	7.01
	113	-60	7.21	0.88	6.03

	113	-100	9.10	1.04	7.40
	113	-120	8.77	1.00	7.60
LL2	113	0	8.24	1.04	8.81
	113	-5	7.92	0.94	8.61
	113	-10	8.08	1.09	9.42
	113	-20	7.90	1.06	7.60
	113	-40	8.55	1.06	9.22
	113	-60	8.68	1.02	7.01
LL0	113	0	6.65	0.98	6.61
	113	-5	7.68	1.01	10.67
	113	-10	7.77	1.16	7.01
	113	-20	8.74	1.10	7.21
	113	-38	8.56	1.20	6.41
LM10	113	0	7.10	0.88	6.61
	113	-5	7.55	0.94	7.01
	113	-10	7.60	0.95	5.44
	113	-20	8.23	0.92	6.03
	113	-30	8.51	0.99	7.60
	113	-50	8.27	1.02	6.03
	113	-70	8.42	1.10	6.22
	113	-90	8.18	1.01	8.99
LL21	120	0	6.92	1.01	8.99
	120	-5	4.07	0.91	5.57
	120	-10	7.14	1.17	7.26
	120	-15	7.64	1.17	7.45
	120	-20	6.08	1.12	6.13
LL20	120	0	5.70	0.99	9.76
	120	-5	7.60	1.20	8.21
	120	-10	7.82	1.20	7.44
LL19	120	0	6.55	0.96	12.16
	120	-5	5.59	1.06	6.67
	120	-10	6.54	1.05	6.67
	120	-20	7.38	1.15	8.00
	120	-40	6.65	1.08	6.49
LL16	120	0	5.10	0.86	8.76
	120	-5	6.45	1.05	7.41
	120	-10	6.33	1.08	6.85
	120	-20	7.00	1.25	6.85
	120	-40	3.30	0.79	3.91
	120	-60	5.21	0.89	5.73
	120	-100	8.28	1.24	7.99
LL14	120	0	3.55	0.61	5.98
	120	-5	3.99	0.74	5.13
	120	-15	4.60	0.85	5.36
	120	-35	5.61	0.95	5.91
	120	-55	4.60	0.87	5.17
	120	-115	5.61	1.01	6.28
LL10	120	0	4.48	0.61	7.45
	120	-5	4.38	0.68	5.53
	120	-10	5.35	0.71	6.24
	120	-20	2.41	0.54	3.41
	120	-40	8.15	0.99	7.31
	120	-60	8.21	1.01	7.51
	120	-130	6.29	1.02	6.64
LL7	120	0	4.28	0.88	5.33
	120	-5	5.81	0.91	6.99
	120	-10	5.82	0.83	6.39
	120	-20	5.57	0.69	5.92
	120	-40	4.03	0.74	4.55
	120	-60	8.08	1.05	7.59
	120	-130	7.13	0.90	6.58
LL4	120	0	5.23	0.86	6.92
	120	-5	5.08	0.87	5.70
	120	-10	4.61	0.78	5.02

	120	-20	8.40	1.09	7.73
	120	-40	6.25	0.88	5.92
	120	-60	8.32	1.04	7.59
	120	-120	8.01	1.04	6.99
LL2	120	0	7.51	1.10	8.41
	120	-5	5.81	0.88	5.73
	120	-15	5.35	0.78	5.87
	120	-35	8.69	1.13	7.59
	120	-55	5.52	0.97	5.60
	120	-95	6.05	0.94	5.99
LL0	120	0	4.47	0.79	5.34
	120	-5	5.77	0.81	5.41
	120	-10	9.18	1.19	6.93
	120	-20	10.85	1.25	6.66
LL21	127	0	5.65	0.79	7.98
	127	-5	8.36	0.19	8.71
	127	-10	8.72	0.14	8.19
	127	-15	8.63	0.01	7.82
	127	-20	8.58	0.01	7.60
LL20	127	0	5.75	0.62	7.93
	127	-5	8.41	0.78	7.99
	127	-10	8.85	0.76	7.92
	127	-15	8.72	0.76	7.91
LL19	127	0	6.46	0.66	10.26
	127	-5	8.26	0.79	7.28
	127	-10	9.03	0.78	8.08
	127	-20	9.25	0.81	8.07
	127	-40	9.29	0.82	7.91
LL16	127	0	7.04	0.69	10.44
	127	-5	7.96	0.78	8.03
	127	-10	9.29	0.85	8.10
	127	-20	9.56	0.86	7.95
	127	-40	9.29	0.88	7.65
	127	-60	9.20	0.78	7.22
	127	-100	8.94	0.78	7.00
LL14	127	0	7.96	0.79	8.43
	127	-5	9.16	0.91	7.92
	127	-10	9.91	0.91	8.28
	127	-15	10.13	0.91	8.42
	127	-35	9.99	0.90	8.94
	127	-55	9.56	0.88	8.41
	127	-110	9.42	0.88	7.24
LL10	127	0	7.04	0.90	8.46
	127	-5	8.76	0.88	7.93
	127	-10	9.42	0.91	9.20
	127	-20	10.31	0.96	8.45
	127	-40	10.13	1.02	8.75
	127	-60	10.44	0.96	7.26
	127	-140	9.51	0.91	7.30
LL7	127	0	8.68	0.94	8.79
	127	-5	8.18	0.95	8.34
	127	-10	8.28	0.92	8.34
	127	-20	10.20	1.04	8.63
	127	-40	10.92	1.11	9.76
	127	-60	10.69	1.05	12.33
	127	-135	10.03	1.05	8.85
LL4	127	0	7.15	0.86	8.90
	127	-5	6.31	0.76	8.29
	127	-10	9.63	1.07	7.92
	127	-20	11.28	1.19	8.73
	127	-40	11.00	1.20	7.97
	127	-60	10.95	1.17	7.97
	127	-115	10.76	1.15	7.45
LL2	127	0	7.47	0.91	10.54

	127	-5	8.02	0.96	9.23
	127	-10	10.08	1.11	8.24
	127	-20	11.68	1.20	8.61
	127	-40	11.25	1.25	7.86
	127	-60	11.05	1.18	7.56
	127	-80	11.01	1.24	7.77
LL0	127	0	10.29	1.23	6.90
	127	-5	10.24	1.23	6.49
	127	-10	11.44	1.34	6.69
	127	-20	11.79	1.37	6.91
	127	-40	11.44	1.32	7.20
LM10	127	0	7.70	1.16	6.72
	127	-5	8.85	1.15	6.50
	127	-10	9.22	1.13	6.64
	127	-20	9.68	1.22	5.03
	127	-40	9.45	1.18	6.49
	127	-60	9.31	1.15	6.05
	127	-90	9.56	1.27	4.61
LL19	164	0	3.38	0.82	1.46
	164	-5	3.41	0.83	1.89
	164	-10	3.67	0.81	1.09
	164	-20	3.25	0.63	2.26
LL16	164	0	2.45	0.52	2.32
	164	-5	0.95	0.23	1.59
	164	-10	1.23	0.24	2.39
	164	-15	1.53	0.39	7.50
	164	-20	2.45	0.45	1.28
	164	-40	2.12	0.53	1.34
	164	-60	2.19	0.48	2.90
LL14	164	0	0.62	0.17	1.90
	164	-5	1.06	0.32	0.79
	164	-10	0.99	0.41	1.28
	164	-20	1.37	0.29	0.85
	164	-40	1.72	0.55	1.46
	164	-60	2.06	0.62	1.22
	164	-110	2.89	0.70	1.66
LL10	164	0	1.92	0.42	1.34
	164	-5	1.76	0.44	0.85
	164	-10	1.59	0.35	0.55
	164	-20	1.86	0.41	4.78
	164	-40	8.18	0.80	11.17
	164	-60	2.42	0.68	1.97
	164	-100	2.77	0.74	7.21
	164	-135	3.39	0.82	2.47
LL7	164	0	1.31	0.54	1.41
	164	-5	1.44	0.57	0.92
	164	-10	1.62	0.60	1.28
	164	-20	2.73	0.70	0.97
	164	-40	2.54	0.67	1.21
	164	-60	2.75	0.74	1.21
	164	-100	3.31	0.72	1.89
LL4	164	0	1.39	0.53	0.99
	164	-10	1.92	0.70	1.02
	164	-20	2.26	0.74	0.99
	164	-40	2.52	0.79	1.10
	164	-60	2.74	0.86	1.24
	164	-100	3.08	0.92	1.36
LL2	164	0	1.66	0.68	0.99
	164	-5	1.58	0.58	0.98
	164	-10	1.84	0.71	0.80
	164	-20	2.21	0.75	0.92
	164	-40	2.35	0.80	1.10
	164	-60	2.68	0.83	1.35
	164	-90	2.60	0.80	1.23

LL0	164	0	1.95	0.59	0.98
	164	-5	0.96	0.46	0.79
	164	-10	0.81	0.45	0.73
	164	-20	1.32	0.52	0.85
	164	-35	1.82	0.58	0.85
LL19	171	0	1.34	0.48	4.91
	171	-5	1.70	0.70	3.64
	171	-10	2.07	0.83	3.65
	171	-20	2.44	0.96	3.11
	171	-40	2.88	1.10	3.12
LL16	171	0	1.40	0.69	4.03
	171	-5	0.88	0.66	1.72
	171	-10	1.80	0.72	1.72
	171	-20	2.50	0.90	2.07
	171	-40	2.64	0.97	1.73
	171	-60	2.86	1.05	1.91
	171	-100	3.13	1.13	2.44
	171	-115	3.29	1.13	2.28
LL14	171	0	1.02	0.65	4.27
	171	-5	0.44	0.54	1.23
	171	-10	1.31	0.62	1.41
	171	-20	2.55	0.83	1.77
	171	-40	2.65	0.91	1.60
	171	-60	2.83	1.04	1.96
	171	-110	3.01	1.04	1.96
LL10	171	0	0.98	0.53	3.23
	171	-5	0.47	0.36	1.80
	171	-10	1.08	0.39	0.93
	171	-20	2.42	0.48	1.99
	171	-40	2.81	0.62	1.11
	171	-60	2.88	0.66	2.00
	171	-100	2.66	0.69	1.30
	171	-150	2.95	0.68	1.66
LL7	171	0	0.93	0.45	3.64
	171	-5	0.79	0.38	0.96
	171	-10	1.54	0.35	1.15
	171	-20	2.25	0.33	1.15
	171	-40	2.54	0.36	1.33
	171	-60	2.78	0.46	1.69
	171	-100	2.69	0.53	1.73
	171	-150	2.94	0.48	1.92
LL4	171	-5	1.32	0.45	1.03
	171	-10	2.27	0.45	1.21
	171	-20	2.56	0.47	1.22
	171	-40	2.66	0.42	1.40
	171	-60	2.73	0.45	1.41
	171	-100	2.83	0.48	1.60
	171	-115.00	2.96	0.46	1.97
LL2	171	0.00	0.94	0.32	1.08
	171	-5.00	1.44	0.33	1.27
	171	-10.00	2.66	0.33	1.46
	171	-20.00	2.44	0.32	1.46
	171	-40.00	2.75	0.35	1.46
	171	-60.00	2.96	0.38	1.46
	171	-100.00	2.92	0.36	1.83
LL0	171	0.00	1.75	0.29	1.30
	171	-5.00	1.88	0.25	1.49
	171	-10.00	2.33	0.24	0.96
	171	-20.00	2.57	0.24	1.51
	171	-35.00	3.85	0.24	2.23

APPENDIX 5.3

NUTRIENT DATA COLLECTED AT STATION LLO IN 1991

J.DAY	DEPTH (m)	NITRATE	PHOSPHATE	SILICATE	N:P
		MICROMOLAR CONCENTRATIONS			
79	0	8.21	0.71	11.35	11.5
79	-10	10.39	0.66	9.76	15.81
79	-20	10.94	0.78	7.86	14.02
79	-40	10.59	0.65	7.73	16.39
85	0	6.06	0.71	8.25	8.49
85	-10	6.14	0.71	6.04	8.6
85	-20	5.74	0.74	5.02	7.8
85	-40	6.58	0.77	6.54	8.55
93	0	7.93	1	8.5	7.9
93	-10	6.17	0.98	6.38	6.27
93	-20	6.31	1.01	5.62	6.22
93	-40	7.42	1.18	5.67	6.31
98	0	2.25	0.35	12.88	6.4
98	-10	5.61	0.88	7.39	6.39
98	-20	5.99	0.78	6.68	7.68
98	-40	9.08	0.96	8.44	9.43
107	0	7.51	0.78	8.12	9.63
107	-5	7.49	0.72	7.57	10.33
107	-10	7.6	0.79	6.16	9.61
107	-20	8.23	0.82	6.57	9.99
107	-35	8.36	0.82	5.47	10.15
113	0	6.65	0.98	6.61	6.76
113	-5	7.68	1.01	10.67	7.57
113	-10	7.77	1.16	7.01	6.72
113	-20	8.74	1.1	7.21	7.97
113	-38	8.56	1.2	6.41	7.16
120	0	4.47	0.79	5.34	5.65
120	-5	5.77	0.81	5.41	7.1
120	-10	9.18	1.19	6.93	7.74
120	-20	10.85	1.25	6.66	8.66
120	-40	4.91	0.88	3.61	5.59
127	0	10.29	1.23	6.9	8.34
127	-5	10.24	1.23	6.49	8.3
127	-10	11.44	1.34	6.69	8.55
127	-20	11.79	1.37	6.91	8.58
127	-40	11.44	1.32	7.2	5.57

APPENDIX 5.3

NUTRIENT DATA COLLECTED AT STATION LL4 IN 1991

J.DAY	DEPTH (m)	NITRATE	PHOSPHATE	SILICATE	N:P
		MICROMOLAR CONCENTRATIONS			
79	0	6.57	0.51	25.98	12.95
79	-10	9.57	0.80	99.00	11.93
79	-20	9.81	0.88	8.58	11.17
79	-40	11.65	0.98	99.00	11.84
85	0	3.52	0.33	13.78	10.75
85	-10	5.94	0.63	8.74	9.36
85	-20	7.06	0.76	7.29	9.31
85	-40	6.34	0.75	8.37	8.49
85	-60	7.57	0.82	7.75	9.19
93	0	4.6	0.45	11.65	10.27
93	-10	6.55	0.67	10.02	9.80
93	-20	7.44	0.79	7.01	9.40
93	-40	7.34	0.82	7.43	8.91
93	-60	7.77	0.90	7.11	8.64
98	0	5.44	0.51	14.27	10.73
98	-10	7.29	0.75	7.72	9.76
98	-20	8.93	0.93	7.08	9.59
98	-40	8.96	0.97	6.65	9.21
98	-60	8.96	0.97	6.90	9.21
107	0	7.71	0.81	10.69	9.48
107	-5	7.94	0.83	9.90	9.51
107	-10	7.82	0.81	10.84	9.62
107	-20	8.17	0.87	10.58	9.42
107	-40	8.36	0.93	9.01	8.98
107	-60	5.87	0.68	7.59	8.63
113	0	7.91	0.97	8.00	8.13
113	-5	7.8	0.94	8.21	8.28
113	-10	8.59	1.01	7.60	8.47
113	-20	7.31	0.91	8.40	8.03
113	-40	7.89	1.02	7.01	7.70
113	-60	7.21	0.88	6.03	8.21
120	0	5.23	0.86	6.92	6.11
120	-5	5.08	0.87	5.70	5.86
120	-10	4.61	0.78	5.02	5.91
120	-20	8.4	1.09	7.73	7.73
120	-40	6.25	0.88	5.92	7.12
120	-60	8.32	1.04	7.59	8.04
127	0	7.15	0.86	8.90	8.35
127	-5	6.31	0.76	8.29	8.32
127	-10	9.63	1.07	7.92	9.04
127	-20	11.28	1.19	8.73	9.52
127	-40	11	1.20	7.97	9.13
127	-60	10.95	1.17	7.97	9.39

APPENDIX 5.3

NUTRIENT DATA COLLECTED AT STATION LL10 IN 1991

J.DAY	DEPTH (m)	NITRATE MICROMOLAR CONCENTRATIONS	PHOSPHATE	SILICATE
79	0	4.4	0.34	25.98
79	-10	8.9	0.8	8.75
79	-20	10.55	0.86	99
79	-40	8.59	0.75	99
85	0	4.43	0.55	12.2
85	-10	4.84	0.77	8.59
85	-20	5.34	0.94	7.54
85	-40	5.78	0.92	6.89
85	-60	5.86	0.89	6
93	0	3.61	0.46	15.14
93	-10	6.13	0.54	9.75
93	-20	7.29	0.7	7.84
93	-40	7.74	0.63	7.53
93	-60	8.29	0.66	7.17
98	0	2.72	0.25	15.63
98	-10	7	0.23	7.86
98	-20	7.81	0.88	7.97
98	-40	6.47	0.8	5.93
98	-60	7.43	0.9	6.61
107	0	7.68	99	11.01
107	-5	8.28	99	8.57
107	-10	8.3	99	8.19
107	-20	8.47	99	6.88
107	-40	8.52	99	6.85
107	-60	8.63	0.95	7
113	0	7.23	0.85	9.63
113	-5	7.67	0.7	8.87
113	-10	99	99	99
113	-20	8.3	0.77	7.97
113	-40	9.42	0.98	8.2
113	-60	8.55	0.99	7.39
120	0	4.48	0.61	7.45
120	-5	4.38	0.68	5.53
120	-10	5.35	0.71	6.24
120	-20	2.41	0.54	3.41
120	-40	8.15	0.99	7.31
120	-60	8.21	1.01	7.51
127	0	7.04	0.9	8.46
127	-5	8.76	0.88	7.93
127	-10	9.42	0.91	9.2
127	-20	10.31	0.96	8.45
127	-40	10.13	1.02	8.75
127	-60	10.44	0.96	7.26

APPENDIX 5.3

NUTRIENT DATA COLLECTED AT STATION LL14 IN 1991

J.DAY	DEPTH (m)	NITRATE	PHOSPHATE	SILICATE	N:P
		MICROMOLAR CONCENTRATIONS			
79	0	5.47	0.3	25.98	18.06
79	-10	9.21	0.79	10.65	11.64
79	-20	9.79	0.76	10.28	12.91
79	-40	10.94	0.94	9.01	11.62
85	0	3.6	0.45	9.96	8.04
85	-10	4.48	0.72	8	6.18
85	-20	4.43	0.78	6.54	5.68
85	-40	3.91	0.82	6.92	4.75
85	-60	4.16	1.11	8.36	3.76
93	0	4.7	0.51	14	9.27
93	-10	6.12	0.83	8.41	7.33
93	-20	6.61	0.91	7.59	7.26
93	-40	6.24	0.88	7.46	7.11
93	-60	6.88	0.72	6.96	9.49
93	0	1.7	0.11	13.64	14.78
98	-10	7.31	0.79	8.61	9.24
98	-20	7.42	0.79	8.85	9.38
98	-40	8.51	0.92	7	9.24
98	-60	2.72	0.99	7.6	8.59
107	0	7.68	99	12.12	0.08
107	-5	8.13	99	9.83	0.08
107	-10	8.36	99	7.66	0.08
107	-20	8.08	99	7.77	0.09
107	-40	8.48	99	7.13	0.08
107	-60	8.01	99	99	0.09
113	0	7.52	0.83	10.1	9.01
113	-5	7.39	0.59	8.42	12.55
113	-10	7.27	0.63	8.12	11.46
113	-20	8.16	0.71	7.66	11.43
113	-40	7.74	0.74	7.18	10.52
113	-60	7.74	0.67	8.21	11.58
120	0	3.55	0.61	5.98	5.8
120	-5	3.99	0.74	5.13	5.42
120	-15	4.6	0.85	5.36	5.44
120	-35	5.61	0.95	5.91	5.89
127	0	7.96	0.79	8.43	10.06
127	-5	9.16	0.91	7.92	10.07
127	-10	9.91	0.91	8.28	10.89
127	-15	10.13	0.91	8.42	11.13
127	-35	9.99	0.9	8.94	11.11
127	-55	9.56	0.88	8.41	10.89

APPENDIX 5.3

NUTRIENT DATA COLLECTED AT STATION LL19 IN 1991

J.DAY	DEPTH (m)	NITRATE	PHOSPHATE	SILICATE	N:P
		MICROMOLAR CONCENTRATIONS			
79	0	5.71	0.46	25.98	12.41
79	-10	6.35	0.72	9.42	8.76
79	-20	7.19	0.68	9.1	10.57
79	-40	11.11	1.00	99	11.06
85	0	3.6	0.7	15.17	5.12
85	-10	3.64	1.38	9.51	2.63
85	-20	3.86	0.53	8.35	7.27
85	-40	4.56	1	6.82	4.54
93	0	3.82	0.24	16.77	15.85
93	-10	7.01	0.77	10.33	9.11
93	-20	7.2	0.82	8.47	8.74
93	-40	7.59	0.68	7.53	11.16
98	0	2.12	0.29	6.4	7.3
98	-10	6.98	0.93	8.51	7.5
98	-20	7.62	0.94	7.3	8.09
98	-40	8.02	0.91	6.88	8.81
107	0	5.98	0.7	13.41	8.51
107	-5	7.41	0.95	8.81	7.78
107	-10	7.22	0.94	8.73	7.67
107	-20	7.03	0.97	8.32	7.22
107	-40	6.78	0.96	8.13	7.04
113	0	5.67	0.46	10.12	12.33
113	-5	7.37	0.54	13.17	13.59
113	-9	7.9	0.99	8.47	7.95
113	-19	6.47	0.59	5.89	10.99
113	-44	8.06	0.99	7.66	8.11
120	0	6.55	0.96	12.16	6.8
120	-5	5.59	1.06	6.67	5.3
120	-10	6.54	1.05	6.67	6.26
120	-20	7.38	1.15	8	6.44
120	-40	6.65	1.08	6.49	6.18
127	0	6.46	0.66	10.26	9.83
127	-5	8.26	0.79	7.28	10.44
127	-10	9.03	0.78	8.08	11.57
127	-20	9.25	0.81	8.07	11.38
127	-40	9.29	0.82	7.91	11.27

APPENDIX 5.4

UNIMAP SETTINGS FOR FIGURES 5.17 TO 5.21: TEMPORAL VARIABILITY OF NUTRIENT CONCENTRATIONS, CONTOUR PLOTS.

The files from which the timeseries plots are made up contain data arranged in columns. It is of the format:

Time (Julian Day) Depth (m) Nitrate (μM) Phosphate (μM) Silicate (μM)

Therefore nitrate, phosphate and silicate data are read into UNIMAP as three z variables. The basic set-up within the UNIMAP software is as follows:

DATA:	IRREGULAR	
	FORMAT:	NUMBER OF Z VARIABLES = 3
		COLUMNS
		FORTRAN FORMAT = *
	RATIO:	X = 1.6
		Y = 1
		Z = 1
	READ	
INTERPOLATE:	METHOD:	BILINEAR
	OPTIONS:	DISTANCE WEIGHTED
	GRIDCELLS:	X DIRECTION = 7 (weeks)
		Y DIRECTION = 5 (LL0), 6 (LL4 - 60 m), 6 (LL10 - 60 m), 6 (LL14 - 60 m), 5 (LL19)
MAP:	GALLERY:	2D LINE
SMOOTH:	SMOOTHING LEVEL:	MED
STYLE:	ANNOTATE	
	METHOD:	OVERLAY
CLASS:	LIMITS:	AS ON PLOTS

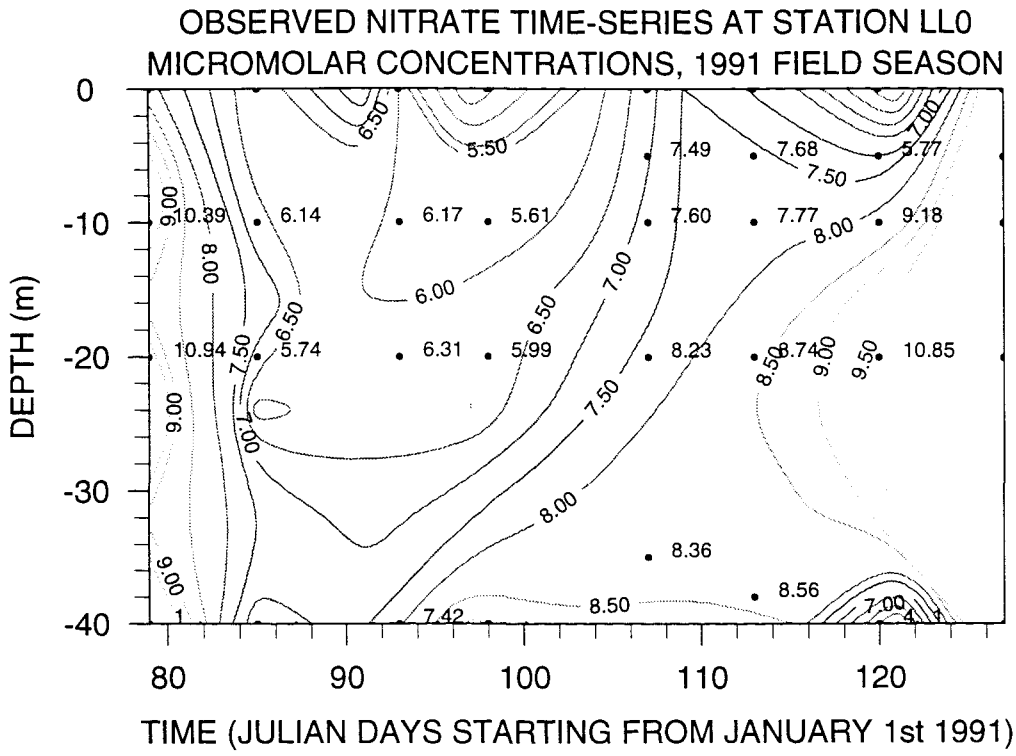
OBSERVED NITRATE TIME-SERIES AT STATION LL0
MICROMOLAR CONCENTRATIONS, 1991 FIELD SEASON
DEPTH (m)
0
-10
-20
-30
-40
80
90
100
110
120
TIME (JULIAN DAYS STARTING FROM JANUARY 1st 1991)

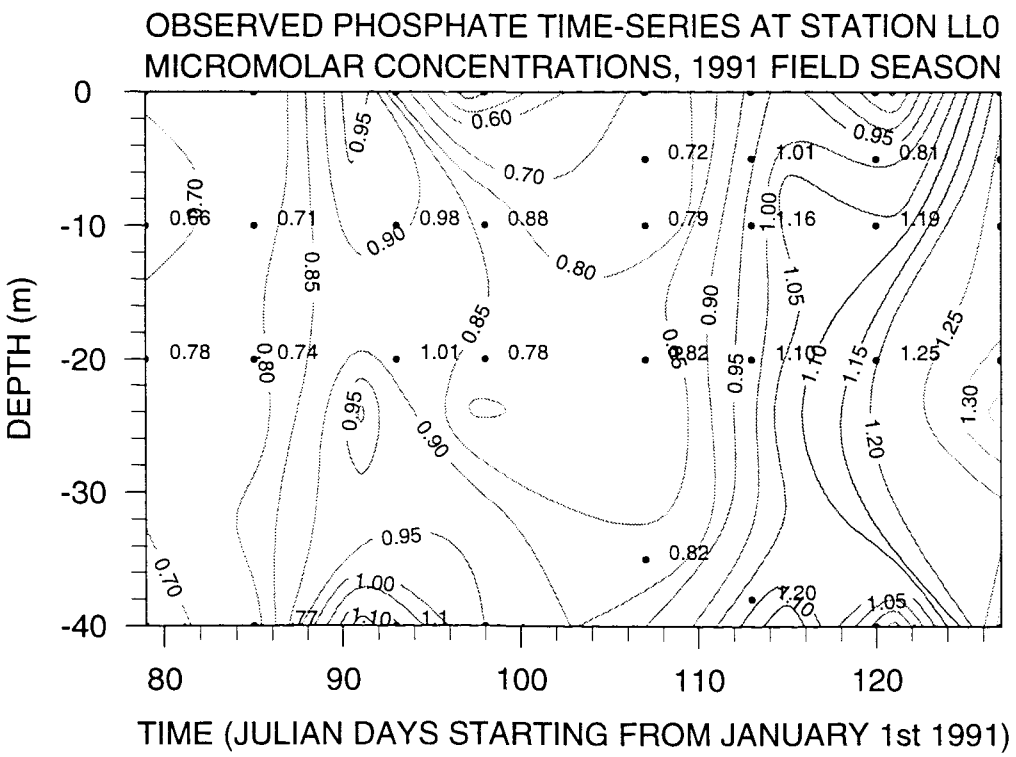
OBSERVED PHOSPHATE TIME-SERIES AT STATION LL0
MICROMOLAR CONCENTRATIONS, 1991 FIELD SEASON
DEPTH (m)
0
-10
-20
-30
-40
80
90
100
110
120
TIME (JULIAN DAYS STARTING FROM JANUARY 1st 1991)

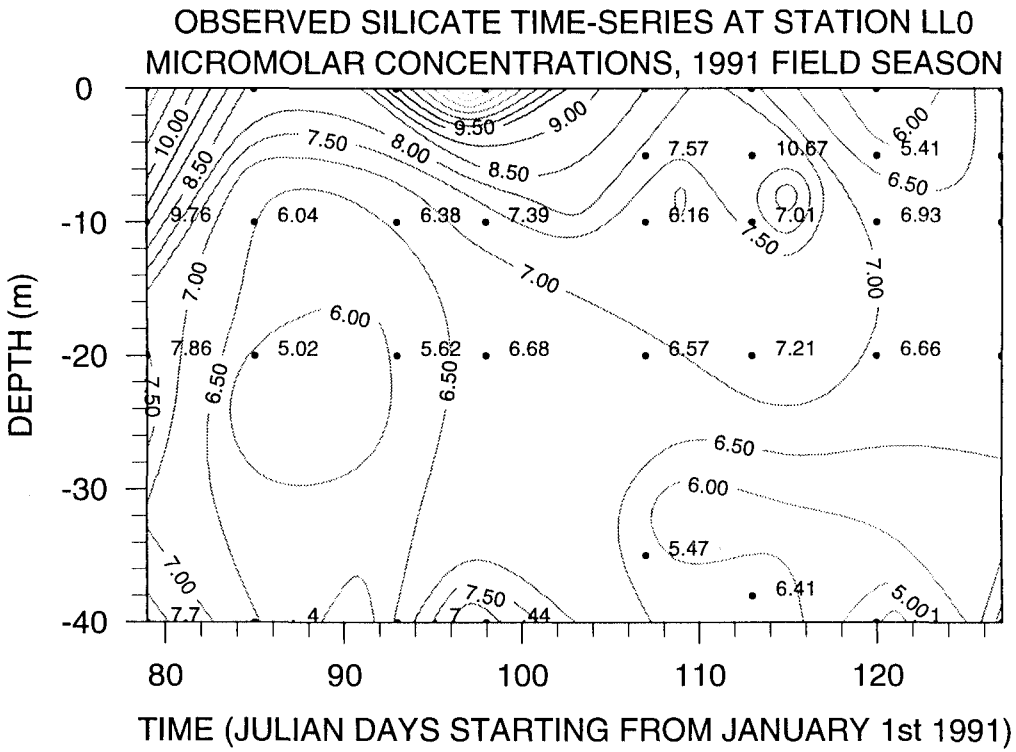
OBSERVED SILICATE TIME-SERIES AT STATION LL0
MICROMOLAR CONCENTRATIONS, 1991 FIELD SEASON
DEPTH (m)
0
-10
-20
-30
-40
80
90
100
110
120
TIME (JULIAN DAYS STARTING FROM JANUARY 1st 1991)
10.00
9.50
9.00
8.50
8.00
7.50
7.00
6.50
6.00
5.50
9.76
6.04
6.38
7.39
7.57
6.16
10.67
7.01
5.41
6.93
7.86
5.02
5.62
6.68
6.57
7.21
6.66
5.47
6.41
7.7
4
7
44
1

OBSERVED NITRATE TIME-SERIES AT STATION LL4
MICROMOLAR CONCENTRATIONS, 1991 FIELD SEASON

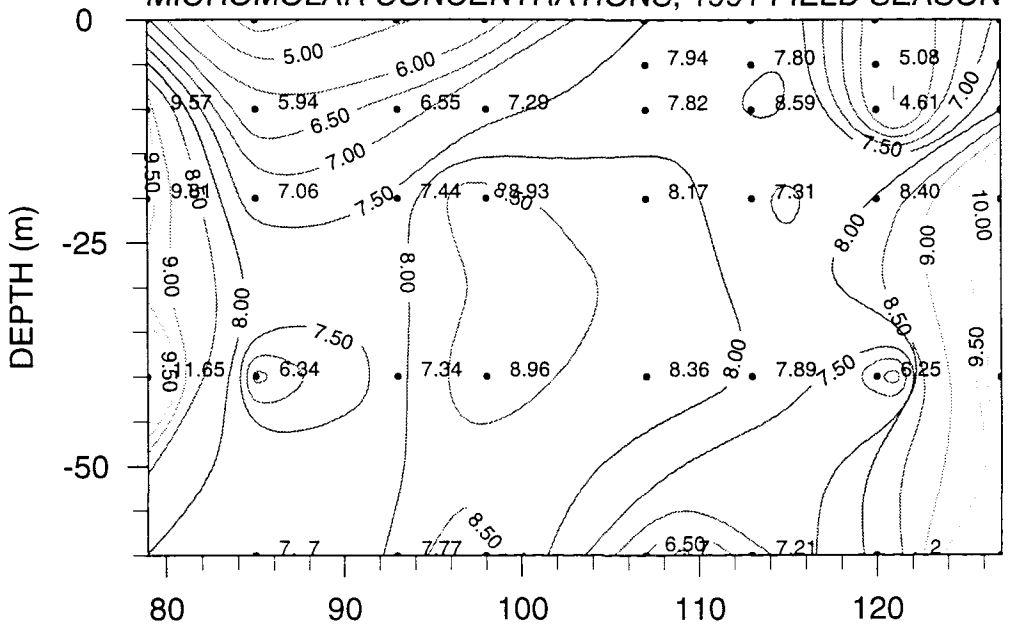

OBSERVED PHOSPHATE TIME-SERIES AT STATION LL4
MICROMOLAR CONCENTRATIONS, 1991 FIELD SEASON

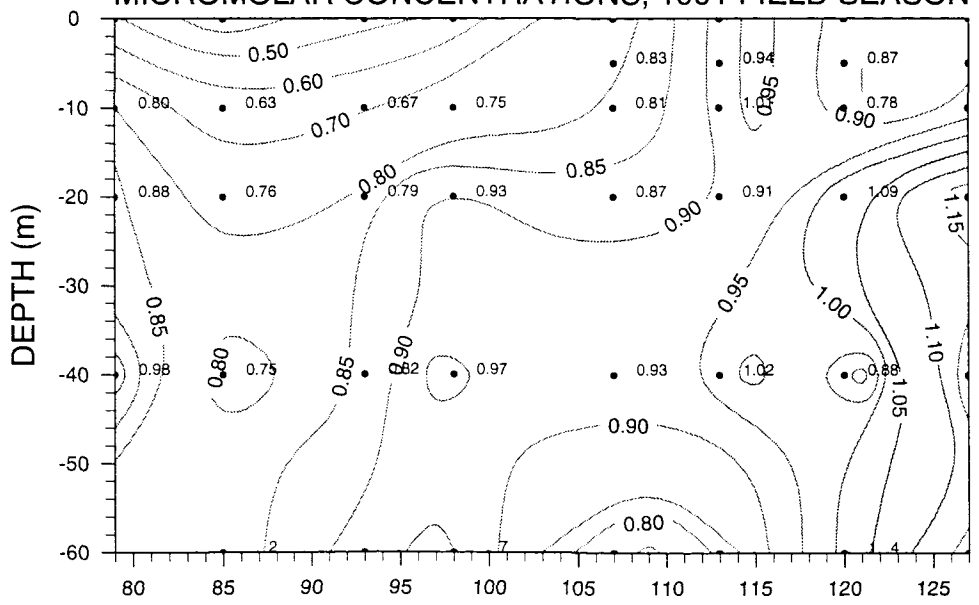

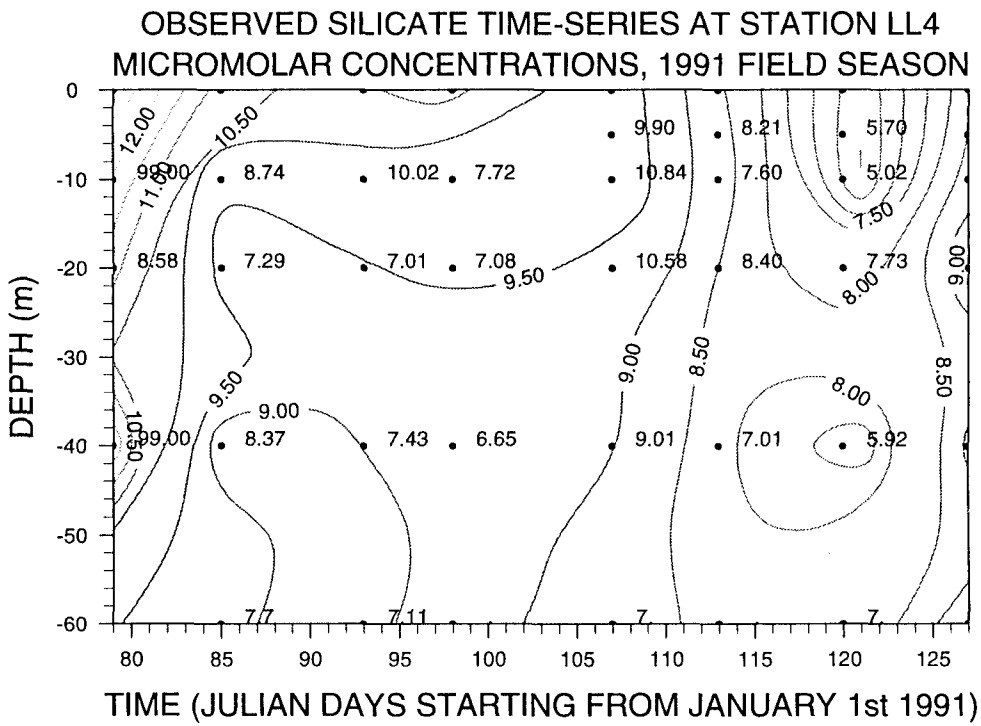
OBSERVED SILICATE TIME-SERIES AT STATION LL4
MICROMOLAR CONCENTRATIONS, 1991 FIELD SEASON
DEPTH (m)
0
-10
-20
-30
-40
-50
-60
80
85
90
95
100
105
110
115
120
125
TIME (JULIAN DAYS STARTING FROM JANUARY 1st 1991)
12.00
10.50
9.50
9.00
8.50
8.00
7.50
10.00
11.00
9.90
8.21
5.70
8.74
10.02
7.72
10.84
7.60
5.02
8.58
7.29
7.01
7.08
10.58
8.40
7.73
8.37
7.43
6.65
9.01
7.01
5.92

OBSERVED NITRATE TIME-SERIES AT STATION LL10
MICROMOLAR CONCENTRATIONS, 1991 FIELD SEASON

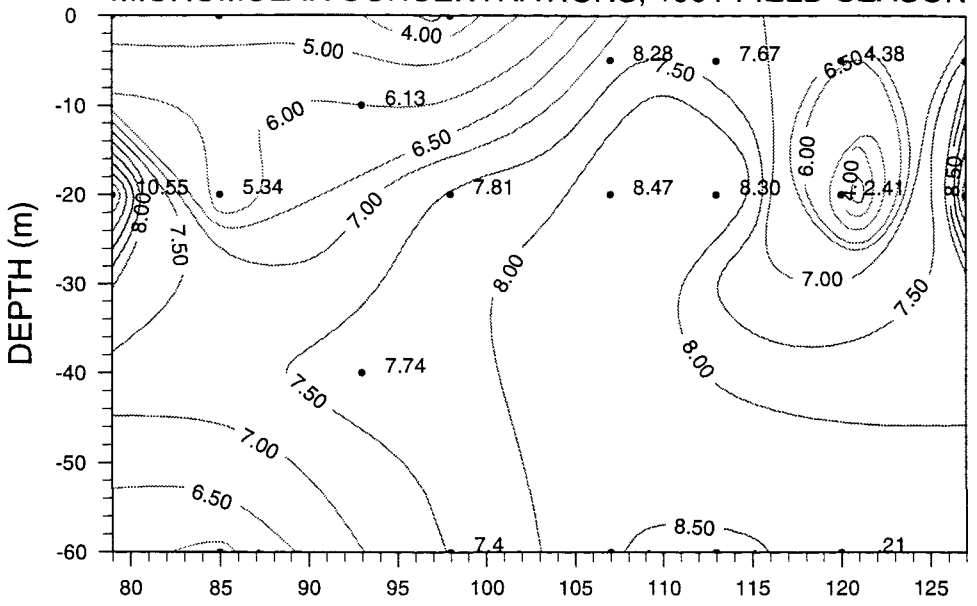

TIME (JULIAN DAYS STARTING FROM JANUARY 1st 1991)

OBSERVED PHOSPHATE TIME-SERIES AT STATION LL10
MICROMOLAR CONCENTRATIONS, 1991 FIELD SEASON

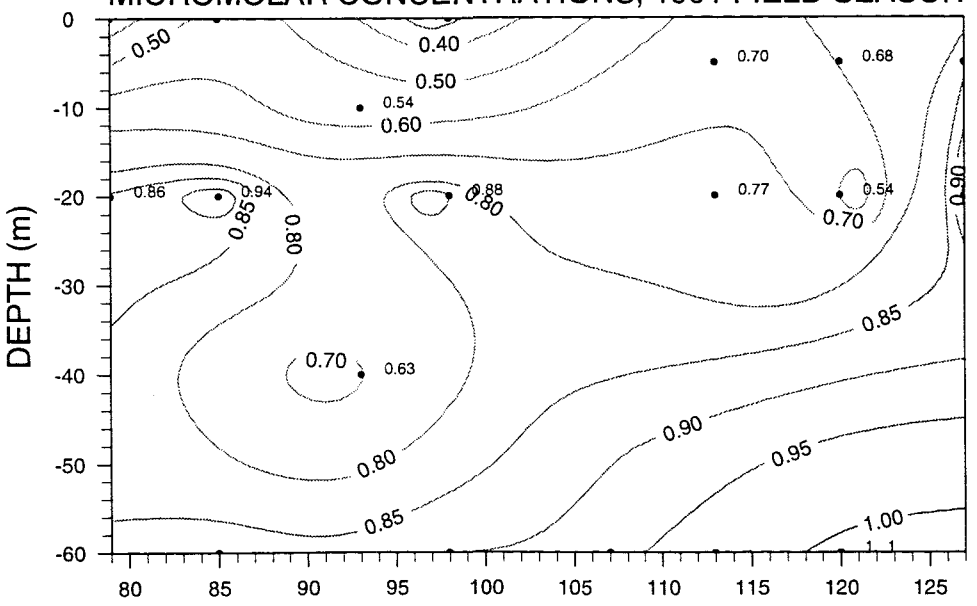

TIME (JULIAN DAYS STARTING FROM JANUARY 1st 1991)

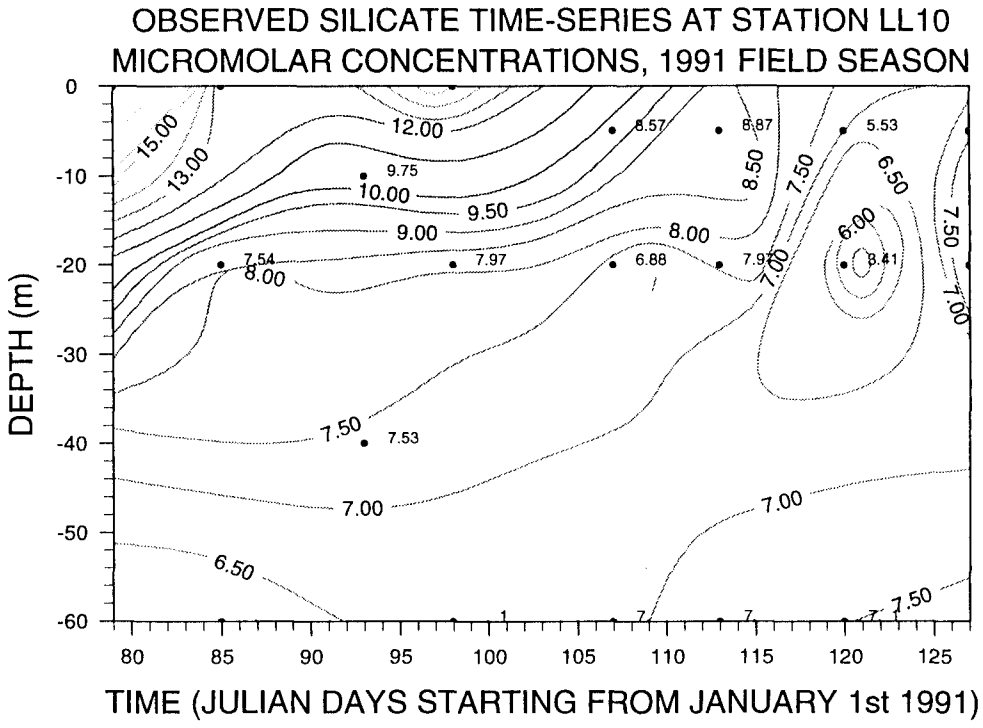
OBSERVED SILICATE TIME-SERIES AT STATION LL10
MICROMOLAR CONCENTRATIONS, 1991 FIELD SEASON
DEPTH (m)
0
-10
-20
-30
-40
-50
-60
80
85
90
95
100
105
110
115
120
125
TIME (JULIAN DAYS STARTING FROM JANUARY 1st 1991)
15.00
13.00
12.00
10.00
9.75
9.50
9.00
8.00
8.57
8.87
5.53
8.50
7.50
6.50
6.00
8.41
7.54
7.97
6.88
7.97
7.00
7.53
6.50

OBSERVED NITRATE TIME-SERIES AT STATION LL14
MICROMOLAR CONCENTRATIONS, 1991 FIELD SEASON

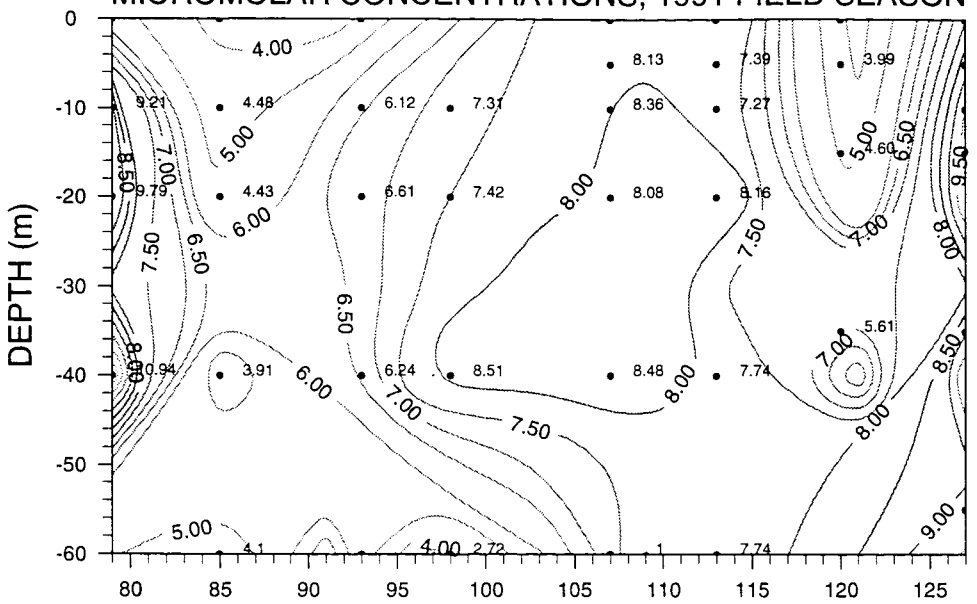

TIME (JULIAN DAYS STARTING FROM JANUARY 1st 1991)

OBSERVED PHOSPHATE TIME-SERIES AT STATION LL14
MICROMOLAR CONCENTRATIONS, 1991 FIELD SEASON

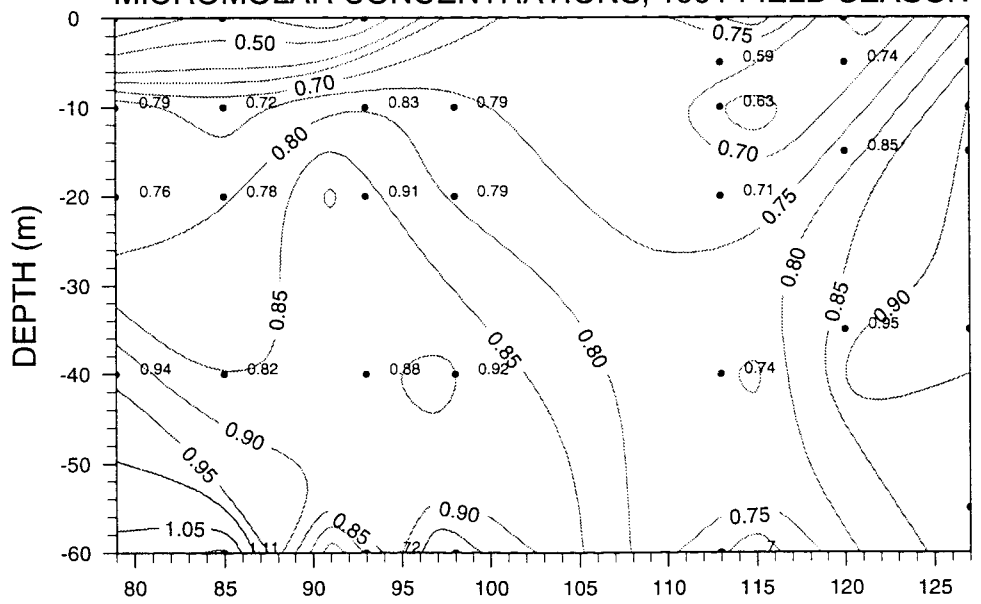

TIME (JULIAN DAYS STARTING FROM JANUARY 1st 1991)

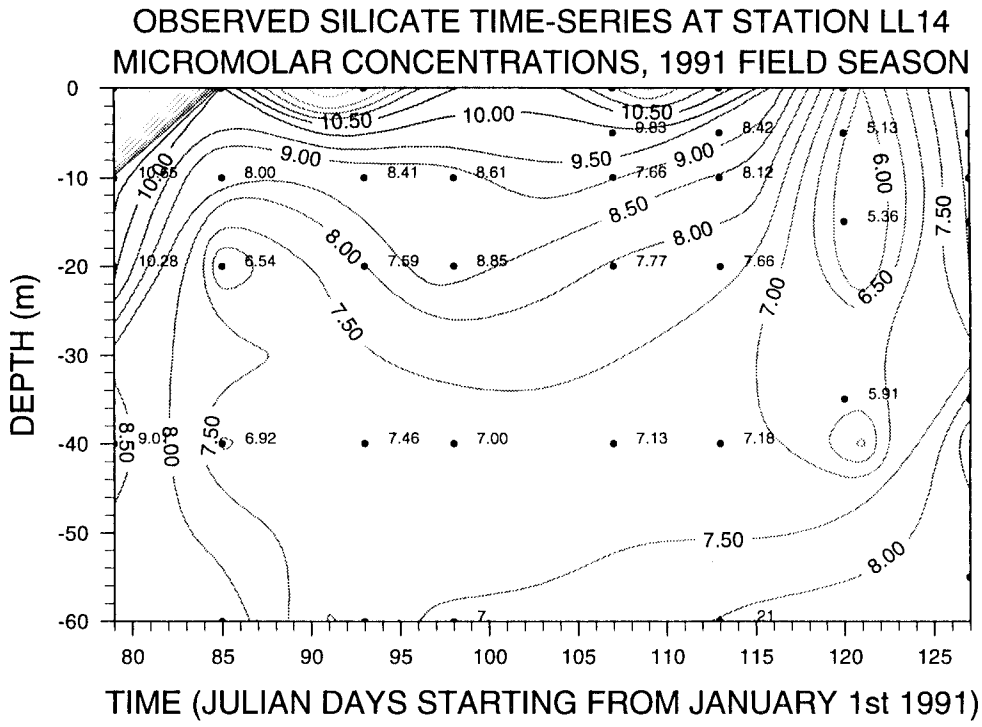
OBSERVED SILICATE TIME-SERIES AT STATION LL14
MICROMOLAR CONCENTRATIONS, 1991 FIELD SEASON
DEPTH (m)
0
-10
-20
-30
-40
-50
-60
80
85
90
95
100
105
110
115
120
125
TIME (JULIAN DAYS STARTING FROM JANUARY 1st 1991)
10.50
10.00
9.00
9.50
8.50
8.00
7.50
7.00
6.50
6.00
8.00
8.41
8.61
7.66
8.12
5.36
10.28
6.54
7.59
8.85
7.77
7.66
5.91
9.07
6.92
7.46
7.00
7.13
7.18

OBSERVED NITRATE TIME-SERIES AT STATION LL19
MICROMOLAR CONCENTRATIONS, 1991 FIELD SEASON

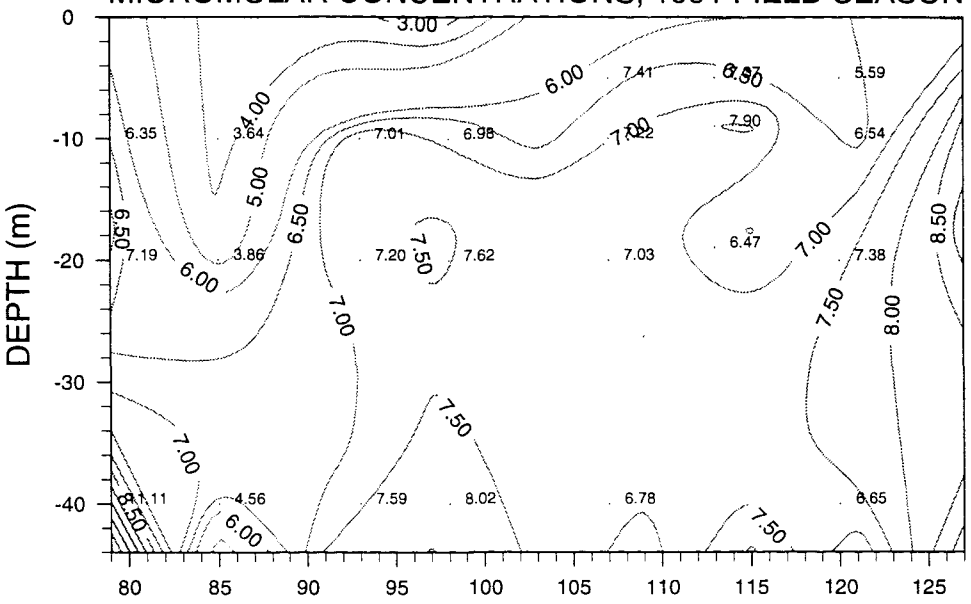

TIME (JULIAN DAYS STARTING FROM JANUARY 1st 1991)

OBSERVED PHOSPHATE TIME-SERIES AT STATION LL19
MICROMOLAR CONCENTRATIONS, 1991 FIELD SEASON

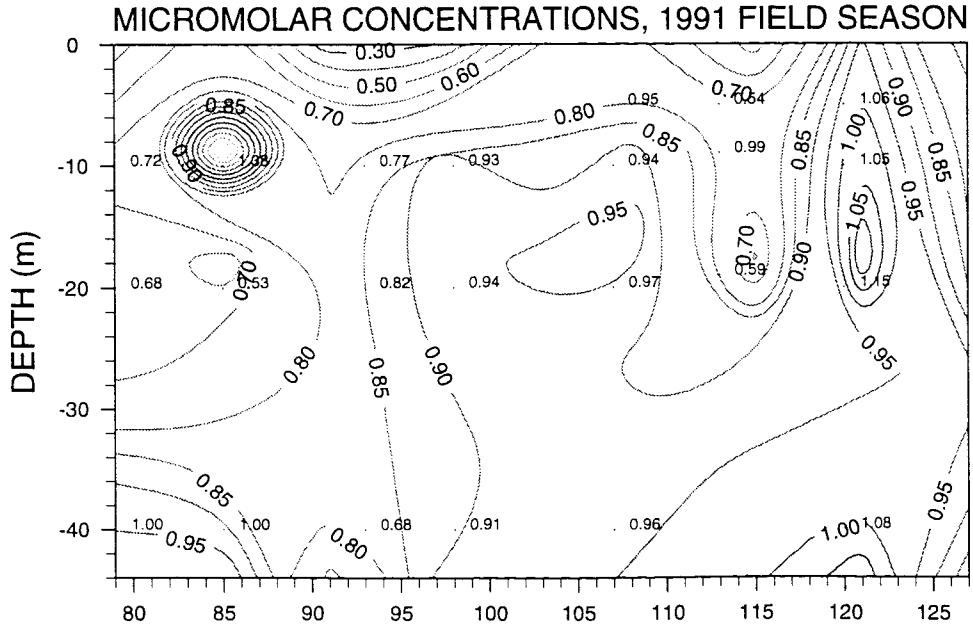

TIME (JULIAN DAYS STARTING FROM JANUARY 1st 1991)

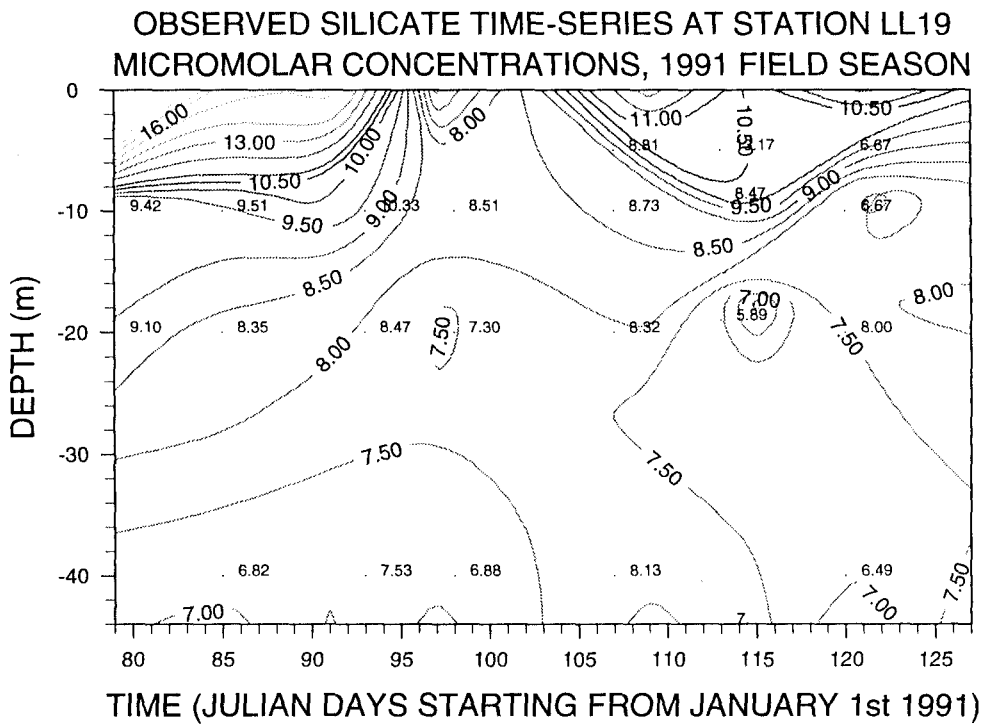
OBSERVED SILICATE TIME-SERIES AT STATION LL19
MICROMOLAR CONCENTRATIONS, 1991 FIELD SEASON
DEPTH (m)
0
-10
-20
-30
-40
16.00
13.00
10.50
10.00
8.00
11.00
10.50
9.42
9.51
9.50
9.00
8.33
8.51
8.73
9.50
9.00
6.67
8.50
8.50
9.10
8.35
8.47
7.50
7.30
8.32
7.00
5.89
8.00
8.00
7.50
7.50
6.82
7.53
6.88
8.13
6.49
7.00
7.00
7.50
80
85
90
95
100
105
110
115
120
125
TIME (JULIAN DAYS STARTING FROM JANUARY 1st 1991)

APPENDIX 5.5

UNIMAP SETTINGS FOR FIGURE 5.22: TEMPORAL VARIABILITY OF NUTRIENT CONCENTRATIONS, CONTOUR PLOTS.

The file from which this timeseries plot is made up contains data arranged in columns. It is of the format:

Time (Julian Day) Depth (m) Nitrate (µM) Phosphate (µM) Silicate (µM)

Therefore nitrate, phosphate and silicate data are read into UNIMAP as three z variables. The basic set-up within the UNIMAP software is as follows:

DATA:	IRREGULAR	
	FORMAT:	NUMBER OF Z VARIABLES = 3
		COLUMNS
		FORTRAN FORMAT = *
	RATIO:	X = 1.6
		Y = 1
		Z = 1
	READ	
INTERPOLATE:	METHOD:	BILINEAR
	OPTIONS:	DISTANCE WEIGHTED
	GRIDCELLS:	X DIRECTION = 8 (weeks)
		Y DIRECTION = 3
MAP:	GALLERY:	2D LINE
SMOOTH:	SMOOTHING LEVEL: MED	
STYLE:	ANNOTATE	
	METHOD:	OVERLAY
CLASS:	LIMITS:	AS ON PLOTS]

APPENDIX 6.2

UNIMAP SETTINGS FOR FIGURES 6.1 TO 6.3: SPATIAL VARIABILITY OF HYDROGRAPHIC PROPERTIES.

The file from which the plots are made up contains data from six stations arranged in columns and each column has a 1 m depth resolution. It is of the format:

Distance from LL0 (Km) Depth (m) Temperature (°C) Salinity (PSU) Density (Kg m^{-3}) Chlorophyll (Micrograms per litre)

Therefore temperature, salinity, density and chlorophyll data are read into UNIMAP as four z variables. A file containing distance data of the stations from station LL0 is also read into UNIMAP as a fault file. The basic set-up within the UNIMAP software is as follows:

DATA:	IRREGULAR	
	FORMAT:	NUMBER OF Z VARIABLES = 4
		COLUMNS
		FORTRAN FORMAT = *
	RATIO:	X = 1.6
		Y = 1
		Z = 1
	READ	
INTERPOLATE:	METHOD:	BILINEAR
	OPTIONS:	DISTANCE WEIGHTED
	GRIDCELLS:	X DIRECTION = 5 (for the 6 stations used)
		Y DIRECTION = 115
MAP:	GALLERY:	2D LINE
SMOOTH:	SMOOTHING LEVEL: MED	
STYLE:	ANNOTATE	
	METHOD:	OVERLAY
CLASS:	LIMITS:	AS ON PLOTS]

APPENDIX 6.2

UNIMAP SETTINGS FOR FIGURES 6.5 TO 6.7: TEMPORAL VARIABILITY OF HYDROGRAPHIC PROPERTIES, CONTOUR PLOTS.

The files from which the timeseries plots are made up contain data arranged in columns and each column has a 1 m depth resolution. It is of the format:

Time (Julian Day) Depth (m) Temperature (°C) Salinity (PSU) Density (Kg m^{-3}) Chlorophyll (µg l^{-1})

Therefore temperature, salinity, density and chlorophyll data are read into UNIMAP as four z variables. The basic set-up within the UNIMAP software is as follows:

DATA:	IRREGULAR	
	FORMAT:	NUMBER OF Z VARIABLES = 4
		COLUMNS
		FORTRAN FORMAT = *
	RATIO:	X = 1.6
		Y = 1
		Z = 1
	READ	
INTERPOLATE:	METHOD:	BILINEAR
	OPTIONS:	DISTANCE WEIGHTED
	GRIDCELLS:	X DIRECTION = 11 (weeks)
		Y DIRECTION = 36 (LL0), 110 (LL14), 40 (LL19).
MAP:	GALLERY:	2D LINE
SMOOTH:	SMOOTHING LEVEL: MED	
STYLE:	ANNOTATE	
	METHOD:	OVERLAY
CLASS:	LIMITS:	AS ON PLOTS]

APPENDIX 6.4

NUTRIENT DATA COLLECTED AT STATIONS LL0 AND LL14 IN 1992
FRESHWATER DATA RELEVANT TO THE TIME-PERIOD ALSO INCLUDED

	JDAY	DEPTH (m)	PHOSP	NITRAT	SILICATE
			MICROMOLAR CONCENTRATIONS		
STATION LL0	59	0	0.42	3.98	5.69
	64	0	0.53	4.93	7.84
	86	0	0.42	4.7	5.59
	99	0	0.91	6.38	8.97
	105	0	0.47	7.24	7.02
	114	0	0.34	4.97	4.36
	125	0	0.65	3.07	3.34
	132	0	0.2	1.74	1.86
	139	0	0.2	1.73	1.33
	59	-5	0.55	5.67	7.29
	64	-5	0.38	4.39	8.84
	86	-5	0.68	4.79	7.04
	99	-5	0.88	5.68	7.31
	105	-5	2.26	7.63	12.89
	114	-5	0.34	4.87	4.35
	125	-5	0.22	2.72	1.2
	132	-5	0.32	4.38	2.24
	139	-5	0.34	3.13	1.71
	59	-10	0.48	4.64	6.89
	64	-10	0.4	4.8	6.52
	86	-10	0.94	6.74	9.04
	99	-10	1.18	7.72	7.82
	105	-10	2.42	10.35	14.51
	114	-10	0.8	8.53	6.4
	125	-10	0.55	5.19	4
	132	-10	0.51	6.02	1.99
	139	-10	0.33	3.19	1.62
	59	-20	0.53	6.43	6.43
	64	-20	0.5	5.63	5.24
	86	-20	0.53	7.5	6.16
	99	-20	0.44	4.25	3.34
	105	-20	0.53	7.91	5.31
	114	-20	0.47	6.73	3.59
	125	-20	0.43	5.75	2.28
	132	-20	0.38	5.08	1.61
	139	-20	0.5	6.49	2.65
	59	-40	1.53	5.56	9.23
	64	-40	0.57	7.52	6.88
	86	-40	0.46	7.12	6.17
	99	-40	1.13	9.33	8.76
	105	-40	0.55	7.31	4.62
	114	-40	0.53	6.21	4.9
	125	-40	0.5	7.8	4.25
	132	-40	0.45	6.14	2.47
	139	-30	0.45	4.97	2.25
STATION LL14	59	0	0.21	6.58	14.98
	64	0	0.91	4.86	15.26
	79	0	0.39	3.92	9.64
	86	0	0.38	5.09	8.74
	99	0	0.43	6.62	8.63
	105	0	0.25	3.5	8
	114	0	0.2	3.45	7.56
	125	0	0.17	2.11	2.63
	132	0	0.14	0.44	4.88

139	0	0.4	2.34	9.07
59	-5	0.36	4.34	10.68
64	-5	0.23	6.56	16.26
79	-5	1.6	6.39	13.05
86	-5	0.84	5.08	6.84
105	-5	0.51	5.5	7.5
114	-5	0.53	6.35	7.56
125	-5	0.14	2.5	2.18
132	-5	0.14	1.14	0.87
139	-5	0.26	2.6	1.67
59	-10	0.8	6.8	8.19
79	-10	0.44	8.17	11.17
86	-10	0.54	8.66	8.17
99	-10	0.43	6.7	6.27
105	-10	0.51	5.5	6.15
114	-10	0.53	5.63	4.92
125	-10	0.17	2.74	1.43
132	-10	0.2	2.62	1.3
139	-10	0.6	3.2	2.54
59	-20	0.51	6.71	6.61
64	-20	0.64	7.13	7.49
79	-20	0.38	6.62	7.02
86	-20	0.54	7.08	5.96
99	-20	0.43	6.09	4.93
114	-20	0.53	5.71	4.57
125	-20	0.78	3.86	3.48
132	-20	0.45	5.23	2.18
139	-20	1.14	4.92	4.6
59	-40	0.61	8.83	8.82
64	-40	0.81	6.7	7.89
79	-40	0.46	6.61	6.05
86	-40	0.84	5.33	6.23
99	-40	0.55	7.75	6.42
105	-40	1.19	8.5	10
114	-40	0.5	8	6
125	-40	0.36	5.47	2.29
132	-40	0.48	6.44	3.65
139	-40	0.39	4.57	2.22
64	-60	0.51	6.69	6.31
86	-60	0.58	7.42	6.55
79	-65	0.48	7.11	6.59
99	-60	0.45	6.08	4.93
105	-60	1.03	9	11
114	-60	0.6	6.42	7.95
125	-60	0.54	7.07	5.08
132	-60	0.51	7.39	5.26
139	-60	0.66	7.67	5.02
59	-76	0.53	7.61	7.48
64	-77	0.5	6.16	6.4
64	-92	0.63	7.77	8.16
79	-90	0.48	7.25	7.53
86	-90	0.89	9.54	9.37
59	-106	0.65	6.48	8.57
64	-107	0.93	9.2	9.76
79	-105	0.55	8.01	8.23
86	-80	0.86	7.24	8.03
99	-80	0.48	7.13	5.82
114	-80	0.65	6.32	6.91
125	-80	0.6	7.21	8.16
132	-80	0.54	7.04	5.4
139	-80	0.62	8.86	6.78
99	-100	0.48	7.82	6.42
105	-100	0.67	7.86	6.71
125	-100	0.7	8.56	7.41
132	-100	0.68	9.2	7.75
105	-110	0.66	8.09	6.4
125	-110	0.66	8.21	7.25

	139	-109	0.69	8.58	7.64
FRESHWATER	77		0.135	3	
DATA	92		0.135	5.56	
	104		0.135	6	
	133		0.135	2.71	

APPENDIX 6.5

UNIMAP SETTINGS FOR FIGURES 6.23 TO 6.25: TEMPORAL VARIABILITY OF NUTRIENT CONCENTRATIONS, CONTOUR PLOTS.

The files from which the timeseries plots are made up contain data arranged in columns. It is of the format:

Time (Julian Day) Depth (m) Nitrate (µM) Phosphate (µM) Silicate (µM)

Therefore nitrate, phosphate and silicate data are read into UNIMAP as three z variables. The basic set-up within the UNIMAP software is as follows:

DATA:	IRREGULAR	
	FORMAT:	NUMBER OF Z VARIABLES = 3
		COLUMNS
		FORTRAN FORMAT = *
	RATIO:	X = 1.6
		Y = 1
		Z = 1
	READ	
INTERPOLATE:	METHOD:	BILINEAR
	OPTIONS:	DISTANCE WEIGHTED
	GRIDCELLS:	X DIRECTION = 11 (weeks)
		Y DIRECTION = 5 for station LL0 and 9 for LL14
MAP:	GALLERY:	2D LINE
SMOOTH:	SMOOTHING LEVEL: MED	
STYLE:	ANNOTATE	
	METHOD:	OVERLAY
CLASS:	LIMITS:	AS ON PLOTS]

OBSERVED PHOSPHATE TIME-SERIES AT STATION LL14
MICROMOLAR CONCENTRATIONS, 1992 FIELD SEASON

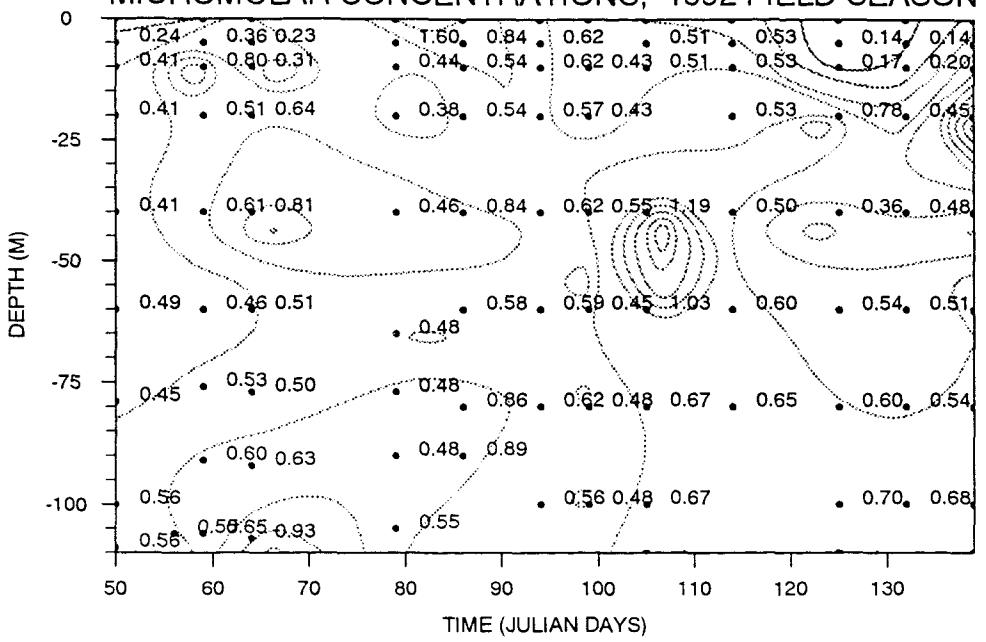

OBSERVED PHOSPHATE TIME-SERIES AT STATION LL0
MICROMOLAR CONCENTRATIONS, 1992 FIELD SEASON

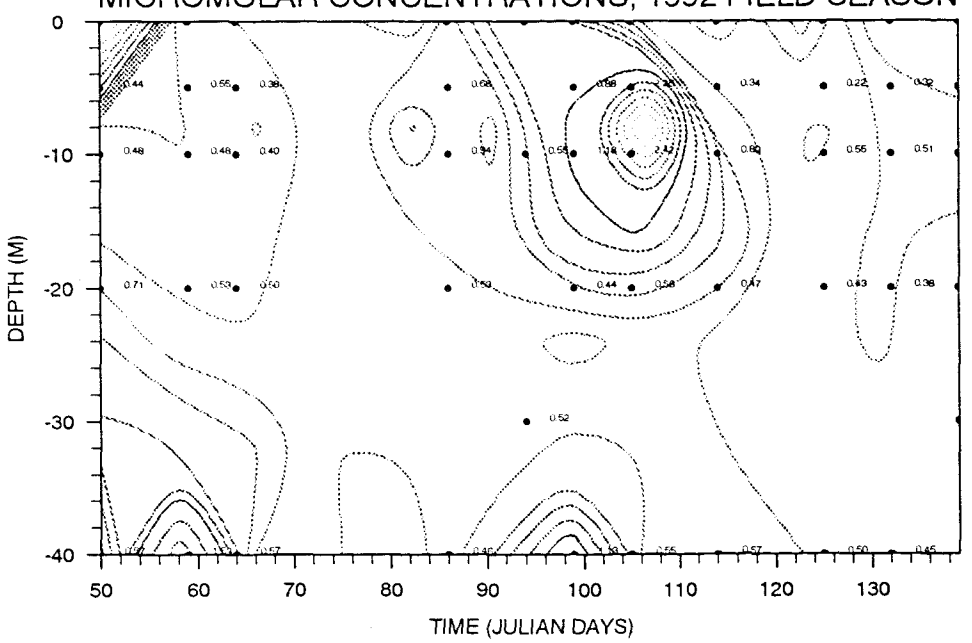

OBSERVED NITRATE TIME-SERIES AT STATION LL14
MICROMOLAR CONCENTRATIONS, 1992 FIELD SEASON

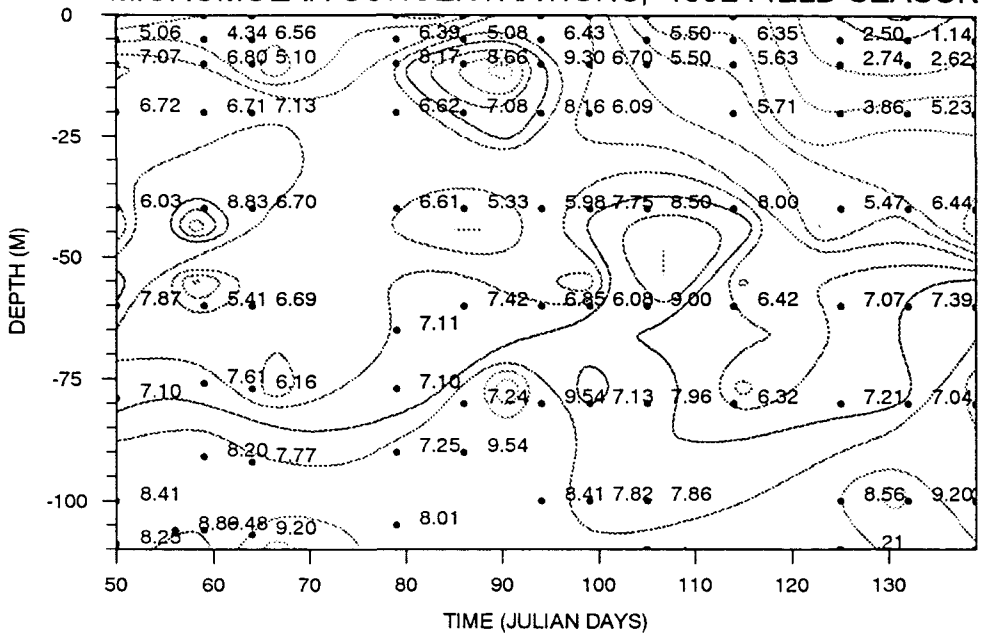

OBSERVED NITRATE TIME-SERIES AT STATION LL0
MICROMOLAR CONCENTRATIONS, 1992 FIELD SEASON

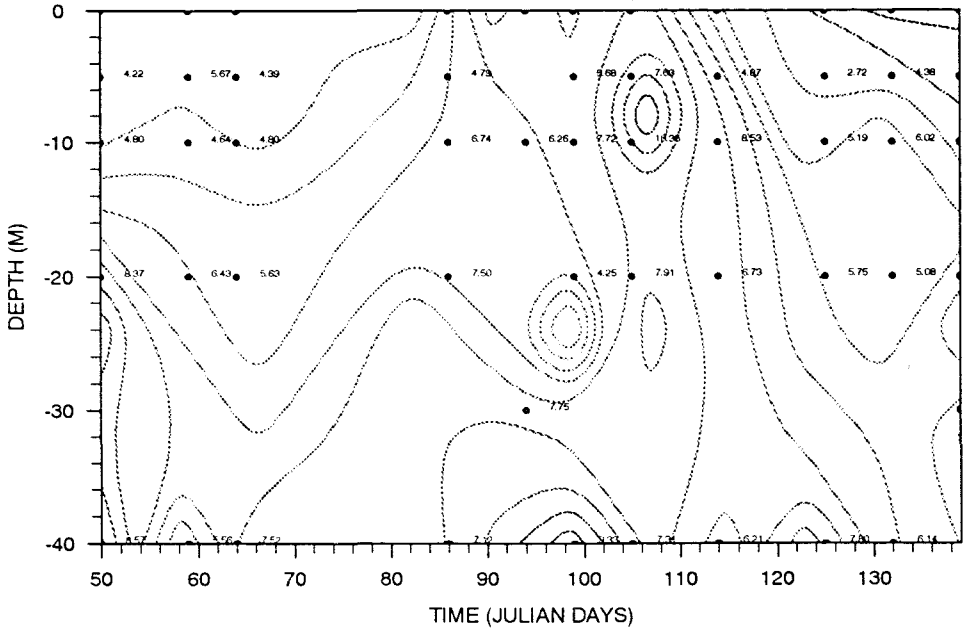

OBSERVED SILICATE TIME-SERIES AT STATION LL14
MICROMOLAR CONCENTRATIONS, 1992 FIELD SEASON

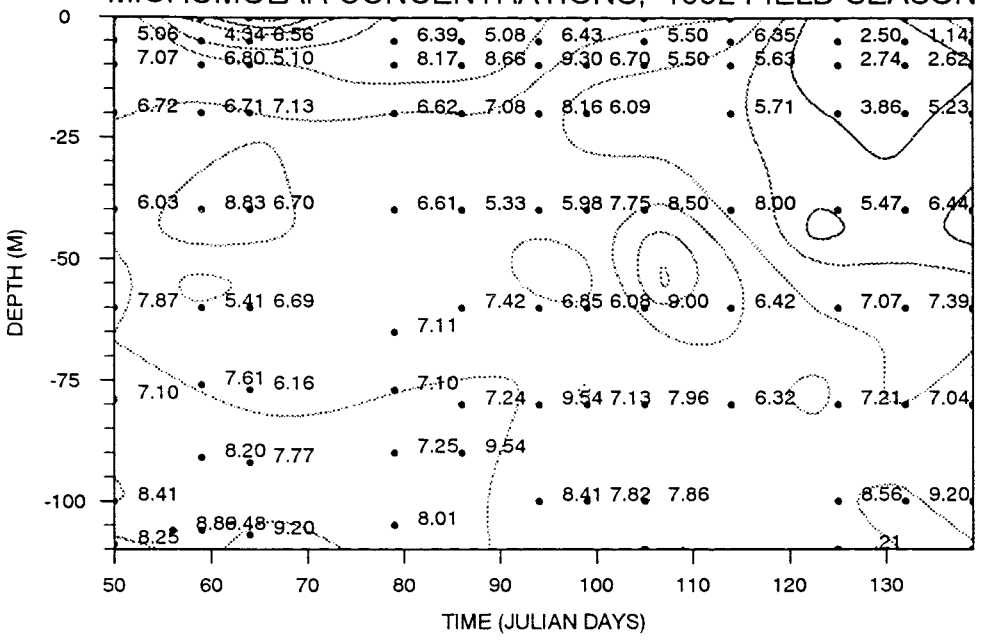

OBSERVED SILICATE TIME-SERIES AT STATION LL0
MICROMOLAR CONCENTRATIONS, 1992 FIELD SEASON

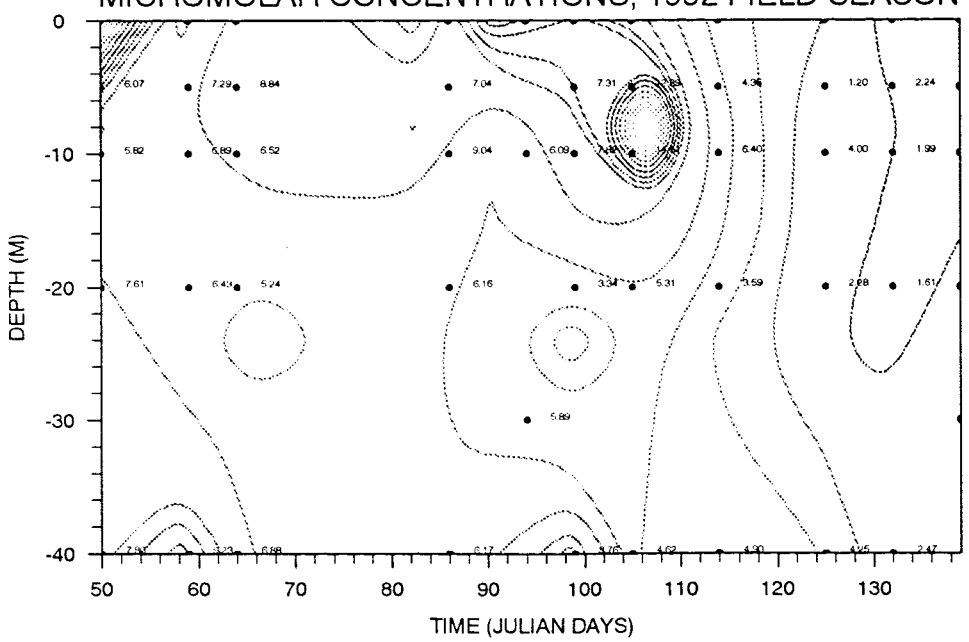

APPENDIX 6.6

CORING DATA 1993 LOCH LINNHE

XRD RESULTS
% WEIGHT

STATION	DISTANCE FROM LL0 (Km)	QUARTZ	FELD-SPAR	TOTAL COARSE	CLAYS	HAEM TITE
RIVER LOCHY	21	30.4	51.5	81.9	17.1	0.6
LL20	20	58.6	20.6	79.2	19.5	1.1
LL19	18	39.7	28	67.7	31.3	0.5
LL14	13	31.7	18.7	50.4	48.1	1.47
LL2	8	29.9	34.8	64.7	31.3	3.5
LL0	0	34.6	39.7	74.3	18.8	0.9

XRF RESULTS
% WEIGHT

	DISTANCE FROM LL0 (Km)	P205	Al203	Fe2O3	Fe:Al	P:Al
RIVER LOCHY	21	0.115	10.359	2.877	0.27773	0.011101
LL20	20	0.132	8.918	2.884	0.323391	0.014802
LL19	18	0.167	10.543	3.197	0.303234	0.01584
LL14	13	0.264	13.365	5.47	0.409278	0.019753
LL2	8	0.164	10.23	3.655	0.357283	0.016031
LL0	0	0.15	9.568	2.802	0.292851	0.015677

APPENDIX 7.1

DATA FILE CHECK 92.RUN:

J.DAY	SALINITY (PSU)	TEMP (oC)	IRRAD (mW hrs cm-2)	DEW POINT TEMP (oC)	RIVER TEMP. (oC)	WIND VEL. (KNOTS)	FRESHWATER VOL. (CUMECS)
56.	28.476	7.883	111.700	1.000	4.633	11.000	156.178
57.	28.279	7.886	179.200	3.000	4.689	11.000	180.668
58.	28.081	7.889	83.200	5.600	4.744	11.000	257.712
59.	27.883	7.892	167.100	1.000	4.800	11.000	147.613
60.	27.737	7.895	60.700	5.000	4.911	11.000	120.577
61.	27.591	7.898	62.900	5.000	5.022	6.700	122.882
62.	27.444	7.902	39.500	3.400	5.133	9.000	177.382
63.	27.298	7.905	240.400	7.000	5.244	10.200	149.673
64.	27.152	7.908	55.000	8.000	5.356	12.500	180.977
65.	26.842	7.911	87.000	7.000	5.467	9.700	177.055
66.	26.532	7.914	74.900	4.600	5.578	11.700	226.603
67.	26.222	7.917	98.800	6.000	5.689	11.900	273.178
68.	25.912	7.920	292.600	4.000	5.800	5.100	176.536
69.	25.602	7.923	96.400	6.200	5.911	9.400	173.863
70.	25.293	7.926	200.900	1.000	6.022	15.500	147.949
71.	24.983	7.929	166.400	1.000	6.133	14.000	264.626
72.	24.673	7.932	96.700	2.400	6.244	24.200	254.276
73.	24.363	7.936	207.400	0.000	6.356	18.200	162.537
74.	24.053	7.939	138.900	0.000	6.467	12.500	101.304
75.	23.743	7.942	288.200	0.000	6.578	2.400	77.114
76.	23.433	7.945	126.700	8.000	6.689	8.800	150.795
77.	23.124	7.948	135.800	8.000	6.800	10.800	192.646
78.	22.814	7.951	172.500	7.000	6.050	10.000	236.479
79.	22.504	7.954	66.700	4.000	5.300	10.100	323.976
80.	22.194	7.957	186.500	8.800	5.262	9.700	254.808
81.	23.461	7.960	185.200	2.000	5.223	10.700	216.525
82.	24.728	7.963	273.500	3.000	5.185	10.700	158.999
83.	25.995	7.966	355.000	0.800	5.146	11.000	155.067
84.	27.262	7.970	284.000	-0.400	5.108	9.300	61.032
85.	28.528	7.973	81.500	6.600	5.069	12.000	40.205
86.	29.795	7.976	272.700	1.000	5.031	12.500	104.970
87.	30.011	7.979	185.000	0.200	4.992	7.100	78.110
88.	30.226	7.982	204.600	7.000	4.954	4.500	50.968
89.	30.442	7.985	98.800	0.600	4.915	9.200	41.190
90.	30.657	7.988	188.100	2.000	4.877	12.000	32.213
91.	30.873	7.991	59.700	0.200	4.838	18.000	30.537
92.	31.088	7.994	328.700	-3.800	4.800	24.400	16.170
93.	31.303	7.997	264.600	-4.400	4.900	10.300	12.768
94.	31.519	8.000	310.300	-2.000	5.000	5.900	10.589
95.	31.734	8.004	244.800	2.600	5.140	6.000	14.062
96.	31.950	8.007	173.000	5.000	5.280	7.900	18.202
97.	32.165	8.010	200.100	7.000	5.420	5.300	34.661
98.	32.381	8.013	314.200	3.600	5.560	5.300	36.605
99.	32.596	8.016	370.900	4.400	5.700	4.200	33.999
100.	32.529	8.019	194.900	5.000	6.000	7.900	32.275
101.	32.461	8.022	116.000	9.000	6.300	4.900	34.876
102.	32.394	8.025	115.700	7.000	6.600	5.800	38.553
103.	32.326	8.028	311.500	4.000	6.900	8.600	46.702
104.	32.259	8.031	329.100	1.600	7.200	10.500	27.977
105.	32.191	8.034	142.900	2.000	7.090	10.700	24.176
106.	32.108	8.038	492.200	0.800	6.980	9.400	24.440

107.	32.024	8.041	222.600	-2.000	6.870	8.900	32.146
108.	31.941	8.044	64.100	6.400	6.760	9.300	90.964
109.	31.857	8.047	400.100	5.000	6.650	17.500	47.782
110.	31.774	8.050	492.400	0.800	6.540	6.700	33.221
111.	31.690	8.053	92.100	2.000	6.430	11.500	33.267
112.	31.607	8.056	295.000	8.600	6.320	11.200	40.508
113.	31.523	8.059	308.700	3.000	6.210	6.400	19.589
114.	31.440	8.062	319.100	6.000	6.100	10.400	14.187
115.	31.353	8.065	255.600	7.000	6.161	9.300	45.997
116.	31.267	8.068	412.900	7.000	6.222	10.500	59.384
117.	31.181	8.072	365.100	5.000	6.283	10.000	129.657
118.	31.094	8.075	354.000	6.000	6.344	12.500	153.149
119.	31.008	8.078	377.000	5.000	6.406	7.000	107.607
120.	30.922	8.081	317.900	4.000	6.467	8.500	75.021
121.	30.749	8.084	168.300	9.000	6.528	9.500	75.884
122.	30.663	8.087	322.200	5.800	6.589	19.000	114.782
123.	30.577	8.090	421.200	2.800	6.650	13.900	87.222
124.	30.490	8.093	112.800	6.800	6.711	6.900	59.200
125.	30.490	8.096	133.900	9.400	6.772	7.800	86.796
126.	30.519	8.099	369.900	5.400	6.833	8.900	108.976
127.	30.547	8.102	50.200	9.800	6.894	11.700	164.737
128.	30.576	8.106	238.100	8.000	6.956	14.400	163.442
129.	30.604	8.109	529.000	2.000	7.017	19.000	114.966
130.	30.633	8.112	563.100	2.000	7.078	5.700	104.482
131.	30.661	8.115	665.000	2.000	7.139	4.500	91.366
132.	30.690	8.118	364.100	6.000	7.200	8.000	83.257
133.	30.681	8.121	240.100	5.000	8.400	10.300	116.577
134.	30.671	8.124	525.900	11.400	8.583	10.000	127.980
135.	30.662	8.127	422.900	11.000	8.767	12.300	57.727
136.	30.653	8.130	388.100	4.000	8.950	13.500	41.867
137.	30.644	8.133	749.000	4.200	9.133	5.100	40.442
138.	30.635	8.136	721.700	8.000	9.317	3.300	37.523
139.	30.626	8.140	738.100	6.200	9.500	8.200	35.607

DATA FILE CHECK92.STR:

J.DAY	DEPTH (m)	TEMP (oC)	SALINITY (PSU)	DENS (Kg/m3)	TRANS (VOLTS)	FLUOR (VOLTS)
56	0	6.019	8.779	6.89	1.228	1.076
56	-1	6.019	8.779	6.89	1.228	1.076
56	-2	6.133	10.849	8.514	2.189	1.048
56	-3	6.651	16.093	12.596	1.99	0.852
56	-4	7.253	21.394	16.696	1.326	0.584
56	-5	7.455	23.286	18.156	2.216	0.457
56	-6	7.579	24.772	19.306	2.929	0.389
56	-7	7.653	25.783	20.09	3.097	0.321
56	-8	7.697	26.377	20.55	3.254	0.264
56	-9	7.724	26.679	20.783	3.409	0.234
56	-10	7.748	27.015	21.044	3.525	0.201
56	-11	7.778	27.494	21.415	3.593	0.23
56	-12	7.808	27.923	21.747	3.637	0.206
56	-13	7.831	28.184	21.949	3.682	0.138
56	-14	7.846	28.399	22.115	3.722	0.107
56	-15	7.868	28.69	22.341	3.746	0.086
56	-16	7.894	28.929	22.524	3.8	0.072
56	-17	7.91	29.036	22.607	3.872	0.068
56	-18	7.916	29.098	22.655	3.918	0.062
56	-19	7.92	29.233	22.76	3.92	0.051
56	-20	7.939	29.476	22.948	3.901	0.04
56	-21	7.961	29.703	23.122	3.929	0.034
56	-22	7.973	29.852	23.238	3.962	0.026
56	-23	7.984	29.947	23.311	3.965	0.009
56	-24	7.991	30.016	23.364	3.964	0.013
56	-25	7.999	30.091	23.421	3.965	0.015
56	-26	8.015	30.21	23.513	3.975	-0.001
56	-27	8.033	30.35	23.62	4.005	-0.02
56	-28	8.036	30.429	23.682	4.026	-0.026
56	-29	8.035	30.465	23.71	4.002	0.005
56	-30	8.043	30.502	23.737	3.982	-0.011
56	-31	8.052	30.532	23.76	3.996	-0.029
56	-32	8.058	30.561	23.782	4.01	-0.033
56	-33	8.062	30.595	23.808	4.015	-0.04
56	-34	8.073	30.632	23.835	4.018	-0.034
56	-35	8.084	30.66	23.856	4.029	-0.036
56	-36	8.095	30.686	23.875	4.052	-0.036
56	-37	8.104	30.705	23.888	4.071	-0.028
56	-38	8.107	30.718	23.898	4.079	-0.039
56	-39	8.11	30.726	23.904	4.079	-0.054
56	-40	8.113	30.736	23.911	4.076	-0.057
56	-41	8.119	30.752	23.923	4.076	-0.05
56	-42	8.126	30.766	23.933	4.078	-0.047
56	-43	8.136	30.779	23.942	4.081	-0.053
56	-44	8.147	30.794	23.952	4.081	-0.058
56	-45	8.151	30.815	23.967	4.084	-0.05
56	-46	8.153	30.831	23.98	4.09	-0.041
56	-47	8.16	30.856	23.999	4.088	-0.04
56	-48	8.174	30.89	24.023	4.078	-0.05
56	-49	8.184	30.914	24.041	4.067	-0.068
56	-50	8.189	30.927	24.05	4.059	-0.077
56	-51	8.194	30.939	24.059	4.052	-0.062
56	-52	8.199	30.95	24.067	4.043	-0.054
56	-53	8.204	30.968	24.08	4.035	-0.06
56	-54	8.218	31.002	24.105	4.029	-0.072
56	-55	8.23	31.019	24.117	4.029	-0.076
56	-56	8.238	31.03	24.124	4.028	-0.062
56	-57	8.246	31.049	24.138	4.025	-0.045

56	-58	8.259	31.074	24.155	4.026	-0.055
56	-59	8.273	31.095	24.17	4.025	-0.072
56	-60	8.288	31.118	24.186	4.019	-0.068
56	-61	8.311	31.144	24.203	4.018	-0.066
56	-62	8.322	31.15	24.206	4.027	-0.067
56	-63	8.325	31.152	24.207	4.033	-0.06
56	-64	8.327	31.163	24.216	4.035	-0.06
56	-65	8.331	31.166	24.217	4.032	-0.075
56	-66	8.33	31.165	24.217	4.027	-0.067
56	-67	8.329	31.164	24.216	4.025	-0.055
56	-68	8.327	31.165	24.217	4.021	-0.06
56	-69	8.331	31.176	24.225	4.013	-0.06
56	-70	8.341	31.19	24.235	4.01	-0.067
56	-71	8.352	31.196	24.237	4.009	-0.081
56	-72	8.359	31.201	24.241	4.006	-0.078
56	-73	8.359	31.214	24.25	4.003	-0.059
56	-74	8.361	31.216	24.252	4.001	-0.062
56	-75	8.366	31.225	24.258	4.001	-0.059
56	-76	8.375	31.24	24.269	4	-0.058
56	-77	8.382	31.251	24.276	3.996	-0.06
56	-78	8.386	31.257	24.28	3.991	-0.064
56	-79	8.39	31.264	24.285	3.985	-0.068
56	-80	8.397	31.27	24.289	3.981	-0.069
56	-81	8.4	31.272	24.29	3.98	-0.082
56	-82	8.402	31.275	24.293	3.977	-0.052
56	-83	8.406	31.279	24.295	3.974	-0.049
56	-84	8.41	31.282	24.296	3.975	-0.064
56	-85	8.418	31.288	24.3	3.978	-0.062
56	-86	8.427	31.296	24.305	3.977	-0.046
56	-87	8.431	31.304	24.311	3.974	-0.048
56	-88	8.432	31.309	24.315	3.969	-0.046
56	-89	8.434	31.312	24.317	3.965	-0.041
56	-90	8.437	31.318	24.321	3.963	-0.055
56	-91	8.442	31.323	24.324	3.961	-0.058
56	-92	8.448	31.333	24.331	3.956	-0.055
56	-93	8.455	31.352	24.345	3.946	-0.057
56	-94	8.466	31.364	24.352	3.933	-0.052
56	-95	8.459	31.359	24.35	3.929	-0.049

DATA FILE LINNHE.RUN

```
0.07000                    ! inflow mixing efficency (ei)
0.00125   66400            ! dt (days) and no.timesteps (1992)
1.0         152            ! dz (mtrs) and no. of depth interval
15.000000                        ! sill depth (m)
20.1e6                     ! surface area (m2)
```

NOTE: No. of timesteps is changed to 90400 for year 1990 and 64000 for nutrient model

DATA FILE LINNHE.AREA

Depth (m)	Area (Km2)	Fraction of surface area
0	20.1	1.000
2	19.5	0.970
4	18.96	0.943
6	18.45	0.918
8	17.8	0.886
10	17.16	0.854
12	16.65	0.828
14	16	0.796
16	15.45	0.769
18	14.8	0.736
20	14.25	0.709
22	13.65	0.679
24	13.15	0.654
26	12.65	0.629
28	12.15	0.604
30	11.74	0.584
32	11.4	0.567
34	11.05	0.550
36	10.65	0.530
38	10.33	0.514
40	10.03	0.499
42	9.72	0.484
44	9.4	0.468
46	9.05	0.450
48	8.72	0.434
50	8.4	0.418
52	8.2	0.408
54	7.95	0.396
56	7.75	0.386
58	7.53	0.375
60	7.3	0.363
62	7.1	0.353
64	6.9	0.343
66	6.7	0.333
68	6.5	0.323
70	6.27	0.312
72	6.05	0.301
74	5.85	0.291
76	5.65	0.281
78	5.45	0.271
80	5.25	0.261
82	5.05	0.251
84	4.9	0.244
86	4.7	0.234
88	4.59	0.228
90	4.41	0.219
92	4.25	0.211
94	4.1	0.204
96	3.93	0.196
98	3.78	0.188
100	3.65	0.182
102	3.49	0.174
104	3.33	0.166
106	3.2	0.159
108	3.04	0.151
110	2.9	0.144
112	2.75	0.137
114	2.63	0.131

116	2.49	0.124
118	2.35	0.117
120	2.2	0.109
122	2.1	0.104
124	1.95	0.097
126	1.8	0.090
128	1.7	0.085
130	1.57	0.078
132	1.43	0.071
134	1.3	0.065
136	1.18	0.059
138	1.05	0.052
140	0.93	0.046
142	0.8	0.040
144	0.69	0.034
146	0.55	0.027
148	0.45	0.022
150	0.32	0.016
152	0.22	0.011

DATA FILE CHECK90.RUN

J.day	Salinity (PSU)	Temp (oC)	Irrad	Dew Point Temp(oC)	River Temp(oC)	Wind Vel. (knots)	Freshwater Vol (CUMECS)
38	25.140	7.238	100	3	5	5.7	370.516
39	25.706	7.299	100	0	5	13.9	258.228
40	25.737	7.201	100	3.8	5	12.1	299.605
41	25.767	7.103	100	4	5	13.7	289.332
42	25.798	7.006	100	1	5	14	216.509
43	25.828	6.908	100	-0.6	5	15.1	129.712
44	25.859	6.810	100	-0.2	5	8.1	70.124
45	28.174	7.136	100	0.6	5	5.6	56.786
46	30.490	7.462	100	1	5	9	52.089
47	27.622	7.316	100	0	5	5.3	51.428
48	27.344	7.180	100	4.8	5	12.7	141.44
49	27.066	7.044	100	1.6	5	15.1	216.011
50	26.787	6.908	100	3	5	17.7	450.487
51	26.509	6.772	100	4	5	14.9	350.195
52	26.231	6.636	100	2	5	14.8	310.432
53	24.461	6.532	100	5	5	15.6	363.641
54	25.003	6.573	100	6.2	5	9.5	347.874
55	25.546	6.614	100	3	5	5.6	277.049
56	26.088	6.654	100	5.2	5	13.4	312.187
57	26.631	6.695	100	0.6	5	24.4	269.427
58	27.174	6.736	100	2	5	23.7	166.63
59	27.716	6.777	100	-0.8	5	10.8	71.537
60	28.259	6.818	100	-3.2	5	10.7	58.098
61	27.637	6.775	100	2.8	5	11.8	61.567
62	27.015	6.733	100	4.2	5	14.5	437.71
63	26.392	6.691	100	2.8	5	14	342.107
64	25.770	6.649	100	5.8	5	22	702.681
65	25.148	6.607	100	8	5	14.6	932.96
66	26.620	6.768	100	8.6	5	11.9	861.783
67	28.093	6.929	100	3	5	6.5	395.946
68	25.712	6.808	100	-0.2	5	10.2	315.209
69	25.398	6.814	100	8.8	5	11.9	971.062
70	25.084	6.820	100	2.8	5	20.9	595.763
71	24.770	6.826	100	4	5	7.8	369.752
72	24.456	6.832	100	5	5	14.2	321.679
73	23.021	6.847	100	5.2	5	15.5	322.456
74	21.585	6.861	100	7.4	5	13.6	702.753
75	23.047	7.066	100	9.4	5	14.8	543.077
76	23.263	7.095	100	7	5	10	339.246
77	23.480	7.125	100	7.6	5	12.3	364.29
78	23.696	7.154	100	2.4	5	12.9	284.833
79	23.913	7.183	100	5	5	12.9	374.722
80	23.234	7.151	100	3	5	17.4	362.4
81	22.556	7.118	100	3.6	5	15.4	295.439
82	23.090	7.094	100	7	5	19.1	508.512
83	23.623	7.070	100	1	5	23.6	297.139
84	24.157	7.046	100	3.8	5	13.3	193.895
85	24.691	7.022	100	5	5	4.4	138.574
86	25.225	6.998	100	2	5	14.4	129.584
87	25.552	7.052	100	2.6	5	5.8	76.237
88	25.879	7.107	100	5.4	5	9	62.105
89	27.304	7.279	100	8.8	5	6.7	68.587
90	28.228	7.279	100	6.2	5	1.8	58.284
91	29.153	7.279	100	7.6	5	2.5	56.113
92	30.078	7.279	100	6	5	14.3	76.875
93	31.003	7.279	100	-6	5	11.3	55.41
94	30.241	7.243	100	-8.6	5	7.3	40.06
95	29.479	7.207	100	4.6	5	8.1	61.164

96	28.299	7.222	100	5.2	5	3.5	54.413
97	28.248	7.306	100	4	5	2.3	52.551
98	28.197	7.390	100	5	5	4.3	46.066
99	28.146	7.474	100	6	5	9.4	69.83
100	28.094	7.559	100	6	5	17.4	133.247
101	28.397	7.547	100	8.8	5	10.3	116.942
102	28.699	7.536	100	3.6	5	10.3	79.513
103	29.001	7.525	100	3	5	8.5	57.125
104	29.304	7.514	100	3	5	7.9	49.336
105	29.606	7.503	100	3	5	12.7	65.112
106	29.909	7.492	100	2	5	9.2	104.777
107	30.211	7.480	100	2.6	5	7.6	103.263
108	30.513	7.469	100	2.6	5	9.3	66.053
109	28.732	7.359	100	4	5	8.4	107.286
110	29.189	7.468	100	3.8	5	6.5	127.047
111	29.646	7.578	100	0.8	5	2.7	59.766
112	30.104	7.687	100	7	5	4.3	48.35
113	30.561	7.797	100	7	5	2.9	53.592
114	31.018	7.906	100	5	5	4.5	55.85
115	29.819	7.914	100	5	5	9.8	71.853
116	28.619	7.922	100	2.4	5	12.8	60.558
117	31.356	7.887	100	1	5	7.5	42.497
118	31.466	7.920	100	9	5	8.9	51.894
119	31.576	7.954	100	9.8	5	8.4	62.325
120	31.576	7.954	100	9	5	2.5	30.638
121	31.686	7.987	100	12	5	5.5	25.126
122	31.796	8.021	100	12	5	3.5	25.387
123	31.906	8.055	100	10	5	4	23.56
124	32.016	8.088	100	11	5	5.4	18.868
125	32.126	8.122	100	5	5	9.7	19.588
126	32.236	8.155	100	6	5	7.4	19.425
127	32.345	8.189	100	5.2	5	4.9	23.251
128	32.455	8.223	100	5.4	5	3.3	39.145
129	32.565	8.256	100	6.4	5	2.7	38.7
130	32.675	8.290	100	7	5	3.3	34.405
131	32.785	8.323	100	12.8	5	5.1	32.392
132	32.895	8.357	100	6.6	5	4.1	31.086
133	33.005	8.391	100	6	5	4.2	30.214
134	33.115	8.424	100	8.6	5	4.9	27.415
135	33.225	8.458	100	7.2	5	8.4	27.571
136	31.082	8.849	100	8.2	5	8.5	24.454
137	31.180	8.870	100	6	5	3.2	23.491
138	31.278	8.892	100	7.2	5	4.1	19.788
139	31.376	8.913	100	6.8	5	4.2	18.505
140	31.474	8.935	100	7.6	5	4.8	18.151
141	31.572	8.957	100	8	5	5	17.919
142	31.670	8.978	100	7	5	5.3	18.262
143	31.768	9.000	100	7.4	5	10.9	19.083
144	31.866	9.022	100	2	5	6.5	17.258
145	31.964	9.043	100	4	5	3.9	9.308
146	32.062	9.065	100	6	5	4.3	5.907
147	32.160	9.086	100	9	5	3.8	5.698
148	32.258	9.108	100	10	5	6.1	5.686
149	32.356	9.130	100	13	5	4.5	6.333
150	32.454	9.151	100	10	5	6.5	6.296
151	32.552	9.173	100	9	5	9.6	6.229

APPENDIX 7.2

UNIMAP SETTINGS FOR HYDROGRAPHIC MODEL-PREDICTED TIMESERIES CONTOUR PLOTS.

The output file from the model from which the timeseries plots are made up contains predicted data in columns and each column has a 1 m depth resolution. Data are output to a depth of 110 m. It is of the format:

Time (Julian Day) Depth (m) Temperature (°C) Salinity (PSU) Density (Kg m^{-3})

Therefore temperature, salinity and density data are read into UNIMAP as three z variables. The basic set-up within the UNIMAP software is as follows:

DATA:	IRREGULAR	
	FORMAT:	NUMBER OF Z VARIABLES = 3
		COLUMNS
		FORTRAN FORMAT = *
	RATIO:	X = 1.6
		Y = 1
		Z = 1
	READ	
INTERPOLATE:	METHOD:	BILINEAR
	OPTIONS:	DISTANCE WEIGHTED
	GRIDCELLS:	X DIRECTION = 83 for 1992 data, 113 for 1990
		Y DIRECTION = 110 for 1992 and 1990 data
MAP:	GALLERY:	2D LINE
SMOOTH:	SMOOTHING LEVEL: MED	
STYLE:	ANNOTATE	
	METHOD:	OVERLAY
CLASS:	LIMITS:	AS ON PLOTS]

DATA FILE: CHECK90.STR

J.DAY	DEPTH (m)	TEMP (oC)	SALINITY (PSU)	DENSITY (kg/m3)	TRANS	FLUOR
38	0	4.705	3.841	3.037	1000	1000
38	-1	4.732	3.915	3.096	1000	1000
38	-2	4.938	4.253	3.359	1000	1000
38	-3	5.072	4.423	3.489	1000	1000
38	-4	5.115	4.719	3.722	1000	1000
38	-5	5.38	6.893	5.433	1000	1000
38	-6	5.862	10.594	8.329	1000	1000
38	-7	6.275	15.554	12.204	1000	1000
38	-8	6.565	20.711	16.231	1000	1000
38	-9	6.792	23.642	18.51	1000	1000
38	-10	6.929	24.516	19.181	1000	1000
38	-11	7.039	25.073	19.607	1000	1000
38	-12	7.145	25.52	19.945	1000	1000
38	-13	7.274	26.13	20.409	1000	1000
38	-14	7.381	26.621	20.781	1000	1000
38	-15	7.445	26.874	20.971	1000	1000
38	-16	7.495	27.097	21.14	1000	1000
38	-17	7.555	27.352	21.332	1000	1000
38	-18	7.61	27.559	21.488	1000	1000
38	-19	7.652	27.723	21.611	1000	1000
38	-20	7.703	27.913	21.753	1000	1000
38	-21	7.76	28.116	21.905	1000	1000
38	-22	7.801	28.261	22.014	1000	1000
38	-23	7.825	28.376	22.1	1000	1000
38	-24	7.851	28.501	22.195	1000	1000
38	-25	7.904	28.67	22.321	1000	1000
38	-26	7.943	28.835	22.445	1000	1000
38	-27	7.985	28.979	22.552	1000	1000
38	-28	8.01	29.066	22.616	1000	1000
38	-29	8.032	29.198	22.717	1000	1000
38	-30	8.071	29.361	22.839	1000	1000
38	-31	8.097	29.427	22.887	1000	1000
38	-32	8.09	29.457	22.912	1000	1000
38	-33	8.077	29.519	22.962	1000	1000
38	-34	8.105	29.626	23.042	1000	1000
38	-35	8.155	29.674	23.073	1000	1000
38	-36	8.172	29.728	23.113	1000	1000
38	-37	8.195	29.781	23.151	1000	1000
38	-38	8.238	29.821	23.176	1000	1000
38	-39	8.271	29.861	23.204	1000	1000
38	-40	8.283	29.909	23.239	1000	1000
38	-41	8.293	29.953	23.272	1000	1000
38	-42	8.32	30.037	23.334	1000	1000
38	-43	8.348	30.128	23.402	1000	1000
38	-44	8.377	30.206	23.459	1000	1000
38	-45	8.414	30.273	23.505	1000	1000
38	-46	8.448	30.336	23.55	1000	1000
38	-47	8.498	30.399	23.592	1000	1000
38	-48	8.546	30.512	23.674	1000	1000
38	-49	8.597	30.654	23.778	1000	1000
38	-50	8.668	30.854	23.923	1000	1000
38	-51	8.762	31.045	24.059	1000	1000
38	-52	8.847	31.184	24.155	1000	1000
38	-53	8.895	31.272	24.217	1000	1000
38	-54	8.925	31.321	24.25	1000	1000
38	-55	8.954	31.375	24.288	1000	1000
38	-56	8.978	31.439	24.335	1000	1000
38	-57	9.005	31.511	24.386	1000	1000
38	-58	9.031	31.556	24.418	1000	1000

38	-59	9.056	31.602	24.45	1000	1000
38	-60	9.079	31.634	24.472	1000	1000
38	-61	9.095	31.65	24.482	1000	1000
38	-62	9.104	31.672	24.498	1000	1000
38	-63	9.111	31.696	24.515	1000	1000
38	-64	9.133	31.748	24.553	1000	1000
38	-65	9.174	31.832	24.612	1000	1000
38	-66	9.211	31.866	24.633	1000	1000
38	-67	9.23	31.872	24.635	1000	1000
38	-68	9.244	31.918	24.668	1000	1000
38	-69	9.261	31.966	24.703	1000	1000
38	-70	9.284	32.009	24.733	1000	1000
38	-71	9.305	32.023	24.741	1000	1000
38	-72	9.31	32.028	24.744	1000	1000
38	-73	9.314	32.046	24.757	1000	1000
38	-74	9.323	32.106	24.802	1000	1000
38	-75	9.329	32.104	24.8	1000	1000
38	-76	9.336	32.093	24.791	1000	1000
38	-77	9.342	32.099	24.794	1000	1000
38	-78	9.345	32.094	24.79	1000	1000
38	-79	9.347	32.106	24.799	1000	1000
38	-80	9.355	32.125	24.812	1000	1000
38	-81	9.364	32.13	24.815	1000	1000
38	-82	9.368	32.131	24.815	1000	1000
38	-83	9.369	32.11	24.798	1000	1000
38	-84	9.372	32.106	24.795	1000	1000
38	-85	9.375	32.131	24.814	1000	1000
38	-86	9.376	32.122	24.806	1000	1000
38	-87	9.377	32.128	24.811	1000	1000
38	-88	9.377	32.132	24.815	1000	1000
38	-89	9.378	32.132	24.814	1000	1000
38	-90	9.379	32.125	24.809	1000	1000
38	-91	9.381	32.136	24.817	1000	1000
38	-92	9.384	32.159	24.834	1000	1000
38	-93	9.387	32.155	24.83	1000	1000
38	-94	9.389	32.178	24.849	1000	1000
38	-95	9.389	32.178	24.848	1000	1000
38	-96	9.391	32.168	24.84	1000	1000
38	-97	9.395	32.18	24.849	1000	1000
38	-98	9.397	32.183	24.851	1000	1000
38	-99	9.399	32.169	24.84	1000	1000
38	-100	9.401	32.162	24.834	1000	1000
38	-101	9.401	32.175	24.845	1000	1000
38	-102	9.402	32.193	24.858	1000	1000
38	-103	9.402	32.199	24.862	1000	1000
38	-104	9.402	32.208	24.87	1000	1000

DATA FILE NUTSAL.92

Concentrations in micromoles per litre.

J.Day	Saline PO4	Saline NO3	Saline Si04	River PO4	River NO3	River Si04
59	0.495	5.18	6.575	0.088398	5.8648	13.78
60	0.484375	5.119375	6.70875	0.089373	5.839281	13.78
61	0.47375	5.05875	6.8425	0.090378	5.813494	13.78
62	0.463125	4.998125	6.97625	0.091411	5.787445	13.78
63	0.4525	4.9375	7.11	0.092473	5.761144	13.78
64	0.461548	4.984881	7.102738	0.093562	5.734597	13.78
65	0.470595	5.032262	7.095476	0.09468	5.707813	13.78
66	0.479643	5.079643	7.088214	0.095824	5.680799	13.78
67	0.48869	5.127024	7.080952	0.096996	5.653564	13.78
68	0.497738	5.174405	7.07369	0.098194	5.626115	13.78
69	0.506786	5.221786	7.066429	0.099419	5.59846	13.78
70	0.515833	5.269167	7.059167	0.100669	5.570609	13.78
71	0.524881	5.316548	7.051905	0.101946	5.542568	13.78
72	0.533929	5.363929	7.044643	0.103247	5.514347	13.78
73	0.542976	5.41131	7.037381	0.104573	5.485953	13.78
74	0.552024	5.45869	7.030119	0.105924	5.457396	13.78
75	0.561071	5.506071	7.022857	0.107298	5.428683	13.78
76	0.570119	5.553452	7.015595	0.108697	5.399824	13.78
77	0.579167	5.600833	7.008333	0.110118	5.370826	13.78
78	0.588214	5.648214	7.001071	0.111563	5.341698	13.78
79	0.597262	5.695595	6.99381	0.113029	5.312449	13.78
80	0.60631	5.742976	6.986548	0.114518	5.283088	13.78
81	0.615357	5.790357	6.979286	0.116028	5.253623	13.78
82	0.624405	5.837738	6.972024	0.117559	5.224063	13.78
83	0.633452	5.885119	6.964762	0.11911	5.194417	13.78
84	0.6425	5.9325	6.9575	0.120682	5.164694	13.78
85	0.652778	6.02	7.067778	0.122274	5.134901	13.78
86	0.663056	6.1075	7.178056	0.123884	5.105049	13.78
87	0.673333	6.195	7.288333	0.125514	5.075146	13.78
88	0.683611	6.2825	7.398611	0.127161	5.045201	13.78
89	0.693889	6.37	7.508889	0.128826	5.015222	13.78
90	0.704167	6.4575	7.619167	0.130509	4.985219	13.78
91	0.714444	6.545	7.729444	0.132208	4.955201	13.78
92	0.724722	6.6325	7.839722	0.133924	4.925176	13.78
93	0.735	6.72	7.95	0.135655	4.895153	13.78
94	0.754583	6.60125	7.768333	0.137401	4.865142	13.78
95	0.774167	6.4825	7.586667	0.139162	4.835151	13.78
96	0.79375	6.36375	7.405	0.140938	4.805188	13.78
97	0.813333	6.245	7.223333	0.142727	4.775264	13.78
98	0.832917	6.12625	7.041667	0.144529	4.745386	13.78
99	0.8525	6.0075	6.86	0.146344	4.715564	13.78
100	0.947083	6.386667	7.372083	0.14817	4.685806	13.78
101	1.041667	6.765833	7.884167	0.150009	4.656122	13.78
102	1.13625	7.145	8.39625	0.151858	4.626519	13.78
103	1.230833	7.524167	8.908333	0.153717	4.597008	13.78
104	1.325417	7.903333	9.420417	0.155587	4.567596	13.78
105	1.42	8.2825	9.9325	0.157466	4.538292	13.78
106	1.316389	8.059444	9.348333	0.159353	4.509105	13.78
107	1.212778	7.836389	8.764167	0.161249	4.480044	13.78
108	1.109167	7.613333	8.18	0.163152	4.451117	13.78
109	1.005556	7.390278	7.595833	0.165063	4.422333	13.78
110	0.901944	7.167222	7.011667	0.16698	4.3937	13.78
111	0.798333	6.944167	6.4275	0.168903	4.365227	13.78
112	0.694722	6.721111	5.843333	0.170831	4.336922	13.78
113	0.591111	6.498056	5.259167	0.172764	4.308794	13.78
114	0.4875	6.275	4.675	0.174701	4.280851	13.78
115	0.485227	6.084773	4.495909	0.176642	4.253101	13.78
116	0.482955	5.894545	4.316818	0.178586	4.225552	13.78

117	0.480682	5.704318	4.137727	0.180533	4.198213	13.78
118	0.478409	5.514091	3.958636	0.182481	4.171092	13.78
119	0.476136	5.323864	3.779545	0.184431	4.144197	13.78
120	0.473864	5.133636	3.600455	0.186382	4.117535	13.78
121	0.471591	4.943409	3.421364	0.188332	4.091115	13.78
122	0.469318	4.753182	3.242273	0.190283	4.064944	13.78
123	0.467045	4.562955	3.063182	0.192232	4.039031	13.78
124	0.464773	4.372727	2.884091	0.19418	4.013383	13.78
125	0.4625	4.1825	2.705	0.196125	3.988007	13.78
126	0.446786	4.2	2.593571	0.198068	3.962911	13.78
127	0.431071	4.2175	2.482143	0.200008	3.938102	13.78
128	0.415357	4.235	2.370714	0.201944	3.913589	13.78
129	0.399643	4.2525	2.259286	0.203875	3.889377	13.78
130	0.383929	4.27	2.147857	0.205802	3.865475	13.78
131	0.368214	4.2875	2.036429	0.207723	3.841889	13.78
132	0.3525	4.305	1.925	0.209638	3.818626	13.78
133	0.351071	4.209286	1.911071	0.211546	3.795694	13.78
134	0.349643	4.113571	1.897143	0.213446	3.773098	13.78
135	0.348214	4.017857	1.883214	0.215339	3.750846	13.78
136	0.346786	3.922143	1.869286	0.217224	3.728945	13.78
137	0.345357	3.826429	1.855357	0.219099	3.7074	13.78
138	0.343929	3.730714	1.841429	0.220965	3.686219	13.78
139	0.3425	3.635	1.8275	0.222821	3.665407	13.78

DATA FILE NUTPRO.PRN

NOTE: Concentrations are in micromoles per litre

J. Day	Depth (m)	PO4	NO3	SiO4
59	0	0.21	6.58	14.98
59	-1	0.21	6.58	14.98
59	-2	0.213509	6.527602	14.87942
59	-3	0.219023	6.445263	14.72135
59	-4	0.244211	6.069123	13.9993
59	-5	0.36	4.34	10.68
59	-6	0.413222	4.637562	10.37881
59	-7	0.494605	5.092563	9.918259
59	-8	0.63287	5.865594	9.135802
59	-9	0.749946	6.52015	8.473262
59	-10	0.8	6.8	8.19
59	-11	0.735969	6.780128	7.841139
59	-12	0.693101	6.766824	7.607585
59	-13	0.657188	6.755679	7.411923
59	-14	0.61564	6.742785	7.185555
59	-15	0.579427	6.731546	6.988259
59	-16	0.559043	6.72522	6.877199
59	-17	0.539677	6.71921	6.771691
59	-18	0.524149	6.714391	6.687089
59	-19	0.516895	6.71214	6.647565
59	-20	0.51	6.71	6.61
59	-21	0.517438	6.867686	6.77438
59	-22	0.5242	7.011037	6.923817
59	-23	0.532915	7.1958	7.116424
59	-24	0.544786	7.447461	7.378768
59	-25	0.553201	7.625853	7.564733
59	-26	0.55831	7.734162	7.677641
59	-27	0.56402	7.855214	7.803832
59	-28	0.568077	7.941225	7.893494
59	-29	0.572059	8.025642	7.981495
59	-30	0.575214	8.092539	8.051232
59	-31	0.577769	8.146694	8.107686
59	-32	0.580849	8.211998	8.175763
59	-33	0.584681	8.293231	8.260443
59	-34	0.589865	8.403133	8.375011
59	-35	0.594673	8.505071	8.481277
59	-36	0.59843	8.584711	8.564298
59	-37	0.60121	8.643644	8.625733
59	-38	0.603914	8.700984	8.685507
59	-39	0.607145	8.769474	8.756905
59	-40	0.61	8.83	8.82
59	-41	0.594516	8.476968	8.438065
59	-42	0.582903	8.212194	8.151613
59	-43	0.576129	8.057742	7.984516
59	-44	0.572742	7.980516	7.900968
59	-45	0.568871	7.892258	7.805484
59	-46	0.562581	7.748839	7.650323
59	-47	0.555323	7.583355	7.47129
59	-48	0.546129	7.373742	7.244516
59	-49	0.537903	7.186194	7.041613
59	-50	0.530645	7.02071	6.862581
59	-51	0.524839	6.888323	6.719355
59	-52	0.512258	6.601484	6.409032
59	-53	0.497742	6.270516	6.050968
59	-54	0.488548	6.060903	5.824194
59	-55	0.481774	5.906452	5.657097
59	-56	0.476452	5.785097	5.525806

59	-57	0.472581	5.696839	5.430323
59	-58	0.46871	5.608581	5.334839
59	-59	0.463871	5.498258	5.215484
59	-60	0.46	5.41	5.12
59	-61	0.464345	5.546552	5.266483
59	-62	0.472069	5.78931	5.526897
59	-63	0.482207	6.107931	5.86869
59	-64	0.487034	6.259655	6.031448
59	-65	0.488483	6.305172	6.080276
59	-66	0.489448	6.335517	6.112828
59	-67	0.49331	6.456897	6.243034
59	-68	0.497172	6.578276	6.373241
59	-69	0.502483	6.745172	6.552276
59	-70	0.50731	6.896897	6.715034
59	-71	0.508276	6.927241	6.747586
59	-72	0.51069	7.003103	6.828966
59	-73	0.513586	7.094138	6.926621
59	-74	0.516	7.17	7.008
59	-75	0.524207	7.427931	7.28469
59	-76	0.53	7.61	7.48
59	-77	0.534959	7.563306	7.525041
59	-78	0.537934	7.535289	7.552066
59	-79	0.547851	7.441901	7.642149
59	-80	0.556777	7.357851	7.723223
59	-81	0.564711	7.28314	7.795289
59	-82	0.570661	7.227107	7.849339
59	-83	0.574628	7.189752	7.885372
59	-84	0.578595	7.152397	7.921405
59	-85	0.584545	7.096364	7.975455
59	-86	0.592479	7.021653	8.047521
59	-87	0.595455	6.993636	8.074545
59	-88	0.597438	6.974959	8.092562
59	-89	0.599421	6.956281	8.110579
59	-90	0.599421	6.956281	8.110579
59	-91	0.599421	6.956281	8.110579
59	-92	0.601405	6.937603	8.128595
59	-93	0.60438	6.909587	8.15562
59	-94	0.611322	6.844215	8.218678
59	-95	0.62124	6.750826	8.30876
59	-96	0.630165	6.666777	8.389835
59	-97	0.63314	6.63876	8.41686
59	-98	0.635124	6.620083	8.434876
59	-99	0.639091	6.582727	8.470909
59	-100	0.639091	6.582727	8.470909
59	-101	0.641074	6.56405	8.488926
59	-102	0.641074	6.56405	8.488926
59	-103	0.640083	6.573388	8.479917
59	-104	0.64405	6.536033	8.51595
59	-105	0.645041	6.526694	8.524959
59	-106	0.65	6.48	8.57

DATA FILE NUTLIN.PRN

NOTE: Concentrations are in micromoles/litre
Simulated linear profiles 1:1 with initial salinity profile

J.Day	Depth (m)	PO4	NO3	SiO4
59	0	0.21	6.58	14.98
59	-1	0.21	6.58	14.98
59	-2	0.210539	6.59688	15.01843
59	-3	0.211385	6.623404	15.07881
59	-4	0.215252	6.744575	15.35467
59	-5	0.23303	7.3016	16.62279
59	-6	0.26212	8.213094	18.69789
59	-7	0.306602	9.60686	21.87094
59	-8	0.382175	11.97482	27.26182
59	-9	0.446166	13.97986	31.8265
59	-10	0.473525	14.8371	33.77808
59	-11	0.494072	15.48093	35.24383
59	-12	0.507829	15.91197	36.22511
59	-13	0.519353	16.27307	37.04719
59	-14	0.532686	16.69083	37.99828
59	-15	0.544307	17.05495	38.82723
59	-16	0.550848	17.25992	39.29385
59	-17	0.557063	17.45463	39.73714
59	-18	0.562046	17.61077	40.0926
59	-19	0.564374	17.68371	40.25866
59	-20	0.566586	17.75304	40.41649
59	-21	0.568491	17.81272	40.55236
59	-22	0.570223	17.86698	40.67588
59	-23	0.572454	17.93691	40.83508
59	-24	0.575494	18.03215	41.05192
59	-25	0.577649	18.09967	41.20564
59	-26	0.578957	18.14067	41.29896
59	-27	0.58042	18.18648	41.40327
59	-28	0.581459	18.21903	41.47738
59	-29	0.582478	18.25098	41.55011
59	-30	0.583286	18.2763	41.60776
59	-31	0.58394	18.2968	41.65442
59	-32	0.584729	18.32152	41.71069
59	-33	0.58571	18.35226	41.78068
59	-34	0.587038	18.39386	41.87538
59	-35	0.588269	18.43244	41.96321
59	-36	0.589231	18.46258	42.03184
59	-37	0.589943	18.48489	42.08261
59	-38	0.590636	18.50659	42.13202
59	-39	0.591463	18.53251	42.19104
59	-40	0.592194	18.55542	42.24319
59	-41	0.59281	18.57471	42.28711
59	-42	0.593272	18.58918	42.32004
59	-43	0.593541	18.59762	42.33926
59	-44	0.593676	18.60184	42.34886
59	-45	0.59383	18.60666	42.35984
59	-46	0.59408	18.6145	42.37769
59	-47	0.594368	18.62354	42.39827
59	-48	0.594734	18.63499	42.42435
59	-49	0.595061	18.64524	42.44768
59	-50	0.59535	18.65428	42.46827
59	-51	0.59558	18.66152	42.48473
59	-52	0.596081	18.67719	42.52042
59	-53	0.596658	18.69528	42.56159
59	-54	0.597023	18.70673	42.58767

59	-55	0.597293	18.71517	42.60688
59	-56	0.597504	18.7218	42.62198
59	-57	0.597658	18.72663	42.63296
59	-58	0.597812	18.73145	42.64394
59	-59	0.598005	18.73748	42.65766
59	-60	0.598158	18.7423	42.66864
59	-61	0.598332	18.74773	42.68099
59	-62	0.598639	18.75737	42.70295
59	-63	0.599044	18.77003	42.73177
59	-64	0.599236	18.77606	42.7455
59	-65	0.599294	18.77787	42.74961
59	-66	0.599332	18.77907	42.75236
59	-67	0.599486	18.7839	42.76334
59	-68	0.59964	18.78872	42.77432
59	-69	0.599852	18.79535	42.78941
59	-70	0.600044	18.80138	42.80314
59	-71	0.600082	18.80258	42.80588
59	-72	0.600179	18.8056	42.81274
59	-73	0.600294	18.80921	42.82098
59	-74	0.60039	18.81223	42.82784
59	-75	0.600717	18.82248	42.85117
59	-76	0.600948	18.82971	42.86764
59	-77	0.601044	18.83273	42.8745
59	-78	0.601102	18.83453	42.87862
59	-79	0.601295	18.84056	42.89234
59	-80	0.601468	18.84599	42.9047
59	-81	0.601622	18.85081	42.91568
59	-82	0.601737	18.85443	42.92391
59	-83	0.601814	18.85684	42.9294
59	-84	0.601891	18.85925	42.93489
59	-85	0.602006	18.86287	42.94312
59	-86	0.60216	18.86769	42.9541
59	-87	0.602218	18.8695	42.95822
59	-88	0.602257	18.8707	42.96097
59	-89	0.602295	18.87191	42.96371
59	-90	0.602295	18.87191	42.96371
59	-91	0.602295	18.87191	42.96371
59	-92	0.602333	18.87312	42.96646
59	-93	0.602391	18.87492	42.97057
59	-94	0.602526	18.87914	42.98018
59	-95	0.602718	18.88517	42.9939
59	-96	0.602891	18.8906	43.00626
59	-97	0.602949	18.89241	43.01037
59	-98	0.602988	18.89361	43.01312
59	-99	0.603065	18.89602	43.01861
59	-100	0.603065	18.89602	43.01861
59	-101	0.603103	18.89723	43.02135
59	-102	0.603103	18.89723	43.02135
59	-103	0.603084	18.89663	43.01998
59	-104	0.603161	18.89904	43.02547
59	-105	0.60318	18.89964	43.02684
59	-106	0.603276	18.90266	43.0337

APPENDIX 7.4

UNIMAP SETTINGS FOR NUTRIENT CONCENTRATION MODEL-PREDICTED TIMESERIES CONTOUR PLOTS.

The output file from the model from which the timeseries plots are made up contains predicted data in columns and each column has a 1 m depth resolution. Data are output to a depth of 110 m. It is of the format:

Time (Julian Day) Depth (m) Temperature (°C) Salinity (PSU) Density (Kg m^{-3}) Phosphate (μM) Nitrate (μM) Silicate (μM)

Therefore phosphate, nitrate and silicate data are read into UNIMAP as part of six z variables. The basic set-up within the UNIMAP software is as follows:

DATA:	IRREGULAR	
	FORMAT:	NUMBER OF Z VARIABLES = 6
		COLUMNS
		FORTRAN FORMAT = *
	RATIO:	X = 1.6
		Y = 1
		Z = 1
	READ	
INTERPOLATE:	METHOD:	BILINEAR
	OPTIONS:	DISTANCE WEIGHTED
	GRIDCELLS:	X DIRECTION = 83 for 1992 data, 113 for 1990
		Y DIRECTION = 110 for 1992 and 1990 data
MAP:	GALLERY:	2D LINE
SMOOTH:	SMOOTHING LEVEL: MED	
STYLE:	ANNOTATE	
	METHOD:	OVERLAY
CLASS:	LIMITS:	AS ON PLOTS]

REFERENCES

Aarseth I. 1980, Glaciomarine sedimentation in a fjord environment: example from Sognefjord. In: "Glaciation and Deglaciation in Central Norway. Field Guide to Excursion. Symposium on Processes of Glacier Erosion and Sedimentation, Geilo, Norway". (Orheim O., ed.), Norsk Polar Institutt, Oslo.

Aksnes D.L. and Lie U. 1990, A coupled physical-biological pelagic model of a shallow sill fjord. Est. Coast. Shelf Sci., 31: 459-486.

Alvarez-Salgado X.A., Fraga F. and Pérez F.F. 1992, Determination of nutrient salts by automatic methods both in seawater and brackish water: the phosphate blank. Marine Chem., 39: 311-319.

Andrae M.O. and Andrae T.W. 1989, Dissolved arsenic species in the Schelde Estuary and watershed, Belgium Est. Coast. Shelf Sci., 29: 421-433.

Atlas E.L., Gordon L.I., Hager S.W. and Park P.K. 1971, A practical manual for use of the Technicon autoanalyser in sea water nutrient analysis, (revised). Technical Report 215. Department of Oceanography, School of Science, Oregon state University

Balls P.W. 1992, Nutrient behaviour in two contrasting Scottish estuaries, the Forth and Tay. Oceanologica Acta, 15, no. 3: 261-277.

Balzer W. 1980, Redox dependent processes in the transition from oxic to anoxic conditions: An in situ study concerning remineralisation, nutrient release and heavy metal solubilization. In: "Fjord Oceanography". (Freeland H.J., Farmer D.M. and Levings C.D., eds.), 659-666. Plenum Press, New York and London.

Banse K. 1974[1], On the interpretation of data for the carbon-to-nitrogen ratio of phytoplankton. Limnol. Oceanogr., 19: 695-699.

Banse K. 1974[2], The nitrogen to phosphorus ratio in the photic zone of the sea and the elemental composition of the plankton. Deep-Sea Res., 21: 767-771.

Banwell C.N. 1983, Electron spectroscopy of atoms. In: "Fundamentals of Molecular Spectroscopy". McGraw-Hill Book Comapny (U.K.) Limited, London.

Beck K.C., Reuter J.H. and Perdue E.M. 1974, Organic and inorganic geochemistry of some coastal plain rivers in the southeastern United States. Geochim. Cosmochim. Acta, 38: 341-364.

Bendschneider K. and Robinson R.J. 1952, A new spectrophotometric determination of nitrite in sea water. Jour. Mar. Res., 11: 87-96.

Berry A.W. 1993, A response to the Scottish Office Consultation Paper on proposed amendments to the Control of Pollution Act, 1974 and the Reservoirs Act, 1975. Unpublished report from Knapdale Seafarms Limited, Achnamara, Argyll, Scotland.

Billen G., Lancelot C. and Meybeck M. 1990, N, P and Si retention along the aquatic continuum from land to ocean. In: "Ocean Margin Processes in Global Change". Dahlem Conference, Berlin.

Billen G., Lancelot C. and Meybeck M. 1991, N, P and Si retention along the aquatic continuum from land to ocean. In: "Ocean Margin Processes in Global Change". (Mantoura R.F.C., Martin J.M. and Wollast R., eds.). John Wiley and Sons Limited.

Boulton G.S., Chroston P.N. and Jarvis J. 1981, A marine seismic study of the late Quaternary sedimentation and inferred glacier fluctuations along western Inverness-shire, Scotland. Boreas, 10: 39-51.

Bowden K.F. 1948, The processes of heating and cooling in a section of the Irish Sea. Monthly Not. Roy. Astron. Soc. Geophys. Suppl., 5: 270-281.

Bowden K.F. 1983, The stress of the wind on the sea surface. In: "Physical Oceanography of Coastal Waters". (Allan T.D., ed.), 122-128. Ellis Horwood Limited, Chichester.

Boyle E.A., Edmond J.M. and Sholkovitz E.R. 1977, The mechanism of iron removal in estuaries. Geochim. Cosmochim. Acta, 41: 1313-1324.

Brady D.K., Graves W.L., Geyer J.C. 1969, Surface heat exchange st power plant cooling lakes. Cooling Water Discharge Project Report No. 5. Edison Electric Institute Publication No. 69-901, New York.

Brewer P.G. 1975, Minor elements in seawater. In: "Chemical Oceanography, Second Edition". (Riley J.P. and Skirrow, eds.), p 453. Academic Press, London, New York, San Francisco.

Brewer P.G. and Riley J.P. 1965, The automatic determination of nitrate in seawater. Deep-Sea Res., 12: 765.

Brockmann U., Billen M. and Gieskes W.W.C. 1988, North Sea nutrients and eutrophication. In: "Pollution of the North Sea. An Assessment". (Salomons W., Bayne B.L., Duursma E. and Forstener U., eds.). Springer-Verlag.

Broecker W.S. 1982, Ocean chemistry during glacial time. Geochim. Cosmochim. Acta, 46: 1689-1705.

Broecker W.S. and Peng T.H. 1982, Internal cycling and Throughput. In: "Tracers in the Sea". Eldigio Press.

Brogersma-Sanders M. 1957, Mass mortality in the sea. In: "Treaties on Marine Ecology and Paleoecology". (Hedgepath, J.W., ed.), Geol. Soc. Am. Mem., 67: 941-1010.

Burton J.D. 1976, Basic properties and processes in estuarine chemistry. In: "Estuarine Chemistry". (Burton J.D. and Liss P.S., eds.), 1-36. Academic Press, London.

Burton J.D. 1980, Factors limiting primary production: nutrients. In: "Plankton and Productivity in the Oceans". (Raymont J.E.G., ed.), second edition, volume 1. Pergamon Press.

Burton J.D. 1988, Riverborne materials and the continent-ocean interface. In: "Physical and Chemical Weathering in Geochemical Cycles". (Lerman A. and Meybeck M., eds.),299-321. Kluwer Academic Publishers.

Burton J.D., Leatherland T.M. and Liss P.S. 1970, The reactivity of dissolved silicon in some natural waters. Limnol. Oceanogr., 15: 472-476.

Butler E.I. and Tibbitts S. 1972, Chemical survey of the Tamar Estuary. I. Properties of the waters. J. Mar. Biol. Assoc. U.K., 52: 681-699.

Cannon G.A. and Ebbesmeyer C.C. 1978, Winter replacement of bottom water in Puget Sound. In: "Estuarine Transport Processes". (Kjerfve B., ed.), 229-238. Univ. S. Carolina Press, Columbia.

Carman R. and Wulff F. 1989, Adsorption capacity of phosphorus in Baltic Sea sediments. Est. Coast. Shelf Sci., 29: 447-456.

Carpenter P.D. and Smith J.D. 1984, Effect of pH, iron and humic acid on behaviour of phosphate. Environ. Tech. Lett., 6: 65-72.

Carritt D.E. and Goodgal S. 1954, Sorption reactions and source ecological implications. Deep-Sea Res., 1: 224-243.

Chase E.M. and Sayles F.L. 1980, Phosphorus in suspended sediments of the Amazon River. Est. Coast. Mar. Sci., 11: 383-391.

Chen Y.S.R., Butler J.N. and Stumm W. 1973, Kinetic study of phosphate reaction with aluminium oxide and kaolinite. Environ. Sci. Technol., 7: 327-332.

Chester R. 1990, The global journey: material sources. In: "Marine Geochemistry", 9-77. Unwin Hyman Limited, London.

Choppin G.R. and Clark S.B. 1991, The kinetic interactions of metal ions with humic acids. Mar. Chem., 36: 27-38.

Cifuentes L.A., Schemel L.E. and Sharp J.H. 1990, Qualitative and numerical analyses of the effects if river inflow variations on mixing diagrams in estuaries. Est. Coast. Shelf Sci., 30: 411-427.

Collos Y., Yin K. and Harrison P.J. 1992, A note of caution on reduction conditions when using the cadmium-copper column for nitrate determinations in aquatic environments of varying salinities. Mar. Chem., 38: 325-329.

Craib J.S. 1965, A sampler for taking short, undisturbed marine cores. J. Cons. Perm. Int. Explor. Mer. 30: 34-39.

Craig R.E. 1954, A first study of the detailed hydrography of some Scottish West Highland sea-lochs (Loch Inard, Kanaird and the Cairnbaan group). Int. Council Explor. sea., Annates Biol., 10: 16-19.

Craig R.E. 1959, Hydrography of Scottish coastal waters. Mar. Res. No. 2. Scottish Home Department.

Degobbis D. 1990, A stoichiometric model of nutrient cycling in the northern Adriatic Sea and its relation to regeneration processes. Mar. Chem., 29: 235-253.

Dortch O. and Rabalais N.N., Turner E., Redalje D.G. and Lohrenz S.E. 1992, Silicate availability, direct sinking of phytoplankton and hypoxia on the Louisiana continental shelf. A paper presented at the ECSA/ERF meeting, Plymouth, September 1992.

Dyer K.R. 1979, Estuaries and estuarine sedimentation. In: "Estuarine Hydrography and Sedimentation". (Dyer K.R., ed.), 1-18. Cambridge University Press, Cambridge. London, New York and Melbourne.

Eckert J.M. and Sholkovitz E.R. 1976, The flocculation of iron, aluminium and humates from river water by electrolytes. Geochim. Cosmochim. Acta, 40: 847-848.

Edinger J.E., Brady D.K. and Geyer J.C. 1968, The response of water temperatures to meteorological conditions. Water Resour. Res., 4: 1137-1145.

Edinger J.E., Brady D.K. and Geyer J.C. 1974, Heat exchange and transport in the environment. Cooling WAter Dischrge Project Report, No. 14. Electric Power Research Institute Publication No. 74-049-00-3, Palo Alto.

Edwards A. and Edelsten D.J. 1977, Deep water renewal of Loch Etive: A three basin Scottish fjord. Estuar. Coast. Mar. Sci., 5: 575-595.

Edwards A., Edelsten D.J., Saunders M.A. and Stanley S.O. 1980, Renewal and entrainment in Loch Eil: A periodically ventilated Scottish fjord. In: "Fjord Oceanography". (Freeland H.J., Farmer D.M. and Levings C.D., eds.), 523 530. Plenum Press, New York and London.

Edwards A. and Grantham B.E. 1986, Inorganic nutrient regeneration in Loch Etive bottom water. In: "The Role of Freshwater Outflow in Coastal Marine Ecosystems". (Skreslet S., ed.), 195-204. Springer-Verlag, Berlin, Heidelberg.

Edwards A. and Sharples F. 1986, Scottish sea-lochs: A catalogue. SMBA Publication.

Edwards A.M.C. 1973, The variation of dissolved constituents with discharge in some Norfolk rivers. J. Hydrol., 18: 219-242.

Ellett D.J. and Martin J.H.A. 1973, The physical and chemical oceanography of the Rockall Channel. Deep-Sea Res., 20: 585-625.

Falconer R.A. 1989, Numerical modelling of the vertical tidal current and salinity structure in a deep water Scottish loch. Ocean Shore. Manag., 12: 61-80.

Farmer D.M. and Freeland H.J. 1983, The physical oceanography of fjords. Prog. Oceanogr., 12: 147-220.

Fisher T.R., Harding L.W., Stanley D.W. and Ward L.G. 1988, Phytoplankton, nutrients and turbidity in the Chesapeake, Delaware and Hudson estuaries. Est. Coast. Shelf. sci., 27: 61-93.

Fitzgerald G.P. and Faust S.L. 1967, Effect of water sample preservation methods on the release of phosphorus from algae. Limnol. Oceanogr., 12: 332-334.

Fleischer M. 1975, "Glossary of Mineral Species". U.S. Geological Survey.

Foster P. 1984, Nutrient distributions in the winter regime of the northern Irish Sea. Mar. Environ. Res., 13: 81-95.

Fox L.E. 1988, A model for inorganic control of phosphate concentrations in river waters. Geochim. Cosmochim. Acta, 53: 417-428.

Fox L.E. 1991, Phosphorus chemistry in the Hudson tidal river. Geochim. Cosmochim. Acta, 55: 1529-1538.

Fox L.E., Sager S.L. and Wofsy S.C. 1985, Factors controlling the concentrations of soluble phosphorus in the Mississippi Estuary. Limnol. Oceanogr., 30: 826-832.

Fox L.E., Sager S.L. and Wofsy S.C. 1986, The chemical control of soluble phosphorus in the Amazon Estuary. Geochim. Cosmochim. Acta, 50: 783-794.

Froelich P.N. 1988, Kinetic control of dissolved phosphate in natural rivers and estuaries: A primer on the phosphate buffer mechanism. Limnol. Oceanogr., 33: 649-668.

Froelich P.N., Bender M.L., Leudtke N.A., Heath G.R. and Devries T. 1982, The marine phosphorus cycle. Amer. J. Sci., 282: 474-511.

Gade H.G. 1970, Hydrodynamic investigation in the Oslofjord; a study of water circulation and exchange processes. Geophysical Institute, Bergen. Report No. 24: pp 193.

Gade H.G. 1976, Transport mechanism in fjords. In: "Freshwater on the Sea". (Skreslet S., Leinebø R., Matthews J.B.L. and Sakshaug E.,eds.), 51-56. Assoc. Norweg. Oceanogr., Oslo.

Gade H.G. and Edwards A. 1980, Deep-water renewal in fjords. In: "Fjord Oceanography". (Freeland H.J., Farmer D.M. and Levings C.D., eds.), 453-490. Plenum Press, New York and London.

Gade H.G., Lake R.A., Lewis E.L. and Walker E.R. 1974, Oceanography of an Arctic bay. Deep Sea Res., 21: 547-571.

Gardner W.S., Wynne D.S. and Dunstan W.M. 1976, Simplified procedure for the manual analysis of nitrate in seawater. Mar. Chem., 4: 393-396.

Gargett A.E. 1984, Vertical eddy diffusivity in the ocean interior. J. Mar. Res., 42: 359-393.

Gillibrand P.A. 1993, Circulation and mixing in a Scottish sea-loch. Ph.D. Thesis submitted to the University of Wales.

Glibert P.L and Loder T.C. 1977, Automated analysis of nutrients in seawater: a manual of techniques. Technical Report reference WHOI-77-47, Woods Hole Institution, Masachusetts.

Goldman J.C, McCarthy J.J. and Peavey D.G. 1979, Growth rate influence on the chemical composition of phytoplankton in oceanic waters. Nature, 279: 210-215.

Gowen R. 1988, A *Chaetoroceros* bloom and associated mortalities of farmed salmon in Lochs Torridon and Diabeg during July 1988. Confidential Report to Marine Harvest Limited, pp 39.

Gowen R. 1990, An assessment of the effects of fish-farming on the nutrient status and levels of phytoplankton biomass in Loch Sween. Internal Report to the Clyde River Purification Board.

Gowen R.J. and Bradbury N.B. 1987, The ecological impact of salmon farming in coastal waters: a review. Oceanogr. Mar. Biol. Ann. Review, 25: 563-575.

Gowen R., Lewis J. and Bullock A.M. 1982, A flagellate bloom and associated mortalities of farmed trout and salmon in upper Loch Fyne. Scottish Mar. Biol.

Assoc., Internal Reports no. 71.

Grantham B.E. 1981, The Loch Eil project: chlorophyll a and nutrients in the water column of Loch Eil. J. Exp. Mar. Biol. Ecol., 55: 283-297.

Grantham B.E. 1986, Nutrient regeneration in the deep water of sea-lochs. M. Phil thesis, Open University.

Grantham B.E. 1991, Loch Linnhe nutrient results; 6th February-12th June 1990. Dunstaffnage Marine Laboratory Internal Report No. 177.

Grantham B.E. 1992, Nutrient flux in a Scottish sea-loch. Dunstaffnage Marine Laboratory Internal Report. Unpublished.

Grantham B.E. and Tett P. 1993, The nutrient status of the Clyde Sea in winter. Est., Coast. and Shelf Sci., 36: 449-462.

Grasshoff K. 1964, Zur Bestimmung von Nitrat in Meer-und Trinkwasser. Kieler Meeresforschungen, 20: 5-11.

Grasshoff K. 1976, Determination of nutrients . In: "Methods of Seawater Analysis". (Giesler G. and Sosath S., eds.), pp 117. Verlag Chemie, Weinheim, New York.

Grasshoff K. 1983, Determination of nutrients . In: "Methods of Seawater Analysis". (Giesler G. and Sosath S., eds.), pp 117. Verlag Chemie, Weinheim, New York.

Haig A.J.N. 1986, Use of the Clyde Estuary and Firth for the disposal of effluents. Proceedings of The Royal Society of Edinburgh, Series B, 90: 393-405.

Heath M. 1990, An ecosystem research programme in Loch Linnhe on the west coast of Scotland. DAFS Internal Report. Unpublished.

Hingston F.J., Posner A.M. and Quirk J.P. 1974, Anion adsorption by goethite and gibsite II. J. Soil. Sci., 25: 16-26.

Hogg N., Biscaye P., Gardner W. and Schmitz W.J. 1982, On the transport and modification of Antarctic Bottom Water in the Vema Channel. J. Mar. Res., 40: 231-263.

Hooton D.H. and Giorgetta N.E. 1977, Quantitative x-ray diffraction analysis by a direct calculation method. X-Ray Spectr., 6: No.1, 2-5.

Hydes D.J. 1984, A manual of methods for the continuous flow determination of ammonia, nitrate-nitrite, phosphate and silicate. Institute of Oceanographic Science Internal Report No. 177.

Hygrometric Tables. 1970, Meteorological Office, Part II, second edition. Her Majesty's Stationery Office, London.

Ivanoff A. 1977, Oceanic adsorption of solar energy. In: "Modelling and Prediction of the Upper Layers of the Ocean". (Kraus E.B., ed.). Pergamon Press, London.

Jitts H.R. 1959, The adsorption of phosphate by estuarine bottom deposits. Aust J. Mar. Freshwat. Res. 10: 7-21.

Jones M.A. 1988, Sedimentary phosphorus and its exchange with seawater in the English Channel. Ph.D Thesis, Reading University.

de Jonge V.N. and Villerius L.A. 1989, Possible role of carbonate dissolution in estuarine phosphate dynamics. Limnol. Oceanogr., 34: 332-340.

Kafkafi U., Posner A.M. and Quirk J.P. 1967, Desorption of phosphate from kaolinite. Soil Sci. Soc. Am. Proc., 31: 348-353.

Kaul W.W. and Froelich P.N. 1984, Modelling estuarine nutrient geochemistry in a simple system. Geochim. Cosmochim Acta, 48: 1417-1433.

Kirkwood D.S. 1992, Stability of solutions of nutrient salts during storage. Mar. Chem., 38: 151-164.

Koroleff F. 1976, Determination of nutrients: determination of silicon. In: Grasshoff K. "Methods of Seawater Analysis". (Giesler G. and Sosath S., eds.), p149-158. Verlag Chemie, Weinheim, New York. "

Kramer J.R., Herbes S.E. and Allen H.E. 1972, Phosphorus: Analysis of water, biomass and sediment. In: "Nutrients in Natural Waters". (Allen H.E. and Kramer J.R., eds.), 51-100. Wiley, New York.

Kremling K. and Wenck A. 1986, On the storage of dissolved inorganic nitrate and phosphorus and reactive silicate in Atlantic Ocean water samples. Meeresforssch, 31: 69-74.

Krom M.D. and Berner R.A. 1981, The diagenesis of phosphorus in a nearshore marine sediment. Geochim. Cosmochim. Acta, 45: 207-216.

Låg J. 1976, Influence of soils on freshwater. In: "Freshwater on the Sea". (Skreslet S., Leinebø R., Matthews J.B.L. and Sakshaug E.,eds.), 21-25. Assoc. Norweg. Oceanogr., Oslo.

Lavin-Peregrina M.F. 1984, The seasonal cycle and variability of stratification in the western Irish Sea. Ph.D thesis, submitted to the University College of North Wales.

Lawrence M. 1990, The Yachtsman's Pilot to the West Coast of Scotland. Crinan to Canna. Imray Laurie Norie & Wilson Ltd, St. Ives, Cambridgeshire.

Lebo M.E. 1991, Particle-bound phosphorus along an urbanised coastal plain estuary. Mar. Chem., 34: 225-246.

Lebo M.E. and Sharp J.H. 1992, Modeling phophorus cycling in a well-mixed coastal plain estuary. Est. Coast. Shelf Sci., 35: 235-252.

Lerat Y., Lasserre P. and le Corre P. 1990, Seasonal changes in porewater concentrations of nutrients and their diffusive fluxes at the sediment-water interface. J. Exp. Mar. Biol. ecol., 135: 136-160.

Linden P.F. and Simpson J.E. 1986, Gravity driven flows in a turbulent fluid. J. Fluid Mechs., 172: 481-497.

Linden P.F. and Simpson J.E. 1988, Modulated mixing and frontogenesis in shallow seas and estuaries. Cont. Shelf Res., 8: 1107-1127.

Liss P.S. 1976, Conservative and non-conservative behaviour of dissolved constituents during estuarine mixing. In: "Estuarine Chemistry". (Burton J.D. and Liss P.S., eds.), 93-129. Academic Press, London.

Liss P.S. and Spencer C.P. 1970, Abiological processes in the removal of silicate from seawater. Geochim. Cosmochim. Acta., 34: 1073-1088.

Livingstone D.A. 1963, Chemical composition of rivers and lakes. Prog. Paper. US. Geol. Surv., 440: pp. 64.

Loder T.C. and Reichard R.P. 1981, The dynamics of conservative mixing in estuaries. Estuaries, 4: 64-69.

Lucotte M. and d'Anglejan B. 1988, Processes controlling phosphate adsorption by iron hydroxides in estuaries. Chem. Geol., 67: 75-83.

Macdonald R.W. and McLaughlin F.A. 1982, The effect of storage by freezing on dissolved inorganic phosphate, nitrate and reactive silicate for samples from coastal and estuarine waters. Water Res., 16: 95-104.

Mackay D.W. and Halcrow W. 1976, The distribution of nutrients in relation to water movements in the Firth of Clyde. In: "Freshwater on the Sea". (Skreslet S., Leinebø R., Matthews J.B.L. and Sakshaug E.,eds.), 109-118. Assoc. Norweg. Oceanogr., Oslo.

Mackay D.W. and Leatherland T.M. 1976, Chemical processes in an estuary receiving major inputs of industrial and domestic wastes. In: "Estuarine Chemistry". (Burton J.D. and Liss P.S., eds.), 185-218. Academic Press, London.

Mackay W.A. and Baxter M.S. 1985, Water transport from the north-east Irish Sea to western Scottish coastal waters: Further observations from time-trend matching of Sellafield radiocaesium. Est. Coast. Shelf Sci., 21: 471-480.

Mackay W.A., Baxter M.S., Ellett D.J. and Meldrum D.T. 1986, Radiocaesium and circulation patterns west of Scotland. J. Environ. Radioactivity, 4: 205-232.

Mantoura R.F.C. and Woodward E.M.S. 1983, Conservative behaviour of riverine dissolved organic carbon in the Severn estuary: Chemical and geochemical implications. Geochim. Cosmochim. Acta, 47: 1293-1309.

McAlister W.B., Rattray M. and Barnes C.A. 1959, the dynamics of a fjord estuary: Silver Bay, Alaska. Dept of Oceanog. Tech. Rep. No. 62. University of Washington, Seattle, Washington.

McClimans T.A. 1978, On the energetics of tidal inlets to land-locked fjords. Mar. Sci. Comm., 4: 121-137.

McElroy M.B. 1983, Marine biological controls on atmospheric CO_2 and climate. Nature, 302: 328-329.

Meybeck M. 1979, Concentrations des eaux fluviales en elements majeurs et apports en solution aux oceans. Rev. Geol. Dyn. Geogr. Phys., 21: 215-246.

Meybeck M. 1982, C, N and P transport by world rivers. Am. J. Sci., 282: 401-450.

Meybeck M. 1983, Atmospheric inputs and river transport of dissolved substances. In: "Dissolved Loads of Rivers and Surface Water Quantity/Quality Relationships". International Association of Hydrological Sciences Publ., 141: 173-192.

Meybeck M. 1988, How to establish and use world budgets of river material. In: "Physical and Chemical Weathering in Geochemical Cycles". (Lerman A. and Meybeck M., eds.). Dordrecht, Reidel.

Miller A.E.J. and Mantoura R.F.C. 1992, Investigation of dissolved organic carbon in the Tamar Estuary, using high temperature catalytic oxidation and persulphate-promoted ultra-violet photo-oxidation techniques. A paper presented at the Oceanography U.K. meeting, Liverpool, U.K., September 1992.

Milliman J.D. 1993, Water and sediment discharge from rivers to the oceans: new perspectives on old problems. A paper presented at the E.C, MAST workshop entitled Biogeochemical Processes in Estuarine and Shelf Seas, Plymouth, U.K. September 1993.

Milne P.H. 1972, Hydrography of Scottish west coast sea-lochs. Mar. Res. Rep. DAFS, 3: pp. 40

Molvaer J. 1980, Deep-water renewals in the Frierfjord - an intermittently anoxic basin. In: "Fjord Oceanography". (Freeland H.J., Farmer D.M. and Levings C.D., eds.), 531-539. Plenum Press, New York and London.

Moore R.M., Burton J.D., LeB Williams P.J. and Young M.L. 1979, The behaviour of dissolved organic material, iron and manganese in estuarine mixing. Geochim. Cosmochim. Acta, 43: 919-926.

Morris A.W. 1988, The estuaries of the Humber and Thames. In: "Pollution of the North Sea. An Assessment." (Salomons W., Bayne B.L., Duursma E.K. and Forstner U., eds.). Springer-Verlag.

Morris A.W. and Riley J.P. 1963, The determination of nitrate in sea-water. Analyt. Chim. Acta, 29: 272-279.

Morris A.W., Bale A.J. and Howland J.M. 1981, Nutrient Distributions in an estuary: Evidence of chemical precipitation of dissolved silicate and phosphate. Est. Coast. Shelf Sci., 12: 205-216.

Muller F, Tranter M., Burton J.D., Statham P. and Fones G. 1992, The cycling and fate of toxic trace metals within the Clyde Estuary and the Firth of Clyde: The role of suspended particulates enriched in manganese. MAFF Report. Unpublished.

Mullin J.B. and Riley J.P. 1965, Colorimetric determination of silicate with special reference to sea and natural waters. Analyt. Chim. Acta, 12: 162-175.

Munday B., Eleftheriou A., Kentouri M. and Divanach P. 1992, The Interactions of Aquaculture and the Environment. A Bibliographical Review. Report prepared for the Commission of European Communities, Directorate General for Fisheries. Ref. XIV/D/3,003218 - 12.02.92.

Murphy J. and Riley J.P. 1962, A modified single solution method for the determination of phosphate in natural waters. Anal. Chim. Acta, 27: 31-36.

Nowicki B.L. and Oviatt C.A. 1990, Are estuaries traps for anthropogenic nutrients? Evidence from estuarine mesocosms. Marine Ecology Progress Series, 66: 131-146.

Officer C.B. 1983, Physics of estuarine circulation. In: "Ecosystems of the World. Estuaries and Enclosed Seas. No. 26". (Ketchum B.H., ed.), 15-41. Elsevier Scientific Publishing Company, Amsterdam, Oxford, New York.

Officer C.B. and Kester D.R. 1991, On estimating the non-advective tidal exchanges and advective gravitational circulation exchanges in an estuary. Est. Coast. Shelf Sci., 32: 99-103.

Officer C.B. and Lynch D.R. 1981, Dynamics of mixing in estuaries. Est. Coast. Shelf Sci., 12: 525-533.

Officer and Ryther J.H. 1980, The possible importance of silicon in marine eutrophication. Mar. Ecol. Progr. Ser., 3: 83-91.

Open University. 1989, "Ocean Chemistry and Deep-Sea Sediments". Pergamon Press PLC.

Oviatt C.A., Pilson M.E.Q., Nixon S.W., Frithsen J.B., Rudnick D.T., Kelly J.R., Grassle J.F. and Grassle J.P. 1984, Recovery of a polluted estuarine system: A mesocosm experiment. Mar. Ecol. Progress Ser., 16: 203-217.

Parsons T.R., Takahashi M. and Hargrave B. 1984, "Biological Oceanographic Processes". Pergamon Press.

Parsons T.R., Maita Y. and Lalli C.M. 1985, Determination of chlorophylls and total cartenoids: Spectrophotometric method. In: "A Manual of Chemical and Biological Methods for Seawater Analysis". Pergamon Press Publishers. Oxford, New York, Toronto, Sydney and Frankfurt.

Pearson T.H. 1970, The benthic ecology of Loch Linnhe and Loch Eil, a sea-loch system on the west coast of Scotland. I. The physical environment and distribution of macrobenthic fauna. J. Exp. Mar. Biol. Ecol., 5: 1-34.

Pearson T.H. 1988, Energy flow through fjord systems. Lecture Notes on Coastal and Estuarine Studies, 22: 188-208.

Pei-Yuan Chen. 1977, Table of Key Lines in X-ray Powder Diffraction Patterns of Minerals and Associated Rocks. Department of Natural Resources, Geological Survey. Occassional paper no. 21. Printed by the Authority of the State, Bloomington.

Pejrup M., Bartholdy J. and Jensen A. 1993, Supply and nutrient exchange of water and nutrients in the Grådyb tidal area, denmark. Est. Coast. Shelf Sci., 36: 221-234.

Pickard G.L. and Emery W.J. 1982, Physical properties of seawater. In: "Descriptive Physical Oceanography, An Introduction". pp 17-19. Fourth edition (in S.I. units). Pergamon Press.

Pomeroy L.R., Smith E.E. and Grant C.M. 1965, The exchange of phosphate between estuarine waters and sediments. Limnol. Oceanogr., 10: 167-172.

Pratt D.M. 1965, The winter-spring diatom flowering in Narragansett Bay. Limnol. Oceanogr., 10: pp173.

Price N.B. 1976, Chemical diagenesis in sediments. In: "Chemical Oceanography". (Riley J.P. and Chester R., eds.), 1-58. Second edition, vol 6. Academic Press, New

York.

Pritchard D.W. 1952, Estuarine hydrography. Adv. Geophys., 1: 243-280.

Rabalais N.N. 1992, Mississippi River quality changes and consequences to coastal ecosystems. A paper presented at the ERF/ECSA meeting in Plymouth, U.K., September 1992.

Raymont J.E.G. 1963, "Plankton and Productivity in the Oceans". (McMillan Co., New York), pp 660.

Redfield A.C. 1934, In: "James Johnstone Memorial Volume". (Daniel R.J., ed.), 177-192. Liverpool University Press.

Redfield A.C., Ketchum B.H. and Richards F.A. 1963, The influence of organisms on the composition of seawater. In: "The Sea. Ideas and Observations on Progress in the Study of the Seas". (Hill M.N., ed.), 26-49. Interscience Publishers, John Wiley and Sons. New York, London.

Richards F.A. 1958, Dissolved silicate and related properties of some Western North Atlantic and Caribbean waters. J. Mar. Res., 17: 449-465.

Richards F.A. 1965, Anoxic basins and fjords. In: "Chemical Oceanography". (Riley J.P. and Skirrow G. eds.), 1: 611-645. Academic Press, London.

Rigler F.H. 1973, A dynamic view of the phosphorus cycle in lakes. In: "Environmental Chemistry Handbook". (Griffith, ed.), 539-572. John Wiley, New York.

Riley J.P. and Chester R. 1971, "Introduction to Marine Chemistry", Ch.7. Academic Press, New York.

Roberts G., Hudson J.A. and Blackie J.R. 1983, Nutrient cycling in the Wye and Severn at Plynlimon. Institue of Hydrology. Report No. 86.

Robinson R.J. and Thompson T.G. 1948, J. Mar. Res., 7: pp 49.

Ross A.H., Gurney W.S.C. and Heath M.R.[1] 1993, Ecosystem models of Scottish sea-lochs for assessing the impact of nutrient enrichment. ICES J. Mar. Sci., 50: 359-367.

Ross A.H., Gurney W.S.C. and Heath M.R.[2] 1993, A comparative study of the ecosystem dynamics of four fjordic sea-lochs. In press, Limnol. Oceanogr.

Sakshaug E. and Myklestad S. 1973, Studies on the phytoplankton ecology of the Trondheimsfjord, III. Dynamics of phytoplankton blooms in relation to environmental factors, bioassay experiments and parameters for the physiological state of the populations. J. Exp. Mar. Biol. Ecol., 11: 157-188.

SCOR Working Group. 1988, River inputs to ocean systems: Status and recommendations for research. (Burton, J.D., ed.), UNESCO Technical Papers in Marine Science, 55.

Seitzinger S.P. 1991, The effect of pH on the release of phosphorus from Potomac Estuary sediments: Implications for blue-green algae blooms. Est. Coast. Shelf Sci., 33: 409-418.

Sharp J.H., Pennock J.R., Church T.M., Tramontano J.M. and Cifuentes L.A. 1984, The estuarine interaction of nutrients, organics and metals: A case study in the Delaware Estuary. In: "The Estuary as a Filter". (Kennedy V.S., ed.), 241-258. Academic Press, London.

Sharples J. and Tett P.B. 1992, Modelling observations of the seasonal cycle of primary productivity: the importance of short-term physical variability. Internal

Report University College of North Wales. Unpublished.

Sharples J., Simpson J.H. and Brubaker J.M. 1994, Observations and modelling of periodic stratification in the upper York River Estuary, Virginia. Est. Coast. Shelf Sci., 38: 301-312.

Shinn M.B. 1941, A colorimetric method for the determination of nitrate. Industrial and Engineering Chemistry, Analytical edition, 13: 33-35.

Sholkovitz E.R. 1976, Flocculation of dissolved organic and inorganic matter during the mixing of river water and seawater. Geochim. Cosmochim. Acta, 40: 831-845.

Sholkovitz E.R. 1979, Chemical and Physical processes controlling the chemical composition of suspended material in the River Tay estuary. Estuar. Coast. Shelf Sci., 8: 523-545.

Sholkovitz E.R. and Copland D. 1981, The coagulation, solubility and adsorption properties of Fe, Mn, Cu, Ni, Cd, Co and humic acids in river water. Geochim. Cosmochim. Acta, 45: 181-189.

Sholkovitz E.R., Boyle E.A. and Price N.B. 1977, The removal of dissolved humic acids and iron during estuarine mixing. Earth Plan. Sci. Lett., 40: 130-136.

Sieburth J. and Jensen A. 1968, Studies on algal substances in the sea. I. Gelbstoff (humic material) in terrestrial and marine waters. J. Exp. Mar. Biol. Ecol., 2: 174-189.

Simpson J.H.. and Bowers D.G. 1981, Models of stratification and frontal movement in shelf seas. Deep-Sea Res., 28A, No. 7: 727-738.

Simpson J.H. and Bowers D.G. 1984, The role of tidal stirring in controlling the

seasonal heat cycle in shelf seas. Annal. Geophys., 2: 411-416.

Simpson J.H. and Rippeth T.P. 1993, The Clyde Sea: A model of the seasonal cycle of stratification and mixing. Est. Coastal. Shelf Sci., 37: 129-144.

Simpson J.H. and Sharples J. 1991, Dynamically-active models in the prediction of estuarine stratification. In: "Dynamics and Exchanges in Estuaries and the Coastal Zone". (Prandle D., ed.), 101-113. Springer-Verlag, New York.

Smayda T.J. 1983, The phytoplankton of estuaries. In: "Ecosystems of the World. Estuaries and Enclosed Seas". (Ketchum B.H., ed.), pp 70. Elsevier Scientific Publishing Company.

Smith D.J. and Longmore A.R. 1980, Behaviour of phosphate in estuarine water. Nature, 287: 532-534.

Solorzano L. and Ehrlich B. 1977, Chemical investigations of Loch Etive, Scotland. I. Inorganic nutrients and pigments. J. Exp. Mar. Biol. Ecol., 9: 45-64.

Solorzano L. and Grantham B. 1975, Surface nutrients, chlorophyll a and phaeopigment in some Scottish sea-lochs. J. Exp. Mar. Biol. Ecol. 20: 63-76.

Spiegel M. R. 1972, Correlation theory. In: "Schaums Outline Series of Theory and Problems of Statistics". 241-244. McGraw-Hill Book Company.

Stainton M.P. 1974, Simple, efficient reduction column for use in automated determination of nitrate in water. Anal. Chem., 46: 1616.

Stefansson U. and Richards F.A. 1963, Processes contributing to the nutrient distributions off the Columbia River and Strait of Juan de Fuca. Limnol. Oceanogr., 8: pp 394.

Stigebrandt A. 1976, Vertical diffusion driven by internal waves in a sill fjord. J. Phys. Oceanogr., 6: 486-495.

Stigebrandt A. 1977, On the effect of barotropic current fluctuations on the two-layer transport capacity of a constriction. J. Phys. Oceanogr., 7: 118-122.

Stigebrandt A. 1979, Observational evidence for vertical diffusion driven by internal waves of tidal origin in the Oslofjord. J. Phys. Oceanogr., 9: 435-441.

Stigebrandt A. and Aure J. 1989, Vertical mixing in basin waters of fjords. J. Phys. Oceanogr., 19: 917-926.

Stigebrandt A. and Wulff F. 1987, A model for the dynamics of nutrients and oxygen in the Baltic proper. J. Mar. Res., 45: 729-759.

Strickland J.D.H. and Parsons T.R. 1968, "A Practical Handbook of Seawater Analysis" Bulletin 167, Fisheries Research Board of Canada.

Strickland J.D.H. and Parsons T.R. 1977, "A Practical Handbook of Seawater Analysis" Bulletin 167, Fisheries Research Board of Canada.

Stumm W. and Morgan J.J. 1970, Case studies: Phosphorus, iron and manganese. In: "Aquatic Chemistry", 514-563. Wiley, New York.

Stumm W. and Morgan J.J. 1981, Specific chemical interaction with cations and anions at the oxide surface. In: "Aquatic Chemistry", 632-639. Second edition, Wiley, New York.

Sundby B., Gobeil C., Silverberg N., Mucci A. 1992, The phosphorus cycle in coastal marine sediments. Limnol. Oceanogr., 37: 1129-1145.

Svensson T. 1980, Tracer measurements of mixing in the deepwater of a small stratified sill-fjord. In: "Fjord Oceanography". (Freeland H.J., Farmer D.M. and Levings C.D., eds.), 355-362. Plenum Press, New York and London.

Syvitski J.P.M., Burrell D.C. and Skei J.M. 1986, "Fjords: Processes and Products". Springer-Verlag, Berlin, Heihelberg, New York.

Takahashi M. and Fukazawa N. 1982, A mechanism of "red tide" formation. II. Effect of selective stimulation on the growth of different phytoplankton species in natural water. Mar. Biol., 70: 267-273.

Tett P. 1980, Phytoplankton and the fish kills in Loch Striven. SMBA Internal Report No. 25.

Tett P. 1987, Modelling the growth and distribution of marine microplankton. In: "Ecology of Microbial Communities". 387-425. Cambridge University Press.

Tett P. and Edwards A. 1984, Mixing and plankton: An interdisciplinary theme in oceanography. Oceanogr. Mar. Biol. Ann. Rev., 22: 99-123.

Tett P. and Grantham B. 1978, A simple guide to the measurement and interpretation of chlorophyll concentration, temperature and salinity in coastal waters. SMBA Internal Report.

Tett P., Edwards A. and Jones K. 1986, A model for the growth of shelf-sea phytoplankton in summer. Est. Coastal Shelf Sci., 23: 641-672.

Tett P., Gowen R., Grantham B., Jones K. and Miller B.S. 1985, The phytoplankton ecology of the Firth of Clyde sea-lochs Striven and Fyne. Symposium on the Environment of the Estuary and Firth of Clyde, Glasgow, 1-2 Oct. 1985.

Thompson R.E. 1981, Oceanography of the British Columbian coast. Can. Fish. Aquat. Sci., 56: 1-291.

Tritton D.J. 1977, Free convection. In: "Physical Fluid Dynamics". Published by Van Nostran Reinhold Company. pp. 141.

UNESCO. 1991, Processing of oceanographic station data. UNESCO, ISBN 92-3-102756-5. pp 137.

UNESCO Programme on Harmful Algal Blooms. 1991, IOC-SCOR workshop on programme development for harmful algal blooms. Newport, Rhode Island, USA, 2-3 November, 1991.

UNESCO Technical Report in Marine Science. 1981, No. 36.

UNESCO Technical Papers in Marine Sciences Nos. 37, (1981) and 44 (1983). Algorithms for computation of fundamental properties of seawater.

Upchurch J.B., Edzwald J.K. and O' Melia C.R. 1974, Phosphates in sediments of Pamlico Estuary. Environ. Sci. Technol., 8: 56-58.

Van Bennekon A.J. and Wetsjen F.J. 1990, The winter distribution of nutrients in the Southern Bight of the North sea (1961-1978) and in the estuaries of the Scheldt and the Rhine/Meuse. Neth. J. Sea Res., 25: 75-87.

Vaz R.A., Lennon G.W. and Samarasinghe J. 1989, The negative role of turbulence in estuarine mass transport. Est. Coast. Shelf Sci., 28: 361-377.

Walling D.E. and Webb B.W. 1983, The dissolved loads of rivers: A global overview. In: "Dissolved Loads of Rivers and Surface Water Quantity/Quality Relationships". International Assoc. Hydrol. Sci. Publ., 141: 3-20.

Walling D.E. and Webb B.W. 1984, Local variation of nitrate levels in the Exe Basin, Devon, U.K. Betrage Zur Hydrol., 71-100.

Webb B.W. and Walling D.E. 1985, Nitrate behaviour in streamflow from a grassland catchment in Devon, U.K. Water Res., 19(8): 1005-1016.

Welander P. 1974, Theory of a two-layer fjord type estuary with special reference to the Baltic Sea. J. Phys. Oceanogr., 4: 542-556.

West Coast of Scotland Pilot. West Coast of Scotland from Mull of Galloway to Cape Wrath including the Inner and Outer Hebrides and off-lying Islands. 1974. Published by the Hydrographer of the Navy.

Wood E.D., Armstrong F.A.J. and Richards F.A. 1967, Determination of nitrate in seawater by cadmium-copper reduction to nitrite. J. Mar Biol. Assoc. UK., 47: 23-31.

Yen T.F. and Tang J.I.S. 1977, Chemical aspects of marine sediments. In: "Chemistry of Marine Sediments" (Yen T.F., ed.), 1-39. Ann Arbor Sci. Publ., Michigan.

Youden W.J. 1951, "Statistical Methods for Chemists" (Stewhart W.A., ed.), pp.15. John Wiley and Sons Publ., New York.

Zhiliang S., Xingjan L., Jiaping L. and Haunxiang D. 1985, Changes in inorganic phosphate concentrations during water sample storage. Mar. Sci., 9: 29-33

Zussman J. 1977, "Physical Methods in Determinative Mineralology". Academic press.

Zwolsman J.J.G. 1986, Nutrient biogeochemistry in estuaries, with an emphasis on the Scheldt Estuary. Internal Report for the State University of Utrecht,

Unpublished.

Zwolsman, J.J.G. 1992, Behaviour of phosphorus in the Scheldt Estuary, SW-Netherlands. A paper presented at the ECSA/ERF meeting, Plymouth, U.K., September 1992.